



World Journal of Gastroenterology®



Volume 11 Number 10
March 14, 2005



National Journal Award

Contents

LIVER CANCER

- 1411** Co-administration of cyclosporine A alleviates thioacetamide-induced liver injury
Fan S, Weng CF
- 1420** Sirolimus inhibits growth of human hepatoma cells alone or combined with tacrolimus, while tacrolimus promotes cell growth
Schumacher G, Oidtmann M, Rueggeberg A, Jacob D, Jonas S, Langrehr JM, Neuhaus R, Bahra M, Neuhaus P
- 1426** Comparison between combination therapy of percutaneous ethanol injection and radiofrequency ablation and radiofrequency ablation alone for patients with hepatocellular carcinoma
Kurokohchi K, Watanabe S, Masaki T, Hosomi N, Miyauchi Y, Himoto T, Kimura Y, Nakai S, Deguchi A, Yoneyama H, Yoshida S, Kuriyama S
- 1433** Impact of pre-operative transarterial embolization on the treatment of hepatocellular carcinoma with liver transplantation
Cheng YF, Huang TL, Chen TY, Chen YS, Wang CC, Hsu SL, Tsang LLC, Sun PL, Chiu KW, Jawan B, Eng HL, Chen CL
- 1439** Factors for early tumor recurrence of single small hepatocellular carcinoma after percutaneous radiofrequency ablation therapy
Yu HC, Cheng JS, Lai KH, Lin CP, Lo GH, Lin CK, Hsu PI, Chan HH, Lo CC, Tsai WL, Chen WC
- 1445** Clinicopathological significance of expression of paxillin, syndecan-1 and EMMPRIN in hepatocellular carcinoma
Li HG, Xie DR, Shen XM, Li HH, Zeng H, Zeng YJ
- 1452** Impact of prolonged fraction dose-delivery time modeling intensity-modulated radiation therapy on hepatocellular carcinoma cell killing
Zheng XK, Chen LH, Yan X, Wang HM
- 1457** Are polymorphisms of N-acetyltransferase genes susceptible to primary liver cancer in Luoyang, China?
Zhang XF, Bian JC, Zhang XY, Zhang ZM, Jiang F, Wang QM, Wang QJ, Cao YY, Tang BM
- 1463** Identify lymphatic metastasis-associated genes in mouse hepatocarcinoma cell lines using gene chip
Song B, Tang JW, Wang B, Cui XN, Hou L, Sun L, Mao LM, Zhou CH, Du Y, Wang LH, Wang HX, Zheng RS, Sun L

COLORECTAL CANCER

- 1473** Vegetable/fruit, smoking, glutathione S-transferase polymorphisms and risk for colorectal cancer in Taiwan
Yeh CC, Hsieh LL, Tang R, Chang-Chieh CR, Sung FC
- 1481** Clinical phenotype and prevalence of hereditary nonpolyposis colorectal cancer syndrome in Chinese population
Zhang YZ, Sheng JQ, Li SR, Zhang H

Contents

BASIC RESEARCH

- 1489** Toll-like receptor 4 and NOD2/CARD15 mutations in Hungarian patients with Crohn's disease: Phenotype-genotype correlations
Lakatos PL, Lakatos L, Szalay F, Willheim-Polli C, Österreicher C, Tulassay Z, Molnar T, Reinisch W, Papp J, Mozsik G, Hungarian IBD Study Group, Ferenci P
- 1496** Hepatocyte growth factor gene therapy prevents radiation-induced liver damage
Chi CH, Liu IL, Lo WY, Liaw BS, Wang YS, Chi KH
- 1503** Protective effects of *Rheum tanguticum* polysaccharide against hydrogen peroxide-induced intestinal epithelial cell injury
Liu LN, Mei QB, Liu L, Zhang F, Liu ZG, Wang ZP, Wang RT
- 1508** Activation of nuclear factor-kappa B and effects of pyrrolidine dithiocarbamate on TNBS-induced rat colitis
Chen K, Long YM, Wang H, Lan L, Lin ZH
- 1515** Effects of drug serum of anti-fibrosis I herbal compound on calcium in hepatic stellate cell and its molecular mechanism
Xiao YH, Liu DW, Li Q

CLINICAL RESEARCH

- 1521** Synergistic effects of interferon-alpha in combination with chemoradiation on human pancreatic adenocarcinoma
Ma JH, Patrut E, Schmidt J, Knaebel HP, Büchler MW, Märten A
- 1529** Aspartate aminotransferase-immunoglobulin complexes in patients with chronic liver disease
Tameda M, Shiraki K, Ooi K, Takase K, Kosaka Y, Nobori T, Tameda Y
- 1532** Efficacy of multislice computed tomography for gastroenteric and hepatic surgeries
Ohtani H, Kawajiri H, Arimoto Y, Ohno K, Fujimoto Y, Oba H, Adachi K, Hirano M, Terakawa S, Tsubakimoto M
- 1535** Hypoxia-inducible factor 1 alpha and vascular endothelial growth factor overexpression in ischemic colitis
Okuda T, Azuma T, Ohtani M, Masaki R, Ito Y, Yamazaki Y, Ito S, Kuriyama M
- 1540** A blind, randomized comparison of racecadotril and loperamide for stopping acute diarrhea in adults
Wang HH, Shieh MJ, Liao KF

BRIEF REPORTS

- 1544** Connexin 26 correlates with Bcl-xL and Bax proteins expression in colorectal cancer
Kanczuga-Koda L, Sulkowski S, Koda M, Skrzydlewska E, Sulkowska M
- 1549** *Helicobacter pylori* strain-specific modulation of gastric inflammation in Mongolian gerbils
Ohnita K, Isomoto H, Honda S, Wada A, Wen CY, Nishi Y, Mizuta Y, Hirayama T, Kohno S
- 1554** Anatomic and technical skill factor of gastroduodenal complication in post-transarterial embolization for hepatocellular carcinoma: A retrospective study of 280 cases
Leung TK, Lee CM, Chen HC
- 1558** Laparoscopic Heller myotomy with or without partial fundoplication: A matter of debate
Ramacciato G, D'Angelo FA, Aurello P, Gaudio MD, Varotti G, Mercantini P, Bellagamba R, Ercolani G
- 1562** Immunocytochemical detection of HoxD9 and Pbx1 homeodomain protein expression in Chinese esophageal squamous cell carcinomas
Liu DB, Gu ZD, Cao XZ, Liu H, Li JY

<div> <div>World Journal of Gastroenterology®</div> <div>Volume 11 Number 10 March 14, 2005</div> </div>	
Contents	
CASE REPORT	<div>1567 Effect of <i>Helicobacter pylori</i> eradication on gastric hyperplastic polyposis in Cowden's disease</div> <div>Isomoto H, Furusu H, Ohnita K, Takehara Y, Wen CY, Kohno S</div>
ACKNOWLEDGEMENTS	1570 Acknowledgements to reviewers for this issue
APPENDIX	<div>1A Meetings</div> <div>2A Instructions to authors</div> <div>4A <i>World Journal of Gastroenterology</i> standard of quantities and units</div>
FLYLEAF	I-V Editorial Board
INSIDE FRONT COVER	ISI journal citation reports 2003-GASTROENTEROLOGY AND HEPATOLOGY
INSIDE BACK COVER	15 th World Congress of the International Association of Surgeons and Gastroenterologists
<p><i>World Journal of Gastroenterology</i> (<i>World J Gastroenterol</i>, <i>WJG</i>), a leading international journal in gastroenterology and hepatology, has an established reputation for publishing first class research on esophageal cancer, gastric cancer, liver cancer, viral hepatitis, colorectal cancer, and <i>Helicobacter pylori</i> infection, providing a forum for both clinicians and scientists, and has been indexed and abstracted in Index Medicus, MEDLINE, PubMed, Chemical Abstracts, EMBASE, Abstracts Journals, Nature Clinical Practice Gastroenterology and Hepatology, CAB Abstracts and Global Health. Impact factor of ISI JCR during 2000-2003 is 0.993, 1.445, 2.532 and 3.318 respectively. <i>WJG</i> is a weekly journal published jointly by The <i>WJG</i> Press and Elsevier Inc. The publication date is on 7th, 14th, 21st, and 28th every month. The <i>WJG</i> is supported by The National Natural Science Foundation of China, No. 30224801 and No.30424812, which was founded with a name of <i>China National Journal of New Gastroenterology</i> on October 1,1995, and renamed as <i>WJG</i> on January 25, 1998.</p>	
HONORARY EDITORS-IN-CHIEF Ke-Ji Chen, <i>Beijing</i> Dai-Ming Fan, <i>Xi'an</i> Zhi-Qiang Huang, <i>Beijing</i> Nicholas F LaRusso, <i>Rochester</i> Jie-Shou Li, <i>Nanjing</i> Geng-Tao Liu, <i>Beijing</i> Fa-Zu Qiu, <i>Wuhan</i> Eamonn M Quigley, <i>Cork</i> David S Rampton, <i>London</i> Rudi Schmid, <i>California</i> Nicholas Joseph Talley, <i>Rochester</i> Zhao-You Tang, <i>Shanghai</i> Guido NJ Tytgat, <i>Amsterdam</i> Meng-Chao Wu, <i>Shanghai</i> Xian-Zhong Wu, <i>Tianjin</i> Hui Zhuang, <i>Beijing</i> Jia-Yu Xu, <i>Shanghai</i>	EDITORIAL BOARD See full details flyleaf I-V DEPUTY EDITOR Michelle Gabbe, Xian-Lin Wang ASSOCIATE MANAGING EDITORS Jan-Zhong Zhang, Shi-Yu Guo EDITORIAL OFFICE MANAGER Jing-Yun Ma EDITORIAL ASSISTANT Juan Li TECHNICAL EDITORS Meng Li, Shao-Hua Li, Hu-Jun Mei, Hu Wang PROOFREADERS Hong Li, Li Ding, Shi-Yu Guo PUBLISHED JOINTLY BY The WJG Press and Elsevier Inc PRINTING GROUP Printed in Beijing on acid-free paper by Beijing Kexin Printing House COPYRIGHT © 2005 Published jointly by The WJG Press and Elsevier Inc. All rights reserved; no part of this publication may be reproduced, stored in a retrieval system, or transmitted in any form or by any means, electronic, mechanical, photocopying, recording, or otherwise without the prior permission of
PRESIDENT AND EDITOR-IN-CHIEF Lian-Sheng Ma, <i>Beijing</i> EDITOR-IN-CHIEF Bo-Rong Pan, <i>Xi'an</i> ASSOCIATE EDITORS-IN-CHIEF Bruno Annibale, <i>Roma</i> Henri Bismuth, <i>Villejuif</i> Jordi Bruix, <i>Barcelona</i> Roger William Chapman, <i>Oxford</i> Alexander L Gerbes, <i>Munich</i> Shou-Dong Lee, <i>Taipei</i> Walter Edwin Longo, <i>New Haven</i> You-Yong Lu, <i>Beijing</i> Masao Omata, <i>Tokyo</i> Harry H-X Xia, <i>Hong Kong</i>	The <i>WJG</i> Press and Elsevier Inc. Author are required to grant <i>WJG</i> an exclusive licence to publish. Print ISSN 1007-9327 CN 14-1219/R. SPECIAL STATEMENT All articles published in this journal represent the viewpoints of the authors except where indicated otherwise. EDITORIAL OFFICE Editor: <i>World Journal of Gastroenterology</i> , The WJG Press, Apartment 1066 Yishou Garden, 58 North Langxinzhuang Road, PO Box 2345, Beijing 100023, China Telephone: +86-(0)10-85381892 Fax: +86-10-85381893 E-mail: wjg@wjgnet.com http://www.wjgnet.com Public Relationship Manager Shi-Yu Guo The WJG Press, Apartment 1066 Yishou Garden, 58 North Langxinzhuang Road, PO Box 2345, Beijing 100023, China Telephone: +86-(0)10-85381892 Fax: +86-10-85381893 E-mail: s.y.guo@wjgnet.com http://www.wjgnet.com SUBSCRIPTION INFORMATION Foreign Elsevier (Singapore) Pte Ltd, 3 Killiney Road #08-01, Winsland House I, Singapore 239519 Telephone: +65-6349 0200 Fax: +65-6733 1817
	E-mail: r.garcia@elsevier.com http://asia.elsevierhealth.com Institutional Rates Print-2005 rates: USD1 500.00 Personal Rates Print-2005 rates: USD700.00 Domestic Local Post Offices Code No. BM 82-261 Author Reprints and Commercial Reprints The WJG Press, Apartment 1066 Yishou Garden, 58 North Langxinzhuang Road, PO Box 2345, Beijing 100023, China Telephone: +86-(0)10-85381892 Fax: +86-10-85381893 E-mail: wjg@wjgnet.com http://www.wjgnet.com ADVERTISING Rosalia Da Carcia Elsevier Science Journals Marketing & Society Relations Health Science Asia 3 Killiney Road #08-01, Winsland House 1 Singapore 239519 Telephone: +65-6349 0200 Fax: +65-6733 1817 E-mail: r.garcia@elsevier.com http://asia.elsevierhealth.com INSTRUCTIONS TO AUTHORS Full instructions are available online at http://www.wjgnet.com/wjg/help/ instructions.jsp If you do not have web access please contact the editorial office.

World Journal of Gastroenterology®

Editorial Board

2004-2006



Published by The WJG Press and Elsevier Inc., PO Box 2345, Beijing 100023, China
Fax: +86-(0)10-85381893 E-mail: wjg@wjgnet.com <http://www.wjgnet.com>

HONORARY EDITORS-IN-CHIEF

Ke-Ji Chen, *Beijing*
Dai-Ming Fan, *Xi'an*
Zhi-Qiang Huang, *Beijing*
Nicholas F LaRusso, *Rochester*
Jie-Shou Li, *Nanjing*
Geng-Tao Liu, *Beijing*
Fa-Zu Qiu, *Wuhan*
Eamonn M Quigley, *Cork*
David S Rampton, *London*
Rudi Schmid, *California*
Nicholas Joseph Talley, *Rochester*
Zhao-You Tang, *Shanghai*
Guido NJ Tytgat, *Amsterdam*
Meng-Chao Wu, *Shanghai*
Xian-Zhong Wu, *Tianjin*
Hui Zhuang, *Beijing*
Jia-Yu Xu, *Shanghai*

PRESIDENT AND EDITOR-IN-CHIEF

Lian-Sheng Ma, *Beijing*

EDITOR-IN-CHIEF

Bo-Rong Pan, *Xi'an*

ASSOCIATE EDITORS-IN-CHIEF

Bruno Annibale, *Roma*
Henri Bismuth, *Villesuif*
Jordi Bruix, *Barcelona*

Roger William Chapman, *Oxford*
Alexander L Gerbes, *Munich*
Shou-Dong Lee, *Taipei*
Walter Edwin Longo, *New Haven*
You-Yong Lu, *Beijing*
Masao Omata, *Tokyo*
Harry H-X Xia, *Hong Kong*

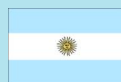
MEMBERS OF THE EDITORIAL BOARD



Albania
Bashkim Resuli, *Tirana*



Algeria
Hocine Asselah, *Algiers*



Argentina
Julio Horacio Carri, *Córdoba*



Australia
Darrell HG Crawford, *Brisbane*
Robert JL Fraser, *Daw Park*
Yik-Hong Ho, *Townsville*
Gerald J Holtmann, *Adelaide*
Michael Horowitz, *Adelaide*

www.wjgnet.com

Riordan SM, *Sydney*
IC Roberts-Thomson, *Adelaide*
James Tooili, *Adelaide*



Austria
Dragosics BA, *Vienna*
Peter Ferenci, *Vienna*
Alfred Gangl, *Vienna*
Michael Trauner, *Graz*
Harald Vogelsang, *Vienna*



Belarus
Yury K Marakhouski, *Minsk*



Belgium
Geerts AEC, *Brussels*
Cremer MC, *Brussels*
Yves J Horsmans, *Brussels*
Yvan Vandenplas, *Brussels*
Eddie Wisse, *Keerbergen*



Brazil
Heitor Rosa, *Goiania*

**Bulgaria**Zahariy Alexandrov Krastev, *Sofia***Canada**Wang-Xue Chen, *Ottawa*
Richard N Fedorak, *Edmonton*
Hugh James Freeman, *Vancouver*
Samuel S Lee, *Calgary*
Philip Martin Sherman, *Toronto*
Alan BR Thomson, *Edmonton*
Eric M Yoshida, *Vancouver***Egypt**Abdel-Rahman El-Zayadi, *Giza***Finland**Pentti Sipponen, *Espoo***Greece**Arvanitakis C, *Thessaloniki*
Elias A Kouroumalis, *Heraklion***China**Francis KL Chan, *Hong Kong*
Xiao-Ping Chen, *Wuhan*
Jun Cheng, *Beijing*
Chi-Hin Cho, *Hong Kong*
Zong-Jie Cui, *Beijing*
Da-Jun Deng, *Beijing*
Er-Dan Dong, *Beijing*
Sheung-Tat Fan, *Hong Kong*
Xue-Gong Fan, *Changsha*
Jin Gu, *Beijing*
De-Wu Han, *Taiyuan*
Shao-Heng He, *Shantou*
Fu-Lian Hu, *Beijing*
Wayne HC Hu, *Hong Kong*
Ching Lung Lai, *Hong Kong*
Kam Chuen Lai, *Hong Kong*
Wai-Keung Leung, *Hong Kong*
Zhi-Hua Liu, *Beijing*
Ai- Ping Lu, *Beijing*
Jing-Yun Ma, *Beijing*
Lun-Xiu Qin, *Shanghai*
Yu-Gang Song, *Guangzhou*
Peng Shang, *Xi'an*
Qin Su, *Beijing*
Yuan Wang, *Shanghai*
Benjamin Wong, *Hong Kong*
Wai-Man Wong, *Hong Kong*
Hong Xiao, *Shanghai*
Dong-Liang Yang, *Wuhan*
Xue-Biao Yao, *Hefei*
Yuan Yuan, *Shenyang*
Man-Fung Yuen, *Hong Kong*
Jian-Zhong Zhang, *Beijing*
Zhi-Rong Zhang, *Chengdu*
Xiao-Hang Zhao, *Beijing*
Shu Zheng, *Hangzhou***France**Charles Paul Balabaud, *Bordeaux*
Jacques Belghiti, *Clichy*
Pierre Brissot, *Rennes*
Franck Carbonnel, *Besancon*
Bruno Clément, *Rennes*
Jacques Cosnes, *Paris*
Francoise Degos, *Clichy*
Francoise Lunel Fabian, *Angers*
Gérard Feldmann, *Paris*
Jean Fioramonti, *Toulouse*
Rene Lambert, *Lyon*
Didier Lebrec, *Clichy*
Francis Mégraud, *Bordeaux*
Richard Moreau, *Clichy*
Jose Sahel, *Marseille*
Jean-Yves Scoazec, *Lyon*
Jean-Pierre Henri Zarski, *Grenoble***Hungary**Simon A László, *Szekszárd*
János Papp, *Budapest***Iceland**Hallgrímur Gudjonsson, *Reykjavik***India**Sujit Kumar Bhattacharya, *Kolkata*
Chawla YK, *Chandigarh*
Radha Dhiman K, *Chandigarh*
Sri Prakash Misra, *Allahabad*
Kartar Singh, *Lucknow***Iran**Reza Malekzadeh, *Tehran***Israel**Abraham Rami Eliakim, *Haifa*
Yaron Niv, *Pardesia***Italy**Giovanni Addolorato, *Roma*
Alfredo Alberti, *Padova*
Annese V, *San Giovanni Rotondo*
Giovanni Barbara, *Bologna*
Gabrio Bassotti, *Perugia*
Franco Bazzoli, *Bologna*
Adolfo Francesco Attili, *Roma*
Antonio Benedetti, *Ancona*
Giovanni Cammarota, *Roma*
Antonino Cavallari, *Bologna*
Dario Conte, *Milano*
Gino Roberto Corazza, *Pavia*
Guido Costamagua, *Roma*
Antonio Craxi, *Palermo*
Fabio Farinati, *Padua*
Giovanni Gasbarrini, *Roma*
Paolo Gentilini, *Florence*
Eduardo G Giannini, *Genoa***Costa Rica**Edgar M Izquierdo, *San José***Croatia**Marko Duvnjak, *Zagreb***Denmark**Flemming Burcharth, *Herlev*
Peter Bytzer, *Copenhagen*
Hans Gregersen, *Aalborg*

Paolo Gionchetti, *Bologna*
 Roberto De Giorgio, *Bologna*
 Mario Guslandi, *Milano*
 Giovanni Maconi, *Milan*
 Giulio Marchesini, *Bologna*
 Giuseppe Montalto, *Palermo*
 Luisi Pagliaro, *Palermo*
 Fabrizio R Parente, *Milan*
 Perri F, *San Giovanni Rotondo*
 Raffaele Pezzilli, *Bologna*
 Pilotto A, *San Giovanni Rotondo*
 Massimo Pinzani, *Firenze*
 Gabriele Bianchi Porro, *Milano*
 Piero Portincasa, *Bari*
 Giacomo Laffi, *Firenze*
 Enrico Roda, *Bologna*
 Massimo Rugge, *Padova*
 Vincenzo Savarino, *Genova*
 Vincenzo Stanghellini, *Bologna*
 Calogero Surrenti, *Florence*
 Roberto Testa, *Genoa*
 Dino Vaira, *Bologna*

Junji Kato, *Sapporo*
 Mototsugu Kato, *Sapporo*
 Shinzo Kato, *Tokyo*
 Sunao Kawano, *Osaka*
 Yoshikazu Kinoshita, *Izumo*
 Masaki Kitajima, *Tokyo*
 Tsuneo Kitamura, *Chiba*
 Seigo Kitano, *Oita*
 Hironori Koga, *Kurume*
 Satoshi Kondo, *Sapporo*
 Shoji Kubo, *Osaka*
 Shigeki Kuriyama, *Kagawa*
 Masato Kusunoki, *Mie*
 Takashi Maeda, *Fukuoka*
 Shin Maeda, *Tokyo*
 Osamu Matsui, *Kanazawa*
 Yasushi Matsuzaki, *Tsukuba*
 Hiroto Miwa, *Hyogo*
 Masashi Mizokami, *Nagoya*
 Motowo Mizuno, *Hiroshima*
 Morito Monden, *Suita*
 Hisataka S Moriwaki, *Gifu*
 Yoshiharu Motoo, *Kanazawa*
 Akihiro Munakata, *Hirosaki*
 Kazunari Murakami, *Oita*
 Kunihiko Murase, *Tusima*
 Masato Nagino, *Nagoya*
 Yuji Naito, *Kyoto*
 Hisato Nakajima, *Tokyo*
 Hiroki Nakamura, *Yamaguchi*
 Shotaro Nakamura, *Fukuoka*
 Akimasa Nakao, *Nagoya*
 Mikio Nishioka, *Niihama*
 Susumu Ohmada, *Maebashi*
 Masayuki Ohta, *Oita*
 Tetsuo Ohta, *Kanazawa*
 Susumu Okabe, *Kyoto*
 Katsuhisa Omagari, *Nagasaki*
 Saburo Onishi, *Nankoku*
 Morikazu Onji, *Ehime*
 Hiromitsu Saisho, *Chiba*
 Hidetsugu Saito, *Tokyo*
 Takafumi Saito, *Yamagata*
 Isao Sakaida, *Yamaguchi*
 Michie Sakamoto, *Tokyo*
 Iwao Sasaki, *Sendai*
 Motoko Sasaki, *Kanazawa*
 Chifumi Sato, *Tokyo*
 Shuichi Seki, *Osaka*
 Hiroshi Shimada, *Yokohama*
 Mitsuo Shimada, *Tokushima*
 Hiroaki Shimizu, *Chiba*
 Tooru Shimosegawa, *Sendai*
 Tadashi Shimoyama, *Hirosaki*
 Ken Shirabe, *Iizuka City*
 Yoshio Shirai, *Niigata*
 Katsuya Shiraki, *Mie*
 Yasushi Shiratori, *Okayama*
 Yasuhiko Sugawara, *Tokyo*
 Toshiro Sugiyama, *Toyama*
 Kazuyuki Suzuki, *Morioka*
 Hidekazu Suzuki, *Tokyo*
 Tadatoshii Takayama, *Tokyo*
 Tadashi Takeda, *Osaka*

Koji Takeuchi, *Kyoto*
 Kiichi Tamada, *Tochigi*
 Akira Tanaka, *Kyoto*
 Eiji Tanaka, *Matsumoto*
 Noriaki Tanaka, *Okayama*
 Shinji Tanaka, *Hiroshima*
 Kyuichi Tanikawa, *Kurume*
 Tadashi Terada, *Shizuoka*
 Akira Terano, *Shimotsugagun*
 Kazunari Tominaga, *Osaka*
 Hidenori Toyoda, *Ogaki*
 Akihito Tsubota, *Chiba*
 Shingo Tsuji, *Osaka*
 Takato Ueno, *Kurume*
 Shinichi Wada, *Tochigi*
 Hiroyuki Watanabe, *Kanazawa*
 Sumio Watanabe, *Akita*
 Toshio Watanabe, *Osaka*
 Yuji Watanabe, *Ehime*
 Chun-Yang Wen, *Nagasaki*
 Koji Yamaguchi, *Fukuoka*
 Takayuki Yamamoto, *Yokkaichi*
 Takashi Yao, *Fukuoka*
 Hiroshi Yoshida, *Tokyo*
 Masashi Yoshida, *Tokyo*
 Norimasa Yoshida, *Kyoto*
 Kentaro Yoshika, *Toyoake*
 Masahide Yoshikawa, *Kashiwara*

Japan

Kyoichi Adachi, *Izumo*
 Takashi Aikou, *Kagoshima*
 Taiji Akamatsu, *Matsumoto*
 Takafumi Ando, *Nagoya*
 Akira Andoh, *Otsu*
 Taku Aoki, *Tokyo*
 Masahiro Arai, *Tokyo*
 Tetsuo Arakawa, *Osaka*
 Yasuji Arase, *Tokyo*
 Masahiro Asaka, *Sapporo*
 Hitoshi Asakura, *Tokyo*
 Yutaka Atomi, *Tokyo*
 Takeshi Azuma, *Fukui*
 Nobuyuki Enomoto, *Yamanashi*
 Kazuma Fujimoto, *Saga*
 Toshio Fujioka, *Oita*
 Yoshihide Fujiyama, *Otsu*
 Hiroyuki Hanai, *Hamamatsu*
 Kazuhiro Hanazaki, *Nagano*
 Naohiko Harada, *Fukuoka*
 Makoto Hashizume, *Fukuoka*
 Tetsuo Hayakawa, *Nagoya*
 Kazuhide Higuchi, *Osaka*
 Ichiro Hirata, *Osaka*
 Keiji Hirata, *Kitakyushu*
 Takafumi Ichida, *Shizuoka*
 Kenji Ikeda, *Tokyo*
 Kohzoh Imai, *Sapporo*
 Fumio Imazeki, *Chiba*
 Masayasu Inoue, *Osaka*
 Hiromi Ishibashi, *Nagasaki*
 Shunji Ishihara, *Izumo*
 Toru Ishikawa, *Niigata*
 Kei Ito, *Sendai*
 Masayoshi Ito, *Tokyo*
 Hiroaki Itoh, *Akita*
 Hiroshi Kaneko, *Aichi-Gun*
 Shuichi Kaneko, *Kanazawa*
 Takashi Kanematsu, *Nagasaki*

Lithuania

Sasa Markovic, *Japljeva*

Macedonia

Vladimir Cirko Serafimovski, *Skopje*

Malaysia

Andrew Seng Boon Chua, *Ipoh*
 Jayaram Menon, *Sabah*
 Khean-Lee Goh, *Kuala Lumpur*

Monaco

Patrick Rampal, *Monaco*

Netherlands

Louis MA Akkermans, *Utrecht*
 Karel Van Erpecum, *Utrecht*
 Albert K Groen, *Amsterdam*
 Dirk Joan Gouma, *Amsterdam*
 Jan BMJ Jansen, *Nijmegen*
 Evan Anthony Jones, *Abcoude*
 Ernst Johan Kuipers, *Rotterdam*
 Chris JJ Mulder, *Amsterdam*
 Michael Müller, *Wageningen*

Pena AS, *Amsterdam*
Andreas Smout, *Utrecht*
RW Stockbrugger, *Maastricht*
GP Vanberge-Henegouwen,
Utrecht



New Zealand

Ian David Wallace, *Auckland*



Norway

Trond Berg, *Oslo*
Helge Lyder Waldum, *Trondheim*



Pakistan

Muhammad S Khokhar, *Lahore*



Philippines

Eulenia Rasco Nolasco, *Manila*



Poland

Tomasz Brzozowski, *Cracow*
Andrzej Nowak, *Katowice*



Portugal

Miguel Carneiro De Moura, *Lisbon*



Russia

Vladimir T Ivashkin, *Moscow*
Leonid Lazebnik, *Moscow*
Vasily I Reshetnyak, *Moscow*



Singapore

Bow Ho, *Kent Ridge*
Francis Seow-Choen, *Singapore*



Slovakia

Anton Vavrecka, *Bratislava*



South Africa

Michael C Kew, *Parktown*



South Korea

Jin-Hong Kim, *Suwon*
Myung-Hwan Kim, *Seoul*
Yun-Soo Kim, *Seoul*
Yung-Il Min, *Seoul*

Jae-Gahb Park, *Seoul*
Dong Wan Seo, *Seoul*



Spain

Abraldes JG, *Barcelona*
Fernando Azpiroz, *Barcelona*
Ramon Bataller, *Barcelona*
Josep M Bordas, *Barcelona*
Maria Buti, *Barcelon*
Xavier Calvet, *Sabadell*
Antoni Castells, *Barcelona*
Manuel Daz-Rubio, *Madrid*
Juan C Garcia-Pagán, *Barcelona*
Genover JB, *Barcelona*
Javier P Gisbert, *Madrid*
Jaime Guardia, *Barcelona*
Angel Lanas, *Zaragoza*
Ricardo Moreno-Otero, *Madrid*
Julian Panes, *Barcelona*
Miguel Perez-Mateo, *Alicante*
Josep M Pique, *Barcelona*
Jesus Prieto, *Pamplona*
Luis Rodrigo, *Oviedo*



Sri Lanka

Janaka De Silva, *Ragama*



Swaziland

Gerd Kullak-Ublick, *Zurich*



Sweden

Lars Christer Olbe, *Molndal*
Curt Einarsson, *Huddinge*
Lars R Lundell, *Stockholm*
Xiao-Feng Sun, *Linkoping*



Switzerland

Christoph Beglinger, *Basel*
Michael W Fried, *Zurich*
Bruno Stieger, *Zurich*
Arthur Zimmermann, *Berne*



Turkey

Yusuf Bayraktar, *Ankara*
Figen Gurakan, *Ankara*
Cihan Yurdaydin, *Ankara*



United Kingdom

Axon ATR, *Leeds*
Paul Jonathan Ciclitira, *London*
Amar Paul Dhillon, *London*



United States

Firas H Ac-Kawas, *Washington*
Gianfranco D Alpini, *Temple*
Paul Angulo, *Rochester*
Jamie S Barkin, *Miami Beach*
Todd Baron, *Rochester*
Kim Elaine Barrett, *San Diego*
Jennifer D Black, *Buffalo*
Xu Cao, *Birmingham*
David L Carr-Locke, *Boston*
Marc F Catalano, *Milwaukee*
Xian-Ming Chen, *Rochester*
James M Church, *Cleveland*
Vincent Coghlan, *Beaverton*
James R Connor, *Hershey*
Pelayo Correa, *New Orleans*
John Cuppoletti, *Cincinnati*
Peter V Danenberg, *Los Angeles*
Kiron Moy Das, *New Brunswick*
Hala El-Zimaity, *Houston*
Ronnie Fass, *Tucson*
Emma E Furth, *Pennsylvania*
John Geibel, *New Haven*
Graham DY, *Houston*
Joel S Greenberger, *Pittsburgh*
Anna S Gukovskaya, *Los Angeles*
Gavin Harewood, *Rochester*
Atif Iqbal, *Omaha*
Hajime Isomoto, *Rochester*
Dennis M Jensen, *Los Angeles*
Leonard R Johnson, *Memphis*
Peter James Kahrilas, *Chicago*
Anthony Nicholas Kallou, *Baltimore*
Neil Kaplowitz, *Los Angeles*
Emmet B Keefe, *Palo Alto*
Joseph B Kirsner, *Chicago*
Burton I Korelitz, *New York*
Robert J Korst, *New York*
Richard A Kozarek, *Seattle*
Shiu-Ming Kuo, *Buffalo*
Frederick H Leibach, *Augusta*
Andreas Leodolter, *La Jolla*
Ming Li, *New Orleans*
Lenard M Lichtenberger, *Houston*
Gary R Lichtenstein, *Philadelphia*
Josep M Llovet, *New York*
Martin Lipkin, *New York*

Robin G Lorenz, *Birmingham*
 James David Luketich, *Pittsburgh*
 Henry Thomson Lynch, *Omaha*
 Paul Martiw, *New York*
 Richard W McCallum, *Kansas City*
 Timothy H Moran, *Baltimore*
 Hiroshi Nakagawa, *Philadelphia*
 Douglas B Neison, *Minneapolis*
 Juan J Nogueras, *Weston*
 Curtis T Okamoto, *Los Angeles*
 Pankaj Jay Pasricha, *Galveston*
 Zhiheng Pei, *New York*
 Pitchumoni CS, *New Brunswick*
 Satish Rao, *Iowa City*
 Adrian Reuben, *Charleston*

Victor E Reyes, *Galveston*
 Richard E Sampliner, *Tucson*
 Vijay H Shah, *Rochester*
 Stuart Sherman, *Indianapolis*
 Stuart Jon Spechler, *Dallas*
 Michael Steer, *Boston*
 Gary D Stoner, *Columbus*
 Rakesh Kumar Tandon, *New Delhi*
 Tchou-Wong KM, *New York*
 Paul Joseph Thuluvath, *Baltimore*
 Swan Nio Thung, *New York*
 Travagli RA, *Baton Rouge-La*
 Triadafilopoulos G, *Stanford*
 David Hoffman Vanthiel, *Mequon*
 Jian-Ying Wang, *Baltimore*

Kenneth Ke-Ning Wang, *Rochester*
 Judy Van De Water, *Davis*
 Steven David Wexner, *Weston*
 Russell Harold Wiesner, *Rochester*
 Keith Tucker Wilson, *Baltimore*
 George Y Wu, *Farmington*
 Jian Wu, *Sacramento*
 Chung Shu Yang, *Piscataway*
 David Yule, *Rochester*
 Michael Zenilman, *Brooklyn*



Yugoslavia

Jovanovic DM, *Sremska Kamenica*

Manuscript reviewers of *World Journal of Gastroenterology*

Yogesh K Chawla, *Chandigarh*
 Chiung-Yu Chen, *Tainan*
 Gran-Hum Chen, *Taichung*
 Li-Fang Chou, *Taipei*
 Jennifer E Hardingham, *Woodville*
 Ming-Liang He, *Hong Kong*
 Li-Sung Hsu, *Taichung*
 Guang-Cun Huang, *Shanghai*
 Shinn-Jang Hwang, *Taipei*
 Jia-Horng Kao, *Taipei*
 Aydin Karabacakoglu, *Konya*
 Sherif M Karam, *Al-Ain*
 Tadashi Kondo, *Tsukiji*
 Jong-Soo Lee, *Nam-yang-ju*
 Lein-Ray Mo, *Tainan*
 Kpozehouen P Randolph, *Shanghai*
 Bin Ren, *Boston*
 Tetsuji Sawada, *Osaka*
 Cheng-Shyong Wu, *Cha-Yi*
 Ming-Shiang Wu, *Taipei*
 Wei-Guo Zhu, *Beijing*

Co-administration of cyclosporine A alleviates thioacetamide-induced liver injury

Sabrina Fan, Ching-Feng Weng

Sabrina Fan, Ching-Feng Weng, Institute of Biotechnology, National Dong Hwa University, Taiwan, China
Supported by NSC (Taiwan) under grant 91-2317-B-259-001 and Council of Agriculture (Taiwan) under grant 92-Agr-5.1.3-F-Z1 [10].
Correspondence to: Ching-Feng Weng, Institute of Biotechnology, National Dong Hwa University, Hualien 974, Taiwan, China. cfweng@mail.ndhu.edu.tw
Telephone: +886-3-8633637 Fax: +886-3-8630255
Received: 2004-11-06 Accepted: 2004-11-19

Abstract

AIM: To investigate the effects of cyclosporine A (CsA) on thioacetamide (TAA)-induced liver injury.

METHODS: CsA was co-administrated (7.5 µg/kg body weight per day, i.p.) into rat to investigate the role of CsA on TAA-(200 mg/kg body weight per 3 d for 30 d, i.p.) induced liver injury.

RESULTS: The data show that TAA caused liver fibrosis in rat after 30 d of treatment. CsA alleviates the morphological changes of TAA-induced fibrosis in rat liver. The blood glutamyl oxaloacetic transaminase (GOT)/glutamyl pyruvic transaminase (GPT) in the TAA-injury group is elevated compared to that of the normal rat. Compared with the TAA-injury group, the blood GOT/GPT and TGFβ1 (by RT-PCR analysis) are reduced in the CsA plus TAA-treated rat. The level of the transforming growth factor receptor I (TGFβ-R1) in the CsA plus TAA-treated group shows higher than that in the TAA only group, but shows a lower level of the fibroblast growth factor receptor 4 (FGFR4) in the CsA plus TAA-treated group, when using the Western blot analysis. After immunostaining of the frozen section, TGFβ-R1 and FGFR4 are more concentrated in rat liver after CsA plus TAA injury.

CONCLUSION: This result suggests that CsA has an alleviated effect on TAA-induced liver injury by increasing the multidrug resistance P-glycoprotein and could be through the regulation of TGFβ-R1 and FGFR4.

© 2005 The WJG Press and Elsevier Inc. All rights reserved.

Key words: Cyclosporine A; Thioacetamide; Liver injury; P-glycoprotein; TGFβ1; TGFβ-R1; FGFR4

Fan S, Weng CF. Co-administration of cyclosporine A alleviates thioacetamide-induced liver injury. *World J Gastroenterol* 2005; 11(10): 1411-1419
<http://www.wjgnet.com/1007-9327/11/1411.asp>

INTRODUCTION

Thioacetamide [TAA, CH₃-C(S)NH₂], a hepatotoxin, was first used to control the decay of oranges and then as a fungicide^[1]. In the liver, TAA is S-oxidized at the thioamide group to TAA sulfoxide [CH₃-C(SO)NH₂] and subsequently to di-S-oxide [CH₃-C(SO₂)NH₂]. Reactive intermediates in this pathway covalently bind to hepatic macromolecules and eventually cause liver injury^[2,3]. TAA undergoes an extensive metabolism to acetamide shortly after administration and to the hepatotoxic metabolite TAA-S-oxide by the mixed function oxidase system^[2-4]. Free radical-mediated lipid peroxidation contributes to the development of TAA-induced liver fibrosis^[5,6]. In chronic TAA intoxication, substantial liver fibrosis and prominent regenerative nodules develop after 3 mo of TAA administration and are associated with portal hypertension and the hyperdynamic circulation characteristic of liver cirrhosis^[7]. Concerning biochemical and morphological observations, the TAA-induced rat liver cirrhosis has been shown to resemble the human disease and serves as a suitable animal model for studying the causes of human liver fibrosis and cirrhosis^[8]. The transforming growth factor beta-1 (TGFβ1) is synthesized in non-parenchymal cells such as hepatic stellate cell (HSC) and inhibits hepatocellular DNA synthesis, both in culture and *in vivo*. Picomolar concentrations of TGFβ1 suppress hepatocyte DNA synthesis in culture. Moreover, injection of TGFβ1 into partially hepatectomized rats significantly delays the onset of DNA synthesis. TGFβ1 mediates the transformation of quiescent HSCs into myofibroblast-like cells with an increased production of extracellular matrix (ECM) proteins, including type I collagen^[9-13]. In addition, TGFβ1 increases the synthesis and deposition of ECM proteins such as fibronectin by HSC, and is closely associated with the progression of hepatic fibrosis.

Cyclosporine A (CsA), a fungal cyclic polypeptide and used clinically as an immunosuppressive agent^[14,15] following renal, cardiac, pancreatic, bone marrow, and hepatic transplantation, has a number of adverse effects including renal, hepatic, cardiovascular, alimentary, skin and neural toxicity^[16,17]. The alterations of dilatation of the endoplasmic reticulum, loss of ribosomes, centrilobular fatty infiltration and focal hepatocyte necrosis have been observed microscopically in livers from CsA-treated animals^[16,18]. Inhibition of the ATP-dependent bile salt export carrier in the canalicular membrane and the P-glycoprotein (P-gp) transporter is probably involved in cholestasis caused by CsA^[19,20]. Despite extensive research on the sideeffects of CsA including hypertension, hepatotoxicity and nephrotoxicity, the exact mechanisms of CsA-induced hepatotoxicity remain

obscure. Fibroblast growth factors (FGFs) comprise a growing family of structurally related polypeptide growth factors, currently consisting of 23 members^[21]. They transduce their signals through four high-affinity transmembrane protein tyrosine kinases, FGF receptors 1-4 (FGFR1-4)^[21-24], which bind the different FGFs with different affinities. Of the four FGFR isotypes, only FGFR4 is expressed in mature hepatocytes^[25]. It has become increasingly clear that the ubiquitous and extremely diverse members of the FGF family of activating FGF polypeptides, FGFR transmembrane kinases and heparan sulfate oligosaccharide chains combine in a tissue-specific mode to sense perturbation and maintain homeostasis, both in diverse developing and adult tissues^[22,25,26]. Recently, an agonist role for FGF1 and FGF2 is seen in specifically insult-induced liver matrix deposition and hepatic fibrogenesis and as a potential target for the prevention of hepatic fibrosis by acute CCl₄ exposure^[27]. The aim of this study was to investigate whether co-administration of CsA with liver fibrotic agent TAA had any beneficial or deleterious effects on TAA-induced liver injury.

MATERIALS AND METHODS

Animals

Male Sprague-Dawley rats (250-300 g) were obtained from the National Laboratory Animal Center, Taipei, Taiwan, and were kept in a temperature-controlled environment (22 °C) and fed ad libitum with standard rat chow. Rats were randomly allotted into TAA-, CsA-, CsA plus TAA- and placebo-treated groups ($n = 5$ in each group). Liver cirrhosis in rats was induced by intraperitoneal (i.p.) injection of TAA (200 mg/kg) every 3 d for 30 d is previously described. Animals assigned to the CsA (Neoral[®]; Sandimmune[®]) group were given a daily dose of CsA (7.5 µg/kg body weight, i.p.) dissolved in olive oil. The control group received the vehicle (normal saline solution) only. Treatments were carried out for 30 d. Rats were bled for blood test and sacrifices were treated with carbon dioxide gas anesthesia in closed chamber after the end of the experiment. One part of the liver was sampled for immunohistology. The remainder of the liver was rapidly removed and stored at -80 °C for RT-PCR and Western blot analysis.

GOT/GPT

The level of glutamyl oxaloacetic transaminase (GOT) and glutamyl pyruvic transaminase (GPT) in the blood, as a hepatic index for determining the status of liver function, was measured by using the Johnson and Johnson assay on the Vitros 750 (J and J/Vitros 750), a kinetic enzymatic assay in which the rate of formation of the final oxidized leuco dye is monitored at 670 nm. All assays were performed according to the procedures described by the manufacturers.

Semi-quantitative RT-PCR

The liver was weighed before being homogenized with a motorized Teflon pestle at 1 000 r/min for 2 min on ice, in cold sterile water (W:V = 1:2), or in a Trizol reagent (Invitrogen, USA) in order to isolate total RNA. After centrifugation (12 902 g for 30 min at 4 °C), the supernatant was kept at -70 °C until the assay. Total RNA was extracted, and 5 µg of each RNA was soon thereafter reverse transcribed to

first strand cDNA in 20 µL of reaction mixture using a SuperScript[™] First-Strand Synthesis System for RT-PCR kit (Invitrogen). Sets of PCR primers for selected genes and β-actin were designed based on the NCBI database of conserved coding regions (Table 1). One microliter of cDNA solution and two sets (β-actin and selected gene) of primers were used in 25 µL of PCR reaction samples. The parameters of the β-actin PCR reaction were 25 cycles at 95 °C for 45 s, 50 °C for 45 s and 72 °C for 1 min. After 25 cycles of amplification and sampling, 10 additional cycles under the same condition for the selected gene were amplified with a single cycle at 72 °C for 10 min. PCR products were separated in 12 g/L agarose gel. After ethidium bromide (EtBr, 0.5 µg/mL) staining and photographing, the data were analyzed by phoretix ID standard software, after β-actin (as an internal control) internalization.

Table 1 Primer sequence and expected lengths of fragments in RT-PCR analysis of rat liver selected genes and β-actin

Gene		Primer sequence	Expected lengths of fragments
β-actin	Forward	5'-GTCTTCCCTCCATCGTG-3'	992 bp
	Reverse	5'-TGCTTGCTGATCCACATCTG-3'	
FGFR2	Forward	5'-GGACAGACCCAAGGAGGAG-3'	667 bp
	Reverse	5'-GCCAGCAGTCCCTCATCATC-3'	
FGFR4	Forward	5'-GGAGGTGCTGTATCTGAGGAACGTG-3'	599 bp
	Reverse	5'-TGTCGGAGGCATTGTCTTTCAG-3'	
TGFβ R1	Forward	5'-CGTCGCTGCTGCTTCTCATC-3'	646 bp
	Reverse	5'-CCGCCATTTCCTCGCC-3'	
TGFβ R2	Forward	5'-CGACAACCTGCGCCATCATCC-3'	649 bp
	Reverse	5'-GGCCATGTATCTCGCTGTCCC-3'	
TGFβ R3	Forward	5'-GGTGTGGCATCTGAAGACGGAG-3'	787 bp
	Reverse	5'-GCTCAGGAGGAATGGTGTGGACT-3'	
Collagen1	Forward	5'-GCGAAGGCAACAGTCGATTC-3'	69 bp
	Reverse	5'-CCCAAGITCCGGTGTGACTC-3'	
Collagen3	Forward	5'-CAGCTGGCCTTCTCAGACTT-3'	70 bp
	Reverse	5'-GCTGTTTTTGCAGTGGTATGTAATG-3'	
Abcb1	Forward	5'-GGACCCACAGCGGAGG-3'	634 bp
	Reverse	5'-GCAGGGTGTGTAGGGCTCA-3'	

Sequence analysis

To confirm the nucleotide sequence of the PCR-amplified product selected, the product was cloned into plasmid following a cloning procedure as previously described. Plasmid DNA of the recombinant colonies was isolated and purified, using a Qiagen Plasmid Mini Kit. Fifty vectors were sequenced at once, from the 5' end using a Dye Terminator Cycle Sequence FS Ready Kit and a T7 primer from Applied Biosystems (Applied Biosystems ABI 377 sequencer). Sequence files were processed electronically to remove vector sequences, and were then analyzed using an automatic BLAST algorithm, to screen the public nucleotide databases.

Western blotting

The liver was homogenized in a homogenization solution (137 mmol/L NaCl, 1 mmol/L CaCl₂, 1 mmol/L MgCl₂, 0.1 mmol/L sodium ortho-vanadate, 20 mmol/L Tris-HCl pH 7.4, 10 g/L NP-40, 1 mmol/L PMSF) with a motorized Teflon pestle at 600 r/min for 20 strokes, on ice. After centrifugation (at 12 902 g for 30 min at 4 °C), the supernatant

was kept at -70 °C until the assay. Total protein was determined using the Bradford protein assay kit (Bio-Rad, Hercules, CA) and calculated using bovine serum albumin (Sigma, St. Louis, MO) as a standard. The whole liver homogenate (total protein 40 µg) was mixed with 6× electrophoresis sample buffer, containing 1,4-dithiothreitol (DTT, Sigma). The proteins were separated by electrophoresis on a 40-120 g/L gradient polyacrylamide slab gel, and then electrophoretically transferred to a PVDF membrane (NENTM Life Science Products, Boston, MA). The blots were incubated for 2 h in blocking buffer (30 g/L BSA in TBST buffer) and were washed twice in TBST buffer (8 g/L NaCl, 0.2 g/L KCl, 3 g/L Tris-base, pH 7.5, 0.24 g/L KH₂PO₄ and 2 g/L Tween-20). Membranes were incubated overnight at 4 °C with the first antibody as shown in Table 2. After incubation with a secondary antibody (alkaline phosphatase-conjugated goat anti-rabbit/sheep antibody, 1:4 000, ZYMED, San Francisco), the protein bands were analyzed by ECL autoradiography.

Table 2 Antibodies used in current investigation

Antibody ¹	Dilution	Protein size (ku)
β-actin, mouse polyclone	1:500	41
FGFR-2, rabbit polyclone, sc-122	1:500	119
FGFR-4, rabbit polyclone, sc-124	1:500	93
TGFβR1, rabbit polyclone, sc-402	1:1 000	53

¹All antibodies were purchased from Santa Cruz Biotechnology (CA, USA).

Immunohistochemistry

Fresh tissues were carefully embedded in OCT (Optimal Cutting Temperature, 4583, Tissue-Tek, SAKURA) in a plastic mold, without air bubbles surrounding the tissue. The mold was then put on top of liquid nitrogen until 70-80% of the block turned white, and then the block was put on top of dry ice. Prior to being sectioned, the frozen block was equilibrated in the cryostat chamber for about 5 min. Sections, 10-µm thick, were mounted on glass slides, dried at room temperature (RT) for at least 30 min. After washing with PBS twice, the tissue slide was incubated with 30 mL/L H₂O₂ for 10 min to cut down the endogenous peroxidase. The slide was blocked with 70-100 g/L BSA for 20 min after washing. The primary antibodies (diluted in 0.05 mol/L Tris-saline, pH 7.4, 250 mL/L serum) as shown in Table 2 were directly added onto the sections and incubated overnight at 4 °C. The antibodies were removed, and the tissue slide was washed thrice, for 10 min each time, with PBS buffer, at RT. The secondary antibody, diluted in Tris-saline/25 mL/L serum, was added and incubated for an additional 45 min. After washing, an ABC (avidin and biotinylated horseradish peroxidase macromolecular complex, PK-6105, VECTOR) reagent was added for 30 min of incubation. Methyl green was counterstained for less than 5 min after washing. The slide was sequentially fixed with 700, 850, 950 and 1 000 mL/L ethanol and xylene. The slide was then washed with deionized water for 5 min and left on a bench to air dry. The stained slide was mounted with VectaMountTM, P0505, (VECTOR, CA, USA), and microscopic examinations were carried out.

Sirius red staining (collagen)

The tissue slide was stained with Weigert's hematoxylin for cell nuclear staining prior to the Sirius red staining. After a 10-min wash, the slide was incubated with Pico Sirius red at RT for 1 h. The slide was then washed twice with acidified water before dehydration with ethanol absolute anhydrous. Afterwards, the tissue slide was washed with xylene and fixed in a permanent mounting medium (VECTOR).

Statistical analysis

All data are expressed as the mean±SE. Differences among the groups were determined by one-way analysis of variance (ANOVA) using SuperANOVA, statistical software from MICROSOFT (Abacus Concepts Inc., Berkeley, CA), and the means among them were compared with control values by the Student's *t* test. *P* values <0.05 were chosen to be significant.

RESULTS

Morphology/blood GOT/GPT

After carbon dioxide anesthetic, the internal organ was removed immediately and a photograph was taken. The data showed that TAA obviously induced morphological injury in the liver after 30-d treatment. CsA alleviated the morphological changes of TAA-induced fibrosis in rat liver. The GOT/GPT of the blood in the TAA-injury group was elevated compared to that of the normal rat. Compared with the TAA-injury group, the blood GOT/GPT declined in the CsA plus TAA-treated rat (Figures 1A, B).

Collagen

After Sirius red staining of the frozen sections, the collagen in the CsA plus TAA group was lower than that in the TAA group (Figure 2A). After RT-PCR of collagen I and III, the data showed that TAA induced collagen I and III in the RNA level compared to that of the control group. The collagen I expression of the CsA plus TAA group was lower than that in the TAA group (Figure 2B). However, the collagen III level was not significantly different between the TAA and the CsA plus TAA groups (Figure 2C).

TGFβ1 and receptor

TGFβ1 appears to be an important regulator in both normal and pathological conditions in the liver. In the TAA or CsA group, the expression of the TGFβ1 level was elevated compared to that of the control group. Conversely, the TGFβ1 in the CsA plus TAA group was lower than that in CsA or TAA alone (Figure 3A). The expression levels of TGFβ-R2 and TGFβ-R3 are not significantly different among treatments (Figures 3B, C). The protein level of TGFβ-R1 in CsA plus TAA-treated liver is higher than that of the TAA group (Figure 4B), but not significantly different in RNA level among treatments (Figure 4A). The aggregations of TGFβ-R1 immunostaining in liver caused by the TAA or the CsA group were sparse and scattered compared with those by the CsA plus TAA group (Figure 4C). This result implies that CsA might have a protective effect on TAA-induced liver injury through the regulation of the TGFβ1 receptor.

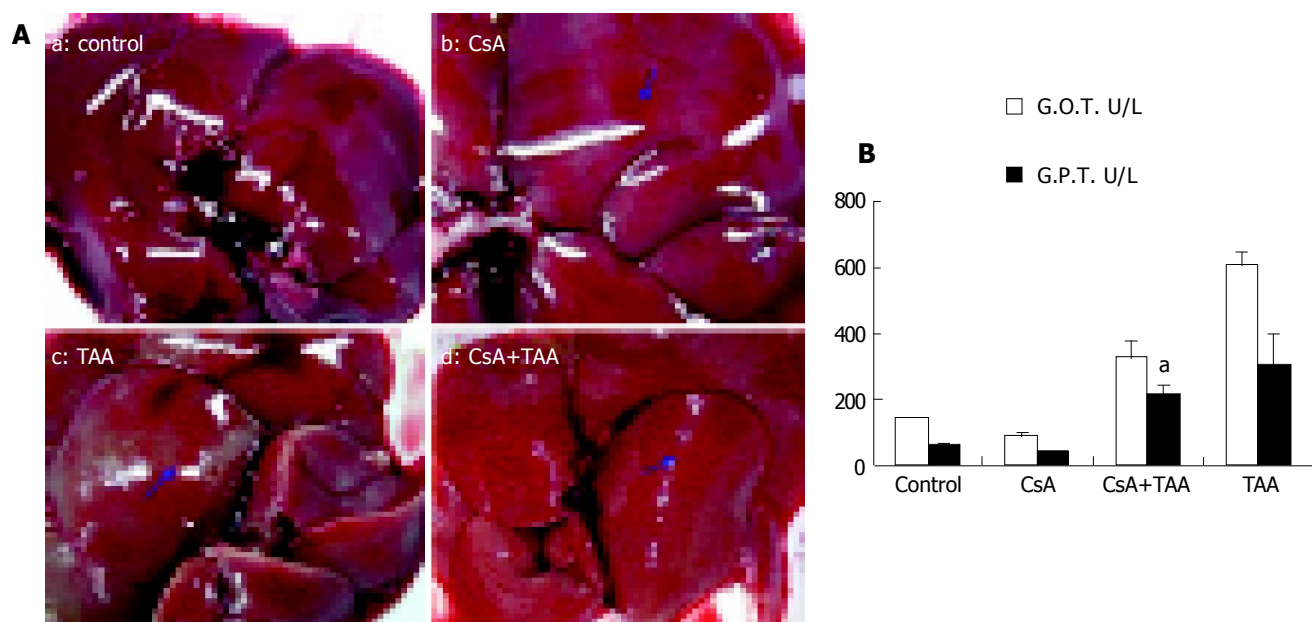


Figure 1 (A) morphology of liver, and the (B) alterations of blood GOT/GPT in (a) control, (b) CsA treatment, (c) TAA-induced, (d) CsA plus TAA treatment rats. The regimens of CsA, TAA or CsA plus TAA treatment were as described in Materials and Methods. ^a $P < 0.05$ between TAA and TAA plus CsA treatments.

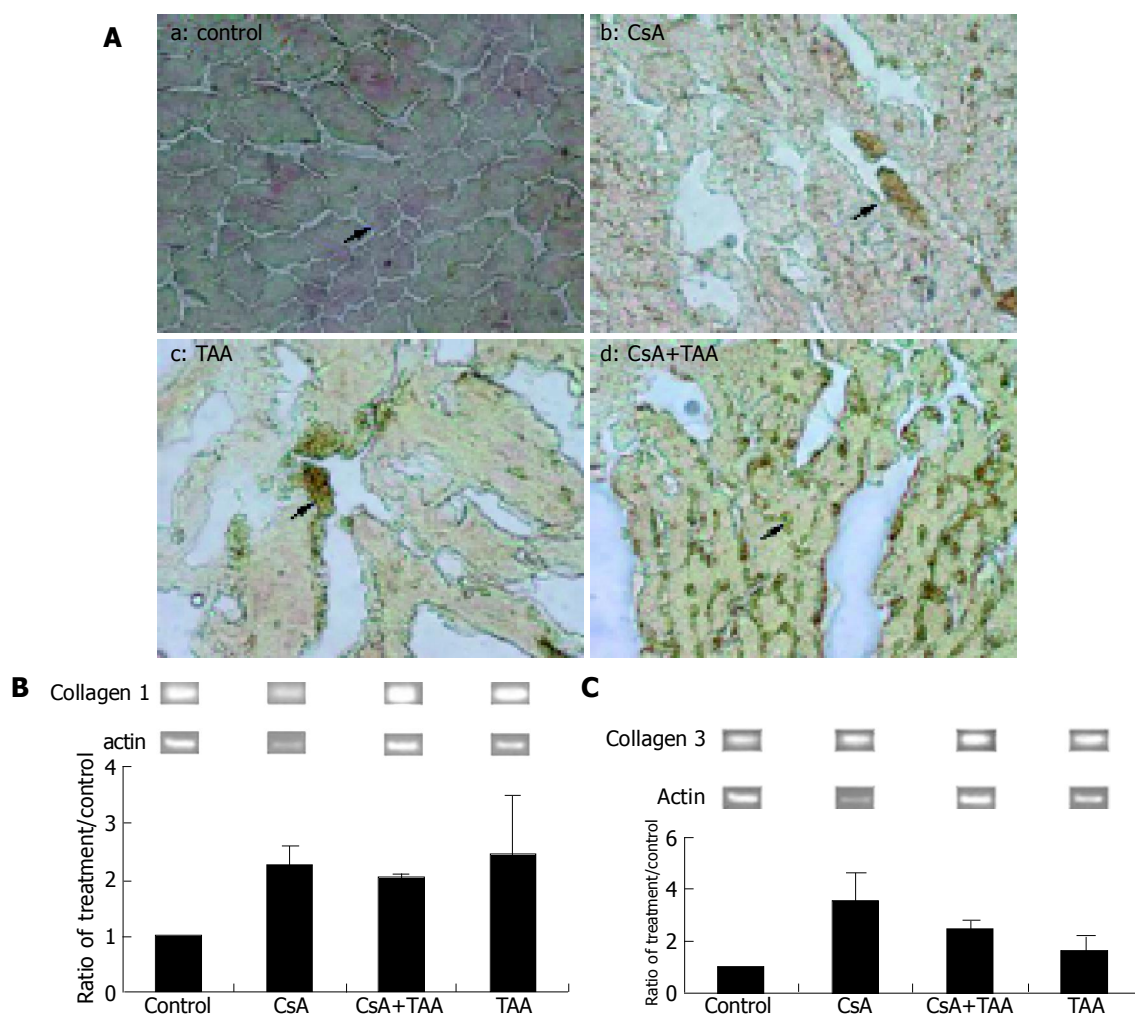


Figure 2 Levels of (A) collagen staining, (B) collagen 1 RNA expression, and (C) collagen 3 RNA expression in rat liver after various treatments. Immunocytochemistry of collagen (red) was stained by using Sirius red. Magnification = $\times 200$. The expression levels of collagen 1 and 3 were measured by using semi-quantitative PCR.

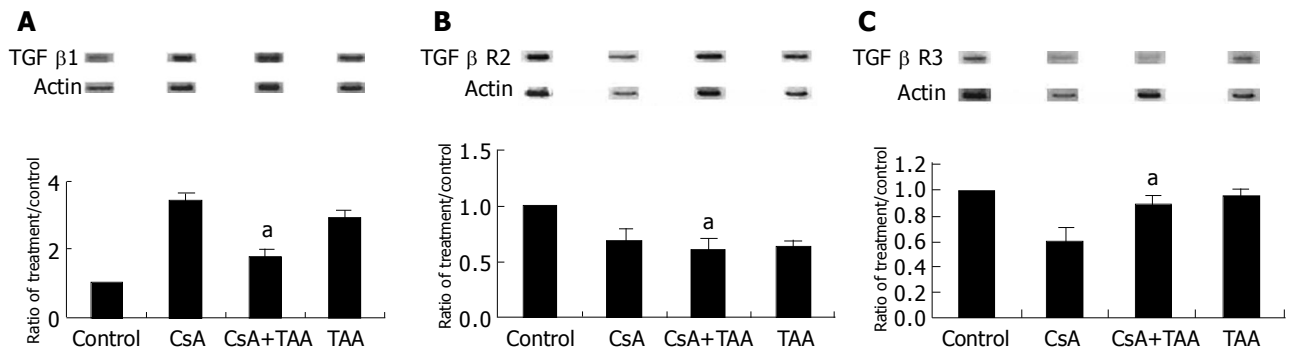


Figure 3 The RNA expression levels of (A) TGF β 1, (B) TGF β R2 and (C) TGF β R3 in rat liver after various treatments by using semi-quantitative PCR. 1 represents the significant difference $^aP<0.05$ between TAA and TAA plus CsA treatments.

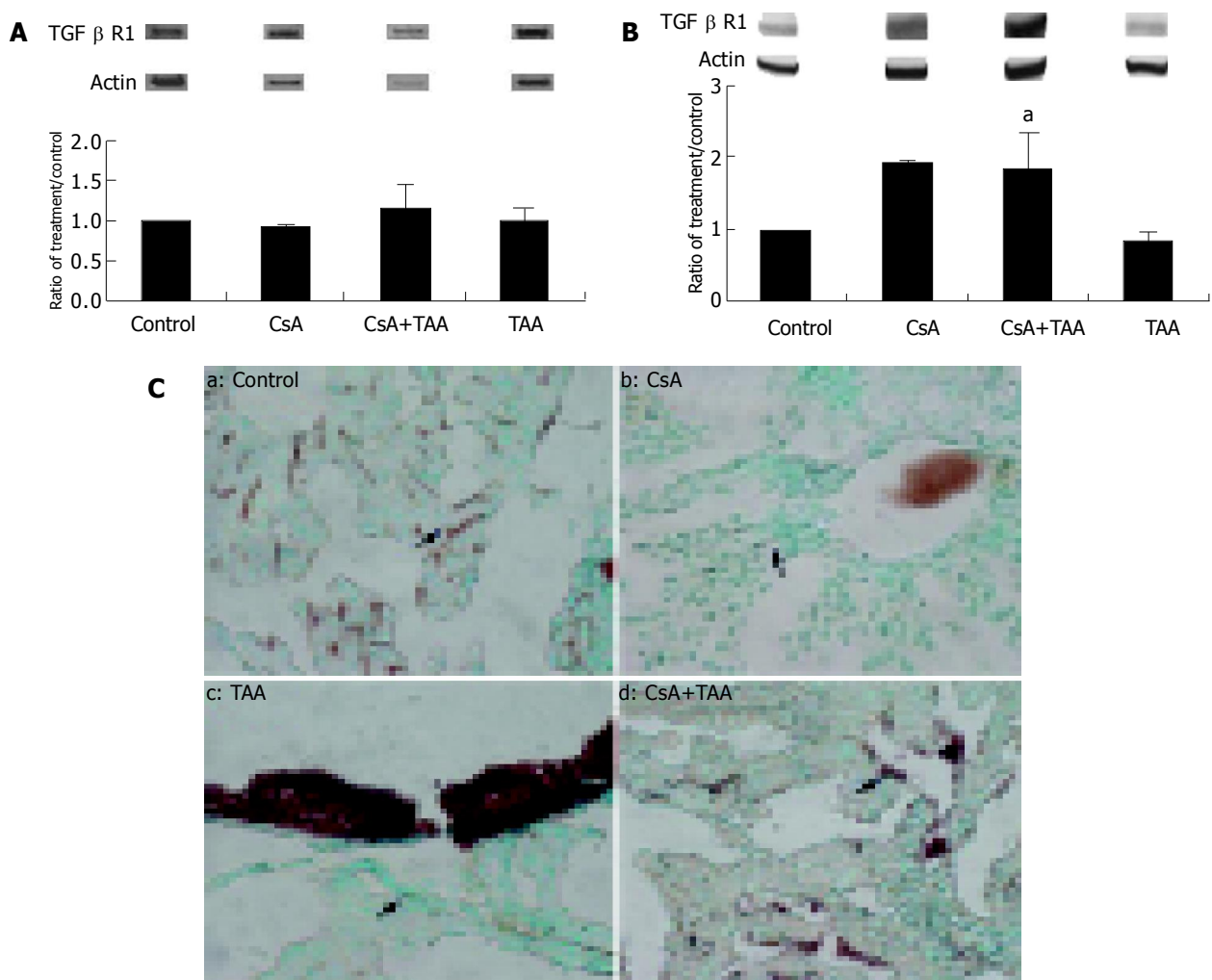


Figure 4 The levels of (A) semi-quantitative PCR for TGF β R1 RNA expression, (B) Western blot for TGF β R1 protein expression and (C) immunostaining for TGF β R1 in rat liver after various treatments. $^aP<0.05$ between TAA and TAA plus CsA treatments. Blue arrows indicate the positive staining and methyl green (green) for cell nuclear stained. Magnification = $\times 200$.

Fibroblast growth factor receptor (FGFR2, 4)

RT-PCR, Western blot and immunostaining of FGFR2 analysis showed that the FGFR2 was not significantly different among treatments (Figures 5A, B). The aggregations of FGFR2 in liver, caused by TAA or CsA treatment, are reduced when treated with CsA plus TAA (Figure 5C). CsA or TAA treatment increased the FGFR4 in the RNA and

protein levels, but this trend was reduced in the CsA plus TAA group (Figures 6A, B). Interestingly, the FGFR4 expression of liver was scattered in the CsA plus TAA treatment after immunostaining (Figure 6C). The RNA level of P-gp ATP binding cassette (ABC) transporter in CsA plus TAA-treated liver is higher than that of the TAA or CsA group (Figure 7).

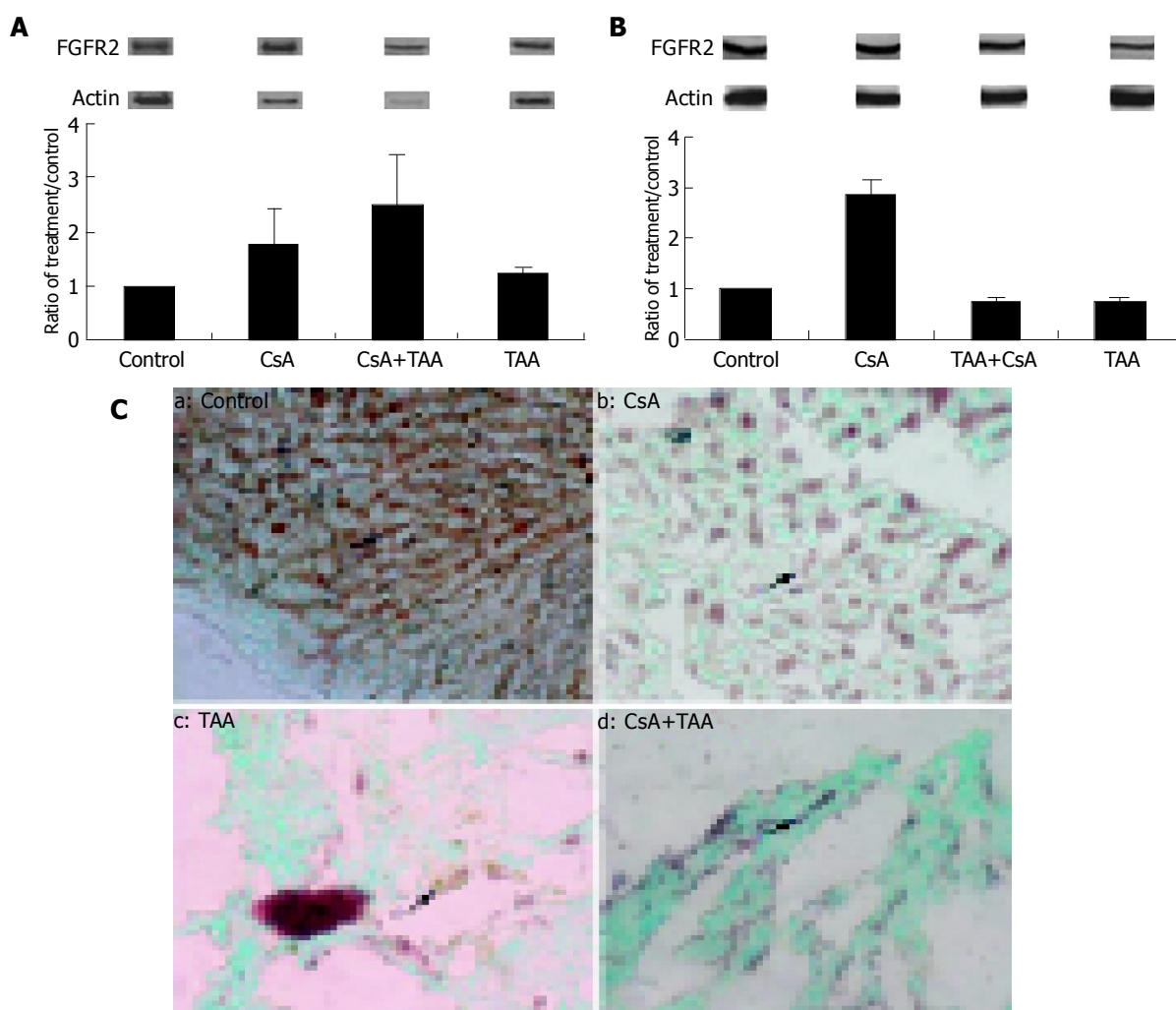


Figure 5 Levels of (A) semi-quantitative PCR for FGF receptor R2 RNA expression, (B) Western blot for FGF receptor R2 protein expression and (C) immunostaining for FGF receptor R2 in rat liver after various treatments. Blue arrows indicate the positive staining and methyl green (green) for cell nuclear stained. Magnification = $\times 200$.

DISCUSSION

After CsA plus TAA treatment, the blood GOT/GPT of the liver function index is shown to have improved significantly, and the collagen of liver is scattered after being stained with Sirius red. In the present study, the fact that TAA caused the increment of blood GOT/GPT, agrees with previous studies in TAA administration^[28-32] and in CsA treatment^[33]. The collagen I level in liver of rat is reduced after the CsA plus TAA treatment in this study. CsA can alleviate the collagen formation in liver of TAA-induced rat. Collagens are the major components of liver ECM^[34]. In the normal liver, interstitial collagen I and III are present in approximately equal quantities, constituting about 80% of the total^[35] and are mainly located within the portal areas^[34,36]. In a normal liver, HSCs are non-parenchymal, quiescent cells whose main function is to store vitamin A. When liver injury associated with the activation of HSCs, undergoes an activation process in which they lose vitamin A, they become highly proliferative and synthesize a fibrotic matrix rich in type I collagen, exhibiting features of myofibroblasts. HSCs are the key matrix-producing cells of a normal or fibrotic liver and are intimately regulated by

TGF- β ^[37]. HSC produces and secretes TGF- β , and responds to this cytokine with an increased production of type I collagen, the predominant ECM protein in liver fibrosis^[38,39]. In chronic injury, stellate cell activation and the consequent secretion of the matrix by activated stellate cells result in liver fibrosis and ultimately cirrhosis.

TGF- β 1 is a cytokine that plays a pivotal role in liver fibrosis by regulating the matrix synthesis and deposition^[40]. The hepatic expression of TGF- β 1 in liver fibrosis is markedly increased in animal models, and in human patients with chronic liver disease^[9,40-47]. Recent investigations have shown that TGF- β is one of the most powerful profibrogenic mediators playing a major role in the development of liver cirrhosis^[48]. Although TGF- β is also an important negative regulator of proliferation and an inducer of hepatocyte apoptosis, TGF- β up regulates the expression of collagens I, II and IV, fibronectin and laminin in HSCs, and accelerates the transformation of quiescent HSCs into myofibroblasts. In addition to accelerating activation and stimulating matrix synthesis, TGF- β down regulates the degradation of ECM proteins by matrix metalloproteinases through the up-regulation of tissue inhibitors of metalloproteinases in activated HSCs. TGF- β 1 is considered to be the most potent

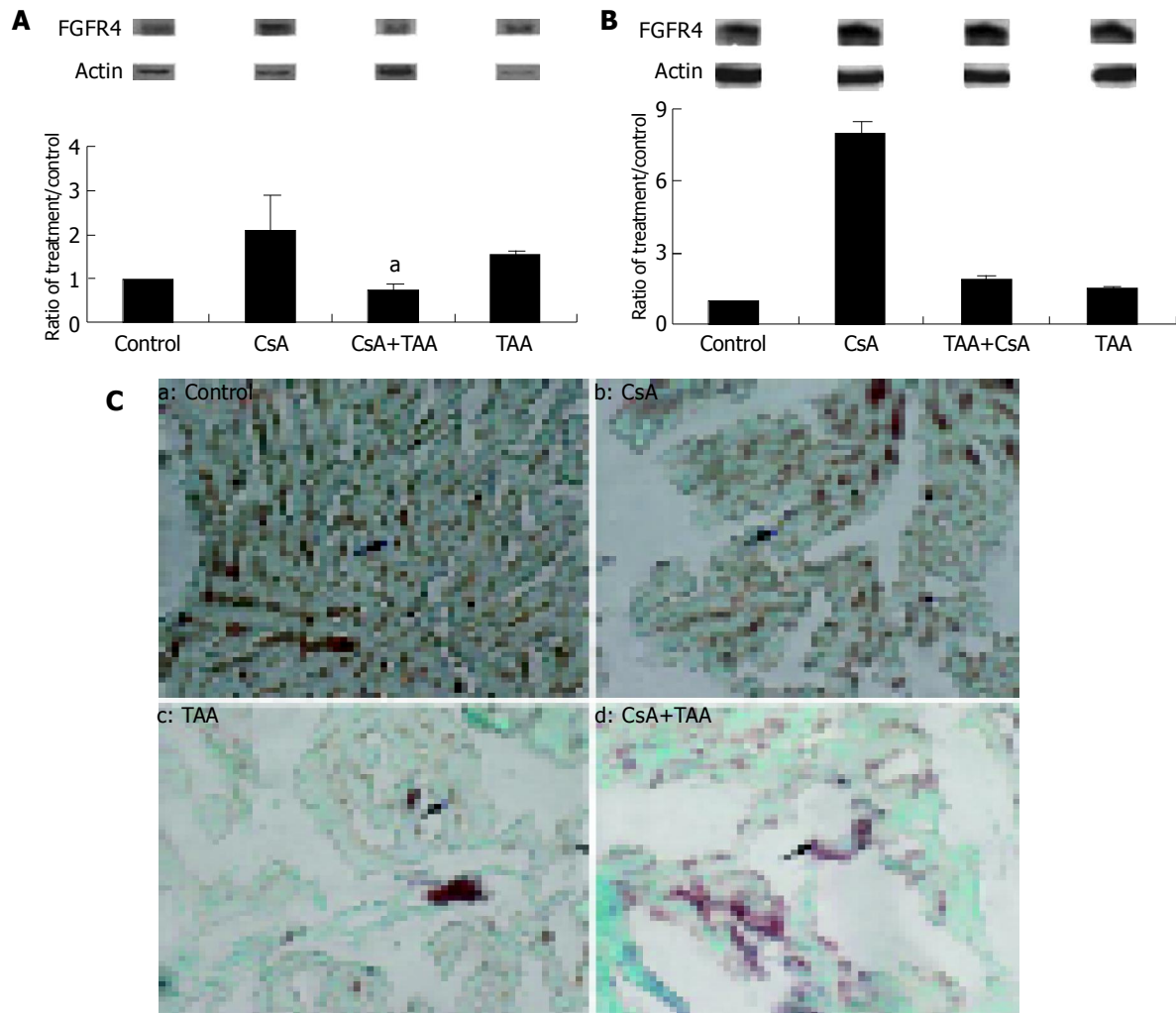


Figure 6 Levels of (A) semi-quantitative PCR for FGF receptor R4 RNA expression, (B) Western blot for FGF receptor R4 protein expression and (C) immunostaining for FGF receptor R4 in rat liver after various treatments. ^a $P < 0.05$ between TAA and TAA plus CsA treatments. Blue arrows indicate the positive staining and methyl green (green) for cell nuclear stained. Magnification $\times 200$.

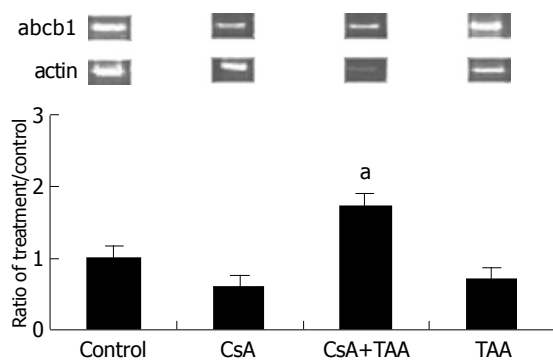


Figure 7 Levels of semi-quantitative PCR for P-gp RNA expression in rat liver after various treatments. ^a $P < 0.05$ between TAA and TAA plus CsA treatments.

profibrogenic cytokine in liver fibrosis through activation of HSCs that apparently includes the stimulation of an increase in cell numbers, migratory behavior, and the deposition of ECM components both *in vitro* and *in vivo*^[49-52]. The function of this cytokine is dependent on the interaction

with TGF surface receptor types 1, 2 and 3 (TGF β -Rs 1-3). TGF β -R3 is proposed to be involved in regulating the access of ligands to TGF β -Rs 1 and 2. The activation of TGF β -R2 leads to the phosphorylation of TGF β -R1, which, in turn, phosphorylates Smad proteins that transduce the signal to the nucleus^[53-57]. TGF- β is reduced in the CsA plus TAA group, while TGF β -R1 is increased. This implies that CsA might alleviate the collagen formation via the down-regulation of TGF- β and the up-regulation of TGF β -R1. In CCl₄-induced liver regeneration, the up-regulation of both TGF- β 1 and TGF β -Rs 1 to 3 may ensure that cycling hepatocytes stop proliferation, thereby preventing overshoots in liver growth^[58]. The levels of TGF β -R1 and TGF β -R2 mRNA expression changes occurred in the hepatocytes of rat livers injured by CCl₄ administration, while TGF β -R3 mRNA decreased only in non-parenchymal cells^[59].

In this study, CsA possesses the stimulatory effects on the RNA level of P-gp in TAA-treated liver. The ABC superfamily of membrane transporters is one of the largest protein classes known, and counts numerous proteins involved in the trafficking of biological molecules across cell membranes. The first known human ABC transporter

was P-gp, which confers multidrug resistance (MDR) to anticancer drugs (reviewed in Ref.^[60]). Previous studies showed that the immunosuppressive agent CsA modulates the MDR protein P-gp and exerts a hepatotrophic influence in the regenerating liver^[61-63]. CsA has an additive effect on the expression of P-gp during liver regeneration in the rat. The induction of P-gp might be considered in patients receiving CsA after liver transplantation for hepatocellular carcinoma and chemotherapy as an adjuvant treatment for the prevention of tumor recurrence^[64]. Following acute CCl₄ exposure, FGFR4 acts promoting processes that restore hepatobular architecture rather than cellularity, while limiting the damage due to prolonged CYP2E1 activity. In the present study, the CsA or TAA treatment increased FGFR4 in RNA and in the protein levels, but this trend was decreased in the CsA plus TAA group. A dual role for hepatocyte FGFR4 occurs as a consequence of toxic insult, in limiting the product-induced damage during biochemical detoxification and by the reconstitution of normal architecture. The modulation of hepatocyte FGFR4 signaling may be a useful target for the therapeutic mediation of toxin-induced liver injury and fibrosis, while the FGFR4-deficient mice is a useful model for the study of both high-level acute and low-level chronic liver insult, including cirrhosis. These results suggest that the up-regulation of hepatic regeneration with CsA pre-treatment might be attributed in part to changes in the production of these mitogenic and mitoinhibitory cytokines. Furthermore, CsA stimulates rat liver cell proliferation *in vivo* without inducing liver cell necrosis. This effect may contribute to accelerate the development of hepatocellular carcinomas in rats fed a CsA diet. As previously observed with BR 931, a hypolipidemic peroxisome proliferator, stimulation of liver cell growth by CsA does not entail changes in the production of HGF, TGF α or TGF β ^[63].

In conclusion, immunosuppressive molecules such as CsA, when co-administrated with TAA-treated liver, inhibited TGF- β activation by a mechanism that may involve down regulation of transglutaminase and collagen expression. The augmentation of the MDR protein P-gp by CsA-induced could protect TAA injury in rat liver. CsA indeed alleviates the damage caused by TAA in the rat liver, and this might be because of the mediating expressions of the growth factor and its receptor.

REFERENCES

- 1 **Childs JF**, Siegler EA. Compounds for control of orange decays. *Science* 1945; **102**: 68
- 2 **Hunter AL**, Holscher MA, Neal RA. Thioacetamide-induced hepatic necrosis: I. Involvement of the mixed-function oxidase enzyme system. *J Pharmacol Exp Ther* 1977; **200**: 439-448
- 3 **Porter WR**, Neal RA. Metabolism of thioacetamide and thioacetamide S-oxide by rat liver microsomes. *Drug Metab Dispos* 1978; **6**: 379-388
- 4 **Chieli E**, Malvaldi G. Role of the microsomal FAD-containing monooxygenase in the liver toxicity of thioacetamide S-oxide. *Toxicology* 1984; **31**: 41-52
- 5 **Sanz N**, Díez-Fernández C, Valverde AM, Lorenzo M, Benito M, Cascales M. Malic enzyme and glucose-6-phosphate dehydrogenase gene expression increases in rat liver cirrhogenesis. *Br J Cancer* 1997; **75**: 487-492
- 6 **Bruck R**, Aeed H, Shirin H, Matas Z, Zaidel L, Avni Y, Halpern Z. The hydroxyl radical scavengers dimethylsulfoxide and dimethylthiourea protect rats against thioacetamide-induced fulminant hepatic failure. *J Hepatol* 1999; **31**: 27-38
- 7 **Hori N**, Okanou T, Sawa Y, Mori T, Kashima K. Hemodynamic characterization in experimental liver cirrhosis induced by thioacetamide administration. *Dig Dis Sci* 1993; **38**: 2195-2202
- 8 **Muller A**, Machnik F, Zimmermann T, Schubert H. Thioacetamide-induced cirrhosis-like liver lesions in rats--usefulness and reliability of this animal model. *Exp Pathol* 1988; **34**: 229-236
- 9 **Matsuoka M**, Tsukamoto H. Stimulation of hepatic lipocyte collagen production by Kupffer cell-derived transforming growth factor beta: implication for a pathogenetic role in alcoholic liver fibrogenesis. *Hepatology* 1990; **11**: 599-605
- 10 **Wu J**, Zern MA. Hepatic stellate cells: a target for the treatment of liver fibrosis. *J Gastroenterol* 2000; **q35**: 665-672
- 11 **Casini A**, Pinzani M, Milani S, Grappone C, Galli G, Jezequel AM, Schuppan D, Rotella CM, Surrenti C. Regulation of extracellular matrix synthesis by transforming growth factor beta 1 in human fat-storing cells. *Gastroenterology* 1993; **105**: 245-253
- 12 **Hasegawa T**, Yoneda M, Nakamura K, Makino I, Terano A. Plasma transforming growth factor-beta1 level and efficacy of alpha-tocopherol in patients with non-alcoholic steatohepatitis: a pilot study. *Aliment Pharmacol Ther* 2001; **15**: 1667-1672
- 13 **Paradis V**, Dargere D, Vidaud M, De Gouville AC, Huet S, Martinez V, Gauthier JM, Ba N, Sobesky R, Ratzin V, Bedossa P. Expression of connective tissue growth factor in experimental rat and human liver fibrosis. *Hepatology* 1999; **30**: 968-976
- 14 **Borel JF**, Feurer C, Gubler HU, Stahelin H. Biological effects of cyclosporin A: a new antilymphocytic agent. 1976. *Agents Actions* 1994; **43**: 179-186
- 15 **Margreiter R**, Huber C, Spielberger M, Konig P. Cyclosporine in the treatment of acute cadaveric kidney graft rejection refractory to high-dose methylprednisolone. *Transplantation* 1983; **36**: 203-204
- 16 **Farthing MJ**, Clark ML. Nature of the toxicity of cyclosporin A in the rat. *Biochem Pharmacol* 1981; **30**: 3311-3316
- 17 **Sibley RK**, Rynasiewicz J, Ferguson RM, Fryd D, Sutherland DE, Simmons RL, Najarian JS. Morphology of cyclosporine nephrotoxicity and acute rejection in patients immunosuppressed with cyclosporine and prednisone. *Surgery* 1983; **94**: 225-234
- 18 **Ryffel B**, Donatsch P, Madorin M, Matter BE, Ruttimann G, Schon H, Stoll R, Wilson J. Toxicological evaluation of cyclosporin A. *Arch Toxicol* 1983; **53**: 107-141
- 19 **Bohme M**, Muller M, Leier I, Jedlitschky G, Keppler D. Cholestasis caused by inhibition of the adenosine triphosphate-dependent bile salt transport in rat liver. *Gastroenterology* 1994; **107**: 255-265
- 20 **Thalhammer T**, Stapf V, Gajdzik L, Graf J. Bile canalicular cationic dye secretion as a model for P-glycoprotein mediated transport. *Eur J Pharmacol* 1994; **270**: 213-220
- 21 **Ornitz DM**, Itoh N. Fibroblast growth factors. *Genome Biol* 2001; **2**: REVIEWS3005
- 22 **Johnson DE**, Williams LT. Structural and functional diversity in the FGF receptor multigene family. *Adv Cancer Res* 1993; **60**: 1-41
- 23 **McKeehan WL**, Wang F, Kan M. The heparan sulfate-fibroblast growth factor family: diversity of structure and function. *Prog Nucleic Acid Res Mol Biol* 1998; **59**: 135-176
- 24 **Powers CJ**, McLeskey SW, Wellstein A. Fibroblast growth factors, their receptors and signaling. *Endocr Relat Cancer* 2000; **7**: 165-197
- 25 **Kan M**, Wu X, Wang F, McKeehan WL. Specificity for fibroblast growth factors determined by heparan sulfate in a binary complex with the receptor kinase. *J Biol Chem* 1999; **274**: 15947-15952
- 26 **Wang F**, McKeehan WL. The fibroblast growth factor (FGF) signaling complex. Handbook of Cell Signaling Vol. I, Chap. 46 (R. Bradshaw and E. Dennis, eds.), Academic/Elsevier Press, 2003: 265-270
- 27 **Yu C**, Wang F, Jin C, Huang X, Miller DL, Basilico C, McKeehan

- WL. Role of fibroblast growth factor type 1 and 2 in carbon tetrachloride-induced hepatic injury and fibrogenesis. *Am J Pathol* 2003; **163**: 1653–1662
- 28 **Shakoori AR**, Cheema IA, Rani A, Ali SS. Evaluation of liver function after thioacetamide treatment of partially hepatectomized rabbits. *Acta Physiol Pharmacol Latinoam* 1984; **34**: 301–312
 - 29 **Younes M**, Albrecht M, Siegers CP. Interrelationship between *in vivo* lipid peroxidation, microsomal Ca²⁺-sequestration activity and hepatotoxicity in rats treated with carbon tetrachloride, cumene hydroperoxide or thioacetamide. *Res Commun Chem Pathol Pharmacol* 1983; **40**: 405–415
 - 30 **Akbay A**, Cinar K, Uzunalimoglu O, Eranil S, Yurdaydin C, Bozkaya H, Bozdayi M. Serum cytotoxin and oxidant stress markers in N-acetylcysteine treated thioacetamide hepatotoxicity of rats. *Hum Exp Toxicol* 1999; **18**: 669–676
 - 31 **Bergasa NV**, Borque MJ, Wahl LM, Rabin L, Jones EA. Modulation of thioacetamide-induced hepatocellular necrosis by prostaglandins is associated with novel histologic changes. *Liver* 1992; **12**: 168–174
 - 32 **Osada J**, Aylagas H, Sanchez-Vegazo I, Gea T, Millan I, Palacios-Alaiz E. Effect of S-adenosyl-L-methionine on thioacetamide-induced liver damage in rats. *Toxicol Lett* 1986; **32**: 97–106
 - 33 **Al-Nasser IA**. *In vivo* prevention of adriamycin cardiotoxicity by cyclosporin A or FK506. *Toxicology* 1998; **131**: 175–181
 - 34 **Martinez-Hernandez A**, Amenta PS. The hepatic extracellular matrix. II. Ontogenesis, regeneration and cirrhosis. *Virchows Arch A Pathol Anat Histopathol* 1993; **423**: 77–84
 - 35 **Biagini G**, Ballardini G. Liver fibrosis and extracellular matrix. *J Hepatol* 1989; **8**: 115–124
 - 36 **Rojkind M**, Giambrone MA, Biempica L. Collagen types in normal and cirrhotic liver. *Gastroenterology* 1979; **76**: 710–719
 - 37 **Knittel T**, Mehde M, Kobold D, Saile B, Dinter C, Ramadori G. Expression patterns of matrix metalloproteinases and their inhibitors in parenchymal and non-parenchymal cells of rat liver: regulation by TNF- α and TGF- β 1. *J Hepatol* 1999; **30**: 48–60
 - 38 **Sanderson N**, Factor V, Nagy P, Kopp J, Kondaiah P, Wakefield L, Roberts AB, Sporn MB, Thorgeirsson SS. Hepatic expression of mature transforming growth factor β 1 in transgenic mice results in multiple tissue lesions. *Proc Natl Acad Sci USA* 1995; **92**: 2572–2576
 - 39 **Clouthier DE**, Comerford SA, Hammer RE. Hepatic fibrosis, glomerulosclerosis, and a lipodystrophy-like syndrome in PEPCK-TGF- β 1 transgenic mice. *J Clin Invest* 1997; **100**: 2697–2713
 - 40 **Bedossa P**, Paradis V. Transforming growth factor- β (TGF- β): a key-role in liver fibrogenesis. *J Hepatol* 1995; **22**: 37–42
 - 41 **Czaja MJ**, Weiner FR, Flanders KC, Giambrone MA, Wind R, Biempica L, Zern MA. *In vitro* and *in vivo* association of transforming growth factor- β 1 with hepatic fibrosis. *J Cell Biol* 1989; **108**: 2477–2482
 - 42 **Nakatsukasa H**, Evarts RP, Hsia CC, Thorgeirsson SS. Transforming growth factor- β 1 and type I procollagen transcripts during regeneration and early fibrosis of rat liver. *Lab Invest* 1990; **63**: 171–180
 - 43 **Nakatsukasa H**, Nagy P, Evarts RP, Hsia CC, Marsden E, Thorgeirsson SS. Cellular distribution of transforming growth factor- β 1 and procollagen types I, III, and IV transcripts in carbon tetrachloride-induced rat liver fibrosis. *J Clin Invest* 1990; **85**: 1833–1843
 - 44 **Rieder H**, Armbrust T, Meyer zum Buschenfelde KH, Ramadori G. Contribution of sinusoidal endothelial liver cells to liver fibrosis: expression of transforming growth factor- β 1 receptors and modulation of plasmin-generating enzymes by transforming growth factor- β 1. *Hepatology* 1993; **18**: 937–944
 - 45 **Friedman SL**, Yamasaki G, Wong L. Modulation of transforming growth factor β receptors of rat lipocytes during the hepatic wound healing response. Enhanced binding and reduced gene expression accompany cellular activation in culture and *in vivo*. *J Biol Chem* 1994; **269**: 10551–10558
 - 46 **Knittel T**, Janneck T, Muller L, Fellmer P, Ramadori G. Transforming growth factor β 1-regulated gene expression of Ito cells. *Hepatology* 1996; **24**: 352–360
 - 47 **Castilla A**, Prieto J, Fausto N. Transforming growth factors β 1 and α in chronic liver disease. Effects of interferon α therapy. *N Engl J Med* 1991; **324**: 933–940
 - 48 **Flisiak R**, Pytel-Krolczuk B, Prokopowicz D. Circulating transforming growth factor β (1) as an indicator of hepatic function impairment in liver cirrhosis. *Cytokine* 2000; **12**: 677–681
 - 49 **Hellerbrand C**, Stefanovic B, Giordano F, Burchardt ER, Brenner DA. The role of TGF β 1 in initiating hepatic stellate cell activation *in vivo*. *J Hepatol* 1999; **30**: 77–87
 - 50 **Gressner AM**, Weiskirchen R, Breitkopf K, Dooley S. Roles of TGF β in hepatic fibrosis. *Front Biosci* 2002; **7**: d793–d807
 - 51 **Win KM**, Charlotte F, Mallat A, Cherqui D, Martin N, Mavrier P, Preaux AM, Dhumeaux D, Rosenbaum J. Mitogenic effect of transforming growth factor- β 1 on human Ito cells in culture: evidence for mediation by endogenous platelet-derived growth factor. *Hepatology* 1993; **18**: 137–145
 - 52 **Fibbi G**, Pucci M, D'Alessio S, Grappone C, Pellegrini G, Salzano R, Casini A, Milani S, Del Rosso M. Transforming growth factor β -1 stimulates invasivity of hepatic stellate cells by engagement of the cell-associated fibrinolytic system. *Growth Factors* 2001; **19**: 87–100
 - 53 **Nakao A**, Roijer E, Imamura T, Souchelnytskyi S, Stenman G, Heldin CH, ten Dijke P. Identification of Smad2, a human Mad-related protein in the transforming growth factor β signaling pathway. *J Biol Chem* 1997; **272**: 2896–2900
 - 54 **Inagaki M**, Moustakas A, Lin HY, Lodish HF, Carr BI. Growth inhibition by transforming growth factor β (TGF- β) type I is restored in TGF- β -resistant hepatoma cells after expression of TGF- β receptor type II cDNA. *Proc Natl Acad Sci USA* 1993; **90**: 5359–5363
 - 55 **Bassing CH**, Yingling JM, Howe DJ, Wang T, He WW, Gustafson ML, Shah P, Donahoe PK, Wang XF. A transforming growth factor β type I receptor that signals to activate gene expression. *Science* 1994; **263**: 87–89
 - 56 **Tsuchida K**, Lewis KA, Mathews LS, Vale WW. Molecular characterization of rat transforming growth factor- β type II receptor. *Biochem Biophys Res Commun* 1993; **191**: 790–795
 - 57 **Wang XF**, Lin HY, Ng-Eaton E, Downward J, Lodish HF, Weinberg RA. Expression cloning and characterization of the TGF- β type III receptor. *Cell* 1991; **67**: 797–805
 - 58 **Grasl-Kraupp B**, Rossmannith W, Ruttkay-Nedecky B, Mullauer L, Kammerer B, Bursch W, Schulte-Hermann R. Levels of transforming growth factor β and transforming growth factor β receptors in rat liver during growth, regression by apoptosis and neoplasia. *Hepatology* 1998; **28**: 717–726
 - 59 **Date M**, Matsuzaki K, Matsushita M, Sakitani K, Shibano K, Okajima A, Yamamoto C, Ogata N, Okumura T, Seki T, Kubota Y, Kan M, McKeehan WL, Inoue K. Differential expression of transforming growth factor- β and its receptors in hepatocytes and nonparenchymal cells of rat liver after CCl₄ administration. *J Hepatol* 1998; **28**: 572–581
 - 60 **Litman T**, Druley TE, Stein WD, Bates SE. From MDR to MXR: new understanding of multidrug resistance systems, their properties and clinical significance. *Cell Mol Life Sci* 2001; **58**: 931–959
 - 61 **Kahn D**, Makowka L, Lai H, Eagon PK, Dindzans V, Starzl TE, Van Thiel DH. Cyclosporine augments hepatic regenerative response in rats. *Dig Dis Sci* 1990; **35**: 392–398
 - 62 **Delle Monache MD**, Gigliozzi A, Benedetti A, Marucci L, Bini A, Francia C, Papa E, Di Cosimo E, Fraioli F, Jezequel AM, Alvaro D. Effect of pharmacological modulation of liver P-glycoproteins on cyclosporin A biliary excretion and cholestasis: a study in isolated perfused rat liver. *Dig Dis Sci* 1999; **44**: 2196–2204
 - 63 **Morii Y**, Kawano K, Kim YI, Aramaki M, Yoshida T, Kitano S. Augmentative effect of cyclosporin A on rat liver regeneration: influence on hepatocyte growth factor and transforming growth factor- β (1). *Eur Surg Res* 1999; **31**: 399–405
 - 64 **Daoudaki M**, Fouzas I, Stapf V, Ekmekcioglu C, Imvrios G, Andoniadis A, Demetriadou A, Thalhammer T. Cyclosporine augments P-glycoprotein expression in the regenerating rat liver. *Biol Pharm Bull* 2003; **26**: 303–307

• LIVER CANCER •

Sirolimus inhibits growth of human hepatoma cells alone or combined with tacrolimus, while tacrolimus promotes cell growth

Guido Schumacher, Marijke Oidtmann, Anne Rueggeberg, Dietmar Jacob, Sven Jonas, Jan M. Langrehr, Ruth Neuhaus, Marcus Bahra, Peter Neuhaus

Guido Schumacher, Marijke Oidtmann, Dietmar Jacob, Sven Jonas, Jan M. Langrehr, Ruth Neuhaus, Marcus Bahra, Peter Neuhaus, Departments of General, Visceral, and Transplantation Surgery, Charité Campus Virchow Klinikum, Berlin, Germany
Anne Rueggeberg, Department of Anesthesiology, Charité Virchow Klinikum, Berlin, Germany

Correspondence to: Guido Schumacher, M.D., Department of General, Visceral, and Transplantation Surgery, Charité Campus Virchow Klinikum, Humboldt University, Augustenburger Platz 1, Berlin 13353, Germany. guido.schumacher@charite.de

Telephone: +49-30-450-552001 Fax: +49-30-450-552900

Received: 2004-08-13 Accepted: 2004-09-30

Growth inhibition; Apoptosis; SK-Hep 1; Hep3B

Schumacher G, Oidtmann M, Rueggeberg A, Jacob D, Jonas S, Langrehr JM, Neuhaus R, Bahra M, Neuhaus P. Sirolimus inhibits growth of human hepatoma cells alone or combined with tacrolimus, while tacrolimus promotes cell growth. *World J Gastroenterol* 2005; 11(10): 1420-1425

<http://www.wjgnet.com/1007-9327/11/1420.asp>

Abstract

AIM: Standard immunosuppression after organ transplantation stimulates tumor growth. Sirolimus has a strong antiproliferative and a tumor inhibiting effect. The purpose is to assess the effect on tumor growth of the immunosuppressive compounds sirolimus and tacrolimus alone and in combination on cells of human hepatocellular carcinoma.

METHODS: We used the human cell lines SK-Hep 1 and Hep 3B derived from hepatocellular carcinoma. Proliferation analyses after treatment with sirolimus, tacrolimus, or the combination of both were performed. FACS analyses were done to reveal cell cycle changes and apoptotic cell death. The expression of apoptosis-related proteins was estimated by Western blots.

RESULTS: Sirolimus alone or combined with tacrolimus inhibited the growth of both cell lines after 5 d by up to 35% in SK-Hep 1 cells, and by up to 68% in Hep 3B cells at 25 ng/mL. Tacrolimus alone stimulated the growth by 12% after 5 ng/mL and by 25% after 25 ng/mL in Hep 3B cells. We found an increase of apoptotic Hep 3B cells from 6 to 16%, and a G1-arrest in SK-Hep 1 cells with an increase of cells from 61 to 82%, when sirolimus and tacrolimus were combined. Bcl-2 was down-regulated in Hep 3B, but not in SK-Hep 1 cells after combined treatment.

CONCLUSION: Sirolimus appears to inhibit the growth of hepatocellular carcinoma cells alone and in combination with tacrolimus. Sirolimus seems to inhibit the growth stimulation of tacrolimus.

INTRODUCTION

The five-year survival rate of patients suffering from hepatocellular carcinoma (HCC) stands at about 50-75% considering all available treatment modalities^[1]. In addition to the tumor burden, patients who are considered as candidates for liver transplantation (LTX) usually suffer from progressive disease and advanced cirrhosis. In such cases, LTX can successfully treat both the tumor and the cirrhosis. LTX for hepatocellular carcinoma is the best treatment option when the tumor stage is limited. Multifocal growth, large tumors of more than 5 cm of diameter, high grading, and angioinvasion are factors which indicate a poor prognosis. The exact extent of the disease often becomes evident only after LTX through the pathological examination. When the result shows the presence of an advanced stage of the disease, a recurrence rate of up to 70% can be expected. No promising therapy is available for those patients, resulting in 100% fatality rate within months. New approaches to prevent tumor recurrence are of high interest for these patients.

Sirolimus, an immunosuppressive compound, has been successfully used for immunosuppression in kidney^[2,3] and liver^[4] transplant recipients. It has been successfully combined with other compounds such as cyclosporin^[5] and tacrolimus^[6]. In spite of the same receptor of sirolimus and tacrolimus, namely the FKBP-12, no clinically apparent competitive inhibition can be revealed. Thus, a combination of sirolimus and tacrolimus has achieved sufficient immunosuppression^[7,8]. The sirolimus-FKBP-12 complex acts differently from those including calcineurin inhibitors. This complex binds to a specific cell cycle regulatory protein, the mammalian target of rapamycin (mTOR), and inhibits its action. This inhibition causes growth inhibition of tumor cells which is achieved by different mechanisms^[9]. Briefly, the inhibition of mTOR inhibits the G1 to S phase transition in the cell cycle. It also inhibits the translation of an mRNA family, which encodes essential cell cycle regulatory proteins. Further mechanisms are an inhibition of the IL-2 induced transcription of the

proliferating cell nuclear antigen (PCNA), which is essential for DNA replication, and inhibition of the kinase activity of cdk4/cyclin D and cdk2/cyclin E complexes, causing decreased synthesis of the cell cycle proteins cdc2 and Cyclin A for cell cycle progression^[10]. The inhibition of the kinase activity is caused by the prolonged half-life of the tumor suppressor protein p27^{KIP1}, which is overexpressed in this situation, causing cell cycle inhibition in the G1-Phase^[11]. Sirolimus also reduces intimal proliferation following vascular injury in pigs^[12]. A strong antiangiogenic effect by a decrease in production of the vascular endothelial growth factor (VEGF) was observed in experiments using colon cancer cells^[13]. The growth of different cancer types could be inhibited by sirolimus, namely rhabdomyosarcoma cells^[14], osteosarcoma cells^[15], hepatoma cells^[16,17], lung cancer cells^[18], B lymphoma cells^[19], and renal cancer metastases^[20]. Conversely, the calcineurin inhibitors tacrolimus and cyclosporine promote cell cycle progression by a cell-autonomous mechanism^[21] such as an increase in cdk4 kinase activity^[22]. The purpose of our study was to examine the effect on tumor cell proliferation of hepatoma cells after treatment with sirolimus and tacrolimus alone or in combination of both, since this combination is regularly used in the clinic. We present an *in vitro* study that shows growth inhibition after incubation with sirolimus alone or in combination with tacrolimus in human hepatocellular carcinoma cells. We also show some of the possible mechanisms of growth inhibition.

MATERIALS AND METHODS

Cell lines and tissue culture

Two cell lines derived from human hepatocellular carcinoma were purchased from the American Type Tissue Collection (ATCC) harboring wild-type p53 (SK-Hep 1) or mutated p53 (Hep 3B). The cells were grown in Modified Eagle Medium (MEM) supplemented with 10% fetal calf serum, antibiotics, antimycotics, sodium pyruvate, non-essential aminoacids, and glutamine.

Drugs

Sirolimus and tacrolimus were generously provided by Wyeth-Pharma GmbH Münster, Germany and Fujisawa Healthcare, Inc., Munich, Germany respectively. Both were pure drugs, which were dissolved in absolute alcohol. The final concentrations were achieved by diluting the stock solution in culture medium.

Proliferation assays

Cells were set up from a 70–80% confluent T-flask in 24-well plates in MEM medium as described above at a density of 1 000 cells/well. Three wells per treatment group were used. Two days later, cells were incubated in serum-free medium with different concentrations of sirolimus and tacrolimus alone and also combined with each other. Serum-free medium was used to avoid interactions of proteins with sirolimus or tacrolimus. Doses were 5 or 25 ng/mL for each group. Additional groups treated with PBS or absolute alcohol at the same concentrations served as control groups. The medium was replaced by fresh medium

containing 10% serum 24 h after treatment. Cell counts were done on day five after incubation with the drugs. Average cell numbers were calculated from three counts per treatment group.

Western blot analysis

A standardized protocol to measure the quantities of cell proteins was used^[23]. Briefly, cells were set-up and treated in 5-cm dishes at the same doses as done for the proliferation assays. After 2 d, cell lysates were harvested and the analysis was performed. The detection of different protein expression patterns was performed using Western blot analysis. The antibodies used were p53 (p53 Ab-3, NeoMarkers) with a 1:500 dilution, p21^{WAF1} (Ab-1, Oncogene Research Products Calbiochem) with a dilution of 1:300, bcl-2 (PharMingen) with a dilution of 1:200, and β -actin (monoclonal anti- β -actin, Sigma-Aldrich) with a dilution of 1:700. As a secondary antibody we used the HRP-conjugated antibody (ImmunoPure, anti-goat, mouse IgG, Pierce) with a dilution of 1:5.000. The loading quantity of the proteins was 50 μ g/well for p53, 100 μ g/well for p21^{WAF1}, 100 μ g/well for bcl-2, and 15 μ g/well for β -actin detection. Western Blot analyses for these protein expressions were repeated at least thrice.

FACS analysis

To examine the presence or absence of apoptotic cell death, FACS analyses were performed. Furthermore, a possible G1-arrest after treatment with sirolimus alone or in combination with tacrolimus should be proved. Cells were seeded in 100-mm diameter dishes at 1×10^6 cells per dish and incubated with sirolimus, tacrolimus, or the combination of both at 25 ng/mL each compound. After one day of incubation, cells were trypsinized, washed in PBS, and fixed in 70% ice-cold ethanol for 60 min and stored at 4 °C until used. The procedure for FACS analysis was performed according to a protocol described previously^[24]. Briefly, fixed cells were incubated with 1 mg/mL of RNase (Sigma Chemical Co., Deidenhofen, Germany) for 15 min at room temperature. Thereafter, 0.5 mL PI solution (Sigma; 100 ng/mL PBS) was added for 15 min at room temperature in the dark. Cells were washed once in PBS and kept at 4 °C in the dark until measurement. We analyzed 10 000 cells using a FACS scan flow cytometer (Becton-Dickinson). These experiments were repeated twice.

Statistical analyses

A one-way ANOVA was used for statistical analyses for proliferation assays.

RESULTS

Sirolimus inhibits growth of hepatocellular carcinoma cells

Growth inhibition after treatment with sirolimus was dose-dependent in both cell lines after five days (Figure 1). When treated with 5 or 25 ng/mL sirolimus alone, we found an inhibition of 20–30% in SK-Hep 1 cells ($P = 0.0105$), and a growth inhibition of 55–65% in Hep 3B cells ($P < 0.0001$). Conversely, an increased cell proliferation was observed in the tacrolimus-treated group to up to 46% in SK-Hep 1 cells ($P = 0.0156$) and 15% in Hep 3B cells ($P = 0.0654$)

compared to non-treated control cells. The combination of sirolimus and tacrolimus showed a similar degree of cell growth inhibition as the groups treated with sirolimus alone. In Hep 3B cells, we found a highly significant inhibition of cells as compared to control cells of 55-61% when treated with 5 and 25 ng/mg ($P = 0.0002$). The growth inhibition in the combination group of both compounds was 18% and did not reach statistical significance in SK-Hep 1 cells. When the level of growth inhibition of the combination treatment with sirolimus and tacrolimus was compared to the tacrolimus alone group, there was a significant difference of the cell numbers in Hep 3B cells ($P < 0.0001$) and SK-Hep 1 cells ($P = 0.0005$).

G1-arrest and induction of apoptosis

To understand more about mechanisms of growth inhibition, cell cycle analyses were performed as shown in Figure 2 and Table 1. In Hep 3B cells, we found only a slight increase of cells in the G1-phase from 69 to 73% after treatment with sirolimus alone when compared to control non-treated cells. After treatment with tacrolimus alone, the amount of cells in the G1-phase decreased slightly from 69 to 65%, but increased in the S-phase from 10 to 17% indicating an increased DNA synthesis. As sirolimus and tacrolimus were combined at a dose of 25 ng/mL each, an increase of apoptotic cells from 6 to 16% was observed as compared to control non-treated cells. A decrease of cells in G2/M

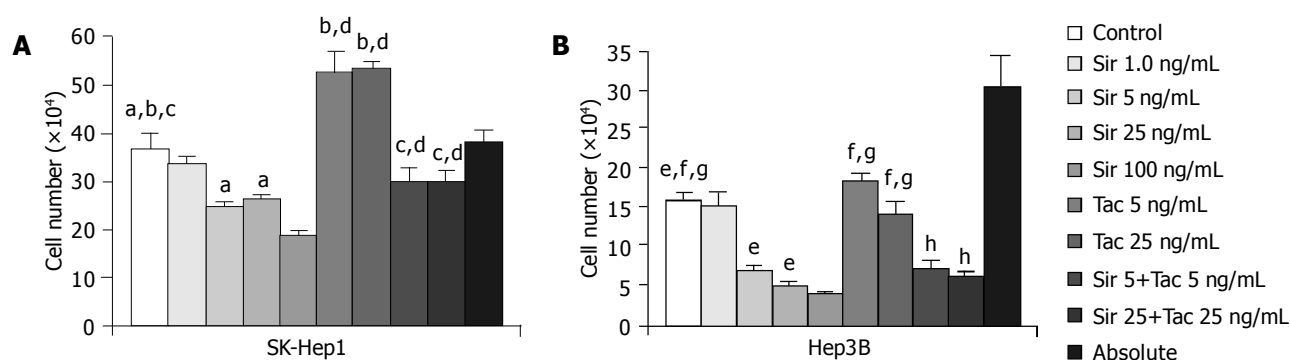


Figure 1 Proliferation assays showing cell numbers from mean counts of three experiments. Cells were treated as described in Materials and Methods with sirolimus, tacrolimus, or the combination of both. Sir = sirolimus; Tac = tacrolimus. Data are expressed as mean±SE. (A: SK-Hep 1: ^a $P = 0.0105$; ^b $P = 0.0156$; ^c $P = 0.254$; ^d $P < 0.0001$; B: Hep 3B: ^e $P < 0.0001$; ^f $P = 0.0654$; ^g $P = 0.0002$; ^h $P < 0.0001$).

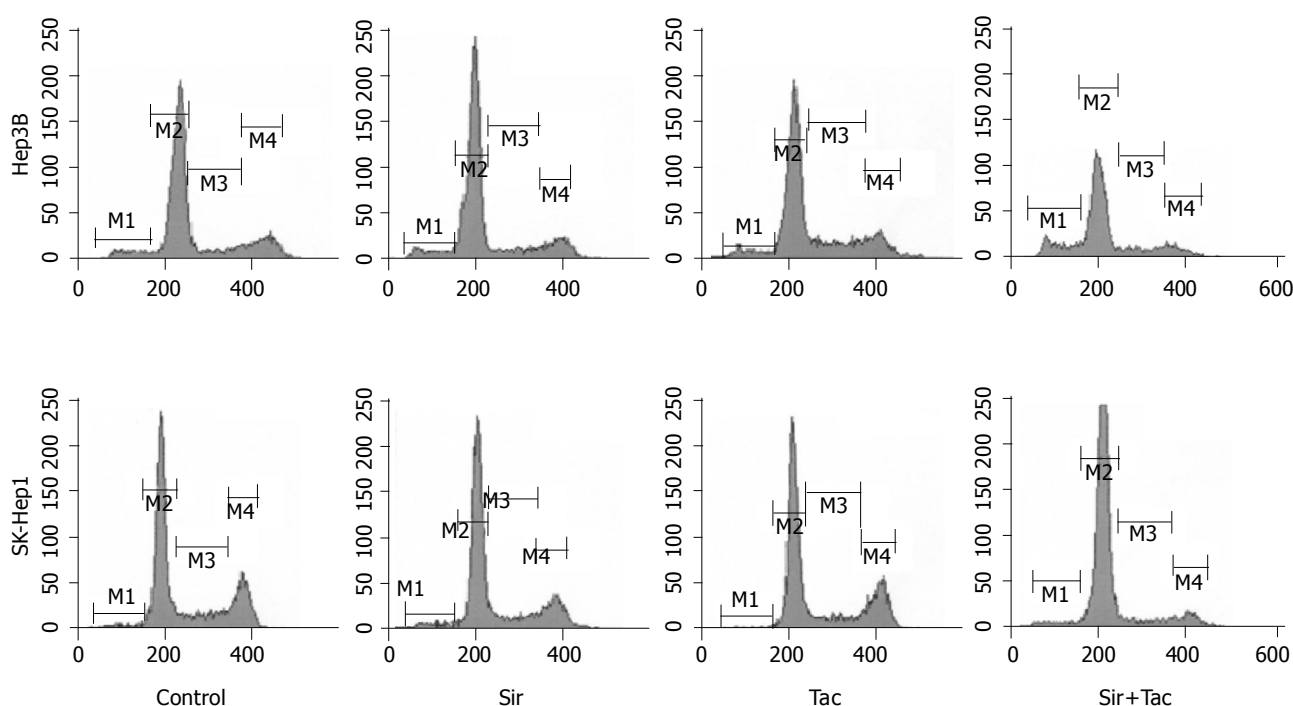


Figure 2 Cell-cycle analysis of both cell lines after treatment for 24 h with sirolimus, tacrolimus, or the combination of both at a dose of 25 ng/mL each compound. M1 = Sub-G1 region, indicating cells with small DNA fragments, a typical feature of apoptosis; M2 = G1-Phase; M3 = S-Phase; M4 = G2/M-Phase. The different cell cycle phases (M1-M4) were set in a reference analysis and kept constant throughout the measurements.

phase from 14 to 9% suggests an inhibition of mitosis in this treatment group. In contrast to Hep 3B cells, we found more changes of cells in the G1-phase in SK-Hep 1 cells with an increase from 61 to 69% after sirolimus alone. Tacrolimus resulted in a decrease of cells in the G1-phase from 61 to 54%. The combination of sirolimus and tacrolimus at a dose of 25 ng/mL resulted in a G1-arrest with an increase of cells from 61 to 82%. No induction of apoptosis was observed after treatment with sirolimus alone or in combination with tacrolimus in SK-Hep 1 cells.

Table 1 Relative cell numbers in different cell-cycle phases after treatment with sirolimus, tacrolimus and the combination of both. The doses used in these experiments were 25 ng/mL for each compound. Results of one representative experiment are shown

Cell cycle	Sub-G1	G1	S	G2/M
Hep3B				
Control	6	69	10	14
Sir	6	73	10	10
Tac	4	65	17	13
Sir + Tac	16	63	10	9
SK-Hep1				
Control	1	61	16	22
Sir	2	69	12	16
Tac	2	54	13	20
Sir + Tac	2	82	8	7

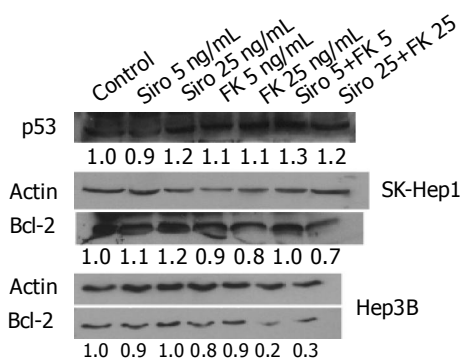


Figure 3 Western blot analysis of p53 and bcl-2. SK-Hep 1 cells express wild-type p53. Hep 3B cells harbor a deletion of the p53 gene and express no p53 protein. Expression levels were analyzed by densitometry referring to levels of actin. Relative values to controls are shown.

Expression of apoptosis-related proteins

In Figure 3, Western blot analysis of apoptosis-related proteins are shown to explain the induction of apoptosis in Hep 3B cells. SK-Hep 1 cells express a wild-type p53 gene. Since changes of p53 protein expression can be responsible for a p53-dependent induction of apoptosis, we measured the expression levels after treatment with sirolimus and tacrolimus alone or in combination with each other. There was no change of the expression levels of the p53 protein in all treatment groups. Bcl-2, a strong antiapoptotic gene, also showed no change in the expression levels in all treatment groups in SK-Hep 1 cells. Hep 3B cells expressed a deletion of the p53 gene. The expression of the bcl-2 protein in Hep 3B cells did not change after treatment with sirolimus or tacrolimus alone. When sirolimus and tacrolimus were

combined, we found a decrease of the bcl-2 protein expression by 55% in Hep 3B cells as measured by densitometry.

DISCUSSION

We hereby show that sirolimus is able to inhibit cell growth of human hepatocellular carcinoma *in vitro* by 50% in a concentration of 5 ng/mL. This low concentration may correspond to clinical serum levels considering a daily dose of 5 mg per patient. A dose-dependent growth inhibition was observed when cells were treated with doses ranging from 1 to 100 ng/mL. Control groups using absolute alcohol as the solvent at the same doses were not inhibited in growth. As shown previously, sirolimus is able to inhibit cell growth of different tumor cells^[13,14]. However, tacrolimus has been shown to promote cell growth^[21] through induction of cell cycle proteins such as cdk-4^[22]. For patient treatment after organ transplantation, a combination of sirolimus and tacrolimus has been shown to be effective for immunosuppression. No episodes of organ rejection were observed^[25]. Our experiments show that the combination of sirolimus and tacrolimus inhibits growth of hepatocellular carcinoma cells to a similar degree as sirolimus alone, while growth was stimulated after tacrolimus alone. In SK-Hep 1 cells, the combination of sirolimus and tacrolimus inhibited growth to 18% compared to control cells, which was not statistically significant. However, in this cell line, there was a large increase in cell numbers after treatment with tacrolimus alone ($P = 0.0156$). The cell numbers of combination treatment compared to treatment with tacrolimus alone were significantly lower in SK-Hep 1 cells ($P = 0.0005$). In Hep 3B, we found a significant decrease in cell numbers in the combination treatment group compared to control ($P = 0.0002$) and to the tacrolimus alone group ($P < 0.0001$). Thus, sirolimus inhibits the growth of HCC cells alone and in combination with tacrolimus. In SK-Hep 1 cells, which are strongly stimulated in growth by tacrolimus, sirolimus inhibits this proliferation significantly ($P = 0.0005$). According to these results, a combination of sirolimus and tacrolimus may prevent recurrence of HCC after LTX as much as treatment with sirolimus alone. The mechanisms of the observed G1-arrest in SK-Hep 1 and apoptosis in Hep 3B cells in the groups with combined treatment with sirolimus and tacrolimus are still not completely understood. Induction of apoptosis was observed in rhabdomyosarcoma cells^[14] and B lymphoma cells^[19] after incubation with sirolimus. We found a down-regulation of bcl-2 in Hep 3B cells as a possible mechanism of apoptosis. Since Hep 3B cells are deleted for the p53 gene, the induction of apoptosis appears to be p53-independent.

Cell cycle arrest after treatment with sirolimus has been described before^[11]. The mechanisms of an arrest in the G1-phase after the combined treatment with tacrolimus and sirolimus compared to sirolimus alone are not clear. The observed cell cycle arrest in SK-Hep 1 cells in our system may be p53-independent, because no change in the expression level of p53 was observed. In a different cell system, the observed induction of apoptosis in rhabdomyosarcoma cells was p53-independent^[14]. Also the G1 arrest, which is induced by both p53 and sirolimus appears to act through a different

mechanism^[26]. Another group showed that p53 and sirolimus cooperate in the induction of G1 arrest^[27]. Besides a decreased cell number in the G1-phase in Hep 3B cells after treatment with tacrolimus alone, an increase of cells in the S-Phase was observed, indicating cell proliferation. On the other hand, sirolimus caused a reduction of cells in the G2/M phase in SK-Hep 1 and Hep 3B cells, which corresponds to a reduced number of cells in mitosis with the subsequent reduced proliferation rate.

The growth inhibition of cells from hepatocellular carcinoma and their mechanisms in the present study are phenomena observed *in vitro*. Other mechanisms such as an antiangiogenic effect, which has been described in colon cancer^[13], could occur, which may increase the anti-tumor effect *in vivo*. The combination of sirolimus and tacrolimus resulted in a greater inhibition of intimal thickening in rat carotid arteries than sirolimus alone or the combination of sirolimus and cyclosporin^[28]. At low doses of tacrolimus, the growth inhibition of mesangial cell proliferation in kidneys observed after treatment with sirolimus could not be reversed. However, when cells were treated with higher doses of tacrolimus, such as 1 000 $\mu\text{mol/L}$, the cell inhibiting effect of sirolimus could be partially antagonized^[29]. Lymphocyte proliferation and IL-2 expression could be inhibited by sirolimus when combined with tacrolimus or cyclosporine. TGF- β was induced in this combination. These results show that combination treatments of sirolimus and calcineurin inhibitors can be used for immunosuppression^[30]. These studies demonstrate that the above-mentioned combinations of sirolimus and calcineurin inhibitors may be used for immunosuppression after organ transplantation, regardless of the transplanted organ or the disease which led to transplantation. The antiproliferative effect of sirolimus is a general phenomenon affecting both normal and tumor cells. A sirolimus-based immunosuppressive regimen in patients after liver transplantation due to HCC showed a beneficial effect on tumor recurrence and survival with an acceptable rate of rejection and toxicity^[31].

In conclusion, our data show that the two major mechanisms of sirolimus, namely immunosuppression and tumor inhibition, make this compound highly interesting for clinical application in patients who received a liver transplant for HCC. In the case of recurrence, no cure could be achieved so far. Thus, prevention of cancer recurrence is essential in the treatment of those patients. As we have shown, the combination of sirolimus and tacrolimus had a similar effect on cell growth inhibition as sirolimus alone *in vitro*. In the clinical situation, it has to be verified whether the recurrence rate of HCC correlates to the use of different immunosuppressive compounds, namely sirolimus and tacrolimus. In a long-term situation after liver transplantation, immunosuppression in these patients would be a sirolimus monotherapy or a combination of sirolimus and tacrolimus at low doses.

REFERENCES

- Llovet JM, Fuster J, Bruix J. The Barcelona approach: diagnosis, staging, and treatment of hepatocellular carcinoma. *Liver Transpl* 2004; **10**: S115-S120
- Podbielski J, Schoenberg L. Use of sirolimus in kidney transplantation. *Prog Transplant* 2001; **11**: 29-32
- Gonwa TA, Hricik DE, Brinker K, Grinyo JM, Schena FP. Improved renal function in sirolimus-treated renal transplant patients after early cyclosporine elimination. *Transplantation* 2002; **74**: 1560-1567
- Neuhaus P, Klupp J, Langrehr JM. mTOR inhibitors: an overview. *Liver Transpl* 2001; **7**: 473-484
- Kahan BD, Stepkowski SM, Napoli KL, Katz SM, Knight RJ, Van Buren C. The development of sirolimus: The University of Texas-Houston experience. *Clin Transpl* 2000: 145-158
- Gaston RS. Potential utility of rapamycin and tacrolimus in long-term, low-toxicity regimens. *Transplant Proc* 1999; **31**: 175-225
- McAlister VC, Gao Z, Peltekian K, Domingues J, Mahalati K, MacDonald AS. Sirolimus-tacrolimus combination immunosuppression. *Lancet* 2000; **355**: 376-377
- McAlister VC, Peltekian KM, Malatjalian DA, Colohan S, MacDonald S, Bitter-Suermann H, MacDonald AS. Orthotopic liver transplantation using low-dose tacrolimus and sirolimus. *Liver Transpl* 2001; **7**: 701-708
- Dumont FJ, Su Q. Mechanism of action of the immunosuppressant rapamycin. *Life Sci* 1996; **58**: 373-395
- Sherr CJ. G1 phase progression: cycling on cue. *Cell* 1994; **79**: 551-555
- Toyoshima H, Hunter T. p27, a novel inhibitor of G1 cyclin-Cdk protein kinase activity, is related to p21. *Cell* 1994; **78**: 67-74
- Gallo R, Padurean A, Jayaraman T, Marx S, Roque M, Adelman S, Chesebro J, Fallon J, Fuster V, Marks A, Badimon JJ. Inhibition of intimal thickening after balloon angioplasty in porcine coronary arteries by targeting regulators of the cell cycle. *Circulation* 1999; **99**: 2164-2170
- Guba M, von Breitenbuch P, Steinbauer M, Koehl G, Flegel S, Hornung M, Bruns CJ, Zuelke C, Farkas S, Anthuber M, Jauch KW, Geissler EK. Rapamycin inhibits primary and metastatic tumor growth by antiangiogenesis: involvement of vascular endothelial growth factor. *Nat Med* 2002; **8**: 128-135
- Hosoi H, Dilling MB, Shikata T, Liu LN, Shu L, Ashmun RA, Germain GS, Abraham RT, Houghton PJ. Rapamycin causes poorly reversible inhibition of mTOR and induces p53-independent apoptosis in human rhabdomyosarcoma cells. *Cancer Res* 1999; **59**: 886-894
- Ogawa T, Tokuda M, Tomizawa K, Matsui H, Itano T, Konishi R, Nagahata S, Hatase O. Osteoblastic differentiation is enhanced by rapamycin in rat osteoblast-like osteosarcoma (ROS 17/2.8) cells. *Biochem Biophys Res Commun* 1998; **249**: 226-230
- Price DJ, Grove JR, Calvo V, Avruch J, Bierer BE. Rapamycin-induced inhibition of the 70-kilodalton S6 protein kinase. *Science* 1992; **257**: 973-977
- Schumacher G, Oidtmann M, Rosewicz S, Langrehr J, Jonas S, Mueller AR, Rueggeberg A, Neuhaus R, Bahra M, Jacob D, Gerlach H, Neuhaus P. Sirolimus inhibits growth of human hepatoma cells in contrast to tacrolimus which promotes cell growth. *Transplant Proc* 2002; **34**: 1392-1393
- Seufferlein T, Rozengurt E. Rapamycin inhibits constitutive p70s6k phosphorylation, cell proliferation, and colony formation in small cell lung cancer cells. *Cancer Res* 1996; **56**: 3895-3897
- Muthukkumar S, Ramesh TM, Bondada S. Rapamycin, a potent immunosuppressive drug, causes programmed cell death in B lymphoma cells. *Transplantation* 1995; **60**: 264-270
- Luan FL, Ding R, Sharma VK, Chon WJ, Lagman M, Suthanthiran M. Rapamycin is an effective inhibitor of human renal cancer metastasis. *Kidney Int* 2003; **63**: 917-926
- Hojo M, Morimoto T, Maluccio M, Asano T, Morimoto K, Lagman M, Shimbo T, Suthanthiran M. Cyclosporine induces cancer progression by a cell-autonomous mechanism. *Nature* 1999; **397**: 530-534
- Baksh S, DeCaprio JA, Burakoff SJ. Calcineurin regulation of the mammalian G0/G1 checkpoint element, cyclin dependent kinase 4. *Oncogene* 2000; **19**: 2820-2827
- Hamada K, Alemany R, Zhang WW, Hittelman WN, Lotan

- R, Roth JA, Mitchell MF. Adenovirus-mediated transfer of a wild-type p53 gene and induction of apoptosis in cervical cancer. *Cancer Res* 1996; **56**: 3047-3054
- 24 **Weber AK**, Wahn U, Renz H. Superantigen-induced T cell death by apoptosis: analysis on a single cell level and effect of IFN-gamma and IL-4 treatment. *Int Arch Allergy Immunol* 2000; **121**: 215-223
- 25 **Shapiro AM**, Lakey JR, Ryan EA, Korbutt GS, Toth E, Warnock GL, Kneteman NM, Rajotte RV. Islet transplantation in seven patients with type 1 diabetes mellitus using a glucocorticoid-free immunosuppressive regimen. *N Engl J Med* 2000; **343**: 230-238
- 26 **Metcalfe SM**, Canman CE, Milner J, Morris RE, Goldman S, Kastan MB. Rapamycin and p53 act on different pathways to induce G1 arrest in mammalian cells. *Oncogene* 1997; **15**: 1635-1642
- 27 **Huang S**, Liu LN, Hosoi H, Dilling MB, Shikata T, Houghton PJ. p53/p21(CIP1) cooperate in enforcing rapamycin-induced G(1) arrest and determine the cellular response to rapamycin. *Cancer Res* 2001; **61**: 3373-3381
- 28 **Waller JR**, Murphy GJ, Bicknell GR, Toomey D, Nicholson ML. Effects of the combination of rapamycin with tacrolimus or cyclosporin on experimental intimal hyperplasia. *Br J Surg* 2002; **89**: 1390-1395
- 29 **Wang W**, Chan YH, Lee W, Chan L. Effect of rapamycin and FK506 on mesangial cell proliferation. *Transplant Proc* 2001; **33**: 1036-1037
- 30 **Khanna AK**. Mechanism of the combination immunosuppressive effects of rapamycin with either cyclosporine or tacrolimus. *Transplantation* 2000; **70**: 690-694
- 31 **Kneteman NM**, Oberholzer J, Al Saghier M, Meeberg GA, Blitz M, Ma MM, Wong WW, Gutfreund K, Mason AL, Jewell LD, Shapiro AM, Bain VG, Bigam DL. Sirolimus-based immunosuppression for liver transplantation in the presence of extended criteria for hepatocellular carcinoma. *Liver Transpl* 2004; **10**: 1301-1311

Edited by Guo SY Language Editor Elsevier HK

Comparison between combination therapy of percutaneous ethanol injection and radiofrequency ablation and radiofrequency ablation alone for patients with hepatocellular carcinoma

Kazutaka Kurokohchi, Seishiro Watanabe, Tsutomu Masaki, Naoki Hosomi, Yoshiaki Miyauchi, Takashi Himoto, Yasuhiko Kimura, Seiji Nakai, Akihiro Deguchi, Hirohito Yoneyama, Shuhei Yoshida, Shigeki Kuriyama

Kazutaka Kurokohchi, Seishiro Watanabe, Tsutomu Masaki, Naoki Hosomi, Yoshiaki Miyauchi, Takashi Himoto, Yasuhiko Kimura, Seiji Nakai, Akihiro Deguchi, Hirohito Yoneyama, Shuhei Yoshida, Shigeki Kuriyama, Third Department of Internal Medicine, Kagawa University School of Medicine, 1750-1 Ikenobe, Miki-cho, Kita-gun, Kagawa 761-0793, Japan

Correspondence to: Shigeki Kuriyama, Third Department of Internal Medicine, Kagawa University School of Medicine, 1750-1 Ikenobe, Miki-cho, Kita-gun, Kagawa 761-0793, Japan. skuriyam@med.kagawa-u.ac.jp

Telephone: +81-878-91-2156 Fax: +81-878-91-2158

Received: 2004-08-17 Accepted: 2004-10-18

Key words: Combination therapy; Percutaneous ethanol injection; Radiofrequency ablation; Energy requirement

Kurokohchi K, Watanabe S, Masaki T, Hosomi N, Miyauchi Y, Himoto T, Kimura Y, Nakai S, Deguchi A, Yoneyama H, Yoshida S, Kuriyama S. Comparison between combination therapy of percutaneous ethanol injection and radiofrequency ablation and radiofrequency ablation alone for patients with hepatocellular carcinoma. *World J Gastroenterol* 2005; 11 (10): 1426-1432

<http://www.wjgnet.com/1007-9327/11/1426.asp>

Abstract

AIM: In the present study, the characteristics of PEI-RFA treatment were further elucidated by analyzing the relationship between the volume of coagulated necrosis and the energy requirement for ablation or the amount of ethanol injected into HCC.

METHODS: The volume of coagulated necrosis, total energy requirement and energy requirement for coagulation of per unit volume were examined in the groups of PEI-RFA and RFA alone using the Cool-tip RF system.

RESULTS: The results showed that the volume of coagulated necrosis induced was significantly larger in PEI-RFA group than in routine RFA group, when the total energy administered was comparable in both groups. In PEI-RFA, enlargement of coagulated necrosis was admitted in 3 dimensions and the amount of energy requirement per unit volume of coagulated necrosis was negatively correlated with the amount of ethanol injected into HCC.

CONCLUSION: These results suggest that, compared to RFA alone, PEI-RFA enables to induce comparable coagulated necrosis with smaller energy requirement, and that PEI-RFA is likely to be less invasive than RFA alone irrespective of inducing enhanced coagulated necrosis. Thus, simple prior injection of ethanol may make RFA treatment more effective and less invasive for the treatment of patients with HCC.

INTRODUCTION

Hepatocellular carcinoma (HCC) is one of the most serious problems worldwide. Although intensive efforts have been made for the treatment of HCC, the mortality of patients with HCC is still high. Tumor ablation technologies such as microwave, laser and radio frequency have been shown to be reliable and effective for inducing thermally-mediated coagulation necrosis for primary HCC^[1-4] and metastatic liver cancer^[5,6]. Percutaneous ethanol injection (PEI) therapy, more frequently performed in the past, is considered to be effective for the treatment of patients with relatively small-sized encapsulated HCC below 3 cm in the longest diameter. Recently, it has become possible to obtain larger areas of coagulated necrosis by the innovation of radiofrequency (RFA) technologies^[7,8]. Much effort has been applied to enhance the therapeutic effects of RFA by the combination of RFA with other modalities. For example, combined use of transcatheter arterial chemoembolization^[9-13] or saline injection^[14-17] with RFA therapy was shown to be effective to enhance the coagulated necrosis. We also developed a novel combination therapy of PEI and RFA (PEI-RFA) and reported that this combination therapy could induce wider coagulated necrosis without much efforts and adverse effects. Furthermore, this therapy can be applied to the tumors that are difficult to treat with RFA alone^[18,19]. Furthermore, this enhancing effect for inducing the coagulated necrosis has been experimentally confirmed using bovine liver^[20]. Recently, we have reported that percutaneous ethanol and lipiodol injection therapy (PELIT), considered to be a milder therapy than RFA, was important as a supportive treatment modality for HCCs

especially for those lacking the vascularity or for patients with severely impaired hepatic reserve and useful for the treatment of HCCs that were difficult to treat with RFA alone^[21]. After developing PEI-RFA treatment, we have experienced so far some cases that were satisfactorily treated by use of relatively low-power output control. Thus, in the present study, PEI-RFA treatment was further characterized from the standpoint of the energy requirement for total and unit volume ablation as well as of the amount of ethanol injected, using the RF system with cool-tip type electrodes.

MATERIALS AND METHODS

Patients

PEI-RFA was performed against 75 cases (53 males and 22 females; mean age of 69 years) with biopsy-proven HCC. The patients were also diagnosed as having HCC by helical dynamic computed tomography (CT). Among the total subjects, RFA alone was done in 15 patients and PEI-RFA was in 60. The characteristics of the subjects are shown in Table 1. All of these studies were conducted with informed consent at the time of the enrollment for this study.

Table 1 Characteristics of patients enrolled in the present study

	RFA alone	PEI-RFA
Total number of patient	15	60
Male/Female	10/5	45/15
Age (yr)		
Mean	63	69
Range	47-74	44-86
Tumor size (cm)		
Mean	2.5	3.0
Range	1.5-3.5	1.0-8.0
Injected ethanol (mL)		
Mean	0	7.1
Range	0-0	0-37
Child-Pugh grade		
A	7	38
B	7	21
C	1	1

Equipments and RFA procedures

PEI-RFA was performed under the real-time ultrasonography (US) guidance with a 3.5-MHz sector probe (Power Vision 5000; Toshiba Medical, Tokyo, Japan). RFA was performed by Cool-tip RF System (RADIONICS, Burlington, USA)^[22] according to the method described in our previous manuscripts^[18,19]. Briefly, a 17-gauge RFA needle with an electrode of 3 cm in length was first inserted into the tumor, and then a 21-gauge PEI needle was inserted into the tumor in the liver through the same hole of the attachment beside the echo probe, and then pure ethanol was slowly injected into the tumor till the whole area of tumor was filled with the ethanol (Figure 1). Ethanol injection into the tumor was ceased when resistance to the injection was felt. The volume of injected ethanol was always kept below the double of estimated tumor volume. The ablation was performed under the impedance control and the power output was increased stepwise and the ablation was terminated after the high echic shadow sufficiently covered the tumor margin.

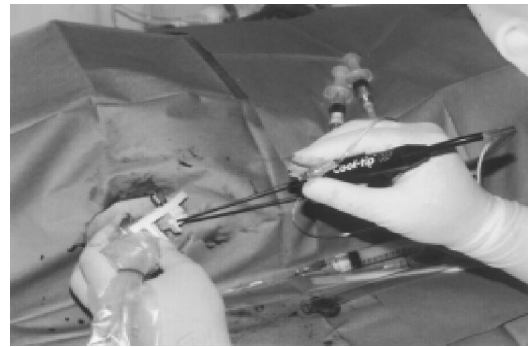


Figure 1 Appearance of PEI-RFA treatment. A 17-gauge RFA needle with 2 or 3 cm electrode was first inserted into the tumor through the hole of the attachment beside the echo probe, and then 21-gauge PEI needle was inserted through the same hole. RFA was performed immediately after injecting the ethanol into the tumor. The ablation was performed under the impedance control. The amount of ethanol injected into the tumors was always kept below the double of the estimated tumor volume and the injection of ethanol was ceased if resistance to the injection was felt.

Evaluation of therapeutic efficacy

The efficacy of the RFA was assessed by using helical dynamic contrast-enhanced CT five to seven days after the treatment. Tumor necrosis was considered to be complete if no enhancing areas were observed based on images obtained during early and late phases of dynamic contrast-enhanced CT.

Evaluation of energy requirement for ablation

Energy requirement needed for ablation was calculated as follows: energy (J) = Watt (W) × duration of ablation (s). The length of coagulated necrosis of the lesion was measured from the late phase of helical dynamic CT. Approximation volume of whole coagulated necrosis area and energy requirement for ablation per unit volume were calculated as follows: whole coagulated volume (cm³) = $\frac{4}{3} \times r^1(\text{cm}) \times r^2(\text{cm}) \times r^3(\text{cm})$; (r^1 = longest diameter/2; r^2 = shortest diameter/2; r^3 = height/2) and energy requirement for coagulation per unit volume (J/cm³) = energy/whole coagulated necrosis.

Statistical analysis

Statistical analysis was performed using Macintosh software StatView II (Version 5.0). Regression analysis was used to calculate the correlation coefficients and *P* values. Statistical significance was accepted when *P* < 0.05.

RESULTS

Comparison of the volume of coagulated area, and energy requirement and the energy requirement for total and unit volume coagulation in the groups of PEI-RFA and RFA alone

Seventy-five patients were divided randomly into two groups. One group (60 patients) received PEI-RFA, while the other (15 patients) RFA alone. All of these patients underwent RFA therapy by means of the Cool-tip RF system. No major complications or adverse effects were observed in both groups. The volume of coagulated necrosis areas, the total amount of energy requirement and the energy requirement

Table 2 Comparison of the volume of coagulated necrosis, total energy requirement and the energy requirement for inducing coagulation of per unit volume in the groups of PEI-RFA and RFA alone

	EtOH (mL)	L (cm)	S (cm)	H (cm)	V (cm ³)	T-ENE (J)	T-ENE/V (J/cm ³)
RFA alone (n = 15)	0±0	2.3±0.6	2.1±0.6	2.4±0.4	6.5±3.6	38 700±12 549	10 010±11 124
PEI-RFA (n = 60)	6.9±6.6	4.2±1.2	3.5±1.0	4.0±1.1	34.0±29.3	53 828±28 144	2 355±1 690
P	<0.0001	<0.0001	<0.0001	0.0002	<0.0001	0.73	<0.0001

Sixty patients with HCC were treated with PEI-RFA by Cool-tip RF System, while 15 patients were treated with RFA alone using the same system. After the treatment, the longest and shortest diameters and the height of the coagulated necrosis were estimated by the contrast-enhanced CT scan. Each abbreviation in the table is expressing as follows: EtOH, the amount of ethanol; L, longest diameter; S, shortest diameter; H, height; V, the volume of coagulated necrosis; T-ENE, total energy requirement; T-ENE/V, the energy requirement for inducing coagulation of per unit volume. The coagulated necrosis in PEI-RFA group was enlarged in 3 dimensions compared with the group of RFA alone, although the total energy requirement was comparable between groups.

Table 3 Comparative study of coagulated necrosis in the groups classified according to the amount of ethanol injected in PEI-RFA

	EtOH (mL)	L (cm)	S (cm)	H (cm)	V (cm ³)	T-ENE (J)	T-ENE/V (J/cm ³)
EtOH <6.9 mL (n = 41)	3.1±1.6	3.8±0.9	3.0±0.6	3.6±0.9	22.3±14.3 (1)	48 901±23 219	2 796±1 752
EtOH >6.9 mL (n = 19)	14.9±6.1	5.1±1.3	4.3±1.2	4.8±1.1	57.6±38.2 (2.6)	63 931±34 744	1 460±1 016
P	<0.0001	0.0002	<0.0001	0.0003	<0.0001	0.11	0.0014

The mean volume of ethanol injected in PEI-RFA was 6.9 mL. Therefore, 60 patients treated with PEI-RFA were divided into two groups according to the amount of ethanol injected. One group (high EtOH group) consisted of 19 cases administered with 6.9 mL and more ethanol, and the other (low EtOH group) of 41 cases less than 6.9 mL ethanol. Each abbreviation in the table is expressing as follows: EtOH, the amount of ethanol; L, longest diameter; S, shortest diameter; H, height; V, the volume of coagulated necrosis; T-ENE, total energy requirement; T-ENE/V, the energy requirement for inducing coagulation of per unit volume. The volume of coagulated necrosis in the high EtOH group was 2.6 times larger than that in the low EtOH group, although the total energy requirement was comparable between groups.

Table 4 Comparative study of coagulated necrosis in the groups classified according to the total energy requirement in PEI-RFA

	EtOH (mL)	L (cm)	S (cm)	H (cm)	V (cm ³)	T-ENE (J)	T-ENE/V (J/cm ³)
T-ENE <53828 J (n = 32)	5.8±5.8	3.6±0.8	3.2±0.8	3.6±1.0	24.6±17.3 (1)	32 003±12 743	2 038±1 638
T-ENE >53828 J (n = 28)	8.1±7.3	4.8±1.2	3.8±1.2	4.4±1.2	44.0±36.4 (1.8)	77 884±19 567	2 727±1 687
P	0.23	0.0002	0.04	0.0028	0.014	<0.0001	0.052

All cases treated with PEI-RFA were divided into two groups. One was high energy group and the other low energy group according to the mean amount of total energy requirement (53828 Joule). Each abbreviation in the table is expressing as follows: EtOH, the amount of ethanol; L, longest diameter; S, shortest diameter; H, height; V, the volume of coagulated necrosis; T-ENE, total energy requirement; T-ENE/V, the energy requirement for inducing coagulation of per unit volume. The amount of ethanol injected was statistically comparable in both groups. The volume of coagulated necrosis in the high energy group was 1.8 times larger than that in the low energy group. The degree of the enhancing effect was smaller compared with that in cases classified by the mean amount of injected ethanol as shown in Table 3. Furthermore, the energy requirement for coagulation of per unit volume was comparable between groups.

for inducing coagulation of per unit volume in the groups of PEI-RFA and RFA alone are shown in Table 2. The longest and shortest diameters as well as the height of the coagulated necrosis areas and the coagulated volume evaluated by dynamic contrast-enhanced CT scan were significantly larger in cases treated with PEI-RFA than in those treated with RFA alone. By contrast, the total amount of energy requirement was comparable between groups. Thus, the energy requirement for coagulation of per unit volume was significantly smaller in PEI-RFA group compared to the group of RFA alone. The energy requirement for coagulation of per unit volume in PEI-RFA was approximately three-fourths of that in RFA alone.

Comparative study of the coagulated necrosis and the energy requirement for coagulation of per unit volume between PEI-RFA and RFA groups

As shown in Table 3, the mean volume of ethanol injected in PEI-RFA group was 6.9 mL. Therefore, 60 patients

treated with PEI-RFA were divided into two groups according to the amount of ethanol injected. One group (high-EtOH group) consisted of 19 cases administered with 6.9 mL and more ethanol and the other (low-EtOH group) of 41 cases less than 6.9 mL ethanol. Between these two groups, the total energy requirement was also comparable as shown in Table 1. However, the volume of coagulated necrosis was significantly larger in the high-EtOH group than in the low-EtOH group. The volume of coagulated necrosis in the high-EtOH group was 2.6 times larger than that in the low-EtOH group. Accordingly, the energy requirement for coagulation per unit volume in the high-EtOH group was significantly lower in the high-EtOH group than in the low-EtOH group.

All cases treated with PEI-RFA were divided into two groups. One was high-energy group and the other low-energy group according to the mean amount of total energy requirement (53 828 J). As shown in Table 4, in this classification, the amount of ethanol injected was statistically

comparable in both groups. The volume of coagulated necrosis in the high-energy group was 1.8 times larger than that in the low-energy group. The degree of the enhancing effect was smaller compared to that in cases classified by the mean amount of ethanol injected as shown in Table 2. Furthermore, the energy requirement for coagulation of per unit volume was comparable between groups.

Relationship between the amount of ethanol and the volume of coagulated necrosis or the energy requirement for coagulation of per unit volume

Relationship between the amount of ethanol injected and the volume of coagulated necrosis or the energy requirement for coagulation of per unit volume was analyzed in the total subjects treated with PEI-RFA (60 cases). As shown in Figure 2, the amount of ethanol injected into tumor significantly and positively correlated with the volume of coagulated necrosis with high correlation coefficient ($r = 0.71$, $P < 0.0001$). Then, the amount of ethanol injected negatively, although weak, correlated with the energy requirement for coagulation of per unit volume ($r = -0.41$, $P = 0.014$). These results suggest that, according to the amount of ethanol injected into tumor, larger coagulated necrosis can be obtained and less amount of energy is required for coagulation of per unit volume.

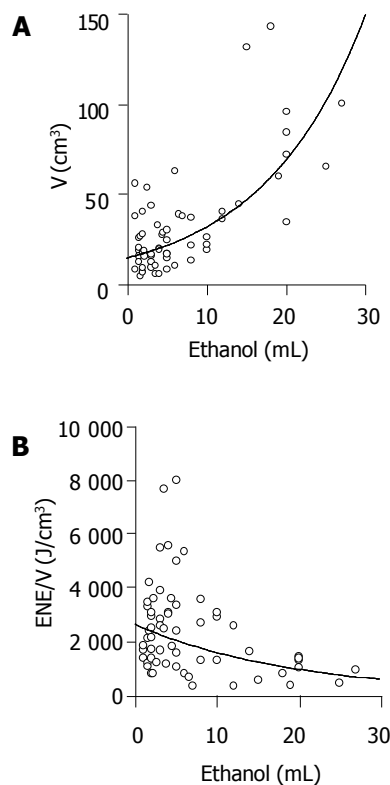


Figure 2 Relationship between the amount of ethanol injected and the volume of coagulated necrosis or the energy requirement for inducing per unit volume of coagulated necrosis in PEI-RFA. PEI-RFA was performed on 60 patients with HCC. The ablation was done by using the Cool-tip RF system. The amount of ethanol injected into tumors positively correlated with the volume of coagulated necrosis (A: $r = 0.71$, $P < 0.0001$) and it negatively correlated with the energy requirement for inducing per unit volume of coagulated necrosis (B: $r = -0.41$, $P = 0.014$).

Relationship between the total required energy for ablation and the volume of coagulated necrosis or the energy requirement for coagulation of per unit volume

Relationship between the total required energy and the volume of the coagulated necrosis or the energy requirement for coagulation of per unit volume was analyzed in the total subjects treated with PEI-RFA (60 cases). As shown in Figure 3, the total required energy significantly and positively correlated with the volume of coagulated necrosis ($r = 0.47$, $P = 0.0013$). However, this correlation coefficient was smaller than that between the amount of ethanol injected and the volume of coagulated necrosis. Moreover, the total required energy and the energy requirement for coagulation of per unit volume did not show significant correlation ($r = 0.35$, $P = 0.13$).

Representative cases with HCC treated with PEI-RFA

By analyzing the relationship between the energy requirement and the amount of ethanol injected in PEI-RFA, two characteristic points have been turned out: (1) PEI-RFA enables to induce wider coagulated necrosis by increasing the amount of ethanol injected into tumor; (2) PEI-RFA is able to obtain comparative therapeutic effects by means of lower energy compared to RFA alone.

Four cases with HCC treated with PEI-RFA expressing

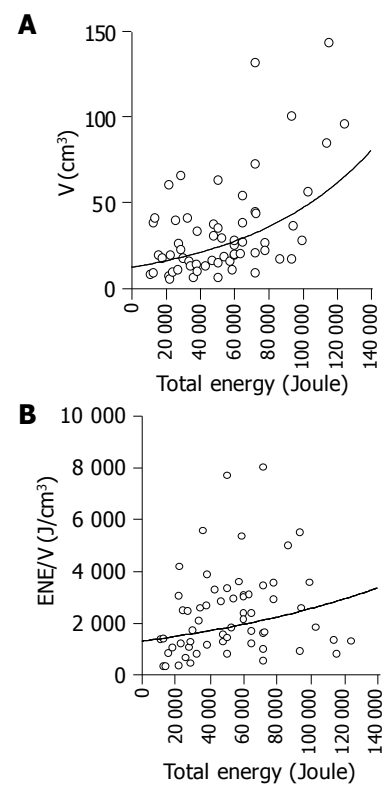


Figure 3 Relationship between the amount of total energy requirement and the volume of coagulated necrosis or the energy requirement for inducing per unit volume of coagulated necrosis in PEI-RFA. PEI-RFA was performed on 60 patients with HCC. The ablation was done by using the Cool-tip RF system. The amount of total energy requirement positively correlated with the volume of coagulated necrosis ($r = 0.47$, $P = 0.0013$), whereas no significant correlation was admitted between the total amount of energy requirement and the energy requirement for inducing per unit volume of coagulated necrosis ($r = 0.35$, $P = 0.13$) in PEI-RFA.

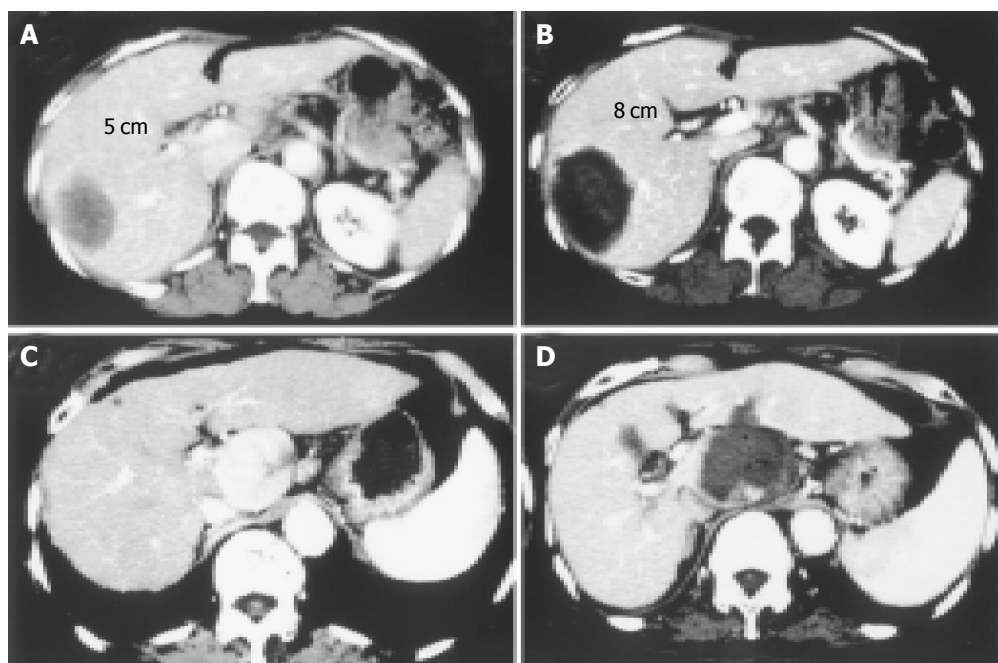


Figure 4 Two cases with large-sized HCC treated with PEI-RFA are shown. Contrast-enhanced CT before (A: delay phase, C: early vascular phase) and after (B: delay phase, D: delay phase) PEI-RFA. Massive HCCs of 5 cm in the longest diameter were located in the right lobe of the liver in both cases. In the first case (A and B), RFA was started at 30 W and the power output was increased stepwise to 100 W every two min and the ablation was performed for 20 min. In the second case (C and D), because the tumor was located close by blood vessel such as inferior vena cava, portal tract and aorta, it was likely to be difficult to treat with RFA under high power control. After injecting 19 mL of ethanol into the tumor, one session of RFA was performed at 30 W for 12 min. The massive tumor was completely eliminated by PEI-RFA.

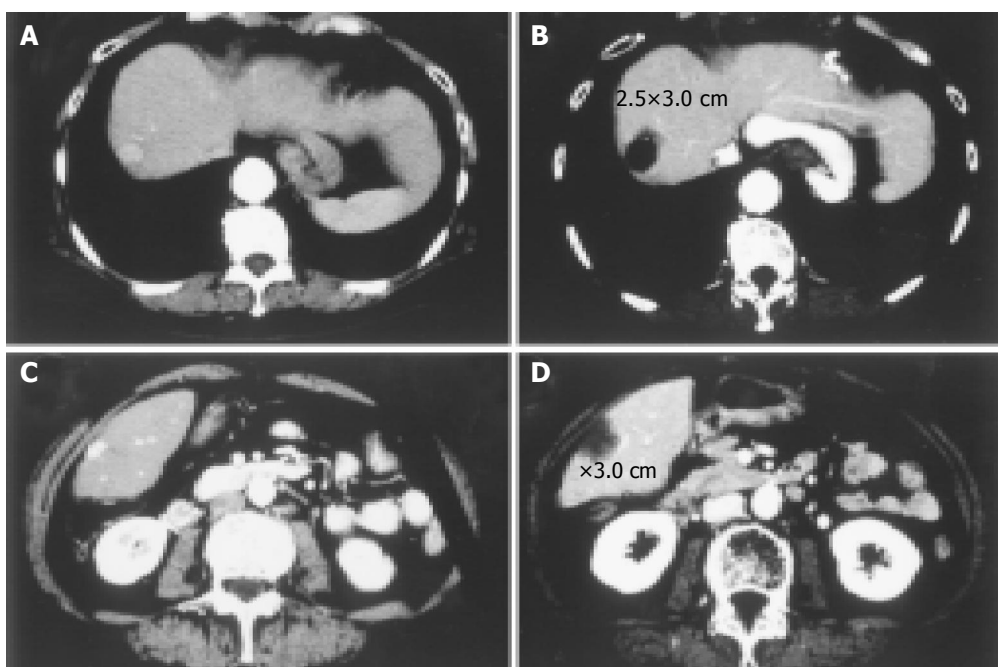


Figure 5 Two cases with small-sized HCCs treated with PEI-RFA under low power output control are shown. Contrast-enhanced CT before (A, C) and after (B, D) PEI-RFA. Small HCCs of 1.5 cm in the longest diameter were located in the S8 region of the liver in both cases. In both cases, RFA was performed at 40 W for 5 min. Though the ablation was performed at relatively low power output for short duration, the coagulated necrosis larger than 2.5 cm was induced after the treatment.

these characteristic points are shown in Figures 4, 5. The large-sized HCCs (5 cm in diameter) of the first and second cases were located in S7 (Figure 4A) and S1 regions (Figure 4C) respectively. In the first case, RFA was performed at 30-100 W for 10 min after injecting 10 mL

of ethanol homogeneously into the tumor. The RFA electrode was reinserted into the tumor and the RFA was performed for further 10 min. Contrast-enhanced CT after the treatment showed the achievement of coagulated necrosis of 8 cm in diameter and the ablated region covered

the entire region of the tumor including the safety margin (Figure 4B). In the second case, contrast-enhanced CT showed the enhancement in the early vascular phase of dynamic CT (Figure 4C). It was likely to be difficult to treat with RFA under high power output, because the tumor was surrounded by inferior vena cava, portal tract and aorta. Therefore, PEI-RFA under a relatively low power output after injecting high amount of ethanol was chosen as a treatment modality. After injecting 19 mL of ethanol into the tumor, one session of RFA was performed at 30 W for 12 min. Contrast-enhanced CT after the treatment showed that the ablated region reached the most of the entire region of the tumor in this case as well (Figure 4D).

The HCCs of the third and fourth cases are located in S8 (Figure 5A) and S6 (Figure 5C) respectively and the size of both HCCs was 1.5 cm in diameter. To obtain over 0.5 cm of the safety margin area from the edge of the tumor, the coagulated necrosis wider than 2.5 cm in diameter was required for the ablation. In both cases, after injecting 2 mL of ethanol into the tumors, RFA was performed at 40 W for 5 min. Although RFA was performed under a relatively low power output and for a short time period, dynamic CT after PEI-RFA in both cases indicated the induction of coagulated necrosis larger than 2.5 cm in diameter (Figure 5B, D). In the third case, the energy requirement for coagulation of per unit volume was an extremely low level of 1244 (J/cm³), a half-value of the mean in PEI-RFA group as shown in the Table 2.

DISCUSSION

RFA is a promising technique for local control of liver malignancy such as primary hepatocellular carcinoma^[4,23,24] and metastatic liver cancers^[25]. This technique has become the main stream of the treatment of non-surgical treatment modalities in clinical settings^[3]. In contrast to its efficacy, the region of coagulated necrosis induced by RFA is still limited and tumors within 3 cm in diameter are thought to be the good application sites of RFA therapy. Underestimated complication was sometimes observed after RFA treatment. To enhance the therapeutic effect of RFA, several treatment modalities have been applied as additional treatments on local treatment. It has been reported that combined use of transcatheter arterial chemoembolization or saline injection therapy with RFA enhanced the extent of induced coagulation^[11-14,17,26,27]. Recently, Pawlik *et al* have reported that resection combined with RFA provides a surgical option to a group of patients with unresectable liver metastases^[28]. As one of the optional combination therapies, we have shown that the injection of ethanol prior to RFA markedly increased the induced coagulated necrosis in human^[18,19] and bovine livers^[20]. In the present study, we further evaluated the usefulness of PEI-RFA using the system equipped with a cool-tip type electrode, instead of the system with an expandable type electrode. Especially, the characteristics of PEI-RFA were assessed from the standpoint of energy requirement for inducing the coagulated necrosis and the amount of ethanol injected. In our previous manuscript, we have shown that the longest and the shortest diameters as well as the height of the coagulated necrosis areas, and

the coagulated volume evaluated by dynamic contrast-enhanced CT scan were significantly larger in cases treated with PEI-RFA than in those treated with RFA alone using the system equipped with an expandable type of electrode (RITA-500PA)^[18]. Similar enhancing effects of ethanol injection were observed in the present study using the Cool-tip RF system. The volume of coagulated necrosis in PEI-RFA was approximately four times larger than that in RFA alone in the Cool-tip RF system. This degree of enhancement of coagulated necrosis area was quite similar to that detected in the system with the expandable type of electrode in our previous manuscript^[18]. These results suggest that injection of ethanol prior to RFA therapy may equally enhance the volume of coagulated necrosis in 3 dimensions to the same extent regardless of types of RFA instruments.

More importantly and interestingly, it should be noted that the volume and diameters of coagulated necrosis were significantly larger in PEI-RFA than in RFA alone, although the amount of total energy requirement was comparable between groups. Thus, the energy requirement for coagulation of per unit volume was significantly lower in PEI-RFA than in RFA alone. The degree of enhancement of coagulated necrosis was higher between the groups classified according to the amount of injected ethanol than between those classified according to the amount of total energy requirement. The former was 2.6-times enhancement and the latter was 1.8 times. Furthermore, the volume of coagulated necrosis showed a stronger correlation with the amount of ethanol injected than the total energy requirement ($r = 0.71$ vs 0.47) respectively. While the amount of injected ethanol, negatively correlated with the energy requirement for coagulation of per unit volume, the total required energy did not show negative correlation with the energy requirement for coagulation of per unit volume. Taken together, these results clearly indicate that smaller energy is required in PEI-RFA to induce comparable coagulated necrosis to RFA alone, and the use of ethanol injection prior to RFA is likely to alter the RFA therapy to a milder one for the treatment of patients with HCC. These results may be one of the explanations that PEI-RFA is able to induce wider coagulated necrosis compared to RFA alone under the same power output condition.

Although it is possible to say that RFA is less invasive compared to surgical treatment, we have experienced some patients whose liver function tests declined after RFA treatment. Furthermore, RFA treatment has sometimes been obliged to be ceased due to the pain complained by patients during the treatment^[29]. Therefore, it is very important to develop less invasive treatments than those currently used. It is needless to say that less invasive and more effective treatment is desirable for local control of HCC in patients treated with RFA.

When thinking of the medical treatment, it should be important to take both efficacy and the adverse reactions into consideration. In this regard, PEI-RFA is thought to be a less invasive and more effective treatment modality for local control of hepatic malignancies than RFA alone. PEI-RFA is expected to contribute to the local treatment of patients with hepatic malignancy from the standpoint of not only the effectiveness but also the reduction of adverse events.

REFERENCES

- 1 Nagata Y, Hiraoka M, Akuta K, Abe M, Takahashi M, Jo S, Nishimura Y, Masunaga S, Fukuda M, Imura H. Radiofrequency thermotherapy for malignant liver tumors. *Cancer* 1990; **65**: 1730-1736
- 2 Allgaier HP, Deibert P, Zuber I, Olschewski M, Blum HE. Percutaneous radiofrequency interstitial thermal ablation of small hepatocellular carcinoma. *Lancet* 1999; **353**: 1676-1677
- 3 Goldberg SN, Gazelle GS, Solbiati L, Livraghi T, Tanabe KK, Hahn PF, Mueller PR. Ablation of liver tumors using percutaneous RF therapy. *AJR Am J Roentgenol* 1998; **170**: 1023-1028
- 4 Curley SA, Izzo F, Ellis LM, Nicolas Vauthey J, Vallone P. Radiofrequency ablation of hepatocellular cancer in 110 patients with cirrhosis. *Ann Surg* 2000; **232**: 381-391
- 5 Solbiati L, Goldberg SN, Ierace T, Livraghi T, Meloni F, Dellanoce M, Sironi S, Gazelle GS. Hepatic metastases: percutaneous radio-frequency ablation with cooled-tip electrodes. *Radiology* 1997; **205**: 367-373
- 6 Solbiati L, Ierace T, Goldberg SN, Sironi S, Livraghi T, Fiocca R, Servadio G, Rizzatto G, Mueller PR, Del Maschio A, Gazelle GS. Percutaneous US-guided radio-frequency tissue ablation of liver metastases: treatment and follow-up in 16 patients. *Radiology* 1997; **202**: 195-203
- 7 Livraghi T, Goldberg SN, Lazzaroni S, Meloni F, Solbiati L, Gazelle GS. Small hepatocellular carcinoma: treatment with radio-frequency ablation versus ethanol injection. *Radiology* 1999; **210**: 655-661
- 8 Goldberg SN, Gazelle GS, Compton CC, Mueller PR, Tanabe KK. Treatment of intrahepatic malignancy with radiofrequency ablation: radiologic-pathologic correlation. *Cancer* 2000; **88**: 2452-2463
- 9 Rossi S, Garbagnati F, Lencioni R, Allgaier HP, Marchian^o A, Fornari F, Quaretti P, Tolla GD, Ambrosi C, Mazzaferro V, Blum HE, Bartolozzi C. Percutaneous radio-frequency thermal ablation of nonresectable hepatocellular carcinoma after occlusion of tumor blood supply. *Radiology* 2000; **217**: 119-126
- 10 Buscarini L, Buscarini E, Di Stasi M, Quaretti P, Zangrandi A. Percutaneous radiofrequency thermal ablation combined with transcatheter arterial embolization in the treatment of large hepatocellular carcinoma. *Ultraschall Med* 1999; **20**: 47-53
- 11 Yamasaki T, Kurokawa F, Shirahashi H, Kusano N, Hironaka K, Okita K. Percutaneous radiofrequency ablation therapy with combined angiography and computed tomography assistance for patients with hepatocellular carcinoma. *Cancer* 2001; **91**: 1342-1348
- 12 Koda M, Murawaki Y, Mitsuda A, Oyama K, Okamoto K, Idobe Y, Suou T, Kawasaki H. Combination therapy with transcatheter arterial chemoembolization and percutaneous ethanol injection compared with percutaneous ethanol injection alone for patients with small hepatocellular carcinoma: a randomized control study. *Cancer* 2001; **92**: 1516-1524
- 13 Kitamoto M, Imagawa M, Yamada H, Watanabe C, Sumioka M, Satoh O, Shimamoto M, Kodama M, Kimura S, Kishimoto K, Okamoto Y, Fukuda Y, Dohi K. Radiofrequency ablation in the treatment of small hepatocellular carcinomas: comparison of the radiofrequency effect with and without chemoembolization. *AJR Am J Roentgenol* 2003; **181**: 997-1003
- 14 Livraghi T, Goldberg SN, Monti F, Bizzini A, Lazzaroni S, Meloni F, Pellicano S, Solbiati L, Gazelle GS. Saline-enhanced radio-frequency tissue ablation in the treatment of liver metastases. *Radiology* 1997; **202**: 205-210
- 15 Honda N, Guo Q, Uchida H, Ohishi H, Hiasa Y. Percutaneous hot saline injection therapy for hepatic tumors: an alternative to percutaneous ethanol injection therapy. *Radiology* 1994; **190**: 53-57
- 16 Burdío F, Guemes A, Burdío JM, Navarro A, Sousa R, Castiella T, Cruz I, Burzaco O, Guirao X, Lozano R. Large hepatic ablation with bipolar saline-enhanced radiofrequency: an experimental study in in vivo porcine liver with a novel approach. *J Surg Res* 2003; **110**: 193-201
- 17 Hansler J, Frieser M, Schaber S, Kutschall C, Bernatik T, Muller W, Becker D, Hahn EG, Strobel D. Radiofrequency ablation of hepatocellular carcinoma with a saline solution perfusion device: a pilot study. *J Vasc Interv Radiol* 2003; **14**: 575-580
- 18 Kurokohchi K, Watanabe S, Masaki T, Hosomi N, Funaki T, Arima K, Yoshida S, Miyauchi Y, Kuriyama S. Combined use of percutaneous ethanol injection and radiofrequency ablation for the effective treatment of hepatocellular carcinoma. *Int J Oncol* 2002; **21**: 841-846
- 19 Kurokohchi K, Watanabe S, Masaki T, Hosomi N, Funaki T, Arima K, Yoshida S, Nakai S, Murota M, Miyauchi Y, Kuriyama S. Combination therapy of percutaneous ethanol injection and radiofrequency ablation against hepatocellular carcinomas difficult to treat. *Int J Oncol* 2002; **21**: 611-615
- 20 Watanabe S, Kurokohchi K, Masaki T, Miyauchi Y, Funaki T, Inoue H, Himoto T, Kita Y, Uchida N, Touge T, Tatsukawa T, Kuriyama S. Enlargement of thermal ablation zone by the combination of ethanol injection and radiofrequency ablation in excised bovine liver. *Int J Oncol* 2004; **24**: 279-284
- 21 Kurokohchi K, Masaki T, Miyauchi Y, Funaki T, Yoneyama H, Miyoshi H, Yoshida S, Himoto T, Morishita A, Uchida N, Watanabe S, Kuriyama S. Percutaneous ethanol and lipiodol injection therapy for hepatocellular carcinoma. *Int J Oncol* 2004; **24**: 381-387
- 22 Francica G, Marone G. Ultrasound-guided percutaneous treatment of hepatocellular carcinoma by radiofrequency hyperthermia with a 'cooled-tip needle'. A preliminary clinical experience. *Eur J Ultrasound* 1999; **9**: 145-153
- 23 Goldberg SN, Gazelle GS, Comon CC, Mueller PR, Tanabe KK. Treatment of intrahepatic malignancy with radiofrequency ablation: radiologic-pathologic correlation. *Cancer* 2000; **88**: 2452-2463
- 24 Jiang HC, Liu LX, Piao DX, Xu J, Zheng M, Zhu AL, Qi SY, Zhang WH, Wu LF. Clinical short-term results of radiofrequency ablation in liver cancers. *World J Gastroenterol* 2002; **8**: 624-630
- 25 Curley SA, Izzo F, Delrio P, Ellis LM, Granchi J, Vallone P, Fiore F, Pignata S, Daniele B, Cremona F. Radiofrequency ablation of unresectable primary and metastatic hepatic malignancies: results in 123 patients. *Ann Surg* 1999; **230**: 1-8
- 26 Yasuda S, Ito H, Yoshikawa M, Shinozaki M, Goto N, Fujimoto H, Nasu K, Uno T, Itami J, Isobe K, Shigematsu N, Ebara M, Saisho H. Radiotherapy for large hepatocellular carcinoma combined with transcatheter arterial embolization and percutaneous ethanol injection therapy. *Int J Oncol* 1999; **15**: 467-473
- 27 Okano H, Shiraki K, Inoue H, Ito T, Yamanaka T, Deguchi M, Sugimoto K, Sakai T, Ohmori S, Murata K, Takase K, Nakano T. Combining transcatheter arterial chemoembolization with percutaneous ethanol injection therapy for small size hepatocellular carcinoma. *Int J Oncol* 2001; **19**: 909-912
- 28 Pawlik TM, Izzo F, Cohen DS, Morris JS, Curley SA. Combined resection and radiofrequency ablation for advanced hepatic malignancies: results in 172 patients. *Ann Surg Oncol* 2003; **10**: 1059-1069
- 29 Curley SA, Marra P, Beaty K, Ellis LM, Vauthey JN, Abdalla EK, Scaife C, Raut C, Wolff R, Choi H, Loyer E, Vallone P, Fiore F, Scordino F, De Rosa V, Orlando R, Pignata S, Daniele B, Izzo F. Early and late complications after radiofrequency ablation of malignant liver tumors in 608 patients. *Ann Surg* 2004; **239**: 450-458

• LIVER CANCER •

Impact of pre-operative transarterial embolization on the treatment of hepatocellular carcinoma with liver transplantation

Yu-Fan Cheng, Tung-Liang Huang, Tai-Yi Chen, Yaw-Sen Chen, Chih-Chi Wang, Sheng-Lung Hsu, Leo Leung-Chit Tsang, Po-Lin Sun, King-Wah Chiu, Bruno Jawan, Hock-Liew Eng, Chao-Long Chen

Yu-Fan Cheng, Tung-Liang Huang, Tai-Yi Chen, Sheng-Lung Hsu, Leo Leung-Chit Tsang, Po-Lin Sun, Department of Diagnostic Radiology, Kaohsiung Medical Center, Chang Gung Memorial Hospital, Chang Gung University, Kaohsiung 83305, Taiwan, China
Yaw-Sen Chen, Chih-Chi Wang, Chao-Long Chen, Department of Surgery, Kaohsiung Medical Center, Chang Gung Memorial Hospital, Chang Gung University, Kaohsiung 83305, Taiwan, China
King-Wah Chiu, Department of Hepatogastroenterology, Kaohsiung Medical Center, Chang Gung Memorial Hospital, Chang Gung University, Kaohsiung 83305, Taiwan, China
Bruno Jawan, Department of Anesthesiology, Kaohsiung Medical Center, Chang Gung Memorial Hospital, Chang Gung University, Kaohsiung 83305, Taiwan, China
Hock-Liew Eng, Department of Pathology, Kaohsiung Medical Center, Chang Gung Memorial Hospital, Chang Gung University, Kaohsiung 83305, Taiwan, China
Supported by Project Grant NHRI-EX94-9228SP from the National Health Research Institutes and NSC 93-2314-B-182A-084 from the National Science Council, Taiwan, China
Correspondence to: Chao-Long Chen, M.D., Department of Surgery, Chang Gung Memorial Hospital, 123 Taipei Road, Niao-Sung, Kaohsiung 83305, Taiwan, China. cheng.yufan@msa.hinet.net
Received: 2004-09-18 Accepted: 2004-10-08

100% at 3 years, which was significantly better than the others who showed <85% tumor necrosis (57.1% at 3 years) or who did not have TAE (75% at 3 years).

CONCLUSION: TAE is an effective treatment for HCC before LT. Excellent long-term survival was achieved in patients that did not fit Milan criteria. Our results broadened and redefined the selection policy for LT among patients with HCC. Meticulous pre-LT TAE helps in further reducing the rate of dropout from waiting lists and should be considered for patients with advanced HCC.

© 2005 The WJG Press and Elsevier Inc. All rights reserved.

Key words: Hepatocellular carcinoma; Liver transplantation; Transarterial embolization

Cheng YF, Huang TL, Chen TY, Chen YS, Wang CC, Hsu SL, Tsang LC, Sun PL, Chiu KW, Jawan B, Eng HL, Chen CL. Impact of pre-operative transarterial embolization on the treatment of hepatocellular carcinoma with liver transplantation. *World J Gastroenterol* 2005; 11(10): 1433-1438
<http://www.wjgnet.com/1007-9327/11/1433.asp>

Abstract

AIM: To determine the effectiveness of pre-liver transplant (LT) transarterial embolization (TAE) in treating hepatocellular carcinoma (HCC) and the patient categories, which are likely to have a good outcome after LT.

METHODS: Twenty-nine patients with hepatitis-related cirrhosis and unresectable HCC after LT were studied over a 7-year period. The patients were divided into two groups: group A patients (19/29) received pre-LT TAE, whereas group B (10/29) underwent LT without prior TAE. According to Milan criteria, group A patients were further subdivided into: group A1 (12/19) who met the criteria, and group A2 (7/19) who did not. Patient survivals were compared.

RESULTS: In the explanted liver, CT images correlated well with pathological specimens showing that TAE induced massive tumor necrosis (>85%) in 63.1% of patients in group A and all 7 patients in group A2 exhibited tumor downgrading that met Milan criteria. The overall 5-year actuarial survival rate was 80.6%. The TAE group had a better survival (84% at 5 years) than the non-TAE (75% at 4 years). The 3-year survival of group A2 (83%) was also higher than that of group A1 (79%). Tumor necrosis >85% was associated with excellent survival of

INTRODUCTION

Hepatocellular carcinoma (HCC) is the most common form of primary liver cancer worldwide and has been the leading cause of cancer death in Taiwan in recent years. HCC caused by the current epidemic of hepatitis B virus-related cirrhosis claims the lives of 5 000 people each year in Taiwan. The number of new cases is still steadily increasing^[1]. For patients with early disease, primary treatment is surgical resection whenever possible. Unfortunately, in patients with large and multiple tumors at the time of initial presentation, surgery is not feasible and their overall survival is usually less than 6 mo^[2]. With the advance of surgical techniques in the past few years, LT is now commonly accepted as the optimal therapeutic measure because not only does it remove the cancer, but it also treats the underlying disease with eradication of the cirrhotic tissue that may progress to dysplastic nodules or HCC in the future^[3]. The current United Network of Organ Sharing (UNOS) policy for organ allocation among patients with HCCs favors those potential recipients with limited number and diameter of tumor nodule defined by Milan criteria: (A) solitary tumor <5 cm, or (B) three or less lesions, none of them >3 cm^[4]. LT can therefore be offered with a good chance of success to only a relatively small proportion of patients, and there is a need for

associated treatment regimens to improve the operation rate and to diminish the incidence of recurrence after transplantation.

Various non-surgical therapeutic options for advanced HCC have been introduced, including TAE, percutaneous ethanol injection, systemic chemotherapy, hormone therapy, immunotherapy, and radiotherapy, among which TAE plays the major role as a widely accepted treatment^[5]. Transarterial embolization (TAE) is a procedure involving the injection of lipiodol and chemotherapeutic agent into the hepatic artery, followed by embolization with absorbable gelatin particles. It produces a selective ischemic and pharmacologic injury to the tumor that relies mainly on the arterial circulation. TAE was first introduced as a palliative treatment for patients with inoperable disease and achieved good results. In the past few years, the concept of blocking collateral blood supply to the tumor through complete embolization of liver tissue surrounding the tumor to achieve curative treatment for hepatic malignancies has been proposed. Moreover, the transarterial administration of a mixture of lipiodol and ethanol to create dual hepatic arterial and portal venous embolization to attain the effect of lobar ablation has been documented^[6]. More importantly, TAE has also been applied to improve the resectability of primary unresectable tumors^[7] because it effectively decreases tumor size, causes compensatory hepatic hypertrophy, and improves ICGR15 that allows a wider range of patients to undergo liver surgery with the achievement of a better survival. Pre-transplant adjuvant treatments, therefore, plays an important role in reducing the dropout rate of the waiting list for LT. Hence, not only is TAE the treatment of choice for unresectable HCC to induce tumor necrosis and to control tumor progression, it may also be beneficial for enlisted patients for LT while waiting for the suitable grafts. The aim of this study is to evaluate the effect of pre-transplantation TAE on patients with HCC.

MATERIALS AND METHODS

Patient selection

Patients with histologically proven HCC or a clinical and radiological presentation strongly suggestive of HCC were considered for the protocol. All were deemed unresectable, either because of anatomic considerations or inadequacy of hepatic reserve. The absence of metastatic tumor was documented with computed tomography (CT) of the chest, abdomen, and pelvis. Tumor invasion of the portal vein was assessed with ultrasound, CT angiography and magnetic resonance scans. Invasion to portal vein was an exclusion criterion. If the patients fully fit the Milan criteria and liver graft was available, then LT proceeded. Otherwise, the patients were included into the TAE group. TAE was performed in the absence of contraindications and poor liver function in the Child's class C. If the TAE was well tolerated, it was repeated if necessary until a donor organ became available.

Method of embolization

All patients received complete celiac and superior mesenteric artery injection for the localization of hepatomas in the

liver before embolization. The 4 F catheter was advanced into the feeding artery as distally as possible. Throughout this study, coaxial 3F catheter was used in all patients. By using syringe pump (Razel Scientific Instruments Inc., Stamford, CT) which can control the injection rate ranging from 0.1 to 1.2 mL/min, a mixture of iodized oil/ethanol (99.5%) in the ratio of 2:1 was infused selectively into the supplying artery at a flow rate of 0.5 to 1 mL/min until the adjacent portal branches of the segmental or lobar liver were demonstrated. The process was under remote manual fluoroscopic guidance outside the angiographic room. The results of embolization were evaluated by CT in all patients 2 wk after the procedure. We classified the results as complete if lipiodol occupied the whole tumor (100%), above 85% as partial embolization, 85% or below as incomplete embolization. All cases with partial or incomplete embolization received second embolization 3 to 4 wk later after liver function was resumed. Following radiological restaging after TAE, the patients underwent liver transplantation when a graft became available either from a cadaveric or a living donor. The discovery of extrahepatic tumor either during radiological staging or at laparotomy precluded LT.

Histopathologic and radiologic studies

The explanted liver specimens were examined for features of tumor disease, including the size, number of nodules, presence of portal vein thrombosis and percentage of tumor necrosis. The tumor size and number were also measured on the pre-TAE/LT sonography and CT. The size and number of the tumor on the explanted liver were taken as the basis for staging to be compared with Milan criteria. Downgrading was defined as the size and number of the tumors in the explanted liver fully fit the criteria: A) solitary tumor <5 cm or B) ≤ 3 lesions none of them >3 cm, but the initial pretreatment images exceeded these criteria.

Post transplantation management and follow-up

Immunosuppressive therapy after LT consisted of a triple drug regimen of tacrolimus, corticosteroids, and either azathioprine or mycophenolate mofetil. Corticosteroids were gradually tapered and were discontinued in 3 mo. All patients were followed up weekly in the outpatient clinic in the first few months after discharge. The frequency of the outpatient clinic visits thereafter varied according to the patients' conditions and types of complications. Screening for tumor recurrence was assessed by the measurement of serum alpha fetal protein (AFP) and abdominal sonography every 2-3 mo. CT scans of the abdomen and chest were performed if HCC recurrence was suspected.

Statistical analysis

The biomedical statistical program Statistica 4.0 (Statsoft, Tulsa, OK) was used for statistical analysis where appropriate. The Kaplan-Meier method was used to calculate survival and groups were compared with the log-rank test. *P* value less than 0.05 was considered significant.

RESULTS

In the 8-year period from 1996 to 2003, 29 patients in our

program underwent LT treatment for histologically confirmed HCC associated with cirrhosis. There are 28 male and 1 female with age of 50.03 ± 8.93 years (mean \pm SD, range: 24-67). The nature of underlying liver cirrhosis was hepatitis B in 21 (HBsAg positive), hepatitis C (determined by HCV RNA testing) in 7, and combined hepatitis B and C in 1.

In group A, 19 patients (19 males and 0 female, age: 52.4 ± 7.61 years) with sufficient hepatic function underwent TAE in the treatment of HCC before LT. Of these 19 patients, 12 met the Milan criteria (group A1) and 7 exceeded the criteria (group A2). In group B, 10 patients (9 males and 1 female, age: 45.5 ± 9.89 years) received LT without prior TAE because of available liver graft. Of these 10 patients who met the criteria for transplant, 4 had inadequate liver function for TAE. The mean waiting time from diagnosis to LT was 19.7 ± 18.2 mo in the TAE group and 12.6 ± 12.7 mo in the non-TAE group (Table 1 and Figure 1).

Table 1 Demographics of patients with hepatocellular carcinoma for liver transplantation

	TAE (group A, %)	No TAE (group B, %)	P
Number of patient	19 (66)	10 (34)	
Age (yr) (mean \pm SD)	52.4 ± 7.61	45.5 ± 9.89	0.045
Follow-up time (d)	769 ± 395	708 ± 403	0.697
Time from diagnosis to liver transplant	19.7 ± 18.2	12.6 ± 12.7	0.281
Male/Female	19 (100)/0 (0)	9 (90)/1 (10)	0.345
Hepatitis virus			0.787
Hepatitis B	14 (74)	7 (70)	
Hepatitis C	4 (21)	3 (30)	
Hepatitis B & C	1 (5)	0 (0)	
Initial tumor size (cm)			0.597
≤ 3 cm (number of patient)	12 (63)	8 (80)	
$>3, \leq 5$ cm	4 (21)	2 (20)	
>5 cm	3 (16)	0 (0)	
Tumor number			0.481
1 nodule	9 (47)	7 (70)	
2 nodule	7 (37)	2 (20)	
3 nodule	1 (5)	1 (10)	
>3 nodule	2 (11)	0	
TAE (number of courses)			
1 (number of patient)	10 (53)	--	
2	3 (16)	--	
>2	6 (32)	--	
Above Milan criteria before TAE or transplantation	7 ¹ (group A2)	--	

¹All downgraded below Milan criteria after TAE.

Histopathologic and radiologic findings

The explanted liver of all 19 patients in group A with pre-LT TAE showed tumor necrosis. Significant tumor necrosis from $>85\%$ to 100% was observed in 12 of the 19 patients (63.1%) after TAE. In the other 7 cases, $<85\%$ of tumor necrosis was found. The estimated median percentage of tumor necrosis was well correlated with the post-TAE CT finding and pathological specimen. Microscopic tumor

invasion to the portal vein was found in 2 cases that were underestimated by the pre-operative imaging studies. Pathological evaluation of the explanted liver shows no discrepancy between the clinical staging and pathological finding. Downgrading of HCC was achieved in all 7 patients in group A2 to meet the Milan criteria (Figure 1).

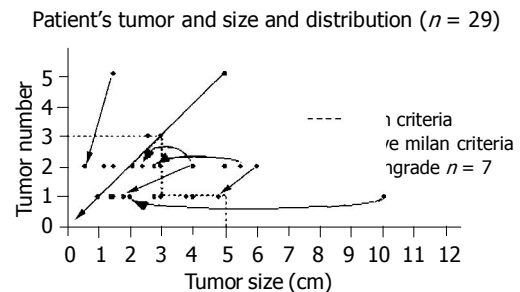


Figure 1 Staging of hepatocellular carcinoma before and after TAE. Twenty-nine patients received embolization before liver transplantation. Seven patients exceeding criteria (group A2) (outside the box) were downgraded to acceptable limits (inside the box with arrow).

Patient survival and disease-free survival

After LT, all 29 patients were followed for 747.83 ± 391.66 d (mean \pm SD, range: 204-1920) in the outpatient clinic with ultrasound, CT, and liver function tests. The overall 5-year actuarial survival rate was 80.6% (Figure 2). The survival rates were different between group A (i.e., TAE group) and group B (i.e., non-TAE group) with the former showing a better 5-year survival (84%) than the 4-year survival in the latter (75%) (Figure 3). The 3-year survival of the 7 patients who exceeded the Milan criteria pre-LT and were downgraded by TAE (group A2) was 83% which is better than the patients that met the criteria pre-LT ($n = 22$) (Figure 4). In group A1, one patient suffered from lung metastasis 6 mo after LT and died one year later. Microscopic tumor invasion to the portal vein was also noted in the explanted liver of that patient. The other mortality occurred 2.2 years after LT in the downgraded group (group A2). However, the mortality was due to primary lung cancer unrelated to recurrent HCC. In the non-TAE group (group B), one patient was lost due to the recurrence of hepatitis C.

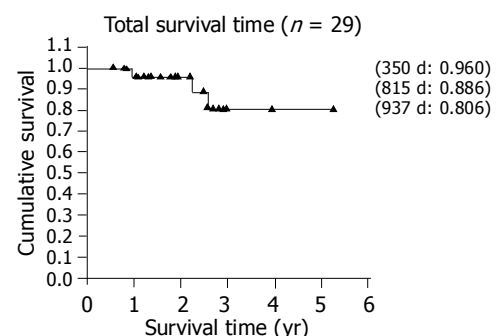


Figure 2 The 5-year actuarial survival rate of patients with hepatocellular carcinoma after liver transplantation.

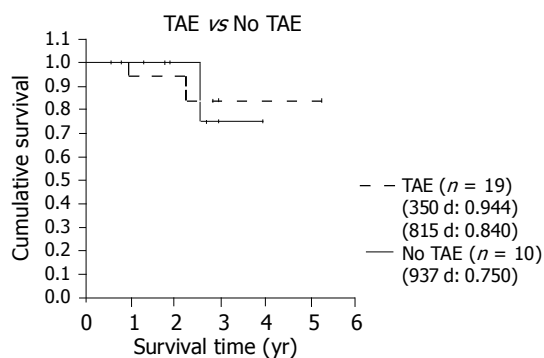


Figure 3 Patient and graft survival by Kaplan-Meier analysis shows higher 4-year survival in hepatocellular carcinoma that received pre-transplantation TAE (group A) compared to non-TAE (group B). Log-rank: $P = 0.95$.

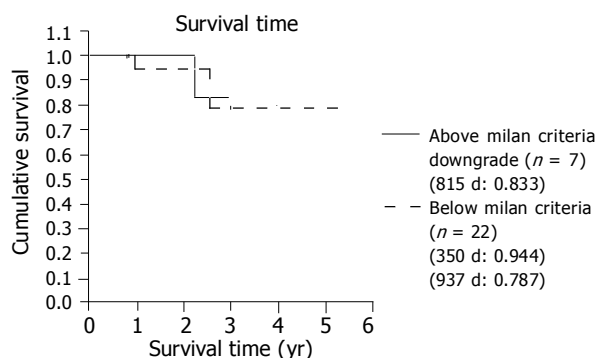


Figure 4 Patient and graft survival by Kaplan-Meier analysis shows a higher 3-year survival in patients with hepatocellular carcinoma previously above the Milan criteria and downgraded by TAE (group A2) than the patients that originally met the criteria (group A1 + group B). Log-rank: $P = 0.81$.

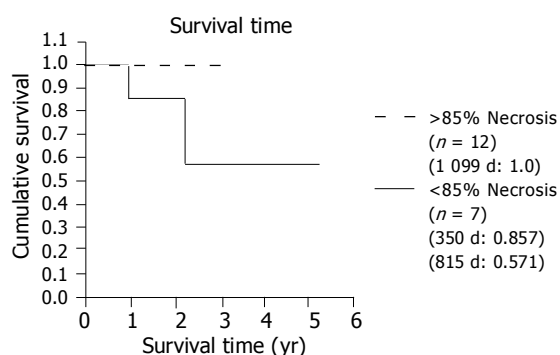


Figure 5 Patient and graft survival by Kaplan-Meier analysis shows a significantly higher 3-year survival in patients with hepatocellular carcinoma with tumor necrosis >85% compared to those with tumor necrosis <85% after TAE. Log-rank: $P = 0.060$.

Among the 12 patients, whose tumors had undergone necrosis >85%, no recurrent tumor was found and their disease-free survival (100% at 3 years) was significantly better than the others who showed <85% tumor necrosis (57.1% at 3 years) (Figure 5) or who did not have TAE (75% at 3 years).

DISCUSSION

Although the outcome of LT has proved encouraging in the treatment of advanced HCC, the shortage of organs dissuades the policy for organ allocation for malignant disease in Taiwan. The number and size of tumors are considered major factors associated with the risk of tumor recurrence and survival^[4]. For patients with liver tumor size and number exceeding the Milan criteria for LT, TAE was beneficial in controlling tumor growth, effectively decreasing tumor size, and allowing a wider range of patients to undergo liver surgery and achieve better survival. Downgrading or total necrosis of the tumor induced by TAE was also associated with improved disease-free survival after resection. In this study, we investigated the influence of TAE on patients undergoing LT for HCC associated with liver cirrhosis. Although the overall 5-year survival in LT for HCC is 80.6%, which is far behind the overall patients' survival (after undergoing LT in our program) of 95% at 5 years, preoperative TAE followed by LT is associated with a better outcome and may be a sensible therapeutic strategy for selected patients with HCC. In our study, TAE before LT appears to be most useful in patients who exceed selection criteria of a single lesion smaller than 5 cm or three lesions smaller than 3 cm. Response to TAE in the form of downgrading or necrosis >85% of the tumor was observed in 63% (12/19) of patients and associated with increased disease-free survival. Response to TAE in these patients has important clinical implications as patients with large tumors are generally considered poor candidates for LT, especially when presenting with multinodular disease. Our results showed that downgrading by TAE is associated with low incidence of recurrence after LT comparable to that in patients with smaller tumors and should be regarded as a strong argument for patients with advanced HCC to proceed to LT.

The significance of the role of TAE in pre-LT treatment was further underscored by the fact that although group A patients had more advanced HCC and were significantly older compared to those in group B ($P < 0.05$, Table 1), the former actually enjoyed a better survival rate than the latter after transplant.

Cadaveric LT is an excellent treatment for early HCC. Its use, however, is limited by the shortage of grafts. As a result of prolonged waiting period before transplantation, tumor progression may counteract the benefit of LT. An estimated 30% of patients develop contra-indications to the procedure while waiting for a suitable donor and up to 10% of patients with HCC on transplant waiting list die before undergoing LT^[8,9]. Surgical resection of the tumor is an optimal bridging treatment, which has been anecdotally proposed in many centers^[10]. However, acceptable liver function is the prerequisite for hepatectomy or tumor resection. In fact, less than 30% of patients who have advanced liver cirrhosis would tolerate liver resection^[1,2]. So TAE is another treatment of choice in these cirrhotic patients to halt or delay tumor progression and to reduce the impact of a long waiting list and donor shortage. Presence of vascular invasion, number of satellite nodules, natural history of tumor behavior and response to TAE are powerful predictors of survival in patients with HCC.

Angiography and TAE can demonstrate and offer that additional information. Patients with poor prognostic criteria may be removed from the waiting list.

From the experience using animal model, the nature of the injected material and the rate of injection had a significant impact on the actual amount of embolizer that reaches the tumor, the adjacent parenchyma, and the portal vein. The pharmacokinetics is especially important for those liquid materials that are not soluble in blood, such as lipiodol/ethanol mixture, to pass from the hepatic artery and to the portal vein through the presinusoidal communication to create a dual artery and portal vein embolization^[11,12]. On the kinetics of the flow, slow injection can produce small droplets of the liquid embolizer that are carried along with the high velocity main stream towards the feeding vessels of the tumor. When the velocity of the main blood flow slows down during embolization, the embolizer will be evenly distributed inside the tumor and also the adjacent liver parenchyma according to the velocity of the blood vessels. Our results suggest that preoperative TAE can achieve better results than those cases with similar tumor sizes but received LT without prior TAE. It indicates that the therapeutic effect of the transhepatic artery approach by using lipiodol/ethanol mixture is an effective modality in the treatment of HCC especially when combined with LT.

Significant tumor necrosis is an important factor that contributed to the excellent outcome after TAE in our study. Our data revealed that recurrence was infrequent in those patients with TAE-induced extensive tumor necrosis who showed an excellent 100% disease-free survival at 3 years. It is superior to the incomplete embolization group with less than 85% tumor necrosis (57.1% at 3 years) or who did not have TAE (75% at 3 years) before LT. Almost all of our patients showed a marked response to pre-transplant TAE, 63% (12/19) of the patients had >85% tumor necrosis or at least greater than 50% tumor size reduction in the explanted livers. This high response rate can possibly be explained by the superselective embolization, slow injection of the embolizer, dual hepatic artery and portal vein embolization, and the strategy of repeated TAE sessions within a short period of time to achieve maximal necrosis. The procedure was well-tolerated in the majority of patients and caused almost no significant complications.

Hepatic artery injury during TAE is considered a risk factor for LT that may impair post-transplant survival especially in the living donor liver transplant. Delicate interventional technique, highly specific selection of intrahepatic artery by using microcatheter, and slow injection of embolizer using microinfusion pump to prevent reflux of the agents can minimize injury to the major hepatic artery. From our experience, TAE prior to LT did not increase surgical difficulty in hepatic artery dissection and anastomosis. No graft loss due to hepatic artery injury was observed in our 19 TAE patients.

In addition to the tumor size and number, vascular invasion is another important predictor of outcome after transplant. Early lung metastasis was also noted in one of our cases with microscopic tumor invasion to the portal vein. Although TAE was performed by slowly infusing the mixture of lipiodol and ethanol into the artery supplying

the tumor until dual hepatic artery and portal vein embolization, early distant metastasis still cannot be prevented. Unfortunately, the diagnosis of microscopic vascular invasion can only be made under microscope *in vitro* and cannot be predicted or detected by any laboratory tests, imaging modalities, and even invasive procedures such as biopsy and angiography. Since advanced HCC (stage 4) may still achieve 20% 5-year survival post-LT in comparison with 100% mortality without operation^[13], all HCC patients without extrahepatic spread should be offered LT. The major limiting factors have been organ shortage and cost. On the basis of the probability of early recurrence, candidates with vascular invasion should be excluded from the transplantation waiting list.

Pathologic analysis showed that the percentage of tumor necrosis correlated with the results of post-TAE CT. Besides, post-TAE CT, with lipiodol stasis in HCC, can show nodules previously ignored by CT, ultrasound, and angiography, contributing to a more accurate staging of the disease^[14,15]. It indicated that post-TAE CT is a good examination modality that can be used in the pre-transplant survey that includes patient selection and outcome prediction after LT. Precise assessment of the size, number, and percentage of tumor necrosis after TAE are among the most powerful predictors of survival in patients with HCC. In addition to these factors, natural history of tumor behavior can be incorporated into future treatment planning. Uncontrolled tumor growth after TAE that does not meet the criteria and macroscopic vascular invasion may not be good candidates for transplantation and could therefore be removed from the waiting list. Other patients with insufficient tumor necrosis after TAE but within the criteria may be selected for early transplantation.

In conclusion, our results show a low risk of recurrent HCC in patients treated with preoperative TAE before LT. These results also provide evidence to redefine the current rationale behind organ allocation for malignant liver diseases. The combination of the improved survival rate noted in this study and the development of living donor LT may potentially revolutionize the current scoring system and scheme of organ allocation that would advocate organ allocation for patients with advanced HCC. For those patients, Pre-LT TAE may be considered the therapeutic strategy of choice that may reduce their dropout rate for LT to achieve better patient survival and quality of life.

REFERENCES

- 1 **Lin TM**, Chen CJ, Tsai SF, Tsai TH. Hepatoma in Taiwan. *J Natl Public Health Asso* 1988; **8**: 91-100
- 2 **Okuda K**, Ohtsuki T, Obata H, Tomimatsu M, Okazaki N, Hasegawa H, Nakajima Y, Ohnishi K. Natural history of hepatocellular carcinoma and prognosis in relation to treatment. Study of 850 patients. *Cancer* 1985; **56**: 918-928
- 3 **Gondolesi GE**, Roayaie S, Munoz L, Kim-Schluger L, Schiano T, Fishbein TM, Emre S, Miller CM, Schwartz ME. Adult living donor liver transplantation for patients with hepatocellular carcinoma: extending UNOS priority criteria. *Ann Surg* 2004; **239**: 142-149
- 4 **Mazzaferro V**, Regalia E, Doci R, Andreola S, Pulvirenti A, Bozzetti F, Montalto F, Ammatuna M, Morabito A, Gennari L. Liver transplantation for the treatment of small hepatocellular carcinomas in patients with cirrhosis. *N Engl J Med* 1996;

- 334: 693-699
- 5 **Lin DY**, Lin SM, Liaw YF. Non-surgical treatment of hepatocellular carcinoma. *J Gastroenterol Hepatol* 1997; **12**: S319-S328
- 6 **Kan Z**, Wallace S. Transcatheter liver lobar ablation: an experimental trial in an animal model. *Eur Radiol* 1997; **7**: 1071-1075
- 7 **Cheng Y**, Kan Z, Chen C, Huang T, Chen T, Yang B, Ko S, Lee T. Efficacy and safety of preoperative lobar or segmental ablation via transarterial administration of ethiodol and ethanol mixture for treatment of hepatocellular carcinoma: clinical study. *World J Surg* 2000; **24**: 844-850; discussion 850
- 8 **Sarasin FP**, Majno PE, Llovet JM, Bruix J, Mentha G, Hadengue A. Living donor liver transplantation for early hepatocellular carcinoma: A life-expectancy and cost-effectiveness perspective. *Hepatology* 2001; **33**: 1073-1079
- 9 **Llovet JM**, Fuster J, Bruix J. Intention-to-treat analysis of surgical treatment for early hepatocellular carcinoma: resection versus transplantation. *Hepatology* 1999; **30**: 1434-1440
- 10 **Belghiti J**, Cortes A, Abdalla EK, Regimbeau JM, Prakash K, Durand F, Sommacale D, Dondero F, Lesurtel M, Sauvanet A, Farges O, Kianmanesh R. Resection prior to liver transplantation for hepatocellular carcinoma. *Ann Surg* 2003; **238**: 885-892; discussion 892-893
- 11 **Kan Z**, Wallace S. Sinusoidal embolization: impact of iodized oil on hepatic microcirculation. *J Vasc Interv Radiol* 1994; **5**: 881-886
- 12 **Kan Z**, Ivancev K, Lunderquist A. Peribiliary plexa--important pathways for shunting of iodized oil and silicon rubber solution from the hepatic artery to the portal vein. An experimental study in rats. *Invest Radiol* 1994; **29**: 671-676
- 13 **Penn I**. Hepatic transplantation for primary and metastatic cancers of the liver. *Surgery* 1991; **110**: 726-734; discussion 734-735
- 14 **Ohishi H**, Uchida H, Ohue S, Yoshimura H, Yoshioka T, Matsuo N, Yoshida H, Fukai Y. Computed tomography detection of small daughter nodules in hepatocellular carcinoma after iodized oil infusion into the hepatic artery. *J Comput Tomogr* 1988; **12**: 129-134
- 15 **Novell R**, Dusheiko G, Hilson A, Dick R, Begent R, Hobbs K. Lipiodol computed tomography for small hepatocellular carcinomas. *Lancet* 1991; **337**: 729

Edited by Li WZ Language Editor Elsevier HK

• LIVER CANCER •

Factors for early tumor recurrence of single small hepatocellular carcinoma after percutaneous radiofrequency ablation therapy

Hsien-Chung Yu, Jin-Shiung Cheng, Kwok-Hung Lai, Chi-Pin Lin, Gin-Ho Lo, Chiun-Ku Lin, Ping-I Hsu, Hoi-Hung Chan, Ching-Chu Lo, Wei-Lun Tsai, Wen-Chi Chen

Hsien-Chung Yu, Jin-Shiung Cheng, Kwok-Hung Lai, Gin-Ho Lo, Chiun-Ku Lin, Ping-I Hsu, Hoi-Hung Chan, Ching-Chu Lo, Wei-Lun Tsai, Wen-Chi Chen, Division of Gastroenterology, Department of Internal Medicine, Kaohsiung Veterans General Hospital and National Yang-Ming University, Taiwan, China
Chi-Pin Lin, Division of Gastroenterology, Department of Internal Medicine, God's Help Hospital, Taiwan, China
Supported by the Research Grants VGHKS-92104 from Kaohsiung Veterans General Hospital, Taiwan, China

Co-first-authors: Jin-Shiung Cheng

Correspondence to: Dr. Jin-Shiung Cheng, Division of Gastroenterology, Kaohsiung Veterans General Hospital, 386, Ta-Chung 1st Road, Kaohsiung 813, Taiwan, China. jcheng@isca.vghks.gov.tw
Telephone: + 86-7-3422121-2075 Fax: + 86-7-3468237

Received: 2004-09-08 Accepted: 2004-09-15

Abstract

AIM: To evaluate the factors affecting the early tumor recurrence within one year in cirrhotic patients having a single small hepatocellular carcinoma (HCC) after complete tumor necrosis by radiofrequency ablation (RFA) therapy.

METHODS: Thirty patients with a single small HCC received RFA therapy by a RFA 2000 generator with LeVeen needle. Tri-phase computerized tomogram was followed every 2 to 3 mo after RFA. The clinical effects and tumor recurrence were recorded.

RESULTS: The initial complete tumor necrosis rate was 86.7%. Twenty-two patients were followed for more than one year. The local and overall recurrence rates were 13.6% and 36.4%, 33.3% and 56.2%, 46.6% and 56.2% at 12, 24 and 30 mo, respectively. No major complication or procedure-related mortality was found. The risk factors for early local tumor recurrence within one year were larger tumor size, poor pathologic differentiation of tumor cells and advanced tumor staging. The age of patients with new tumor formation within one year was relatively younger (55.1 ± 8.3 vs 66.7 ± 10.8 , $P = 0.029$).

CONCLUSION: Large tumor size, poor pathologic differentiation of tumor cells and advanced tumor staging are the risk factors for early local tumor recurrence within one year, and young age is the positive predictor for new tumor formation within one year.

© 2005 The WJG Press and Elsevier Inc. All rights reserved.

Key words: Recurrence; Radiofrequency; Hepatocellular

carcinoma

Yu HC, Cheng JS, Lai KH, Lin CP, Lo GH, Lin CK, Hsu PI, Chan HH, Lo CC, Tsai WL, Chen WC. Factors for early tumor recurrence of single small hepatocellular carcinoma after percutaneous radiofrequency ablation therapy. *World J Gastroenterol* 2005; 11(10): 1439-1444

<http://www.wjgnet.com/1007-9327/11/1439.asp>

INTRODUCTION

Hepatocellular carcinoma (HCC) is a common malignancy worldwide and about 70% of HCC is found in Asia^[1]. There is an increasing incidence in the western countries^[2]. In Taiwan, HCC is a leading neoplasm due to the high prevalence of chronic viral hepatitis^[3-5].

Surgical resection, liver transplantation and local ablation therapy are considered potentially curative therapies for HCC nowadays^[6,7]. However, only 9% to 27% of patients are suitable for operation^[8,9]. For the patients who are not candidates for surgical treatment, local ablation therapy is another choice for controlling this neoplasm. Many modalities, such as percutaneous ethanol injection (PEI), percutaneous acetic acid injection (PAI), cryotherapy, percutaneous microwave coagulation therapy (PMCT), and radiofrequency ablation (RFA) are available for local therapy. These minimally invasive techniques have the advantages of preserving the uninvolved liver parenchyma with less complication and mortality than surgery. However, inadequate treatment and recurrence of tumor are still common.

RFA first described by Rossi and coworkers^[10] is a new technique of local thermal ablation therapy for HCC. It allows focal coagulation necrosis of hepatic tumors by producing thermal energy with an alternating electric current generator at a radiofrequency of 200 to 1 200 kHz through a needle electrode. Tumor cells are destroyed by heating to a temperature of about 80 °C to 100 °C. Previous reports have shown that RFA has a better complete necrosis rate, lower local recurrence rate, fewer treatment sessions and longer survival interval than PEI^[11,12]. However, despite the high complete necrosis rate of RFA, early tumor recurrence within one year, either local tumor recurrence or new tumor formation, can still be found. A series of studies discussed the factors for tumor recurrence including the tumor size, subcapsular lesion, operative procedure, underlying liver disease and alpha-fetoprotein (AFP) levels, but the results were not well documented^[13-15,23]. The factors for the early

tumor recurrence within one year were never discussed independently.

In our study, we followed our patients with a single small HCC after RFA and analyzed the results including complete tumor necrosis, local and overall tumor recurrence, safety of procedure, clinical morbidity and mortality and the factors responsible for early tumor recurrence within one year.

MATERIALS AND METHODS

Patients

From September 2000 to February 2003, 30 cirrhotic patients with a single small HCC received ultrasound-guided percutaneous RFA therapy in our hospital. The enrolled criteria included: (1) HCC was pathologically proved before therapy by ultrasound-guided cutting biopsy; (2) the largest tumor size was smaller than 4 cm in diameter and the number of tumor was single; (3) there was no bleeding tendency (prolongation of prothrombin time was ≤ 3 s and platelet count was $\geq 60\ 000/\text{mm}^3$) or uncontrollable ascites; (4) no extra-hepatic metastases could be found by clinical or image studies (computed tomogram, abdominal ultrasound and chest X-ray) before procedure; (5) tumor location was detectable under ultrasound-guided approach and was far away from major vessels and main bile ducts at least by 1.0 cm (to prevent major complication and heat-sink effect by major vessels); (6) patients refused surgery or were not candidates for surgical treatment and (7) there was no previous therapy for HCC.

Patients were given full explanation of the procedure and written consent was obtained from each patient. This study was approved by the Department of Medical Research and Education of Kaohsiung Veterans General Hospital.

The cirrhotic condition was defined by Child-Pugh classification and the tumor staging was defined by BCLC staging system^[6]. The pathologic grading was defined by Edmondson and Steiner classification^[7] and the grade I and II was defined as well-differentiation and the grade III and IV was defined as poor differentiation.

Procedure of RFA

All patients received intra-muscular injection of pethidine 50 mg and oral diclofenac potassium 25 mg (if serum creatinine level was < 2 mg/dL and no peptic ulcer by endoscopy) about 30 min before RFA after they had fasted for 4 h. In patients with impaired renal function (serum creatinine was ≥ 2 mg/dL) or peptic ulcers, diclofenac potassium would be held to prevent the advanced effect and acetaminophen 500 mg would be given orally. Local anesthesia with 10 CC of 2% Xylocaine was injected at the puncture site before introducing the needle. RFA machine of 2000 generator (Boston Scientific Co.) and LeVeen needle electrode (15 gauge, 25 cm in length, 8-10 hooks, maximum dimension 2.0, 3.0 and 3.5 cm on full expanded) were used. Under real-time ultrasound guidance, the electrode needle was introduced percutaneously into the center or lower part of hepatic tumor, and then expanded the tines of the tip fully before ablation. The selection of needle size depended on the location and diameter of the tumor.

The initial output was set at 30-50 W with an increment

of 10 W every 60 s till the power of about 60-90 W, which was maintained for 5 min, and then, increasing the power again to the maximum level (90-130 W) step by step. The selection of the power level depended on the size of needle. Ablation was maintained for at least 15 min unless there was a rapid drop in the power output coincident with marked increase in tissue impedance due to coagulation necrosis (roll-off phenomenon). If no roll-off occurred after ablation for 15 min, the second ablation as the previous procedure would be performed till the roll-off occurred or 10 min of the treatment time had elapsed. No more than 25 min of radiofrequency energy was applied with each deployment of the needle electrode.

After initial ablation, the tines of the tip were fully retracted and if needed, the needle was withdrawn about 1 to 2 cm along the needle tract and re-expanded the tines for another ablation to cover the main tumor area and to create the safe margin of about 0.5 to 1 cm as possible. If no more ablation was needed, we withdrew the needle to the point about 1 cm near the liver surface and re-expanded the tines about 1/4 to 1/5 on extensions. Then, another ablation with initial power was performed till roll-off occurred (usually within 2 min) for coagulating the needle tract to prevent bleeding and needle tract tumor seeding. Patients received sand bag compression for 2 h to prevent internal bleeding after procedure. The complete course of procedure was defined as one therapeutic session. The number of sessions needed for ablating the whole tumor was dependent on the tumor size and needle introducing position. The second session would be performed within one week if indicated. For subcapsular lesions, we inserted the electrode into the HCC nodule through non-cancerous liver tissue without making artificial ascites. Heat coagulation was performed carefully under real-time ultrasound monitor to prevent adjacent organ injury. Intra-muscular injection of ketoprofen 50 mg (in patients with serum creatinine < 2 mg/dL and no peptic ulcer) or pethidine 50 mg (in patients with serum creatinine ≥ 2 mg/dL or peptic ulcer) for further pain control during or after procedure would be given, if needed. Any complications, associated symptoms and signs were recorded and treated.

Follow-up studies

Tri-phase computerized tomography (CT) was performed after RFA therapy one month later for detecting the effect. Successful complete tumor necrosis was defined as no enhanced lesion could be found at previous ablative site. (Figure 1). On the other hand, patients with enhanced lesions were considered as treatment failure; another course of RFA or shifted to other therapies such as transcatheter arterial embolization (TAE), PAI or PEI would be arranged.

Regular follow-up with the tri-phase CT scan, liver biochemistries and AFP level every 2-3 mo was performed after initial successful treatment. The local recurrence was defined as enhanced lesions over the previous ablative area. Enhanced lesions over different segments or faraway from the previous ablative site were defined as new tumor formation. If any recurrence or new tumor developed, proper therapy would be performed according to the patient's condition.

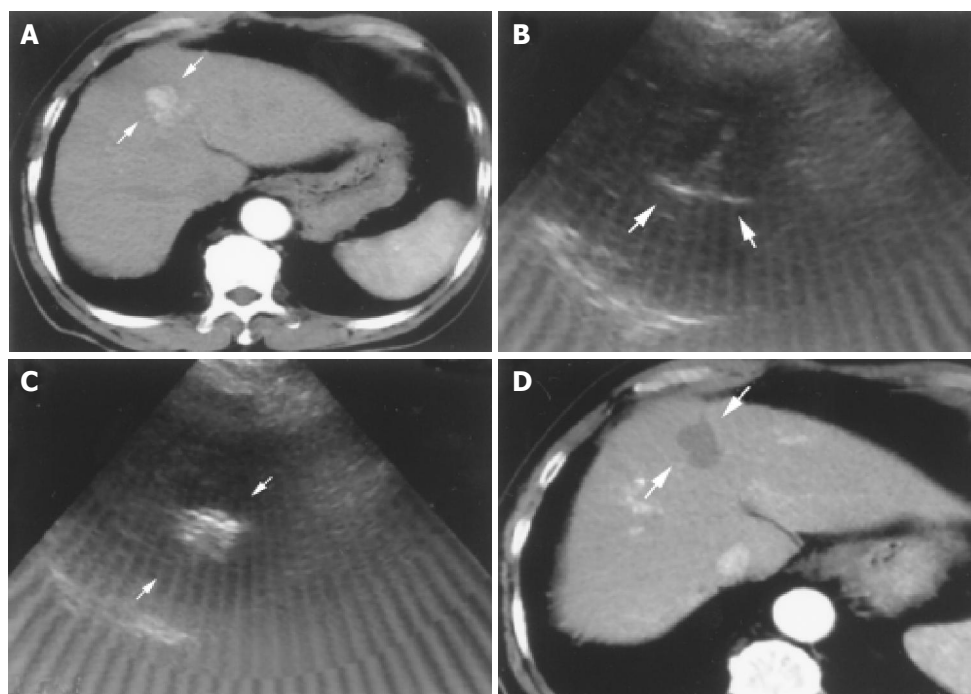


Figure 1 Successful RFA in an 82-year-old male patient with HCC. A: Tri-phase CT scan showed an enhanced nodule in hepatic arterial phase about 2.8 cm in size before RFA (arrows); B: Radiofrequency ablation was performed in one session. The needle was introduced into the lower part of the tumor first with fully expanded tines under real-time ultrasound-guidance (arrows); C: Complete ablation after 2 ablative courses within 37 min was done. The tumor showed hyperechoic signals after RFA under ultrasound (arrows); D: Tri-phase CT scan showed complete necrosis of this tumor without enhancement in hepatic arterial phase one month after RFA (arrows).

Statistical analysis

The data were expressed as mean \pm SD. χ^2 test and Fisher's exact test (*F*-test) were used for comparison of categorical data. Mann-Whitney analysis was performed for comparisons of continuous variables. Statistical significance was defined as $P < 0.05$. Kaplan-Meier analysis was used for tumor recurrent curve.

RESULTS

Thirty patients with single HCC were enrolled for RFA therapy. The tumor size ranged from 1.1 to 3.9 cm. There were 37 sessions totally (one session in 24 tumors, two sessions in 6 tumors). Ablative duration ranged from 3 to 48 min. One patient developed severe pain during RFA and the procedure was prematurely terminated. Three patients failed to reach successful complete tumor necrosis after RFA by CT images one month later. They were excluded from our follow-up study. Further RFA therapy was refused and they were referred for TAE therapy. The initial successfully completed tumor necrosis rate was 86.7% (26 in 30).

In the 26 patients with successful initial complete tumor necrosis, three patients were lost for follow-up within 6 mo. One patient died of sepsis 9 mo after RFA without tumor recurrence. These patients were also excluded from our study. There were 22 patients who received long-term regular follow-up for more than one year. The baseline data was shown in Table 1. The results of RFA were shown in Table 2. The mean follow-up duration was 28.8 \pm 9.0 mo (from 15 to 45 mo). The accumulative local tumor recurrence rates were 13.6%, 33.3% and 46.6% at 12, 24 and 30 mo

respectively. Overall tumor recurrence rates (including new tumor formation and local tumor recurrence) were 36.4%, 56.2% and 56.2% at 12, 24 and 30 mo respectively (Figure 2). The tumor-free interval was 18.5 \pm 11.4 mo (from 2 to 45 mo) (Table 2). One patient died of hepatic failure 15 mo after RFA. The survival interval was 28.7 \pm 9.1 mo (from 15 to 45 mo). Except for three patients lost for follow-up, 25 of 27 patients survived till July 2004. The accumulative mortality rate was 7.4% (2 in 27).

Table 1 Baseline data of 22 patients with long-term follow-up

Sex (male/ female)	16/6
Age (yr, range)	62.5 \pm 11.3 (40-82)
HBV/HCV/HBV+HCV/others	9/10/2/1
Child's classification	
A / B / C	18/4/0
Esophageal varices (+/-)	11/11
Ascites (+/-)	1/21
Tumor size (cm, range)	2.3 \pm 0.7 (1.1-3.9)
≤ 2 cm / > 2 cm	10/12
Tumor location	
Right lobe/ Left lobe	16/6
Subcapsular lesion (+/-)	4/18
Histological classification	
Well ¹ /Poor ²	21/1
Tumor staging (BCLC stage) ³	
Ia / Ib / Ic	11/10/1

Grading of HCC by Edmondson and Steiner classification^[17] ¹Well: well differentiated (grade I, II). ²Poor: poorly differentiated (grade III, IV) ³BCLC stage: staging system from conclusions of the Barcelona-2000 EASL conference^[16].

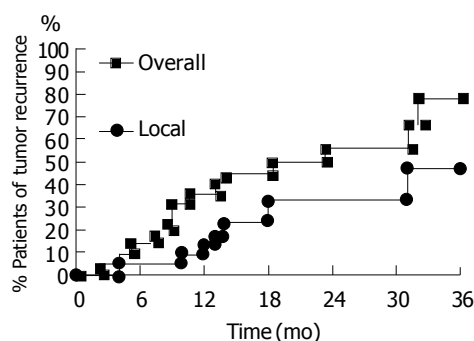


Figure 2 Accumulated tumor recurrence curves of 22 patients with small HCC after RFA. Local tumor recurrence (triangle line) and overall tumor recurrence (including local tumor recurrence, new tumor formation and both) (dot line) are shown.

Table 2 Results of RFA in 22 patients with long-term follow-up

Total sessions of RFA	26
One session/ Two sessions	18/4
Average sessions	1.2±0.4
Ablative time (min, range)	21.3±13.7 (3-48)
F/U ¹ duration (mo, range)	28.8±9.0 (15-45)
Roll-off (+/-)	21/1
Complications	
Local pain	11
Nausea/vomiting	4
Fever	1
Local-free interval (M ² , range)	22.2±10.0 (4-45)
Tumor-free interval (M ² , range)	18.5±11.4 (2-45)
Local recurrence rate	
12M/24M/30M	13.6% / 33.3% / 46.6%
Overall recurrence rate	
12M/24M/30M	36.4%/56.2%/56.2%
Survival interval (M ² , range)	28.7±9.1 (15-45)
Pre-RFA / Post-RFA ³	
Albumin (g/dL)	3.8±0.5/4.2±0.6
GOT (U/L)	63.5±32.9/70.4±34.2
GPT (U/L)	71.1±40.0/79.2±34.2
T. Bili. ⁴ (mg/dL)	1.1±0.5/1.0±0.5
Alk-P ⁵ (U/L)	116.0±46.3/123.5±46.1
AFP ⁶ level (ng/mL)	
Pre-treatment (range)	223.5±663.1 (3-2870)
Post-treatment	41.3±90.6 (3-422)
Decrease AFP > 50% post RFA	
Yes / No	8/14

¹F/U: Follow-up ²M: months ³Data of pre-RFA / Data of post-RFA ⁴T. Bili: total bilirubin level ⁵Alk-P: alkaline phosphatase level ⁶AFP: alpha-fetoprotein.

Eight patients had new tumor formation within one year and 14 patients had no new tumor formation. By analysis, young age (55.1 ± 8.3 vs 66.7 ± 10.8 , $P = 0.029$, Mann-Whitney test) was the independent risk factor for early new tumor formation within one year. There were no differences in sex, age, Child-Pugh classification, underlying etiology of cirrhosis, presentation of esophageal varices, duration of tumor ablation, tumor size, tumor location, tumor staging, therapeutic sessions, roll-off phenomenon, histological classification, follow-up duration and the liver biochemistries and AFP level before and after RFA (Table 3).

Table 3 Factors affecting the new tumor formation within one year in 22 patients after RFA

	New tumor (n = 8)	No new tumor (n = 14)	P
Age (yr)	55.1±8.3	66.7±10.8	0.029
Sex (male/female)	6/2	10/4	NS ⁶
Child ¹ (A/B)	5/3	13/1	0.076
Right lobe/Left lobe	5/3	11/3	NS
Subcapsular (+/-)	2/6	2/12	NS
HBV/HCV/others	3/4/1	6/6/2	NS
EV ² (+/-)	2/6	9/5	0.076
Tumor size (cm)	2.4±0.8	2.2±0.8	NS
Tumor > 2 cm (+/-)	5/3	7/7	NS
Histology			
(Well/Poor) ³	7/1	14/0	NS
BCLC stage ⁴ Ia/Ib/Ic	2/5/1	9/5/0	NS
Roll-off (+/-)	8/0	13/1	NS
Ablative time (min)	20.8±10.8	21.6±15.5	NS
Sessions	1.1±0.4	1.2±0.4	NS
Follow-up (mo)	26.8±10.4	30.0±8.3	NS
Pre-RFA / Post-RFA			
Albumin (g/dL)	3.6±0.5/4.1±0.7	4.0±0.4/4.2±0.5	0.059/NS
T.Bili (mg/dL)	1.3±0.6/1.0±0.3	1.0±0.4/1.1±0.6	NS/NS
GOT (U/L)	54.3±18.1/61.0±23.1	68.7±38.5/75.8±38.9	NS/NS
GPT (U/L)	63.3±36.5/82.1±41.1	75.6±42.5/77.6±31.1	NS/NS
Alk-P (U/L)	117.0±33.3/126.9±45.1	115.5±53.5/121.6±48.2	NS/NS
AFP ⁵ (ng/mL)	388.5±1 003.2/77.9±142.4	129.2±376.8/20.4±32.4	NS/NS
Decrease AFP > 50%	4/4	4/10	NS
Post-RFA(+/-)			

¹Child: Child-Pugh classification. ²EV: esophageal varices ³Well/Poor: Well differentiated/Poor differentiated ⁴BCLC stage: staging system from conclusions of the Barcelona-2000 EASL conference^[16] ⁵AFP: alpha-fetoprotein ⁶NS: not significant.

Three patients had early local tumor recurrence within one year after RFA. Tumor size was the significant factor for early local tumor recurrence within one year. (3.2 ± 0.7 vs 2.2 ± 0.7 , $P = 0.03$, Mann-Whitney test). Besides, poor differentiation of tumor cells ($P = 0.01$, χ^2 test) and advanced tumor staging ($P = 0.036$, χ^2 test) were other risk factors for early local tumor recurrence within one year (Table 4).

Some minor advanced events such as local heat and pain (11 cases), low-grade fever ($< 38^\circ\text{C}$) (1 case) and nausea or vomiting (4 cases) were found (Table 2). They were controlled by conservative treatment. No procedure-related mortality was noted.

DISCUSSION

In our study, the high complete tumor necrosis rate (86.7%) after RFA is comparable with other trials (65-100%, average 83%)^[18,22-24]. The local recurrence rates of HCC after RFA are 2.1 to 39% for variable methods, variable follow-up duration and tumor characters reported by several studies^[22-28]. Our local tumor recurrence rates are 13.6% and 33.3% at 12 and 24 mo respectively, which are comparable with other reports. However, the local tumor recurrence rate increases to 46.6% at 30 mo after the so-called "complete necrosis" by RFA therapy.

As we know, successful RFA therapy requires an adequate safe margin to prevent the local tumor recurrence due to

Table 4 Factors affecting the local tumor recurrence within 1 year in 22 patients after RFA

	Local recurrence (<i>n</i> = 3)	No local recurrence (<i>n</i> = 19)	<i>P</i>
Age (yr)	57.7±9.3	63.3±11.6	NS ⁶
Sex (Male/Female)	2/1	14/5	NS
Child ¹ (A/B)	3/0	15/4	NS
Right lobe/Left lobe	2/1	14/5	NS
Subcapsular (+/-)	1/2	3/16	NS
HBV/HCV/others	1/2/0	8/8/3	NS
EV ² (+/-)	1/2	10/9	NS
Tumor size (cm)	3.2±0.7	2.2±0.7	0.03
Tumor >2 cm (+/-)	3/0	9/10	0.089
Histology			
(Well/Poor) ³	2/1	19/0	0.01
BCLC stage ⁴ Ia/Ib/Ic	1/1/1	10/9	0.036
Roll-off (+/-)	3/0	18/1	NS
Ablative time (min)	27.0±12.3	20.4±14.0	NS
Sessions	1.3±0.6	1.2±0.4	NS
Follow-up (mo)	35.0±6.6	27.8±9.1	NS
Pre-RFA/post-RFA			
Albumin (g/dL)	3.6±0.3/4.0±1.0	3.9±0.5/4.2±0.5	NS/NS
T. Bili. (mg/dL)	1.2±0.6/1.1±0.2	1.0±0.5/1.0±0.5	NS/NS
GOT (U/L)	56.3±16.2/49.3±14.0	64.6±34.9/73.3±35.4	NS/NS
GPT (U/L)	50.0±24.4/56.3±20.1	74.4±41.4/82.8±34.9	NS/NS
Alk-P (U/L)	106.3±26.3/109.3±31.0	117.6±49.1/125.7±48.3	NS/NS
AFP ⁵ (ng/mL)	967.7±1647.5/145.0±240.0	106.0±323.3/24.9±33.3	NS/NS
Decrease AFP > 50%	2/1	6/13	NS
Post-RFA(+/-)			

¹ Child: child-Pugh classification ² EV: esophageal varices ³ Well/Poor: well differentiated/Poor differentiated ⁴ BCLC stage: staging system from conclusions of the Barcelona-2000 EASL conference^[16] ⁵ AFP: alpha-fetoprotein

⁶ NS: not significant.

microscopic invasion around the periphery of the tumor. Just like hepatic resection, 0.5 to 1.0 cm is the acceptable thickness for this purpose when RFA is performed^[20,21]. Two or more sessions and a longer ablative duration will be needed to create the area compared to only ablating the main tumor area without adequate safe margin. Unfortunately, repeated insertion and positioning of an electrode may result in inaccurate positioning because the safe margin is difficult to identify after the first treatment under sonogram, probably due to echogenic gas formation by the initial RFA^[29]. Inadequate safe margin may be created due to the interference especially for larger tumor that needs repeated sessions. So, further studies for development of a new technique or a protocol to create enough ablative area and a safe margin with lesser sessions may increase the success rate^[30]. Chen and his colleagues reported protocol and clinical application for RFA therapy^[31] and Poon and his colleagues reported the learning curve for RFA therapy^[32]. Both suggest the need to improve the technique to reach the goal for an adequate creation of safe margins. The incomplete treatment due to technical defect may be one of the causes for high local recurrence rate for our study after 2.5 years post-RFA therapy.

On the other hand, despite the high initial complete necrosis rate of RFA therapy, early local tumor recurrence still can be found in some cases. Some trials reported risk factors relating to local tumor recurrence but the early tumor recurrence within one year was not discussed independently, earlier. In our study, we evaluated the factors for this issue. Larger tumor size, poor pathologic differentiation of tumor cells and advanced tumor staging are the major risk factors

for early local tumor recurrence within one year as per our analysis.

Komorizono and colleagues reported that the tumor of more than 2 cm in size and the subcapsular lesions were the risk factors of local tumor recurrence^[13]. In our study, tumor size >2 cm has the trend for early local tumor recurrence ($P = 0.089$, Mann-Whitney test) (Table 4). We also performed RFA for subcapsular lesions without making artificial ascites. However, no significant relation to early tumor recurrence was found by analysis ($P = 0.464$, χ^2 test). Harrison and colleagues reported frequent local tumor recurrence after RFA for HCC in 46 patients^[14]. They found that the independent predictors of tumor recurrence are tumor size, serum AFP levels and presence of hepatitis. In our study, the AFP level or presence of hepatitis were not related to early local tumor recurrence (Table 4). Kosari and his colleagues^[15] and Llovet and his coworkers^[23] also reported that the tumor size was the independent predictor for tumor recurrence after RFA. Our results are comparable with them (3.2 ± 0.7 vs 2.2 ± 0.7 , $P = 0.03$, Mann-Whitney test).

As we know, the cooling effect due to heat-sink by blood flow when lesions are adjacent to major vessels will decrease the efficacy of RFA. In our study, we excluded lesions near the main portal vein or major vessels (<1 cm in distance) to avoid the cooling effect. These patients received other treatments such as TAE or PEI. In addition, except for the tumor size that is comparable to other trials, poor pathologic differentiation of tumor cells ($P = 0.01$, χ^2 test) and advanced tumor staging ($P = 0.036$, χ^2 test) are the other predictors for early local tumor recurrence within one year (Table 4). The results are reasonable due to the usually poor prognosis and aggressive tumor progression in patients with poorly differentiated tumor cells and advanced tumor stage.

New tumor formation is frequent in patients with chronic liver disease such as cirrhosis. Ikeda and colleagues reported that the new tumor formation invariably reflected the advanced stage of chronic liver disease. In our study, the markers of advanced cirrhosis such low pre-treatment albumin level ($P = 0.059$, Mann-Whitney test), advanced Child-Pugh classification ($P = 0.076$, χ^2 test) and presence of portal hypertension (esophageal varices) ($P = 0.076$, χ^2 test) were shown to have the trend related to the early new tumor formation after RFA therapy (Table 3). In addition, the most important process in hepatocarcinogenesis is genomic instability caused by chronic hepatitis associated with repeated destruction and regeneration of hepatocytes. In our study, younger age (55.1 ± 8.3 vs 66.7 ± 10.8 , $P = 0.029$, Mann-Whitney test) was found in the early new tumor formation group (Table 3). The cellular reproductive ability and the growth of tumor cells may be faster in younger patients than the old. There is no study that reported earlier the relationship between young age and rapid new tumor formation. It may need further study with larger case numbers to evaluate.

The complication rates in other studies are around 2-5.7% and 6-6.3% in minor and major complications^[18,19]. The procedure-related mortality rate is 0.5-1.4%^[18,19]. In our study, no major complication or procedure-related mortality could be noted. One patient died of sepsis about 9 mo

after RFA and one patient died of hepatic failure due to rapid tumor progression 15 mo after RFA. The accumulative mortality rate is 7.4% (2 in 27). All minor complications are tolerable and mild. They subsided after supportive treatment.

In conclusion, RFA therapy is an effective treatment for small HCC. Large tumor size, poor pathologic differentiation of tumor cells and advanced tumor staging are the risk factors for early local tumor recurrence taking place within one year, after initial successful complete tumor necrosis by RFA therapy. In addition, young age is the predictor for new tumor formation within one year.

ACKNOWLEDGEMENTS

This study was sponsored by the grants from Kaohsiung Veterans General Hospital (VGHKS 92104). The authors would like to thank Miss Wan-Ling Li for her kind help in data collection.

REFERENCES

- 1 **Bosch FX**. Global epidemiology of hepatocellular carcinoma. In: Okuda K, Tabor E. Liver Cancer. New York: Churchill Livingstone 1997; 13-28
- 2 **Bosch FX**, Ribes J, Borrás J. Epidemiology of primary liver cancer. *Semin Liver Dis* 1999; **19**: 271-285
- 3 **Beasley RP**. Hepatitis B virus. The major etiology of hepatocellular carcinoma. *Cancer* 1988; **61**: 1942-1956
- 4 **Yeh FS**, Yu MC, Mo CC, Luo S, Tong MJ, Henderson BE. Hepatitis B virus, aflatoxins, and hepatocellular carcinoma in southern Guangxi, China. *Cancer Res* 1989; **49**: 2506-2509
- 5 **Liaw YF**, Tai DI, Chu CM, Lin DY, Sheen IS, Chen TJ, Pao CC. Early detection of hepatocellular carcinoma in patients with chronic type B hepatitis. A prospective study. *Gastroenterology* 1986; **90**: 263-267
- 6 **Poon RT**, Fan ST, Lo CM, Ng IO, Liu CL, Lam CM, Wong J. Improving survival results after resection of hepatocellular carcinoma: a prospective study of 377 patients over 10 years. *Ann Surg* 2001; **234**: 63-70
- 7 **Roayaie S**, Haim MB, Emre S, Fishbein TM, Sheiner PA, Miller CM, Schwartz ME. Comparison of surgical outcomes for hepatocellular carcinoma in patients with hepatitis B versus hepatitis C: a western experience. *Ann Surg Oncol* 2000; **7**: 764-770
- 8 **Primary liver cancers in Japan**. *Cancer* 1980; **45**: 2663-2669
- 9 **Lai EC**, Fan ST, Lo CM, Chu KM, Liu CL, Wong J. Hepatic resection for hepatocellular carcinoma. An audit of 343 patients. *Ann Surg* 1995; **221**: 291-298
- 10 **Rossi S**, Fornari F, Buscarini L. Percutaneous ultrasound-guided radiofrequency electrocautery for the treatment of small hepatocellular carcinoma. *J Interv Radiol* 1993; **8**: 97-103
- 11 **Lencioni RA**, Allgaier HP, Cioni D, Olschewski M, Deibert P, Crocetti L, Frings H, Laubenderger J, Zuber I, Blum HE, Bartolozzi C. Small hepatocellular carcinoma in cirrhosis: randomized comparison of radio-frequency thermal ablation versus percutaneous ethanol injection. *Radiology* 2003; **228**: 235-240
- 12 **Livraghi T**, Goldberg SN, Lazzaroni S, Meloni F, Solbiati L, Gazelle GS. Small hepatocellular carcinoma: treatment with radio-frequency ablation versus ethanol injection. *Radiology* 1999; **210**: 655-661
- 13 **Komorizono Y**, Oketani M, Sako K, Yamasaki N, Shibata T, Maeda M, Kohara K, Shigenobu S, Ishibashi K, Arima T. Risk factors for local recurrence of small hepatocellular carcinoma tumors after a single session, single application of percutaneous radiofrequency ablation. *Cancer* 2003; **97**: 1253-1262
- 14 **Harrison LE**, Koneru B, Baramipour P, Fisher A, Barone A, Wilson D, Dela Torre A, Cho KC, Contractor D, Korogodsky M. Locoregional recurrences are frequent after radiofrequency ablation for hepatocellular carcinoma. *J Am Coll Surg* 2003; **197**: 759-764
- 15 **Kosari K**, Gomes M, Hunter D, Hess DJ, Greeno E, Sielaff TD. Local, intrahepatic, and systemic recurrence patterns after radiofrequency ablation of hepatic malignancies. *J Gastrointest Surg* 2002; **6**: 255-263
- 16 **Befeler AS**, Di Bisceglie AM. Hepatocellular carcinoma: diagnosis and treatment. *Gastroenterology* 2002; **122**: 1609-1619
- 17 **Edmondson HA**, Steiner PE. Primary carcinoma of the liver: a study of 100 cases among 48,900 necropsies. *Cancer* 1954; **7**: 462-503
- 18 **Scaife CL**, Curley SA. Complication, local recurrence, and survival rates after radiofrequency ablation for hepatic malignancies. *Surg Oncol Clin N Am* 2003; **12**: 243-255
- 19 **de Baere T**, Risse O, Kuoch V, Dromain C, Sengel C, Smayra T, Gamal El Din M, Letoublon C, Elias D. Adverse events during radiofrequency treatment of 582 hepatic tumors. *AJR Am J Roentgenol* 2003; **181**: 695-700
- 20 **Regimbeau JM**, Kianmanesh R, Farges O, Dondero F, Sauvanet A, Belghiti J. Extent of liver resection influences the outcome in patients with cirrhosis and small hepatocellular carcinoma. *Surgery* 2002; **131**: 311-317
- 21 **Poon RT**, Fan ST, Ng IO, Wong J. Significance of resection margin in hepatectomy for hepatocellular carcinoma: A critical reappraisal. *Ann Surg* 2000; **231**: 544-551
- 22 **Curley SA**, Izzo F, Ellis LM, Nicolas Vauthey J, Vallone P. Radiofrequency ablation of hepatocellular cancer in 110 patients with cirrhosis. *Ann Surg* 2000; **232**: 381-391
- 23 **Llovet JM**, Vilana R, Bru C, Bianchi L, Salmeron JM, Boix L, Ganau S, Sala M, Pages M, Ayuso C, Sole M, Rodes J, Bruix J. Increased risk of tumor seeding after percutaneous radiofrequency ablation for single hepatocellular carcinoma. *Hepatology* 2001; **33**: 1124-1129
- 24 **Solbiati L**, Livraghi T, Goldberg SN, Ierace T, Meloni F, Dellanoce M, Cova L, Halpern EF, Gazelle GS. Percutaneous radio-frequency ablation of hepatic metastases from colorectal cancer: long-term results in 117 patients. *Radiology* 2001; **221**: 159-166
- 25 **Rossi S**, Buscarini E, Garbagnati F, Di Stasi M, Quaretti P, Rago M, Zangrandi A, Andreola S, Silverman D, Buscarini L. Percutaneous treatment of small hepatic tumors by an expandable RF needle electrode. *AJR Am J Roentgenol* 1998; **170**: 1015-1022
- 26 **Rossi S**, Di Stasi M, Buscarini E, Quaretti P, Garbagnati F, Squassante L, Paties CT, Silverman DE, Buscarini L. Percutaneous RF interstitial thermal ablation in the treatment of hepatic cancer. *AJR Am J Roentgenol* 1996; **167**: 759-768
- 27 **Poggi G**, Gatti C, Cupella F, Fiori M, Avanza F, Baldi M. Percutaneous US-guided radiofrequency ablation of hepatocellular carcinomas: results in 15 patients. *Anticancer Res* 2001; **21**: 739-742
- 28 **Buscarini L**, Buscarini E, Di Stasi M, Vallisa D, Quaretti P, Rocca A. Percutaneous radiofrequency ablation of small hepatocellular carcinoma: long-term results. *Eur Radiol* 2001; **11**: 914-921
- 29 **Cha CH**, Lee FT, Gurney JM, Markhardt BK, Warner TF, Kelcz F, Mahvi DM. CT versus sonography for monitoring radiofrequency ablation in a porcine liver. *AJR Am J Roentgenol* 2000; **175**: 705-711
- 30 **Kuvshinov BW**, Ota DM. Radiofrequency ablation of liver tumors: influence of technique and tumor size. *Surgery* 2002; **132**: 605-611; discussion 611-612
- 31 **Chen MH**, Yang W, Yan K, Zou MW, Solbiati L, Liu JB, Dai Y. Large liver tumors: protocol for radiofrequency ablation and its clinical application in 110 patients--mathematic model, overlapping mode, and electrode placement process. *Radiology* 2004; **232**: 260-271
- 32 **Poon RT**, Ng KK, Lam CM, Ai V, Yuen J, Fan ST, Wong J. Learning curve for radiofrequency ablation of liver tumors - prospective analysis of initial 100 patients in a tertiary institution. *Ann Surg* 2004; **239**: 441-449

Clinicopathological significance of expression of paxillin, syndecan-1 and EMMPRIN in hepatocellular carcinoma

Hai-Gang Li, De-Rong Xie, Xi-Ming Shen, Hong-Hao Li, Hong Zeng, Yun-Jie Zeng

Hai-Gang Li, Xi-Ming Shen, Hong Zeng, Yun-Jie Zeng, Department of Pathology, The Second Affiliated Hospital to Sun Yat-Sen University, Guangzhou 510120, Guangdong Province, China
De-Rong Xie, Department of Oncology, The Second Affiliated Hospital to Sun Yat-Sen University, Guangzhou 510120, Guangdong Province, China

Hong-Hao Li, Department of Surgery, The Second Affiliated Hospital to Sun Yat-Sen University, Guangzhou 510120, Guangdong Province, China

Supported by the Major Programs of Health Bureau of Guangdong Province, No. A200194

Co-first-authors: De-Rong Xie

Correspondence to: De-Rong Xie, Department of Oncology, Second Affiliated Hospital to Sun Yat-Sen University, Guangzhou 510120, Guangdong Province, China. xiederong@21cn.com

Telephone: +86-20-81332616 Fax: +86-20-81332781

Received: 2004-08-30 Accepted: 2004-12-03

Abstract

AIM: To evaluate the relationship of expression of paxillin, syndecan-1 and EMMPRIN proteins with clinicopathological features in hepatocellular carcinoma (HCC).

METHODS: Fifty-one patients who underwent HCC resection were recruited in the study. Paxillin, syndecan-1 and EMMPRIN proteins in HCC tissues were detected with immunohistochemical staining.

RESULTS: Of 51 cases of HCC, 23 (45%) exhibited paxillin protein positive expression. Of 42 cases of adjacent non-tumor liver tissues, 24 (57%) exhibited positive expression. Positive paxillin protein expression was associated with low differentiation ($r = 0.406$, $P = 0.004$), with the presence of portal vein thrombosis ($r = 0.325$, $P = 0.021$), with extra-hepatic metastasis ($r = 0.346$, $P = 0.014$). Of 51 cases of HCC, 28 (55%) exhibited syndecan-1 protein positive expression. Of 42 cases of adjacent non-tumor liver tissues, 23 (55%) exhibited positive expression. Positive syndecan-1 protein expression was associated with well differentiation ($r = 0.491$, $P = 0.001$), with no extra-hepatic metastasis ($r = 0.346$, $P = 0.014$). Of 51 cases of HCC, 28 (55%) exhibited EMMPRIN protein positive expression. Of 42 cases of adjacent non-tumor liver tissues, 21 (50%) exhibited positive expression. Expression of EMMPRIN protein was not associated with serum AFP level, HBsAg status, presence of microsatellite nodule, tumor size, presence of cirrhosis and necrosis, differentiation, presence of portal vein thrombosis, extra-hepatic metastasis, disease-free survival and overall survival ($P > 0.05$). Expression of paxillin protein was

correlated conversely with the expression of syndecan-1 protein in HCC ($r = -0.366$, $P = 0.010$).

CONCLUSION: Expression of paxillin and syndecan-1 proteins in HCC may affect its invasive and metastatic ability of the tumor. There may be a converse correlation between the expression of paxillin and syndecan-1 protein in HCC. Expression of EMMPRIN protein may be detected in HCC, but it may play little role in the invasion and metastasis of HCC.

© 2005 The WJG Press and Elsevier Inc. All rights reserved.

Key words: Hepatocellular carcinoma; Paxillin; Syndecan-1; EMMPRIN; Immunohistochemistry

Li HG, Xie DR, Shen XM, Li HH, Zeng H, Zeng YJ. Clinicopathological significance of expression of paxillin, syndecan-1 and EMMPRIN in hepatocellular carcinoma. *World J Gastroenterol* 2005; 11(10): 1445-1451

<http://www.wjgnet.com/1007-9327/11/1445.asp>

INTRODUCTION

Primary cancers of the liver in adults are of two main histological types: hepatocellular carcinoma (HCC) and cholangiocarcinoma. HCC is a frequently occurring tumor in individuals in many developing countries^[1]. It ranks fifth in frequency worldwide among all malignancies and causes one million deaths annually^[2], yet its incidence is increasing steadily in various countries^[3-5]. Epidemiology studies showed that primary liver cancer is the second major cause of mortality in China^[6] and it accounts for 53% of all liver cancer deaths worldwide^[7]. Though with great development in diagnosis and therapy, the prognosis of patients with HCC remains dismal for its high rate of metastasis and recurrence. For patients in the advanced stages, the median survival is less than 6 mo, no matter what kinds of therapy were managed^[8-12]. So it is urgent to further explore the mechanism of HCC occurrence, progress and metastasis.

Progression and metastasis are malignant characteristics of malignant tumors. It includes the cellular adhesion (between tumor cell and normal cell, also between tumor cells) and the destruction of extracellular matrix (ECM) in the progressive and metastatic process of malignant tumor. During the process, the molecules existing in ECM and the receptors or ligands existing on the surfaces of tumor cells play critical roles^[13,14].

Focal adhesions form a structural link between the ECM

and the actin cytoskeleton and are also important sites of signal transduction; their components propagate signals arising from the activation of integrins following their engagement with ECM proteins, such as fibronectin, collagen and laminin. Paxillin is a central protein within the focal adhesion^[15]. Its primary function is as a molecular adapter or scaffold protein that provides multiple docking sites at the plasma membrane for an array of signaling and structural proteins. For example, it provides a platform for protein tyrosine kinases such as focal adhesion kinase (FAK) and SRC, which are activated as a result of adhesion or growth factor stimulation. Paxillin binds to many proteins that are involved in effecting changes in the organization of the actin cytoskeleton, which are necessary for cell motility events associated with embryonic development, wound repair and tumor metastasis^[16,17].

Syndecans comprise a gene family of transmembrane proteoglycans that regulate cellular behavior through interactions with various effectors including heparin-binding growth factors and insoluble matrix components. Syndecan-1, a transmembrane heparin sulfate proteoglycan, localizes in epithelial cells and has been shown to be present in normal hepatocytes^[18]. It interacts with growth factors, matrix components, and other extracellular proteins and is thought to be involved in processes such as cell growth, differentiation and adhesion. The expression of syndecan-1 appears generally downregulated in human carcinomas and in experimental cancer models, whereas transfectional expression of syndecan-1 in cultured cancer cells has been shown to inhibit their growth and other aspects of malignant behavior^[19].

Extracellular matrix metalloproteinase inducer (EMMPRIN), which is also called CD147 and basigin, is a transmembrane glycoprotein with two immunoglobulin-like domains and forms a family with embigin and neuropilin. EMMPRIN in tumor cells triggers the production or release of matrix metalloproteinases in the surrounding mesenchymal cells and tumor cells, thereby contributing to tumor invasion^[20-23].

MATERIALS AND METHODS

Patients

Fifty-one patients (32 men and 19 women; mean age 51 ± 11 years, range 24-69 years) who underwent resection of HCC in the Department of Surgery of Second Affiliated Hospital to Sun Yat-Sen University were studied. None of 51 patients had received any preoperative treatment. Classified according to the Chinese Diagnosis and Treatment Standard for Common Malignant Tumors, 35 carcinomas were well-differentiated (Edmonson grade 1-2) and 16 carcinomas were low-differentiated (Edmonson grade 3-4). Tissue specimens were fixed promptly with 100 g/L formaldehyde solution, embedded in paraffin and cut into 4 μ m sections. Sections of 42 carcinomas were excised from the marginal part of the tumor containing both HCC and normal liver tissues.

Immunohistochemistry

Fifty-one patients, who underwent HCC resection, were

recruited in the study. A 3-step immunoperoxidase technique, using the streptavidin-peroxidase (S-P), was employed for paxillin, syndecan-1 and EMMPRIN detection. All the sections were routinely deparaffinized and re-hydrated; then the sections were rinsed in phosphate-buffered saline (PBS, pH 7.4) and subsequently were treated for antigen retrieve. Sections for paxillin and syndecan-1 staining were treated in EDTA (1 mmol/L, pH 8.0) in water bath. Sections for EMMPRIN staining were treated in sodium citrate buffered saline (0.001 mol/L, pH 6.0) with microwave. After cooling at room temperature for 20 min, the sections were rinsed in PBS, then immersed in 3% H₂O₂ for 15 min to block the endogenous enzymes. After being rinsed in PBS, the sections were incubated with normal goat serum at 37 °C for 15 min to block nonspecific antibodies. After interaction with anti-paxillin antibody (No. 5H11, Maxim Biological and Technical Company, Fujian, China; ready-to-use), anti-syndecan-1 and anti-EMMPRIN antibodies (No.5F7 and polyclonal antibody, Zhongshan Biological and Technical Company, Beijing, China; diluted 1:70), the sections were rinsed in PBS, then incubated with biotinylated secondary antibodies and rinsed in PBS again. After interaction with streptavidin-HRP and being rinsed in PBS, the sections were visualized by reaction with 3,3'-diaminobenzidine and counter-stained with hematoxylin.

The determination, whether the tumor and the normal tissues were positive or not, was performed by two persons. A tumor or normal tissue, more than 10% of cancer cells or normal hepatic cells, stained with those antibodies was recognized as positive. The sections of lung carcinoma and bladder carcinoma tissues known for those antibodies stained positive were used as positive controls and normal goat serum and PBS substituting the primary antibody were used as negative controls.

Clinicopathological and follow-up data

Clinicopathological classification of the investigated HCC was made according to the criteria described by the Chinese Diagnosis and Treatment Standard for Common Malignant Tumors. Some clinicopathological findings (presence of cirrhosis and necrosis, histological grading and metastasis) were judged by two pathologists, others (presence of microsatellite nodule and tumor size) were judged by ultrasonic examination.

Postoperative follow-up included monitoring for disease recurrence by serum AFP level and chest X-ray detection, together with ultrasonography or computed tomography (CT) scan every 3 mo. Recurrence of tumor was diagnosed by the detection of any intra-hepatic or extra-hepatic tumor with a typical enhancement pattern of HCC in contrast CT scan and elevation of serum AFP level compared with the previous level. Disease-free survival was calculated from the date of hepatic resection to the date when recurrence was diagnosed or, in the absence of detectable recurrence, to the date of death or last follow-up.

Statistical analysis

Statistical analysis was performed by the generalized Wilcoxon's test (or the Fisher's exact test, where appropriate). Postoperative prognosis was evaluated with the Kaplan-

Meier method and compared between groups by the log-rank test; the significance of the prognostic value of the variables was estimated with Cox's multivariate proportional hazard model. All statistical analyses were performed using SPSS Win program package 8.0. Differences were considered as significant when the *P* value was less than 0.05.

RESULTS

Correlation between expression of paxillin protein and clinicopathological features in HCC

Of 51 cases that we assayed for paxillin protein expression in HCC, 23 (45%) exhibited positive expression (Figure 1A). Of 42 cases of adjacent non-tumor liver tissues, 24 (57%) exhibited positive expression. If paxillin expression was compared between HCC and the adjacent non-tumor liver tissues, there was no significant difference ($P = 0.415$). Positive paxillin expression was associated with low differentiation ($r = 0.406$, $P = 0.004$), with the presence of portal vein thrombosis ($r = 0.325$, $P = 0.021$), with extra-hepatic metastasis ($r = 0.346$, $P = 0.014$). Expression of paxillin protein was not associated with serum AFP level ($P = 0.604$), HBsAg status ($P = 0.638$), presence of microsatellite nodule ($P = 0.991$), tumor size ($P = 0.272$), presence of cirrhosis and necrosis ($P = 0.886$ and 0.922 , respectively, Table 1).

Correlation between expression of syndecan-1 protein and clinicopathological features in HCC

Of 51 cases that we assayed for syndecan-1 protein expression in HCC, 28 (55%) exhibited positive expression (Figure 1B). Of 42 cases of adjacent non-tumor liver tissues, 23 (55%) exhibited positive expression. If syndecan-1 expression was compared between HCC and the adjacent non-tumor liver tissues, there was no significant difference ($P = 0.842$). Positive syndecan-1 expression was associated with well differentiation ($r = 0.491$, $P = 0.001$), with no extra-hepatic metastasis ($r = 0.346$, $P = 0.014$). Expression of syndecan-1 protein was not associated with serum AFP level ($P = 0.280$), HBsAg status ($P = 0.465$), presence of microsatellite nodule ($P = 0.578$), tumor size ($P = 0.607$), presence of cirrhosis and necrosis ($P = 0.640$ and 0.646 , respectively), presence of portal vein thrombosis ($P = 0.292$). (Table 2).

Table 1 Expression of paxillin protein categorized by pathological variables

Variables	Paxillin		<i>P</i>
	-	+	
Serum AFP level			
≤25 ng/mL (<i>n</i> = 22)	13	9	0.604
>25 ng/mL (<i>n</i> = 29)	15	14	
HBsAg			
Positive (<i>n</i> = 16)	8	8	0.638
Negative (<i>n</i> = 35)	20	15	
Microsatellite nodule			
Absent (<i>n</i> = 31)	17	14	0.991
Present (<i>n</i> = 20)	11	9	
Tumor size			
≤3 cm (<i>n</i> = 18)	8	10	0.272
>3 cm (<i>n</i> = 33)	20	13	
Cirrhosis			
Absent (<i>n</i> = 36)	20	16	0.886
Present (<i>n</i> = 15)	8	7	
Necrosis			
Absent (<i>n</i> = 24)	13	11	0.922
Present (<i>n</i> = 27)	15	12	
Portal vein thrombosis			
Absent (<i>n</i> = 37)	24	13	0.021
Present (<i>n</i> = 14)	4	10	
Differentiation			
Well (<i>n</i> = 35)	24	11	0.004
Low (<i>n</i> = 16)	4	12	
Extra-hepatic metastasis			
Absent (<i>n</i> = 41)	26	15	0.014
Present (<i>n</i> = 10)	2	8	

Correlation between expression of EMMPRIN protein and clinicopathological features in HCC

Of 51 cases that we assayed for EMMPRIN protein expression in HCC, 28 (55%) exhibited positive expression (Figure 1C). Of 42 cases of adjacent non-tumor liver tissues, 21 (50%) exhibited positive expression. If EMMPRIN expression was compared between HCC and the adjacent non-tumor liver tissues, there was no significant difference ($P = 0.842$). Expression of EMMPRIN protein was not associated with serum AFP level ($P = 0.242$), HBsAg status ($P = 0.284$), presence of microsatellite nodule ($P = 0.576$), tumor size ($P = 0.607$), presence of cirrhosis and necrosis ($P = 0.281$ and 0.992 , respectively), differentiation ($P = 0.897$), presence of portal vein thrombosis and extra-hepatic metastasis ($P = 0.292$ and 0.721 , respectively). (Table 3).

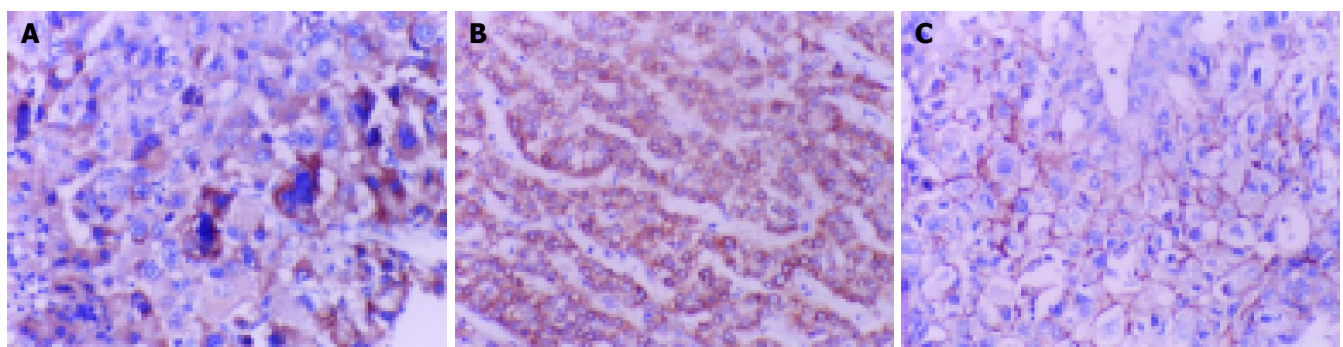


Figure 1 Immunohistochemical detection. A: Paxillin protein positive locates in cytoplasm of low-differentiated HCC cells (×200); B: Syndecan-1 protein positive locates in cytoplasm of well-differentiated HCC cells (×200); C: EMMPRIN protein positive locates in cytomembrane of well-differentiated HCC cells (×200).

Table 2 Expression of syndecan-1 protein categorized by pathological variables

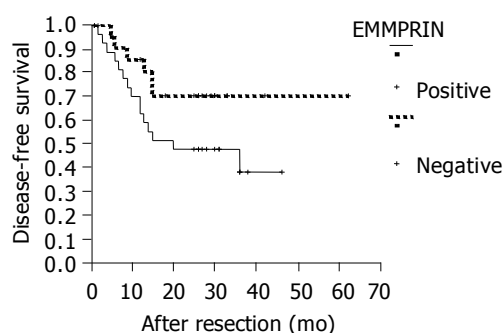
Variables	Syndecan-1		P
	-	+	
Serum AFP level			
≤25 ng/mL (n = 22)	8	14	0.280
>25 ng/mL (n = 29)	15	14	
HBsAg			
Positive (n = 16)	6	10	0.465
Negative (n = 35)	17	18	
Microsatellite nodule			
Absent (n = 31)	13	18	0.578
Present (n = 20)	10	10	
Tumor size			
≤3 cm (n = 18)	9	9	0.607
>3 cm (n = 33)	14	19	
Cirrhosis			
Absent (n = 36)	17	19	0.640
Present (n = 15)	6	9	
Necrosis			
Absent (n = 24)	10	14	0.646
Present (n = 27)	13	14	
Portal vein thrombosis			
Absent (n = 37)	15	22	0.292
Present (n = 14)	8	6	
Differentiation			
Well (n = 35)	10	25	0.001
Low (n = 16)	13	3	
Extra-hepatic metastasis			
Absent (n = 41)	15	26	0.014
Present (n = 10)	8	2	

Table 3 Expression of EMMPRIN protein categorized by pathological variables

Variables	EMMPRIN		P
	-	+	
Serum AFP level			
≤25 ng/mL (n = 22)	12	10	0.242
>25 ng/mL (n = 29)	11	18	
HBsAg			
Positive (n = 16)	9	7	0.284
Negative (n = 35)	14	21	
Microsatellite nodule			
Absent (n = 31)	13	18	0.576
Present (n = 20)	10	10	
Tumor size			
≤3 cm (n = 18)	9	9	0.607
>3 cm (n = 33)	14	19	
Cirrhosis			
Absent (n = 36)	18	18	0.281
Present (n = 15)	5	10	
Necrosis			
Absent (n = 24)	11	13	0.992
Present (n = 27)	12	15	
Portal vein thrombosis			
Absent (n = 37)	15	22	0.292
Present (n = 14)	8	6	
Differentiation			
Well (n = 35)	16	19	0.897
Low (n = 16)	7	9	
Extra-hepatic metastasis			
Absent (n = 41)	19	22	0.721
Present (n = 10)	4	6	

Prognostic value of paxillin, syndecan-1 and EMMPRIN proteins on disease-free survival and overall survival

Of 51 cases of HCC, median follow-up of the patients was 26 mo (range 5-90 mo). At the time of analysis, 21 of the 51 HCC patients had postoperative recurrence. The disease-free survival and overall survival were compared between two groups of patients who were segregated in positive and negative expression of those proteins. Patients with negative expression of EMMPRIN protein had better disease-free survival than those with positive expression, but the difference was not statistically significant ($P = 0.087$, Figure 2). The disease-free survival of the 51 HCC patients was not related to the expression of paxillin and syndecan-1 proteins ($P = 0.350$ and 0.654 , respectively). The overall survival of those HCC patients was not related to the expression of paxillin, syndecan-1 and EMMPRIN proteins ($P = 0.916$, 0.538 , and 0.476 , respectively).

**Figure 2** Disease-free analyses of HCC patients segregated into negative and positive expression of EMMPRIN protein ($P = 0.087$).

The expression of paxillin, syndecan-1 and EMMPRIN proteins was enabled to enter into a Cox's regression analysis of disease-free survival and overall survival together with serum AFP level, HBsAg status, presence of microsatellite nodule, tumor size, presence of cirrhosis and necrosis, differentiation, presence of portal vein thrombosis and extra-hepatic metastasis. No significant prognostic factor was found for disease-free survival and overall survival ($P > 0.05$, data not shown).

Correlation among expression of paxillin, syndecan-1 and EMMPRIN protein in HCC

Expression of paxillin protein was correlated conversely with the expression of syndecan-1 protein in HCC ($r = -0.366$, $P = 0.010$, Table 4). Expression of EMMPRIN protein was not correlated with the expression of paxillin and syndecan-1 protein in HCC ($P = 0.184$ and 0.141 , respectively, Table 5).

Table 4 Association between paxillin and syndecan-1 protein

Paxillin	Syndecan-1		P
	-	+	
Negative	8	20	0.010
Positive	15	8	

Table 5 Association between EMMPRIN and paxillin, syndecan-1 protein

	EMMPRIN		<i>P</i>
	-	+	
Paxillin			
Negative	15	13	0.184
Positive	8	15	
Syndecan-1			
Negative	13	10	0.141
Positive	10	18	

DISCUSSION

Evaluation of adhesion and proteolytic destruction of ECM and basement membranes (BM) has shown important clinical implications in the invasive and metastatic process of many types of malignant tumors. Immunohistochemical detection of factors attributed to adhesion and proteolytic destruction of ECM and BM might provide important prognostic values, independent of conventional pathological factors in cancer patients^[24,25]. HCC is a highly invasive and metastatic malignancy. HCC quickly permeates the liver through the portal venous system; portal vein thrombosis is found at a high proportion in the advanced cases. Metastases to regional lymph nodes are also common. Paxillin, syndecan-1 and EMMPRIN proteins appear to be promising immunohistochemical markers that might have a value to evaluate malignancy in other types of cancers^[17,21,26-29]. To our knowledge, this is the first study that evaluated the clinical significance of paxillin and EMMPRIN proteins in HCC patients.

Paxillin acts as an adaptor molecule in integrin signaling. Tyrosine phosphorylation of paxillin is a prominent event on integrin activation in normal epithelial cells^[30-32]. Similarly, paxillin protein might be detected in normal (non-tumor) liver tissues. Although the percentage of adjacent non-tumor liver tissues that were positive for paxillin protein was higher than that of HCC, no significant difference was found between those two percentages. This finding suggested that paxillin protein existed in both the non-tumor liver cells and HCC cells, and interfered in their activities. Both adjacent non-tumor liver tissues and HCC tissues have the same chance to encounter carcinogenic factors and oncogenes. The paxillin-binding protein might attribute to the presence of paxillin protein in both normal (non-tumor) liver tissues and HCC. Furthermore, paxillin protein expression was associated with low differentiation, in the presence of portal vein thrombosis, along with extra-hepatic metastasis. Low differentiation, presence of portal vein thrombosis and extra-hepatic metastasis means high malignancy in HCC. So positivity of paxillin protein was related to the malignancy of HCC. Previous studies showed that protein kinase C (PKC) activator and 12-O-tetradecanoylphorbol-13-acetate (TPA) increased the expression of tyrosine phosphorylation of several proteins including the FAK and paxillin, which increased the invasion ability of human hepatocellular carcinoma cells *in vitro*^[33-35]. However, paxillin protein was not related to the disease-free survival and overall survival in HCC patients. This finding suggested that detection of paxillin in HCC probably had little prognostic value, though

this protein was related to the malignancy of HCC. Moreover, paxillin protein was not related to serum AFP level, HBsAg status, presence of microsatellite nodule, tumor size, and the presence of cirrhosis and necrosis.

Previous study has demonstrated that syndecan-1 expressed in normal epithelial cells^[36]. Syndecan-1 protein was also detected in the adjacent non-tumor liver tissues^[37]. This study showed that syndecan-1 exhibited positive expression in HCC. Interestingly, the percentage of syndecan-1 protein that were positive in both HCC and the adjacent non-tumor liver tissues was the same, and no significant difference was found between the percentages of those two kinds of tissues. Previous study showed that the expression of syndecan-1 reduced in HCC with intra-hepatic or extra-hepatic metastasis^[37]. Similarly, this study had the same finding, in which there was a higher percentage of well differentiated HCC or HCC without extra-hepatic metastasis. This finding suggested that syndecan-1 protein was conversely related to the malignancy of HCC. Previous study had demonstrated that syndecan-1 was reduced both on the level of mRNA and protein levels in other cancers, and the reduction altered in different carcinomas^[36]. Previously, it had been revealed that the expression of syndecan-1 was reduced in human hepatocellular carcinomas with high metastatic potential and speculated that syndecan-1 played an important role in inhibition of invasion and metastasis^[26,36,37]. However, syndecan-1 protein was not related to the disease-free survival and overall survival in HCC patients, which suggested that it probably had little prognostic value in HCC. Furthermore, syndecan-1 protein was not related to serum AFP level, HBsAg status, the presence of microsatellite nodule, tumor size, presence of cirrhosis and necrosis, and the presence of portal vein thrombosis.

Matrix metalloproteinases (MMPs) play critical roles in the process of carcinogenesis, carcinoma invasion and metastasis by way of the proteolytic destruction of ECM and basement membranes^[38]. There is a positive correlation between MMPs expression and the invasive and metastatic potential of malignant tumors, including colorectal, lung, prostate, bladder, HCC, pancreatic carcinomas, astrocytic and oligodendroglial gliomas^[39-45]. EMMPRIN is a heavily glycosylated transmembrane glycoprotein containing two immunoglobulin superfamily domains, which induces MMPs production in the adjacent stromal cells. Some results implied that an EMMPRIN counter-receptor might have existed on the fiber cell surface, but such a counter-receptor has not been identified. This study showed that EMMPRIN protein was detected in the adjacent non-tumor liver tissues frequently, which was contrary to the finding of low expression in normal liver tissues. The percentage of EMMPRIN protein expression in HCC was higher than that in the adjacent non-tumor liver tissues. However, no significant reduction of EMMPRIN protein was found in adjacent non-tumor liver tissues compared with that in HCC. Other studies showed that EMMPRIN also acted in an autocrine fashion to increase productions of MMPs and invasiveness in tumor cells themselves. Previous studies demonstrated that EMMPRIN enriched in HCC tissue and these might be a potential target for anti-invasion and metastasis therapies. It was also shown that HAB18G/

CD147 was highly expressed in HCC tissues and lowly expressed in normal tissues. HAb18G/CD147, not only participated in adhesion of cell-cell or cell-matrix but also enhanced metastatic potentials of human hepatoma cells by disrupting the regulation of store-operated Ca^{2+} entry by NO/cGMP^[13,14]. This study showed that EMMPRIN protein might express in HCC. However, EMMPRIN protein was not related to differentiation, presence of portal vein thrombosis and extra-hepatic metastasis. These findings suggested that the expression of EMMPRIN protein was not associated with the malignancy of HCC, which was contrary to the findings of MMPs expression^[25]. Though those MMPs played an important role in the degradation of extracellular matrix of HCC, tissue inhibitor of matrix metalloproteinase proteins (TIMPs) also played an important role that inhibited the activities of MMPs in the degradation of extracellular matrix^[25]. Moreover, this study showed that EMMPRIN was not related to the differentiation, presence of portal vein thrombosis and extra-metastasis. This was probably attributable to the finding that EMMPRIN protein was not related to the malignancy of HCC and the prognosis of HCC patients. Moreover, this study showed that patients with negative expression of EMMPRIN protein had better disease-free survival than those with positive expression, but the difference was not statistically significant. This was probably attributable to that EMMPRIN protein was only the inducer of MMPs, and the activity of MMPs was regulated by many factors such as TIMPs. This probably made the association of EMMPRIN protein with biological behaviors of HCC complicated. This study also showed that EMMPRIN might be detected in the HCC patients whose AFP serum levels were >25 ng/mL. And no significant difference of the expression of EMMPRIN protein was found between the patients with AFP serum levels >25 ng/mL and with those ≤ 25 ng/mL. This finding was not in agreement with the previous study. Moreover, EMMPRIN protein was not related to HBsAg status, presence of microsatellite nodule, tumor size and presence of cirrhosis and necrosis.

This study demonstrated that the expression of paxillin protein correlated with the expression of syndecan-1 protein conversely, which suggested that the two proteins played a contrary role in the progression and metastasis of HCC. Paxillin protein increased and syndecan-1 protein decreased the malignancy of HCC.

In conclusion, our data demonstrated that the expression of paxillin protein correlated with differentiation, the presence of portal vein thrombosis and extra-hepatic metastasis in HCC. Furthermore, the expression of syndecan-1 protein correlated with differentiation and extra-hepatic metastasis in HCC. Hence, both paxillin and syndecan-1 correlated with the malignancy of HCC, and those proteins played a contrary role in the progression and metastasis of HCC. Though EMMPRIN protein might express in HCC, no association was found between this protein and the malignancy of HCC.

REFERENCES

- 1 **Srivatanakul P**, Sriplung H, Deerasamee S. Epidemiology of liver cancer: an overview. *Asian Pac J Cancer Prev* 2004; **5**: 118-125
- 2 **Yu AS**, Keffe EB. Management of hepatocellular carcinoma. *Rev Gastroenterol Disord* 2003; **3**: 8-24
- 3 **El-Serag HB**, Mason AC. Rising incidence of hepatocellular carcinoma in the United States. *N Engl J Med* 1999; **340**: 745-750
- 4 **Kiyosawa K**, Tanaka E. Characteristics of hepatocellular carcinoma in Japan. *Oncology* 2002; **62** Suppl 1: 5-7
- 5 **Tang ZY**. Hepatocellular carcinoma-cause, treatment and metastasis. *World J Gastroenterol* 2001; **7**: 445-454
- 6 **Zhang S**, Li L, Lu F. Mortality of primary liver cancer in China from 1990 through 1992. *Zhonghua Zhongliu Zazhi* 1999; **21**: 245-249
- 7 **Pisani P**, Parkin DM, Bray F, Ferlay J. Estimates of the world-wide mortality from 25 cancers in 1990. *Int J Cancer* 1999; **83**: 18-29
- 8 **Johnson PJ**. Hepatocellular carcinoma: is current therapy really altering outcome? *Gut* 2002; **51**: 459-462
- 9 **Watanabe T**, Omori M, Fukuda H, Takada H, Miyao M, Mizuno Y, Ohsawa I, Sato Y, Hasegawa T. Analysis of sex, age and disease factors contributing to prolonged life expectancy at birth, in cases of malignant neoplasms in Japan. *J Epidemiol* 2003; **13**: 169-175
- 10 **Ziparo V**, Balducci G, Lucandri G, Mercantini P, Di Giacomo G, Fernandes E. Indications and results of resection for hepatocellular carcinoma. *Eur J Surg Oncol* 2002; **28**: 723-728
- 11 **Kanematsu T**, Furui J, Yanaga K, Okudaira S, Shimada M, Shirabe K. A 16-year experience in performing hepatic resection in 303 patients with hepatocellular carcinoma: 1985-2000. *Surgery* 2002; **131**: S153-158
- 12 **Aguayo A**, Patt YZ. Liver cancer. *Clin Liver Dis* 2001; **5**: 479-507
- 13 **Yano H**, Mazaki Y, Kurokawa K, Hanks SK, Matsuda M, Sabe H. Roles played by a subset of integrin signaling molecules in cadherin-based cell-cell adhesion. *J Cell Biol* 2004; **166**: 283-295
- 14 **Romanova LY**, Hashimoto S, Chay KO, Blagosklonny MV, Sabe H, Mushinski JF. Phosphorylation of paxillin tyrosines 31 and 118 controls polarization and motility of lymphoid cells and is PMA-sensitive. *J Cell Sci* 2004; **117**: 3759-3768
- 15 **Sattler M**, Pisick E, Morrison PT, Salgia R. Role of the cytoskeletal protein paxillin in oncogenesis. *Crit Rev Oncog* 2000; **11**: 63-76
- 16 **Turner CE**. Paxillin interactions. *J Cell Sci* 2000; **113** Pt 23: 4139-4140
- 17 **Della Morte R**, Squillacioti C, Garbi C, Derkinderen P, Belisario MA, Girault JA, Di Natale P, Nitsch L, Staiano N. Echinostatin inhibits pp125FAK autophosphorylation, paxillin phosphorylation and pp125FAK-paxillin interaction in fibronectin-adherent melanoma cells. *Eur J Biochem* 2000; **267**: 5047-5054
- 18 **Roskams T**, De Vos R, David G, Van Damme B, Desmet V. Heparan sulphate proteoglycan expression in human primary liver tumours. *J Pathol* 1998; **185**: 290-297
- 19 **Kiviniemi J**, Kallajoki M, Kujala I, Matikainen MT, Alanen K, Jalkanen M, Salmivirta M. Altered expression of syndecan-1 in prostate cancer. *APMIS* 2004; **112**: 89-97
- 20 **Muramatsu T**, Miyauchi T. Basigin (CD147): a multifunctional transmembrane protein involved in reproduction, neural function, inflammation and tumor invasion. *Histol Histopathol* 2003; **18**: 981-987
- 21 **Marieb EA**, Zoltan-Jones A, Li R, Misra S, Ghatak S, Cao J, Zucker S, Toole BP. Emmprin promotes anchorage-independent growth in human mammary carcinoma cells by stimulating hyaluronan production. *Cancer Res* 2004; **64**: 1229-1232
- 22 **Dalberg K**, Eriksson E, Enberg U, Kjellman M, Backdahl M. Gelatinase A, membrane type 1 matrix metalloproteinase, and extracellular matrix metalloproteinase inducer mRNA expression: correlation with invasive growth of breast cancer. *World J Surg* 2000; **24**: 334-340
- 23 **Sun J**, Hemler ME. Regulation of MMP-1 and MMP-2 production through CD147/extracellular matrix metalloproteinase

- inducer interactions. *Cancer Res* 2001; **61**: 2276–2281
- 24 **Hefler LA**, Concin N, Mincham D, Thompson J, Swarte NB, van Eijkeren MA, Sie-Go DM, Hammond I, McCartney AJ, Tempfer CB, Speiser P. The prognostic value of immunohistochemically detected CD44v3 and CD44v6 expression in patients with surgically staged vulvar carcinoma: a multicenter study. *Cancer* 2002; **94**: 125–130
 - 25 **Wei QY**, Wu YQ, Fan SQ. Expression of matrix metalloproteinases and tissue inhibitors of matrix metalloproteinases in the hepatocellular carcinomas. *Huan Yike Daxue Xuebao* 2003; **28**: 212–216
 - 26 **Ohtake T**, Fujimoto Y, Ikuta K, Saito H, Ohhira M, Ono M, Kohgo Y. Proline-rich antimicrobial peptide, PR-39 gene transduction altered invasive activity and actin structure in human hepatocellular carcinoma cells. *Br J Cancer* 1999; **81**: 393–403
 - 27 **Leyton J**, Garcia-Marin LJ, Tapia JA, Jensen RT, Moody TW. Bombesin and gastrin releasing peptide increase tyrosine phosphorylation of focal adhesion kinase and paxillin in non-small cell lung cancer cells. *Cancer Lett* 2001; **162**: 87–95
 - 28 **Mennerich D**, Vogel A, Klamann I, Dahl E, Lichtner RB, Rosenthal A, Pohlenz HD, Thierauch KH, Sommer A. Shift of syndecan-1 expression from epithelial to stromal cells during progression of solid tumours. *Eur J Cancer* 2004; **40**: 1373–1382
 - 29 **Han JL**, Xie WL, Huang J, Yao YS. Expression of extracellular matrix metalloproteinase inducer in human bladder transitional cell carcinoma. *Aizheng* 2003; **22**: 1158–1161
 - 30 **Yano H**, Uchida H, Iwasaki T, Mukai M, Akedo H, Nakamura K, Hashimoto S, Sabe H. Paxillin alpha and Crk-associated substrate exert opposing effects on cell migration and contact inhibition of growth through tyrosine phosphorylation. *Proc Natl Acad Sci USA* 2000; **97**: 9076–9081
 - 31 **Yu CF**, Sanders MA, Basson MD. Human caco-2 motility redistributes FAK and paxillin and activates p38 MAPK in a matrix-dependent manner. *Am J Physiol Gastrointest Liver Physiol* 2000; **278**: G952–G966
 - 32 **Umino T**, Wang H, Zhu Y, Liu X, Manouilova LS, Spurzem JR, Patricia Leuschen M, Rennard SI. Modification of type I collagenous gels by alveolar epithelial cells. *Am J Respir Cell Mol Biol* 2000; **22**: 702–707
 - 33 **Imamura F**, Mukai M, Ayaki M, Akedo H. Y-27632, an inhibitor of rho-associated protein kinase, suppresses tumor cell invasion via regulation of focal adhesion and focal adhesion kinase. *Jpn J Cancer Res* 2000; **91**: 811–816
 - 34 **Tu LC**, Chou CK, Chen HC, Yeh SF. Protein kinase C-mediated tyrosine phosphorylation of paxillin and focal adhesion kinase requires cytoskeletal integrity and is uncoupled to mitogen-activated protein kinase activation in human hepatoma cells. *J Biomed Sci* 2001; **8**: 184–190
 - 35 **Yoon WH**, Song IS, Lee BH, Jung YJ, Kim TD, Li G, Lee TG, Park HD, Lim K, Hwang BD. Differential regulation of vimentin mRNA by 12-O-tetradecanoylphorbol 13-acetate and all-trans-retinoic acid correlates with motility of Hep 3B human hepatocellular carcinoma cells. *Cancer Lett* 2004; **203**: 99–105
 - 36 **Watari J**, Saitoh Y, Fujiya M, Shibata N, Tanabe H, Inaba Y, Okamoto K, Maemoto A, Ohta T, Yasuda A, Ayabe T, Ashida T, Yokota K, Obara T, Kohgo Y. Reduction of syndecan-1 expression in differentiated type early gastric cancer and back-ground mucosa with gastric cellular phenotype. *J Gastroenterol* 2004; **39**: 104–112
 - 37 **Matsumoto A**, Ono M, Fujimoto Y, Gallo RL, Bernfield M, Kohgo Y. Reduced expression of syndecan-1 in human hepatocellular carcinoma with high metastatic potential. *Int J Cancer* 1997; **74**: 482–491
 - 38 **Freije JM**, Balbin M, Pendas AM, Sanchez LM, Puente XS, Lopez-Otin C. Matrix metalloproteinases and tumor progression. *Adv Exp Med Biol* 2003; **532**: 91–107
 - 39 **Tutton MG**, George ML, Eccles SA, Burton S, Swift RI, Abulafi AM. Use of plasma MMP-2 and MMP-9 levels as a surrogate for tumour expression in colorectal cancer patients. *Int J Cancer* 2003; **107**: 541–550
 - 40 **Lee SJ**, Sakurai H, Oshima K, Kim SH, Saiki I. Anti-metastatic and anti-angiogenic activities of a new matrix metalloproteinase inhibitor, TN-6b. *Eur J Cancer* 2003; **39**: 1632–1641
 - 41 **London CA**, Sekhon HS, Arora V, Stein DA, Iversen PL, Devi GR. A novel antisense inhibitor of MMP-9 attenuates angiogenesis, human prostate cancer cell invasion and tumorigenicity. *Cancer Gene Ther* 2003; **10**: 823–832
 - 42 **Gakiopoulou H**, Nakopoulou L, Siatelis A, Mavrommatis I, Panayotopoulou EG, Tsirompa I, Stravodimos C, Giannopoulos A. Tissue inhibitor of metalloproteinase-2 as a multifunctional molecule of which the expression is associated with adverse prognosis of patients with urothelial bladder carcinomas. *Clin Cancer Res* 2003; **9**: 5573–5581
 - 43 **Ishii Y**, Nakasato Y, Kobayashi S, Yamazaki Y, Aoki T. A study on angiogenesis-related matrix metalloproteinase networks in primary hepatocellular carcinoma. *J Exp Clin Cancer Res* 2003; **22**: 461–470
 - 44 **Harvey SR**, Hurd TC, Markus G, Martinick MI, Penetrante RM, Tan D, Venkataraman P, DeSouza N, Sait SN, Driscoll DL, Gibbs JF. Evaluation of urinary plasminogen activator, its receptor, matrix metalloproteinase-9, and von Willebrand factor in pancreatic cancer. *Clin Cancer Res* 2003; **9**: 4935–4943
 - 45 **Thorns V**, Walter GF, Thorns C. Expression of MMP-2, MMP-7, MMP-9, MMP-10 and MMP-11 in human astrocytic and oligodendroglial gliomas. *Anticancer Res* 2003; **23**: 3937–3944

Impact of prolonged fraction dose-delivery time modeling intensity-modulated radiation therapy on hepatocellular carcinoma cell killing

Xiao-Kang Zheng, Long-Hua Chen, Xiao Yan, Hong-Mei Wang

Xiao-Kang Zheng, Long-Hua Chen, Xiao Yan, Hong-Mei Wang, Department of Radiation Oncology, Nanfang Hospital, The Southern Medical University, Guangzhou 510515, Guangdong Province, China Supported by the Natural Science Foundation of Guangdong Province, No. 013056

Correspondence to: Long-Hua Chen, Department of Radiation Oncology, Nanfang Hospital, The Southern Medical University, Guangzhou 510515, Guangdong Province, China. zkn1268@fimmu.com

Telephone: +86-20-61642136 Fax: +86-20-61642131

Received: 2004-08-31 Accepted: 2004-11-26

Abstract

AIM: To explore the impact of prolonged fraction dose-delivery time modeling intensity-modulated radiation therapy (IMRT) on cell killing of human hepatocellular carcinoma (HCC) HepG2 and Hep3B cell lines.

METHODS: The radiobiological characteristics of human HCC HepG2 and Hep3b cell lines were studied with standard clonogenic assays, using standard linear-quadratic model and incomplete repair model to fit the dose-survival curves. The identical methods were also employed to investigate the biological effectiveness of irradiation protocols modeling clinical conventional fractionated external beam radiotherapy (EBRT, fraction delivery time 3 min) and IMRT with different prolonged fraction delivery time (15, 30, and 45 min). The differences of cell surviving fraction irradiated with different fraction delivery time were tested with paired *t*-test. Factors determining the impact of prolonged fraction delivery time on cell killing were analyzed.

RESULTS: The α/β and repair half-time ($T_{1/2}$) of HepG2 and Hep3b were 3.1 and 7.4 Gy, and 22 and 19 min respectively. The surviving fraction of HepG2 irradiated modeling IMRT with different fraction delivery time was significantly higher than irradiated modeling EBRT and the cell survival increased more pronouncedly with the fraction delivery time prolonged from 15 to 45 min, while no significant differences of cell survival in Hep3b were found between different fraction delivery time protocols.

CONCLUSION: The prolonged fraction delivery time modeling IMRT significantly decreased the cell killing in HepG2 but not in Hep3b. The capability of sub-lethal damage repair was the predominant factor determining

the cell killing decrease. These effects, if confirmed by clinical studies, should be considered in designing IMRT treatments for HCC.

© 2005 The WJG Press and Elsevier Inc. All rights reserved.

Key words: Prolonged delivery time; Hepatocellular carcinoma; Radiation therapy

Zheng XK, Chen LH, Yan X, Wang HM. Impact of prolonged fraction dose-delivery time modeling intensity-modulated radiation therapy on hepatocellular carcinoma cell killing. *World J Gastroenterol* 2005; 11(10): 1452-1456
<http://www.wjgnet.com/1007-9327/11/1452.asp>

INTRODUCTION

With the popularization of intensity-modulated radiation therapy (IMRT), an irradiation technique developed to improve target dose conformity and normal tissue sparing^[1-4], more and more patients with hepatocellular carcinoma (HCC) would receive radiotherapy^[5]. IMRT optimized the physical dose distribution of radiotherapy, which thereby could enhance the tumor local control and lower the radiation-induced hepatitis. However, the radiobiological effectiveness of IMRT might be different from conventional external beam radiation therapy (EBRT) especially considering the prolonged fraction delivery time in IMRT. IMRT delivers dose, either dynamically or statically (e.g., step-and-shoot), using many beam apertures (segments) that are shaped with multileaf collimator^[1,4,6]. It takes a much longer time to deliver a single fraction dose with IMRT than EBRT. Generally, EBRT takes about 2-5 min to deliver a single fractional dose, whereas IMRT with static delivery requires 15-45 min to deliver the same fractional dose. According to radiobiological theory, cell killing tends to decrease with fraction delivery time increasing because of ongoing sublethal damage repair (SLDR) processes during dose delivery. Wang *et al*^[7] calculated the cell-killing efficiency of simulated and clinical IMRT plans with the generalized linear-quadratic (LQ) model, which indicated that fraction delivery times in the range of 15-45 min may significantly decrease tumor cell killing and may have a significant impact on treatment outcome for tumors with a low α/β ratio and short repair half-time ($T_{1/2}$). However, such calculation lacks confirmation of studies *in vitro*. To clarify the impact of prolonged fraction delivery time in IMRT on tumor cell

killing, more detailed studies *in vitro* are required.

In this study, we attempt to ascertain the impact of prolonged fraction delivery time modeling IMRT on survival of human HCC cell lines HepG2 and Hep3B, so as to provide radiobiological basis for optimizing IMRT plans for this disease.

MATERIALS AND METHODS

Cell culture

Human HCC cell lines including HepG2 and Hep3b were employed in this study. Both cell lines were cultured in plastic flasks at 37 °C in a humidified atmosphere of 50 mL/L CO₂ and 95% air with the 1 640 medium containing 10-15% fetal calf serum with 100 U/mL penicillin and 100 µg/mL streptomycin. Results of regular tests for mycoplasma contamination were negative. When they become confluent, cells were sub-cultured (1:4 dilution). Exponentially growing cells were used for experiments.

Immediately prior to irradiation, single-cell suspension was prepared by trypsinization and cell number was counted using a hemocytometer. Cells were then seeded in varying amounts onto 6-well tissue culture dishes with 1 640 medium. Three parallel samples were set at each radiation dose of various irradiation schedules.

Irradiation scheme

Irradiation was carried out at room temperature using a 6-MeV X-ray. To learn the radiobiological characteristics, doses of 0 Gy, 1 Gy, 2 Gy, 4 Gy, 6 Gy, 8 Gy and 10 Gy were given as single, continuous doses at a dose rate of 3.2 Gy/min for generating standard dose-survival curves and acquiring a variety of mathematic model parameters. To achieve the $T_{1/2}$, doses of 0 Gy, 1 Gy, 2 Gy, 4 Gy, 6 Gy, 8 Gy and 10 Gy were given as single, continuous doses at a dose rate of 0.066 Gy/min. To compare the cell killing effectiveness of fraction delivery time modeling EBRT and IMRT, fractionated irradiation of 0 Gy, 1 Gy×1, 2 Gy×1, 2 Gy×2, 2 Gy×3, 2 Gy×4 and 2 Gy×5, were given with one fraction per day just like clinical dose-time-fractionation pattern. In irradiation modeling EBRT, the fraction delivery time was 3 min, with two 1.18 min intervals modeling 3 portals irradiation. In irradiation modeling IMRT with different fraction delivery times, each fraction dose was given in seven equal sub-fractions; the total fraction delivery time was 15, 30 or 45 min.

Clonogenic assays

Standard clonogenic assays were used to acquire the standard dose-survival curves of HepG2 and Hep3b and to determine the effect of irradiation modeling EBRT and IMRT with fraction delivery time of 15, 30 and 45 min. Cells plated in 6-well tissue culture dishes were incubated in an undisturbed state for 10 d. Cell fixation and staining used methanol and 0.5% crystal violet in deionized water and colony counts were performed by visual inspection. A colony was defined as 50 or more cells. Colony plating efficiency was calculated to be the number of viable nucleated cells plated and expressed as a percentage. The surviving fraction at each dose of each irradiation protocols was determined by

dividing the plating efficiency of the irradiated cells by that of the untreated control. All data points were the mean results of experiments.

Survival curve fitting and calculation

Dose-survival curves for each experiment were constructed by semi-logarithmically plotting the mean surviving fractions as a function of irradiation dose. The data were analyzed, and survival curves were plotted following the standard linear-quadratic model [$S = \exp(-\alpha D - \beta D^2)$] or incomplete repair model [$S = \exp(-\alpha D - \beta_g D^2)$]^[8] using GraphPad Prism 4.0 software (GraphPad Software, Inc., USA). α and β resulted from the best fitting survival curves and were used to calculate surviving fraction at 2 Gy (SF₂).

Differences of surviving fraction treated with different irradiation protocols were tested with paired *t*-test. Statistical significance was assumed when $P < 0.05$.

RESULTS

Radiobiological characteristics of HepG2 and Hep3b

Standard dose-survival curves of HepG2 and Hep3b fitted with the standard LQ model are shown in Figure 1. The survival curves with irradiation at a low dose rate of 0.066 Gy/min fitted with incomplete repair model to acquire the $T_{1/2}$ of both cell lines were shown in Figure 2. The radiobiological characteristics of both cell lines described with the parameters of the mathematic models are listed in Table 1.

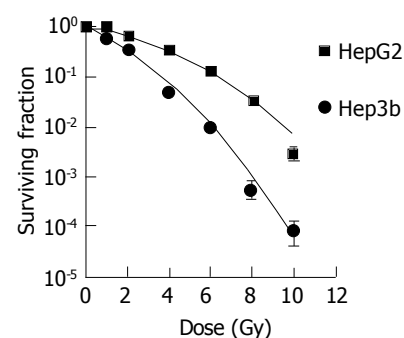


Figure 1 Standard dose-survival curves of HepG2 and Hep3b fitted with standard two parameter LQ model.

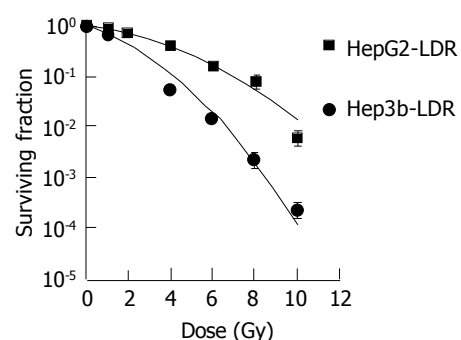


Figure 2 Dose-survival curves of HepG2 and Hep3b irradiated at a low dose rate of 0.067 Gy/min fitted with incomplete repair model.

Table 1 Radiobiological characteristics of HepG2 and Hep3b described with parameters derived from the dose-survival curves fitted with standard LQ model and incomplete repair model

Cell	Parameters					
	SF _{2read} (%)	SF _{2est} (%)	α (Gy ⁻¹)	β (Gy ⁻²)	α/β (Gy)	T _{1/2} (min)
HepG2	89.0	67.6	0.118	0.038	3.1	22
Hep3b	60.0	34.6	0.413	0.056	7.4	19

Cell surviving fraction irradiated modeling EBRT and IMRT

Surviving fraction of HepG2 and Hep3b irradiated modeling fractionated EBRT of 0Gy, 1Gy×1, 2Gy×1, 2Gy×2, 2Gy×3, 2Gy×4 and 2Gy×5, as well as modeling IMRT given in seven equal sub-fractions per fraction delivered within a total fraction delivery time of 15, 30 or 45 min are listed in Table 2. The dose-survival curves of both cell lines with different fractionated irradiation schedules fitted with standard LQ model are shown in Figure 3. The surviving fractions of HepG2 irradiated modeling IMRT with different fraction delivery times were significantly higher than irradiated modeling EBRT ($P<0.05$), and the cell irradiated modeling IMRT with longer fraction delivery time has a significant higher survival than that with shorter fraction delivery time ($P<0.05$). No significant survival differences of Hep3b were found between different fraction delivery time protocols ($P>0.05$) (Table 3).

DISCUSSION

This study demonstrated that the prolonged fraction delivery time modeling IMRT decreased the cell killing of HepG2; the cell killing decreased more pronouncedly with the fraction delivery time being prolonged from 15 min to 45 min. These phenomena, however, were not obvious in Hep3b.

Essence of the impact of prolonged fraction delivery time on cell killing

The intrinsic reason for increasing of the cell survival treated with IMRT like protocols is the ongoing SLDR processes during dose delivery. Irradiated tumor cells may be lethally or not lethally damaged. Cells that are not lethally damaged may undergo repair. SLDR is an important type of damage repair that is defined as the enhancement in survival when a dose of radiation is separated over a period time. Generally, SLDR experiments divide a single dose into two relatively equal doses spaced at variable time intervals. Elkind *et al* investigated this phenomenon in great detail^[9,10]. An enhancement in survival after two doses separated in time was observed. This enhancement in survival was due to SLDR.

Factors determining the impact degree of prolonged fraction delivery time on cell killing

The survival increasing of cells irradiated with a prolonged fraction delivery time is mainly associated with the capacity

Table 2 Surviving fraction of HepG2 and Hep3B irradiated modeling fractionated EBRT, as well as modeling IMRT with a total fraction delivery time of 15, 30 or 45 min

Dose	Survival fraction of HepG2 and Hep3b							
	Modeling EBRT-03'		Modeling IMRT-15'		Modeling IMRT-30'		Modeling IMRT-45'	
	HepG2	Hep3b	HepG2	Hep3b	HepG2	Hep3b	HepG2	Hep3b
0.0 Gy	1.0000	1.0000	1.0000	1.0000	1.0000	1.0000	1.0000	1.0000
1.0 Gy×1	0.8700	0.4800	0.8800	0.4800	0.8800	0.4800	0.9100	0.4800
2.0 Gy×1	0.6636	0.3559	0.6747	0.4123	0.7012	0.4389	0.7133	0.4500
2.0 Gy×2	0.4669	0.0507	0.5123	0.0546	0.5181	0.0550	0.5498	0.0590
2.0 Gy×3	0.2578	0.0550	0.2906	0.0200	0.3006	0.0208	0.3236	0.0230
2.0 Gy×4	0.1321	0.0027	0.1700	0.0033	0.1987	0.0049	0.2137	0.0051
2.0 Gy×5	0.0547	0.0005	0.0671	0.0007	0.0851	0.0009	0.0996	0.0011

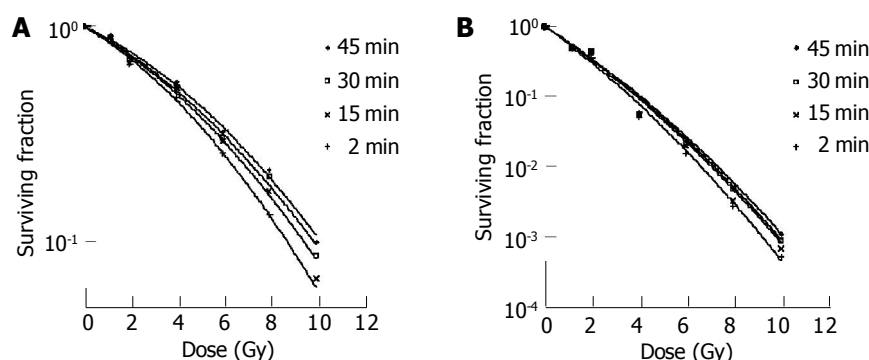
**Figure 3** Effects of fractionated irradiation modeling EBRT and IMRT on survival of HepG2 and Hep3b. A: Cell survival curve of HepG2 fitted with LQ model; B: Cell survival curve of Hep3b fitted with LQ model. Cells were irradiated modeling fractionated EBRT [•] with doses of 0.0Gy, 1Gy×1, 2Gy×1, 2Gy×2, 2Gy×3, 2Gy×4 and 2Gy×5 delivered within a fraction time of 3 min, as well as modeling IMRT with the corresponding doses delivered within a fraction time of [×] 15 min, [□] 30 min or [◆] 45 min.

Table 3 Results of t-tests for surviving fractions between different fraction delivery time protocols

Fraction delivery time protocols	HepG2		Hep3b	
	<i>t</i>	<i>P</i>	<i>t</i>	<i>P</i>
EBRT-03' <i>vs</i> IMRT-15'	-3.308	0.016	-1.199	0.276
EBRT-03' <i>vs</i> IMRT-30'	-3.909	0.008	-1.179	0.283
EBRT-03' <i>vs</i> IMRT-45'	-4.814	0.003	-1.240	0.261
IMRT-15' <i>vs</i> IMRT-30'	-2.823	0.030	-1.133	0.301
IMRT-15' <i>vs</i> IMRT-45'	-5.686	0.001	-1.301	0.241
IMRT-30' <i>vs</i> IMRT-45'	-4.308	0.005	-1.644	0.151

and rate of the SLDR during the dose delivery as well as the fraction dose delivery time.

The capacity of a cell to undergo SLDR, which is associated with the intrinsic radiobiological characteristics of the cell, may be represented by the quadratic term in LQ model. A cell with a small α/β is considered having a large ability to undergo SLDR. Most human tumor cell lines studied *in vitro* have a relatively small ability to undergo SLDR^[11-15]. Yet, a large capacity for SLDR has been reported for some human tumor cell lines^[12,16-20]. According to this study, HepG2 has a relatively large capacity for SLDR with a α/β of 3.1, which is much lower than what was expected, while Hep3b has a smaller capacity for SLDR with a α/β of 7.4.

The rate of SLDR can be represented with $T_{1/2}$. Apparently, cells with short $T_{1/2}$ have more repairs during a certain fraction delivery time. For human tumor cell lines, the characteristic $T_{1/2}$ ranges from a few minutes to several hours^[21-23]. In a review article, Steel *et al.*^[21] pointed out that the repair time for many tumors appears different when measured from a split-dose experiment *vs* a low-dose-rate exposure. They attributed this difference to the presence of two or more repair components. Others have confirmed that non-exponential or multi-exponential SLDR kinetics are involved in cell killing^[24-28]. In split-dose survival experiments, the fast and slow rates of SLDR kinetics can be reasonably approximated by a single (average) first-order repair term. In low-dose-rate experiments, cell killing is more sensitive to the fast repair component. For fraction delivery times in the range of 15 to 45 min (i.e., comparable to IMRT treatment times), the fast repair component is important and the slow repair component has little impact on cell killing. Brenner and Hall^[22] have compiled *in vitro* data on the $T_{1/2}$ of human cancer cell lines under low-dose-rate exposure conditions. They have found that the most probable $T_{1/2}$ is approximately 20 min. For prostate cancer, Wang *et al.*^[17] used clinical data to derive a $T_{1/2}$ of 16 min. In this study, the $T_{1/2}$ of HepG2 and Hep3b were 22 and 19 min respectively. They are just within the general fraction delivery time of IMRT (15-45 min). Although cells, with shorter $T_{1/2}$ (Hep3b), could not be proved as having more SLDR than that with longer $T_{1/2}$ (HepG2) in this study for the much larger SLDR capability of HepG2 than Hep3b, the importance of SLDR rate should not be neglected only if the $T_{1/2}$ of cell lines being considered were similar just like that in this study and the study of Brenner and Hall^[22].

The fraction dose delivery time is another factor that impacts the effect of cell survival. For HepG2 in this study,

the differences of surviving fraction in each group irradiated with different prolonged fraction delivery time were small but significant ($P < 0.05$).

These important factors synthetically affect the effect of prolonged fraction delivery time on cell killing. According to the results of this study, HepG2 and Hep3b have similar $T_{1/2}$. The predominant factor that affects the effect of prolonged fraction delivery time on cell killing apparently should be the SLDR capability of the cells.

In conclusion, the prolonged fraction delivery time modeling IMRT significantly decreased the cell killing in HepG2 but not in Hep3b. The capability of SLDR was the predominant factor determining the cell killing decrease. These effects, if confirmed by clinical studies, should be considered in designing IMRT treatments.

REFERENCES

- 1 Bortfeld TR, Kahler DL, Waldron TJ, Boyer AL. X-ray field compensation with multileaf collimators. *Int J Radiat Oncol Biol Phys* 1994; **28**: 723-730
- 2 Brahme A. Recent advances in light ion radiation therapy. *Int J Radiat Oncol Biol Phys* 2004; **58**: 603-616
- 3 Siochi RA. Minimizing static intensity modulation delivery time using an intensity solid paradigm. *Int J Radiat Oncol Biol Phys* 1999; **43**: 671-680
- 4 Webb S. The physical basis of IMRT and inverse planning. *Br J Radiol* 2003; **76**: 678-689
- 5 Wu DH, Liu L, Chen LH. Therapeutic effects and prognostic factors in three-dimensional conformal radiotherapy combined with transcatheter arterial chemoembolization for hepatocellular carcinoma. *World J Gastroenterol* 2004; **10**: 2184-2189
- 6 Galvin JM, Chen XG, Smith RM. Combining multileaf fields to modulate fluence distributions. *Int J Radiat Oncol Biol Phys* 1993; **27**: 697-705
- 7 Wang JZ, Li XA, D'Souza WD, Stewart RD. Impact of prolonged fraction delivery times on tumor control: a note of caution for intensity-modulated radiation therapy (IMRT). *Int J Radiat Oncol Biol Phys* 2003; **57**: 543-552
- 8 Thames HD. An "incomplete-repair" model for survival after fractionated and continuous irradiations. *Int J Radiat Biol Relat Stud Phys Chem Med* 1985; **47**: 319-339
- 9 Elkind MM. The initial part of the survival curve: does it predict the outcome of fractionated radiotherapy? *Radiat Res* 1988; **114**: 425-436
- 10 Elkind MM, Sutton HG. X-ray damage and recovery in mammalian cells in culture. *Nature* 1959; **184**: 1293-1295
- 11 Boothman DA, Bouvard I, Hughes EN. Identification and characterization of X-ray-induced proteins in human cells. *Cancer Res* 1989; **49**: 2871-2878
- 12 Carney DN, Mitchell JB, Kinsella TJ. *In vitro* radiation and chemotherapy sensitivity of established cell lines of human small cell lung cancer and its large cell morphological variants. *Cancer Res* 1983; **43**: 2806-2811
- 13 Kelland LR, Bingle L, Edwards S, Steel GG. High intrinsic radiosensitivity of a newly established and characterised human embryonal rhabdomyosarcoma cell line. *Br J Cancer* 1989; **59**: 160-164
- 14 Weichselbaum RR, Beckett MA, Vijayakumar S, Simon MA, Awan AM, Nachman J, Panje WR, Goldman ME, Tybor AG, Moran WJ. Radiobiological characterization of head and neck and sarcoma cells derived from patients prior to radiotherapy. *Int J Radiat Oncol Biol Phys* 1990; **19**: 313-319
- 15 Weichselbaum RR, Rotmensch J, Ahmed-Swan S, Beckett MA. Radiobiological characterization of 53 human tumor cell lines. *Int J Radiat Biol* 1989; **56**: 553-560
- 16 Barranco SC, Romsdahl MM, Humphrey RM. The radiation response of human malignant melanoma cells grown *in vitro*. *Cancer Res* 1971; **31**: 830-833

- 17 **Wang JZ**, Guerrero M, Li XA. How low is the alpha/beta ratio for prostate cancer? *Int J Radiat Oncol Biol Phys* 2003; **55**: 194-203
- 18 **Brenner DJ**, Hall EJ. Fractionation and protraction for radiotherapy of prostate carcinoma. *Int J Radiat Oncol Biol Phys* 1999; **43**: 1095-1101
- 19 **Fowler J**, Chappell R, Ritter M. Is alpha/beta for prostate tumors really low? *Int J Radiat Oncol Biol Phys* 2001; **50**: 1021-1031
- 20 **Brenner DJ**, Martinez AA, Edmundson GK, Mitchell C, Thames HD, Armour EP. Direct evidence that prostate tumors show high sensitivity to fractionation (low alpha/beta ratio), similar to late-responding normal tissue. *Int J Radiat Oncol Biol Phys* 2002; **52**: 6-13
- 21 **Steel GG**, Deacon JM, Duchesne GM, Horwich A, Kelland LR, Peacock JH. The dose-rate effect in human tumour cells. *Radiother Oncol* 1987; **9**: 299-310
- 22 **Brenner DJ**, Hall EJ. Conditions for the equivalence of continuous to pulsed low dose rate brachytherapy. *Int J Radiat Oncol Biol Phys* 1991; **20**: 181-190
- 23 **Kampinga HH**, Hiemstra YS, Konings AW, Dikomey E. Correlation between slowly repairable double-strand breaks and thermal radiosensitization in the human HeLa S3 cell line. *Int J Radiat Biol* 1997; **72**: 293-301
- 24 **Ang KK**, Jiang GL, Guttenberger R, Thames HD, Stephens LC, Smith CD, Feng Y. Impact of spinal cord repair kinetics on the practice of altered fractionation schedules. *Radiother Oncol* 1992; **25**: 287-294
- 25 **Millar WT**, Canney PA. Derivation and application of equations describing the effects of fractionated protracted irradiation, based on multiple and incomplete repair processes. Part 2. Analysis of mouse lung data. *Int J Radiat Biol* 1993; **64**: 293-303
- 26 **van Rongen E**, Thames HD, Travis EL. Recovery from radiation damage in mouse lung: interpretation in terms of two rates of repair. *Radiat Res* 1993; **133**: 225-233
- 27 **Stewart RD**. Two-lesion kinetic model of double-strand break rejoining and cell killing. *Radiat Res* 2001; **156**: 365-378
- 28 **Guerrero M**, Stewart RD, Wang JZ, Li XA. Equivalence of the linear-quadratic and two-lesion kinetic models. *Phys Med Biol* 2002; **47**: 3197-3209

Edited by Li WZ Language Editor Elsevier HK

• LIVER CANCER •

Are polymorphisms of N-acetyltransferase genes susceptible to primary liver cancer in Luoyang, China?

Xiu-Feng Zhang, Jian-Chao Bian, Xiao-Yan Zhang, Zhu-Mei Zhang, Feng Jiang, Qi-Min Wang, Qi-Jun Wang, Yan-Yan Cao, Bo-Ming Tang

Xiu-Feng Zhang, Jian-Chao Bian, Xiao-Yan Zhang, Zhu-Mei Zhang, Feng Jiang, Yan-Yan Cao, Department of Epidemiology, School of Public Health, Fudan University, Shanghai 200032, China
Qi-Min Wang, Qi-Jun Wang, Bo-Ming Tang, Department of Epidemiology, Luoyang Center for Disease Control and Prevention, Luoyang 471000, Henan Province, China

Supported by the National Natural Science Foundation of China, No. 39870654

Correspondence to: Dr. Jian-Chao Bian, Department of Epidemiology, School of Public Health, Fudan University, Shanghai 200032, China. jcbian@shmu.edu.cn

Telephone: +86-21-54237294

Received: 2004-08-30 Accepted: 2004-09-03

© 2005 The WJG Press and Elsevier Inc. All rights reserved.

Key words: Polymorphisms; N-acetyltransferase genes; Primary liver cancer

Zhang XF, Bian JC, Zhang XY, Zhang ZM, Jiang F, Wang QM, Wang QJ, Cao YY, Tang BM. Are polymorphisms of N-acetyltransferase genes susceptible to primary liver cancer in Luoyang, China? *World J Gastroenterol* 2005; 11(10): 1457-1462

<http://www.wjgnet.com/1007-9327/11/1457.asp>

Abstract

AIM: To identify whether the polymorphisms of the N-acetyltransferase (NAT) genes are susceptible to primary liver cancer (PLC) in Luoyang, a PLC low-incidence area of China.

METHODS: The NAT1 and NAT2 genotypes of 96 PLC cases and 173 controls were determined by PCR-RFLP. Both interaction between NAT1 or NAT2 and environmental risk factors were analyzed based on case control study.

RESULTS: Compared to the control group, the frequencies of alleles NAT1*3, NAT1*4, NAT1*10, NAT1*14B and alleles NAT2*4, NAT2*6, NAT2*7 in PLC group showed no statistically significant difference ($\chi^2 = 2.61$ and 4.16 , respectively, both $P > 0.05$). The frequencies of NAT1 genotypes NAT1*3/*3, NAT1*3/*4, NAT1*3/*10, NAT1*3/*14B, NAT1*4/*4, NAT1*4/*10, NAT1*4/*14B, NAT1*10/*10, NAT1*10/*14B, and NAT2 genotypes NAT2*4/*4, NAT2*4/*6, NAT2*4/*7, NAT2*6/*6, NAT2*6/*7 and NAT2*7/*7 also had no statistically significant difference between the two groups ($\chi^2 = 11.86$ and 2.94 respectively both, $P > 0.05$). Neither the frequencies of rapid and slow NAT1 acetylators nor the frequencies of rapid and slow NAT2 acetylators were significantly different between the two groups ($\chi^2 = 0.598$ and 0.44 , respectively, both $P > 0.05$). The interaction between NAT1*10 and occupational exposures was found significant with an odds ratio of 3.40 ($\chi^2 = 8.42$, $P = 0.004$, OR 95%CI:1.03-11.22). But no interaction was found between NAT2 and any environmental risk factors.

CONCLUSION: The polymorphisms of NAT1 and NAT2 are not susceptible to PLC in Luoyang. Allele NAT1*10 interacts with occupational exposures.

INTRODUCTION

Primary liver cancer (PLC), most of which refers to primary hepatocellular carcinoma (HCC), following lung cancer and stomach cancer, ranked the third of cancer mortality worldwide, accounting for an estimated 357 000 deaths in 1990^[1]. In China, PLC ranked the second of cancer mortality since 1990s^[2]. The incidence of PLC in China has also been found to be increasing, covering about 42.5% of the new global 260 000 cases each year^[3]. To explore the risk factors of PLC in mainland China has remained an attractive target.

The pathogenesis of PLC remains unknown although much progress has been made in the past decades. Many studies have suggested that PLC is a multi-factorial disease induced by interactions between genetic and environmental factors. Researches in molecular genetics have revealed that polymorphisms of some metabolizing enzyme genes may related to the development of PLC. N-acetyltransferase (NAT) is a kind of enzyme family, which catalyzes acetylation reactions of nitrogenous compounds. It can activate or inactivate extrinsic nitrogenous substances especially amine carcinogens^[4]. NAT is encoded by two isozyme genes, NAT1 and NAT2.

Much work has been reported on the relationship between NAT1 genetic polymorphisms and some cancers such as bladder or colon cancer, a few of which were focused on PLC in high incidence areas. In contrast, little has been reported on association between NAT2 genetic polymorphisms and PLC. Bian *et al*^[5] who studied the genotypes, phenotypes and polymorphism of NAT2 for 65 HCC cases in high incidence area of China, found out that slow NAT2 acetylators (NAT2*4 allele) increased the risk of HCC. However, no such works have been reported in PLC low incidence areas of China or other countries. In order to know whether polymorphisms of NAT1 and NAT2 are susceptible to PLC, and to know the interaction between

environmental risk factors and NAT1 or NAT2 in such areas, we selected Luoyang City as our research site, which is located in the west of Henan Province, China.

MATERIALS AND METHODS

Subjects and standard of enrollment

We collected 96 newly diagnosed PLC patients as the case group from more than ten hospitals of Luoyang city during 1999-2002. All the patients met the diagnosis criteria for PLC established by Chinese Anti-Cancer Association^[6]. Meanwhile, we collected 65 controls from hospitals and another 108 controls from communities who were all excluded for any hepatic diseases or cancers. Hospital and community controls were merged as the control group based on their balance in gender, age and resident area. All the controls had no kinship with each other. Both groups were of local residents.

Data collection and blood sampling

All of the subjects gave verbal informed consent for the survey. A same questionnaire was applied to both groups to investigate their general information, health condition, smoking history, occupational exposures *etc.* We defined smoking as consuming at least one cigarette each day for more than 6 mo, and occupational exposures as contact history with suspicious carcinogens such as benzene, paint and dust.

All cases and controls were interviewed and their medical records were reviewed by trained field workers. They also had 5 mL peripheral blood drawn, which was non-coagulated and kept in -20 °C.

Genomic DNA extraction

Genomic DNA was extracted from peripheral blood leucocytes by general phenol-chloroform method.

PCR amplification

Primers were synthesized based on relevant literatures^[7,8] (Table 1). The NAT1 amplification reaction was carried out in a 30 µL solution containing 0.1-0.3 µg DNA, 2.5 mmol/L 4×dNTP (Shanghai Bioasia Company), 0.2 µmol/L NAT1a and NAT1b primer each (Shanghai Sangon Company), 1.5 U *Taq* DNA polymerase (Beijing Sbsbio Company) and 3.0 µL 10×PCR reaction buffer. The PCR condition consisted of an initial denaturation at 94 °C for 5 min and extension at 72 °C for 7 min followed 30 cycles of denaturation at 94 °C, annealing at 55 °C and extension at 72 °C each for 60 s.

For NAT2, the amplification reaction was carried out in a 100 µL solution containing 1-3 µg DNA, 2.4 mmol/L 4×dNTP, 0.3 µmol/L NAT2a and NAT2b primer each, 0.8 µL *Taq* DNA polymerase (5 U/µL) and 10 µL 10×PCR

reaction buffer. The PCR condition consisted of an initial denaturation at 94 °C and extension at 72 °C each for 5 min followed 30 cycles of denaturation at 94 °C, annealing at 55 °C and extension at 72 °C each for 60 s.

Restriction fragment length polymorphism analysis

The 5-20 µL of NAT1 PCR product was then digested by *Aba*26I, *Ase*I and *Hinf*I, and NAT2 by *Taq*I and *Bam* HI, for 12-16 h at 37 °C water. The reaction products were separated by electrophoresis under 200 V of constant voltage for 30 min through 2.5-3.0% agarose gel with 10 mg/µL ethidium bromide, which was examined under ultraviolet irradiation.

Genotype determinations

The genotypes of single nucleotide polymorphisms (SNPs) of NAT1 at nucleotide 560, 1 088 and 1 095, and SNPs of NAT2 at nucleotide 590 and 857 were determined and divided into wild homozygote (w/w), heterozygote (w/m) and mutant homozygote (m/m) according to the pictures of electrophoresis. Then the genotypes of NAT1 (NAT1*3, *4, *10, *14A, 14B) and NAT2 (NAT2*4, 6, 7) of all subjects were determined based on relevant literature.

Genotype and phenotype

The NAT1*10 phenotype and its association with cancer susceptibility remain poorly understood. Commonly NAT1*10 may increase enzyme activity and was found to increase risk of some cancers. In this study individuals with NAT1*10 were classified as rapid NAT1 acetylators and others were slow NAT1 acetylators as usual^[9]. As for NAT2, those without NAT2*4 could increase susceptibility to some cancers, and were regarded as slow NAT2 acetylators, those with NAT2*4 were rapid acetylators^[8].

Statistical analysis

Data are presented as mean±SD. Database was built by Epi Info 6.0 and the analysis of data was accomplished using SPSS 10.0 software. The genotype distribution of NAT1 and NAT2 in controls was compared with that as expected from Hardy-Weinberg equilibrium by χ^2 tests. The difference in frequency distributions of genotypes and phenotypes between the two groups was tested by χ^2 test. Odds ratios (ORs) and 95% confidence intervals (CIs) were calculated to assess the strength of interaction between environmental risk factors and polymorphisms of NAT1 or NAT2. *P* values of less than 0.05 were considered to be statistically significant.

RESULTS

Balance test and goodness-of-fit test for Hardy-Weinberg law

In the case group, the age span was 20-75 years old, mean

Table 1 Primer sequence of NAT1 and NAT2

Primer	Position	Length (bp)	Primer sequence
NAT1a	-10-29	1 158	5'-TTAGGAATTCATGGACATTGAAGCATATCTTGAAAGAAT-3'
NAT1b	1 127-1 148		5'-GCTTCTAGCATAAAATCACCA-3'
NAT2a	1-30	895	5'-ATGGACATTTGAAGCATATTTTGAAAGAATT-3'
NAT2b	867-895		5'-AAGGGTTATTTTGTTCCTTATTCTAAAT-3'

Table 2 Goodness-of-fit test for Hardy-Weinberg law for genotype frequencies of NAT1 in control group

Genotypes	Observed number	Expected number
NAT1*3/ *3	20	11
NAT1*3/ *4	30	40
NAT1*3/ *10	15	22
NAT1*3/ *14B	4	4
NAT1*4/ *4	50	37
NAT1*4/ *10	27	39
NAT1*4/ *14B	5	6
NAT1*10/ *10	19	10
NAT1*10/ *14B	4	3
Total	173	173

 $\chi^2 = 7.24$, $P > 0.05$.**Table 3** Goodness-of-fit test for Hardy-Weinberg law for genotype frequencies of NAT2 in control group

Genotypes	Observed number	Expected number
NAT2*4/ *4	100	91
NAT2*4/ *6	23	33
NAT2*4/ *7	28	34
NAT2*6/ *6	6	4
NAT2*6/ *7	12	7
NAT2*7/ *7	4	4
Total	173	173

 $\chi^2 = 4.51$, $P > 0.05$.

age was (58.20±10.71) years old, and gender ratio was 3:1. While in the control group, the age span was 26-80 years, mean age was (57.68±10.03) years old and gender ratio was 2.5:1. Case group and control group had similar frequency for distribution of age and sex ($P > 0.05$). As for the control group, the frequencies of NAT1 and NAT2 genotypes fitted well with the Hardy-Weinberg equilibrium, indicating that the control group were sufficiently representative (Tables 2, 3).

PLC and polymorphisms of NAT1 or NAT2

The RFLP results of NAT1 and NAT2 Figures 1-5. Neither 3 SNPs of NAT1 (C1095A, T1088A and G560A) nor 2 SNPs of NAT2 (G857A and G590A) were found to be associated to PLC ($\chi^2 = 1.170$, 0.190, 0.047, 3.33 and 0.95, respectively, all $P > 0.05$).

Similarly, we did not find any association between PLC and NAT1 or NAT2 alleles ($\chi^2 = 2.61$ and 4.16, both $P > 0.05$). We failed to observe NAT1*14A alleles in both groups. The genotypes of NAT1 and NAT2 also showed no association with PLC (Tables 4, 5).

The phenotypes of NAT1 and NAT2 also showed no difference in frequencies between case group and control group (Table 6), suggesting that the phenotypes of NAT1 and NAT2 were not associated with PLC.

Interaction between NAT1 or NAT2 genotypes and environmental risk factors in development of PLC

The metabolism of carcinogenic arylamines in tobacco smoke, occupational exposure, fried food or meat is mediated

Table 4 Genotype frequencies of NAT1 in case group and control group

Genotypes	Cases (%)	Controls (%)	Total
NAT1*3/ *3	4 (4.2)	20 (11.5)	24
NAT1*3/ *4	24 (25.0)	30 (17.2)	54
NAT1*3/ *10	3 (3.1)	15 (8.6)	18
NAT1*3/ *14B	4 (4.2)	4 (2.3)	8
NAT1*4/ *4	30 (31.3)	50 (28.7)	80
NAT1*4/ *10	10 (10.4)	27 (15.5)	37
NAT1*4/ *14B	3 (3.1)	5 (2.9)	8
NAT1*10/ *10	14 (14.7)	19 (10.9)	33
NAT1*10/ *14B	4 (4.2)	4 (2.3)	8
Total	96 (100.0)	173 (100.0)	269

 $\chi^2 = 11.86$, $P > 0.05$.**Table 5** Genotype frequencies of NAT2 in case group and control group

Genotypes	Cases (%)	Controls (%)	Total
NAT2*4/ *4	57 (59.4)	100 (57.8)	157
NAT2*4/ *6	9 (9.4)	23 (13.3)	32
NAT2*4/ *7	15 (15.6)	28 (16.2)	43
NAT2*6/ *6	2 (2.1)	6 (3.5)	8
NAT2*6/ *7	8 (8.3)	12 (6.9)	20
NAT2*7/ *7	5 (5.2)	4 (2.3)	9
Total	96 (100.0)	173 (100.0)	269

 $\chi^2 = 2.94$, $P > 0.05$.**Table 6** Frequency distribution of phenotypes of NAT1 and NAT2 in case and control group

NAT phenotypes	Cases (%)	Controls (%)	Total
NAT1 rapid acetylators	31 (32.3)	64 (37.0)	95
NAT1 slow acetylators	65 (67.7)	109 (63.0) ¹	174
Total	96 (100.0)	173 (100.0)	269
NAT2 rapid acetylators	81 (84.4)	151 (87.3)	232
NAT2 slow acetylators	15 (15.6)	22 (12.7) ²	37
Total	96 (100.0)	173 (100.0)	269

¹ $\chi^2 = 0.598$, $P > 0.05$; ² $\chi^2 = 0.44$, $P > 0.05$.

by enzymes including NAT1 and NAT2. Both NAT1 and NAT2 are genotypically and phenotypically polymorphic with variable genotype frequencies in different ethnic groups.

In our case control study design, we classified all the environmental risk factors into two levels (0 and 1); then calculated odds ratios (OR) of different levels among both groups after setting down those without NAT1*10 and without exposures as referential baseline. We then judged the interaction between susceptible allele and environmental carcinogens. The results suggested that interaction between NAT1*10 and occupational exposures had statistical significance with an OR of 3.40 (Table 7). Interactions between NAT1*10 and other risk factors showed no statistical significance. We also analyzed relationship between HBV infection and NAT1*10, but failed to get positive result.

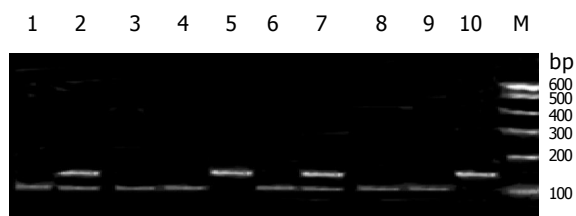


Figure 1 RFLP product of NAT1 C1095A site digested by *Alw26I*. Lanes 1, 3, 4, 6, 8, and 9: wild homozygotes; lanes 2, 7: heterozygotes; lanes 5, 10: mutant homozygotes; M: 100 bp DNA Ladder I; the fragments from up to down are 600, 500, 400, 300, 200 and 100 bp, respectively.

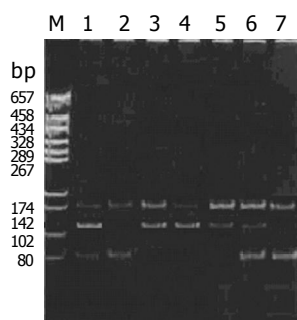


Figure 2 RFLP product of NAT1 G560A site digested by *HinfI*. Lanes 1, 6, 7: heterozygotes; lane 2: wild homozygote; lanes 3, 4, 5: mutant homozygotes; M: pGEM-7Zf(+) DNA/HaeIII Markers; the fragments from up to down are 657, 458, 434, 328, 289, 267, 174, 142, 102 and 80 bp.

As for NAT2, we analyzed interaction between NAT2 and environmental risk factors by case-only study. That is, in the case group, both genotypes and environmental risk factors were classified into two levels (0 and 1), then OR and its 95% CI were calculated. However, we failed to find any positive results. In addition, we applied case control study design method as the above for NAT1 to analyze the interaction between HBV infection and NAT1 or NAT2 genotypes. We found that there was no relationship between NAT1 genotypes and HBV infection. After being stratified by HBV infection, NAT2 genotypes were found to be related to PLC, which suggested that HBV infection interacted with NAT2 genotypes (Table 8). But it needed to be verified because the sample in each level was very small.

DISCUSSION

As an important enzyme involved in the phaseII biotransformation, NAT metabolically activates or inactivates aromatic amines through acetylation. NAT has two isozymes, NAT1 and NAT2. Both genes are located on human chromosome 8p21.3 and 8p23.1 respectively, and their coding area owns 87% homology.

To select a low incidence area of PLC in mainland China as research field to analyze the relationship between NAT1 and NAT2 genetic polymorphisms and PLC is a new attempt. We should explain that some of our cases had accepted

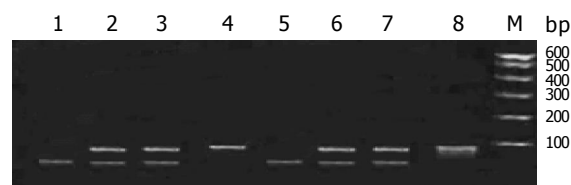


Figure 3 RFLP product of NAT1 T1088A site digested by *AseI*. Lanes 1, 5: wild homozygotes; lanes 2, 3, 6, 7: heterozygotes; lanes 4, 8: mutant homozygotes; M: 100 bp DNA Ladder I; the fragments from up to down are 600, 500, 400, 300, 200 and 100 bp respectively.

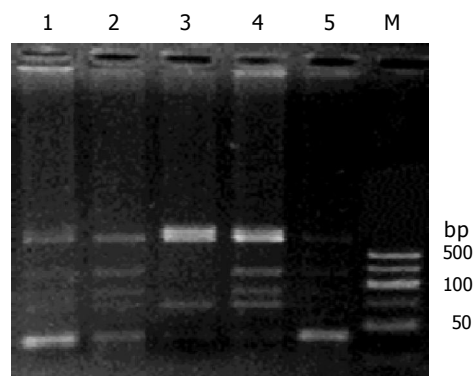


Figure 4 RFLP product of NAT2 G560A site digested by *TaqI*. Lanes 1, 4: NAT2*4/*6; lane 3: NAT2*6/*6; lanes 2, 5: NAT2*4/*4; M: 50 bp DNA Ladder; the fragments from up to down are 500, 300, 200, 150, 100 and 50 bp.

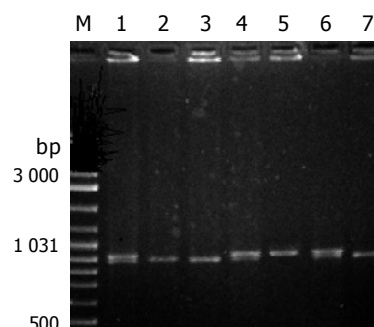


Figure 5 RFLP product of NAT2 G857A site digested by *BamHI*. Lanes 1, 4, 6: NAT2*4/*7; lane 5: NAT2*7/*7; lanes 2, 3, 7: NAT2*4/*4; M: DNA Ladder Mix; the fragments from up to down are 3 000, 2 000, 1 500, 1 200, 1 031, 900, 800, 700, 600 and 500 bp.

chemotherapy or radiotherapy before our research. Considering that genes are stable and not so changeable genetic substances, and reports showed that the null GSTM1 genotype frequency of HCC patients were not affected by chemotherapy or radiotherapy^[10], we did not take into account the effect of these two therapies on NAT genotypes. In this study, the genotype frequencies of NAT1 and NAT2 in the control group fit the Hardy-Weinberg equilibrium very well, suggesting that the study sample was good enough to represent the source communities of Luoyang city.

Compared with relevant research in Taiwan^[11], the frequencies of NAT1*3 and NAT2*4 alleles are higher, while frequency of NAT1*10 is lower in both groups than

Table 7 Interaction between occupational exposure and NAT1*10 allele

Occupational exposures	NAT1*10	Cases	Controls	OR	95%CI
-	-	51	124	1.00	
-	+	11	34	0.79	0.37-1.67
+	-	15	15	2.43	1.11-5.34
+	+	7	5	3.40	1.03-11.22

$\chi^2 = 8.42$, $P = 0.004$.

Table 8 Interaction between NAT2 genotypes and HBV infection

Genotypes	HBV infection (-)		HBV infection (+)	
	Cases	Controls	Cases	Controls
NAT2*4/*4	33	100	24	1
NAT2*4/*6	5	24	4	2
NAT2*4/*7	6	28	11	0
NAT2*6/*6	1	5	1	1
NAT2*7/*7	6	4	1	0
NAT2*6/*7	2	8	2	0

HBV infection (-): $\chi^2 = 8.26$, $P = 0.143$; HBV infection (+): $\chi^2 = 11.13$, $P = 0.049$.

those of Taiwanese. In the control group, the frequency of NAT2*6 is lower than those of Taiwanese. Other alleles are commonly the same between the two ethnic groups. This kind of similarity and difference suggest that NAT genetic polymorphisms could be variable in the same race but of different geographic areas.

Compared to other Chinese people, NAT1*3, NAT1*4 and NAT1*10 allele frequencies of Luoyang people showed little difference, while NAT2*4 and NAT2*6 showed much difference from them^[12,13]. Compared to other ethnic groups such as the whites, blacks or Japanese, the NAT1 and NAT2 alleles of Luoyang people are quite different^[14-16]. This means that different race or ethnic group owns different genetic composition.

NAT1*10 has been verified to be associated with many cancers and regarded as a high activity allele, whose phenotype is rapid NAT1 acetylators. While few reports could be found on PLC and NAT1 genetic polymorphism, Yu *et al*^[17] in Taiwan found that NAT1*10 is not associated with PLC. Our result supports the same argument. Besides, we found that those with NAT1*10 together with occupational exposure has an increased risk of PLC, and the OR is 3.40 (95%CI = 1.03-11.22). Although we failed to find literatures to support this finding, many reports have similar results when analyzing interactions between NAT1*10 and some risk factors in different cancers. For example, a six-fold of increased risk in colorectal adenoma was found among rapid NAT1 acetylators (with NAT1*10 allele) who consume high temperature cooking of red meats often and the OR is 6.50 (95%CI = 2.16-19.7)^[18,19]. The association of the NAT1*10 allele with breast cancer was mainly confirmed to former smokers (OR = 3.3, 95%CI = 1.2-9.5). All these suggest that NAT1 affect carcinogenic process through some way.

In this study, we find that NAT2 genetic polymorphisms are not susceptible to PLC. There are some arguments on their relationship however. Bian *et al*^[5] found that in PLC

high incidence area of China, slow NAT2 acetylators had an increased risk of PLC. Yu *et al*^[17] investigated all the HBV carriers in HCC cases and controls, finding that among smokers, for those with NAT2*4/*4 genotype, the odds ratio of developing HCC was 2.58 (95%CI, 1.04-6.43), for those with NAT2*4 allele, the OR was 2.67 (95%CI, 1.15-6.22), so they concluded that rapid NAT2 acetylators had an increased risk of HCC. Huang *et al*^[20] in Taiwan did not find association between the susceptibility of HCC and the overall NAT2 genotypes. However, the interaction between red meat intake and the NAT2*4 acetylators status for an increased risk of HCC was significant in those with chronic viral hepatitis-related cirrhosis. While Spanish researchers found that slow NAT2 acetylators were susceptible to HCC^[21], in Fujian Province of China, the smokers with slow acetylation genotype of NAT2 were found to be the population with high risk for HCC^[22]. These two conclusions are similar to that of Bian *et al*^[5]. In our study, slow acetylation genotype of NAT2 was not found to be a risk factor of PLC in Luoyang city, NAT2 genotypes did not interact with environmental risk factors. All of the above results suggest that NAT2 gene may play different roles in hepatocarcinogenesis between PLC high and low incidence areas, mainland China and Taiwan, or among different ethnic groups.

All of the different or similar findings lead to such interpretations: First, NAT1 and NAT2 genetic polymorphisms in low incidence area of PLC do have no association with PLC. Second, different regional or ethnic groups have different exposures to the environment, and the metabolism of carcinogens also involves a number of other enzymes, so it is impossible to explain the hepatocarcinogenesis by only genetic polymorphism of one enzyme and its interaction with environmental risk factors. Third, the sample of our study is not big enough to reveal the real truth of the relationship between NAT polymorphism and PLC.

Although most of our results were negative, our research gained the argument from a whole new perspective that NAT1 and NAT2 genes are not negligible in hepatocarcinogenesis study in different areas. Our study also revealed some new questions that need further worthwhile examination.

REFERENCES

- Murray CJ, Lopez AD. Mortality by cause for eight regions of the world: Global Burden of Disease Study. *Lancet* 1997; **349**: 1269-1276
- Tang ZY. Hepatocellular carcinoma-cause, treatment and metastasis. *World J Gastroenterol* 2001; **7**: 445-454
- Xiao KY, Peng MH. Advances in epidemiologic study of primary liver cancer. *Zhongguo Puwai Jichu Yu Linchuang Zazhi* 2000; **7**: 272-274
- Hein DW. N-Acetyltransferase genetics and their role in pre-disposition to aromatic and heterocyclic amine-induced carcinogenesis. *Toxicol Lett* 2000; **112-113**: 349-356
- Bian JC, Shen FM, Wang JB, Wu Y, Zhang BC. Relationship between genetic polymorphism of N-acetyltransferase and genetic susceptibility to primary hepatocellular carcinoma. *Zhonghua Yixue Yichuanxue Zazhi* 1997; **14**: 16-20
- Chinese Anti-Cancer Association. Diagnostic criteria for primary liver cancer. *Zhonghua Ganzangbing Zazhi* 2000; **8**: 135
- Deitz AC, Doll MA, Hein DW. A restriction fragment length polymorphism assay that differentiates human N-

- acetyltransferase-1 (NAT1) alleles. *Anal Biochem* 1997; **253**: 219-224
- 8 **Doll MA**, Fretland AJ, Deitz AC, Hein DW. Determination of human NAT2 acetylator genotype by restriction fragment-length polymorphism and allele-specific amplification. *Anal Biochem* 1995; **231**: 413-420
- 9 **Hein DW**, Leff MA, Ishibe N, Sinha R, Frazier HA, Doll MA, Xiao GH, Weinrich MC, Caporaso NE. Association of prostate cancer with rapid N-acetyltransferase 1 (NAT1*10) in combination with slow N-acetyltransferase 2 acetylator genotypes in a pilot case-control study. *Environ Mol Mutagen* 2002; **40**: 161-167
- 10 **Bian JC**, Wang JB, Wu Y, Zhang BC, Shen FM. Relationship between GSTM1 null genotype and genetic susceptibility to primary hepatocellular carcinoma. *Zhonghua Yixue Yichuanxue Zazhi* 1996; **13**: 353-356
- 11 **Hsieh FI**, Pu YS, Chern HD, Hsu LI, Chiou HY, Chen CJ. Genetic polymorphisms of N-acetyltransferase 1 and 2 and risk of cigarette smoking-related bladder cancer. *Br J Cancer* 1999; **81**: 537-541
- 12 **Zhao B**, Lee EJ, Yeoh PN, Gong NH. Detection of mutations and polymorphism of N-acetyltransferase 1 gene in Indian, Malay and Chinese populations. *Pharmacogenetics* 1998; **8**: 299-304
- 13 **Lee EJ**, Zhao B, Seow-Choen F. Relationship between polymorphism of N-acetyltransferase gene and susceptibility to colorectal carcinoma in a Chinese population. *Pharmacogenetics* 1998; **8**: 513-517
- 14 **Millikan RC**, Pittman GS, Newman B, Tse CK, Selmin O, Rockhill B, Savitz D, Moorman PG, Bell DA. Cigarette smoking, N-acetyltransferases 1 and 2, and breast cancer risk. *Cancer Epidemiol Biomarkers Prev* 1998; **7**: 371-378
- 15 **Bouchardy C**, Mitrunen K, Wikman H, Husgafvel-Pursiainen K, Dayer P, Benhamou S, Hirvonen A. N-acetyltransferase NAT1 and NAT2 genotypes and lung cancer risk. *Pharmacogenetics* 1998; **8**: 291-298
- 16 **Kato T**, Kaneko S, Boissy R, Watson M, Ikemura K, Bell DA. A pilot study testing the association between N-acetyltransferases 1 and 2 and risk of oral squamous cell carcinoma in Japanese people. *Carcinogenesis* 1998; **19**: 1803-1807
- 17 **Yu MW**, Pai CI, Yang SY, Hsiao TJ, Chang HC, Lin SM, Liaw YF, Chen PJ, Chen CJ. Role of N-acetyltransferase polymorphisms in hepatitis B related hepatocellular carcinoma: impact of smoking on risk. *Gut* 2000; **47**: 703-709
- 18 **Ishibe N**, Sinha R, Hein DW, Kulldorff M, Strickland P, Fretland AJ, Chow WH, Kadlubar FF, Lang NP, Rothman N. Genetic polymorphisms in heterocyclic amine metabolism and risk of colorectal adenomas. *Pharmacogenetics* 2002; **12**: 145-150
- 19 **Zheng W**, Deitz AC, Campbell DR, Wen WQ, Cerhan JR, Sellers TA, Folsom AR, Hein DW. N-acetyltransferase 1 genetic polymorphism, cigarette smoking, well-done meat intake, and breast cancer risk. *Cancer Epidemiol Biomarkers Prev* 1999; **8**: 233-239
- 20 **Huang YS**, Chern HD, Wu JC, Chao Y, Huang YH, Chang FY, Lee SD. Polymorphism of the N-acetyltransferase 2 gene, red meat intake, and the susceptibility of hepatocellular carcinoma. *Am J Gastroenterol* 2003; **98**: 1417-1422
- 21 **Agundez JA**, Olivera M, Ladero JM, Rodriguez-Lescure A, Ledesma MC, Diaz-Rubio M, Meyer UA, Benitez J. Increased risk for hepatocellular carcinoma in NAT2-slow acetylators and CYP2D6-rapid metabolizers. *Pharmacogenetics* 1996; **6**: 501-512
- 22 **Gao JP**, Huang YD, Lin JA, Zhu QC, Liang JP. Relationship between genetic polymorphisms of N-acetyltransferase and susceptibility to hepatocellular carcinoma. *Zhonghua Ganzhangbing Zazhi* 2003; **11**: 20-22

Edited by Li WZ Language Editor Elsevier HK

Identify lymphatic metastasis-associated genes in mouse hepatocarcinoma cell lines using gene chip

Bo Song, Jian-Wu Tang, Bo Wang, Xiao-Nan Cui, Li Hou, Lu Sun, Li-Min Mao, Chun-Hui Zhou, Yue Du, Li-Hui Wang, Hua-Xin Wang, Ren-Shu Zheng, Lei Sun

Bo Song, Jian-Wu Tang, Bo Wang, Xiao-Nan Cui, Li Hou, Li-Min Mao, Chun-Hui Zhou, Yue Du, Li-Hui Wang, Hua-Xin Wang, Ren-Shu Zheng, Lei Sun, Department of Pathology, Dalian Medical University, Dalian 116027, Liaoning Province, China
Lu Sun, Shanghai Jingtai Biotechnology Corporation Ltd, Shanghai 200000, China

Supported by the National Natural Science Foundation of China, No. 30371583

Correspondence to: Dr. Jian-Wu Tang, Department of Pathology, Dalian Medical University, Dalian 116027, Liaoning Province, China. yr0806@yahoo.com.cn

Telephone: +86-411-84720610 Fax: +86-411-84720610

Received: 2004-10-09 Accepted: 2004-11-19

Abstract

AIM: In order to obtain lymphogenous metastasis-associated genes, we compared the transcriptional profiles of mouse hepatocarcinoma cell lines Hca-F with highly lymphatic metastasis potential and Hca-P with low lymphatic metastasis potential.

METHODS: Total RNA was isolated from Hca-F and Hca-P cells and synthesized into double-stranded cDNA. *In vitro* transcription double-stranded cDNA was labeled with biotin (i.e., biotin-labeled cRNA, used as the probe). The cRNA probes hybridized with Affymetrix GeneChip® MOE430A (containing 22 690 transcripts, including 14 500 known mouse genes and 4 371 ESTs) respectively and the signals were scanned by the GeneArray Scanner. The results were then analyzed by bioinformatics.

RESULTS: Out of the 14 500 known genes investigated, 110 (0.8%) were up regulated at least 2³ fold. Among the total 4 371 ESTs, 17 ESTs (0.4%) (data were not presented) were up regulated at least 2³ fold. According to the Gene Ontology and TreeView analysis, the 110 genes were further classified into two groups: differential biological process profile and molecular function profile.

CONCLUSION: Using high-throughput gene chip method, a large number of genes and their cellular functions about angiogenesis, cell adhesion, signal transduction, cell motility, transport, microtubule-based process, cytoskeleton organization and biogenesis, cell cycle, transcription, chaperone activity, motor activity, protein kinase activity, receptor binding and protein binding might be involved in the process of lymphatic metastasis and deserve to be used as potential candidates for further investigation. Cyclin D1, Fos11, Hsp47, EGFR and AR, and Cav-1 are

selected as the possible candidate genes of the metastatic phenotype, which need to be validated in later experiments. ESTs (data were not presented) might indicate novel genes associated with lymphatic metastasis. Validating the function of these genes is helpful to identify the key or candidate gene/pathway responsible for lymphatic metastasis, which might be used as the diagnostic markers and the therapeutic targets for lymphatic metastasis.

© 2005 The WJG Press and Elsevier Inc. All rights reserved.

Key words: Hepatocarcinoma; Lymphatic metastasis; Cell lines Hca-F and Hca-P; Gene chip

Song B, Tang JW, Wang B, Cui XN, Hou L, Sun L, Mao LM, Zhou CH, Du Y, Wang LH, Wang HX, Zheng RS, Sun L. Identify lymphatic metastasis-associated genes in mouse hepatocarcinoma cell lines using gene chip. *World J Gastroenterol* 2005; 11(10): 1463-1472

<http://www.wjgnet.com/1007-9327/11/1463.asp>

INTRODUCTION

Metastasis is the major cause of cancer morbidity and mortality^[1]. Metastasis formation is a complex process, involving invasion, transport, arrest, adherence, extravasation and tumor cell proliferation^[2]. High-throughput methods are needed to display the molecular changes involved in this complicated series of steps. Recent development of cDNA microarray technology has opened a new era in this field^[3]. It can provide massive datasets simultaneously. Except this, suitable models for cancer metastasis are necessary for analysis of mechanisms^[4]. Because majority of malignant tumors are carcinomas and lymph node metastases often represent the first step in the metastatic process, whereas the molecular mechanism of lymphatic metastasis remains poorly understood, the clones of lymphatic metastasis are prone to be established. A mouse hepatocarcinoma cell line named Hca-F with highly lymphogenous metastatic potential and its syngeneic cell line named Hca-P^[5] with low lymphogenous metastatic potential have been isolated from hepatocarcinomas in mice. Using gene chip combination with lymphatic metastasis models, we investigated the transcriptional profiles of the mouse hepatocarcinoma cell lines Hca-F with a metastasis rate over 70% and its syngeneic cell line Hca-P with a metastasis rate less than 30% in order to identify lymphatic metastasis-associated genes. Although several metastasis-associated genes have already been

screened with these two cell lines using suppression subtractive hybridization method, we decided to detect the expression profiles of cell lines Hca-F and Hca-P using Affymetrix Genechip® array technology in purpose of extending the panel of candidate genes.

MATERIALS AND METHODS

Animals and cell lines

Hepatocarcinoma cell lines, Hca-F and Hca-P were established and stored by our department. Inbred 615-mice were bred and provided by our department. Forty 615-mice were equally divided into two groups. Hca-F and Hca-P cells were inoculated into 20 mice in each group respectively (2×10^6 cells per mouse). On the 28th d after inoculation, mice were killed and their lymph nodes were collected and stained using HE and examined by light microscope. Then the lymph node metastasis rates of Hca-F and Hca-P cell lines were calculated and tested.

RNA collection and probe preparation for oligonucleotide array hybridization

Total RNA was isolated from Hca-F and Hca-P cells respectively using TRIzol reagent (Invitrogen Life Technologies, P/N 15596-018) and cleaned with Rneasy Mini Kit (Qiagen, P/N 74104). cDNA was synthesized using the T7-Oligo(dT)₂₄ primer (5'-GGCCAGTGAATTGT AATACGACTCACTATAGGGAGGCGG-(dT)₂₄-3'). Double-stranded cDNA was purified with Phase Lock Gel (Eppendorf, P/N 0032 007.953)-phenol/chloroform extraction (Ambion, P/N 9732). Then *in vitro* transcription labeling was performed using the Enzo RNA Transcript Labeling Kit (Affymetrix, P/N 900182). The biotin-labeled cRNA was purified with the Qiagen Rneasy Mini Kit and fragmented randomly to an average size of approximately 50-200 bases by mild alkaline treatment at 94 °C for 35 min in fragmentation buffer. The hybridization solution was composed of 0.05 µg/µL fragmented cRNA, 1 µL herring sperm DNA, 1 µL acetylated BSA and 50 µL 2× hybridization buffer. In addition, the hybridization solution contained a mixture of four control cRNAs for bacterial and phage genes (bioB, bioC, bioD and cre at 5, 5, 25 and 100 pmol/L, respectively) to serve as comparison tools for hybridization efficiency between arrays. A biotinylated oligonucleotide B2, which specifically hybridized to features at the center and corners of the chip, was also added to the solution to allow correct orientation and recognition of the probe sets.

Array hybridization and scanning

The hybridization cocktail was heated to 99 °C for 5 min in a heat block, followed by a 45 °C heat block for 5 min and centrifugation for 5 min to remove any insoluble material. Meanwhile, the arrays were wet with appropriate volume 1× hybridization and incubated by 1× hybridization buffer at 45 °C for 10 min with rotation. The buffer solution was then removed from the probe array and the clarified-hybridization cocktail was added. Fragmented cRNA (5 µg) was hybridized to Affymetrix MOE430A array (containing 22 690 transcripts, almost 14 500 known genes and 4 371

ESTs) for 16 h in Affymetrix®Fluidics Station 400. The arrays were then scanned using the GeneArray Scanner (G2500AgeneArray Scanner, Affymetrix). The cRNA probe was first hybridized to a “test chip” before to the MOE430A array and the quality was confirmed.

Statistical analysis

The data obtained through GeneChip® scanning was analyzed using Affymetrix® Microarray Suit Software 5.0^[6,7]. Before the two arrays were compared, the GeneChip® software conducted normalization and scaling of the data for each array. The mRNA expression level of a transcript is directly related to the signal which is a quantitative metric calculated for each probe set and measures the mean difference of fluorescence intensity between perfect match and central mismatch oligonucleotides of a probe set. Signal log ratio, which estimates the magnitude and direction of change of a transcript when two arrays are compared, of at least three (that indicates an increase of the transcript level by 2³-fold change), and changing *P*-value, which measures the probability that the expression levels of a probe set in two different arrays are the same or not, ≤ 0.05 (that means the expression level in the experiment array is higher than that of the baseline array) were used to select differentially expressed genes. In the following, only up-regulated genes were presented and the assignment “up-regulated” refers to Hca-F in comparison with Hca-P.

RESULTS

The lymph node metastasis rates of Hca-F and Hca-P were 75% (15/20) and 25% (5/20), respectively. The quality of GeneChip® was tested and verified by the positive controls of murine housekeepers β -actin and GAPDH and externally positive controls of spiked bacterial bioB, bioC, bioD and cre (Figure 1). Figure 2A, B indicate the scanning result of real chip (Hca-F and Hca-P, respectively). Figure 3 indicates the comparison of gene expression signal in cell line Hca-F with Hca-P.

To identify genes associated with the lymphatic metastasis, we analyzed the transcriptional profiles of 14 500 mouse genes and 4 371 ESTs from highly lymphatic metastasis potential cell line Hca-F and low lymphatic metastasis potential cell line Hca-P using the Affymetrix GeneChip® array method. On the basis of the selection criteria for up-regulated described above, 110 genes (132 transcripts) and 17 ESTs (21 transcripts) (data were not presented) were obtained. The results about differentially expressed genes are presented in Table 1.

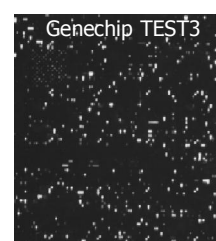


Figure 1 Scanning result of test chip.

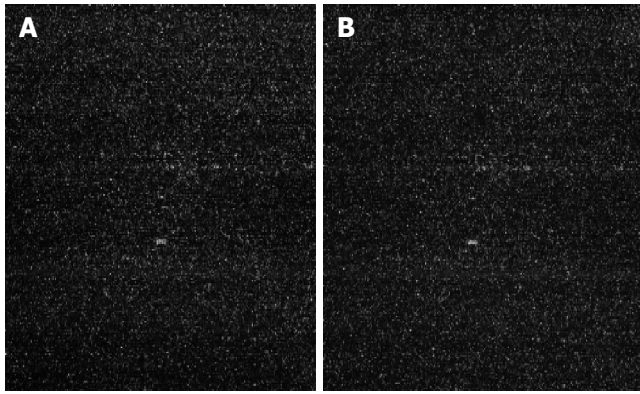


Figure 2 (A) Scanning result of real chip after hybridization with cRNA from Hca-F cell line; (B) Scanning result of real chip after hybridization with cRNA from Hca-P cell line.

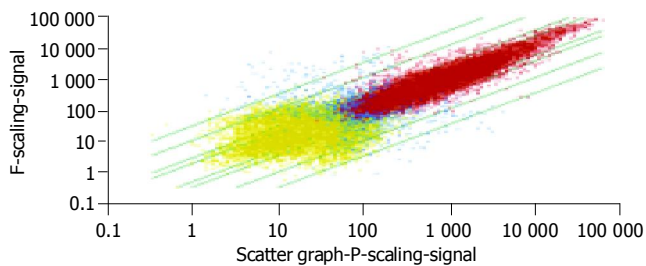


Figure 3 Comparison of gene expression signal in Hca-F cell line with that in Hca-P cell line.

Table 1 Differential gene expression profile in cell lines Hca-F vs Hca-P

Gene	Symbol descriptions	F vs P_Signal log ratio
Slc38a4	Solute carrier family 38, member 4	
	¹ gb: NM_027052	9
	gb: AK003626	3.4
Krt2-8	Keratin complex 2, basic, gene 8	
	gb: M21836	8.6
	gb: NM_031170	4.8
Krt1-19	Keratin complex 1, acidic, gene 19	7.4
Cldn9	Claudin 9	7.4
Gja1	Gap junction membrane channel protein alpha 1	
	gb: M63801	7.2
	gb: BC006894	6.4
Fbp2	Fructose biphosphatase 2	7.1
R75183	Expressed sequence R75183	
	gb: BC004774	7
	gb: BB324973	5.5
Egfr	Epidermal growth factor receptor	
	gb: AF275367	6.9
	gb: U03425	3.6
Lepr	Leptin receptor	6.7
Tm4sf3	Transmembrane 4 superfamily member 3	6.5
Pla2g1b	Phospholipase A2, group IB, pancreas	6.4
Ripk3	Receptor-interacting serine-threonine kinase 3	6.4
Igfbp4	Insulin-like growth factor binding protein 4	
	gb: NM_010517	6.3
	gb: BC019836 ² 1423756_s_at	5.8
	gb: BC019836 1423757_x_at	4.1
	gb: AA119124	4
Piwi2	Piwi-like homolog 2 (Drosophila)	6.3

IL24	Interleukin 24	5.9
Daf1	Decay accelerating factor 1	5.9
Cav	Caveolin, caveolae protein	5.8
Arhgef3	Rho guanine nucleotide exchange factor (GEF) 3	5.7
Efna1	Ephrin A1	
	gb: D38146	5.7
	gb: BC002046	4.2
Ptpn8	Protein tyrosine phosphatase, non-receptor type 8	5.6
Rab3b	RAB3B, member RAS oncogene family	5.6
1190003K14Rik	RIKEN cDNA 1190003K14 gene	5.6
Sh3bp5	SH3-domain binding protein 5 (BTK-associated)	5.5
Fscn1	Fascin homolog 1, actin bundling protein (Strongylocentrotus purpuratus)	
	gb: NM_007984 1416514_a_at	5.4
	gb: BE952057	4.2
	gb: NM_007984 1448378_at	3.7
Fgf15	Fibroblast growth factor 15	5.4
Ehox	ES cell derived homeobox containing gene	5.3
Ankrd1	Ankyrin repeat domain 1 (cardiac muscle)	
	gb: NM_013468	5.3
	gb: AK009959	3.6
1600023A02Rik	RIKEN cDNA 1600023A02 gene	5.3
Cd109	CD109 antigen	5.3
BC037006	cDNA sequence BC037006	5.3
Ltb4dh	Leukotriene B4 12-hydroxydehydrogenase	5.2
Krt2-7	Keratin complex 2, basic, gene 7	5.2
Cnn2	Calponin 2	5.2
Sema3b	Sema domain, immunoglobulin domain (Ig), short basic domain, secreted, (semaphorin) 3B	
	gb: BB116052	5.1
	gb: NM_009153	4.7
Krt1-18	Keratin complex 1, acidic, gene 18	5.1
...	Mouse gene for 18S rRNA	5.1
Fos1	Fos-like antigen 1	
	gb: NM_010235	5
	gb: U34245	4.4
Sncg	Synuclein, gamma	5
Col8a1	Procollagen, type VIII, alpha 1	4.9
Pcdhb7	Protocadherin beta 7	4.9
Msln	Mesothelin	4.9
IL23a	Interleukin 23, alpha subunit p19	4.9
...	Mus musculus adult male tongue cDNA	4.8
Ppp1r14a	Protein phosphatase 1, regulatory (inhibitor) subunit 14A	4.7
Csf3	Colony stimulating factor 3 (granulocyte)	4.7
Nfil3	Nuclear factor, interleukin 3, regulated	4.6
Procr	Protein C receptor, endothelial	4.6
Nr1d1	Nuclear receptor subfamily 1, group D, member 1	4.6
2810003C17Rik	RIKEN cDNA 2810003C17 gene	4.6
MGC27770	Hypothetical protein MGC27770	4.5
Eng	Endoglin	4.5
F2r	Coagulation factor II (thrombin) receptor	4.5
Cdc42ep5	CDC42 effector protein (Rho GTPase binding) 5	4.4
Pla2g7	Phospholipase A2, group VII (platelet-activating factor acetylhydrolase, plasma)	4.4
D18Erttd653e	DNA segment, Chr 18, ERATO Doi 653, expressed	4.4
IL2rg	Interleukin 2 receptor, gamma chain	

	gb: L20048 1416296_at	4.3
	gb: L20048 1416295_a_at	3.3
Smpd2	Sphingomyelin phosphodiesterase 2, neutral	4.3
Areg	Amphiregulin	4.3
Mcam	Melanoma cell adhesion molecule	4.2
Rtn2	Reticulon 2 (Z-band associated protein)	4.2
Gcnt2	Glucosaminyltransferase, I-branching enzyme	4.2
D7Ert458e	DNA segment, Chr 7, ERATO Doi 458, expressed	
	gb: NM_009310	4.2
	gb: BB049138 1423904_a_at	4
	gb: BC013673 1451160_s_at	4
	gb: BB049138 1423905_at	3.9
	gb: BC013673 1423903_at	3.8
Chi3l3	Chitinase 3-like 3	4.1
D4Ert4765e	DNA segment, Chr 4, ERATO Doi 765, expressed	4.1
Ptprr	Protein tyrosine phosphatase, receptor type, R	4.1
Scn8a	Sodium channel, voltage-gated, type VIII, alpha polypeptide	4
AXL	AXL receptor tyrosine kinase	4
Serpinh1	Serine (or cysteine) proteinase inhibitor, clade H, member 1	4
Panx1	Pannexin1	3.9
Tm4sf9	Transmembrane 4 superfamily member 9	3.9
Mak	Male germ cell-associated kinase	3.9
...	Mus musculus transcribed sequences	3.8
9130017N09Rik	RIKEN cDNA 9130017N09 gene	3.8
Lox12	Lysyl oxidase-like 2	3.7
Dok1	Downstream of tyrosine kinase 1	3.6
Abhd3	Abhydrolase domain containing 3	3.6
Ramp3	Receptor (calcitonin) activity modifying protein 3	3.6
Fibp	Fibroblast growth factor (acidic) intracellular binding protein	3.6
Wscr5	Williams-Beuren syndrome chromosome region 5 homolog (human)	3.6
Eppk1	Epiplakin 1	3.6
2010004A03Rik	RIKEN cDNA 2010004A03 gene	3.6
Itgb5	Integrin beta 5	
	gb: NM_010580 1417534_at	3.5
	gb: NM_010580 1417533_a_at	3.3
Mlf1	Myeloid leukemia factor 1	3.5
Tnfrsf22	Tumor necrosis factor receptor superfamily, member 22	3.5
Zdhhc2	Zinc finger, DHHC domain containing 2	3.5
Tnfaip2	Tumor necrosis factor, alpha-induced protein 2	3.4
Rrad	Ras-related associated with diabetes	3.4
A530090O15Rik	RIKEN cDNA A530090O15 gene	3.4
Chi3l4	Chitinase 3-like 4	3.4
Tnfrsf19	Tumor necrosis factor receptor superfamily, member 19	3.4
Myo1b	Myosin IB	
	gb: AI255256	3.4
	gb: BI080370	3.2
Tuba4	Tubulin, alpha 4	3.3
Myo1g	Myosin IG	3.3
Siat10	Sialyltransferase 10 (alpha-2,3-sialyltransferase VI)	3.3
Nol3	Nucleolar protein 3 (apoptosis repressor with CARD domain)	3.3
Tpt1h	tRNA splicing 2' phosphotransferase 1 homolog (S. cerevisiae)	3.3
Igfbp6	Insulin-like growth factor binding protein 6	3.3
Ccnd1	Cyclin D1	
	gb: M64403	3.2
	gb: NM_007631	3.1
BC003236	cDNA sequence BC003236	3.2
2010001C09Rik	RIKEN cDNA 2010001C09 gene	3.2

Chst1	Carbohydrate (keratan sulfate Gal-6) sulfotransferase 1	3.2
Timp1	Tissue inhibitor of metalloproteinase 1	3.2
4921530G04Rik	RIKEN cDNA 4921530G04 gene	3.2
Lxn	Latexin	3.1
Sgk2	Serum/ glucocorticoid regulated kinase 2	3.1
2310047E01Rik	RIKEN cDNA 2310047E01 gene	3.1
2200002N01Rik	RIKEN cDNA 2200002N01 gene	3
Ptpre	Protein tyrosine phosphatase, receptor type, E	3
Psm8	Proteasome (prosome, macropain) subunit, beta type 8 (large multifunctional protease 7)	3
Tm7sf1	Transmembrane 7 superfamily member 1	3

¹Accession number of each gene obtained from PubMed; ²Affymetrix probe identification number.

According to the Gene Ontology (GO) classification and TreeView analysis, the genes are further divided into two groups: differential biological process profile and molecular function profile, as shown respectively in Tables 2, 3. Biological process refers to a biological objective to which the gene or gene product contributes. Molecular function is defined as the biochemical activity (including specific binding to ligands or structures) of a gene product^[8].

Table 2 Differential biological process profile in cell lines Hca-F vs Hca-P

Development					
Itgb5	gb: NM_010580 1417533_a_at	3.3	Ccnd1	gb: M64403	3.2
Mlf1	gb: NM_010580 1417534_at	3.5		gb: NM_007631	3.1
Morphogenesis					
Gja1	gb: BC006894	6.4	Sema3b	gb: BB116052	5.1
	gb: M63801	7.2		gb: NM_009153	4.7
Tnfaip2		3.4	Tm4sf9		3.9
Igfbp6		3.3	Igfbp4	gb: NM_010517	6.3
Egfr	gb: AF275367	6.9		gb: AA119124	4
	gb: U03425	3.6		gb: BC019836 1423756_s_at	5.8
Efna1	gb: D38146	5.7		gb: BC019836 1423757_x_at	4.1
	gb: BC002046	4.2	Eng		4.5
Cellular process					
Cell communication					
Cell adhesion					
Mcam		4.2	Itgb5	gb: NM_010580 1417533_a_at	3.3
Tm4sf9	3.9			gb: NM_010580 1417534_at	3.5
D7Ert458e	gb: BC013673 1423903_at	3.8	Col8a1		4.9
	gb: BB049138 1423904_a_at	4	Eng		4.5
	gb: BB049138 1423905_at	3.9	Pcdhb7		4.9
	gb: NM_009310	4.2			
	gb: BC013673 1451160_s_at	4			
Cell-cell signaling					
Gja1	gb: BC006894	6.4			
	gb: M63801	7.2			
Signal transduction					
IL2rg	gb: L20048 1416295_a_at	3.3	Efna1	gb: BC002046	4.2
	gb: L20048 1416296_at	4.3		gb: D38146	5.7
Itgb5	gb: NM_010580 1417533_a_at	3.3	Egfr	gb: AF275367	6.9
	gb: NM_010580 1417534_at	3.5		gb: U03425	3.6
Dok1		3.6	Fgf15		5.4
Ptpre		3	Cdc42ep5		4.4
Ramp3		3.6	Sh3bp5		5.5
Lepr		6.7	Ptprr		4.1
Eng		4.5	Ripk3		6.4

F2r	4.5	R75183	gb: BC004774	7	Nucleobase, nucleoside, nucleotide and nucleic acid metabolism					
Rrad	3.3		gb: BB324973	5.5	Nol3	3.3	Lepr		6.7	
Rab3b	5.6				Transcription					
<i>Cellular physiological process</i>					Fosl1	gb: NM_010235	5	Ankrd1	gb: NM_013468	5.3
Cell death						gb: U34245	4.4		gb: AK009959	3.6
Ripk3	6.4		Nol3	3.3	Nfil3		4.6	Nr1d1		4.6
Cell motility					<i>Regulation of physiological process</i>					
Tm4sf9	3.9	D7Ert458e	gb: BC013673	1423903_at	3.8	Gja1	gb: BC006894	6.4	Procr	4.6
Cnn2	5.2		gb: BB049138	1423904_a_at	4		gb: M63801	7.2		
			gb: BB049138	1423905_at	3.9	<i>Coagulation</i>				
			gb: NM_009310	4.2	Procr		4.6	F2r		4.5
			gb: BC013673	1451160_s_at	4	<i>Organismal physiological process</i>				
Cell growth and/or maintenance					Chi3l3		4.1	Chi3l4		3.4
Transport					Csf3		4.7	Daf1		5.9
Tuba4	3.3	Slc38a4	gb: NM_027052	9	F2r		4.5	Gja1	gb: BC006894	6.4
Ramp3	3.6		gb: AK003626	3.4	IL24		5.9		gb: M63801	7.2
Rab3b	5.6	Cav		5.8	Pla2g7		4.4	Procr		4.6
Scn8a	4				... Mus musculus					
Cell organization and biogenesis					transcribed sequences		3.8	Psmb8		3
Igfbp6	3.3	Igfbp4	gb: NM_010517	6.3	<i>Response to stimulus</i>					
Egfr	gb: AF275367		gb: AA119124	4	Chi3l3		4.1	Chi3l4		3.4
	gb: U03425		gb: BC019836	1423756_s_at	5.8	Csf3		4.7	Daf1	5.9
...	AFFX-18SRNAMur/X00686_M_at	5.1	gb: BC019836	1423757_x_at	4.1	F2r		4.5	IL24	5.9
Microtubule-based process					Gja1	gb: BC006894	6.4	Krt2-8	gb: NM_031170	4.8
Tua4	3.3					gb: M63801	7.2		gb: M21836	8.6
Cytoskeleton organization and biogenesis					Pla2g1b		6.4	Pla2g7		4.4
Krt1-19	7.4	Krt2-8	gb: M21836	8.6	Psmb8		3	Serpinh1		4
Tuba4	3.3		gb: NM_031170	4.8	... Mus musculus					
Krt2-7	5.2	Myo1b	gb: AI255256	3.4	transcribed sequences		3.8			
Krt1-18	5.1		gb: BI080370	3.2						
<hr/>										
Table 3 Differential molecular function profile in cell lines Hca-F vs Hca-P										
<hr/>										
Transporter activity										
Gja1	gb: BC006894	6.4						Slc38a4	gb: AK003626	3.4
	gb: M63801	7.2							gb: NM_027052	9
Ramp3		3.6						Rab3b		5.6
Scn8a		4								
Tptih		3.3								
Structural molecule activity										
Eppk1		3.6						Cldn9		7.4
Col8a1		4.9						Krt1-19		7.4
Tuba4		3.3						Krt2-7		5.2
Krt2-8	gb: NM_031170	4.8						Krt1-18		5.1
	gb: M21836	8.6								
Chaperone activity										
Serpinh1		4						Sncg		5
Motor activity										
Myo1b	gb: BI080370	3.2						Myo1g		3.3
	gb: AI255256	3.4								
Catalytic activity										
Gcnt2		4.2						Siat10		3.3
Chst1		3.2						Lox12		3.7
Ltb4dh		5.2						2310047E01Rik		3.1
<i>Hydrolase activity</i>										
Pla2g1b		6.4						Smpd2		4.3
Abhd3		3.6						Ptpn8		5.6
Ptpre		3						Chi3l3		4.1
Rrad		3.4						Rab3b		5.6
Chi3l4		3.4						Ptprr		4.1
Pla2g7		4.4						Fbp2		7.1
Psmb8		3								
<i>Kinase activity</i>										
Ccnd1	gb: M64403	3.2						Krt2-8	gb: NM_031170	4.8
	gb: NM_007631	3.1							gb: M21836	8.6
A530090O15Rik		3.4								
Protein-tyrosine kinase activity										
Sgk2		3.1						Egfr	gb: AF275367	6.9

Axl	4	gb: U03425	3.6
Ripk3	6.4		
Transmembrane receptor protein kinase activity			
Egfr	gb: AF275367 6.9		
	gb: U03425 3.6		
Protein serine/threonine kinase activity			
Sgk2	3.1	Mak	3.9
Axl	4	Egfr	gb: AF275367 6.9
Ripk3	6.4		gb: U03425 3.6
Transferase activity			
A530090O15Rik	3.4	Axl	4
Ccnd1	gb: M64403 3.2	Egfr	gb: AF275367 6.9
	gb: NM_007631 3.1		gb: U03425 3.6
Chst1	3.2	Gcnt2	4.2
Krt2-8	gb: NM_031170 4.8	Mak	3.9
	gb: M21836 8.6	Ripk3	6.4
Sgk2	3.1	Siat10	3.3
Enzyme regulator activity			
Ccnd1	gb: M64403 3.2	Lxn	3.1
	gb: NM_007631 3.1	Timp1	3.2
Sh3bp5	5.5	Cd109	5.9
1600023A02Rik	5.3	Serpinh1	4
Binding			
Nucleic acid binding			
Fosl1	gb: NM_010235 5	Ankrd1	gb: NM_013468 5.3
	gb: U34245 4.3		gb: AK009959 3.6
Nr1d1	4.6		
Metal ion binding			
Pla2g1b	6.4	Smpd2	4.3
Ltb4dh	5.2	Scn8a	4
2310047E01Rik	3.1	Pcdhb7	4.9
2810003C17Rik	4.6	Loxl2	3.7
Zdhc2	3.5		
Nucleotide binding			
A530090O15Rik	3.4	Axl	4
Egfr	gb: AF275367 6.9	Krt2-8	gb: NM_031170 4.8
	gb: U03425 3.6		gb: M21836 8.6
Mak	3.9	Rab3b	5.6
Myo1b	gb: BI080370 3.2	Ripk3	6.4
	gb: AI255256 3.4	Rrad	3.4
Scn8a	4	Sgk2	3.1
Tuba4	3.3		
Receptor binding			
Areg	4.3	Csf3	4.7
Dok1	3.6	Fgf15	5.4
Il24	5.9	Pla2g1b	6.4
Protein binding			
Ankrd1	gb: NM_013468 5.3	Ccnd1	gb: M64403 3.2
	gb: AK009959 3.6		gb: NM_007631 3.1
Cav	5.8	Cdc42ep5	4.4
Col8a1	4.9	Eng	4.5
D7Ert458e			
	gb: BC013673 1423903_at 3.8	Egfr	gb: AF275367 6.9
	gb: BB049138 1423904_a_at 4		gb: U03425 3.6
	gb: BB049138 1423905_at 3.9	Fibp	3.6
	gb: NM_009310 4.2	Il2rg	gb: L20048 1416295_a_at 3.3
	gb: BC013673 1451160_s_at 4		gb: L20048 1416296_at 4.3
Itgb5	gb: NM_010580 3.5	Igfbp6	3.3
	gb: NM_010580 3.3	Lepr	6.7
Nol3	3.3	Pcdhb7	4.9
Procr	4.6	Ptpre	3
Rab3b	5.6	Rrad	3.4
Sh3bp5	5.5	Tnfrsf22	3.5
Fscn1	gb: NM_007984 1416514_a_at 5.4	Myo1b	gb: BI080370 3.2
	gb: BE952057 4.2		gb: AI255256 3.4
	gb: NM_007984 1448378_at 3.7	Cnn2	5.2
Carbohydrate binding			
Chi3l3	4.1	Chi3l4	3.4
Signal transducer activity			

Dok1	3.6	Ripk3	6.4
Receptor activity			
Axl	4	Itgb5	gb: NM_010580.1 3.5
D7Ert458e	gb: BC013673 1423903_at 3.8		gb: NM_010580.1 3.3
	gb: BB049138 1423904_a_at 4	Nr1d1	4.6
	gb: BB049138 1423905_at 3.9	Procr	4.6
	gb: NM_009310 4.2	Ptpn8	5.6
	gb: BC013673 1451160_s_at 4	Ptprr	4.1
Ramp3	3.6	Tnfrsf19	3.4
Tnfrsf22	3.5	Lepr	6.7
Il2rg	gb: L20048.1 1416295_a_at 3.3	Egfr	gb: AF275367.1 6.9
	gb: L20048.1 1416296_at 4.3		gb: U03425.1 3.6
F2r	4.5		

DISCUSSION

We used an Affymetrix GeneChip® MOE430A to identify lymphatic metastasis-associated genes in two hepatocarcinoma cell lines with different lymphatic metastasis potential. Based on the selection criteria for up-regulated expression discussed in “MATERIALS AND METHODS”, 110 differential genes were observed in the highly lymphogenous metastatic cell line. The over expressed genes were then classified according to the GO classification and TreeView analysis.

In the category development, we found three genes associated with angiogenesis: endoglin (EDG; CD105), ephrin A1 and Tnfaip2. Tumor angiogenesis plays an important role in tumor growth and metastasis^[9] and certain angiogenesis markers may be useful as metastasis markers and/or the targets for antiangiogenic therapy^[10]. EDG was thought to be a proliferation-associated antigen of endothelial cells and essential for angiogenesis. Elevated serum EDG was associated with metastasis in patients with colorectal, breast, and other solid tumors and chemotherapy exerts a suppression effect on the serum EDG^[11,12]. In endometrial carcinoma, EDG counts correlated significantly with the presence of angiolymphatic invasion, lymph nodes metastasis and tumor stage^[9]. Ephrin-A1, formerly called B61, was found to be up-regulated during melanoma progression and implicated in angiogenesis^[13,14]. Tnfaip2 (B94), originally identified as a tumor necrosis factor alpha-inducible gene in endothelial cells, was highly expressed in marrow from patients with acute myelogenous leukemia French-American-British subtypes M₀-M₂^[15], but its correlation with metastasis requires to be elucidated.

Adaptation of cell adhesion functions of the tumor cells to successfully overcome the different hurdles in the metastatic cascade is a prerequisite for metastasis^[16]. We noted up-regulation of MCAM (CD146; Mel-CAM; Muc18) in Hca-F cell line. Mcam, a member of the immunoglobulin superfamily and homologous to several cell adhesion molecules, was associated with tumor progression and the development of metastasis in human malignant melanoma and also was an important determinant in increasing metastasis of human prostate cancer LNCaP cells to distant organs in a nude mouse model^[17-19]. We also noted over expression of integrin β5, Col8A1 (procollagen, type VIII, alpha 1) and Pcdhb7 (protocadherin beta) in the Hca-F cell line.

In the category signal transduction, we observed up-

regulation of Cdc42ep5 (CEP5; Borg3), Rab3b, Lepr (leptin receptor), Ptprr (protein tyrosine phosphatase, receptor type, R) and F2r (coagulation factor II (thrombin) receptor; Par1; ThrR). Cdc42ep5, one member of CEPs which acts downstream of Cdc42 to induce actin filament assembly leading to cell shape changes, induced pseudopodia formation in NIH-3T3 fibroblasts^[20]. In tumor, it might promote the ability of invasiveness and metastasis. In the highly lymphogenous metastatic pancreatic carcinoma cell line BSp73-ASML, the ras-related rab proteins and protein tyrosine phosphatases were all over expressed^[16]. Lepr positive correlated significantly with distant metastasis and lower survival in breast cancer^[21]. F2r, protease-activated receptor 1, a G protein-coupled receptor for thrombin, was shown to be preferentially expressed in highly lymphogenous metastatic pancreatic carcinoma cell line BSp73-ASML^[16] and correlated with breast carcinoma cell invasion and metastasis^[22,23]. Booden *et al*^[24] also reported that altered trafficking of proteolytically activated PAR1 (F2r) caused sustained activation of phosphoinositide hydrolysis and extracellular signal-regulated kinase signaling, even after thrombin withdrawal, and enhanced breast carcinoma cellular invasion.

The ability to locomote and migrate is fundamental to the acquisition of invasive and metastatic properties by tumor cells^[25]. D7Ertd458e (necl-5), one of the five nectin-like molecules (necls), which have domain structures similar to those of nectins, has recently been identified and appears to play different roles from those of nectins. Experiments showed that enhanced motility and metastasis of V12Ras-NIH3T3 cells (NIH3T3 cells transformed by an oncogenic Ki-Ras) were at least partly the result of up-regulated Necl-5, which does not homophilically trans-interact, but heterophilically trans-interacts with nectin-3, regulates cell migration and adhesion^[26,27].

In the category transport, Slc38a4 was detected to overexpress in the highly metastatic cell line. Recent work has considered SLC38 transporters as therapeutic targets in neoplasia^[28]. Although to date Slc38a4 has not been reported to be correlated with tumor metastasis straightly, the member of the solute carrier family SLC35, which encodes nucleotide sugar transporters, has been shown to be involved in tumor metastasis^[29] and SLC16 and SLC2 were up-regulated in highly lymphogenous metastatic pancreatic carcinoma cell line BSp73-ASML^[16]. Meanwhile, the reason Slc38a4 deserves further attention is that it differs most in our study.

The state of tubulin polymerization associates with tumor metastasis and increased depolymerized form of tubulin could promote metastasis. We noted Tuba4 over expression in Hca-F cell line. Changes in the expression of genes for the cytoskeleton organization and biogenesis mediate adaptation to increased motility and invasion of the metastatic tumor cell^[16]. Krt1-19 (keratin 19), Krt1-18 (keratin 18), Krt2-7 (keratin 7) and Krt2-8 (keratin 8) were up regulated in the highly metastatic cell line Hca-F. Expressive changes of these genes have been reported to be correlated with the invasive and metastatic phenotype^[16,30].

A remarkable feature in our study is the increased steady state level of the mRNA for cyclin D1 in the category cell

cycle. Cyclin D1 is a nuclear protein that plays an important role in regulating the cell cycle by promoting entry of cells from the G1 to S phase due to interaction with its catalytic partner cdk4 or with the extradiol receptor. Over expression of cyclinD1 was associated with the liability of lymph node metastasis and the poor prognosis for patient with laryngeal squamous cell carcinoma, esophageal carcinoma, mammary infiltrating duct carcinoma, oral squamous cell carcinoma and papillary thyroid carcinoma^[31-35]. mRNA for cyclin D1 was also found to be over expressed in lymph node metastases of breast carcinoma by comparison of gene expression profiles with their primary counterparts^[36].

In the category transcription, we observed another feature of our system, i.e., the increased expression of Fos1 (Fra1; fra-1). Fos1 encodes a transcription factor, which was found over expressed in highly aggressive breast carcinoma cell lines and lymphogenous metastatic pancreatic carcinoma^[16,37]. It was reported that Fos1 induces transformation and invasiveness of human epithelial adenocarcinoma cells^[38]. In addition, we identified up-regulation of NR1D1, a member of the orphan receptor superfamily. It was coexpressed with ERBB2 in 34 breast cancer biopsies and also mapped within the same chromosomal location as the ERBB2 gene^[39].

In the present study, we found over expression of heat-shock protein Serpin h1 (HSP47) and SNCG (persyn; breast cancer-specific protein 1) in the category chaperone activity. HSP47 is a stress-inducible glycoprotein of *M*_r 47 000 molecular weight and is assumed to be a collagen-specific molecular chaperone. Tumor cell lines, which were derived from metastatic carcinomas and were still metastatic in animals, synthesized higher levels of HSP47^[40]. SNCG, the third member of a neuronal protein family synuclein, is a new chaperone protein in the Hsp-based multiprotein chaperone complex for the stimulation of ligand-dependent ER-alpha signaling and thus stimulates hormone-responsive mammary tumorigenesis, and is also highly associated with breast or ovarian cancer progression^[41]. In addition, aberrant SNCG gene expression can occur via CpG island demethylation, and tends to occur during the more progressive stages of gastric carcinogenesis^[42].

The motor activity of tumor cell plays an important role in invasiveness and metastasis. Our results revealed the up-regulation of Myosin IB and Myosin IG which are two members of the myosin I family of motor proteins. Myosins are a large family of structurally diverse motor proteins. Each myosin utilizes energy from ATP hydrolysis to generate force for indirectional movement along actin filaments^[43]. It has been reported that myosin VI, a motor protein that regulates border cell migration, was abundantly expressed in high-grade ovarian carcinomas but not in normal ovary and ovarian cancers that behave indolently. Inhibiting myosin VI expression in high-grade ovarian carcinoma cells impeded cell spreading and migration *in vitro*^[44].

Another hallmark of our system is the overexpression of mRNAs coding for kinase activity, such as Sgk2, AXL, Mak and EGFR. EGFR belongs to the family of type I receptor tyrosine kinase. Over expression of EGFR often correlates with an aggressive tumor phenotype and poor prognosis^[16,45-49]. AXL, another member of a family of

receptor tyrosine kinases, has been described to act as a mitogenic factor along with its ligand Gas-6 and has also shown to have a role in apoptosis, cell adhesion, and chemotaxis. There was a significant increase in the steady-state levels of Axl or its mRNA in a variety of cancers. Meanwhile, in colon cancer Axl receptor tyrosine kinase was expressed highly in a peritoneal metastatic nodule than in primary malignant tissues and in papillary thyroid carcinomas solid component and invasive front tended to over express Axl^[50-54]. These indicated that Axl might be related to the tumorigenesis and tumor progression. Sgk, a serine/threonine protein kinase, was found up-regulation in the tumorigenic HeLa cells compared to nontumorigenic HeLa cells which came from fusion of tumorigenic HeLa cells with human skin fibroblasts^[55]. Male germ cell-associated kinase (Mak) was shown to be up-regulated in prostate cancer cell lines than those of normal prostate epithelial cells^[56].

In the category binding, Loxl2 gene expression was up regulated. Loxl2, a copper-containing amine oxidase, belongs to the LOX family which functions as extracellular matrix modulating enzyme. LOX and LOX family members LOXL2, LOXL3, and LOXL4 were observed only in breast cancer cells with a highly invasive/metastatic phenotype but not in poorly invasive/nonmetastatic breast cancer cells^[57]. We also found Areg (AR) over expressed in the highly metastatic hepatocarcinoma cell line. Areg is one of the ligands of EGFR. Concomitant presence of the EGF receptor and its ligands EGF, TGF- α , and/or amphiregulin Areg is associated with enhanced tumor aggressiveness and shorter postoperative survival^[16,58-60]. EGF and AR might modulate invasion by increasing the expression of MMPs^[61] or stimulating directional (chemotactic) and/or random (chemokinetic) motility in malignant cells^[62]. In addition, the mRNA for caveolin (Cav; Cav-1) was up regulated in the highly metastatic cell line. Cav-1 is a major structural component of caveolae of plasma membranes. It was identified as a metastasis-related gene and/or a worse prognostic predictor in prostate carcinoma, renal cell carcinoma, esophageal squamous cell carcinoma, lung adenocarcinoma and colorectal cancer^[63-68]. Cav-1 was reported to be necessary for mediating filopodia formation in lung adenocarcinoma, which may enhance the invasive ability of cancer cells^[67]. In an other study, caveolin-1 was shown to affect angiogenesis during the progression of clear cell renal cell carcinoma^[69].

Taken together, we found that the metastatic phenotype of the highly metastatic mouse hepatocarcinoma cell line Hca-F is accompanied by marked differences in its transcriptional profile in comparison with the low metastatic cell line Hca-P. A large number of genes and their cellular functions, such as angiogenesis, cell adhesion, signal transduction, cell motility, transport, microtubule-based process, cytoskeleton organization and biogenesis, cell cycle, transcription, chaperone activity, motor activity, protein kinase activity, receptor binding and protein binding, might be involved in the process of lymphatic metastasis and deserve to be used as potential candidates for further investigation. We selected cyclin D1, Fos11, Hsp47, EGFR and AR, and Cav-1 as the possible candidate/key genes of

the metastatic phenotype, which needed to be validated in later experiments. Besides these genes, several other genes which have not been validated to contribute to enhanced tumor metastatic properties straightly deserve further attention, for example, Slc38a4 and Cldn9. ESTs (data were not presented) might indicate novel genes associated with lymphatic metastasis and also need attention. Our next work is to identify the candidate genes/pathway responsible for lymphogenous metastasis, because although a large number of genes are associated with the metastasis, some of the changes are believed to be the secondary events; the expression changes as a result of metastasis rather than as an initiator of the metastasis event^[1]. The elucidation of the candidate genes/pathway might not only provide useful diagnostic markers for tumor lymphogenous metastasis, but also more importantly, provide novel therapeutic targets.

REFERENCES

- Cheung ST**, Chen X, Guan XY, Wong SY, Tai LS, Ng IO, So S, Fan ST. Identify metastasis-associated genes in hepatocellular carcinoma through clonality delineation for multinodular tumor. *Cancer Res* 2002; **62**: 4711-4721
- Fidler IJ**. Critical factors in the biology of human cancer metastasis: twenty-eighth G.H.A. Clowes memorial award lecture. *Cancer Res* 1990; **50**: 6130-6138
- Iizuka N**, Oka M, Yamada-Okabe H, Mori N, Tamesa T, Okada T, Takemoto N, Tangoku A, Hamada K, Nakayama H, Miyamoto T, Uchimura S, Hamamoto Y. Comparison of gene expression profiles between hepatitis B virus- and hepatitis C-virus-infected hepatocellular carcinoma by oligonucleotide microarray data on the basis of a supervised learning method. *Cancer Res* 2002; **62**: 3939-3944
- Masui T**, Nakanishi H, Inada K, Imai T, Mizoguchi Y, Yada H, Futakuchi M, Shirai T, Tatematsu M. Highly metastatic hepatocellular carcinomas induced in male F344 rats treated with N-nitrosomorpholine in combination with other hepatocarcinogens show a high incidence of p53 gene mutations along with altered mRNA expression of tumor-related genes. *Cancer Lett* 1997; **112**: 33-45
- Hou L**, Li Y, Jia YH, Wang B, Xin Y, Ling MY, Lü S. Molecular mechanism about lymphogenous metastasis of hepatocarcinoma cells in mice. *World J Gastroenterol* 2001; **7**: 532-536
- Yang MC**, Ruan QG, Yang JJ, Eckenrode S, Wu S, McIndoe RA, She JX. A statistical method for flagging weak spots improves normalization and ratio estimates in microarrays. *Physiol Genomics* 2001; **7**: 45-53
- Li C**, Wong WH. Model-based analysis of oligonucleotide arrays: expression index computation and outlier detection. *Proc Natl Acad Sci USA* 2001; **98**: 31-36
- Ashburner M**, Ball CA, Blake JA, Botstein D, Butler H, Cherry JM, Davis AP, Dolinski K, Dwight SS, Eppig JT, Harris MA, Hill DP, Issel-Tarver L, Kasarskis A, Lewis S, Matese JC, Richardson JE, Ringwald M, Rubin GM, Sherlock G. Gene ontology: tool for the unification of biology. The Gene Ontology Consortium. *Nat Genet* 2000; **25**: 25-29
- Saad RS**, Jasnosz KM, Tung MY, Silverman JF. Endoglin (CD105) expression in endometrial carcinoma. *Int J Gynecol Pathol* 2003; **22**: 248-253
- Seon BK**, Takahashi N, Haba A, Matsuno F, Haruta Y, She XW, Harada N, Tsai H. Angiogenesis and metastasis marker of human tumors. *Rinsho Byori* 2001; **49**: 1005-1013
- Takahashi N**, Kawanishi-Tabata R, Haba A, Tabata M, Haruta Y, Tsai H, Seon BK. Association of serum endoglin with metastasis in patients with colorectal, breast, and other solid tumors, and suppressive effect of chemotherapy on the serum endoglin. *Clin Cancer Res* 2001; **7**: 524-532
- Li C**, Guo B, Wilson PB, Stewart A, Byrne G, Bundred N, Kumar S. Plasma levels of soluble CD105 correlate with me-

- tastasis in patients with breast cancer. *Int J Cancer* 2000; **89**: 122–126
- 13 **Straume O**, Akslen LA. Importance of vascular phenotype by basic fibroblast growth factor, and influence of the angiogenic factors basic fibroblast growth factor/fibroblast growth factor receptor-1 and ephrin-A1/EphA2 on melanoma progression. *Am J Pathol* 2002; **160**: 1009–1019
 - 14 **Easty DJ**, Hill SP, Hsu MY, Fallowfield ME, Florenes VA, Herlyn M, Bennett DC. Up-regulation of ephrin-A1 during melanoma progression. *Int J Cancer* 1999; **84**: 494–501
 - 15 **Rusiniak ME**, Yu M, Ross DT, Tolhurst EC, Slack JL. Identification of B94 (TNFAIP2) as a potential retinoic acid target gene in acute promyelocytic leukemia. *Cancer Res* 2000; **60**: 1824–1829
 - 16 **Tarbe N**, Losch S, Burtscher H, Jarsch M, Weidle UH. Identification of rat pancreatic carcinoma genes associated with lymphogenous metastasis. *Anticancer Res* 2002; **22**: 2015–2027
 - 17 **Sers C**, Kirsch K, Rothbacher U, Riethmuller G, Johnson JP. Genomic organization of the melanoma-associated glycoprotein MUC18: implications for the evolution of the immunoglobulin domains. *Proc Natl Acad Sci USA* 1993; **90**: 8514–8518
 - 18 **Wu GJ**, Peng Q, Fu P, Wang SW, Chiang CF, Dillehay DL, Wu MW. Ectopical expression of human MUC18 increases metastasis of human prostate cancer cells. *Gene* 2004; **327**: 201–213
 - 19 **Wu GJ**, Varma VA, Wu MW, Wang SW, Qu P, Yang H, Petros JA, Lim SD, Amin MB. Expression of a human cell adhesion molecule, MUC18, in prostate cancer cell lines and tissues. *Prostate* 2001; **48**: 305–315
 - 20 **Hirsch DS**, Pirone DM, Burbelo PD. A new family of Cdc42 effector proteins, CEPs, function in fibroblast and epithelial cell shape changes. *J Biol Chem* 2001; **276**: 875–883
 - 21 **Ishikawa M**, Kitayama J, Nagawa H. Enhanced expression of leptin and leptin receptor (OB-R) in human breast cancer. *Clin Cancer Res* 2004; **10**: 4325–4331
 - 22 **Even-Ram S**, Uziely B, Cohen P, Grisaru-Granovsky S, Maoz M, Ginzburg Y, Reich R, Vlodavsky I, Bar-Shavit R. Thrombin receptor overexpression in malignant and physiological invasion processes. *Nat Med* 1998; **4**: 909–914
 - 23 **Henrikson KP**, Salazar SL, Fenton JW, Pentecost BT. Role of thrombin receptor in breast cancer invasiveness. *Br J Cancer* 1999; **79**: 401–406
 - 24 **Booden MA**, Eckert LB, Der CJ, Trejo J. Persistent signaling by dysregulated thrombin receptor trafficking promotes breast carcinoma cell invasion. *Mol Cell Biol* 2004; **24**: 1990–1999
 - 25 **Nabi IR**, Watanabe H, Raz A. Autocrine motility factor and its receptor: role in cell locomotion and metastasis. *Cancer Metastasis Rev* 1992; **11**: 5–20
 - 26 **Takai Y**, Irie K, Shimizu K, Sakisaka T, Ikeda W. Nectins and nectin-like molecules: Roles in cell adhesion, migration, and polarization. *Cancer Sci* 2003; **94**: 655–667
 - 27 **Ikeda W**, Kakunaga S, Takekuni K, Shingai T, Satoh K, Morimoto K, Takeuchi M, Imai T, Takai Y. Nectin-like molecule-5/Tage4 enhances cell migration in an integrin-dependent, Nectin-3-independent manner. *J Biol Chem* 2004; **279**: 18015–18025
 - 28 **Mackenzie B**, Erickson JD. Sodium-coupled neutral amino acid (System N/A) transporters of the SLC38 gene family. *Pflugers Arch* 2004; **447**: 784–795
 - 29 **Ishida N**, Kawakita M. Molecular physiology and pathology of the nucleotide sugar transporter family (SLC35). *Pflugers Arch* 2004; **447**: 768–775
 - 30 **Wauters CC**, Smedts F, Gerrits LG, Bosman FT, Ramaekers FC. Keratins 7 and 20 as diagnostic markers of carcinomas metastatic to the ovary. *Hum Pathol* 1995; **26**: 852–855
 - 31 **Lim SC**. Role of COX-2, VEGF and cyclin D1 in mammary infiltrating duct carcinoma. *Oncol Rep* 2003; **10**: 1241–1249
 - 32 **Zhang L**, Xu Y, Ge Y, Yu Y, Yu L. Expression of p27 protein and cyclinD1 in laryngeal carcinoma. *Linchuang Erbiyanhouke Zazhi* 2002; **16**: 646–647
 - 33 **Nakashima S**, Natsugoe S, Matsumoto M, Kijima F, Miyazono F, Ishigami S, Baba M, Takao S, Aikou T. Biological properties of biopsy specimens are useful for predicting lymph node micrometastasis in esophageal carcinoma. *Anticancer Res* 2002; **22**: 2951–2956
 - 34 **Khoo ML**, Beasley NJ, Ezzat S, Freeman JL, Asa SL. Overexpression of cyclin D1 and underexpression of p27 predict lymph node metastases in papillary thyroid carcinoma. *J Clin Endocrinol Metab* 2002; **87**: 1814–1818
 - 35 **Miyashita H**, Uchida T, Mori S, Echigo S, Motegi K. Expression status of Pin1 and cyclins in oral squamous cell carcinoma: Pin1 correlates with Cyclin D1 mRNA expression and clinical significance of cyclins. *Oncol Rep* 2003; **10**: 1045–1048
 - 36 **Hao X**, Sun B, Hu L, Lahdesmaki H, Dunmire V, Feng Y, Zhang SW, Wang H, Wu C, Wang H, Fuller GN, Symmans WF, Shmulevich I, Zhang W. Differential gene and protein expression in primary breast malignancies and their lymph node metastases as revealed by combined cDNA microarray and tissue microarray analysis. *Cancer* 2004; **100**: 1110–1122
 - 37 **Zajchowski DA**, Bartholdi MF, Gong Y, Webster L, Liu HL, Munishkin A, Beauheim C, Harvey S, Ethier SP, Johnson PH. Identification of gene expression profiles that predict the aggressive behavior of breast cancer cells. *Cancer Res* 2001; **61**: 5168–5178
 - 38 **Kustikova O**, Kramerov D, Grigorian M, Berezin V, Bock E, Lukanidin E, Tulchinsky E. Fra-1 induces morphological transformation and increases in vitro invasiveness and motility of epithelioid adenocarcinoma cells. *Mol Cell Biol* 1998; **18**: 7095–7105
 - 39 **Dressman MA**, Baras A, Malinowski R, Alvis LB, Kwon I, Walz TM, Polymeropoulos MH. Gene expression profiling detects gene amplification and differentiates tumor types in breast cancer. *Cancer Res* 2003; **63**: 2194–2199
 - 40 **Morino M**, Tsuzuki T, Ishikawa Y, Shirakami T, Yoshimura M, Kiyosuke Y, Matsunaga K, Yoshikumi C, Saijo N. Specific expression of HSP47 in human tumor cell lines *in vitro*. *In Vivo* 1997; **11**: 17–21
 - 41 **Jiang Y**, Liu YE, Goldberg ID, Shi YE. Gamma synuclein, a novel heat-shock protein-associated chaperone, stimulates ligand-dependent estrogen receptor alpha signaling and mammary tumorigenesis. *Cancer Res* 2004; **64**: 4539–4546
 - 42 **Yanagawa N**, Tamura G, Honda T, Endoh M, Nishizuka S, Motoyama T. Demethylation of the synuclein gamma gene CpG island in primary gastric cancers and gastric cancer cell lines. *Clin Cancer Res* 2004; **10**: 2447–2451
 - 43 **Voigt H**, Olivo JC, Sansonetti P, Guillen N. Myosin IB from *Entamoeba histolytica* is involved in phagocytosis of human erythrocytes. *J Cell Sci* 1999; **112** (Pt 8): 1191–1201
 - 44 **Yoshida H**, Cheng W, Hung J, Montell D, Geisbrecht E, Rosen D, Liu J, Naora H. Lessons from border cell migration in the *Drosophila* ovary: A role for myosin VI in dissemination of human ovarian cancer. *Proc Natl Acad Sci USA* 2004; **101**: 8144–8149
 - 45 **McKay JA**, Murray LJ, Curran S, Ross VG, Clark C, Murray GI, Cassidy J, McLeod HL. Evaluation of the epidermal growth factor receptor (EGFR) in colorectal tumours and lymph node metastases. *Eur J Cancer* 2002; **38**: 2258–2264
 - 46 **Ito R**, Nakayama H, Yoshida K, Matsumura S, Oda N, Yasui W. Expression of Cbl linking with the epidermal growth factor receptor system is associated with tumor progression and poor prognosis of human gastric carcinoma. *Virchows Arch* 2004; **444**: 324–331
 - 47 **Deng Z**, Ge D, Zhang D, Tan Y, Bai C, Xu Y. The expression of erbB/HER family in lung cancer. *Zhonghua JieHe He HuXi ZaZhi* 2002; **25**: 207–209
 - 48 **Kopp R**, Rothbauer E, Mueller E, Schildberg FW, Jauch KW, Pfeiffer A. Reduced survival of rectal cancer patients with increased tumor epidermal growth factor receptor levels. *Dis Colon Rectum* 2003; **46**: 1391–1399
 - 49 **Niu Y**, Fu X, Lv A, Fan Y, Wang Y. Potential markers predicting distant metastasis in axillary node-negative breast carcinoma. *Int J Cancer* 2002; **98**: 754–760
 - 50 **Chung BI**, Malkowicz SB, Nguyen TB, Libertino JA, McGarvey

- TW. Expression of the proto-oncogene Axl in renal cell carcinoma. *DNA Cell Biol* 2003; **22**: 533-540
- 51 **Sun WS**, Fujimoto J, Tamaya T. Coexpression of growth arrest-specific gene 6 and receptor tyrosine kinases Axl and Sky in human uterine endometrial cancers. *Ann Oncol* 2003; **14**: 898-906
- 52 **Ito M**, Nakashima M, Nakayama T, Ohtsuru A, Nagayama Y, Takamura N, Demedchik EP, Sekine I, Yamashita S. Expression of receptor-type tyrosine kinase, Axl, and its ligand, Gas6, in pediatric thyroid carcinomas around chernobyl. *Thyroid* 2002; **12**: 971-975
- 53 **Berclaz G**, Altermatt HJ, Rohrbach V, Kieffer I, Dreher E, Andres AC. Estrogen dependent expression of the receptor tyrosine kinase axl in normal and malignant human breast. *Ann Oncol* 2001; **12**: 819-824
- 54 **Craven RJ**, Xu LH, Weiner TM, Fridell YW, Dent GA, Srivastava S, Varnum B, Liu ET, Cance WG. Receptor tyrosine kinases expressed in metastatic colon cancer. *Int J Cancer* 1995; **60**: 791-797
- 55 **Tsujimoto H**, Nishizuka S, Redpath JL, Stanbridge EJ. Differential gene expression in tumorigenic and nontumorigenic HeLa x normal human fibroblast hybrid cells. *Mol Carcinog* 1999; **26**: 298-304
- 56 **Xia L**, Robinson D, Ma AH, Chen HC, Wu F, Qiu Y, Kung HJ. Identification of human male germ cell-associated kinase, a kinase transcriptionally activated by androgen in prostate cancer cells. *J Biol Chem* 2002; **277**: 35422-35433
- 57 **Kirschmann DA**, Seftor EA, Fong SF, Nieva DR, Sullivan CM, Edwards EM, Sommer P, Csiszar K, Hendrix MJ. A molecular role for lysyl oxidase in breast cancer invasion. *Cancer Res* 2002; **62**: 4478-4483
- 58 **Friess H**, Kleeff J, Korc M, Buchler MW. Molecular aspects of pancreatic cancer and future perspectives. *Dig Surg* 1999; **16**: 281-290
- 59 **Panico L**, D'Antonio A, Salvatore G, Mezza E, Tortora G, De Laurentiis M, De Placido S, Giordano T, Merino M, Salomon DS, Mullick WJ, Pettinato G, Schnitt SJ, Bianco AR, Ciardiello F. Differential immunohistochemical detection of transforming growth factor alpha, amphiregulin and CRIPTO in human normal and malignant breast tissues. *Int J Cancer* 1996; **65**: 51-56
- 60 **Kopp R**, Rothbauer E, Mueller E, Schildberg FW, Jauch KW, Pfeiffer A. Reduced survival of rectal cancer patients with increased tumor epidermal growth factor receptor levels. *Dis Colon Rectum* 2003; **46**: 1391-1399
- 61 **Kondapaka SB**, Fridman R, Reddy KB. Epidermal growth factor and amphiregulin up-regulate matrix metalloproteinase-9 (MMP-9) in human breast cancer cells. *Int J Cancer* 1997; **70**: 722-726
- 62 **Liu Z**, Klominek J. Chemotaxis and chemokinesis of malignant mesothelioma cells to multiple growth factors. *Anticancer Res* 2004; **24**: 1625-1630
- 63 **Yang G**, Truong LD, Timme TL, Ren C, Wheeler TM, Park SH, Nasu Y, Bangma CH, Kattan MW, Scardino PT, Thompson TC. Elevated expression of caveolin is associated with prostate and breast cancer. *Clin Cancer Res* 1998; **4**: 1873-1880
- 64 **Li L**, Yang G, Ebara S, Satoh T, Nasu Y, Timme TL, Ren C, Wang J, Tahir SA, Thompson TC. Caveolin-1 mediates testosterone-stimulated survival/clonal growth and promotes metastatic activities in prostate cancer cells. *Cancer Res* 2001; **61**: 4386-4392
- 65 **Horiguchi A**, Asano T, Asakuma J, Asano T, Sumitomo M, Hayakawa M. Impact of caveolin-1 expression on clinicopathological parameters in renal cell carcinoma. *J Urol* 2004; **172**: 718-722
- 66 **Kato K**, Hida Y, Miyamoto M, Hashida H, Shinohara T, Itoh T, Okushiba S, Kondo S, Katoh H. Overexpression of caveolin-1 in esophageal squamous cell carcinoma correlates with lymph node metastasis and pathologic stage. *Cancer* 2002; **94**: 929-933
- 67 **Ho CC**, Huang PH, Huang HY, Chen YH, Yang PC, Hsu SM. Up-regulated caveolin-1 accentuates the metastasis capability of lung adenocarcinoma by inducing filopodia formation. *Am J Pathol* 2002; **161**: 1647-1656
- 68 **Lin SY**, Yeh KT, Chen WT, Chen HC, Chen ST, Chang JG. Promoter CpG methylation of caveolin-1 in sporadic colorectal cancer. *Anticancer Res* 2004; **24**: 1645-1650
- 69 **Joo HJ**, Oh DK, Kim YS, Lee KB, Kim SJ. Increased expression of caveolin-1 and microvessel density correlates with metastasis and poor prognosis in clear cell renal cell carcinoma. *BJU Int* 2004; **93**: 291-296

• COLORECTAL CANCER •

Vegetable/fruit, smoking, glutathione S-transferase polymorphisms and risk for colorectal cancer in Taiwan

Chih-Ching Yeh, Ling-Ling Hsieh, Reiping Tang, Chung Rong Chang-Chieh, Fung-Chang Sung

Chih-Ching Yeh, Institute of Environmental Health, National Taiwan University, Taipei 100, Taiwan, China

Ling-Ling Hsieh, Chung Rong Chang-Chieh, Department of Public Health, Chang Gung University, Tao-Yuan 333, Taiwan, China
Reiping Tang, Colorectal Section, Chang Gung Memorial Hospital, Taipei 244, Taiwan, China

Fung-Chang Sung, Institute of Environmental Health, China Medical University, Taichung 404, Taiwan, China

Supported by National Science Council No. 89-2314-B-002-373, 90-2320-B-002-123 and 91-2320-B-002-121; National Health Research Institute No. 85-HR-516, 86-HR-516, and 87-HR-516

Correspondence to: Dr. Fung-Chang Sung, Institute of Environment Health, China Medical University, 91 Hsueh-Shih Road, Taichung 404, Taiwan, China. fcsung@mail.cmu.edu.tw

Telephone: +886-4-2205-4070 Fax: +886-4-2201-9901

Received: 2004-08-26 Accepted: 2004-09-25

genotypes with OR = 0.17 and 0.21 respectively.

CONCLUSION: This study suggests that the GSTT1 gene can modulate the colorectal cancer risk and vegetable/fruit-related colorectal cancer risk, particularly in men of no smoking history.

© 2005 The WJG Press and Elsevier Inc. All rights reserved.

Key words: Colorectal cancer; Glutathione S-transferase; Polymorphisms; Vegetables; Smoking

Yeh CC, Hsieh LL, Tang R, Chang-Chieh CR, Sung FC. Vegetable/fruit, smoking, glutathione S-transferase polymorphisms and risk for colorectal cancer in Taiwan. *World J Gastroenterol* 2005; 11(10): 1473-1480

<http://www.wjgnet.com/1007-9327/11/1473.asp>

Abstract

AIM: To investigate the colorectal cancer risk associated with polymorphic GSTM1, GSTT1 and GSTP1 and the effect of diet and smoking.

METHODS: With consents, genotypes of the genes were determined using PCR methods for 727 cases and 736 sex and age-matched healthy controls recruited at a medical center in the Northern Taiwan. Nurses who were blind to the study hypothesis conducted interviews with study participants for the information of socio-demographic variables, diet and smoking.

RESULTS: There was no significant association between GSTM1 genotypes and the disease. Men, not women, with GSTT1 null genotype were at significant risk of colorectal cancer, but limited to rectal tumor, and in men aged 60 years and less. The corresponding association with the GSTP1 with G allele compared to GSTP1 A/A genotype was at borderline significance. Compared to men with GSTT1 present and GSTP1 A/A combined, men with both GSTT1 null and GSTP1 with G allele genotypes were at significant risk (odds ratio (OR) = 1.91, 95% confidence interval (CI) = 1.21-3.02), also limited to the rectal tumor and younger men. The beneficial effects of vegetable/fruit intake on colorectal cancer were much higher for men with GSTT1 present (OR = 0.32, 95%CI = 0.20-0.50) or GSTP1 A/A genotypes (OR = 0.40, 95%CI = 0.25-0.64). These effects remained significant for women. But, the greatest protective effect from vegetable/fruit intake for women was observed in those with GSTT1 null or GSTP1 with G allele genotypes. In addition, non-smoking men benefitted significantly from combined effect of higher vegetable/fruit intake and GSTT1 present or GSTP1 A/A

INTRODUCTION

Human glutathione S-transferase (GST) consists of four main classes, alpha (A), mu (M), pi (P) and theta (T)^[1], involving in the detoxification of many electrophilic compounds by conjugation reaction with glutathione^[2]. Most GST substrates are thought as xenobiotics or products of oxidative stress, including polycyclic aromatic hydrocarbons present in the diet or from tobacco smoke^[2]. The GST enzymes also conjugate isothiocyanates, potent enzyme inducers, detoxifying mutagens^[3] to glutathione and divert them from the enzyme induction pathway to excretion^[4,5]. Functional polymorphisms known in most studies are GSTM1, GSTT1 and GSTP1^[6-8]. The absence of GSTM1 and GSTT1 enzyme activity correlates with homozygosity for deletions in these genes, termed the null genotype^[6,7]. For GSTP1, a polymorphic Ile105Val (resulting from an A to G substitution at base 1 578) has been found to modify the enzyme's activity and affinity for electrophilic substrates^[8]. Studies have shown that higher levels of DNA damage are associated with the GSTM1/T1 null genotype and GSTP1 with G allele^[9,10].

Several studies have examined the relationship between the GSTM1 null genotype and susceptibility to colorectal cancer^[11-15]. The first study by Zhong *et al*^[16] found significantly increased colon cancer risk associated with the GSTM1 null genotype, particular for cancers of the proximal colon. A significant risk for distal colorectal cancer was observed later in a Japanese study^[17]. Sgambato *et al*^[15] also reported strongest association between GSTM1 null genotype and colon cancer and with a younger age (<60 years) of

onset. Other studies failed to find similar associations^[11-14]. Several studies also examined whether the GSTT1 null genotype exhibition conferred susceptibility to colorectal cancer^[11-15]. Only the largest study^[18], with 252 cases and 577 controls, demonstrated an increased risk for the GSTT1 null genotype due to excess GSTT1 deletion for cases with left colon and rectal cancer. Five studies examined the GSTP1 A/G polymorphism for colorectal cancer. None reported a significant association^[11,12,19-21].

Differences in carcinogen metabolism might explain the differences in cancer susceptibility especially as most cancers are influenced by environmental factors^[22]. Etiological studies have attributed more than 85% of colorectal cancer to environmental factors^[23,24], particularly dietary factors^[25]. These dietary effects might be modulated by genetic polymorphisms of the metabolic genes^[26]. For instance, Lin *et al*^[27] found that the protective effect of broccoli for colorectal adenoma was observed only among subjects with the GSTM1 null genotype. Recent GST polymorphism studies have focused on gene-environment interactions in the occurrence of colorectal cancer^[14,28-30]. Slattery *et al*^[30] reported that the beneficial effect of cruciferous vegetable intake was stronger for subjects aged less than 55 years old, with GSTM1 null genotype than with GSTM1 present genotype.

Three studies linking these GST polymorphisms with colorectal cancer for Chinese subjects^[31-33] were limited to small sample sizes or no control for potential confounders. In addition, the incidence of colorectal cancer increased 2.6 folds in the past decade in Taiwan and dietary behavior has changed by increasing meat consumption. The present hospital-based case-control study examined the role of polymorphisms of GSTM1, GSTT1 and GSTP1 genes in colorectal cancer and their combined effects with environmental factors such as meat consumption, cigarette smoking and vegetable/fruit intake.

MATERIALS AND METHODS

Subjects

Detailed descriptions for the study participants have been published previously^[34]. In brief, the colorectal adenocarcinoma cancer cases ($n = 776$) were newly diagnosed and histologically confirmed at the Chang Gung Memorial Hospital between January 1995 and January 1999. Patients with familial adenomatous polyposis ($n = 11$), hereditary nonpolyposis colorectal cancer ($n = 18$), or inflammatory bowel disease and other malignancies ($n = 20$) were excluded from the data analysis. Seven hundred and twenty-seven cases (94%) were included (56.4% men) in this study. During the same period, seven hundred and forty-seven subjects were recruited as controls from the Physical Check-Up Department for comprehensive health examinations including colonoscopies matched by same age and sex. After excluding individuals diagnosed with other colorectal diseases ($n = 5$) and with a history of other cancers ($n = 6$), 736 controls (98%) were included (55.6% men) in this study.

Questionnaire

Professional nurses employed were trained to conduct

interviews with all participants in the hospital prior to surgical operations for cases and colonoscopies for the controls. These nurses were blind to the study hypothesis regarding diet, lifestyle and colorectal cancer. All interviews were administered uniformly in the wards. The standardized interview was conducted with informed consent using a structured questionnaire covering socio-demographic characteristics, lifestyle factors (including physical activities, cigarette and alcohol use and coffee intake), dietary consumption and medical history. The reliability (standardized Cronbach's alpha) of this questionnaire was 0.92 based on the lifestyle and dietary variables. This interview took approximately 20 min to complete. Information on usual dietary intake 5 years preceding the date of diagnosis for the cases and the date of selection for the controls was collected. The intake frequency was categorized into six levels ranging from never, less than once a month, 1-3 times a month, once a week, 2-3 times a week to almost everyday.

Cigarette and alcohol use and coffee intake were evaluated in both the amount and duration. Total cigarette smoking and alcohol drinking were estimated in pack-years and bottle-years using daily pack and bottle (600 mL) consumption multiplied by the number of years respectively. Because less than 10% of the subjects in our study had a coffee intake habit (more than one cup of coffee per month), coffee intake was estimated by status ("Yes" or "No") rather than total consumption.

Genotyping

WBC DNA was isolated from 10 mL whole blood using standard procedures with sodium dodecyl sulfate (SDS)-proteinase K-RNase digestion and phenol-chloroform extraction. The extracted DNA was dissolved in Tris-EDTA buffer to a concentration of 500 ng/ μ L. The polymorphisms were analyzed by polymerase chain reaction (PCR) assays for GSTM1 and GSTT1 or combined with restriction fragment length polymorphism (RFLP) assays for GSTP1 Ile105Val. All of the PCR reactions were performed in a 25 μ L final volume containing 200 ng of each primer, 100 ng genomic DNA, 1.5 mmol/L $MgCl_2$, 200 μ mol/L dNTPs and 1.0 unit of Taq DNA Polymerase in the buffer provided by the manufacturer. Amplification was performed in a Programmable Thermal Controller (MJ Research, Waltham, MA) for the PCR reaction.

The multiple PCR used to detect the presence or absence of the GSTM1 and GSTT1 genes was determined using the following primers: GSTT1 (5'-TTCCCTTACTGGTCC-TCACATCTC-3' and 5'-CACCGGATCATGGCCAGCA-3'), GSTM1 (5'-TGCCCTACTTGATTGATGGG-3' and 5'-CTGGATTGTAGCAGATCATGC-3') and the internal control, β -globin (5'-CACAACGTGTGTTCACTAGC-3' and 5'-CAACTTCATCCACGTTTACC-3'). The PCR program was a 5-min denaturing step at 94 °C followed by 30 cycles of 30 s at 94 °C, 30 s at 59 °C and 60 s at 72 °C. Individuals without intact GSTT1 or GSTM1 genes showed no amplification of the 480 bp GSTT1 fragment or the 273 bp GSTM1 fragment and a positive internal control^[35]. The GSTP1 A/G (Ile105Val) polymorphism was determined using the following primers: sense, 5'-CCTCTCCCTTTCCT-CTGTTTC-3'; antisense, 5'-CAGGTGAGGGGGACATCT-

3'. PCR program was a 5-min denaturing step at 95 °C followed by 30 cycles of 30 s at 94 °C, 30 s at 55 °C and 30 s at 72 °C. The 176 bp PCR product was digested with Alw26I (New England BioLabs, Beverly, MA): the Val allele was cut into 91 and 85 bp fragments (Ile allele not digested)^[36].

Statistical analysis

Food items were coded into three major groups: staples (rice, noodles and instant noodles), meat (red meat and white meat), and vegetables and fruits. Viscera fish and shrimp were considered separate food items in the data analysis. The consumption of each food item was scored from 1 for "almost ate every day" to 6 for "never ate". The group score was the total sum of scores from the intake frequency for the individual food items. Because of etiological differences between colon cancer and rectal cancer and between men and women^[37], all analyses in this study were estimated separately by sex and cancer site. Most risk factors were dichotomized into "Low" and "High" according to the median of the controls in the data analysis. Only 4% of the women were smokers and only 5.1% of women were alcohol users. The risks for these two factors were therefore calculated only for men.

Some unmatched cases occurred when we were unable to interview an eligible control or controls who were eliminated by the exclusion criteria. Unmatched controls also occurred when cases with hereditary syndromes or other malignancies were excluded. To make the use of information on unmatched subjects, and because we had to break the matches due to stratification by sex and tumor site, unconditional logistic regression was used to control for the matching factor (age as continuous variable) to identify potential risk factors.

The odds ratio (OR) and the 95% confidence interval (CI) were measured. A stepwise selection procedure was applied to determine the covariates included in the final multivariate models beginning with all dietary and non-dietary variables. Multivariate unconditional logistic regressions were also used to examine the association between the GSTM1, GSTT1 and GSTP1 polymorphisms and risk for colorectal cancer controlling for age and selected covariates. We conducted interaction analyses on the basis of a multiplicative scale. The likelihood ratio test was used to evaluate the interaction between GST genes and cigarette smoking, meat consumption and vegetable/fruit intake on the risk for colorectal cancer. Analysis was also conducted separately to observe the differences between age groups at diagnosis. All analyses were performed using the SAS statistical package (version 8.2 for Windows; SAS Institute, Inc., Cary, NC) and all statistical tests were two-sided.

RESULTS

Overall, 410 men and 317 women with eligible colorectal cancer cases and 409 male and 327 female controls were included in this analysis. These four groups of subjects had a similar average age of 60 years (Table 1). The stepwise selection procedure produced six potential covariates, including age, physical activity, coffee use, cigarette smoking, drinking, and meat consumption associated with the disease for men. The three potential risk covariates for women included age, consumption of staples and meat. Vegetable/fruit and fish/shrimp intakes had protective effect for both men and women. The frequencies of the polymorphisms for GSTM1, GSTT1 and GSTP1 genes were also presented in Table 1. Only the GSTT1 null genotype was moderately

Table 1 Selected colorectal cancer case and control distribution by sex in Taiwan

Variable	Men		<i>P</i> ¹	Women		<i>P</i> ¹
	Cases <i>n</i> = 410 (%)	Controls <i>n</i> = 409 (%)		Cases <i>n</i> = 317 (%)	Controls <i>n</i> = 327 (%)	
Age (mean±SD, yr)	60.5±12.2	60.6±12.7		60.2±13.6	60.7±13.4	
Colon/rectum, <i>n</i>	185/225			167/150		
Physical activity	53 (14.1)	95 (23.2)	<0.01	NI ²		
Coffee	63 (16.5)	36 (8.8)	<0.01	NI ²		
Smoking			0.18	NA ³		
Never	122 (31.3)	150 (36.7)				
Ex-smoker	91 (23.3)	98 (24.0)				
Current	177 (45.4)	161 (39.4)				
Alcohol drinking			0.01	NA ³		
Never	186 (48.1)	205 (50.1)				
Ex-drinker	17 (4.4)	37 (9.1)				
Current	184 (47.6)	167 (40.8)				
High staple ⁴	NI ²			156 (49.2)	112 (34.3)	<0.01
High meat ⁴	294 (71.7)	244 (59.7)	<0.01	203 (64.0)	151 (46.2)	<0.01
High vegetable/fruit ⁴	168 (44.7)	266 (65.0)	<0.01	147 (50.2)	197 (60.2)	0.01
Fish/shrimp (almost everyday)	174 (46.3)	256 (62.6)	<0.01	125 (42.8)	167 (51.1)	0.04
GSTM1 null	213 (52.2)	215 (52.7)	0.89	189 (60.0)	195 (60.0)	1.00
GSTT1 null	216 (52.9)	189 (46.3)	0.06	180 (57.1)	171 (52.6)	0.25
GSTP1			0.78			0.39
A/A	277 (67.9)	287 (70.2)		224 (71.3)	226 (69.5)	
A/G	117 (28.7)	109 (26.7)		84 (26.8)	87 (26.8)	
G/G	14 (3.4)	13 (3.2)		6 (1.9)	12 (3.7)	

¹χ²; ²Not included as covariates in the multiple logistic regression model; ³Not available for analysis; ⁴The cut-point of score using the median of the score distribution among controls for high consumption of staple, meat and vegetable/fruit were <10, <5 and <3 respectively.

higher in cases than in controls (0.55 *vs* 0.49, $P = 0.06$). Because of the low frequency of the GSTP1 G/G genotype, we combined heterozygous (GSTP1 A/G) and homozygous (GSTP1 G/G) genotypes, as GSTP1 with G allele, to estimate the cancer risk associated with the G allele.

The ORs of the polymorphisms of GSTM1, GSTT1 and GSTP1 for the colorectal cancer risks in men were shown in Table 2. After controlling for covariates, the risk for colorectal cancer was statistically significantly increased by GSTT1 null genotype (OR = 1.45, 95%CI = 1.07-1.97), compared to GSTT1 present genotype. A moderately increased risk for colorectal cancer was also observed in men with GSTP1 with G allele than those with A/A genotype

(OR = 1.36, 95%CI = 0.98-1.89). Further stratified analysis by tumor site and age at diagnosis showed that, male individuals with the GSTT1 null genotype were at significant risk for rectal cancer with OR = 1.55 (95%CI = 1.08-2.23) and those diagnosed before 60 years old with OR = 2.03 (95%CI = 1.29-3.21) respectively. An increased risk for GSTP1 with G allele was also observed in these subgroups. However, the polymorphism of GSTM1 gene was not associated with colorectal cancer even in the stratified analysis.

The associations between these polymorphisms of GST and the colorectal cancer risks in women were shown in Table 3. No significant difference in proportions of GSTM1

Table 2 Odds ratio (OR) and 95% confidence interval (CI) of the polymorphisms of GSTM1, GSTT1 and GSTP1 for colorectal cancer by age at diagnosis and tumor site in men

	GSTM1		GSTT1		GSTP1	
	Present	Null	Present	Null	A/A	With G ²
Total population						
Cases/Controls	195/193	213/215	192/219	216/189	277/287	131/122
OR (95%CI) ¹	1.0	0.93 (0.68-1.26)	1.0	1.45 (1.07-1.97)	1.0	1.36 (0.98-1.89)
Tumor site						
Colon						
Cases/Controls	82/193	101/215	89/219	94/189	127/287	56/122
OR (95%CI) ¹	1.0	1.00 (0.67-1.48)	1.0	1.24 (0.83-1.83)	1.0	1.15 (0.75-1.76)
Rectum						
Cases/Controls	113/193	112/215	103/219	122/189	150/287	75/122
OR (95%CI) ¹	1.0	0.87 (0.61-1.25)	1.0	1.55 (1.08-2.23)	1.0	1.48 (1.00-2.18)
Age at diagnosis						
≤60 yr						
Cases/Controls	95/85	92/100	86/106	101/79	124/129	63/56
OR (95%CI) ¹	1.0	0.86 (0.53-1.30)	1.0	2.03 (1.29-3.21)	1.0	1.45 (0.89-2.37)
>60 yr						
Cases/Controls	100/108	121/115	106/113	115/110	153/158	68/66
OR (95%CI) ¹	1.0	1.03 (0.67-1.58)	1.0	1.12 (0.73-1.71)	1.0	1.34 (0.84-2.12)

¹ORs and 95% CIs were estimated from multivariate unconditional logistic regressions controlling for age, physical activity, coffee, cigarette, alcohol, meat, vegetable/fruit and fish/shrimp; ² Combined genotype of A/G and G/G.

Table 3 Odds ratio (OR) and 95% confidence interval (CI) of the polymorphisms of GSTM1, GSTT1 and GSTP1 for colorectal cancer by age at diagnosis and tumor site in women

	GSTM1		GSTT1		GSTP1	
	Present	Null	Present	Null	A/A	With G ²
Total population						
Cases/Controls	126/130	189/195	135/154	180/171	224/226	90/99
OR (95%CI) ¹	1.0	0.99 (0.71-1.38)	1.0	1.18 (0.85-1.64)	1.0	1.00 (0.70-1.43)
Tumor site						
Colon						
Cases/Controls	61/130	105/195	72/154	94/171	116/226	49/99
OR (95%CI) ¹	1.0	1.19 (0.78-1.81)	1.0	1.23 (0.82-1.84)	1.0	1.04 (0.67-1.60)
Rectum						
Cases/Controls	65/130	84/195	63/154	86/171	108/226	41/99
OR (95%CI) ¹	1.0	0.84 (0.56-1.27)	1.0	1.20 (0.79-1.81)	1.0	0.93 (0.60-1.46)
Age at diagnosis						
≤60 yr						
Cases/Controls	52/52	84/82	50/55	86/79	99/89	37/45
OR (95%CI) ¹	1.0	1.08 (0.63-1.85)	1.0	1.20 (0.71-2.05)	1.0	0.84 (0.48-1.47)
>60 yr						
Cases/Controls	74/78	105/113	85/99	94/92	125/137	53/54
OR (95%CI) ¹	1.0	0.95 (0.61-1.46)	1.0	1.15 (0.75-1.76)	1.0	1.13 (0.71-1.80)

¹ORs and 95% CIs were estimated from multivariate unconditional logistic regressions controlling for age, sex, physical activity, coffee, cigarette, alcohol, meat, vegetable/fruit and fish/shrimp; ² Combined genotype of A/G and G/G.

null, GSTT1 null and GSTP1 with G allele genotypes were observed between cases and controls for all female subjects and their subgroups by anatomical site and diagnosed age.

Men with more risk genotypes of GSTT1 and GSTP1 had higher risk than those without any risk genotypes (trend test $P < 0.01$) (Table 4). Compared to men with both GSTT1 present and GSTP1 A/A genotypes, those with either or both GSTT1 null and GSTP1 with G allele genotypes had 1.4-fold (OR = 1.42, 95%CI = 1.01-1.99) and 1.9-fold (OR = 1.91, 95%CI = 1.21-3.02) risk of colorectal cancer respectively. A stronger risk of rectal cancer was seen for men with both GSTT1 null and GSTP1 with G allele genotypes (OR = 2.20, 95%CI = 1.28-3.78). The corresponding effect on colorectal cancer for men aged less than 60 years at diagnoses was even greater (OR = 3.05, 95%CI = 1.51-6.12). However, these trends were not observed for women (data not shown).

Table 5 demonstrated a multiplicative synergistic effect for men and an antagonistic effect for women between the GST genes (GSTT1 and GSTP1) and vegetable/fruit intake on the colorectal cancer risk. The protective effect of high vegetable/fruit consumption was enhanced for men with GSTT1 present genotype (OR = 0.32, 95%CI = 0.21-0.50), compared to men with GSTT1 null genotype and low vegetable/fruit consumption. Similarly, the protective effect for men was strongly associated with GSTP1 A/A genotype and high vegetable/fruit consumption (OR = 0.40,

95%CI = 0.25-0.64). However, the beneficial effect of high vegetable/fruit intake was attenuated for women with the protective GSTT1 present or GSTP1 A/A genotypes. The strongest protective effect from vegetable/fruit intake was observed among women having GSTT1 null or GSTP1 with G allele genotypes. The stratification analysis also showed that the multiplicative protective effect was also significant in the rectum and for younger men (data not shown).

The combined effects of GSTT1 present or GSTP1 A/A genotypes, and vegetable/fruit intake on colorectal cancer varied with smoking status (Table 6). Since very few women were smokers (<5%); this stratification analysis by smoking status was calculated only for men. The protective effects of high vegetable/fruit consumption enhanced by the GSTT1 present or GSTP1 A/A genotypes were consistent and the association was robust, particularly for non-smokers. The ORs for these joint effects were 0.17 (95% CI = 0.07-0.42) for GSTT1 and 0.21 (95% CI = 0.09-0.52) for GSTP1. There was no significant interaction between meat intake and GST genes to the risk of colorectal cancer (data not shown).

DISCUSSION

This is the first hospital-based case-control study with a relatively large sample simultaneously examining the association

Table 4 Combined genotype of GSTT1 and GSTP1 on colorectal cancer risk by tumor site and age in men

	GSTT1 / GSTP1					
	Present / (A/A)		Present / with G + null / (A/A)		Null / with G	
	Cases/Controls	OR (95%CI) ¹	Cases/Controls	OR (95%CI) ¹	Cases/Controls	OR (95%CI) ¹
Total population ²	132/157	1.00	205/191	1.42 (1.01-1.99)	71/60	1.91 (1.21-3.02)
Tumor site						
Colon	64/157	1.00	88/191	1.16 (0.75-1.79)	31/60	1.42 (0.79-2.55)
Rectum ²	68/157	1.00	117/191	1.65 (1.09-2.50)	40/60	2.20 (1.28-3.78)
Age at diagnosis						
≤60 yr ²	57/73	1.00	96/89	1.73 (1.04-2.89)	34/23	3.05 (1.51-6.12)
>60 yr	75/84	1.00	109/102	1.25 (0.78-2.02)	37/37	1.41 (0.75-2.64)

¹Adjusted for age, physical activity, coffee, cigarette, alcohol, meat, vegetable/fruit and fish/shrimp; ²Trend test $P < 0.01$.

Table 5 Combined effects of GST genotypes and vegetable/fruit consumption on colorectal cancer risk

Genotype	Vegetable/fruit consumption	Men			Women		
		Cases	Controls	OR (95%CI) ¹	Cases	Controls	OR (95%CI) ²
GSTT1							
Null	Low	106	69	1.00	90	62	1.00
Present	Low	101	74	0.87 (0.55-1.36)	54	66	0.60 (0.36-0.98)
Null	High	110	120	0.57 (0.37-0.88)	90	109	0.47 (0.30-0.75)
Present	High	91	145	0.32 (0.20-0.50)	81	88	0.53 (0.33-0.85)
<i>P</i> for interaction				0.21	0.06		
GSTP1							
With G	Low	60	49	1.00	44	35	1.00
A/A	Low	147	94	1.09 (0.67-1.76)	99	93	0.84 (0.49-1.45)
With G	High	71	73	0.73 (0.43-1.25)	46	64	0.51 (0.28-0.94)
A/A	High	130	193	0.40 (0.25-0.64)	125	133	0.58 (0.34-0.99)
<i>P</i> for interaction				0.03	0.42		

¹Adjusted for age, physical activity, coffee, cigarette, alcohol, meat, vegetable/fruit and fish/shrimp; ²Adjusted for age, staple, meat, vegetable/fruit and fish/shrimp.

Table 6 Smoking specific risk for colorectal cancer for the combined effects of GST genotypes and vegetable/fruit consumption in men

Genotype	Vegetable/fruit consumption	Non-smokers			Smokers		
		Cases	Controls	OR (95% CI) ¹	Cases	Controls	OR (95% CI) ¹
GSTT1							
Null	Low	23	13	1.00	83	56	1.00
Present	Low	28	16	0.85 (0.33-2.21)	73	58	0.85 (0.51-1.41)
Null	High	45	55	0.41 (0.18-0.96)	59	65	0.66 (0.39-1.11)
Present	High	25	65	0.17 (0.07-0.42)	52	80	0.43 (0.25-0.73)
<i>P</i> for interaction				0.23	0.49		
GSTP1							
With G	Low	19	10	1.00	41	39	1.00
A/A	Low	32	19	0.80 (0.30-2.15)	115	75	1.21 (0.69-2.12)
With G	High	25	33	0.41 (0.15-1.10)	40	40	0.96 (0.49-1.88)
A/A	High	45	88	0.21 (0.09-0.52)	71	105	0.55 (0.31-0.98)
<i>P</i> for interaction				0.48	0.07		

¹Adjusted for age, physical activity, coffee, alcohol, meat and fish/shrimp.

between GSTM1, GSTT1 and GSTP1 polymorphisms and colorectal cancer risk for a Chinese population in Taiwan. The results revealed an elevated risk for colorectal cancer for men with GSTT1 null and GSTP1 with G allele genotypes, particularly for rectal cancer and diagnosed before 60 years old. We also found a very significant protective effect for men with GSTT1 present or GSTP1 A/A genotypes and higher consumption of vegetable/fruit. This combined effect reduces the risk for colorectal cancer to 0.40 or less, even for smokers, and further to about 0.20 for non-smokers, suggesting that these metabolic genes can modulate the risk of vegetable/fruit related colorectal cancer.

There is conflicting evidence concerning the role of GST polymorphisms in colorectal cancer susceptibility. It might be associated with the ethnic differences in allele frequency for these polymorphisms^[11]. Carcinogen exposures might vary among populations with the pathogenesis for colorectal cancer differing by tumor site. Moreover, inadequate study design such as non-random sampling, limited sample size and little attempt to adjust for potential confounders should also be considered.

It seems unlikely that the GSTM1 null genotype could predispose an individual to colorectal cancer because GSTM1 is only expressed at low levels in the colon^[38]. Conversely, GSTT1 and GSTP1 seem more likely susceptibility gene candidates because they are the predominant GST isoenzymes in colorectal tissue^[38,39] and are involved in the inactivation of heterocyclic amine^[40]. One previous publication on the GSTP1 A/G (Ile105Val) polymorphism identified that subjects having GSTP1 with G allele are at an elevated risk compared to those with the A/A genotype (OR = 1.77, 95%CI = 1.03-3.06)^[36]. However, one of the Alpha class isoenzymes, GSTA1, abundant in the human liver not colon, can also catalyze the detoxification of *N*-acetoxy-PhIP^[40,41] and increases the risk of colorectal cancer^[41]. Association between the polymorphism of GSTA1 and the risk of colorectal cancer for our subjects needed to be clarified in our future study.

Our results support that GSTT1 and GSTP1 might have a role in colorectal cancer susceptibility. The significant risk of the GSTT1 null genotype for colorectal cancer in our study might be due to the higher prevalence of GSTT1 null (49%) than in Caucasians (15-27%)^[11]. Although the frequency of the GSTP1 G allele in our controls (17%)

was lower than that in Caucasians (23-38%)^[42], the large sample size enabled us to find a moderate relationship between the GSTP1 with G allele and an increased risk of colorectal cancer of men.

Consistent with other studies^[37,43], this study also shows that risk factors for colorectal cancer is different between men and women in Taiwan. The GSTT1 null and GSTP1 with G allele genotypes were associated with increased risk of colorectal cancer, particularly in younger men and rectal cancer. The 2-fold increased risk of the GSTT1 null genotype relative to the GSTT1 present genotype for colorectal cancer in younger men is in line with other studies^[15,19,44]. Studies in human suggest that the detoxification potential of the GST enzymes decreases with age^[45]. It is possible that individuals with the null genotype develop tumors at a younger age than individuals that do express this enzyme. This study showed a slightly stronger genetic effect for the rectum over the colon. This was consistent with findings from previous studies^[17,18]. The risks associated with diet tend to be the strongest in the distal colon for men^[46]. Carcinogenesis within the distal colon has been associated with bulky-adduct-forming (BAF) agents^[47]. The GST polymorphisms of reduced detoxification genotype might thus more likely predispose the rectum rather than the colon to cancer.

In studies on the combined effects of GST polymorphisms and vegetable/fruit consumption on colorectal lesions, three studies indicated that the high isothiocyanates content in cruciferous vegetables enhances the cancer preventive effect for humans with the GSTM1 or T1 null genotypes^[27,28,30]. Potentially slower excretion of isothiocyanates induces GST. Other studies have reported that people with lower levels of enzyme activity (i.e., those with GSTM1 null genotype) obtain less protection from consuming cruciferous vegetables^[48,49]. Our data showed that the greatest protective effect from higher vegetable/fruit consumption was observed for men with GSTT1 present or GSTP1 A/A genotypes, but for women with GSTT1 null or GSTP1 with G allele genotypes. In addition, Lampe *et al*^[50] reported that brassica vegetables increased GSTA and GST activity for the GSTM1 null individuals in a randomized clinical trial. It is warranted to evaluate the gene-gene interactions of the polymorphic GST genes and their interactions with vegetables in further studies.

Because cruciferous vegetables not only induce phase I activating enzyme (e.g., cytochrome P4501A2 (CYP1A2)) and phase II inactivating enzyme (e.g., GST) expression and isothiocyanates themselves are a GST substrate^[51], the delicate balance between phase I, phase II enzymes and their regulators is undoubtedly an important determinant for cancer risk. Although cigarette smoking seems not to interact with GST genes to affect the colorectal cancer risk^[17,20,21,52], smoking can modify the association between GSTM1, cruciferous vegetables and colon cancer^[30]. Because metabolizing enzymes can detoxify carcinogens in cigarette smoke, cigarette smoking might play a role in the balance of these enzymes and their regulators. Smoking might modify this effect by reducing the benefit for approximately 30% for the study subjects. It has been proven that among frequent consumers of cruciferous vegetables, smokers with the GSTM1 null genotype have CYP1A2 activity 2-fold over non-smokers with the GSTM1 present genotype^[49]. Subjects with elevated CYP1A2 activity might be predisposed to colorectal cancer by activating heterocyclic amines and other procarcinogens^[53].

Because GSTT1 and GSTP1 are expressed at higher level in colorectal tissue and were associated with colorectal cancer risk in men, we postulate that people with the genotype for higher detoxified enzyme activity and higher vegetable/fruit consumption exhibit multiplicative synergistic beneficial effect for reduced colorectal cancer risk. This protective effect is extended for non-smokers without enzyme activation or carcinogens exposure. On the other hand, if the detoxifying enzymes were not related to colorectal cancer risk, higher vegetable/fruit consumption could exert their beneficial effect without being excreted by metabolizing enzymes.

This study was limited by obtaining dietary information retrospectively after diagnosis. We cannot exclude the effect of early preclinical disease on the dietary habits in these colorectal cancer cases. This effect might be negligible because the difference in eating habit changes in the previous 10 years among cases and controls was not significant ($P = 0.12$). In addition, the similar interview settings provided reassurance against potential information bias. Other limitations arise from the questionnaire, which included only the diet frequency for major food groups. We could not assess the impact of potential carcinogens derived from processed food or the effects of specific macronutrient or micronutrient.

The strengths of our study are the inclusion of newly diagnosed and histologically confirmed adenocarcinoma colorectal cancer cases and using controls that received colonoscopies. The possibility of misclassification is minimal. This large sample size allowed stratified data analysis. The observed environmental effects in the study population agreed with other published studies^[54] supporting the validity of our results.

Our study results suggest that the GSTT1 null genotype and the GSTP1 with G allele are potential risk alleles for colorectal cancer for the Chinese male population, but of beneficial effect for women with higher vegetable/fruit intake. The beneficial effect of vegetable/fruit on colorectal cancer is enhanced with GSTT1 present and GSTP1 A/A

genotypes for both men and women, in particular for non-smokers. Studies with specific vegetable types, related metabolic enzymes and dietary regulators in different age groups and tumor sites would help to clarify the association.

REFERENCES

- 1 **Mannervik B**, Awasthi YC, Board PG, Hayes JD, Di Ilio C, Ketterer B, Listowsky I, Morgenstern R, Muramatsu M, Pearson WR. Nomenclature for human glutathione transferases. *Biochem J* 1992; **282**(Pt 1): 305-306
- 2 **Ketterer B**. Protective role of glutathione and glutathione transferases in mutagenesis and carcinogenesis. *Mutat Res* 1988; **202**: 343-361
- 3 **Prochaska HJ**, Santamaria AB, Talalay P. Rapid detection of inducers of enzymes that protect against carcinogens. *Proc Natl Acad Sci USA* 1992; **89**: 2394-2398
- 4 **Zhang Y**, Kolm RH, Mannervik B, Talalay P. Reversible conjugation of isothiocyanates with glutathione catalyzed by human glutathione transferases. *Biochem Biophys Res Commun* 1995; **206**: 748-755
- 5 **Kolm RH**, Danielson UH, Zhang Y, Talalay P, Mannervik B. Isothiocyanates as substrates for human glutathione transferases: structure-activity studies. *Biochem J* 1995; **311** (Pt 2): 453-459
- 6 **Seidegard J**, Vorachek WR, Pero RW, Pearson WR. Hereditary differences in the expression of the human glutathione transferase active on trans-stilbene oxide are due to a gene deletion. *Proc Natl Acad Sci USA* 1988; **85**: 7293-7297
- 7 **Pemble S**, Schroeder KR, Spencer SR, Meyer DJ, Hallier E, Bolt HM, Ketterer B, Taylor JB. Human glutathione S-transferase theta (GSTT1): cDNA cloning and the characterization of a genetic polymorphism. *Biochem J* 1994; **300**(Pt 1): 271-276
- 8 **Ali-Osman F**, Akande O, Antoun G, Mao JX, Buolamwini J. Molecular cloning, characterization, and expression in *Escherichia coli* of full-length cDNAs of three human glutathione S-transferase Pi gene variants. Evidence for differential catalytic activity of the encoded proteins. *J Biol Chem* 1997; **272**: 10004-10012
- 9 **Norppa H**. Genetic polymorphisms and chromosome damage. *Int J Hyg Environ Health* 2001; **204**: 31-38
- 10 **Gilliland FD**, Harms HJ, Crowell RE, Li YF, Willink R, Belinsky SA. Glutathione S-transferase P1 and NADPH quinone oxidoreductase polymorphisms are associated with aberrant promoter methylation of P16(INK4a) and O(6)-methylguanine-DNA methyltransferase in sputum. *Cancer Res* 2002; **62**: 2248-2252
- 11 **Cotton SC**, Sharp L, Little J, Brockton N. Glutathione S-transferase polymorphisms and colorectal cancer: a HuGE review. *Am J Epidemiol* 2000; **151**: 7-32
- 12 **Seow A**, Yuan JM, Sun CL, Van Den Berg D, Lee HP, Yu MC. Dietary isothiocyanates, glutathione S-transferase polymorphisms and colorectal cancer risk in the Singapore Chinese health study. *Carcinogenesis* 2002; **23**: 2055-2061
- 13 **Ye Z**, Parry JM. Genetic polymorphisms in the cytochrome P450 1A1, glutathione S-transferase M1 and T1, and susceptibility to colon cancer. *Teratog Carcinog Mutagen* 2002; **22**: 385-392
- 14 **Tiemersma EW**, Kampman E, Bueno de Mesquita HB, Bunschoten A, van Schothorst EM, Kok FJ, Kromhout D. Meat consumption, cigarette smoking, and genetic susceptibility in the etiology of colorectal cancer: results from a Dutch prospective study. *Cancer Causes Control* 2002; **13**: 383-393
- 15 **Sgambato A**, Campisi B, Zupa A, Bochicchio A, Romano G, Tartarone A, Galasso R, Traficante A, Cittadini A. Glutathione S-transferase (GST) polymorphisms as risk factors for cancer in a highly homogeneous population from southern Italy. *Anticancer Res* 2002; **22**: 3647-3652
- 16 **Zhong S**, Wyllie AH, Barnes D, Wolf CR, Spurr NK. Relationship between the GSTM1 genetic polymorphism and susceptibility to bladder, breast and colon cancer. *Carcinogenesis* 1993;

- 14: 1821-1824
- 17 **Katoh T**, Nagata N, Kuroda Y, Itoh H, Kawahara A, Kuroki N, Ookuma R, Bell DA. Glutathione S-transferase M1 (GSTM1) and T1 (GSTT1) genetic polymorphism and susceptibility to gastric and colorectal adenocarcinoma. *Carcinogenesis* 1996; **17**: 1855-1859
- 18 **Deakin M**, Elder J, Hendrickse C, Peckham D, Baldwin D, Pantin C, Wild N, Leopard P, Bell DA, Jones P, Duncan H, Brannigan K, Alldersea J, Fryer AA, Strange RC. Glutathione S-transferase GSTT1 genotypes and susceptibility to cancer: studies of interactions with GSTM1 in lung, oral, gastric and colorectal cancers. *Carcinogenesis* 1996; **17**: 881-884
- 19 **Welfare M**, Monesola Adekun A, Bassendine MF, Daly AK. Polymorphisms in GSTP1, GSTM1, and GSTT1 and susceptibility to colorectal cancer. *Cancer Epidemiol Biomarkers Prev* 1999; **8**: 289-292
- 20 **Yoshioka M**, Katoh T, Nakano M, Takasawa S, Nagata N, Itoh H. Glutathione S-transferase (GST) M1, T1, P1, N-acetyltransferase (NAT) 1 and 2 genetic polymorphisms and susceptibility to colorectal cancer. *J UOEH* 1999; **21**: 133-147
- 21 **Katoh T**, Kaneko S, Takasawa S, Nagata N, Inatomi H, Ikemura K, Itoh H, Matsumoto T, Kawamoto T, Bell DA. Human glutathione S-transferase P1 polymorphism and susceptibility to smoking related epithelial cancer; oral, lung, gastric, colorectal and urothelial cancer. *Pharmacogenetics* 1999; **9**: 165-169
- 22 **Caporaso N**, Landi MT, Vineis P. Relevance of metabolic polymorphisms to human carcinogenesis: evaluation of epidemiologic evidence. *Pharmacogenetics* 1991; **1**: 4-19
- 23 **Doll R**, Peto R. The causes of cancer: quantitative estimates of avoidable risks of cancer in the United States today. *J Natl Cancer Inst* 1981; **66**: 1191-1308
- 24 **Thomas HJ**. Familial colorectal cancer. *BMJ* 1993; **307**: 277-278
- 25 **Armstrong B**, Doll R. Environmental factors and cancer incidence and mortality in different countries, with special reference to dietary practices. *Int J Cancer* 1975; **15**: 617-631
- 26 **Kiyohara C**. Genetic polymorphism of enzymes involved in xenobiotic metabolism and the risk of colorectal cancer. *J Epidemiol* 2000; **10**: 349-360
- 27 **Lin HJ**, Probst-Hensch NM, Louie AD, Kau IH, Witte JS, Ingles SA, Frankl HD, Lee ER, Haile RW. Glutathione transferase null genotype, broccoli, and lower prevalence of colorectal adenomas. *Cancer Epidemiol Biomarkers Prev* 1998; **7**: 647-652
- 28 **Kiss I**, Sandor J, Ember I. Allelic polymorphism of GSTM1 and NAT2 genes modifies dietary-induced DNA damage in colorectal mucosa. *Eur J Cancer Prev* 2000; **9**: 429-432
- 29 **Slattery ML**, Potter JD, Ma KN, Caan BJ, Leppert M, Samowitz W. Western diet, family history of colorectal cancer, NAT2, GSTM-1 and risk of colon cancer. *Cancer Causes Control* 2000; **11**: 1-8
- 30 **Slattery ML**, Kampman E, Samowitz W, Caan BJ, Potter JD. Interplay between dietary inducers of GST and the GSTM-1 genotype in colon cancer. *Int J Cancer* 2000; **87**: 728-733
- 31 **Lee E**, Huang Y, Zhao B, Seow-Choen F, Balakrishnan A, Chan SH. Genetic polymorphism of conjugating enzymes and cancer risk: GSTM1, GSTT1, NAT1 and NAT2. *J Toxicol Sci* 1998; **23 Suppl 2**: 140-142
- 32 **Guo JY**, Wan DS, Zeng RP, Zhang Q. The polymorphism of GSTM1, mutagen sensitivity in colon cancer and healthy control. *Mutat Res* 1996; **372**: 17-22
- 33 **Harris MJ**, Coggan M, Langton L, Wilson SR, Board PG. Polymorphism of the Pi class glutathione S-transferase in normal populations and cancer patients. *Pharmacogenetics* 1998; **8**: 27-31
- 34 **Yeh CC**, Hsieh LL, Tang R, Chang-Chieh CR, Sung FC. Risk factors for colorectal cancer in Taiwan: a hospital-based case-control study. *J Formos Med Assoc* 2003; **102**: 305-312
- 35 **Huang CY**, Huang KL, Cheng TJ, Wang JD, Hsieh LL. The GST T1 and CYP2E1 genotypes are possible factors causing vinyl chloride induced abnormal liver function. *Arch Toxicol* 1997; **71**: 482-488
- 36 **Harries LW**, Stubbins MJ, Forman D, Howard GC, Wolf CR. Identification of genetic polymorphisms at the glutathione S-transferase Pi locus and association with susceptibility to bladder, testicular and prostate cancer. *Carcinogenesis* 1997; **18**: 641-644
- 37 **Tang R**, Wang JY, Lo SK, Hsieh LL. Physical activity, water intake and risk of colorectal cancer in Taiwan: a hospital-based case-control study. *Int J Cancer* 1999; **82**: 484-489
- 38 **Nijhoff WA**, Grubben MJ, Nagengast FM, Jansen JB, Verhagen H, van Poppel G, Peters WH. Effects of consumption of Brussels sprouts on intestinal and lymphocytic glutathione S-transferases in humans. *Carcinogenesis* 1995; **16**: 2125-2128
- 39 **de Bruin WC**, Wagenmans MJ, Board PG, Peters WH. Expression of glutathione S-transferase theta class isoenzymes in human colorectal and gastric cancers. *Carcinogenesis* 1999; **20**: 1453-1457
- 40 **Lin D**, Meyer DJ, Ketterer B, Lang NP, Kadlubar FF. Effects of human and rat glutathione S-transferases on the covalent DNA binding of the N-acetoxy derivatives of heterocyclic amine carcinogens *in vitro*: a possible mechanism of organ specificity in their carcinogenesis. *Cancer Res* 1994; **54**: 4920-4926
- 41 **Coles BF**, Morel F, Rauch C, Huber WW, Yang M, Teitel CH, Green B, Lang NP, Kadlubar FF. Effect of polymorphism in the human glutathione S-transferase A1 promoter on hepatic GSTA1 and GSTA2 expression. *Pharmacogenetics* 2001; **11**: 663-669
- 42 **Coughlin SS**, Hall IJ. Glutathione S-transferase polymorphisms and risk of ovarian cancer: a HuGE review. *Genet Med* 2002; **4**: 250-257
- 43 **Iacopetta B**. Are there two sides to colorectal cancer? *Int J Cancer* 2002; **101**: 403-408
- 44 **Chenevix-Trench G**, Young J, Coggan M, Board P. Glutathione S-transferase M1 and T1 polymorphisms: susceptibility to colon cancer and age of onset. *Carcinogenesis* 1995; **16**: 1655-1657
- 45 **van Lieshout EM**, Peters WH. Age and gender dependent levels of glutathione and glutathione S-transferases in human lymphocytes. *Carcinogenesis* 1998; **19**: 1873-1875
- 46 **McMichael AJ**, Potter JD. Diet and colon cancer: integration of the descriptive, analytic, and metabolic epidemiology. *Natl Cancer Inst Monogr* 1985; **69**: 223-228
- 47 **Breivik J**, Gaudernack G. Carcinogenesis and natural selection: a new perspective to the genetics and epigenetics of colorectal cancer. *Adv Cancer Res* 1999; **76**: 187-212
- 48 **Whalen R**, Boyer TD. Human glutathione S-transferases. *Semin Liver Dis* 1998; **18**: 345-358
- 49 **Probst-Hensch NM**, Tannenbaum SR, Chan KK, Coetzee GA, Ross RK, Yu MC. Absence of the glutathione S-transferase M1 gene increases cytochrome P4501A2 activity among frequent consumers of cruciferous vegetables in a Caucasian population. *Cancer Epidemiol Biomarkers Prev* 1998; **7**: 635-638
- 50 **Lampe JW**, Chen C, Li S, Prunty J, Grate MT, Meehan DE, Barale KV, Dightman DA, Feng Z, Potter JD. Modulation of human glutathione S-transferases by botanically defined vegetable diets. *Cancer Epidemiol Biomarkers Prev* 2000; **9**: 787-793
- 51 **Lampe JW**, Peterson S. Brassica, biotransformation and cancer risk: genetic polymorphisms alter the preventive effects of cruciferous vegetables. *J Nutr* 2002; **132**: 2991-2994
- 52 **Slattery ML**, Potter JD, Samowitz W, Bigler J, Caan B, Leppert M. NAT2, GSTM-1, cigarette smoking, and risk of colon cancer. *Cancer Epidemiol Biomarkers Prev* 1998; **7**: 1079-1084
- 53 **Lang NP**, Butler MA, Massengill J, Lawson M, Stotts RC, Hauer-Jensen M, Kadlubar FF. Rapid metabolic phenotypes for acetyltransferase and cytochrome P4501A2 and putative exposure to food-borne heterocyclic amines increase the risk for colorectal cancer or polyps. *Cancer Epidemiol Biomarkers Prev* 1994; **3**: 675-682
- 54 **Potter JD**, Slattery ML, Bostick RM, Gapstur SM. Colon cancer: a review of the epidemiology. *Epidemiol Rev* 1993; **15**: 499-545

• COLORECTAL CANCER •

Clinical phenotype and prevalence of hereditary nonpolyposis colorectal cancer syndrome in Chinese population

Yuan-Zhi Zhang, Jian-Qiu Sheng, Shi-Rong Li, Hong Zhang

Yuan-Zhi Zhang, Department of Gastroenterology, General Hospital of Perking Military Area and Third Military Medical College, Beijing 10070, China

Jian-Qiu Sheng, Shi-Rong Li, Hong Zhang, Department of Gastroenterology, General Hospital of Perking Military Area, Beijing 10070, China

Correspondence to: Dr. Yuan-Zhi Zhang, Department of Gastroenterology, General Hospital of Perking Military Area, Beijing 10070, China. jianming2000@163.com

Telephone: +86-01-86357923

Received: 2004-08-18 Accepted: 2004-09-18

Abstract

AIM: To describe systematically the clinical characteristics and phenotype of HNPCC families and the prevalence of HNPCC in the general population of CRC patients in China.

METHODS: HNPCC kindreds and CRC patients were from two sources. One was that we consecutively investigated kindreds and patients by ourselves. And the other was the published Chinese and foreign literature related to Chinese HNPCC syndrome. There were 142 HNPCC families fulfilling AC I and/or AC II including 57 families with detailed data, and 3874 general primary CRC patients in all. All statistical tests were two-sided.

RESULTS: In AC I families, the number of Lynch syndrome I and II families were 25 (47.2%) and 28 (52.8%) respectively. There were 215 patients (82.4%) with CRC, 67 patients (25.7%) with extracolonic cancer and 50 patients (19.2%) with multiple primary cancers. In all CRC patients, multiple primary CRC were in 41 patients (19.1%), and the first-CRC was right-sided colorectal cancer in 143 patients (66.5%) and rectal cancer in 44 patients (20.5%). 8.8% and 19.2% of the first cancer were CRC and extracolonic cancers. Among those patients whose first cancer was CRC, 66.8% and 19.9% were right-sided colorectal cancer and rectal cancer, respectively. The similar results were found in AC II families. Normal distribution was only found in the distribution of the age of diagnosis of the first cancer in both AC I families (coefficient of skewness: $u = 0.81$, $0.20 < P < 0.50$; coefficient of kurtosis: $u = 1.13$, $0.20 < P < 0.40$, $\alpha = 0.20$) and AC II families (coefficient of skewness: $u = 0.63$, $P > 0.5$ > 0.20; coefficient of kurtosis: $u = 0.84$, $0.20 < P < 0.50$, $\alpha = 0.20$), but not found in the distribution of the age of diagnosis of the first CRC. When patients with HNPCC-associated cancer suffered from the first malignant tumor in HNPCC families diagnosed by AC I and AC II, the mean age and median age were 45.1 ± 12.7 years and 44.0 years,

45.2 ± 12.7 years and 44.5 years, respectively. The median age of diagnosis of the first tumor of the patients in the later generation was younger than that in the previous generation. Many extracolonic cancers were found to be associated with HNPCC syndrome. Gastric cancer was the most frequent extracolonic cancer followed by endometrial cancer and hepatocarcinoma. In general population of CRC patients, the prevalence of HNPCC diagnosed by AC I and AC II were 1.3% and 2.2%, respectively.

CONCLUSION: The clinical phenotype and prevalence of Chinese HNPCC syndrome are similar to those of Europeans and Americans. Gastric cancer is the most common extracolonic malignant tumor. The age of diagnosis of the first malignant tumor tends to be increasingly younger in patients with HNPCC-related tumors.

© 2005 The WJG Press and Elsevier Inc. All rights reserved.

Key words: Hereditary nonpolyposis colorectal cancer; Phenotype; Prevalence; Normal distribution

Zhang YZ, Sheng JQ, Li SR, Zhang H. Clinical phenotype and prevalence of hereditary nonpolyposis colorectal cancer syndrome in Chinese population. *World J Gastroenterol* 2005; 11(10): 1481-1488

<http://www.wjgnet.com/1007-9327/11/1481.asp>

INTRODUCTION

Colorectal cancer (CRC) is the second most frequent cancers in Western countries^[1], and the third leading cause of cancer deaths in the United States^[2]. In China, the mortality rate of CRC is the fourth to sixth leading cause of cancer deaths^[3]. And its mortality and prevalence are inclined to increase in the coming years. Patients with a familial risk, who have two or more first- or second-degree relatives (or both) with CRC, make up approximately 20 percent of all patients with CRC, whereas approximately 5 to 10 percent of the total annual burden of CRC is Mendelian in nature, that is, it is inherited in an autosomal dominant manner. Hereditary nonpolyposis colorectal cancer (HNPCC) syndrome, also referred to as the Lynch syndrome, is the most common form of hereditary CRC in an autosomal dominant manner^[4]. In addition to CRC, tumors also occur in the endometrium, small bowel, pancreas, biliary tract, stomach, ovary, and urinary tract. Clinically, this disorder is mainly defined by the Amsterdam criteria (AC), which was established by the International

Collaborative Group on HNPCC (ICG-HNPCC) at its meeting in Amsterdam in 1990^[5]. The AC includes the following: (1) at least three relatives with histologically verified CRC, one of them a first-degree relative of the other two (familial adenomatous polyposis excluded); (2) at least two successive generations affected; (3) in one of the individuals, diagnosis of CRC before the age of 50. These criteria were pivotal in identifying kindreds that eventually led to the association of the HNPCC syndrome with germline mismatch repair gene mutations (MMR). However, the criteria are strict and do not account for extracolonic cancers or for small kindreds. In 1998, the set of new clinical criteria for collaborative studies were proposed that included the extracolonic cancers associated with HNPCC and accepted by the majority (85%) of the group^[6]. In addition, it was proposed to keep the classical criteria, which are referred to as Amsterdam Criteria I (AC I). And the revised ICG-HNPCC criteria are referred to as Amsterdam Criteria II (AC II). The AC II includes the following: (1) At least 3 relatives with an HNPCC-associated cancer (CRC, cancer of the endometrium, small bowel, ureter or renal pelvis); (2) One should be a first-degree relative of the other 2; (3) At least 2 successive generations should be affected; (4) At least 1 should be diagnosed before age 50; (5) Familial adenomatous polyposis should be excluded in the CRC case (s) if any and (6) Tumors should be verified by pathological examination. Although there had been many reports on characteristics of HNPCC kindreds in China in the past decade, their samples on fulfilled AC I or AC II kindreds were very small, and most of theirs were only case reports. So there is no systematic and all round clinical research on HNPCC until now. Therefore, it is necessary and urgent to find out the phenotype and prevalence of HNPCC fulfilled AC I or AC II in a larger sample in Chinese populations and the differences between the Chinese patients and the Euro-Americans.

In this study, we on the one hand enrolled kindreds fulfilled AC I or AC II and investigated CRC patients who on our own. On the other hand, in order to provide the overall information on Chinese HNPCC, we reviewed and synthesized the literature on Chinese HNPCC. Based on clinical data, we hoped to find out clinical phenotype and characteristics of HNPCC families in a larger sample and the prevalence of HNPCC in a larger population of CRC patients and to evaluate whether the two sets of criteria for HNPCC are useful in clinical diagnosis and management of HNPCC in modern Chinese society.

MATERIALS AND METHODS

Materials

All subjects could be divided into two groups: HNPCC kindreds and general CRC patients. They were from two sources. One was that we consecutively investigated kindreds and patients by ourselves. During the period from October 2001 to May 2004, we consecutively investigated 25 Chinese families that fulfilled the AC I or AC II. Although there are only four HNPCC-associated cancers (CRC, cancer of the endometrium, small bowel, ureter or renal pelvis) in AC II, ICG definition of HNPCC-associated cancers also included cancers of the stomach, ovary, brain, hepatobiliary tract,

and skin (sebaceous tumors)^[6]. So when we clinically diagnosed HNPCC families that fulfilled AC II, those tumors also were included in the criteria. These families were from Beijing, Henan Province, Inner Mongolia Autonomous Region, Hebei Province, Yunnan Province and Liaoning Province. From January 2002 to December 2002, we also consecutively investigated 594 CRC inpatients with detailed family history in the general hospital of Perking military area. The other source was the published Chinese and foreign literature related to Chinese HNPCC from 1994 to 2004, which were collected by bibliographic searches through Index of Chinese Science, Technology Data and PUBMED. The selection criteria of literature were as follows: the independent kindreds and prevalence of HNPCC were published in Chinese or English magazines, each report should have the detailed kindred data or extracolonic tumor records. Duplicated, poor quality reports or those with little information on each kindred were discarded. Thus, 24 papers were chosen by screening (Table 1), 117 families that fulfilled AC I or AC II and 3 280 general CRC patients were accumulated from 11 districts in China. In Table 1, all or partially reported families have complete data from number 1 to 14; there were detailed data on extracolonic cancer associated with HNPCC from 15 to 21, and HNPCC prevalence data from 20 to 24. In the present study, there were 142 HNPCC families and 3 874 general CRC patients. They were from 15 regions in China, including Beijing, Tianjin, Shanghai, Zhejiang Province, Guangdong Province, Jiangsu Province, Shandong Province, Hebei Province, Henan Province, Hunan Province, Sichuan Province, Yunnan Province, Liaoning Province, Inner Mongolia and Taiwan. Of the HNPCC families, there were 57 families with complete data.

Methods

In 57 fulfilled AC I or AC II families with complete data, common characteristics of HNPCC kindreds were analyzed. In the different criteria, the following were to be analyzed: Distribution of the age of diagnosis of the first tumor and the first CRC, proportion of CRC patients, multiple primary CRC and tumors, proximal cancer to the splenic flexure (or right-sided CRC) and rectal cancer. Extracolonic tumor spectrum associated with HNPCC was analyzed in 142 families, and the prevalence of HNPCC was done in 3 874 general CRC patients.

Statistical analysis

All data were descriptively analyzed by software SPSS 10.0. Test of normality was done by method of movement, and size of the test was $\alpha = 0.20$. When the two values of P on the coefficient of skewness and coefficient of kurtosis are both $P > 0.20$, the data were considered to be normal distribution. All statistical tests were two-sided.

RESULTS

Characterization of HNPCC families

In 57 HNPCC kindreds, there were 53 families that fulfilled AC I and 4 families that only fulfilled AC II. In 53 HNPCC families that fulfilled AC I, the number of Lynch syndrome I and II families were 25 (47.2%) and 28 (52.8%), respectively.

Table 1 Condition of all chosen papers and their studied districts

Number	First authors	District	Source of references
1	Zhen-Jun Wang	Beijing	<i>Journal of Coloproctological Surgery</i> , 2001, 7(3): 3-4
2	Ding-Cun Luo	Zhejiang	<i>China Oncology</i> , 2000, 10(2): 145-146, 152
3	Shi-Lin Wang	Beijing	<i>Journal of General Hospital of Air Force</i> , 2000, 16(1): 33-34, 37
4	Yan-Ting Jian	Guangdong	<i>J First Mil Med Univ</i> , 2001, 21(1): 15-16
5	Shi-Xin Xu	Jiangsu	<i>China Oncology</i> , 1998, 8(1): 56-58
6	Shan-Jing Mo	Shanghai	<i>Chin J Dig</i> , 1996, 16(6): 326-328
7	Jian-Sheng Li	Zhejiang	<i>Journal of Practical Oncology</i> , 2000, 15(1): 46-47
8	Meng-Hong Sun	Shanghai	<i>Natl Med J China</i> , 2001, 81(20): 1268-1269
9	Zhi-Zhuang Li	Shandong	<i>Acta Academiae Medicinae Nantong</i> , 2001, 21(4): 437
10	Chen-Yi Wang	Hunan	<i>Hunan Medical Journal</i> , 1998, 15(1): 64
11	Gang Ye	Zhejiang	<i>Medical Journal of Ningbo</i> , 1997, 9(5): 226
12	Liang Xu	Sichuan	<i>The Practical Journal of Cancer</i> , 2002, 17(4): 395-397
13	Zhen-Jun Wang	Beijing	<i>Chin J Gastrointest Surg</i> , 2000, 3(4): 217-219
14	Yi-Tao Jia	Hebei	<i>Chin J Med Genet</i> , 1999, 16(3): 200
15	Hei-Ying Jin	Shanghai	<i>J Clin Surg</i> , 2001, 9(6): 356-357
16	Shi-Lin Wang	Beijing	<i>Journal of Oncology</i> , 2002, 8(1): 24-26
17	Guo-Fu Chen	Zhejiang	<i>China Oncology</i> , 2003, 13(3): 240-242
18	Li-Xin Liu	Beijing	<i>Chinese Journal of Coal Industry Medicine</i> , 2002, 5(7): 643-644
19	SC Wei	Taiwan	<i>J Formos Med Assoc</i> , 2002, 101(3): 206-209
20	San-Jun Cai	Shanghai	<i>World J Gastroenterol</i> , 2003, 9(2): 284-287
21	Gang Chen	Tianjin	<i>Chinese Journal of Clinical Oncology</i> , 2003, 30(4): 247-249
22	Hua-Wei Jin	Guangdong	<i>Chinese Journal of Practical Surgery</i> , 2000, 20(4): 231-232
23	Zhi-Qiang Xue	Guangdong	<i>Guangdong Medical Journal</i> , 2003, 24(7): 752-753
24	Shi-Lin Wang	Beijing	<i>Chin J Gen Surg</i> , 2000, 15(11): 667-668

There were 261 cancer patients and 343 primary cancers in all. In 261 cancer patients, there were 215 patients (82.4%) with CRC, 67 patients (25.7%) with extracolonic cancer and 50 patients (19.2%) with multiple primary cancers. In 215 CRC patients, there were 41 patients (19.1%) with synchronous (multiple colorectal cancers at or within six months after surgical resection for CRC) or metachronous (CRC occurring more than six months after surgery) CRC and 20 patients (9.3%) with both extracolonic cancer and CRC. In all CRC patients, the first CRC was right-sided CRC in 143 patients (66.5%) and rectal cancer in 44 patients (20.5%). The first cancer was CRC in 211 patients (80.8%) and extracolonic cancer in 50 patients (19.2%). In patients whose first cancer was CRC, 141 patients (66.8%) had right-sided CRC and 42 patients (19.9%) had rectal cancer. There were 270 CRCs (78.7%) and 73 extracolonic cancers (21.3%) in all primary cancers. The proportion of right-sided colorectal cancer and rectal cancer were 62.6% and 21.1% in primary CRCs respectively.

If HNPCC families were diagnosed by AC II, 25 families (43.9%) were Lynch syndrome I and 32 families (56.1%) were Lynch syndrome II. There were 276 cancer patients and 364 primary cancers in all. In all cancer patients, there were 223 CRC patients (80.8%), 75 patients (27.2%) with extracolonic cancer and 52 patients (18.8%) with multiple primary cancers. In 223 CRC patients, there were 43 patients (19.3%) with synchronous or metachronous CRC and 22 patients (9.9%) with both extracolonic cancer and CRC. The first cancer was CRC in 219 patients (79.3%) and extracolonic cancer in 57 patients (20.7%). In patients whose first cancer was CRC, 144 (65.8%) patients had right-sided CRC and 46 patients (21%) had rectal cancer. In 223 CRC patients, proportions of right-sided CRC and rectal cancer of the first CRCs were 65.5% and 21.5% respectively. In

364 primary cancers, there were 282 CRCs (77.5%) and 82 extracolonic cancers (22.5%). In 282 CRCs, the proportion of right-sided CRC and rectal cancer were 63.1% and 21.6% respectively.

Distribution of the age of diagnosis of the first malignant tumor in HNPCC-associated cancer patients and general primary CRC patients

In 57 AC II HNPCC families, the distribution of the age of diagnosis of the first cancer was normal distribution (coefficient of skewness: $u = 0.63$, $P > 0.5$; coefficient of kurtosis: $u = 0.84$, $0.40 < P < 0.50$) (Figure 1A). The mean age and median age were 45.2 ± 12.7 and 44.5 years (range from 5 to 84 years) respectively. The distribution of the age of diagnosis of the first CRC was not normal distribution (coefficient of skewness: $u = 1.85$, $0.05 < P < 0.10$; coefficient of kurtosis: $u = 0.81$, $0.40 < P < 0.50$) in CRC patients in these HNPCC families. Its median age was 43.0 years (range from 12 to 84 years).

In 53 AC I families, the distribution of the age of diagnosis of the first cancer was normal distribution (coefficient of skewness: $u = 0.81$, $0.40 < P < 0.50$; coefficient of kurtosis: $u = 1.13$, $0.20 < P < 0.40$). The mean age and median age of diagnosis of the first cancer were 45.1 ± 12.7 years and 44.0 years (range from 5 to 84 years) respectively. But the distribution of the age diagnosed the first CRC in AC I families was the same as that in the AC II families. It also was not normal distribution (coefficient of skewness: $u = 1.85$, $0.05 < P < 0.10$; coefficient of kurtosis: $u = 0.96$, $0.20 < P < 0.40$). Its median age was 43.0 years (range from 12 to 84 years).

In 594 primary CRC inpatients consecutively investigated, the distribution of the diagnosed age was not normal distribution (coefficient of skewness: $u = 5.03$, $P < 0.001$; coefficient of kurtosis: $u = 1.04$, $0.20 < P < 0.40$) (Figure 1B).

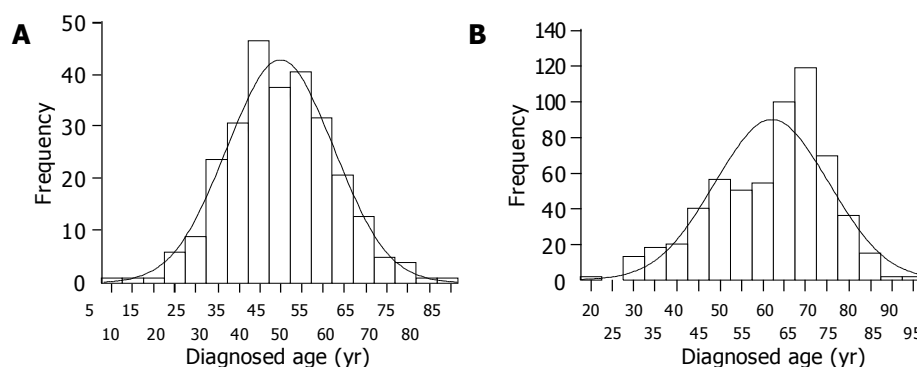


Figure 1 Distribution of the age. A: Distribution of the ages of diagnosis of the first cancer of HNPCC-associated cancer patients in AC II families; B: Distribution of the ages of diagnosis of CRC of 594 general primary CRC patients.

The median age was 65 years (range from 21 to 95 years). There was a statistical significance on the difference of the mean or median age between HNPCC patients and general primary CRC patients ($P < 0.05$).

Age of diagnosis of the first tumor of HNPCC-associated cancer patients in different generations

Because 4 were only fulfilled AC II in 57 AC II HNPCC families, here we only discuss the age of diagnosis of the first tumor of HNPCC-associated cancer patients in different generations in AC II families. At least 2 and at most 5 successive generations should be affected. The numbers of patients in the first, second, third, fourth and fifth generation were 93, 134, 43, 5 and 1 respectively. The distribution of the age of diagnosis of the first tumor of the patients both in the first (coefficient of skewness: $\mu = 0.97$, $0.20 < P < 0.40$; coefficient of kurtosis: $\mu = 1.08$, $0.20 < P < 0.40$) and second generation (coefficient of skewness: $\mu = 0.50$, $P > 0.50$; coefficient of kurtosis: $\mu = 0.59$, $P > 0.50$) were normal distribution, but that in third generation was not normal distribution (coefficient of skewness: $\mu = 1.94$, $0.05 < P < 0.10$; coefficient of kurtosis: $\mu = 1.80$, $0.05 < P < 0.10$). Because the number of patients both in the fourth and fifth generation was too small, their distributions were not analyzed. The mean and median age in the first generation and second generation were 52.7 ± 11.7 and 52.0 , 43.1 ± 11.7 and 43.0 years respectively. The median age in the third generation and fourth generation were 38 years and 31 years respectively. The median age of diagnosis of the first tumor of the patients in the later generation was younger than that in the previous generation.

Spectrum of extracolonic cancer associated with HNPCC and HNPCC prevalence in general primary CRC

In 142 HNPCC families fulfilled AC II, there were 105 families that definitely fulfilled AC I. All these families had the detailed spectrum of extracolonic cancers. There were 125 extracolonic cancers in AC I families and 174 extracolonic cancers in AC II families (Table 2). The spectrum of extracolonic cancers were almost the same in AC I families as in AC II families. Gastric cancer was the most frequent extracolonic cancers in both AC I and AC II families, followed by endometrial cancer, hepatocarcinoma and the other extracolonic cancers.

Table 2 Extracolonic tumors found in HNPCC families

Extracolonic tumor	Number of AC (%)	Number of AC II (%)
Gastric cancer	36 (28.8)	49 (28.2)
Endometrial cancer	28 (22.4)	36 (20.7)
Ovarian cancer	6 (4.8)	9 (5.2)
Small intestinal cancer	3 (2.4)	9 (5.2)
Esophageal cancer	6 (4.8)	9 (5.2)
Pancreatic cancer	5 (4.0)	6 (3.4)
Breast cancer	5 (4.0)	7 (4.0)
Cancer of nasopharynx/larynx	2 (1.6)	3 (1.7)
Malignant lymphoma	2 (1.6)	2 (1.2)
Leukemia	1 (0.8)	1 (0.6)
Thyroid cancer	5 (4.0)	5 (2.9)
Lung cancer	4 (3.2)	8 (4.6)
Hepatocarcinoma	10 (8.0)	11 (6.3)
Bladder carcinoma	1 (0.8)	3 (1.7)
Cancer of brain	3 (2.4)	5 (2.9)
Ureter/renal pelvis cancer	0 (0.0)	1 (0.6)
Carcinoma of kidney	2 (1.6)	2 (1.2)
Skin cancer	2 (1.6)	2 (1.2)
Osteosarcoma	0 (0.0)	2 (1.2)
Carcinoma of prostate	1 (0.8)	1 (0.6)
Malignant teratoma	1 (0.8)	1 (0.6)
Cancer of parotid gland	1 (0.8)	1 (0.6)
Liposarcoma	1 (0.8)	1 (0.6)
Total	125 (100.0)	174 (100.0)

Among 3874 primary CRC patients, the condition of HNPCC patients whose families fulfilled AC I were only analyzed in 942 patients, and the condition of HNPCC patients whose families fulfilled AC II were only analyzed in 1 058 patients. Both of them were analyzed in the other 1 874 patients. So in 2 816 patients who were analyzed the condition of HNPCC patients whose families fulfilled AC I, there were 35 HNPCC patients (1.2%; 95% confidence interval [CI] = 0.8-1.7%). And in 2 932 patients who were analyzed the condition of HNPCC patients whose families fulfilled AC II there were 63 HNPCC patients (2.2%; 95% confidence interval [CI] = 1.6-2.7%).

DISCUSSION

Aldred Warthin first described what is now recognized as the HNPCC or Lynch syndrome in 1913. HNPCC is an autosomal dominantly inherited disorder of cancer

susceptibility with high penetrance (80-85%)^[6], and accounts for approximately 1% to 3% of all cases of colorectal cancer^[7]. This disorder is often characterized by multiple generations being affected and the development of colorectal cancer that is often diagnosed at an early age (mean age, approximately 45 years) and is mostly right-sided colorectal cancer (approximately 70% proximal to the splenic flexure)^[4,6,7]. There is an excess of synchronous CRC and metachronous CRC in 35% of patients^[6]. In addition, there is an excess of extracolonic cancers^[4,6]. The cancer of the endometrium, stomach, ovaries, small bowel, ureter, renal pelvis, brain, and hepatobiliary tract are all clinically associated with HNPCC. But in AC II established in 1998, only CRC, cancer of the endometrium, small bowel, ureter or renal pelvis were thought as HNPCC-associated cancers^[6]. Stomach cancer has a high prevalence in some Asian countries. Occasionally, it results in the chance of familial aggregation of CRC and stomach cancer. But in HNPCC families reported in the Western countries, stomach cancer is uncommon and is observed mainly in patients from older generations. Though stomach cancer was frequently reported in HNPCC families in Asia, there were no studies in these countries revealing the relative risk of developing stomach cancer in carriers of a mutated MMR gene. Therefore, stomach cancer was not included in the spectrum of HNPCC-associated cancers in AC II established by ICG-HNPCC^[6].

HNPCC families can be classically subdivided into Lynch syndrome I and II. Lynch syndrome I only displays colorectal cancer, whereas Lynch syndrome II also exhibits extracolonic tumors. In China, our study showed that the proportion of Lynch syndrome I and II were 43.9% and 56.1% by AC II, 47.2% and 52.8% by AC I respectively. It suggested there were extracolonic cancers in most of Chinese HNPCC families. In AC I families, the overall proportion of CRC, extracolonic cancer, multiple primary cancers and multiple primary CRC patients were 82.4%, 25.7%, 19.2% and 19.1% respectively. The first CRC was right-sided CRC in 66.5% CRC patients. In addition, the first cancer was CRC in 80.8% patients. Among those patients whose first cancer was CRC, 66.8% and 19.9% were right-sided CRC and rectal cancer respectively. At the same time, there were also the similar results in AC II families. It showed that most of HNPCC associated-cancer patients were susceptible to CRC. Moreover, CRC was mainly located in the proximal rather than the distal part of the colon in two-thirds of CRC patients where CRC was the first cancer. It was an important characteristic of HNPCC syndrome. Extracolonic cancer was the first cancer in one-fifth or so of HNPCC associated-cancer patients diagnosed by both AC and AC II. It implied that extracolonic cancers were associated with HNPCC, and many similar results were also reported from other countries^[8-11]. So extracolonic cancers should be included in clinical criteria of HNPCC families. In addition, the proportions of multiple CRC and right-sided CRC patients in the Chinese HNPCC families were similar to those in the Western HNPCC families^[6,12-15].

One of the most important characteristics is that HNPCC-associated cancer is diagnosed at an early age. The mean or median age at cancer diagnosis is approximately

from 41 to 50 years^[4,6-7,12-15]. Mean and median are two most important parameters which statistically describe the central tendency of quantitative data, but there are some differences in their applications. Mean applies to quantitative data of normal distribution. If quantitative data are not normal distribution, mean cannot really describe the central tendency and average level of data. Median applies to all types of quantitative data. If quantitative data are normal distribution, median is theoretically equal to mean. So when we describe the central tendency of some quantitative data, normal distribution should be tested. In HNPCC-associated cancer patients, our study showed that the age distribution of patients diagnosed with the first malignant tumor was normal distribution. The same results were also observed in HNPCC-associated cancer patients of the first and second generations. But the distribution of the age of diagnosis of the first CRC was not normal distribution in all CRC patients. So both mean age and median age could be used to describe the central tendency of the age distribution of patients diagnosed with the first malignant tumor, and median age is the only parameter which can accurately describe the central tendency of the age distribution of patients diagnosed with the first CRC. When patients with HNPCC-associated cancer suffered from the first malignant tumor in Chinese HNPCC families diagnosed by AC and AC II, the mean and median age were 45.1 and 44.0, 45.2 and 44.5 years respectively. When they suffered from the first CRC, the median ages were both 43.0 years. These results were similar to those from other countries^[4,6,7,12-15]. In addition, our findings showed a tendency that HNPCC-associated cancer patients can be diagnosed the first malignancy at an earlier age in later generation than in previous generation. The median ages in the first, second, third and fourth generations were 52, 43, 38 and 31 years respectively.

The other important feature of HNPCC syndrome is frequent occurrence of extracolonic cancers. Many evidences suggest that extracolonic cancers are associated with HNPCC syndrome in clinic and (or) genetics^[4,6,7,9-11,15,16-19]. Our study revealed that about one-fourth of HNPCC-associated cancer patients had extracolonic cancer in China. Its proportion was smaller than in American HNPCC families^[15]. The spectrum of extracolonic cancers included gastric cancer, endometrial cancer, hepatocarcinoma, ovary cancer, esophageal cancer, pancreatic cancer, breast cancer, thyroid cancer, lung cancer, small intestinal cancer, cancer of brain, cancer of nasopharynx/larynx, malignant lymphoma, carcinoma of kidney, skin cancer, leukemia, bladder carcinoma, carcinoma of prostate, malignant teratoma, cancer of parotid gland, liposarcoma, ureter or renal pelvis cancer and osteosarcoma. Ureter or renal pelvis cancer and osteosarcoma were only found in AC II HNPCC families. Gastric cancer, endometrial cancer and hepatocarcinoma were the first, second and third most frequent extracolonic cancers in both AC I HNPCC families and AC II HNPCC families, respectively. They were followed by ovary cancer, esophageal cancer, pancreatic cancer, breast cancer, thyroid cancer, lung cancer, small intestinal cancer, cancer of brain, cancer of nasopharynx/larynx, malignant lymphoma, carcinoma of kidney, skin cancer, leukemia, bladder carcinoma, carcinoma of prostate, malignant teratoma, cancer of parotid gland and liposarcoma

in AC HNPCC families, and gastric cancer, endometrial cancer, hepatocarcinoma, ovary cancer, esophageal cancer, small intestinal cancer, lung cancer, breast cancer, pancreatic cancer, thyroid cancer, cancer of brain, cancer of nasopharynx/larynx, bladder carcinoma, malignant lymphoma, carcinoma of kidney, skin cancer, osteosarcoma, leukemia, ureter/renal pelvis cancer, carcinoma of prostate, malignant teratoma, cancer of parotid gland, and liposarcoma in AC II HNPCC families. Gastric cancer was more common than endometrial cancer in Chinese HNPCC families if difference of sex was not considered. And similar results were reported in Korea and Brazil^[18,19]. It was significantly different from most European and American HNPCC families whose most frequent extracolonic cancer was endometrial cancer^[4,6,7,11]. However, the extracolonic cancers of AC II only included endometrial cancer, small intestinal cancer and ureter or renal pelvis cancer, because gastric cancer was only frequently reported in Asian HNPCC families, and is uncommon and is observed mainly in patients from older generations in western countries. Moreover, there were no studies in these countries revealing the relative risk of developing stomach cancer in carriers of a mutated MMR gene at that time^[6]. In fact, some studies from Europe and America also supported that gastric cancer was associated with HNPCC syndrome^[19,20]. Recently, Kim *et al*^[18] reported gastric cancer was the most common extracolonic malignancy in HNPCC and suspected HNPCC families, and five germline mutations in the hMLH1 and six germline mutations in the hMSH2 were exclusively found in families with gastric cancer. It suggested that gastric cancer was also genetically associated with HNPCC syndrome. Endometrial cancer was the most common extracolonic cancer in Chinese female patients with HNPCC-associated cancer, it is the same in other countries^[4,6,7,11,19]. At the same time, ovarian cancer and breast cancer were also more frequent extracolonic cancer in Chinese HNPCC-associated cancer patients. They were the second and third most frequent extracolonic cancer in female patients. Although they were not included in AC II, they often occurred in HNPCC-associated cancer patients in both China and other countries^[19,21,22]. Moreover, it had been reported that carriers of an hMSH2 mutation developed ovarian cancer^[21]. Compared to the European and American HNPCC families, hepatocarcinoma and esophageal cancer were also more common in Chinese HNPCC families. In addition, Soravia *et al*^[16] reported that prostate cancer was found in HNPCC families, and the MSI and IHC analysis of the prostatic cancer clearly linked its etiology to the germline mutation of mismatch repair genes. The suggestion of other countries, including ours that all extracolonic cancers, which were clinically found in HNPCC families should be included in the malignant tumor spectrum of HNPCC syndrome, though only some of them were genetically confirmed to be HNPCC-associated cancers. First, the selection criteria for HNPCC is that it should be clinical because genetic analyses (MSI and mutation analyses) are not accessible to all families, the techniques are not available in all countries, and the significance of the findings is not completely understood^[6]. Secondly, it is generally accepted that genetic pathogenesis of HNPCC is associated with dysfunction of DNA mismatch repair system

resulting from germline mutation of mismatch repair genes^[4,7,23-26]. Germline mutation of mismatch repair genes was detected in about two third to ninety-two percent in all HNPCC families fulfilled AC I^[25-28], and plays an important role in revealing genetic pathogenesis of HNPCC syndrome and early detection and treatment of HNPCC-associated cancer patients in HNPCC families^[23,29-32]. But definite association between genotype and phenotype has not been found in HNPCC until now^[24-26,28,33]. Thirdly, since AC II was established by ICG-HNPCC in 1998, more extracolonic cancers, which were clinically found to be associated with HNPCC syndrome, have proved genetically to be associated with HNPCC syndrome than before^[16-18,21,34]. Moreover, some of them were rare both in HNPCC-associated tumors and in sporadic cancers^[33,34]. Finally, HNPCC in fact is a syndrome. By analogy with several other genetic disorders, HNPCC encompasses a wide spectrum of different clinical presentations, including Muir-Torre syndrome, Turcot syndrome, and the neurofibromatosis-hematological malignancy association^[33,35]. So, it is improper only to define the extracolonic cancers, which have been genetically ascertained to be associated with HNPCC as the spectrum of HNPCC-associated cancers until genetic pathogenesis of HNPCC syndrome is completely understood.

Members of HNPCC families are high-risk individuals who are more easily predisposed to malignant tumors than members of families with sporadic CRC patients especially CRC. Estimates of the frequency of HNPCC are generally based on clinical criteria including AC I and AC II, and have varied from country to country. In the general population of CRC patients, the prevalence of HNPCC fulfilled AC I vary from 0.3% to 3% in European and American^[36-39]. In China, our study showed that the prevalence of HNPCC fulfilled AC I was 1.2% in general CRC patients, which was similar to that in Europeans and Americans. In addition, the prevalence of HNPCC fulfilled AC II was 2.2% in Chinese general CRC patients.

On the basis of our study, we realize that current AC II has some defects and may result in failure to screen some HNPCC families. So we suggest that the AC II should be revised according to the development of clinical and genetic findings for HNPCC families, and the HNPCC-associated cancers include CRC and extracolonic cancers. Extracolonic cancer is referred to any malignant tumor outside the colorectum. In addition, the other important factors should also be thought when the HNPCC families are screened. With the development of socioeconomics and carrying through Planned Parenthood policy in China, the size of most of Chinese families is growing smaller than before. Under this condition, it is difficult to seek three relatives that one is a first degree relative of the others in a family these days and in future. Therefore, we propose a set of new clinical criteria to diagnose the HNPCC families. It includes the following: 1) at least 3 relatives with an HNPCC-associated cancer (CRC, extracolonic cancer, which can be in any site), at least one must be CRC; 2) One should be a first-degree or second relative of the other 2, at least 2 are first-degree relatives of each other; 3) At least 2 successive generations should be affected; 4) At least 1 should be diagnosed before age 50; 5) Familial adenomatous polyposis

should be excluded in the CRC case(s) if any and 6) Tumors should be verified by pathological examination.

To our knowledge, this report is a first systematic description of HNPCC families and the prevalence of HNPCC in China. As such, it provides a broad and detailed description of general characteristics of HNPCC families in a larger sample, and the prevalence of HNPCC diagnosed by both AC I and AC II in a larger general population of CRC patients in China. We acknowledge that this is not the final answer for characteristics of HNPCC families and HNPCC prevalence figures in the general CRC population in China; however, it is necessary as a first step and provides general data for the scientific community. It will accelerate genetic pathogenesis of HNPCC syndrome and the prevention of HNPCC-associated cancers in members of HNPCC families in China.

REFERENCES

- 1 **Steinert R**, Buschmann T, van der Linden M, Fels LM, Lippert H, Reymond MA. The role of proteomics in the diagnosis and outcome prediction in colorectal cancer. *Technol Cancer Res Treat* 2002; **1**: 297-304
- 2 **Price AS**. Primary and secondary prevention of colorectal cancer. *Gastroenterol Nurs* 2003; **26**: 73-81
- 3 **Zhang YZ**, Li SY. New technologies of early diagnosis on colorectal cancer. *Shijie Huaren Xiaohua Zazhi* 2004; **12**: 1202-1205
- 4 **Lynch HT**, de la Chapelle A. Hereditary colorectal cancer. *N Engl J Med* 2003; **348**: 919-932
- 5 **Vasen HF**, Mecklin JP, Khan PM, Lynch HT. The International Collaborative Group on Hereditary Non-Polypoid Colorectal Cancer (ICG-HNPCC). *Dis Colon Rectum* 1991; **34**: 424-425
- 6 **Vasen HF**, Watson P, Mecklin JP, Lynch HT. New clinical criteria for hereditary nonpolyposis colorectal cancer (HNPCC, Lynch syndrome) proposed by the International Collaborative group on HNPCC. *Gastroenterology* 1999; **116**: 1453-1456
- 7 **Chung DC**, Rustgi AK. The hereditary nonpolyposis colorectal cancer syndrome: genetics and clinical implications. *Ann Intern Med* 2003; **138**: 560-570
- 8 **Vasen HF**, Wijnen JT, Menko FH, Kleibeuker JH, Taal BG, Griffioen G, Nagengast FM, Meijers-Heijboer EH, Bertario L, Varesco L, Bisgaard ML, Mohr J, Fodde R, Khan PM. Cancer risk in families with hereditary nonpolyposis colorectal cancer diagnosed by mutation analysis. *Gastroenterology* 1996; **110**: 1020-1027
- 9 **Vasen HF**, Sanders EA, Taal BG, Nagengast FM, Griffioen G, Menko FH, Kleibeuker JH, Houwing-Duistermaat JJ, Meera Khan P. The risk of brain tumours in hereditary non-polyposis colorectal cancer (HNPCC). *Int J Cancer* 1996; **65**: 422-425
- 10 **Sijmons RH**, Kiemeneij LA, Witjes JA, Vasen HF. Urinary tract cancer and hereditary nonpolyposis colorectal cancer: risks and screening options. *J Urol* 1998; **160**: 466-470
- 11 **Aarnio M**, Mecklin JP, Aaltonen LA, Nyström-Lahti M, Järvinen HJ. Life-time risk of different cancers in hereditary non-polyposis colorectal cancer (HNPCC) syndrome. *Int J Cancer* 1995; **64**: 430-433
- 12 **Bernstein IT**, Bisgaard ML, Myrholm T. Registration of hereditary non-polyposis colorectal cancer. *Ugeskr Laeger* 1999; **161**: 6174-6178
- 13 **Myrholm T**, Bisgaard ML, Bernstein I, Svendsen LB, Sondergaard JO, Bulow S. Hereditary non-polyposis colorectal cancer: clinical features and survival. Results from the Danish HNPCC register. *Scand J Gastroenterol* 1997; **32**: 572-576
- 14 **Box JC**, Rodriguez-Bigas MA, Weber TK, Petrelli NJ. Clinical implications of multiple colorectal carcinomas in hereditary nonpolyposis colorectal carcinoma. *Dis Colon Rectum* 1999; **42**: 717-721
- 15 **Rodriguez-Bigas MA**, Lee PH, O'Malley L, Weber TK, Suh O, Anderson GR, Petrelli NJ. Establishment of a hereditary nonpolyposis colorectal cancer registry. *Dis Colon Rectum* 1996; **39**: 649-653
- 16 **Soravia C**, van der Klift H, Brundler MA, Blouin JL, Wijnen J, Hutter P, Fodde R, Delozier-Blanchet C. Prostate cancer is part of the hereditary non-polyposis colorectal cancer (HNPCC) tumor spectrum. *Am J Med Genet A* 2003; **121A**: 159-162
- 17 **Yamamoto M**, Kashiwai H, Hirata N, Matsuki H, Shimizu K, Tanaka N, Ozono S. Metachronous bilateral ureteral cancer in patient with hereditary nonpolyposis colorectal cancer. *Nihon Hinyokika Gakkai Zasshi* 2004; **95**: 63-66
- 18 **Kim JC**, Kim HC, Roh SA, Koo KH, Lee DH, Yu CS, Lee JH, Kim TW, Lee HL, Beck NE, Bodmer WF. hMLH1 and hMSH2 mutations in families with familial clustering of gastric cancer and hereditary non-polyposis colorectal cancer. *Cancer Detect Prev* 2001; **25**: 503-510
- 19 **Oliveira Ferreira F**, Napoli Ferreira CC, Rossi BM, Toshihiko Nakagawa W, Aguilar S, Monteiro Santos EM, Vierira Costa ML, Lopes A. Frequency of extra-colonic tumors in hereditary nonpolyposis colorectal cancer (HNPCC) and familial colorectal cancer (FCC) Brazilian families: An analysis by a Brazilian Hereditary Colorectal Cancer Institutional Registry. *Fam Cancer* 2004; **3**: 41-47
- 20 **Aarnio M**, Salovaara R, Aaltonen LA, Mecklin JP, Jarvinen HJ. Features of gastric cancer in hereditary non-polyposis colorectal cancer syndrome. *Int J Cancer* 1997; **74**: 551-555
- 21 **Marcelis CL**, van der Putten HW, Tops C, Lutgens LC, Moog U. Chemotherapy resistant ovarian cancer in carriers of an hMSH2 mutation? *Fam Cancer* 2001; **1**: 107-109
- 22 **Gonzalez-Aguilera JJ**, Nejda N, Fernandez FJ, Medina V, Gonzalez-Hermoso F, Barrios Y, Moreno Azcoita M, Fernandez-Peralta AM. Genetic alterations and MSI status in primary, synchronous, and metachronous tumors in a family with hereditary nonpolyposis colorectal cancer (HNPCC). *Am J Clin Oncol* 2003; **26**: 386-391
- 23 **Jarvinen HJ**. Genetic testing for polyposis: practical and ethical aspects. *Gut* 2003; **52** Suppl 2: ii19-ii22
- 24 **Peltomäki P**, Gao X, Mecklin JP. Genotype and phenotype in hereditary nonpolyposis colon cancer: a study of families with different *vs* shared predisposing mutations. *Fam Cancer* 2001; **1**: 9-15
- 25 **Wagner A**, Barrows A, Wijnen JT, van der Klift H, Franken PF, Verkuijen P, Nakagawa H, Geugien M, Jaghmohan-Changur S, Breukel C, Meijers-Heijboer H, Morreau H, van Puijenbroek M, Burn J, Coronel S, Kinarski Y, Okimoto R, Watson P, Lynch JF, de la Chapelle A, Lynch HT, Fodde R. Molecular analysis of hereditary nonpolyposis colorectal cancer in the United States: high mutation detection rate among clinically selected families and characterization of an American founder genomic deletion of the MSH2 gene. *Am J Hum Genet* 2003; **72**: 1088-1100
- 26 **Bisgaard ML**, Jager AC, Myrholm T, Bernstein I, Nielsen FC. Hereditary non-polyposis colorectal cancer (HNPCC): phenotype-genotype correlation between patients with and without identified mutation. *Hum Mutat* 2002; **20**: 20-27
- 27 **Peltomäki P**. Deficient DNA mismatch repair: a common etiologic factor for colon cancer. *Hum Mol Genet* 2001; **10**: 735-740
- 28 **Scott RJ**, McPhillips M, Meldrum CJ, Fitzgerald PE, Adams K, Spigelman AD, du Sart D, Tucker K, Kirk J. Hereditary nonpolyposis colorectal cancer in 95 families: differences and similarities between mutation-positive and mutation-negative kindreds. *Am J Hum Genet* 2001; **68**: 118-127
- 29 **De Jong AE**, Morreau H, Van Puijenbroek M, Eilers PH, Wijnen J, Nagengast FM, Griffioen G, Cats A, Menko FH, Kleibeuker JH, Vasen HF. The role of mismatch repair gene defects in the development of adenomas in patients with HNPCC. *Gastroenterology* 2004; **126**: 42-48
- 30 **Watson P**, Narod SA, Fodde R, Wagner A, Lynch JF, Tinley ST, Snyder CL, Coronel SA, Riley B, Kinarsky Y, Lynch HT.

- Carrier risk status changes resulting from mutation testing in hereditary non-polyposis colorectal cancer and hereditary breast-ovarian cancer. *J Med Genet* 2003; **40**: 591-596
- 31 **Caldes T**, Godino J, Sanchez A, Corbacho C, De la Hoya M, Lopez Asenjo J, Saez C, Sanz J, Benito M, Ramon Y Cajal S, Diaz-Rubio E. Immunohistochemistry and microsatellite instability testing for selecting MLH1, MSH2 and MSH6 mutation carriers in hereditary non-polyposis colorectal cancer. *Oncol Rep* 2004; **12**: 621-629
- 32 **Hendriks YM**, Wagner A, Morreau H, Menko F, Stormorken A, Quehenberger F, Sandkuijl L, Moller P, Genuardi M, Van Houwelingen H, Tops C, Van Puijenbroek M, Verkuijlen P, Kenter G, Van Mil A, Meijers-Heijboer H, Tan GB, Breuning MH, Fodde R, Wijnen JT, Brocker-Vriends AH, Vasen H. Cancer risk in hereditary nonpolyposis colorectal cancer due to MSH6 mutations: impact on counseling and surveillance. *Gastroenterology* 2004; **127**: 17-25
- 33 **Mangold E**, Pagenstecher C, Leister M, Mathiak M, Rutten A, Friedl W, Propping P, Ruzicka T, Kruse R. A genotype-phenotype correlation in HNPCC: strong predominance of msh2 mutations in 41 patients with Muir-Torre syndrome. *J Med Genet* 2004; **41**: 567-572
- 34 **Broaddus RR**, Lynch PM, Lu KH, Luthra R, Michelson SJ. Unusual tumors associated with the hereditary nonpolyposis colorectal cancer syndrome. *Mod Pathol* 2004; **17**: 981-989
- 35 **Lucci-Cordisco E**, Zito I, Gensini F, Genuardi M. Hereditary nonpolyposis colorectal cancer and related conditions. *Am J Med Genet A* 2003; **122A**: 325-334
- 36 **Peel DJ**, Ziogas A, Fox EA, Gildea M, Laham B, Clements E, Kolodner RD, Anton-Culver H. Characterization of hereditary nonpolyposis colorectal cancer families from a population-based series of cases. *J Natl Cancer Inst* 2000; **92**: 1517-1522
- 37 **Hemminki K**, Li X. Familial colorectal adenocarcinoma and hereditary nonpolyposis colorectal cancer: a nationwide epidemiological study from Sweden. *Br J Cancer* 2001; **84**: 969-974
- 38 **Katballe N**, Christensen M, Wikman FP, Orntoft TF, Laurberg S. Frequency of hereditary non-polyposis colorectal cancer in Danish colorectal cancer patients. *Gut* 2002; **50**: 43-51
- 39 **Cornaggia M**, Tibiletti MG, Albarello L, Taborrelli M, Dalla Longa E, Capella C. Low incidence of hereditary nonpolyposis colorectal cancer syndrome in a selected area of the Lombardy Cancer Registry. *Tumori* 2000; **86**: 439-444

Edited by Guo SY Language Editor Elsevier HK

• BASIC RESEARCH •

Toll-like receptor 4 and NOD2/CARD15 mutations in Hungarian patients with Crohn's disease: Phenotype-genotype correlations

Peter Laszlo Lakatos, Laszlo Lakatos, Ferenc Szalay, Claudia Willheim-Polli, Christoph Österreicher, Zsolt Tulassay, Tamas Molnar, Walter Reinisch, Janos Papp, Gyula Mozsik, Hungarian IBD Study Group, Peter Ferenci

Peter Laszlo Lakatos, Ferenc Szalay, Janos Papp, Hungarian IBD Study Group, 1st Department of Medicine, Semmelweis University, Budapest, Hungary
Laszlo Lakatos, 1st Department of Medicine, Csolnoky F. County Hospital, Veszprem, Hungary
Claudia Willheim-Polli, Christoph Österreicher, Walter Reinisch, Peter Ferenci, Department of Internal Medicine 4, University of Vienna, Austria
Zsolt Tulassay, 2nd Department of Medicine, Semmelweis University, Budapest, Hungary
Tamas Molnar, 1st Department of Medicine, University of Szeged, Szeged, Hungary
Gyula Mozsik, 1st Department of Medicine, University of Pecs, Pecs, Hungary
Hungarian IBD Study Group: Semmelweis University, 1st Department of Medicine, Budapest: Peter Fuszek, Peter Vargha; Semmelweis University, 2nd Department of Medicine, Semmelweis University, Budapest: Laszlo Pronai†, Annamaria Nemeth, Pal Miheller; Erzsébet Hospital, 1st Department of Medicine, Budapest: Agota Kovacs, Laszlo Bene; Szent Janos Hospital, 1st Department of Medicine: Gyorgy Szekely; University of Pecs, 1st Department of Medicine, Pecs: Beata Gasztonyi; University of Szeged, 1st Department of Medicine, Szeged: Ferenc Nagy, Janos Lonovics; Semmelweis Hospital, 1st Department of Medicine, Miskolc: Laszlo Ujszaszy; University of Debrecen, 2nd Department of Medicine, Debrecen: Istvan Altorjai, Karoly Palatka; Kenezi Gy. County Hospital, 2nd Department of Medicine, Debrecen: Gyula G. Kiss; County Hospital, 2nd Department of Medicine, Zalaegerszeg: Ferenc Tarnok, Markusovszky Hospital, 2nd Department of Medicine, Szombathely: Zoltan Dobronte; Csolnoky F. County Hospital, 1st Department of Medicine, Veszprem: Zsuzsanna Erdelyi, Tunde Pandur, Gabor Mester
Correspondence to: Peter Laszlo Lakatos, M.D., Ph.D., 1st Department of Medicine, Semmelweis University, Koranyi str. 2/A, H-1083, Hungary. kislakpet@bell.sote.hu
Telephone: +36-1-210-0278/1500-1520 Fax: +36-1-313-0250
Received: 2004-07-26 Accepted: 2004-09-09

Abstract

AIM: To determine common NOD2/CARD15 mutations and TLR4 D299G polymorphism in Hungarian patients with CD.

METHODS: A total of 527 unrelated patients with CD (male/female: 265/262, age: 37.1 (SD 7.6) years) and 200 healthy subjects were included. DNA was screened for possible NOD2/CARD15 mutations by denaturing high-performance liquid chromatography (confirmed by direct sequencing). TLR4 D299G was tested by PCR-RFLP.

RESULTS: NOD2/CARD15 mutations were found in 185 patients (35.1%) and in 33 controls (16.5%, $P < 0.0001$). SNP8/R702W (10.8% vs 6%, $P = 0.02$), SNP13/3020insC (19.4% vs 5%, $P < 0.0001$) and exon4 R703C (2.1% vs 0%, $P = 0.02$) mutations were more frequent in CD, while

the frequency of SNP12/G908R was not increased. The frequency of TLR4 D299G was not different (CD: 9.9% vs controls: 12.0%). Variant NOD2/CARD15 allele was associated with an increased risk for CD ($OR_{net} = 1.71$, 95%CI = 1.12-2.6, $P = 0.0001$, $OR_{two-risk\ alleles} = 25.2$, 95%CI = 4.37- , $P < 0.0001$), early disease onset (carrier: 26.4 years vs non-carrier: 29.8 years, $P = 0.0006$), ileal disease (81.9% vs 69.5%, $OR = 1.99$, 95%CI = 1.29-3.08, $P = 0.02$, presence of NOD2/CARD15 and TLR4: 86.7% vs 64.8%), stricturing behavior ($OR = 1.69$, 95%CI = 1.13-2.55, $P = 0.026$) and increased need for resection ($OR = 1.71$, 95%CI: 1.13-2.62, $P = 0.01$), but not with duration, extra-intestinal manifestations, familial disease or smoking. TLR4 exhibited a modifier effect: age of onset in wt/TLR4 D299G carriers: 27.4 years vs NOD2mut/TLR D299G: 23 years ($P = 0.06$), in NOD2mut/wt: 26.7 years.

CONCLUSION: These results confirm that variant NOD2/CARD15 (R702W, R703C and 3020insC) alleles are associated with earlier disease onset, ileal disease, stricturing disease behavior in Hungarian CD patients. In contrast, although the frequency of TLR4 D299G polymorphism was not different from controls, NOD2/TLR4 mutation carriers tended to present at earlier age.

© 2005 The WJG Press and Elsevier Inc. All rights reserved.

Key words: Crohn's disease; NOD2; CARD15; TLR4; Extraintestinal manifestation; Phenotype

Lakatos PL, Lakatos L, Szalay F, Willheim-Polli C, Österreicher C, Tulassay Z, Molnar T, Reinisch W, Papp J, Mozsik G, Hungarian IBD Study Group, Ferenci P. Toll-like receptor 4 and NOD2/CARD15 mutations in Hungarian patients with Crohn's disease: Phenotype-genotype correlations. *World J Gastroenterol* 2005; 11(10): 1489-1495

<http://www.wjgnet.com/1007-9327/11/1489.asp>

INTRODUCTION

Inflammatory bowel disease (IBD) is a multifactorial polygenic disease with probable genetic heterogeneity. In addition to genetic predisposition, various environmental and host factors (e.g., genetic, epithelial, immune and non-immune factors) play a major role in the pathogenesis of IBD. Crohn's disease (CD) is a chronic inflammatory disorder of the gastrointestinal tract. Extensive heterogeneity is observed in terms of disease presentation, behavior, and response to treatment^[1,2]. Attempts have been made to define clinical subgroups on the basis of age at onset, disease location, extent (diffuse or localized) and behavior (primary

inflammatory, fistulating, or fibrostenotic).

CD has a strong genetic component, with a lifetime risk of 10-20% to develop IBD in the presence of an affected first-degree relative^[1]. The concordance rate of affected siblings for age at onset, disease site, behavior and presence of extra-intestinal manifestation is as high as 80%. Since the first report of Hugot *et al*^[3] in 1996, seven IBD loci have been identified on chromosomes 16q12 (IBD1), 12q13 (IBD2), 6p13 (IBD3), 14q11 (IBD4), 5q31-33 (IBD5), 19p13 (IBD6) and 1p (IBD7)^[4-6]. These seven loci are convincingly replicated. Some genetic markers increase the risk of ulcerative colitis or CD while others are associated with a particular phenotypic expression like disease location and/or behavior. The NOD2/CARD15 gene is located in the IBD1 region. NOD2/CARD15 is a cytoplasmatic protein expressed in peripheral blood monocytes, Paneth cells and intestinal epithelial cells and is related structurally to the well-described R proteins in plants, which mediate host resistance to microbial pathogens^[7] and induce the NF- κ B pathway^[8]. Variant alleles result in reduced NF- κ B activity^[9]. Variant NOD2/CARD15 alleles are also associated with reduced α -defensin release from Paneth cells in response to bacteria^[10]. Of particular importance is the C-terminus leucine-rich repeat domain, reportedly the major structural motif that functions as a pattern-recognition receptor for broad types of microbial components, such as bacterial lipopolysaccharides (LPS) and peptidoglycan (including MDP)^[11].

Two single nucleotide polymorphisms of NOD2/CARD15 (SNP8: Arg702Trp and SNP12: Gly908Arg) and a frame shift mutation (SNP13: Leu1007insC) have been shown by three independent groups to be associated with susceptibility to CD^[12-14]. The presence of one variant allele increases the risk for developing CD 1.5-4.3-fold, and the presence of two copies up to 20-40-fold^[13-15]. It has also been suggested that the presence of variant alleles is associated with ileal disease and fibrostenosing or fistulizing behavior in some^[15,16], but not in all the studies^[17,18].

However, there are significant geographical differences in the frequency of these alleles. They are not found in Japan and China^[19,20] and are less frequent in Finland^[21] than in Western Europe. There are only limited data in patients from Central-Eastern European countries like Hungary. The incidence of CD in Hungary has been steadily elevat in the last decades (from 0.41 in 1977-1981 to 4.68 in 1997-2001), now reaching that of Western European countries.

Toll-like receptors (TLRs) expressed in myeloid cells play a major role both in detecting microbes and in initiating innate immune responses. In contrast, little is known concerning the expression, distribution and function of TLRs in epithelial cells per se. Toll-like receptor 4 (TLR4) is also expressed in the Golgi apparatus of intestinal epithelial cells. Thus, LPS recognition in intestinal epithelial cells may occur in the Golgi apparatus and require LPS internalization^[22]. Recently it has been suggested that the interaction of LPS with TLR4/MD2 contributes to the perpetuation of the inflammatory epithelial cell injury via TNF α -induced alterations of enterocyte turnover in an autocrine/paracrine manner^[23]. TLRs may also influence the nature of the immune response, in particular by skewing T cells toward a Th1 or Th2 profile. Myeloid cells are exquisitely

sensitive to TLR ligands and produce significant IL-12p40 and appear to play key roles in the initiation and possibly the Th1/Th2 skewing of inflammatory responses. In this model the inflammation would normally be controlled by myeloid or lymphocyte-derived IL-10 acting through Stat3 in myeloid cells to block further production of IL-12/IL-23 and skewing to Th1 response^[24].

TLR4 is upregulated in the intestinal epithelial cells in patients with CD. In contrast, the expressions of TLR2 and TLR5 are unchanged, while TLR3 is down-regulated^[25]. The D299G (Asp299Gly) polymorphism of TLR4 gene is associated with LPS hyporesponsiveness^[26] and recently an association between TLR4 mutation and CD was reported in one study^[27], but not in another^[28].

In view of the limited data on the prevalence of NOD2/CARD15 mutations in Eastern European countries, our aim was to investigate the presence of the common three and other exon4 variants of NOD2/CARD15 as well as the presence of functional D299G polymorphism of the TLR4 gene in three large cohorts of Hungarian patients with CD. We also aimed to investigate the possible association between genotype and clinical characteristics of the disease.

MATERIALS AND METHODS

Patients

A total of 527 unrelated Hungarian patients with CD [male/female: 265/262, age: 37.1 (SD 7.6) years] were investigated. The patients were recruited from three Hungarian IBD centers (Szeged [$n = 167$], Budapest [$n = 185$], Veszprem [$n = 175$]). CD patients, with a follow-up time of at least one year were included. The diagnosis was based on the Lennard-Jones criteria^[29]. The clinical characteristics of the patients are summarized in Table 1. The disease phenotype

Table 1 Clinical characteristics of the different cohorts of Crohn's disease (CD) patients

	Budapest ($n = 185$)	Veszprem ($n = 175$)	Szeged ($n = 167$)
Male/Female	98/87	88/87	79/88
Age (yr)	35.6 \pm 11.4	37.8 \pm 13.3	37.1 \pm 12.7
Age at presentation (yr)	27.2 \pm 10.3	30.2 \pm 12.4	28.9 \pm 10.9
Duration (yr)	8.9 \pm 6.6	7.7 \pm 6.8	8.0 \pm 7.3
Familial IBD, n (%)	63 (11.9)	38 (11.1)	25 (13.5)
Location (n)			
L1	43	54	39
L2	37	47	52
L3	103	74	74
L4	2	0	2
Behavior (n)			
B1	88	65	62
B2	40	39	49
B3	56	71	56
Perianal disease, n (%)	41 (22.1)	49 (28.0)	50 (29.9)
Frequent relapse, n (%)	59 (31.9)	72 (41.1)	64 (38.6)
Extraintestinal manifestations, n (%)	67 (36.2)	61 (34.8)	47 (28.2)
Operation, n (%)	77 (41.6)	76 (43.4)	67 (40.1)
Smoking habits (n)			
No	115	96	98
Yes	55	61	55
Previous	15	20	14

(age at onset, duration, location and behavior) was determined according to the Vienna classification^[30]. Perianal involvement, presence of extraintestinal manifestations (EIM; arthritis: peripheral and axial; ocular manifestations: conjunctivitis, uveitis, iridocyclitis; skin lesions: erythema nodosum, pyoderma gangrenosum; hepatic manifestations: primary sclerosing cholangitis [PSC]), frequency of flare-ups (frequent flare-up: >1/year), therapeutic effectiveness (e. g., steroid and/or immunosuppressive resistance), need for surgery (resections). Presence of familial IBD and smoking habits were investigated by filling in a questionnaire.

The control group for mutation analysis consisted of 200 age- and gender-matched healthy subjects [male/female: 102/98, age: 38.05 (SD 10.7) years]. The study was approved by the Semmelweis University Regional and Institutional Committee of Science and Research Ethics (81/2003). Each patient was informed of the nature of the study and signed the informed consent form.

Detection of NOD2/CARD15 SNP8, 12, 13 and exon4 mutations

Genomic DNA was isolated from whole blood according to the QIAamp DNA blood mini kit (QIAGEN GmbH, Germany). Each exon was amplified by PCR using previously published primer sequences^[17]. The initial denaturation step (at 94 °C for 7 min) was to activate AmpliTaq Gold (Applied Biosystems, Foster City, CA, USA), followed by 33 cycles (at 94 °C for 20 s, at 61 °C for 30 s, at 72 °C for 25 s) with a final extension step at 72 °C for 7 min. Then denaturing high-performance liquid chromatography (dHPLC, wave DNA fragment analysis system, Transgenomic Limited, UK) were performed to analyze the exons. PCR products were denatured as a last step at 94 °C for 5 min to induce heteroduplex formation during the following 30 min of slowly cooling down to room temperature. Five microliters of these PCR products were then automatically loaded onto the DNasep cartridge (Transgenomic Limited, UK) in the wave system. The specific acetonitrile gradient to elute each exon was established by using the WaveMaker 3.4.4 software. The particular run temperature for the detection of each SNP was determined using positive controls, which were kindly provided by Dirk Seegert from Kiel, Germany.

Finally, when a sequence variation was observed in the dHPLC profile, the relevant PCR product was sequenced on both strands to confirm the alteration. Sequencing reactions were performed with the ABI BigDye terminator

cycle sequencing kit v1.1 (Applied Biosystems) and samples were sequenced on an ABI Prism 310 genetic analyzer (Applied Biosystems).

Detection of TLR4 D299G polymorphism

The TLR4 D299G polymorphism was detected by PCR-RFLP (PTC-200 thermocycler, MJ Research Inc., MA, USA) using previously published primers and conditions^[31]. For the overnight digestion of the amplified DNA, NcoI enzyme (New England Biolabs, London, UK) was used and the fragments were separated and visualized by gel electrophoresis (3% NuSieve® GTG agarose gel BMA, Rockland, ME, USA).

Statistical analysis

Variables were tested for normality by Shapiro Wilk's *W* test. *t*-test with separate variance estimates, χ^2 -test and χ^2 -test with Yates correction were used to test differences between patients with CD and controls, and also within subgroups of CD patients. Odds ratios (OR) and logistic regression were calculated to compare genetic and clinical data. $P < 0.05$ was considered statistically significant. For the statistical analysis, Statistica 6.1 (Statsoft Inc., OK, USA) was used.

RESULTS

NOD2/CARD15 mutations were more frequently found in CD patients (185/527; 35.1%) than those in controls (16.5%, $P < 0.0001$, Table 2). Heterozygous ($OR_{het} = 1.71$; 95%CI = 1.12–2.6, $P = 0.0001$), homozygous ($OR_{hom} = 14.43$; 95%CI = 2.47– ∞ , $P = 0.0003$) or compound heterozygous ($OR_{compound} = 12.92$; 95%CI = 2.2– ∞ , $P = 0.0006$) carriage of a variant allele was associated with increased risk for CD. The OR for carrying two variant alleles was 25.2 (95%CI: 4.35– ∞ , $P < 0.0001$). SNP8 (11.6% *vs* controls: 6%) and SNP13 (19.4% *vs* controls: 5%, $P < 0.0001$) mutations were more frequent in CD (Table 3), while the frequency of SNP12 variant allele was not different, but consistent in different cohorts (Table 4). The carriage of SNP8, SNP13 ($OR_{SNP8 \text{ allele}} = 2.41$; 95%CI = 1.30–4.44, $OR_{SNP13 \text{ allele}} = 4.78$; 95%CI = 2.50–9.11) and a further exon4 variant allele (R703C_{CD}: 2.1% *vs* controls: 0%, OR = 6.89; 95%CI = 1.18– ∞ , $P = 0.02$) were identified as risk factors for CD (Tables 3 and 5).

Table 2 NOD2/CARD15 and TLR4 D299G genotype in patients with Crohn's disease (CD) and controls, *n* (%)

A	NOD2 genotype				
	Non-carrier	All carrier	Heterozygous	Homozygous	Compound heterozygous
Controls (<i>n</i> = 200)	167 (83.5)	33 (16.5)	33 (16.5)	0	0
CD (<i>n</i> = 527)	342 (64.9)	185 (35.1)	133 (25.2) ¹	30 (5.7) ²	26 (4.9) ³
B	TLR4 D299G				
	Non-carrier	All carrier	Heterozygous	Homozygous	
Controls (<i>n</i> = 200)	176 (88.0)	24 (12.0)	23 (11.5)	1 (0.5)	
CD (<i>n</i> = 527)	475 (90.1)	52 (9.9)	50 (9.5)	2 (0.4)	

$P < 0.0001$ between CD patients and controls, ¹ $OR_{het} = 1.71$ (1.12–2.60), ² $OR_{hom} = 14.43$ (2.47– ∞), ³ $OR_{compound} = 12.92$ (2.2– ∞).

Table 3 NOD2/CARD15 SNP8, 12 and 13 in patients with Crohn's disease (CD) and controls

	R702W (SNP8) ¹		G908R (SNP12)		3020insC (SNP13) ¹	
	CD <i>n</i> (%)	Controls <i>n</i> (%)	CD <i>n</i> (%)	Controls <i>n</i> (%)	CD <i>n</i> (%)	Controls <i>n</i> (%)
Wild type	466 (88.4)	188 (94.0)	494 (96.7)	193 (96.5)	425 (80.6)	190 (95.0)
All carriers	61 (11.6)	12 (6.0)	33 (6.3)	7 (3.5)	102 (19.4)	10 (5.0)
Heterozygous	45 (8.5)	12 (6.0)	33 (6.3)	7 (3.5)	89 (16.9)	10 (5.0)
Homozygous	16 (3.1)	0	0	0	13 (2.5)	0

¹*P* = 0.02 and *P* < 0.0001 between patients and controls for genotype frequency by χ^2 -test, OR_{SNP8 allele} = 2.41 (1.30–4.44), OR_{SNP13 allele} = 4.78 (2.50–9.11).

Table 4 NOD2/CARD15 and TLR4 D299G mutations in different cohorts of CD patients, *n* (%)

	Budapest (<i>n</i> = 185)	Veszprem (<i>n</i> = 175)	Szeged (<i>n</i> = 167)
NOD2/CARD15	64 (34.6) ¹	61 (34.9) ¹	60 (35.9) ¹
SNP8	17 (9.2)	23 (13.1) ²	21 (12.6) ³
SNP12	12 (6.5)	10 (5.7)	11 (6.6)
SNP13	39 (21.1) ¹	33 (18.9) ¹	30 (18.0) ⁴
TLR4 D299G	21 (11.4)	20 (11.4)	11 (6.6)

¹*P* < 0.0001, ²*P* = 0.0002, ³*P* = 0.0005, ⁴*P* = 0.04 cohort *vs* controls (Tables 2, 3).

Table 5 Further exon4 mutations in patients with Crohn's disease (CD) and controls

	CD (<i>n</i> = 527)	Controls (<i>n</i> = 200)
R703C ¹	11 (1 homozygous)	0
R713C	1	0
A755V	2	1
E778K	0	1
R791Q	5	1
V793M	2	1

¹*P* = 0.02 between patients and controls for allele frequency, OR_{R703C} = 6.89 (1.18–∞).

More homozygous (60%) or compound heterozygous (69.2%) patients tended to be females compared to heterozygous (46.6%) patients and non-carriers (49.1%). The use of immunosuppressive drugs (*P* = 0.04) and the need for surgery (resection, *P* = 0.006) were more frequent in carriers of the mutation (Table 6). The percentage of patients with resection was even higher in compound heterozygous patients (65.4%, 17/26, *P* = 0.006 compared to non-carriers by Fischer exact test). The presence of variant NOD2/CARD15 allele affected disease phenotype and was associated with earlier disease onset (26.4 *vs* 29.8 years, *P* = 0.0006), the site of involvement (ileal involvement: 81.6% *vs* non-carriers: 69.0%, OR = 1.99, 95%CI: 1.29–3.08, *P* = 0.02) and with stricturing behavior (OR = 1.69, 95%CI: 1.13–2.55, *P* = 0.02, Tables 6, 7). The presence of NOD2/CARD15 variant alleles was not associated with the presence of perianal manifestation associated disease duration, more frequent relapses, familial disease and presence of EIMs or smoking habits. EIMs were tendentially even less frequent in patients carrying two mutant alleles.

Table 6 Clinical characteristics of CD patients, with respect to the presence or absence of NOD2/CARD15 mutations

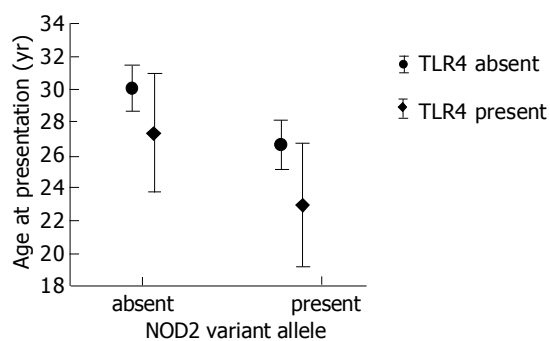
	Total (<i>n</i> = 527)	Non carrier (<i>n</i> = 342)	Carrier (<i>n</i> = 185)	1 allele (<i>n</i> = 133)	2 alleles (<i>n</i> = 52)
Male/Female	265/262	174/168	91/94	71/62	20/32
Age (yr)	36.9±9.1	37.9±13.0	34.9±11.6 ¹	35.2±11.7	34.3±11.4
Age at presentation (yr)	37.1±7.6	29.8±12.1	26.4±9.7 ¹	26.4±9.6	26.5±10.2
Duration (yr)	8.2±5.0	8.1±7.0	8.5±6.7	8.8±7.0	7.9±5.8
Familial IBD <i>n</i> (%)	63 (11.9)	38 (11.1)	25 (13.5)	17 (12.8)	8 (15.4)
Location (<i>n</i>)					
L1	136	84	52 ¹	36 ²	16 ²
L2	136	103	33	26	7
L3	251	152	99	71	28
L4	4	3	1	0	1
Behavior (<i>n</i>)					
B1	216	151	65 ¹	48 ³	17
B2	128	71	57	42	15
B3	183	120	63	43	20
Perianal disease <i>n</i> (%)	140 (26.6)	89 (26.0)	51 (27.6)	36 (27.1)	15 (28.9)
Frequent relapse <i>n</i> (%)	195 (37.1)	126 (36.9)	69 (37.3)	47 (35.3)	22 (42.3)
Extraintestinal manifestations <i>n</i> (%)	175 (33.2)	117 (34.2)	58 (31.3)	45 (33.8)	13 (25)
Arthritis <i>n</i> (%)	147 (27.9)	98 (28.7)	49 (26.5)	36 (27.1)	13 (25)
Ocular <i>n</i> (%)	27 (5.1)	18 (5.2)	9 (4.9)	9 (6.8)	0
Erythema					
nodosum/Pyoderma <i>n</i> (%)	48 (9.1)	30 (8.8)	18 (9.7)	15 (11.3)	3 (5.8)
PSC ^a	18 (3.4)	15 (4.4)	3 (1.6)	3 (2.3)	0
Steroid use/ refractory <i>n</i> (%)	440 (83.5)/ 44 (10)	282 (82.4)/ 28 (9.3)	158 (85.4)/ 16 (10.1)	114 (85.7)/ 10 (8.8)	44 (84.6)/ 6 (13.6)
Azathioprine use/ refractory <i>n</i> (%)	337 (64.1)/ 19 (5.6)	208 (60.8)/ 10 (4.8)	129 (69.7) ¹ / 9 (7.0)	89 (66.9)/ 7 (7.8)	40 (76.9) ⁴ / 2 (5)
Operation <i>n</i> (%)	220 (41.8)	128 (37.4)	92 (49.7) ¹	66 (49.6) ²	26 (50.0) ²
Smoking (<i>n</i>)					
Never	308	191	117	80	37
Active	170	115	55	42	13
Previous	49	36	13	11	2

¹*P* < 0.03 between carriers and non-carriers, ²*P* < 0.03 between patients carrying one or two mutant allele and non-carriers, ³*P* = 0.043 between patients carrying one mutant allele and non-carriers, ⁴*P* = 0.025 between patients carrying two mutant allele and non-carriers.

Table 7 Genotype–phenotype associations with particular NOD2/CARD15 alleles in CD patients

	None (<i>n</i> = 342)	SNP8 (<i>n</i> = 61)	SNP12 (<i>n</i> = 33)	SNP13 (<i>n</i> = 102)
Male/Female	174/168	28/33	14/19	51/51
Age (yr)	37.9±13.0	35.9±13.0	37.1±11.4	33.7±10.4 ¹
Age at presentation (yr)	29.8±12.1	26.6±10.9	28.8±10.0	26.0±8.4 ¹
Duration (yr)	8.1±7.0	9.3±7.6	11.4±6.4 ²	7.7±6.1
Familiar IBD <i>n</i> (%)	38 (11.1)	9 (14.8)	7 (21.1)	11 (10.8)
Location				
L1	84	16	7	32 ²
L2	103	12	5	16
L3	152	33	20	53
L4	3	0	1	1
Behavior				
B1	151	22	8	34
B2	71	15	13	31
B3	120	14	12	37
Perianal disease <i>n</i> (%)	89 (26.0)	18 (29.5)	7 (21.1)	32 (31.4)
Frequent relapse <i>n</i> (%)	126 (36.9)	24 (39.3)	13 (39.4)	38 (37.3)
Extraintestinal manifestations <i>n</i> (%)	117 (34.2)	17 (27.8)	14 (42.4)	31 (30.4)
Arthritis <i>n</i> (%)	98 (28.7)	16 (26.2)	14 (42.2)	24 (23.5)
Occular <i>n</i> (%)	18 (5.2)	1 (1.6)	2 (6.1)	4 (3.9)
Erythema nodosum/ Pyoderma <i>n</i> (%)	30 (8.8)	5 (8.2)	4 (12.1)	7 (6.9)
PSC <i>n</i> (%)	15 (4.4)	1 (1.6)	0	2 (1.9)
Steroid use/ refractory <i>n</i> (%)	282 (82.4)/ 28 (9.3)	51 (83.6)/ 7 (13.7)	31 (93.9)/ 2 (16.1)	88 (86.3)/ 6 (6.8)
Azathioprine use/ refractory <i>n</i> (%)	208 (60.8)/ 10 (4.8)	38 (62.3)/ 4 (10.5)	32 (97) ¹ / 2 (11.1)	69 (67.6)/ 3 (4.3)
Operation <i>n</i> (%)	128 (37.4)	27 (44.3)	23 (69.7) ¹	53 (52.0) ²
Smoking habits				
Never	191	44	21	65
Active	115	12	9	33
Previous	36	5	3	4

¹ $P < 0.001$ between carriers and non-carriers; ² $P < 0.03$ between carriers and non-carriers.

**Figure 1** Association between genetics and age at presentation in patients with CD.

The TLR4 D299G mutation was not different between patients and controls (9.9% *vs* 12.0%, $P = \text{NS}$). The frequency of familial IBD tended to be lower in patients with TLR4 mutation (5.7% *vs* without 12.6%, $P = \text{NS}$). However, the presence of variant TLR4 allele strengthened genotype-phenotype associations (Figure 1; for age of onset: non-carriers [$n = 305$]: 30.2 years, only TLR4 carriers [$n = 37$]: 27.4 years, only NOD2/CARD15 carriers [$n = 170$]: 26.7 years, both NOD2 and TLR4 carriers [$n = 15$]: 23 years, $P = 0.03$ for NOD2/CARD15 variant allele, and $P = 0.06$ for TLR4 variant allele by multiple regression and for ileal involvement; in patients with TLR4 and NOD2/CARD15 mutations: 86.7% *vs* non-carriers: 64.8%).

In a logistic regression model, exploring the effect of NOD2, TLR4 carriage, age at presentation, location, behavior and smoking, presence of NOD2 mutation (coefficient = 0.54, OR = 1.71, 95%CI: 1.13-2.62, $P = 0.01$) and non-inflammatory behavior (coefficient = 1.26, OR = 3.53, 95%CI: 2.76-4.51, $P = 0.001$) but not location, smoking or carriage of TLR4 variant allele were independently associated with the need for surgery. However, the percentage of multiple resections was not different between carriers and non-carriers (13.0% *vs* 11.1%, $P = \text{NS}$).

DISCUSSION

This is the first report on the prevalence of NOD2/CARD15 mutations and TLR4 D299G polymorphism in patients with CD from a Central Eastern European country. The reported rates of 35.1% of patients carrying NOD2/CARD15 mutations in CD and 16.5% in controls are in concordance with previously reported rates of 30-50% in CD and 7-20% in controls from other European regions^[12,15-17,32-35]. Only in Finland (which by language is related to Hungary), the rate of NOD2 mutations was considerably lower (8.7% *vs* 3.5% in controls)^[21]. Similar low frequencies were found in other Northern European countries (8% in Denmark, and 8.9% in patients from Norway)^[28]. The prevalence of SNP8, 12 and 13 was 3.3, 0.6 and 4.8% in the Finish study (in controls it was 1.8%, 0 and 1.7%) with only the SNP13 being more common in CD compared to controls. In our study, the rates were 11.6,

6.3 and 19.4%, which are in concordance with other studies from Europe (6.7-12.5%, 3.3-6.1% and 6.6-16% in CD and 3.5-6.9%, 0.6-3.0% and 1.0-4.4% in controls)^[17,33].

The phenotype-genotype correlations in our cohort were also similar to those reported in various European countries^[6,17,36]. Ileal involvement in Hungarian patients was more frequent in NOD2 mutation carriers (81.6%), while disease confined to the colon alone was less frequent (17.8%), especially in patients with two alleles, in the presence of SNP13 or TLR4 variant allele. Like in other countries, in our study, carriage of variant NOD2/CARD15 allele was associated with stricturing disease (30.8% *vs* 20.8%), while variant alleles were less frequent in patients with inflammatory disease. More patients with stricturing disease carried a mutant NOD2/CARD15 allele (44.5%) than patients without strictures (32.1%, $P < 0.01$). Steroid use and efficacy were similar in mutation carriers and non-carriers, but a higher percentage of patients carrying NOD2/CARD15 variant allele needed azathioprine during the course of the disease, especially in the presence of two risk alleles. There are conflicting data on the association of NOD2/CARD15 mutations and need for surgery in CD patients: association^[37] and also lack of association^[16,17] have been reported.

In a French follow-up study^[18], ileal location was associated with early development of stricturing disease while a high number of flares was associated with a penetrating pattern, but this was not affected by the presence of variant NOD2/CARD15 allele. Active smoking was also associated with early development of penetrating disease. In our study there was no difference in the proportion of smokers between carriers and non-carriers of NOD2/CARD15 variant allele.

The importance of TLR4 D299G polymorphism in CD is less clear. In contrast to Franchimont *et al*^[27] who reported a two-fold elevation in allele frequency of TLR4 D299G (11% *vs* 5%, OR = 2.31), we found no difference in the prevalence of TLR4 D299G polymorphism in CD patients and controls, suggesting that this polymorphism is not essential in the development of the disease. There is also no difference in TLR4 allele frequency between IBD patients and controls in concordance with the preliminary results of the EC-IBD study group^[28]. However, the rate of variant allele is higher in the Hungarian controls compared to the study of Franchimont *et al*^[27]. We also found a tendency of decreased frequency of the TLR4 D299G variant allele in patients with familial disease (6% *vs* sporadic 13%, $P = \text{NS}$).

In our study, no clear-cut phenotype-genotype associations were observed in TLR4 D299G carriers. The presence of variant TLR4 allele tendentially associated with early disease onset ($P = 0.06$), along with a gene-dosage effect. The earliest onset (23 years) was observed in carriers of both variant NOD2/CARD15 and TLR4 alleles (*vs* non-carriers 30.2 years, $P = 0.01$). The presence of TLR4 variant allele did not affect disease behavior (in patients with variant TLR4 allele, stricturing disease was present in 33.3% of NOD2 carriers *vs* 17.1% of NOD2/CARD15 non-carriers).

In summary, this is the first report on the prevalence of NOD2/CARD15 mutations and TLR4 D299G polymorphism in patients with CD from a Central Eastern European country. It confirms that the risk for CD is increased

in carriers of R702W, R703C and 3020insC mutations, while the presence of G908R or TLR4 D299G polymorphism is not different from the controls. The presence of variant NOD2/CARD15 alleles is associated with early disease onset, ileal disease and stricturing disease behavior and increases need for surgery, while the presence of TLR4 D299G variant allele exhibits a disease modifier effect.

ACKNOWLEDGEMENTS

The authors thank Dr. Peter Vargha for performing the statistical analysis.

REFERENCES

- 1 Podolsky DK. Inflammatory bowel disease. *N Engl J Med* 2002; **347**: 417-429
- 2 Lakatos L, Mester G, Erdelyi Z, Balogh M, Szpocs I, Kamaras G, Lakatos PL. Striking elevation in incidence and prevalence of inflammatory bowel disease in a province of western Hungary between 1977-2001. *World J Gastroenterol* 2004; **10**: 404-409
- 3 Hugot JP, Laurent-Puig P, Gower-Rousseau C, Olson JM, Lee JC, Beaugier L, Naom I, Dupas JL, Van Gossum A, Orholm M, Bonaiti-Pellie C, Weissenbach J, Mathew CG, Lennard-Jones JE, Cortot A, Colombel JF, Thomas G. Mapping of a susceptibility locus for Crohn's disease on chromosome 16. *Nature* 1996; **379**: 821-823
- 4 Colombel JF. The CARD15 (also known as NOD2) gene in Crohn's disease: are there implications for current clinical practice? *Clin Gastroenterol Hepatol* 2003; **1**: 5-9
- 5 Bonen DK, Cho JH. The genetics of inflammatory bowel disease. *Gastroenterology* 2003; **124**: 521-536
- 6 Ahmad T, Tamboli CP, Jewell D, Colombel JF. Clinical relevance of advances in genetics and pharmacogenetics of IBD. *Gastroenterology* 2004; **126**: 1533-1549
- 7 Berrebi D, Maudinas R, Hugot JP, Chamaillard M, Chareyre F, De Lagausie P, Yang C, Desreumaux P, Giovannini M, Cezard JP, Zouali H, Emilie D, Peuchmaur M. Card15 gene overexpression in mononuclear and epithelial cells of the inflamed Crohn's disease colon. *Gut* 2003; **52**: 840-846
- 8 Girardin SE, Hugot JP, Sansonetti PJ. Lessons from Nod2 studies: towards a link between Crohn's disease and bacterial sensing. *Trends Immunol* 2003; **24**: 652-658
- 9 Bonen DK, Ogura Y, Nicolae DL, Inohara N, Saab L, Tanabe T, Chen FF, Foster SJ, Duerr RH, Brant SR, Cho JH, Nunez G. Crohn's disease-associated NOD2 variants share a signaling defect in response to lipopolysaccharide and peptidoglycan. *Gastroenterology* 2003; **124**: 140-146
- 10 Aldhous MC, Nimmo ER, Satsangi J. NOD2/CARD15 and the Paneth cell: another piece in the genetic jigsaw of inflammatory bowel disease. *Gut* 2003; **52**: 1533-1535
- 11 Girardin SE, Boneca IG, Viala J, Chamaillard M, Labigne A, Thomas G, Philpott DJ, Sansonetti PJ. Nod2 is a general sensor of peptidoglycan through muramyl dipeptide (MDP) detection. *J Biol Chem* 2003; **278**: 8869-8872
- 12 Hugot JP, Chamaillard M, Zouali H, Lesage S, Cezard JP, Belaiche J, Almer S, Tysk C, O'Morain C, Gassull M, Binder V, Finkel Y, Cortot A, Modigliani R, Laurent-Puig P, Gower-Rousseau C, Macry J, Colombel JF, Sahbatou M, Thomas G. Association of NOD2 leucine-rich repeat variants with susceptibility to Crohn's disease. *Nature* 2001; **411**: 599-603
- 13 Ogura Y, Bonen DK, Inohara N, Nicolae DL, Chen FF, Ramos R, Britton H, Moran T, Karaliuskas R, Duerr RH, Achkar JP, Brant SR, Bayless TM, Kirschner BS, Hanauer SB, Nunez G, Cho JH. A frameshift mutation in NOD2 associated with susceptibility to Crohn's disease. *Nature* 2001; **411**: 603-606
- 14 Hampe J, Cuthbert A, Croucher PJ, Mirza MM, Mascheretti S, Fisher S, Frenzel H, King K, Hasselmeyer A, MacPherson AJ, Bridger S, van Deventer S, Forbes A, Nikolaus S, Lennard-

- Jones JE, Foelsch UR, Krawczak M, Lewis C, Schreiber S, Mathew CG. Association between insertion mutation in NOD2 gene and Crohn's disease in German and British populations. *Lancet* 2001; **357**: 1925–1928
- 15 **Ahmad T**, Armuzzi A, Bunce M, Mulcahy-Hawes K, Marshall SE, Orchard TR, Crawshaw J, Large O, de Silva A, Cook JT, Barnardo M, Cullen S, Welsh KI, Jewell DP. The molecular classification of the clinical manifestations of Crohn's disease. *Gastroenterology* 2002; **122**: 854–866
 - 16 **Brant SR**, Picco MF, Achkar JP, Bayless TM, Kane SV, Brzezinski A, Nouvet FJ, Bonen D, Karban A, Dassopoulos T, Karaliukas R, Beaty TH, Hanauer SB, Duerr RH, Cho JH. Defining complex contributions of NOD2/CARD15 gene mutations, age at onset, and tobacco use on Crohn's disease phenotypes. *Inflamm Bowel Dis* 2003; **9**: 281–289
 - 17 **Lesage S**, Zouali H, Cezard JP, Colombel JF, Belaiche J, Almer S, Tysk C, O'Morain C, Gassull M, Binder V, Finkel Y, Modigliani R, Gower-Rousseau C, Macry J, Merlin F, Chamaillard M, Jannot AS, Thomas G, Hugot JP. CARD15/NOD2 mutational analysis and genotype-phenotype correlation in 612 patients with inflammatory bowel disease. *Am J Hum Genet* 2002; **70**: 845–857
 - 18 **Louis E**, Michel V, Hugot JP, Reenaers C, Fontaine F, Delforge M, El Yafi F, Colombel JF, Belaiche J. Early development of stricturing or penetrating pattern in Crohn's disease is influenced by disease location, number of flares, and smoking but not by NOD2/CARD15 genotype. *Gut* 2003; **52**: 552–557
 - 19 **Inoue N**, Tamura K, Kinouchi Y, Fukuda Y, Takahashi S, Ogura Y, Inohara N, Nunez G, Kishi Y, Koike Y, Shimosegawa T, Shimoyama T, Hibi T. Lack of common NOD2 variants in Japanese patients with Crohn's disease. *Gastroenterology* 2002; **123**: 86–91
 - 20 **Leong RW**, Armuzzi A, Ahmad T, Wong ML, Tse P, Jewell DP, Sung JJ. NOD2/CARD15 gene polymorphisms and Crohn's disease in the Chinese population. *Aliment Pharmacol Ther* 2003; **17**: 1465–1470
 - 21 **Helio T**, Halme L, Lappalainen M, Fodstad H, Paavola-Sakki P, Turunen U, Farkkila M, Krusius T, Kontula K. CARD15/NOD2 gene variants are associated with familiarly occurring and complicated forms of Crohn's disease. *Gut* 2003; **52**: 558–562
 - 22 **Hornef MW**, Normark BH, Vandewalle A, Normark S. Intracellular recognition of lipopolysaccharide by toll-like receptor 4 in intestinal epithelial cells. *J Exp Med* 2003; **198**: 1225–1235
 - 23 **Ruemmele FM**, Beaulieu JF, Dionne S, Levy E, Seidman EG, Cerf-Bensussan N, Lentze MJ. Lipopolysaccharide modulation of normal enterocyte turnover by toll-like receptors is mediated by endogenously produced tumour necrosis factor alpha. *Gut* 2002; **51**: 842–848
 - 24 **Boone DL**, Ma A. Connecting the dots from Toll-like receptors to innate immune cells and inflammatory bowel disease. *J Clin Invest* 2003; **111**: 1284–1286
 - 25 **Cario E**, Podolsky DK. Differential alteration in intestinal epithelial cell expression of toll-like receptor 3 (TLR3) and TLR4 in inflammatory bowel disease. *Infect Immun* 2000; **68**: 7010–7017
 - 26 **Okayama N**, Fujimura K, Suehiro Y, Hamanaka Y, Fujiwara M, Matsubara T, Maekawa T, Hazama S, Oka M, Nohara H, Kayano K, Okita K, Hinoda Y. Simple genotype analysis of the Asp299Gly polymorphism of the Toll-like receptor-4 gene that is associated with lipopolysaccharide hyporesponsiveness. *J Clin Lab Anal* 2002; **16**: 56–58
 - 27 **Franchimont D**, Vermeire S, El Housni H, Pierik M, Van Steen K, Gustot T, Quertinmont E, Abramowicz M, Van Gossum A, Deviere J, Rutgeerts P. Deficient host-bacteria interactions in inflammatory bowel disease? The toll-like receptor (TLR)-4 Asp299gly polymorphism is associated with Crohn's disease and ulcerative colitis. *Gut* 2004; **53**: 987–992
 - 28 **Riis LB**, Wolters F, Solberg C. Regional differences in the prevalence of single nucleotide polymorphisms in CARD15/NOD2 but not in toll-like receptor 4 (TLR4) Asp299Gly polymorphism in patients with inflammatory bowel disease (IBD) across Europe: Results from the EC-IBD study group. *Gastroenterology* 2004; **126**(Suppl S): M1539
 - 29 **Lennard-Jones JE**. Classification of inflammatory bowel disease. *Scand J Gastroenterol Suppl* 1989; **170**: 2–6
 - 30 **Gasche C**, Scholmerich J, Brynskov J, D'Haens G, Hanauer SB, Irvine EJ, Jewell DP, Rachmilewitz D, Sachar DB, Sandborn WJ, Sutherland LR. A simple classification of Crohn's disease: report of the Working Party for the World Congresses of Gastroenterology, Vienna 1998. *Inflamm Bowel Dis* 2000; **6**: 8–15
 - 31 **Lorenz E**, Frees KL, Schwartz DA. Determination of the TLR4 genotype using allele-specific PCR. *Biotechniques* 2001; **31**: 22–24
 - 32 **Annese V**, Palmieri O, Latiano A, Ardizzone S, Castiglione F, Cottone M, D'Inca R, Gionchetti P, Papi C, Riegler G, Vecchi M, Andriulli A. Frequency of NOD2/CARD15 variants in both sporadic and familial cases of Crohn's disease across Italy. An Italian Group for Inflammatory Bowel Disease Study. *Dig Liver Dis* 2004; **36**: 121–124
 - 33 **Cuthbert AP**, Fisher SA, Mirza MM, King K, Hampe J, Croucher PJ, Mascheretti S, Sanderson J, Forbes A, Mansfield J, Schreiber S, Lewis CM, Mathew CG. The contribution of NOD2 gene mutations to the risk and site of disease in inflammatory bowel disease. *Gastroenterology* 2002; **122**: 867–874
 - 34 **Abreu MT**, Taylor KD, Lin YC, Hang T, Gaiennie J, Landers CJ, Vasilias EA, Kam LY, Rojany M, Papadakis KA, Rotter JI, Targan SR, Yang H. Mutations in NOD2 are associated with fibrostenosing disease in patients with Crohn's disease. *Gastroenterology* 2002; **123**: 679–688
 - 35 **Heresbach D**, Gicquel-Douabin V, Birebent B, D'halluin PN, Heresbach-Le Berre N, Dreano S, Siproudhis L, Dabadie A, Gosselin M, Mosser J, Semana G, Bretagne JF, Yaouanq J. NOD2/CARD15 gene polymorphisms in Crohn's disease: a genotype-phenotype analysis. *Eur J Gastroenterol Hepatol* 2004; **16**: 55–62
 - 36 **Torok HP**, Glas J, Lohse P, Folwaczny C. Alterations of the CARD15/NOD2 gene and the impact on management and treatment of Crohn's disease patients. *Dig Dis* 2003; **21**: 339–345
 - 37 **Buning C**, Genschel J, Buhner S, Kruger S, Kling K, Dignass A, Baier P, Bochow B, Ockenga J, Schmidt HH, Lochs H. Mutations in the NOD2/CARD15 gene in Crohn's disease are associated with ileocecal resection and are a risk factor for reoperation. *Aliment Pharmacol Ther* 2004; **19**: 1073–1078

• BASIC RESEARCH •

Hepatocyte growth factor gene therapy prevents radiation-induced liver damage

Chau-Hua Chi, I-Li Liu, Wei-Yu Lo, Bor-Song Liaw, Yu-Shan Wang, Kwan-Hwa Chi

Chau-Hua Chi, I-Li Liu, Bor-Song Liaw, Yu-Shan Wang, Institute of Veterinary Science, National Taiwan University, Taiwan, China
I-Li Liu, Department of General Surgery, Veterans General Hospital-Taipei, National Yang-Ming University, Taipei, Taiwan, China
Wei-Yu Lo, Anawrahta Biotech. Co., Danshuei, Taipei 251, Taiwan, China

Yu-Shan Wang, Kwan-Hwa Chi, Department of Radiation Therapy and Oncology, Shin Kong Wu Ho-Su Memorial Hospital, Taipei, Taiwan, China

Kwan-Hwa Chi, Cancer Center, Veterans General Hospital-Taipei, National Yang-Ming University, Taipei, Taiwan, China

Supported by National Science Council grant NSC-91-275-9075-001 for the development of Boron Neutron Capture Therapy for Hepatoma Treatment

Correspondence to: Kwan-Hwa Chi, M.D., Department of Radiation Therapy and Oncology, Shin Kong Wu Ho-Su Memorial Hospital, 95, Wen-Chang Rd., Shih-Lin, Taipei, Taiwan, China. m006565@ms.skh.org.tw

Telephone: +886-2-28332211-2273 Fax: +886-2-28377582

Received: 2004-10-09 Accepted: 2004-11-19

Abstract

AIM: To transfer human HGF gene into the liver of rats by direct electroporation as a means to prevent radiation-induced liver damage.

METHODS: Rat whole liver irradiation model was accomplished by intra-operative approach. HGF plasmid was injected into liver and transferred by electroporation using a pulse generator. Control rats ($n = 8$) received electroporation (EGT) vehicle plasmid and another 8 rats received HGF-EGT 100 μ g 48 h before WLIR. Expression of HGF in liver was examined by RT-PCR and ELISA methods. Apoptosis was determined by TUNEL assay. Histopathology was evaluated 10 wk after whole liver irradiation.

RESULTS: Marked decrease of apoptotic cells and down-regulation of transforming growth factor-beta 1 (TGF- β 1) mRNA were observed in the HGF-EGT group 2 d after liver irradiation compared to control animals. Less evidence of radiation-induced liver damage was observed morphologically in liver specimen 10 wk after liver irradiation and longer median survival time was observed from HGF-EGT group (14 wk) compared to control rats (5 wk). ($P = 0.031$).

CONCLUSION: For the first time it has been demonstrated that HGF-EGT would prevent liver from radiation-induced liver damage by preventing apoptosis and down-regulation of TGF- β 1.

© 2005 The WJG Press and Elsevier Inc. All rights reserved.

Key words: Hepatocyte growth factor; HGF; Radiation; Liver; Electroporation; Electroporation therapy

Chi CH, Liu IL, Lo WY, Liaw BS, Wang YS, Chi KH. Hepatocyte growth factor gene therapy prevents radiation-induced liver damage. *World J Gastroenterol* 2005; 11(10): 1496-1502
<http://www.wjgnet.com/1007-9327/11/1496.asp>

INTRODUCTION

Radiation-induced liver damage is the end stage of acute liver injury. The damage caused by radiation is characterized by the development of anicteric ascites approximately 2 wk to 4 mo after hepatic irradiation. Radiotherapy traditionally had a limited role in the treatment of unresectable primary or metastatic intrahepatic cancers primarily due to the low liver tolerance to radiotherapy. Radiation-induced liver damage had been observed in 5-10% of patients who had received whole liver radiation dose exceeding 30 Gy^[1]. Although 3-D conformal radiotherapy may greatly reduce the normal liver irradiated volume through dose volume histogram evaluation, the radiation-induced liver damage is the dose-limiting factor for liver tumor irradiation. Recently developed intra-arterial radiolabeled-iododeoxyuridine therapy, lipiodol-¹³¹I therapy, or boron neutron capture therapy for liver cancers are all also potentially limited by the risk of liver damage^[2-4]. The major pathological feature of radiation-induced liver damage is veno-occlusive disease. The biological foundations of radiation-induced liver damage are poorly understood. The standard treatment is limited and has a high mortality rate.

HGF is a pluripotent factor associated with tissue growth and regeneration^[5]. HGF is a strong promoter of cell survival^[6,7]. It promotes the differentiation of mesenchymal cells to epithelial or endothelial cells and plays a pivotal role in the prevention of tissue fibrosis and dysfunction^[8-10]. Moreover, HGF is considered to be a major determinant of whether the epithelium remains in a quiescent state or shifts to a proliferative state associated with development and tissue repair^[8,11].

Under normal conditions, liver, kidney and spleen produce low amounts of HGF. Noticeable pathological changes such as ischemia, toxic injury or tissue loss would result in the increase of HGF and its receptor c-Met during the early stage of injury^[12]. Although endogenous HGF levels are elevated after tissue injury, the amounts are low during the damage occurrence. Furthermore, high and sustained

amounts of HGF are mandatory for subsequent tissue repair. Therefore, the use of exogenous HGF therapy may be an effective treatment for the prevention of tissue injury and the promotion of tissue repair^[13]. Recombinant HGF has a short half life of 3–5 min, local regional continuous infusion by intra-arterial pump would be an appropriate delivery method to achieve high and sustained amount of HGF to liver^[12]. In addition, an alternative method for sustained delivery of pharmacological level of protein in target tissue would be based upon a gene therapy-mediated approach.

Researchers reported that intra-muscular (IM) injection of HGF genes ameliorated chemically-induced liver damage in rabbits^[14]. *In vivo* electrogene transfer (EGT) is considered a highly efficient gene transfer method^[15]. Electricity-mediated HGF gene transfer into muscle has also been reported to accelerate regeneration in cirrhotic livers of mice after partial hepatectomy^[9]. However, there was no report of HGF gene therapy on the protection of radiation damage. The present study was designed to assess the efficacy of direct EGT with HGF gene into livers of rats as a method to prevent radiation-induced liver damage.

MATERIALS AND METHODS

Plasmid DNA

Plasmid PCR3.1/hHGF was constructed by inserting the full length cDNA of human HGF under a human cytomegalovirus promoter. Human HGF cDNA (2.2 kb) was subcloned into two KpnI sites. Plasmids were grown in TOP10F⁺ competent cell, selected by ampicillin and extracted by an EndoFree Plasmid Giga kit (Qiagen, Valencia, CA). Enhanced green fluorescent protein (pIRES2-EGFP) plasmid was obtained commercially (Clontech, Palo Alto, CA, USA). DNA was dissolved in EndoFree TE buffer, and the quality and quantity were assessed by measuring the optical density at 260 and 280 nm.

Liver irradiation

Sprague-Dawley (SD) female rats (180–200 g) received whole liver radiation. The experiment was approved by Animal Committee of Veterans General Hospital-Taipei. Three dosage levels were chosen and each dosage level included eight animals. The measured variables were body weight change, serum aspartate aminotransferase (AST), alkaline aminotransferase (ALT) changes. An autopsy was performed with specific attention to the liver histopathology and animal survival proportion was counted. Before irradiation, each animal was anesthetized with ketamine, and its abdomen was opened. Most of the intestine, stomach, and spleen were not within the radiation field. All organs were kept moist with gauze soaked in lactate Ringer's solution during irradiation of 20 Gy, 40 Gy and 65 Gy with a Cobalt machine. The rats were warmed with a light heater to prevent hypothermia. The animal's muscle layer was sewn together with sterile 3–0 nylon sutures after irradiation. The skin was closed with surgical clips.

EGT-HGF plasmids into liver

In order to observe the HGF protein and mRNA expression

after direct HGF gene transfection by electroporation, we investigated dose-responsive relationship of EGT HGF. The left median or left lateral lobe of the liver was exposed after the abdominal cavity was opened surgically. The center of the lobe was caught between the tweezer-type electrode disks. PCR3.1/hHGF plasmid DNA in 0, 25, 50, 100, 200 µg/100 µL volume was injected with a microinjector into the liver halfway between the two electrode disks. Immediately after the DNA injection, electric pulses were administered. The electrical pulses were delivered using an Electro Square porator (T820, BTX, San Diego, CA)^[16,17]. The rat's liver was electroporated with 8 electrical pulses of 50 ms duration at 50 V. One to eight electric pulses were administered at a rate of one pulse per second. The abdominal wound was then closed. The efficacy of liver EGT was checked with 50 µg EGFP plasmid co-administered with HGF gene 50 µg under fluorescence microscopy. Protein extracts from the liver were prepared 2 d after electroporation. The concentrations of HGF in rat liver extracts after different doses of EGT-HGF were determined by enzyme-linked immunoassay (ELISA) kit for human HGF. (R & D Systems, Inc., Minneapolis, Minnesota, USA).

Therapeutic effect of EGT-HGF for the prevention of radiation-induced liver damage

The liver of each rat received EGT 48 h prior to a liver irradiation of 65 Gy. The experimental groups (10 rats) were transfected with PCR3.1/hHGF plasmid 100 g/liver, and the control group (10 rats) was electroporated with empty vector 100 g/liver. Blood samples were collected weekly for 10 wk to examine the serial AST/ALT and the changes in the transforming growth factor (TGF-β1). One rat from each group was sacrificed 2 d after irradiation to examine the apoptosis formation and TGF-β1 expression in its liver sections. Serum HGF concentrations were determined 7 d after EGT. One rat from each group was sacrificed 10 wk after irradiation to investigate the histopathological changes. The overall survival time was recorded.

Identification of apoptosis

Terminal deoxynucleotidyl transferase-mediated dUTP nick-end labeled (TUNEL) assay was performed for the detection of apoptotic cells. Apoptotic hepatocytes were labeled *in situ* using a FragELTM DNA fragmentation detection kit-TdT enzyme (Oncogene, Boston, MA) according to the manufacturer's stipulations. First, 3 µm thick deparaffinized liver sections were pretreated with proteinase K (20 µg/mL) for 20 min at room temperature. After washing in TBS, the endogenous peroxidase was inactivated in 3% H₂O₂ for 5 min, followed by incubation with TdT labeling reaction mixture at 37 °C for 1.5 h in a humid chamber. After this incubation, sections were incubated with stop solution for 5 min, blocking buffer for 10 min, and 1×conjugate buffer for 30 min. Finally, sections were incubated with diaminobenzidine (DAB) solution for 10–15 min, followed by incubation with methyl green as counterstain. Apoptotic cells were counted using a light microscope at a magnification of ×100. Image quantification was performed using Image-Pro Plus 4.1 program from Media Cybernetics (Silver Spring,

MD) to determine the percent apoptotic cells. In addition, some paraffin-embedded liver sections were stained to assess histopathological changes.

Reverse transcription-polymerase chain reaction (RT-PCR) analysis

Total cellular RNA was isolated from snap-frozen liver tissue by using RNeasyTM B (Tel-Test, Friendswood, TX) according to the manufacturer's instruction. 1-3 µg of RNA was converted to complementary DNA by using SuperscriptTM II RNase H Reverse Transcriptase (Invitrogen, Carlsbad, CA). Primer sequences for human HGF, TGF-β1, and β-globin, used in PCR on complementary DNA in each reaction were shown in Table 1. After the complementary DNA was amplified by using primer HGF-1 and TGF-β1-1, the PCR product was amplified a second time by using primer HGF-2 and TGF-β1-2. The cycle number of PCR was 30 for all genes.

Table 1 Primers for PCR

Gene	Primer sequences
HGF-1	Sense: 5'-CCAGCAGCACCATGTGGG-3' Antisense: 5'-CAGCTATGACTGTGGTACC-3'
HGF-2	Sense: 5'-CTGCTGCTGCAGCATGTCC-3' Antisense: 5'-GGACATCCACGACCAGG-3'
TGFβ	Sense: 5'-GCTGCTGCCGCTTCTGTCC-3' Antisense: 5'-GCACTTGCAGGAGCGCACG-3'
TGF-β1-2	Sense: 5'-GGCTTCTAGTGTGACGCCCG-3' Antisense: 5'-CCACCTTGGGCTTGCGACCC-3'
β-globin	Sense: 5'-CCAATCTGCTCACACAGGATAGAGAGGGCAGG-3' Antisense: 5'-CCTTGAGGCTGTCCAAGTGATTGAGGCCATCG-3'

Histocytochemistry

Autopsies were performed. The liver and adjacent organs were visually examined to determine the possible cause of death. One rat from each group was sacrificed on wk 10. The liver was removed and fixed in buffered formalin and stained with Masson trichrome staining method. Deparaffinized sections were hydrated with distilled water. Each section was rinsed well in distilled water and stained step by step with Weigert's hematoxylin for 10 min. This was followed by a Biebrich scarlet-acid fuchsin solution for 15 min. Then the sample was treated with phosphomolybdic-phosphotungstic acid for 15 min. The next phase was to rinse with aniline blue solution for 10 min at RT. The final process involved differentiation for 2 min in a 1% acetic acid, dehydration and finally mounted with synthetic resin.

Statistical analysis

Results are expressed as mean±SD. Statistical difference was assessed by the unpaired two-tailed Student's *t* test. The survival data was determined by Kaplan-Meier method and a log-rank test was performed to compare the difference. *P*<0.05 was considered significant.

RESULTS

Radiation-induced liver damage model

Single fraction radiation of 20-65 Gy to liver was performed

intra-operatively with Cobalt machine. Rats that received 40 Gy and 65 Gy of irradiation gradually had a decreased body weight and activity. There was no significant weight reduction in the rats that received 20 Gy irradiation. All the groups were observed for three months after radiation. None of the rats in the 20 Gy group died of liver irradiation. Fifty percent of the rats survived after 40 Gy, and only twenty-five percent of the rats survived after 65 Gy of liver irradiation at wk 12. All rats were autopsied and each showed evidence of jaundice as indicated by yellow coloration of the skin, urine and plasma. Ascites and sometimes pleural effusion were also present. No irradiation-related changes of adjacent intra-abdominal organs were seen by macroscopic inspection. The liver surface was adhered to the parietal peritoneum forming dense fibrous tissue. Early deaths (≤6 wk) were associated with hepatic congestion and swelling. Late deaths (≥10 wk) were usually associated with a shrunken and sometimes deformed liver, which indicated fibrosis formation. Microscopically, there were distortion of liver cellular architecture, sinusoid congestion, interstitial fibrosis, inflammatory cell infiltrations, bile duct proliferation and focal hepatocyte necrosis around hepatic veins. The pathology of 20 Gy irradiated animals was not noticeably different from normal control except for the varying congestion and dilatation of sinusoids and slight infiltration of inflammatory cells. There was no significant change of AST/ALT level in all treatment groups. However, the transient elevation of the ALT levels were observed in the second wk in the 65 Gy group, 6th wk in the 40 Gy group and 10th wk in the 20 Gy group. Brown apoptotic hepatocytes stained with TUNEL assay were observed 2 d after radiation and were also visible 2 wk later (data not shown).

Expression of HGF protein and mRNA after direct liver EGT with HGF plasmid

The liver of rats, which had 65 Gy of irradiation were used in the HGF-EGT experiments. PCR3.1/hHGF plasmid DNA in 0, 25, 50, 100, and 200 µg/100 µL were electroporated into the rat's liver and killed them 48 h later. Figure 1 indicated a dose-dependent increase of HGF concentrations in liver protein extracts by ELISA. The HGF expression reached a plateau after 100 µg of plasmid transfection by EGT. Green fluorescent protein can be observed in the cytoplasm of hepatocytes from double-

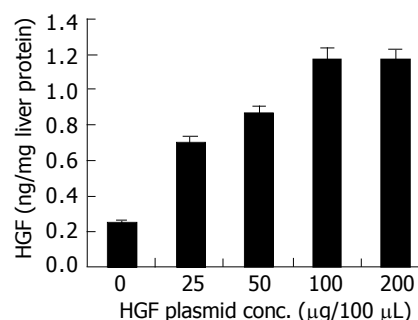


Figure 1 ELISA of human HGF protein concentrations in extracts of liver tissue taken from electroporated area 2 d after EGT-HGF.

gene transfection groups. Green fluorescence protein expressions were detected within 24 h, maximally at 3 d, and persisted for 3 wk but gradually reduced in intensity. The estimated transfection efficiency was around 40% 48 h after EGFP electroporation as assessed by fluorescence intensity under microscopic images examination (data not shown). RT-PCR disclosed human HGF segment of 2.2 kb in length 2 d after the EGT (data not shown).

Therapeutic effect of liver in situ EGT-HGF for the prevention of radiation-induced liver damage

Two days after 65 Gy of irradiation, one rat from each group was killed for an apoptosis study. Overall, there was a mild swelling and a petechial change over the electroporated field. TUNEL staining revealed a significant increase in apoptotic cells in the liver specimen. As shown in Figure 2, pre-administration of HGF plasmid by EGT 48 h before radiation markedly prevented formation of apoptotic cells in the liver. Most apoptosis occurred around the microvascular structures. Ten week after irradiation, one rat from each group was sacrificed for histological study. Grossly, moderate amount of ascites, jaundice, pleural effusion and a shrunken liver were observed in the control group. The degree of gross abnormality was less in the EGT-HGF group. Microscopically, congested hepatic veins, marked proliferation of bile ducts, increased fibrosis and

collagen around hepatic veins, concentric lamellations and subintimal thickening of hepatic arteries were observed in liver sections stained with Masson trichrome method (Figure 3). There were fewer fibrosis in the rats treated with EGT-HGF than radiation alone group. Biochemically, the general patterns of serum ALT/AST showed no significant difference between two groups except for the transient elevation of ALT level one wk after irradiation in the control group (mean 43.6 ± 35.8 vs 53.4 ± 30.8 , $P = 0.2$, Figure 4). EGT-HGF treatment seemed to suppress the initial elevation of ALT level. The relative insensitivity of ALT/AST changes for monitoring radiation-induced liver damage indicated that liver parenchymal cell necrosis was not the major pathological change from radiation damage. The serum TGF- β 1 was also measured without consistent patterns for reliable prediction of liver damage (data not shown). No serum human HGF was detected by the ELISA kit one wk after the administration of EGT. Overproduction of TGF- β 1 is a major cause of radiation-induced tissue fibrosis in liver and TGF- β 1 induces apoptotic cell death in hepatocytes. The expression of TGF- β 1 in liver 48 h after radiation from both groups by RT-PCR was investigated. TGF- β 1 expression was markedly induced in the RT alone group while the TGF- β 1 expression was down-regulated in rats treated with EGT-HGF (Figure 5). Rats, which received whole liver irradiation began to die 4 wk after irradiation.

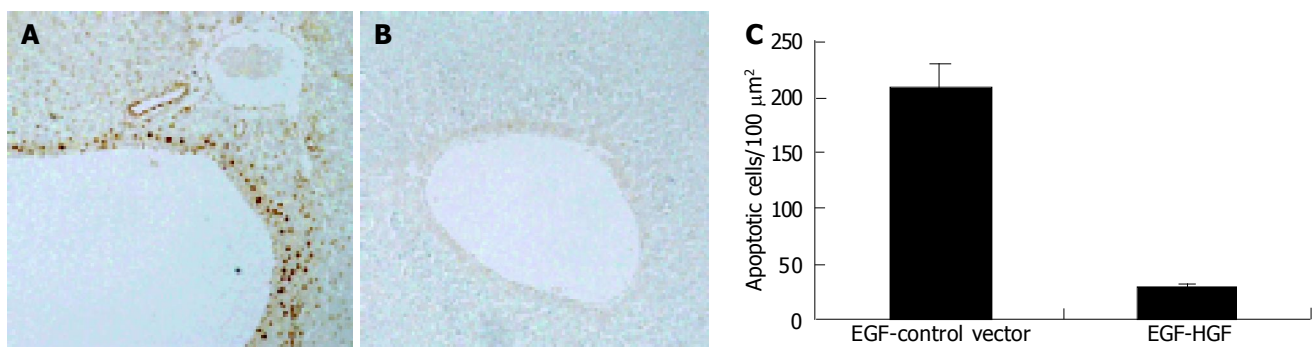


Figure 2 Apoptotic activities (TUNEL analysis) in rat liver after 65 Gy of irradiation. A: EGT-control vector 2 d before liver irradiation; B: EGT-HGF 2 d before irradiation. Rats were sacrificed 2 d after irradiation and stained with TUNEL assay. Note the brown round stain indicated TUNEL-positive cells, which gathered around microvascular region. EGT-HGF almost completely protected rat liver from radiation-induced apoptosis; C: Percent of apoptotic cells were quantitated per 100 μm^2 in areas shown on A and B. ($P < 0.05$).

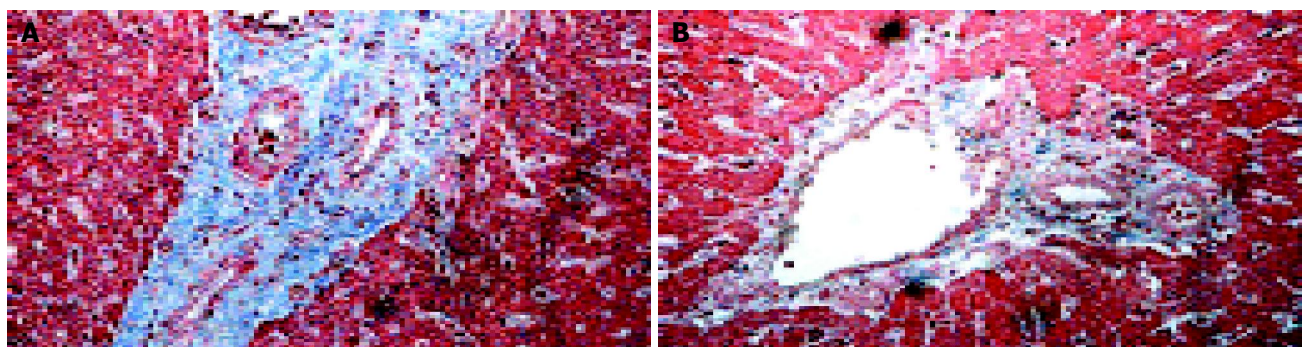


Figure 3 Histopathology of the liver 10 wk after 65 Gy of irradiation. A: rat liver ($\times 200$) receiving EGT-control-vector followed by 65 Gy of liver radiation 48 h later; B: rat liver ($\times 200$) receiving EGT-HGF followed by 65 Gy of liver radiation 48 h later. The blue stain indicated fibrosis formation. Fibrosis is more extensive with evidence of bile duct proliferation, sub-intimal thickening of arterioles with compromise of the vessel lumens. The morphology changes were less severe in HGF gene therapy group.

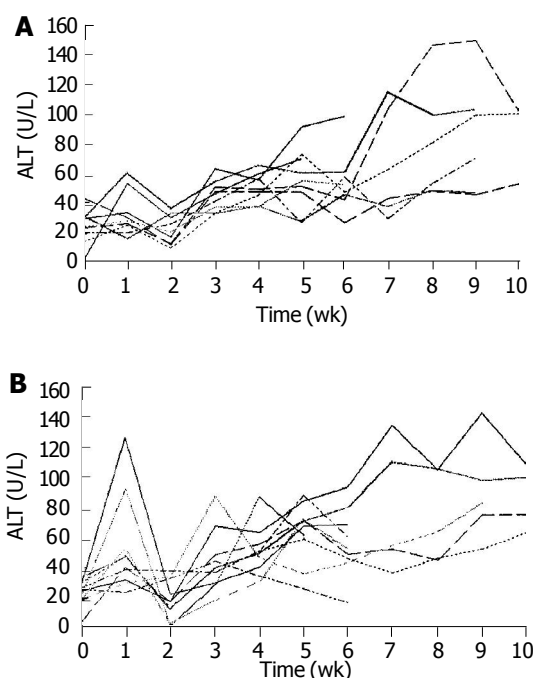


Figure 4 Weekly plasma ALT changes in rats receiving whole liver irradiation. A: Serial plasma ALT changes in EGT-HGF plus radiation group; B: Serial plasma ALT changes in EGT-control vector plus radiation group.

EGT-HGF treatment had prolonged the median survival time from 5 wk to 14 wk. By the end of 24 wk, the overall survival was 0% in the control group and 37.5% in the EGT-HGF group (Figure 6) ($P = 0.031$, Log-rank test).

DISCUSSION

In this study, HGF plasmid gene transferred into liver by electroporation has been demonstrated to be effective in the prevention of RILD in the liver. The introduction of HGF gene by electroporation not only prevented the apoptosis from radiation damage, but also improved overall survival of the rats. Electroporation, a non-viral gene transfer method has been widely used to introduce DNA into various types of cells and organ^[18]. The use of EGT in a liver had been regarded as one of the most efficient method of delivering and expressing high levels of exogenous genes in liver^[19].

HGF gene therapy by EGT HGF plasmid had been successfully reported in prolonging survival time in chemically-induced liver cirrhosis with or without hepatectomy models^[9,14,20]. The expression patterns of HGF transfer involving IM EGT is better than gene transfer using IM high-dose adenoviral vector as it is very difficult to sustain HGF levels due to adverse immune responses^[21]. In case of tumors which are not as permissive to adenovirus, it is difficult to transduce a large number of tumor cells with adenoviral vectors without inducing severe liver damage. In contrast, the systemic toxicity is not a risk with plasmid electroporation as with adenoviral transfection. In this study, the liver electro-transfection efficiency of transferred gene expression was observed from the co-transfection EGFP plasmid by fluorescence microscopic image. Electroporation

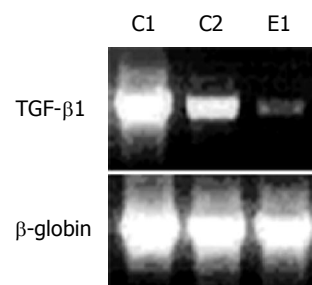


Figure 5 TGF-β1 RT-PCR analysis 2 d after liver irradiation. C1: rats receiving EGT-control vector and 65 Gy of liver irradiation; C2: rats receiving EGT-control vector and 20 Gy of liver irradiation; E1: rats receiving EGT-HGF and 65 Gy of liver irradiation. Figure is the representative of 3 experiments.

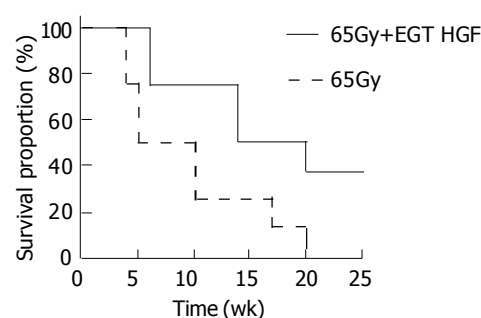


Figure 6 Survival analyses of rats after whole liver irradiation of 65 Gy. Segmented line ($n = 8$) indicated group that received EGT-control vector plus radiation treatment. Solid line ($n = 8$) indicated group that received EGT-HGF plus radiation treatment.

with eight electric pulses of 50 ms duration at 50 V gave a good efficiency of transfection as judged by the induced GFP expression. The transfection efficiency increased as the amount of injected DNA was increased but seemed to reach a plateau after 100 μ g of plasmid per transfection. The volume and techniques of plasmid delivery limited the maximal dose that could be delivered into the liver by direct parenchyma injection. This technical obstacle may be solved by producing micro-encapsulated plasmid injected *via* portal vein in order to increase the plasmid retention in the liver parenchyma before electroporation. The feasibility of HGF gene transfer into the liver *via* the portal vein injection followed by liver parenchyma electroporation has been reported to attenuate rat liver cirrhosis^[22].

In this experiment SD rat could tolerate high dose of whole liver irradiation with an LD₅₀ dose around 50 Gy. Acute lethal intestinal injury was prevented by moving intestine and stomach out of irradiation field. The advantage of intra-operative whole liver irradiation is that one can confirm visually that the liver is in the irradiation field and most of the unnecessary irradiated gastrointestinal tract is out of the irradiation field. Decreased hepatic function, ascites, pleural effusion, jaundice, elevated AST/ALT and histologic changes such as necrosis, parenchymal cell loss, congested sinusoids, hemorrhagic extravasation, portal area fibrosis and collagen around hepatic veins with concentric lamellations and subintimal thickening of hepatic arteries,

which were observed in the present study are similar to veno-occlusive in humans^[23,24]. Gerace *et al.*^[25] had reported similar histological lesion with evidences of injury to hepatic veins after whole liver irradiation of rats. Hebard *et al.*^[26] had reported that the threshold radiation dose for vein damage was less than the threshold dose for direct cell killing of hepatocytes. AST/ALTs are parenchymal intracellular enzymes released into systemic circulation when there is hepatocellular injury and necrosis. Gerace *et al.*^[25] had reported an average of 3 times higher level of elevation of AST/ALT approximately 40 d after irradiation, which coincided with the clearance of rose bengal. Nevertheless, the results of this study indicated that both AST and ALT are not sensitive enough to detect radiation-induced liver damage through out the first 10 wk except some transient elevation of ALT serum levels one wk after 65 Gy of radiation. Apoptosis occurs early after irradiation, which may be a better indicator of radiation damage, yet it needs tissue biopsy. Serum TGF- β 1 may be an alternatives for the early prediction of radiation induced injury. Murase *et al.*^[27] have demonstrated that an elevated plasma TGF- β 1 concentration before transplant predicted the later occurrence of veno-occlusive disease complications. However, the present experiment failed to show correlation of TGF- β 1 dynamic changes between groups with or without HGF after irradiation.

Under normal conditions, liver, kidney and spleen produce low amounts of HGF. Following damage such as ischemia, toxic injury or tissue loss, HGF and its tyrosine kinase receptor c-Met increase during early stage after injury^[12]. HGF and c-Met, forming complex have been shown to interfere with apoptosis induced by ionizing radiation *in vitro*^[28,29]. We found TUNEL-positive signals were reduced compared to those in the radiation alone group by pre-radiation EGT-HGF. This finding indicated that HGF suppresses radiation-induced apoptosis. The apoptotic cells mostly gather around the microvascular structures from TUNEL assay. Recent evidence suggests that microvascular endothelial apoptosis represents the primary lesion in radiation damage^[30]. Endothelial injury of sinusoids and small hepatic veins is considered to be the initial event in genesis of veno-occlusive disease. Emerging data suggest that radiation acts directly on the plasma membrane of several cell types, activating acid sphingomyelinase, which generate ceramide by enzymatic hydrolysis of sphingomyelin. Ceramide, then, acts as a second messenger in initiating an apoptotic response via the mitochondrial system. Radiation-induced DNA damage can also initiate ceramide generation by activation of mitochondrial ceramide synthase and de novo synthesis of ceramide^[30]. HGF acts to stabilize the cell membrane in capillary endothelial cells and may play the most important role in the prevention of radiation induced apoptosis.

In addition to the direct anti-apoptosis effect of HGF during radiation, professionals need to incorporate a therapeutic strategy focused on the promotion of liver regeneration and the prevention of subsequent fibrosis after radiation damage^[5,31]. HGF is a well known hepatotropic factor for liver regeneration and has been reported to increase hepatic collagenase activity, which promotes

degradation of the extracellular matrix components^[5,31]. Another major benefit of HGF treatment after radiation is the reduction of TGF- β 1 mRNA levels. TGF- β 1 is a crucial factor in liver fibrosis and a potent growth inhibitor of hepatocytes. TGF- β 1 is synthesized in non-parenchymal cells such as stellate cells and inhibits hepatocellular DNA synthesis both in culture and *in vivo*^[32]. HGF and TGF- β 1 are key molecules which in general, exert opposite actions^[33]. Geraci *et al.*^[34] had reported the TGF- β 1 mRNA markedly expressed in non-parenchymal cells of rat liver early after radiation and the expression may last for more than 90 d. The present research demonstrated that irradiation rapidly induced TGF- β 1 mRNA expression and HGF gene transfer could antagonize the TGF- β 1 expression early after irradiation. A sustained release of HGF (about 3 wk) from single EGT may provide crucial antagonistic effect on a persistent TGF- β 1 expression after RT. In addition, fibronectin production from injured hepatic stellate cells was greatly reduced^[35].

The incidence of radiation induced liver damage would be expected to increase due to a renewed interest in hepatic irradiation because of the introduction of three dimensional radiation therapy treatment planning and bone marrow transplantation using total body irradiation. The mortality rate of veno-occlusive disease is high ranged from 20 to 50% and is dose-limiting for liver radiotherapy. The data from this study suggests that HGF gene transfer by electroporation may inhibit radiation-induced apoptosis and down-regulate the elevated TGF- β 1 levels after high dose irradiation for the prevention of veno-occlusive disease and liver fibrosis. Administration of HGF gene to normal liver tissue by electroporation during surgical procedure is clinically feasible, which may permit the safe delivery of high doses of radiation to an unresectable or residual hepatoma.

ACKNOWLEDGEMENTS

The work was supported by National Science Council grant NSC-91-275-9075-001 for the development of Boron Neutral Capture Therapy for hepatoma directed by Dr. Lui WY in Veterans General Hospital-Taipei.

REFERENCES

- 1 Dawson LA, Ten Haken RK, Lawrence TS. Partial irradiation of the liver. *Semin Radiat Oncol* 2001; **11**: 240-246
- 2 Chi KH, Wang HE, Chen FD, Chao Y, Liu RS, Chou SL, Wang YS, Yen SH. Preclinical evaluation of locoregional delivery of radiolabeled iododeoxyuridine and thymidylate synthase inhibitor in a hepatoma model. *J Nucl Med* 2001; **42**: 345-351
- 3 Lui WY, Liu RS, Chiang JH, Lo JG, Lai KH, King KL, Cheng HC, Wei YY, Chi CW, P'Eng FK. Report of a pilot study of intra-arterial injection of I-131 lipiodol for the treatment of hepatoma. *Zhonghua Yixue Zazhi (Taipei)* 1990; **46**: 125-133
- 4 Lin WY, Chi CW, Ho YJ, Wu IC, Chung YT, Chen SD, Chou FI, Kai JJ, Lui WY, Chen TJ, Lin Y. Boron-lipiodol: a potential new drug for the treatment of liver tumors. *Anticancer Res* 2002; **22**: 3989-3992
- 5 Michalopoulos GK, DeFrances MC. Liver regeneration. *Science* 1997; **276**: 60-66
- 6 Wang X, DeFrances MC, Dai Y, Pediaditakis P, Johnson C,

- Bell A, Michalopoulos GK, Zarnegar R. A mechanism of cell survival: sequestration of Fas by the HGF receptor Met. *Mol Cell* 2002; **9**: 411-421
- 7 **Derksen PW**, de Gorter DJ, Meijer HP, Bende RJ, van Dijk M, Lokhorst HM, Bloem AC, Spaargaren M, Pals ST. The hepatocyte growth factor/Met pathway controls proliferation and apoptosis in multiple myeloma. *Leukemia* 2003; **17**: 764-774
- 8 **Kopp JB**. Hepatocyte growth factor: mesenchymal signal for epithelial homeostasis. *Kidney Int* 1998; **54**: 1392-1393
- 9 **Xue F**, Takahara T, Yata Y, Kuwabara Y, Shinno E, Nonome K, Minemura M, Takahara S, Li X, Yamato E, Watanabe A. Hepatocyte growth factor gene therapy accelerates regeneration in cirrhotic mouse livers after hepatectomy. *Gut* 2003; **52**: 694-700
- 10 **Fujimoto J**, Kaneda Y. Reversing liver cirrhosis: impact of gene therapy for liver cirrhosis. *Gene Ther* 1999; **6**: 305-306
- 11 **Zarnegar R**, Michalopoulos GK. The many faces of hepatocyte growth factor: from hepatopoiesis to hematopoiesis. *J Cell Biol* 1995; **129**: 1177-1180
- 12 **Kawaida K**, Matsumoto K, Shimazu H, Nakamura T. Hepatocyte growth factor prevents acute renal failure and accelerates renal regeneration in mice. *Proc Natl Acad Sci USA* 1994; **91**: 4357-4361
- 13 **Vijayan A**, Martin DR, Sadow JL, Kissane J, Miller SB. Hepatocyte growth factor inhibits apoptosis after ischemic renal injury in rats. *Am J Kidney Dis* 2001; **38**: 274-278
- 14 **Ueki T**, Kaneda Y, Tsutsui H, Nakanishi K, Sawa Y, Morishita R, Matsumoto K, Nakamura T, Takahashi H, Okamoto E, Fujimoto J. Hepatocyte growth factor gene therapy of liver cirrhosis in rats. *Nat Med* 1999; **5**: 226-230
- 15 **Aihara H**, Miyazaki J. Gene transfer into muscle by electroporation *in vivo*. *Nat Biotechnol* 1998; **16**: 867-870
- 16 **Chi CH**, Wang YS, Lai YS, Chi KH. Anti-tumor effect of *in vivo* IL-2 and GM-CSF electrogene therapy in murine hepatoma model. *Anticancer Res* 2003; **23**: 315-321
- 17 **Chi KH**, Wang HE, Wang YS, Chou SL, Yu HM, Tseng YH, Hwang IM, Lui WY. Antisense thymidylate synthase electrogene transfer to increase uptake of radiolabeled iododeoxyuridine in a murine model. *J Nucl Med* 2004; **45**: 478-484
- 18 **Yamashita YI**, Shimada M, Hasegawa H, Minagawa R, Rikimaru T, Hamatsu T, Tanaka S, Shirabe K, Miyazaki JL, Sugimachi K. Electroporation-mediated interleukin-12 gene therapy for hepatocellular carcinoma in the mice model. *Cancer Res* 2001; **61**: 1005-1012
- 19 **Suzuki T**, Shin BC, Fujikura K, Matsuzaki T, Takata K. Direct gene transfer into rat liver cells by *in vivo* electroporation. *FEBS Lett* 1998; **425**: 436-440
- 20 **Xue F**, Takahara T, Yata Y, Minemura M, Morioka CY, Takahara S, Yamato E, Dono K, Watanabe A. Attenuated acute liver injury in mice by naked hepatocyte growth factor gene transfer into skeletal muscle with electroporation. *Gut* 2002; **50**: 558-562
- 21 **Gao C**, Jokerst R, Gondipalli P, Cai SR, Kennedy S, Ponder KP. Intramuscular injection of an adenoviral vector expressing hepatocyte growth factor facilitates hepatic transduction with a retroviral vector in mice. *Hum Gene Ther* 1999; **10**: 911-922
- 22 **Matsumoto Y**, Iwata H, Umeda Y, Takagi H, Mori Y, Kosugi A, Matsumoto K, Nakamura T, Hirose H. Hepatocyte growth factor gene transfer into the liver via the portal vein using electroporation attenuates rat liver cirrhosis. *Gene Ther* 2003; **10**: 1559-1566
- 23 **Lewin K**, Millis RR. Human radiation hepatitis. A morphologic study with emphasis on the late changes. *Arch Pathol* 1973; **96**: 21-26
- 24 **Reed GB**, Cox AJ. The human liver after radiation injury. A form of veno-occlusive disease. *Am J Pathol* 1966; **48**: 597-611
- 25 **Geraci JP**, Mariano MS, Jackson KL. Hepatic radiation injury in the rat. *Radiat Res* 1991; **125**: 65-72
- 26 **Hebard DW**, Jackson KL, Christensen GM. The chronological development of late radiation injury in the liver of the rat. *Radiat Res* 1980; **81**: 441-454
- 27 **Murase T**, Anscher MS, Petros WP, Peters WP, Jirtle RL. Changes in plasma transforming growth factor beta in response to high-dose chemotherapy for stage II breast cancer: possible implications for the prevention of hepatic veno-occlusive disease and pulmonary drug toxicity. *Bone Marrow Transplant* 1995; **15**: 173-178
- 28 **Fan S**, Ma YX, Wang JA, Yuan RQ, Meng Q, Cao Y, Laterra JJ, Goldberg ID, Rosen EM. The cytokine hepatocyte growth factor/scatter factor inhibits apoptosis and enhances DNA repair by a common mechanism involving signaling through phosphatidylinositol 3' kinase. *Oncogene* 2000; **19**: 2212-2223
- 29 **Fan S**, Wang JA, Yuan RQ, Rockwell S, Andres J, Zlatapolskiy A, Goldberg ID, Rosen EM. Scatter factor protects epithelial and carcinoma cells against apoptosis induced by DNA-damaging agents. *Oncogene* 1998; **17**: 131-141
- 30 **Maj JG**, Paris F, Haimovitz-Friedman A, Venkatraman E, Kolesnick R, Fuks Z. Microvascular function regulates intestinal crypt response to radiation. *Cancer Res* 2003; **63**: 4338-4341
- 31 **Bickel M**, Baringhaus KH, Gerl M, Gunzler V, Kanta J, Schmidts L, Stapf M, Tschank G, Weidmann K, Werner U. Selective inhibition of hepatic collagen accumulation in experimental liver fibrosis in rats by a new prolyl 4-hydroxylase inhibitor. *Hepatology* 1998; **28**: 404-411
- 32 **Bedossa P**, Paradis V. Transforming growth factor-beta (TGF-beta): a key-role in liver fibrogenesis. *J Hepatol* 1995; **22**: 37-42
- 33 **Yasuda H**, Imai E, Shiota A, Fujise N, Morinaga T, Higashio K. Antifibrogenic effect of a deletion variant of hepatocyte growth factor on liver fibrosis in rats. *Hepatology* 1996; **24**: 636-642
- 34 **Geraci JP**, Mariano MS. Radiation hepatology of the rat: parenchymal and nonparenchymal cell injury. *Radiat Res* 1993; **136**: 205-213
- 35 **Date M**, Matsuzaki K, Matsushita M, Tahashi Y, Furukawa F, Inoue K. Modulation of transforming growth factor beta function in hepatocytes and hepatic stellate cells in rat liver injury. *Gut* 2000; **46**: 719-724

• BASIC RESEARCH •

Protective effects of *Rheum tanguticum* polysaccharide against hydrogen peroxide-induced intestinal epithelial cell injury

Lin-Na Liu, Qi-Bing Mei, Li Liu, Feng Zhang, Zhen-Guo Liu, Zhi-Peng Wang, Ru-Tao Wang

Lin-Na Liu, Qi-Bing Mei, Li Liu, Feng Zhang, Zhen-Guo Liu, Zhi-Peng Wang, Ru-Tao Wang, Department of Pharmacology, Fourth Military Medical University, Xi'an 710032, Shaanxi Province, China
Supported by the National Natural Science Foundation of China, No. 30100239

Co-first-authors: Qi-Bing Mei

Co-correspondents: Lin-Na Liu

Correspondence to: Professor Qi-Bing Mei, Department of Pharmacology, Fourth Military Medical University, Xi'an 710032, Shaanxi Province, China. wjg@wjgnet.com

Telephone: +86-10-85381892 Fax: +86-10-85381893

Received: 2004-06-24 Accepted: 2004-07-15

Abstract

AIM: To describe the effect of *Rheum tanguticum* polysaccharide (RTP) on hydrogen peroxide-induced human intestinal epithelial cell injury.

METHODS: Hydrogen peroxide (100 $\mu\text{mol/L}$) was introduced to induce human intestinal epithelial cell injury. Cells were pretreated with RTP (30,100,300 $\mu\text{g/mL}$) for 24 h before exposure to hydrogen peroxide. Cell viability was detected by MTT assay and morphological observation. Acridine orange staining and flow cytometry were performed to assess cell apoptosis. Lactate dehydrogenase (LDH) activity, production of malondialdehyde (MDA) and superoxide dismutase (SOD) activity were measured by spectrophotometry with corresponding assay kits.

RESULTS: Following exposure to H_2O_2 , a marked decrease in cell survival and SOD activity, increased production of MDA, LDH leakage and cell apoptosis were found. Pretreatment of the cells with RTP could significantly elevate cell survival, SOD activity and decrease the level of MDA, LDH activity and cell apoptosis.

CONCLUSION: RTP may have cytoprotective and antioxidant effects against H_2O_2 -induced intestinal epithelial cell injury by inhibiting cell apoptosis and necrosis. This might be one of the possible mechanisms of RTP for the treatment of ulcerative colitis in rats.

against hydrogen peroxide-induced intestinal epithelial cell injury. *World J Gastroenterol* 2005; 11(10): 1503-1507
<http://www.wjgnet.com/1007-9327/11/1503.asp>

INTRODUCTION

Intestinal epithelium acts as a gateway that allows absorption of dietary nutrients and restricts uncontrolled entry of luminal antigens. This selective barrier function is critical for maintaining mucosal immune homeostasis, as evidenced in intestinal inflammation associated with loss of epithelial integrity^[1].

Epithelial apoptosis, in the gastrointestinal tract, is normally restricted to superficial cells, but in pathological states of inflammation or infection, apoptotic cell death can be far more expansive^[2]. Mucosal lesion in inflammatory bowel disease (IBD) is characterized by dense inflammatory cell infiltrate mainly comprised of neutrophils, macrophages and lymphocytes. Although many inflammatory mediators secreted by these cells, including cytokines IL-1, IL-6, IL-8, IL-10, TNF- α and leukotrienes together with luminal bacterial products such as bacterial lipopolysaccharide (LPS) and chemotactic peptide fMLP, have been implicated in the mucosal injury observed in IBD^[3], and the molecules that mediate tissue damage remain poorly understood^[4-7]. Recent indirect evidence has, however, implicated reactive oxygen and nitrogen species (RONS) such as nitric oxide (NO), superoxide (O_2^-), peroxynitrite (ONOO^-), hydrogen peroxide (H_2O_2), and hypochlorite (OCl^-) in the pathogenesis of mucosal lesion^[8-11].

Rheum tanguticum Maxim ex Balf is a well-known traditional Chinese medicine especially for the treatment of gastrointestinal diseases. Polysaccharide is one of its major active ingredients. Our previous studies have demonstrated that polysaccharide extracted from *Rheum tanguticum* (RTP) can prevent 2, 4, 6-trinitrophenyl sulphonic acid (TNBS) - induced ulcerative colitis in rats^[12]. The present study was mainly conducted to describe whether RTP had protective effects on intestinal epithelial cells against hydrogen peroxide-induced acute oxidant stress *in vitro*.

MATERIALS AND METHODS

Cell culture

HIEC cell line derived from normal human intestinal epithelium was used in our experiments. It was provided by Dr. Na Liu (Research Institute of Gastroenterology of Xijing Hospital, Xi'an, China). Cells were grown in media containing RPMI1640 (HyClone, South Logan, UT) with 10% heat-

inactivated fetal bovine serum (FCS, HyClone, South Logan, UT) and antibiotics (100 U/mL penicillin and 100 µg/mL streptomycin) and maintained at 37 °C in a humidified atmosphere containing 50 mL/L CO₂.

Effect of RTP on intestinal epithelial cell morphology

Following pre-treatment with or without RTP (30, 100, 300 µg/mL) for 24 h, HIEC cells were exposed to H₂O₂ (100 µmol/L) for another 2 h. Epithelial monolayers were then photographed with a Nikon camera under an inverted phase contrast microscope (Leica, Germany).

Effect of RTP on intestinal epithelial cell viability

HIEC cells (1×10³/well) were seeded onto 96-well plates. Cultures were then supplemented with or without RTP (30, 100, 300 µg/mL) and incubated for another 24 h before H₂O₂ (100 µmol/L) was added. Colorimetric MTT assay was performed to assess cell viability. Tetrazolium salt thiazolyl blue was added to a final concentration of 5 mg/mL and incubated for 4 h. Cells were washed and lysed with dimethyl sulfoxide (DMSO). Metabolization of MTT correlated directly with the cell number and was quantified by measuring the absorbance at 570 nm (reference wavelength 690 nm) using a microplate-reader. All experiments were performed in triplicate at least.

Determination of apoptotic cells by acridine orange staining

Acridine orange staining was used to confirm the absence or presence of apoptosis by morphological criteria. In brief, cells were inoculated onto the glass slides pre-coated with poly-L-lysine. At the end of experiment, cells from each group were fixed in 95% ethanol for 15 min, and then pre-treated with 1% acetic acid for 30 s before incubation with acridine orange (AO, 2×10⁻⁶ g/mL, Sigma, St. Louis, MO) for 1 min. Cells were visualized for nuclear fragmentation under a phase-contrast inverted microscope (Leica). Induction of apoptosis with H₂O₂ and reduction in extent of the apoptotic response to RTP were confirmed qualitatively.

Determination of cell apoptosis by flow cytometry

Cell apoptosis was examined by flow cytometry using an Annexin V-FITC Apoptosis Detection Kit (Middlefield Way, Mountain View, CA). Cells were treated in a similar manner as described above for the MTT assay, collected and incubated with Annexin V-FITC and propidium iodide (PI) for 5 min in darkness. The double-stained cells were then analyzed by flow cytometry to detect the percentage of apoptotic cells. The excited wavelength was 488 nm and the emission wavelength was 530 nm.

Measurement of lactate dehydrogenase (LDH) activity

Cells were pre-treated with or without RTP (30, 100, 300 µg/mL) for 24 h before exposed to H₂O₂ (100 µmol/L, 2 h). LDH, an indicator of cell injury, was detected by chromatometry with an assay kit (Nanjing Jiancheng Biochemical Reagent Co., Nanjing, China). Briefly, cell medium (50 µL) was gently aspirated and saved for LDH determination. After reaction, each sample was detected and the absorbance was read at wavelength 440 nm. LDH could catalyze the synthesis of pyruvic acid from

lactic acid and pyruvic acid then reacted to form 2,4-dinitrophenyl-hydrazine. The latter showed brownish red color in basic solution.

Measurement of malondialdehyde (MDA) content and superoxide dismutase (SOD) activity

Cells were pre-treated with or without RTP (30, 100, 300 µg/mL) for 24 h before being exposed to H₂O₂ (100 µmol/L, 2 h). The content of MDA, a compound produced during lipid peroxidation, was determined using the thiobarbituric acid method with a commercial kit. The absorbance of each supernatant was measured at 532 nm.

SOD, an important anti-oxidant enzyme that plays a pivotal role in preventing cellular damage caused by ROS, was measured by spectrophotometry using a commercially available detection kit (Nanjing Jiancheng Biochemical Reagent Co. Nanjing, China) according to the manufacturer's instructions.

RESULTS

RTP changed intestinal epithelial cell morphology

Following exposure to hydrogen peroxide, cell numbers decreased markedly; most cells demonstrated round shape and loss of adhesion. Pre-treatment with RTP could significantly alter morphological appearance of HIEC cells and showed cell protective effects (Figure 1).

Effect of RTP on intestinal epithelial cell viability

After exposure to H₂O₂, cell viability decreased significantly compared to normal group ($P<0.05$). Cell viability increased in a dose-dependent manner after being treated with RTP ($P<0.05$). The pre-treatment with RTP at 300 µg/mL could prevent over 80% of H₂O₂-induced cell death (Figure 2).

Morphological changes of cell apoptosis after different treatment

After exposure to H₂O₂ for 2 h, typically morphological characteristics of apoptotic cells were identified with chromatin aggregated in compacted masses, displaying strong green fluorescence in nuclei. Clusters of membrane-bound apoptotic bodies were also present. Cells in normal group showed normal size, shape and greenish structure of nuclei with different shades. When the cells were pre-treated with RTP, apoptosis could be partially inhibited (Figure 3).

Detection of cell apoptosis by flow cytometry

No Annexin V-positive cells were detected in normal group, while a large number of Annexin V-positive cells were detected in H₂O₂ group compared to RTP pre-treated groups. The apoptotic rate of cells in H₂O₂ group was 31.1%. In RTP pre-treated groups (100 and 300 µg/mL), the apoptotic rates were 24.4% and 21.5% respectively. When compared with H₂O₂ group, there was a significant difference ($P<0.05$) (Figure 4).

LDH activity after different treatment

LDH release into the media was used as an index of the integrity of cell membranes or necrosis in response to the oxidant burden.

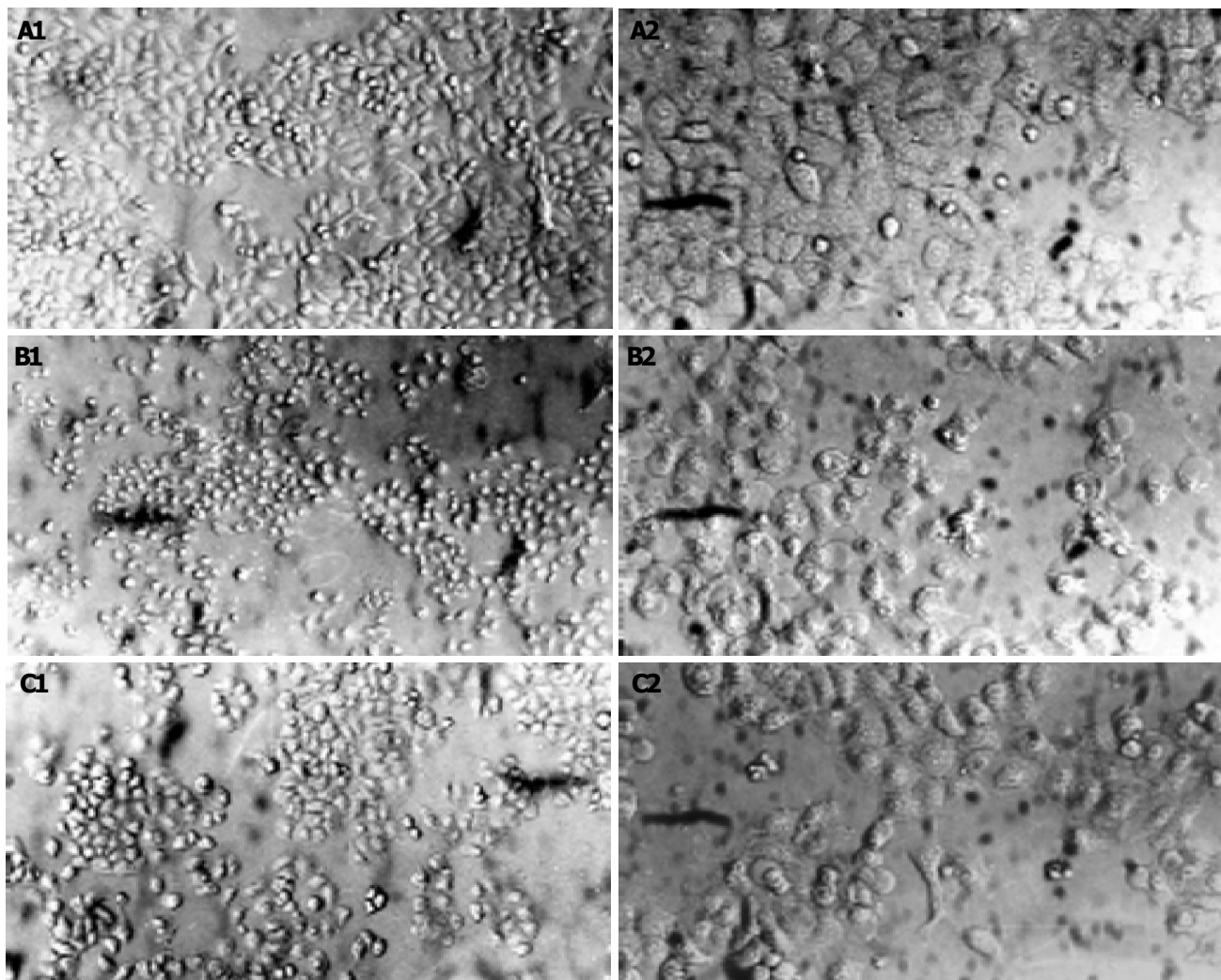


Figure 1 Effect of RTP on cell injury induced by H_2O_2 after different treatment. A: Normal; B: H_2O_2 ; C: H_2O_2 +RTP. 1: 100 \times ; 2: 200 \times .

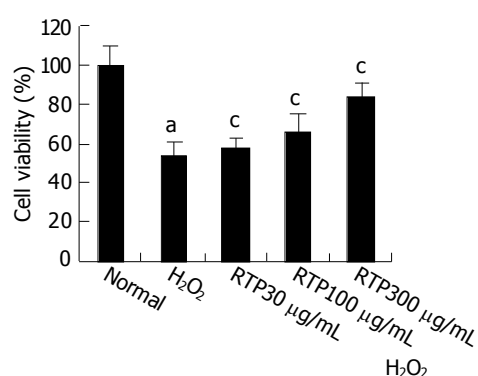


Figure 2 Effect of RTP on cell viability after different treatment. ^a $P < 0.05$ vs normal, ^c $P < 0.05$ vs H_2O_2 .

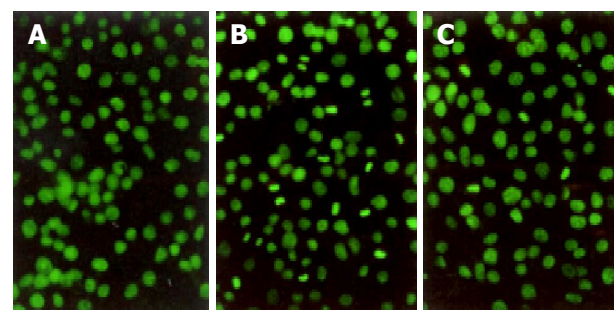


Figure 3 Morphological changes of cell apoptosis detected by acridine orange staining. A: Normal; B: H_2O_2 ; C: H_2O_2 +RTP.

As shown in Figure 5A, there was a marked increase of LDH leakage after addition of H_2O_2 to the culture media. This response was attenuated by RTP in a dose-dependent manner.

MDA content and SOD activity after different treatment

The toxicity caused by H_2O_2 was normally accompanied with the increase of lipid peroxides. As shown in Figure 5B, the intracellular MDA increased after the cultures were

exposed to 100 $\mu mol/L$ H_2O_2 . However, H_2O_2 -induced MDA production was markedly attenuated in a dose-dependent manner by RTP.

In addition, compared to the control cultures, the activity of SOD was decreased by 80% when the cells were exposed to H_2O_2 . Pre-treatment with RTP significantly attenuated the changes of SOD activity in a dose-dependent manner as well (Figure 5C).

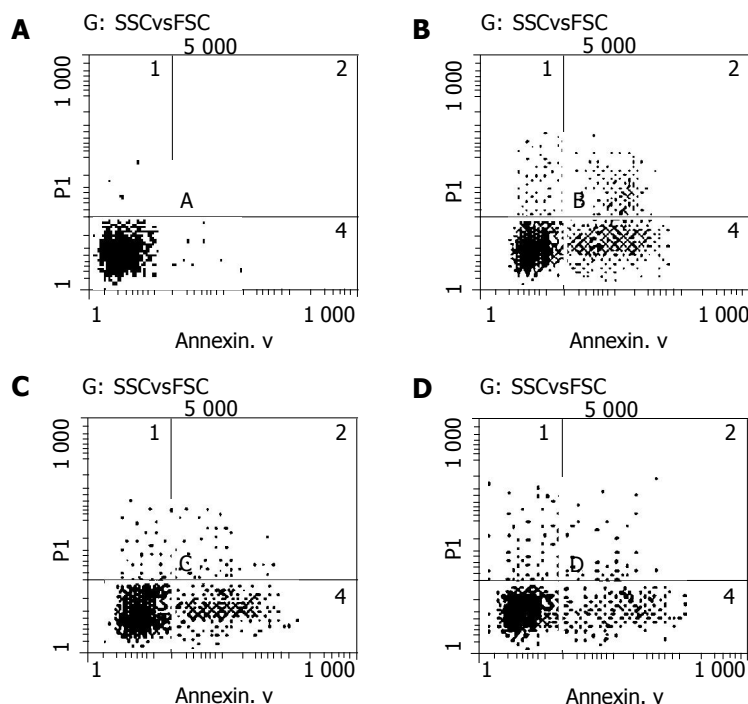


Figure 4 Effect of RTP on cell apoptosis after different treatment detected by flow cytometry. A: Normal; B: H_2O_2 ; C: H_2O_2 +RTP (100 $\mu g/mL$); D: H_2O_2 +RTP (300 $\mu g/mL$).

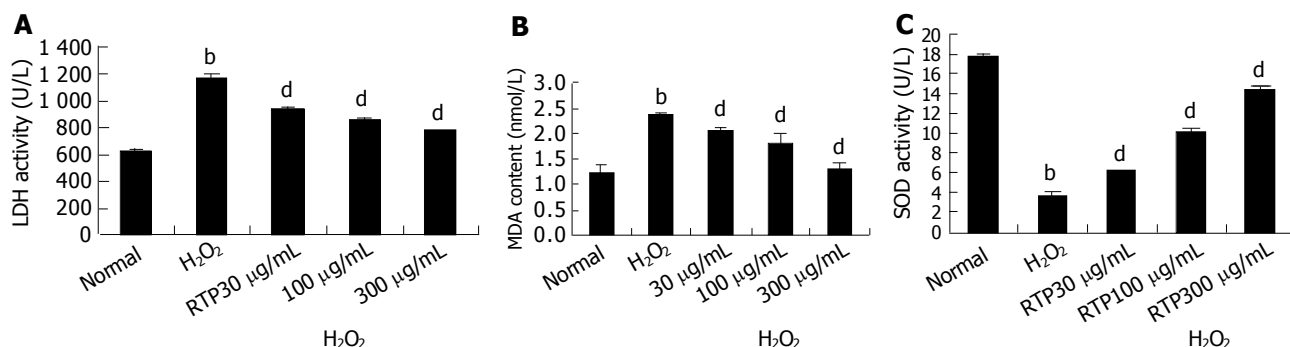


Figure 5 Effect of RTP on LDH activity (A), MDA content (B) and SOD activity (C) after different treatment ^b $P < 0.01$ vs normal, ^d $P < 0.01$ vs H_2O_2 .

DISCUSSION

Epithelial apoptosis is increased in inflammation or infection^[2]. Apoptotic cell death is accompanied with activation of various cell death pathways including caspases, ceramide, altered gene expression, mitochondrial dysfunction and consumption of ATP^[4,5].

Although these signals and metabolic events may be important in the regulation of cell death, cell death pathways are also associated with the secondary production of oxidants that appears to contribute to the magnitude of cell death. The intracellular redox level, in particular, has been shown to play a critical role^[13].

There is ample evidence that cell death is associated with increased intracellular levels of reactive oxygen species (ROS)^[14,15]. This increase in ROS may be due to overproduction of ROS from extracellular or intracellular processes, or there may be a decrease in endogenous antioxidant defense. Much work in recent years has been centered on such intracellular antioxidants as superoxide dismutase, GSH, and

catalase. Alterations in activities of these antioxidant systems have been implicated as causes of diseases as well as cell death^[16].

Evidence for the involvement of reactive oxygen metabolites is found in inflammatory bowel disease in man and in animal models of intestinal inflammation. Superoxide and hydrogen peroxide generated by activated leukocytes cause damage to the mucosa in intestinal inflammation^[15]. Reactive oxygen radicals are unavoidably formed in biochemical processes, and several enzymes are designed to inactivate those metabolites under physiological conditions including cytochrome oxidase, superoxide dismutase and catalase. It has been demonstrated that activated leukocytes form reactive oxygen metabolites and oxidative stress is one of the causes for tissue injury during inflammatory bowel diseases^[17].

Polysaccharide is one of the major active ingredients of *Rheum tanguticum*. Polysaccharide abstracted from *Rheum tanguticum* can stimulate the function of phagocytes, thus

protecting livers function and others^[12,18]. Here, polysaccharide with molecular weight 65-80 kDa, has strong anti-oxidant and protective effects against H₂O₂-induced cell injury in cultured HIEC cells.

Pre-treatment with RTP at 300 µg/mL could preserve over 90% of cell survival after H₂O₂ insult and decrease LDH leakage and cell apoptosis. The isolated polysaccharide also inhibits the production of MDA and the activity of SOD caused by exogenous H₂O₂. Thus, RTP may serve as a useful protective agent that mitigates the oxidative stress.

Free radical molecules can lead to damage or destruction of a variety of tissues. Excessive reactive oxygen species result in lipid peroxidation, oxidation of proteins and damage of DNA. Cells are often equipped with several antioxidants for the prevention of free radical damage. SOD and GSH-Px, along with other non-enzymatic antioxidants, such as ascorbate and GSH, serve as a detoxifying system to prevent cell damage caused by reactive oxygen species, and among these, antioxidant enzymes play a pivotal role. The combined action of GSH-Px and SOD provides a repair mechanism for oxidized membrane components. Exposure of cultured cells to free radicals results in an imbalance in energy metabolism in addition to the deleterious effects of hydroxyl and peroxy radicals on membrane lipids and proteins. Therefore, cellular function is impaired, which finally causes cell death^[19].

In conclusion, H₂O₂-induced decrease in cell survival is correlated with reduction in SOD activity, enhancement in cell apoptosis and MDA content. RTP may have protective effects against H₂O₂-induced intestinal epithelial cell injury. Further studies are needed to confirm the exact mechanism of these effects.

REFERENCES

- 1 **Hermiston ML**, Gordon JI. Inflammatory bowel disease and adenomas in mice expressing a dominant negative N-cadherin. *Science* 1995; **270**: 1203-1207
- 2 **Miller MJ**, Angeles FM, Reuter BK, Bobrowski P, Sandoval M. Dietary antioxidants protect gut epithelial cells from oxidant-induced apoptosis. *BMC Complement Altern Med* 2001; **1**: 11
- 3 **McKenzie SJ**, Baker MS, Buffinton GD, Doe WF. Evidence of oxidant - induced injury to epithelial cells during inflammatory bowel disease. *J Clin Invest* 1996; **98**: 136-141
- 4 **Babbs CF**. Oxygen radicals in ulcerative colitis. *Free Radic Biol Med* 1992; **13**: 169-181
- 5 **Williams JG**, Hughes LE, Hallett MB. Toxic oxygen metabolite production by circulating phagocytic cells in inflammatory bowel disease. *Gut* 1990; **31**: 187-193
- 6 **Mahida YR**, Wu KC, Jewell DP. Respiratory burst activity of intestinal macrophages in normal and inflammatory bowel disease. *Gut* 1989; **30**: 1362-1370
- 7 **Simmonds NJ**, Allen RE, Stevens TR, Van Someren RN, Blake DR, Rampton DS. Chemiluminescence assay of mucosal reactive oxygen metabolites in inflammatory bowel disease. *Gastroenterology* 1992; **103**: 186-196
- 8 **Grisham MB**,aginella TS, von Ritter C, Tamai H, Be RM, Granger DN. Effects of neutrophil-derived oxidants on intestinal permeability, electrolyte transport, and epithelial cell viability. *Inflammation* 1990; **14**: 531-542
- 9 **Middleton SJ**, Shorthouse M, Hunter JO. Increased nitric oxide synthesis in ulcerative colitis. *Lancet* 1993; **341**: 465-466
- 10 **Grisham MB**, Yamada T. Neutrophils, nitrogen oxides, and inflammatory bowel disease. *Ann N Y Acad Sci* 1992; **664**: 103-115
- 11 **Buster BL**, Weintrob AC, Townsend GC, Scheld WM. Potential role of nitric oxide in the pathophysiology of experimental bacterial meningitis in rats. *Infect Immun* 1995; **63**: 3835-3839
- 12 **Liu L**, Wang ZP, Xu CT, Pan BR, Mei QB, Long Y, Liu JY, Zhou SY. Effects of *Rheum tanguticum* polysaccharide on TNBS-induced colitis and CD4⁺T cells in rats. *World J Gastroenterol* 2003; **9**: 2284-2288
- 13 **Slikker W**, Desai VG, Duhart H, Feuers R, Imam SZ. Hypothermia enhances bcl-2 expression and protects against oxidative stress-induced cell death in Chinese hamster ovary cells. *Free Radic Biol Med* 2001; **31**: 405-411
- 14 **Gardner AM**, Xu FH, Fady C, Jacoby FJ, Duffey DC, Tu Y, Lichtenstein A. Apoptotic vs nonapoptotic cytotoxicity induced by hydrogen peroxide. *Free Radic Biol Med* 1997; **22**: 73-83
- 15 **Simonian NA**, Coyle JT. Oxidative stress in neurodegenerative diseases. *Annu Rev Pharmacol Toxicol* 1996; **36**: 83-106
- 16 **Simonian NA**, Coyle JT. Oxidative stress in neurodegenerative diseases. *Annu Rev Pharmacol Toxicol* 1996; **36**: 83-106
- 17 **Jobin C**, Sartor RB. The I kappa B/NF-kappa B system: a key determinant of mucosal inflammation and protection. *Am J Physiol Cell Physiol* 2000; **278**: C451-C462
- 18 **Buffinton GD**, Doe WF. Depleted mucosal antioxidant defences in inflammatory bowel disease. *Free Radic Biol Med* 1995; **19**: 911-918
- 19 **Gotz ME**, Kunig G, Riederer P, Youdim MB. Oxidative stress: free radical production in neural degeneration. *Pharmacol Ther* 1994; **63**: 37-122

Edited by Wang XL Language Editor Elsevier HK

• BASIC RESEARCH •

Activation of nuclear factor-kappa B and effects of pyrrolidine dithiocarbamate on TNBS-induced rat colitis

Ken Chen, You-Ming Long, Hui Wang, Lei Lan, Zhen-He Lin

Ken Chen, You-Ming Long, Department of Clinical Medicine, Guangdong College of Pharmacy, Guangzhou 510224, Guangdong Province, China

Hui Wang, Department of Pharmacology, Guangdong Medical College, Zhanjiang 524023, Guangdong Province, China

Lei Lan, Zhen-He Lin, Department of Digestion, the Affiliated Hospital of Guangdong Medical College, Zhanjiang 524023, Guangdong Province, China

Supported by a Grant From Health Department Foundation of Guangdong Province, No. A2003554

Correspondence to: Professor Ken Chen, Department of Clinical Medicine, Guangdong College of Pharmacy, Guangzhou 510224, Guangdong Province, China. chken@gdpc.edu.cn

Telephone: +86-20-34074077

Received: 2004-06-30 Accepted: 2004-07-11

Abstract

AIM: To explore the changes of nuclear factor-kappa B (NF- κ B) DNA-binding activity, the expression of intercellular adhesion molecule-1 (ICAM-1) regulated by NF- κ B at various times and to evaluate the effects of pyrrolidine dithiocarbamate (PDTC) on trinitrobenzene sulfonic acid (TNBS)-induced rat colitis.

METHODS: TNBS of 0.6 mL was mixed with ethanol of 0.3 mL solution and instilled into the lumen of the rat colon. The rat models were divided into 6 groups, which were killed at 24 h, 3, 7, 14, and 21 d after enema. Colonic inflammation and damage were assessed by macroscopical and histological criteria. Activity of NF- κ B DNA-binding was analyzed by electrophoresis mobility shift assays (EMSA). Expression of ICAM-1 was detected by *in situ* hybridization (ISH) and immunohistochemistry (IH). Then various doses of PDTC were injected into rat abdomen 30 min before enema with TNBS/ethanol as pretreatment. The rats were killed 4 h after enema and the colonic inflammation, myeloperoxidase (MPO) activity, malondialdehyde (MDA) level, and DNA-binding activity of NF- κ B were assessed. Finally, PDTC was injected intraperitoneally after colitis was induced. Changes of morphology were assayed.

RESULTS: During the first week, hyperemia, hemorrhage, edema and ulceration of the colonic mucosa appeared with predominant infiltration of leukocytes. Neutrophils, macrophages, lymphocytes infiltrated in mucosa and submucosa 14 d later. Fibroblasts and granuloma-like structures were also obviously seen. The binding activity of NF- κ B began to increase at 24 h time point and reached a peak at 14 d, then decreased but still was higher than control group at 21 d ($P < 0.01$). Levels of ICAM-1 mRNA

and protein significantly elevated at 24 h and the peak was at 21 d. Pretreatment with PDTC could attenuate the development of inflammation but not by reducing NF- κ B activity. This attenuation of inflammation had a positive relationship with the dose of PDTC. PDTC at the dose of 100 mg/kg had no therapeutic effect after colitis was induced.

CONCLUSION: NF- κ B activation is an important event that may be involved in acute and chronic inflammation development and may contribute to self-protection against early inflammation damage. NF- κ B also regulates ICAM-1 expression during colonic inflammation. Pretreatment of PDTC may attenuate the inflammation development. But PDTC has no therapeutic effect after the colitis is induced.

© 2005 The WJG Press and Elsevier Inc. All rights reserved.

Key words: Nuclear factor; Pyrrolidine dithiocarbamate; Rat; Colitis

Chen K, Long YM, Wang H, Lan L, Lin ZH. Activation of nuclear factor-kappa B and effects of pyrrolidine dithiocarbamate on TNBS-induced rat colitis. *World J Gastroenterol* 2005; 11(10): 1508-1514

<http://www.wjgnet.com/1007-9327/11/1508.asp>

INTRODUCTION

Nuclear factor-kappa B (NF- κ B), which regulates inflammatory and immune processes, is a ubiquitous transcription factor. It has been proved that many inflammatory diseases, such as rheumatoid arthritis, inflammatory bowel disease and systemic inflammatory response syndrome, have the sites at which NF- κ B is highly activated^[1]. Once activated, NF- κ B translocates to the nucleus from the cytosol, then binds to the consensus sequence on promoter or enhancer region of related gene and regulates gene transcription. It is known that several kinds of proinflammatory cytokine genes are regulated by it, such as IL-1, IL-3, IL-6, IL-8, TNF, and ICAM-1. Thus, the event of NF- κ B activation has been the critical position in the inflammatory cascade. In inflammatory bowel disease, a pathogenetically unclear disease, it has been proved that NF- κ B, including p50, c-Rel, and especially p65 is activated in macrophages at lamina propria. And *in vitro* the treatment of these cells with antisense p65 oligonucleotides reduced proinflammatory cytokine production^[2]. Another research showed the administration of antisense phosphorothioate oligonucleotides to p65

subunit of NF- κ B attenuated colitis in IL-10-deficient mice and in trinitrobenzene sulfonic acid-induced colitis model^[3].

Intercellular adhesion molecule-1 (ICAM-1) is a cytokine-inducible glycoprotein belonging to the immunoglobulin supergene family. It is constitutively expressed on a limited number of cell types including endothelial cells and it is induced on a wide variety of cells by inflammatory cytokines such as IL-1, TNF, IFN^[4]. There is a ligand by which the leukocyte integrins leukocyte function associated molecule-1 and Mac-1 and participates in leukocyte adhesion to activated endothelial cells, T cell/antigen presenting cell, T cell/T cell, and T cell/B cell interactions. So when inflammation happens, it can recruit leukocytes to local inflammatory region resulting in acceleration and development of disease. Van der Saag found that there was a specific ICAM-1 gene sequence (TGGAATTCC) bound to NF- κ B and its transcription was regulated by activated NF- κ B^[5].

Pyrrolidine dithiocarbamate (PDTC) represents a kind of antioxidants reported to be an effective NF- κ B inhibitor through its ability to traverse the cell membrane and its prolonged stability in solution at physiological pH. The report by Cuzzocrea showed that it could attenuate acute and chronic inflammatory development induced by activated NF- κ B^[6].

The aims of this study were two-fold. First, to establish a colonic inflammatory rat model similar to human Crohn's disease by the intraluminal instillation of a solution containing 2,4, 6-trinitrobenzenesulfonic acid/ethanol and explore the significance of DNA-binding activity changes of NF- κ B at various times in this model. Meanwhile, to study the expression of ICAM-1 regulated by NF- κ B in colonic tissue. Second, to evaluate the effects (including pretreatment and therapy effects) of pyrrolidine dithiocarbamate (PDTC) on acute and chronic colitis.

MATERIALS AND METHODS

Materials and animals

2,4,6-Trinitrobenzenesulfonic acid 5% was purchased from Sigma (USA). EMSA kit was from Promega (USA). Occult blood test reagents, myeloperoxidase (MPO) and malondialdehyde (MDA) reagent kits were provided by Nanjing Jiancheng Biological Research Unit (China). γ -³²PATP was purchased from Beijing Furui Company (China). *In situ* hybridization (ISH) kit, immunohistochemistry (IH) kit of ICAM-1 and anti-rabbit polyclonal antibody of ICAM-1 was from Wuhan Boshide Biological Company (China). Anti-rat monoclonal antibody of p65 was from Beijing Zhongshan Biological Company (China). All other chemicals were obtained from either Sigma or Beijing Dingguo Company. Male Sprague-Dawley (S-D) rats (170-200 g body wt) were from specific pathogen free unit in Animal Center of Guangdong Medical College.

Establishment of rat colitis model

All rats were maintained at 23 °C on a 12 h light/dark cycle and allowed free access to water and standard laboratory chow. From 12 h before the start of the experiments, the animals were deprived of food except access to water.

For NF- κ B activity study, rats were divided into six groups by randomized block design: (1) enema with 0.9 mL normal saline (NS group, $n = 6$, killed at 24 h), (2) enema with 0.6 mL TNBS+0.3 mL ethanol once (T/E group, $n = 30$, killed at 24 h, 3, 7, 14, 21 d independently). The macroscopic and microscopic damage score criteria were according to Butzner's and Wang's^[7,8].

For the PDTC pretreatment study, 48 rats were divided into six groups: (1) enema with normal saline (N group, $n = 8$), (2) enema with TNBS/ethanol and normal saline given as an intraperitoneal (i.p.) bolus 30 min before enema (M group, $n = 8$), (3) various doses of PDTC, respectively 10, 25, 50, 100 mg/kg, were injected into rat abdomen 30 min before enema (P10, P25, P50, P100 groups, $n = 32$). Rats were bled to death 4 h after enema. The microscopic damage score criteria were according to Millar's^[9].

For the PDTC therapy study, 30 rats were divided into three groups: (1) enema with normal saline and normal saline given i.p. every 48 h starting from d 1 (group A, $n = 10$), (2) enema with TNBS/ethanol and normal saline given i.p. starting from d 1 (group B, $n = 10$), (3) enema with TNBS/ethanol and PDTC given (100 mg/kg) i.p. starting from d 1 (group C, $n = 10$). Rats were killed on d 14. The morphology damage score was according to Butzner's^[7].

The colon was removed, freed from surrounding tissues, opened along the antimesenteric border, rinsed, and weighed. One part was processed for histology, immunohistochemistry and *in situ* hybridization. The other part was stored in liquid nitrogen for NF- κ B, MPO, and MDA detection.

Nuclear protein extractions

Nuclear protein was extracted as described by Gukovsky *et al.*^[10]. Briefly, colon tissue was pounded to pieces in liquid nitrogen, then homogenized in 312 μ L of cold buffer A (10 mmol/L HEPES-KOH, 1.5 mol/L MgCl₂, 10 mmol/L KCl, 1 mmol/L PMSF, 1 mmol/L DTT, 10 μ g/mL leupeptin, 35 μ g/mL aprotinin) for 10-20 times. The samples were separated by centrifugation (0 °C, 2 000 r/min, 15 s) and the supernatant was incubated in ice water for 5 min, and then spun by centrifugation (0 °C, 5 000 r/min, 10 s) again. The supernatant was discarded and 104 μ L buffer B (20 mmol/L HEPES-KOH, 25% glycerol, 420 mmol/L NaCl, 1.5 mmol/L MgCl₂, 1 mmol/L PMSF, 1 mmol/L DTT, 10 μ g/mL leupeptin, 35 μ g/mL pepstatin, 10 μ g/mL aprotinin) was added. The deposits were incubated in ice water for 20 min. Finally, the samples were separated by centrifugation (0 °C, 12 000 g, 15 min). Supernatant liquid was stored at -70 °C. Protein concentrations were determined by Bradford assay.

Electrophoretic mobility shift assays (EMSA) of NF- κ B

The activity of NF- κ B DNA-binding was detected by EMSA as described by Molloy with the following modification^[11]. The double-stranded oligonucleotide sequence of 5'-AGTTGAGGGGACTTTCCAGGC-3, 3'-TCAACTC-CCCTGAAAGGGTCCG-5', which corresponds to the κ B binding site, was end-labeled with [γ -³²P]ATP by T4 polynucleotide kinase (Promega). Labeled probes were purified and counts per minute (CPM) were detected with Whatman DE81 (>5 000 CPM). The nuclear extract

equivalent to 15 μ g was mixed with 5 \times binding buffer 2 μ L (room temperature, 10 min), then labeled probe (0.0175 pmol/L) was added and incubated (room temperature, 20 min). The mixture was then subjected to electrophoresis on 4% polyacrylamide gel at 150 V in 0.5 \times TBE buffer for 40 min at 4 $^{\circ}$ C. After being dried, the gel was exposed to imaging system of FX P screen (Bio-Rad, America) for 24 h. The result was analyzed with software Bandscan 4.0 (denary logarithm of total grey value). Specific competition was performed by addition of specific unlabeled double-stranded oligonucleotide to the reaction mixture in 50-100 fold excess, while nonspecific competition with AP2 oligonucleotide. Supershift assay was performed with the rabbit monoclonal antibody against p65 to verify p65 subunit.

ICAM-1 mRNA and protein detection

In situ hybridization (ISH) and immunohistochemistry (IH) were employed to detect ICAM-1 mRNA and protein, as described from reagent kit. Immunohistochemical score (IHS) was applied to evaluate ISH or IH described by Soslow^[12]. IHS was calculated by combining an estimate of the percentage of immunoreactive cells (quantity score) with an estimate of the staining intensity (staining intensity score), as follows. 0: no staining; 1: 1-10% of cells stained; 2: 11-50% of cells stained; 3: 51-80% of cells stained; 4: 81-100% of cells stained. Staining intensity was rated on a scale of 0-3, with 0 = negative; 1 = weak; 2 = moderate, and 3 = strong. When there was multifocal immunoreactivity and there are significant differences in staining intensities between foci, the average of the least intense and most intense staining was recorded. The raw data were converted to IHS by multiplying the quantity and staining intensity scores.

Detection of MPO, SOD and MDA of colon tissues

MPO, T-SOD and MDA were determined by the methods of the respective kits.

Statistical analysis

Parametric data were presented as mean \pm SD and statistical analyses were performed using the two-way ANOVA or *t*-test with the software package SPSS 8.0. Results were considered significant at a *P* value of less than 0.05.

RESULTS

Severity and morphology of TNBS/ethanol induced colitis

Intracolonic administration of TNBS/ethanol to S-D rats induced a severe illness characterised by bloody diarrhea and a dramatic loss of body weight during the first week. Then the body weight increased but diarrhea still persisted for about two weeks. Two rats died on d 5, 12. No changes could be observed in NS group. Macroscopic evaluation of the colon and rectum up to 24 h after TNBS treatment revealed the presence of mucosal edema and hemorrhagic ulcerations. Conglutination was obvious later. Histologic examination showed predominant infiltration of leukocytes and erythrocytes in mucosa and submucosa in the first week. Neutrophils, macrophages, lymphocytes infiltrated in mucosa, submucosa and muscularis propria 14 d later (Figures 1 A-D). Fibroblasts and granuloma-like structures were also obviously seen. No damage was seen in NS group. The macroscopic and microscopic damage score showed the peak at d 3, then decreased (scores in T/E group at various time points *vs* scores in NS group, *P*<0.01) (Figure 2).

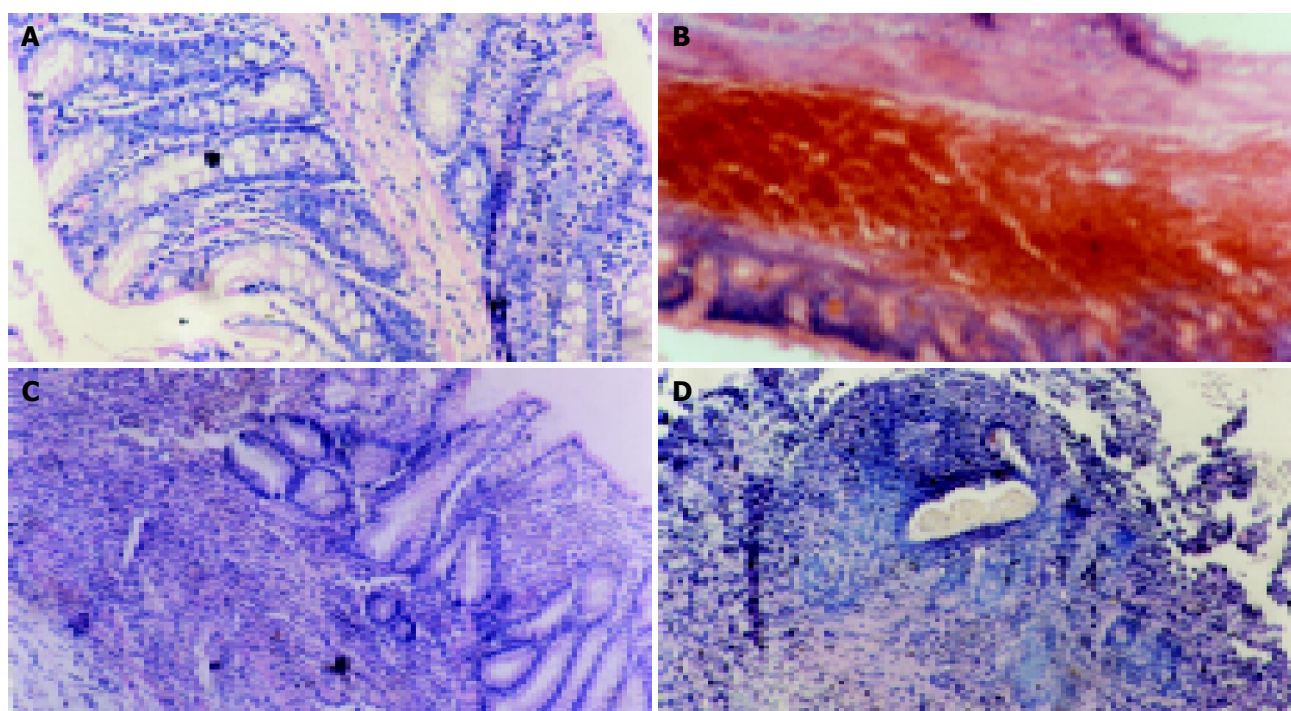


Figure 1 Changes of histological morphology in NS or T/E group. A: No damage in NS group, HE x200; B: Erosion, hemorrhage, edema, and ulceration at mucous and submucous layers at 24 h time point. HE x100; C: Ulcer at 14 d, HE x100; D: Granuloma-like structures and inflammatory cells in submucosa at 14 d, HE x100.

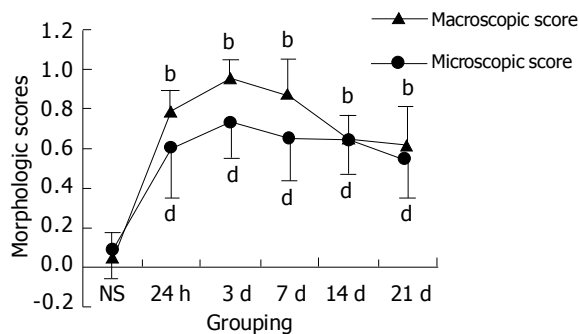


Figure 2 Changes of morphologic scores at various time points. ^b $P < 0.01$ vs macroscopic score in NS group. ^d $P < 0.01$ vs microscopic score in NS group.

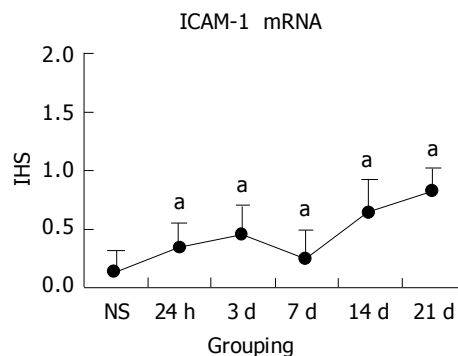


Figure 4 ICAM-1 mRNA expression of colonic tissue in various groups. ^a $P < 0.05$ vs ISH in NS group.

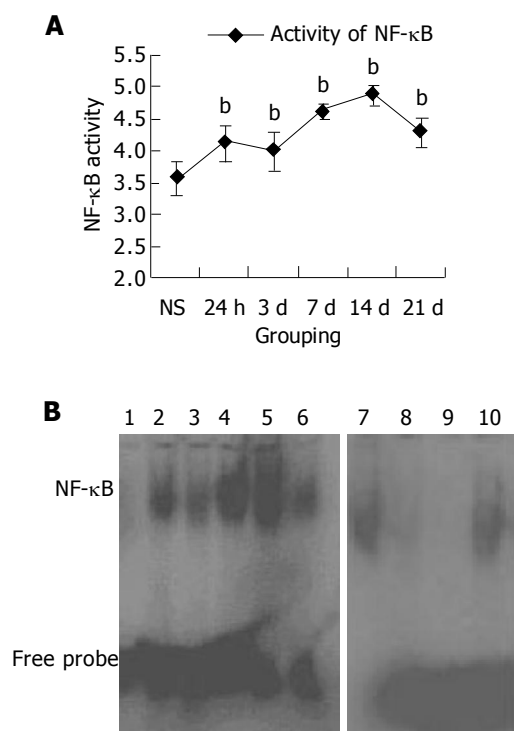


Figure 3 NF- κ B activity of colonic tissue in various groups. **A:** The binding activity of NF- κ B increased with inflammation progression. ^b $P < 0.01$ vs NF- κ B activity in NS group; **B:** The image of EMSA in various group and competition test. lanes 1-6: NF- κ B activity in NS, 21 h, 3 d, 7 d, 14 d, and 21 d groups. lane 7: with the labeled probe. lanes 8-9: specific competition experiment with 50, 100 fold excess of unlabeled probe. lane 10: nonspecific competition experiment with AP2 probe.

EMSA for NF- κ B

Nuclear extracts from normal or inflamed colon tissue at various time points were isolated and analyzed by EMSA. The EMSA analysis showed a strong activation of NF- κ B in rat inflamed colon tissue induced by TNBS/ethanol from 24 h to 21 d. It began to increase sharply at 24 h and the peak was on 14 d. The activity of NF- κ B was very weak in noninflamed colon tissue of NS group. To assess the specificity of the observed DNA-protein, specific and nonspecific competition were performed by addition of unlabeled double-stranded oligonucleotide or AP2 oligonucleotide to the reaction mixture in 50-100 fold excess

(Figure 3). Supershift analysis showed that pre-incubation with the antibodies against p65 was followed by a weakening and lagging of the NF- κ B-DNA complex band. Almost no effect could be seen with the nonspecific antiserum. This indicates that the majority of the dimers in inflammatory intestinal tissue contained a p65 subunit.

Expression of ICAM-1

NS group colon tissue had no or weak ICAM-1 mRNA detected by ISH in endothelial or epithelial cells. Similar to NF- κ B activity, ICAM-1 mRNA increased with inflammation progression in experimental groups. Following 24 h of TNBS/ethanol treatment, ISH showed that expression of ICAM-1 mRNA increased, predominantly associated with endothelial cells. And inflammatory cells also had weak expression in the lamina propria. From the IHS, the maximum of ICAM-1 expression was on 21 d, mainly in either epithelial cells or inflammatory cells from mucosa to submucosa layer. The correlation analysis between ICAM-1 mRNA score and NF- κ B activity indicated that they had significant positive correlation ($r = 0.913$, $P < 0.05$). Colonic ICAM-1 protein was elevated over control group in quantity and intensity after the treatment with TNBS/ethanol. Relatively high ICAM-1 expression occurred at 14 or 21 d, which was stronger in lamina propria than in submucosa (Figures 4 and 5).

Effects of PDTC pretreatment on TNBS/ethanol-induced acute colitis

All rats treated with TNBS/ethanol developed acute colitis characterized by the erosion, edema and bleeding at mucosa and submucosa layers 4 h after TNBS/ethanol administration. It induced a significant increase in the activity of MPO and the level of MDA in colonic tissue. The level of NF- κ B activity was also significantly up-regulated in colonic tissue. Pretreatment of rats with PDTC attenuated the inflammatory degree (histological score according to Millar's criteria^[9]) in a dose-related fashion. Similarly, pretreatment of rats with PDTC significantly reduced both activity of MPO and level of MDA in a dose-dependent fashion (Figures 6A-C, and 8). EMSA analysis of colonic tissue obtained 4 h after TNBS/ethanol administration showed that PDTC almost blocked NF- κ B activity at the dose of 10 mg/kg but not completely reduced histological score at

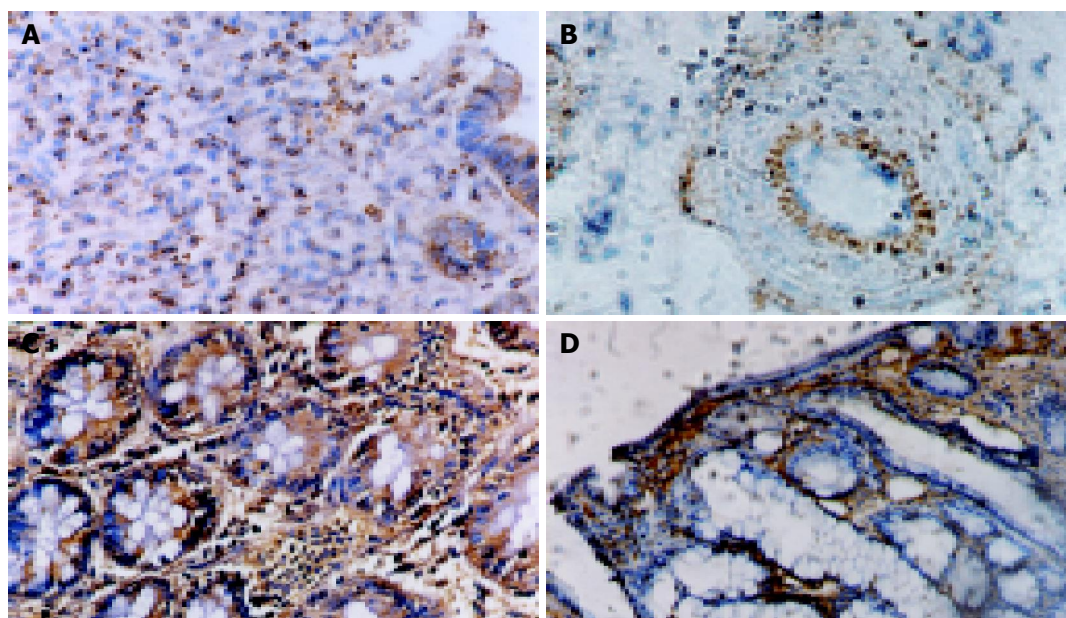


Figure 5 Expression of ICAM-1 mRNA and protein in colonic tissues. A: ICAM-1 mRNA expressed in inflammatory cells at submucosa, ISH x400; B: ICAM-1 mRNA expressed in arterial endothelial cells in submucosa, ISH x400; C: ICAM-1 expressed in epithelial cells in mucosa near inflammatory region, SABC x400; D: ICAM-1 expressed in lamina propria, SABC x200.

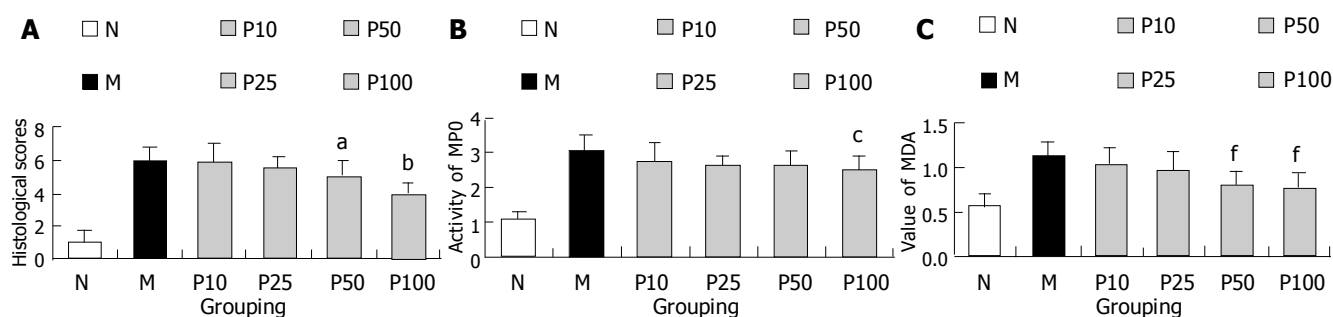


Figure 6 Changes of histological score, MPO activity, and MDA level in various group. A: Histological score. ^a $P < 0.05$ vs histological score in M group. ^b $P < 0.01$ vs histological score in M group; B: MPO activity. ^c $P < 0.05$ vs MPO activity in M group; C: MDA level. ^d $P < 0.01$ vs MDA level in M group.

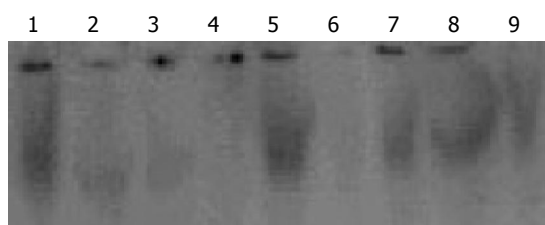


Figure 7 The image of EMSA in various groups and competition test. lanes 1-3: specific competition experiment. lanes 4-9: activity of NF- κ B DNA-Binding in N, M, P10, P25, P100 groups.

the same time. And the added dose of PDTC could attenuate colitis development, consequently MPO activity and MDA level decreased. Interestingly, the added dose of PDTC did not further weaken NF- κ B activity but its effect was stronger than that at 10 mg/kg dose (Figure 7).

Effects of PDTC therapy on TNBS/ethanol-induced colitis

All rats treated with TNBS/ethanol developed a chronic

colitis at 14 d as described above (Figure 1C, D). Both the clinical signs and morphological features of rats were observed in groups A-C. But in PDTC-treated (at the dose of 100 mg/kg) group, there was no significant change in morphology compared with B group (group A vs group B, $P > 0.05$). (Figure 9).

DISCUSSION

Animal colitis which is similar to human Crohn's disease can be induced experimentally in rats, mice, rabbits, pigs, and dogs by TNBS/ethanol introduced via the enema^[13-18]. Trinitrobenzene sulfonic acid is a haptenating agent that couples trinitrophenyl groups to endogenous (self) proteins more or less indiscriminately; the altered self-proteins stimulate a local immunologic response usually called a delayed hypersensitivity reaction. In the colon, this reaction leads to an inflammation marked by a transmural cellular infiltration with T cells and macrophages in a pattern like that described in interleukin-2 knockout mice and Crohn's disease^[19]. Here we induced the model by 5% 0.6 mL TNBS

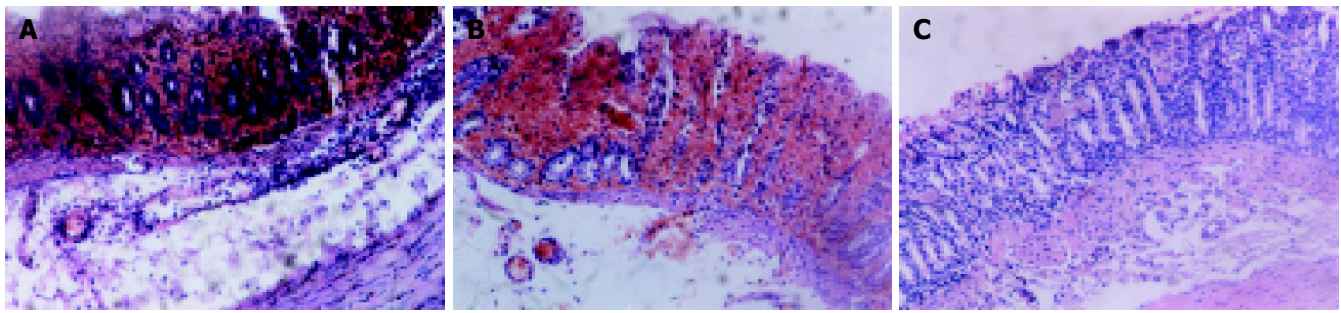


Figure 8 Changes of histological morphology in M, P10, P100 groups. A: The changes of histology in M group. HE x200; B: The changes of histology with PDTC 10 mg/kg. HE x200; C: The changes of histology with PDTC 100 mg/kg. HE x200.

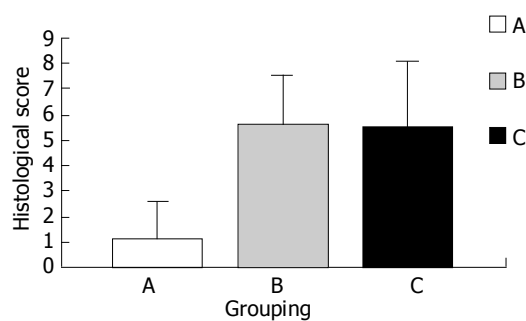


Figure 9 Changes of histological morphology in groups A, B, C. A: enema with normal saline and normal saline given i.p. every 48 h starting from d 1. B: enema with TNBS/ethanol and normal saline given i.p. starting from d 1. C: enema with TNBS/ethanol and PDTC given (100 mg/kg) i.p. starting from d 1.

and 0.3 mL ethanol, rats showed clinical symptoms including diarrhea, occult blood stool, and gross bleeding. Postmortem investigations of both acute and chronic colitis showed that inflammatory changes and multiple erosions appeared in whole colonic walls and were particularly prominent at submucosa layer. Hyperemia, hemorrhage, edema, and ulceration of the colonic mucosa were accompanied with predominant infiltration of leukocytes. Neutrophils, macrophages, lymphocytes infiltrated in mucosa and submucosa. Fibroblasts and granuloma-like structures were also obviously seen. This was consistent with the typical model induced by Morris^[20].

As a nuclear protein, NF- κ B is a eukaryotic transcription factor which was first described as a B-cell specific factor that binds to the motif in the immunoglobulin light-chain intronic enhancer. More and more evidence has confirmed that expression of many cytokines, chemokines, immunoreceptors, adhesion molecules, antiapoptotic/proapoptotic, and transcription factors were regulated by NF- κ B. Once activated, the nuclear localization signal of NF- κ B is uncovered and NF- κ B translocates to the nucleus of the cell from the cytosol to regulate above protein expression. Inflammatory bowel diseases are characterized by the recruitment of humoral and cellular components of the immune system to certain areas of the gut. Excessive cytokines are produced by activated epithelial cells, macrophages, and B and T cells. This process is characterized by NF- κ B induction. As a result, a perpetuation of the

inflammatory reaction was amplified^[21]. Constitutively activated NF- κ B was identified in epithelial cells and lamina propria macrophages from biopsy specimens or cultured cells of patients with inflammatory bowel disease. Further, p65 is the main member closely related to the inflammatory process^[22-25]. Recently it was shown that the administration of antisense phosphorothioate oligonucleotides to the p65 subunit of NF- κ B abrogates colitis in the trinitrobenzene sulfonic acid-induced colitis model^[3]. In our study, we found NF- κ B was activated in TNBS-induced rat early colitis and the binding activity of NF- κ B increased with inflammatory progress in experimental groups at various time points. This result is accorded with the viewpoint that NF- κ B is activated constitutively in IBD. But it did not have significant correlation with the morphology score. Furthermore, we injected PDTC at the dose of 10 mg/kg into rat abdomen 30 min before enema, which almost inhibited NF- κ B DNA-binding activity. As a result, it could not block colonic inflammation development. The reason is not clear. Maybe activation of NF- κ B contributes to self-protection against early inflammation damages^[26].

Leukocytes and endothelial adhesion molecules play a key role in mediating the recruitment of leukocytes to inflammatory site. As a member of immunoglobulin-like, ICAM-1 expresses on endothelial cells, fibroblasts and many other cell types. Evidence has proved that ICAM-1 was up-regulated in inflammatory colonic tissue induced by TNBS^[27-29]. We also found that ICAM-1 mRNA and protein expressions were increased in endothelial, epithelial cells, and inflammatory cells, such as neutrophilic, leukocyte monocytes, lympholeukocyte, with inflammatory progress in TNBS-induced groups. The scores of ICAM-1 mRNA had a significant correlation with NF- κ B activity ($r = 0.913$, $P < 0.05$) indicating its expression was regulated by NF- κ B. Similar to NF- κ B, ICAM-1 scores had no significant correlation with histological score, suggesting that ICAM-1 might be more effective on chronic colitis related to immunity than on nonspecific acute colitis. Further studies are needed.

PDTC attenuated the development of acute and chronic inflammation of pleurisy and arthritis in mice model, which had been reported by Cuzzocrea and his colleagues. The mechanism that PDTC protects against inflammatory injury is that it can inhibit the activation of NF- κ B^[6]. In our study, although we showed pretreatment of rats with PDTC attenuated the inflammatory degree including decrease of histological score, MPO activity, and MDA level in a dose-

dependent fashion, we did not observe its anti-inflammation effect by blocking NF- κ B of activity, because there was no significant effect on inflammation at the dose of 10 mg/kg, while it markedly reduced NF- κ B activity. So other mechanisms of PDTC must be considered. Satriano found that PDTC had the effect to interfere with reactive oxygen metabolism^[30]. When we detected the MPO activity and MDA level which indicate oxidative reaction indirectly, we also found PDTC reduced their level in a dose-related fashion. Furthermore, the chelation of divalent metal ions and influence on intracellular thiol levels also were considered^[6]. Interestingly, PDTC at the dose of 100 mg/kg had no therapeutic effect when we injected it into rat abdomen every 48 h after inducing the model. By different doses, different animal models, and different vehicles, our result did not accord with Cuzzocrea's. The reason for this is not clear.

In conclusion, NF- κ B activation is an important event that may be involved in acute and chronic inflammation development and contribute to self-protection against early inflammation damage. NF- κ B also regulates ICAM-1 expression during colonic inflammation and pretreatment of PDTC may attenuate the inflammatory development but has no therapeutic effect on induced colitis.

REFERENCES

- 1 Tak PP, Firestein GS. NF-kappaB: a key role in inflammatory diseases. *J Clin Invest* 2001; **107**: 7-11
- 2 Neurath MF, Fuss I, Schurmann G, Pettersson S, Arnold K, Muller-Lobeck H, Strober W, Herfarth C, Buschenfelde KH. Cytokine gene transcription by NF-kappa B family members in patients with inflammatory bowel disease. *Ann N Y Acad Sci* 1998; **859**: 149-159
- 3 Neurath MF, Pettersson S, Meyer zum Buschenfelde KH, Strober W. Local administration of antisense phosphorothioate oligonucleotides to the p65 subunit of NF-kappa B abrogates established experimental colitis in mice. *Nat Med* 1996; **2**: 998-1004
- 4 Jones SC, Banks RE, Haidar A, Gearing AJ, Hemingway IK, Ibbotson SH, Dixon MF, Axon AT. Adhesion molecules in inflammatory bowel disease. *Gut* 1995; **36**: 724-730
- 5 van der Saag PT, Caldenhoven E, van de Stolpe A. Molecular mechanisms of steroid action: a novel type of cross-talk between glucocorticoids and NF-kappa B transcription factors. *Eur Respir J Suppl* 1996; **22**: 146s-153s
- 6 Cuzzocrea S, Chatterjee PK, Mazzon E, Dugo L, Serrano I, Britti D, Mazzullo G, Caputi AP, Thiemermann C. Pyrrolidine dithiocarbamate attenuates the development of acute and chronic inflammation. *Br J Pharmacol* 2002; **135**: 496-510
- 7 Butzner JD, Parmar R, Bell CJ, Dalal V. Butyrate enema therapy stimulates mucosal repair in experimental colitis in the rat. *Gut* 1996; **38**: 568-573
- 8 Wang H, Ouyang Q, Hu RW. Establishment of rat colitis model by trinitrobenzenesulfonic acid. *Weichang Bingxue* 2001; **6**: 7-10
- 9 Millar AD, Rampton DS, Chander CL, Claxson AW, Blades S, Coumbe A, Panetta J, Morris CJ, Blake DR. Evaluating the antioxidant potential of new treatments for inflammatory bowel disease using a rat model of colitis. *Gut* 1996; **39**: 407-415
- 10 Gukovsky I, Gukovskaya AS, Blinman TA, Zaninovic V, Pandolfi SJ. Early NF-kappaB activation is associated with hormone-induced pancreatitis. *Am J Physiol* 1998; **275**: G1402-G1414
- 11 Molloy PL. Electrophoretic mobility shift assays. *Methods Mol Biol* 2000; **130**: 235-246
- 12 Soslow RA, Dannenberg AJ, Rush D, Woerner BM, Khan KN, Masferrer J, Koki AT. COX-2 is expressed in human pulmonary, colonic, and mammary tumors. *Cancer* 2000; **89**: 2637-2645
- 13 Hoffmann JC, Peters K, Henschke S, Herrmann B, Pfister K, Westermann J, Zeitz M. Role of T lymphocytes in rat 2,4,6-trinitrobenzene sulphonic acid (TNBS) induced colitis: increased mortality after gamma delta T cell depletion and no effect of alpha beta T cell depletion. *Gut* 2001; **48**: 489-495
- 14 Keates AC, Castagliuolo I, Cruickshank WW, Qiu B, Arseneau KO, Brazer W, Kelly CP. Interleukin 16 is up-regulated in Crohn's disease and participates in TNBS colitis in mice. *Gastroenterology* 2000; **119**: 972-982
- 15 Camoglio L, te Velde AA, de Boer A, ten Kate FJ, Kopf M, van Deventer SJ. Hapten-induced colitis associated with maintained Th1 and inflammatory responses in IFN-gamma receptor-deficient mice. *Eur J Immunol* 2000; **30**: 1486-1495
- 16 Linden DR, Chen JX, Gershon MD, Sharkey KA, Mawe GM. Serotonin availability is increased in mucosa of guinea pigs with TNBS-induced colitis. *Am J Physiol Gastrointest Liver Physiol* 2003; **285**: G207-G216
- 17 Depoortere I, Thijs T, Peeters TL. Generalized loss of inhibitory innervation reverses serotonergic inhibition into excitation in a rabbit model of TNBS-colitis. *Br J Pharmacol* 2002; **135**: 2011-2019
- 18 Shibata Y, Taruishi M, Ashida T. Experimental ileitis in dogs and colitis in rats with trinitrobenzene sulfonic acid-colonoscopy and histopathologic studies. *Gastroenterol Jpn* 1993; **28**: 518-527
- 19 Strober W, Ludviksson BR, Fuss IJ. The pathogenesis of mucosal inflammation in murine models of inflammatory bowel disease and Crohn disease. *Ann Intern Med* 1998; **128**: 848-856
- 20 Morris GP, Beck PL, Herridge MS, Depew WT, Szewczuk MR, Wallace JL. Hapten-induced model of chronic inflammation and ulceration in the rat colon. *Gastroenterology* 1989; **96**: 795-803
- 21 Schottelius AJ, Baldwin AS. A role for transcription factor NF-kappa B in intestinal inflammation. *Int J Colorectal Dis* 1999; **14**: 18-28
- 22 Rogler G, Brand K, Vogl D, Page S, Hofmeister R, Andus T, Knuechel R, Baeuerle PA, Scholmerich J, Gross V. Nuclear factor kappaB is activated in macrophages and epithelial cells of inflamed intestinal mucosa. *Gastroenterology* 1998; **115**: 357-369
- 23 Jobin C, Haskill S, Mayer L, Panja A, Sartor RB. Evidence for altered regulation of I kappa B alpha degradation in human colonic epithelial cells. *J Immunol* 1997; **158**: 226-234
- 24 Schreiber S, Nikolaus S, Hampe J. Activation of nuclear factor kappa B in inflammatory bowel disease. *Gut* 1998; **42**: 477-484
- 25 Cui HH, Chen CL, Wang JD, Yang YJ, Cun Y, Wu JB, Liu YH, Dan HL, Jian YT, Chen XQ. Effects of probiotic on intestinal mucosa of patients with ulcerative colitis. *World J Gastroenterol* 2004; **10**: 1521-1525
- 26 Steinle AU, Weidenbach H, Wagner M, Adler G, Schmid RM. NF-kappaB/Rel activation in cerulein pancreatitis. *Gastroenterology* 1999; **116**: 420-430
- 27 Maric I, Poljak L, Zoricic S, Bobinac D, Bosukonda D, Sampath KT, Vukicevic S. Bone morphogenetic protein-7 reduces the severity of colon tissue damage and accelerates the healing of inflammatory bowel disease in rats. *J Cell Physiol* 2003; **196**: 258-264
- 28 Cuzzocrea S, Mazzon E, Dugo L, Caputi AP, Riley DP, Salvemini D. Protective effects of M40403, a superoxide dismutase mimetic, in a rodent model of colitis. *Eur J Pharmacol* 2001; **432**: 79-89
- 29 Sun FF, Lai PS, Yue G, Yin K, Nagele RG, Tong DM, Krzesicki RF, Chin JE, Wong PY. Pattern of cytokine and adhesion molecule mRNA in hapten-induced relapsing colon inflammation in the rat. *Inflammation* 2001; **25**: 33-45
- 30 Satriano J, Schlondorff D. Activation and attenuation of transcription factor NF-kB in mouse glomerular mesangial cells in response to tumor necrosis factor-alpha, immunoglobulin G, and adenosine 3':5'-cyclic monophosphate. Evidence for involvement of reactive oxygen species. *J Clin Invest* 1994; **94**: 1629-1636

• BASIC RESEARCH •

Effects of drug serum of anti-fibrosis I herbal compound on calcium in hepatic stellate cell and its molecular mechanism

Yong-Hong Xiao, Dian-Wu Liu, Qing Li

Yong-Hong Xiao, Dian-Wu Liu, Qing Li, Department of Epidemiology, Hebei Medical University, Shijiazhuang 050017, Hebei Province, China

Supported by the National Science Foundation of Hebei Province, No. 302489

Correspondence to: Professor Dian-Wu Liu, Department of Epidemiology, Hebei Medical University, Shijiazhuang 050017, Hebei Province, China. liudianw@hebmu.edu.cn

Telephone: +86-311-6265531

Received: 2004-09-23 Accepted: 2004-11-19

Abstract

AIM: To investigate the effects of anti-fibrosis I herbal compound on intracellular Ca^{2+} in activated hepatic stellate cell (HSC) and to try to survey its molecular mechanism in treatment and prevention of hepatic fibrosis and portal hypertension.

METHODS: The activated HSC line was plated on small glass cover slips in 24 wells culture dishes at a density of 5×10^6 /mL, and incubated in RPMI-1640 media for 24 h. After the cells were loaded with Fluo-3/AM, intracellular Ca^{2+} was measured with laser scanning confocal microscopy (LSCM). The dynamic changes of intracellular Ca^{2+} , stimulated by carbon tetrachloride, TGF- β_1 antibody and the drug serum of anti-fibrosis I herbal compound and under orthogonal design were determined by LSCM. The effect of anti-fibrosis I herbal compound on intracellular Ca^{2+} was observed before and after the addition of TGF- β_1 antibody.

RESULTS: The intracellular Ca^{2+} were significantly different in different dosage of carbon tetrachloride anti-fibrosis I formula drug serum, TGF- β_1 antibody and different turn of these substance, but their interval time between CCl_4 and TGF- β_1 antibody, CCl_4 and anti-fibrosis I drug serum had no influence on intracellular Ca^{2+} . The result showed intracellular Ca^{2+} wasn't significantly different between rat serum without anti-fibrosis I and untreated group. After carbon tetrachloride stimulation, intracellular Ca^{2+} of activated HSC increased significantly when the dosage of CCl_4 from 5 to 15 mmol/L, however, decreased significantly after stimulation by 5-20 $\mu\text{g/mL}$ TGF- β_1 antibody or 5-20 mL/L drug serum. Moreover, before and after the addition of TGF- β_1 antibody, intracellular Ca^{2+} was significantly different. These results suggested that the molecular mechanism was independent of blocking TGF- β_1 effects.

CONCLUSION: Anti-fibrosis I herbal compound may treat

hepatic fibrosis and decrease portal hypertension by inhibiting activated HSC contractility through decrease of intracellular Ca^{2+} .

© 2005 The WJG Press and Elsevier Inc. All rights reserved.

Key words: Anti-fibrosis I herbal compound; Transforming growth factor- β_1 antibody; Calcium ion; Hepatic stellate cell; Laser scanning confocal microscopy

Xiao YH, Liu DW, Li Q. Effects of drug serum of anti-fibrosis I herbal compound on calcium in hepatic stellate cell and its molecular mechanism. *World J Gastroenterol* 2005; 11(10): 1515-1520

<http://www.wjgnet.com/1007-9327/11/1515.asp>

INTRODUCTION

Hepatic fibrosis, which may ultimately lead to cirrhosis, is the pathological base of all the chronic hepatic diseases and is characterized by the net accumulation of extracellular matrix (ECM), including collagen, glycoproteins, and proteoglycans^[1]. Lots of data have indicated that the activation of hepatic stellate cell (HSC) is the cytological base of the hepatic fibrosis. Activated HSC plays an important role in the regulation of intrahepatic resistance and microhemodynamics, because of its smooth muscle characteristics, in particular, its contractility^[2,3]. Contractility of HSCs is regulated by intracellular Ca^{2+} and certain vasoactive factors^[3]. Hence, activated HSCs have become a therapeutic target for chronic liver disease. The activation of HSCs is the effect of various cell factors by side secretion or self-secretion, of which, transforming growth factor- β_1 (TGF- β_1) is a key molecule responsible for tissue fibrosis and provides a basis for targeting TGF- β_1 as an anti-fibrotic agent^[4-6]. In the past years, marked progress in the understanding of the pathophysiology of hepatic fibrosis and portal hypertension has opened the door to pharmacological treatments, resulting in dramatic changes in the therapeutic approaches to hepatic fibrosis and portal hypertension. However, few effective drugs can slow the progression of the fibrosis. In the recent study, we have proved from animal experiment that anti-fibrosis I compound have the function of anti-hepatic fibrosis induced by carbon tetrachloride (CCl_4) in rats. This study was performed, using the serum pharmacological method, giving drugs to animals, separating serum with drug and putting them in cultured cells *in vitro*, then the change in intracellular calcium ($[\text{Ca}^{2+}]_i$) was observed with laser scanning confocal

microscope for further studying mechanism of Chinese medicine.

MATERIALS AND METHODS

Preparation of drug and drug serum

Anti-fibrosis I herbal compound included *Salvia miltiorrhiza*, *Sparganium stoloniferum*, *Angelica sinensis*, *Amyda sinensis*, *Curcuma aromatica*, *Carex phacota*. These were purchased from Shijiazhuang Lerentang Pharmacy, China. The herbs were boiled with water and extracted by alcohol: put 95% alcohol in liquid of anti-fibrosis herbs, mixed the alcohol and herbs, filtrate the protein and amylum, then heated the liquid at 90-95 °C to evaporate the remaining alcohol, took the solution of crude drug at 2.5 g/mL final density, which were infused from esophagus into stomach of Wistar rats from Animal Center of Hebei Medical University (Shijiazhuang, China), weighing about 300-400 g, once a day for 3 d, the dose was about 7 times to adult dose whose body weight was 65 kg. After infusion of the drug for 2 h in the last time, rats were given the drug again, 1 h later, blood was collected from inferior vena cava, centrifuged at 2000 r/min for 15 min to get serum, which was put at 56 °C for 30 min to get rid of other possible biological living substance, then removed bacteria by 0.22 µm millipore filtration membrane, sealed up and stored in the -20 °C for further use. Meanwhile, rat serum without anti-fibrosis I was prepared for the negative control.

Main reagents and instrument

Polyclonal rabbit antibody (Ab) to rat TGF-β₁ was bought from Santa Cruz Biotechnology, INC; RPMI-1640 culture medium was purchased from American Gibco Company; Fetal bovine serum was purchased from Sijiqing Biological Products Company (Hangzhou, China); Carbon tetrachloride (CCl₄) was purchased from Tianjin Reagent Factory; Fluo-3/AM(1-[2-Amino-5-(2,7-dichloro-6-hydroxy-3-oxo-9-xanthenyl) phenoxy]-2-(2-amino-5-methylphenoxy) ethane-N, N, N', N'-tetraacetic acid/acetoxymethyl ester), pluronic F-127 were purchased from American Biotium Company; 0.25 % trypsin digestive reagent, dimethylsulfoxide (DMSO), 2-[4-(2-Hydroxyethyl)-1-piperazinyl] ethanesulfonic acid (HEPES) were bought from American Sigma Company.

Main instrument: Laser scanning confocal microscopy (LSCM) (Leica DM IRBE); Bechtol (Suzhou Purify

Equipment Factory), HH CP-T Type CO₂ incubators (Shanghai Fuma Experiment Equipment Company Limited); Inverted Microscope (Chongqin optical instrument factory).

Buffer solution (mmol/L): NaCl 130, KCl 2.7, CaCl₂ 1.5, MgCl₂ 2, HEPES 10, glucose 10, pH 7.4 (NaOH).

Culture of HSCs

HSC strain-CFSC was created and donated by professor Greenwel, whose phenotype was activated HSCs. It was separated from rats with hepatocirrhosis induced by CCl₄, and was well-cultured to gain eternal life^[7]. HSCs frozen in liquid nitrogen were rapidly revived in a 37 °C water bath, then incubated in the RPMI-1640 media containing 10 mL/L fetal bovine serum, 100 U/mL penicillin, 100 U/mL streptomycin sulfate, and cultured at 37 °C, 5 mL/L carbon dioxide (CO₂) condition. Cells were digested by 2.5 g/L trypsin to subculture. Suspending Liquid of cells at a density of 5×10⁶ cells/mL was plated on small glass cover slips in 24 wells culture plate, cultured in a 37 °C, 5 mL/L CO₂ incubator. These cultured cells were used in the following experiments.

Handling HSCs with CCl₄^[8], rat serum without anti-fibrosis I, anti-fibrosis I herbal drug serum and TGF-β₁ antibody

HSCs were handled with CCl₄, rat serum, drug serum, TGF-β₁ antibody for 24 h, respectively, whose dosage CCl₄ was 0, 5, 10, 15 mmol/L, both rat serum and drug serum (volume fraction) were 0, 5, 10, 20 mL/L, TGF-β₁ antibody was 0, 5, 10, 20 µg/mL, 0 was the control group, and loaded with Fluo-3/AM. Then orthogonal trial of mixed level was designed using SPSS/11.5 software, factors-levels were shown in Table 1, the plans of trial in Table 2. After adding second

Table 1 Factor-level for orthogonal design

Level	Factor				
	CCl ₄ (mmol/L)	Durg serum (mL/L)	TGF-β ₁ Ab (µg/mL)	Time ¹ (h)	Turn
1	5	5	5	0.5	Adding CCl ₄ firstly
2	10	10	10	2.0	Adding durg serum /TGF-β ₁ A b firstly
3	15	20	20	4.0	

¹Time is the interval time between CCl₄ and TGF-β₁ antibody or CCl₄ and anti-fibrosis I drug serum.

Table 2 Plan of orthogonal trial and the result of Ca²⁺ assay (mean±SD)

Trial	CCl ₄ (mmol/L)	Drug serum (mL/L)	TGF-β ₁ A b (µg/mL)	Time (h)	Turn	Fluorescence intensity	
						TGF-β ₁ Ab	Drug serum
1	5	5	5	0.5	1	81.03±7.36	78.25±6.84
2	15	20	20	0.5	1	126.52±13.54	109.38±15.63
3	5	10	10	2.0	1	75.84±6.81	72.54±9.52
4	10	20	20	2.0	1	106.46±10.23	88.65±10.38
5	10	5	5	4.0	1	117.65±9.26	102.13±12.45
6	15	10	10	4.0	1	138.24±12.57	113.36±11.82
7	10	10	10	0.5	2	94.53±8.67	84.47±8.23
8	15	10	10	0.5	2	128.67±11.56	96.48±9.65
9	15	5	5	2.0	2	138.21±14.83	118.65±12.34
10	5	20	20	2.0	2	62.17±6.58	50.16±6.48
11	10	5	5	4.0	2	114.28±8.37	92.54±8.75
12	5	20	20	4.0	2	64.23±5.26	46.23±3.64

factor for 24 h, HSCs were loaded with Fluo-3/AM. Using the method of range analysis for orthogonal trial, the best level of every factor was chosen. Firstly HSCs was treated with CCl_4 for certain time, before and after addition of TGF- β_1 antibody for certain time, rat serum or drug serum was added into the cells, 24 h later and HSCs were loaded with Fluo-3/AM.

Measurement of intracellular Ca^{2+}

The cells were loaded with 10 $\mu\text{mol/L}$ Fluo-3/AM for 30 min at 37 °C under a mixed gas containing 95 mL/L air and 5 mL/L CO_2 , washed 2-3 times with buffer solution, then put in 1 mL buffer solution micro-incubation perfusion chamber. One or two cell and their layers were chosen to observe with LSCM. Excitation wave of Fluo-3 was 488 nm and emission wave 525 nm. Fluorescence intensity of $[\text{Ca}^{2+}]_i$ in eight cells chosen randomly was observed using TCS SP2 with LSCM to calculate the average fluorescence intensity of the whole cell. The dynamic changes of $[\text{Ca}^{2+}]_i$ in individual HSC after stimulation with either CCl_4 , anti-fibrosis I drug serum, or TGF- β_1 antibody were recorded using LSCM and a computer. The concentration of HSC $[\text{Ca}^{2+}]_i$ was measured in terms of intracellular fluorescent intensity. This study recorded the relative value of fluorescence intensity for the change of $[\text{Ca}^{2+}]_i$. The larger the fluorescence intensity, the higher the $[\text{Ca}^{2+}]_i$ concentration.

Statistical analysis

All data were expressed as mean \pm SD and analyzed with

SPSS/11.5 statistic software. The mean difference was calculated using the analysis of variance (ANOVA) for orthogonal design, one-way ANOVA and Student-Newman-Keuls test for multiple comparison. The level of significance of hypothesis testing was $P<0.05$.

RESULTS

Effects of CCl_4 , rat serum without anti-fibrosis I, anti-fibrosis I drug serum and TGF- β_1 antibody on $[\text{Ca}^{2+}]_i$ in HSCs, respectively

In the 5 min during observation, there is no obvious change of fluorescence intensity of HSCs, which in untreated group was 69.05 ± 3.16 . In rat serum group, $[\text{Ca}^{2+}]_i$ was not significantly different when the dosage of rat serum was 0, 5, 10, 20 mL/L. While, CCl_4 sharply increased the $[\text{Ca}^{2+}]_i$ when the dosage of CCl_4 from 5 to 15 mmol/L. CCl_4 could make $[\text{Ca}^{2+}]_i$ of HSCs overload, fluorescence intensity increase, what is more, the higher the CCl_4 dosage, the stronger the fluorescence intensity, the higher the $[\text{Ca}^{2+}]_i$ concentration ($F = 760.602$, $P<0.05$) (Figure 1A); After treating HSCs with 5-20 mL/L drug serum, the $[\text{Ca}^{2+}]_i$ dropped ($F = 554.962$, $P<0.05$); with 5-20 $\mu\text{g/mL}$ TGF- β_1 antibody, the $[\text{Ca}^{2+}]_i$ did too ($F = 39.393$, $P<0.05$). The higher drug serum or TGF- β_1 antibody dosage, the less $[\text{Ca}^{2+}]_i$ concentration (Figure 1B,C). The change of fluorescence intensity of HSCs was shown (Figure 2 A-C). Compared with the untreated group, fluorescence intensity of HSCs treated with 10 mmol/L CCl_4 was obviously strong, of which HSCs treated with drug serum of anti-fibrosis I herbal compound was weak.

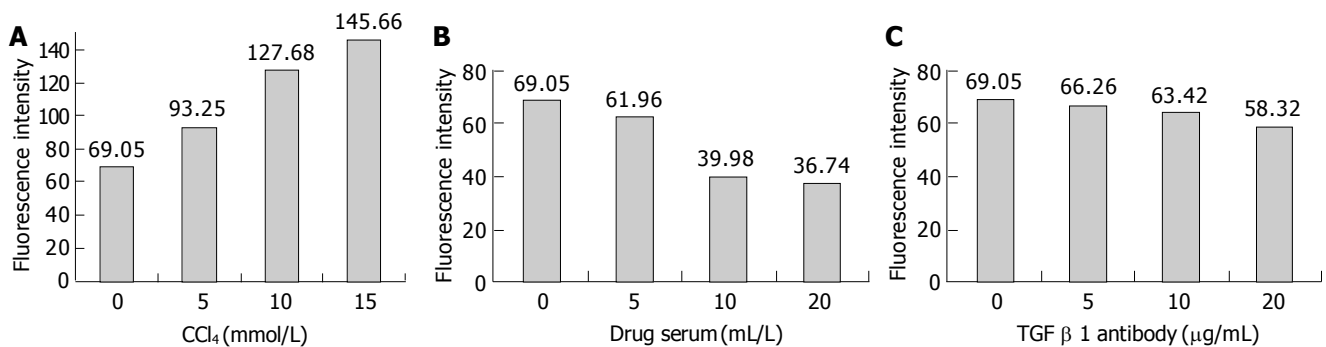


Figure 1 Effect of different dosage of every factor on intracellular Ca^{2+} in HSC. A: Effect of different dosage CCl_4 on intracellular Ca^{2+} in HSC; B: Effect of different dosage drug serum of anti-fibrosis I herbal compound on intracellular Ca^{2+} in HSC; C: Effect of different dosage TGF- β_1 antibody on intracellular Ca^{2+} in HSC.

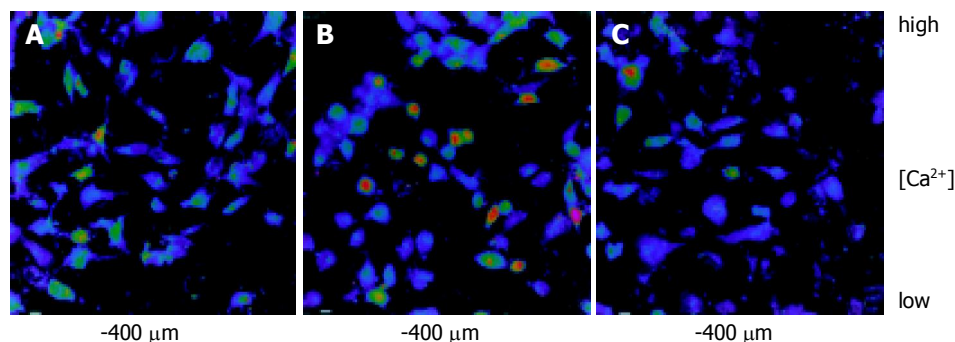


Figure 2 Intracellular Ca^{2+} fluorescent intensity of HSCs in each group. A: Intracellular Ca^{2+} fluorescent intensity of HSCs in untreated group; B: Intracellular Ca^{2+} fluorescent intensity of HSCs in 10 mmol/L CCl_4 group; C: Intracellular Ca^{2+} fluorescent intensity of HSCs in 10 mL/L drug serum group.

Table 3 Results of analysis of variance for orthogonal design

Sources of variation	Sum of squares of deviation from mean	Degree of freedom	Variance	F	P
Variance analysis of TGF- β_1 Ab					
CCl ₄	6 933.936	2	3 466.968	392.639	0.000
TGF- β_1 Ab	378.054	2	189.027	21.408	0.007
Time	67.786	2	33.893	3.838	0.117
Turn	158.777	1	158.777	17.982	0.013
Error	35.320	4	8.830		
Variance analysis of drug serum					
CCl ₄	3 969.848	2	1 984.924	139.437	0.000
Drug serum	656.001	2	328.000	23.041	0.006
Time	55.274	2	27.637	1.941	0.257
Turn	478.551	1	478.551	33.617	0.004
Error	56.941	4	14.235		

Table 4 Range analysis for orthogonal trial

Level	Drug serum				TGF- β_1 Ab			
	CCl ₄	Drug serum	Time	Turn	CCl ₄	TGF- β_1 Ab	Time	Turn
1	61.80	97.89	92.15	94.05	70.82	112.79	107.69	107.62
2	91.95	91.71	82.50	81.42	108.23	109.32	95.67	100.35
3	109.47	73.61	88.57		132.91	89.85	108.60	
R	47.67	24.28	9.65	12.63	37.41	19.47	12.93	7.27

The result of orthogonal trial

The results were shown in Tables 2, 3. From Tables 2, 3, the concentration of $[Ca^{2+}]_i$ were significantly different in different dosage of CCl₄, anti-fibrosis I drug serum, TGF- β_1 antibody and different turn of these substances, but there is no significance in their interval time between CCl₄ and TGF- β_1 antibody, CCl₄ and anti-fibrosis I drug serum. The results of orthogonal design showed that the most important matter that affected $[Ca^{2+}]_i$ was CCl₄, the second important were anti-fibrosis I drug serum and TGF- β_1 antibody (Table 4).

Effects of different treatment on $[Ca^{2+}]_i$

According to results of Orthogonal trial, the method of range analysis was used to find the best level of each factor, which was 15 mmol/L CCl₄, 20 mL/L drug serum, 20 μ g/mL TGF- β_1 antibody. Firstly HSCs were treated with 15 mmol/L CCl₄ for 0.5 h, before and after addition of TGF- β_1 antibody for 2 h, drug serum was added into HSCs, 24 h later, the change of $[Ca^{2+}]_i$ was observed. The results were shown in Table 5. Group 1: HSCs were treated with 15 mmol/L CCl₄ for 0.5 h, added 20 mL/L drug serum; Group 2: HSCs were treated with 15 mmol/L CCl₄ for 0.5 h, added 20 μ g/mL TGF- β_1 antibody; Group 3: HSCs were treated with 15 mmol/L CCl₄ for 0.5 h, after addition of 20 mL/L drug serum for 2 h, add 20 μ g/mL TGF- β_1 antibody; Group 4: HSCs were treated with 15 mmol/L CCl₄ for 0.5 h, after addition of 20 μ g/mL TGF- β_1 antibody for 2 h, add 20 mL/L drug serum. The results of one-way ANOVA showed $[Ca^{2+}]_i$ in HSC treated with drug serum, before and after the addition of TGF- β_1 antibody, were significantly different and also significantly different for multiple comparison.

Table 5 Change of intracellular Ca^{2+} in hepatic stellate cell treated with different methods (mean \pm SD)

Group	Methods of treatment	Fluorescence intensity
1	CCl ₄ +HSC+drug serum	109.38 \pm 15.63
2	CCl ₄ +HSC+TGF- β_1 Ab	126.52 \pm 13.54
3	CCl ₄ +HSC+ drug serum +TGF- β_1 Ab	103.40 \pm 9.87
4	CCl ₄ +HSC+TGF- β_1 Ab+ drug serum	93.77 \pm 6.33

DISCUSSION

For many years, it has been accepted that HSCs play an important role in hepatic fibrosis of chronic liver disease. Many recent studies have made clear that, in chronic liver disease, HSCs also play an important role in the regulation of intrahepatic vascular resistance and blood flow at the sinusoidal level. Accumulating evidence from *in vitro* and *in vivo* studies point to the importance both of the anatomical location of HSCs and of their capacity to contract or relax like smooth muscle cells in response to various vasoactive mediators, including endothelin-1 and nitric oxide^[9-11]. It is the key to the progress of chronic liver disease, hepatic fibrosis and the elevation of intrahepatic vascular resistance. In this process what is called "activation", HSCs get the character of myofibroblast, proliferate and synthesize ECM, however, TGF- β_1 is the strongest factor to facilitate the activation of HSCs. TGF- β_1 activates the static HSCs and turns them into the phenotype of myofibroblast to express α -smooth muscle actin (α -SMA) and possess the character of contraction, so as to enhance the blood resistance in liver sinuses and cause the elevation of portal vein pressure. Therefore, the activation of HSCs is the center tache in the formation of hepatocirrhosis and portal hypertension. In the course of HSCs activation, $[Ca^{2+}]_i$ channels open widely and increase the concentration of $[Ca^{2+}]_i$ which induces obvious contraction of cell. The increase of $[Ca^{2+}]_i$ concentration in HSCs has the direct connection with the contraction of HSCs^[12]. Activated HSCs secrete TGF- β_1 and other many kinds of cell factors by self- secretion. TGF- β_1 stimulates HSCs to synthesize and secrete ECM, which forms the abnormal accumulation to facilitate the activation of HSC, and contributes to the maintenance and aggravation of the hepatic fibrosis.

In this study, the technology of Flou-3/AM fluorescence probe and LSCM were used to observe the influences of anti-fibrosis I on $[Ca^{2+}]_i$ concentration in HSCs. Flou-3 is a kind of sensitive $[Ca^{2+}]_i$ indicator. It can combine with $[Ca^{2+}]_i$ specifically and generate the fluorescence after certain wavelength excitation light, fluorescence spectrum changes after combination with $[Ca^{2+}]_i$, and there is a positive relation between the fluorescence intensity and the concentration of intracellular free $[Ca^{2+}]_i$. Flou-3 is an acid compound and it is difficult to enter cells, but it can enter cells through the cell membrane when Flou-3 is cultivated with cells after that Flou-3 combines with lipophylic AM to become fat-soluble Flou-3/AM, and it can turn back to Flou-3 under the effects of intracellular lipase, Flou-3 combines with intracellular free $[Ca^{2+}]_i$ again.

Our results showed that CCl₄ stimulation significantly increased $[Ca^{2+}]_i$. By contrast, $[Ca^{2+}]_i$ significantly decreased

after anti-fibrosis I drug serum or the TGF- β_1 antibody stimulation. $[Ca^{2+}]_i$ was not significantly different between rat serum without anti-fibrosis I and untreated group. This showed rat serum itself did not affect the activation of HSC. Results of the analysis of variance for orthogonal design indicated that the different concentrations of CC14, anti-fibrosis I drug serum and the TGF- β_1 antibody had great effects to the change of $[Ca^{2+}]_i$ concentration in HSCs. CC14 increased the $[Ca^{2+}]_i$ concentration to cause the cells injury. Activated HSCs secreted many kinds of cell factors. Inactive TGF- β_1 of self-secretion was activated by the enzymes and cell factors in the circumstance of inflammation, afterward, stimulated HSCs to produce TGF- β_1 , in turn to make the magnified effects gradually and lead to the overproduction and activation of TGF- β_1 , which made HSCs contract continuously. TGF- β_1 antibody and drug serum could decrease the $[Ca^{2+}]_i$ elevation caused by CC14. This showed that they could restrain the HSCs injury caused by CC14. If HSCs were pretreated with TGF- β_1 antibody and drug serum, $[Ca^{2+}]_i$ decreased obviously. Therefore, it was considered that TGF- β_1 and drug serum could restrain the contraction of HSCs and reduce the resistance of liver sinuses by decreasing $[Ca^{2+}]_i$. It indicated that TGF- β_1 antibody and drug serum had some effects to the treatment and prevention of hepatic fibrosis and portal vein hypertension.

Since TGF- β_1 is an important factor in hepatic fibrosis, we attempted to treat hepatic fibrosis through restraining the excessive expression or abnormal modulation of TGF- β_1 . In order to explore the mechanism of anti-fibrosis I to prevent and treat hepatic fibrosis and portal vein hypertension from cell factors level, in this study, TGF- β_1 antibody was used to block the action of TGF- β_1 , interrupt the effects of some media or factors on TGF- β_1 primary synthesis, decrease the effect of stimulation on ECM synthesis. TGF- β_1 can facilitate activated HSC to turn into myofibroblast by self-secretion and side secretion. Activated HSCs and myofibroblasts are the major producers of ECM in liver injury, and play a prominent role in liver fibrosis. TGF- β_1 can promote the progression of hepatic fibrosis with tumor necrosis factor- α (TNF- α), insulin like growth factor-1 (IGF-1), platelet derived growth factor (PDGF) *etc.* Anyhow, TGF- β_1 can induce and facilitate hepatic fibrosis through many kinds of approaches and is considered to be a strong cell factor of fibrosis. It had been approved that TGF- β_1 in the cultured HSCs of rats *in vitro* increase two times after addition of extrinsic TGF- β_1 ^[13]. In the progression of hepatic fibrosis, the TGF- β_1 secreted by HSCs itself through self-secretion stimulation made HSC synthesize collagen more obviously. It has been found that the synthesizing and decomposing of ECM was modulated by TGF- β_1 at high degree in recent few years. Animal experiment about hepatic fibrosis showed that the elevation of TGF- β_1 gene expression prior to the increase of collagen synthesis, indicated that TGF- β_1 had some effects to beginning of hepatic fibrosis^[14]. ECM increased and HGF (hepatocyte growth factor) was restrained if TGF- β_1 was added into cultured HSCs, on the contrary, ECM was restrained and HGF increased if TGF- β_1 antibody was added. Rockey *et al.*^[15] found that the degree of liver injury

was consistent with that of HSCs activation and contraction and the contraction of HSCs could lead to the elevation of resistance in cirrhosis liver and pressure of portal vein. One study has proved^[16] that the TGF- β_1 antibody could resist the biology effect of TGF- β_1 at the same time, prevent HSCs from self-secreting TGF- β_1 . Another study has reported^[17] that monoclonal antibody of TGF- β_1 could obviously restrain the proliferation of fibroblast, and had dose-effect relationship in some range. Because of the important effect of TGF- β_1 in the course of fibrosis, the use of TGF- β_1 antibody might give some new clues to the explore the mechanism and therapy of fibrosis. After turning to myofibroblast, HSC itself secreted TGF, PDGF and other cell factors to make its activation go on. Even though, primary activation factors were cancelled, the progress of fibrosis would still last. It indicated that hepatic fibrosis must be treated in the early period. Because, there is mutual promoting or restraining role among cell factors, in the same cell. However, the results are different due to the difference of dosage and lasting time of cell factors. Therefore, according to the results of orthogonal trial, the best level of each factor was chosen to study the mechanism of anti-fibrosis I. After blocking the effects of TGF- β_1 with TGF- β_1 antibody, anti-fibrosis I drug serum decreased $[Ca^{2+}]_i$ most significantly. If drug serum prior to TGF- β_1 antibody was added into HSCs, the $[Ca^{2+}]_i$ was higher than the former, but both were lower than $[Ca^{2+}]_i$ in HSCs treated with drug serum and TGF- β_1 antibody alone. These results suggested Anti-fibrosis I drug serum might induce HSCs relaxation by reducing $[Ca^{2+}]_i$ in activated HSCs, and the mechanism was independent of decreasing TGF- β_1 effects.

Studies have shown that $[Ca^{2+}]_i$ is elevated either by hydrolysis of inositol lipids or by Ca^{2+} influx into the cell through receptor/voltage gated Ca^{2+} channels in the cell plasma membrane. It was reported^[18] that 861 compound decreased the free $[Ca^{2+}]_i$ to modulate the contraction and relaxation of HSCs. 861 compound depressed the expression of HSCs L-type voltage-operated calcium channel (L-VOCC), decreased the concentration of $[Ca^{2+}]_i$, restrained the expression of α -SMA and reduced the contraction of HSCs which might be useful to the therapy of portal vein hypertension in the early time. Yet it was considered^[19]. The pharmacological mechanism of octreotide, used to treat portal hypertension with esophageal variceal bleeding, was via the relaxation of activated HSCs and the consequent decrease in intrahepatic resistance, through the activation of HSCs somatostatin receptors (SSTR), leading to a reduction in intracellular Ca^{2+} , not interdicting the L-VOCC on the membranes of HSCs. Chinese Herbal compound can affect the construction and function of HSCs through the multi-target sites and it is important to prevent and treat hepatic fibrosis and early stage portal vein hypertension. The pharmacological mechanism of anti-fibrosis I herbal compound, used to treat hepatic fibrosis and portal hypertension, is via the relaxation of activated HSCs, and the consequent decrease in intrahepatic resistance, leading to a reduction in $[Ca^{2+}]_i$. Although cell factors play an important role in pathological process of hepatic fibrosis, the interaction between them is very complicated *in vivo*, so the potential mechanism of anti-fibrosis I will be further studied.

REFERENCES

- 1 Liu P, Liu C, Xu LM, Hu YY, Xue HM, Liu CH, Zhang ZQ. Effects of Fuzheng Huayu 319 recipe on liver fibrosis in chronic hepatitis B. *World J Gastroenterol* 1998; **4**: 348-353
- 2 Pinzani M, Marra F, Carloni V. Signal transduction in hepatic stellate cells. *Liver* 1998; **18**: 2-13
- 3 Reynaert H, Thompson MG, Thomas T, Geerts A. Hepatic stellate cells: role in microcirculation and pathophysiology of portal hypertension. *Gut* 2002; **50**: 571-581
- 4 Basile DP. The transforming growth factor beta system in kidney disease and repair: recent progress and future directions. *Curr Opin Nephrol Hypertens* 1999; **8**: 21-30
- 5 Gray MO, Long CS, Kalinyak JE, Li HT, Karliner JS. Angiotensin II stimulates cardiac myocyte hypertrophy via paracrine release of TGF-beta 1 and endothelin-1 from fibroblasts. *Cardiovasc Res* 1998; **40**: 352-363
- 6 Isaka Y, Akagi Y, Ando Y, Tsujie M, Sudo T, Ohno N, Border WA, Noble NA, Kaneda Y, Hori M, Imai E. Gene therapy by transforming growth factor-beta receptor-IgG Fc chimera suppressed extracellular matrix accumulation in experimental glomerulonephritis. *Kidney Int* 1999; **55**: 465-475
- 7 Greenwel P, Schwartz M, Rosas M, Peyrol S, Grimaud JA, Rojkind M. Characterization of fat-storing cell lines derived from normal and CCL₄-cirrhotic livers. Differences in the production of interleukin-6. *Lab Invest* 1991; **65**: 644-653
- 8 Zou Y, Gong DZ, Sun LJ, Mei MH. Protection of hepatocyte growth factor against carbon tetrachloride injury in primary rat hepatocyte culture. *Zhongguo Yiyong Shenglixue Zazhi* 1997; **13**: 228-230
- 9 Gorbis MN, Gines P, Bataller R, Nicolas JM, Garcia-Ramallo E, Cejudo P, Sancho-Bru P, Jimenez W, Arroyo V, Rodes J. Human hepatic stellate cells secrete adrenomedullin: potential autocrine factor in the regulation of cell contractility. *J Hepatol* 2001; **34**: 222-229
- 10 Sakamoto M, Uen T, Nakamura T, Hashimoto O, Sakata R, Kin M, Ogata R, Kawaguchi T, Torimura T, Sata M. Estrogen upregulates nitric oxide synthase expression in cultured rat hepatic sinusoidal endothelial cells. *J Hepatol* 2001; **34**: 858-864
- 11 Bataller R, Gines P, Nicolas JM, Gorbis MN, Garcia-Ramallo E, Gasull X, Bosch J, Arroyo V, Rodes J. Angiotensin II induces contraction and proliferation of human hepatic stellate cells. *Gastroenterology* 2000; **118**: 1149-1156
- 12 Yee HF. Ca²⁺ and rho signaling pathways: two paths to hepatic stellate cell contraction. *Hepatology* 2001; **33**: 1007-1008
- 13 Weiner FR, Giambrone MA, Czaja MJ, Shah A, Annoni G, Takahashi S, Eghbali M, Zern MA. Ito-cell gene expression and collagen regulation. *Hepatology* 1990; **11**: 111-117
- 14 Nakatsukasa H, Nagy P, Evarts RP, Hsia CC, Marsden E, Thorgeirsson SS. Cellular distribution of transforming growth factor-beta 1 and procollagen types I, III, and IV transcripts in carbon tetrachloride-induced rat liver fibrosis. *J Clin Invest* 1990; **85**: 1833-1843
- 15 Rockey DC, Weisiger RA. Endothelin induced contractility of stellate cells from normal and cirrhotic rat liver: implications for regulation of portal pressure and resistance. *Hepatology* 1996; **24**: 233-240
- 16 Eghbali-Fatourehchi G, Sieck GC, Prakash YS, Maercklein P, Gores GJ, Fitzpatrick LA. Type I procollagen production and cell proliferation is mediated by transforming growth factor-beta in a model of hepatic fibrosis. *Endocrinology* 1996; **137**: 1894-1903
- 17 Zhao Y, Tong Z, Xu L, Zhao H, Hou X. The effect of anti-transforming growth factor-beta1 antibody on fibroblast proliferation *in vitro*. *Zhonghua JieHe He HuXi ZaZhi* 1999; **22**: 101-103
- 18 Shen FJ, Tang SZ, Yin CH, Wang P, Ma XM, Li J, Zhang Y, Ma H, Jia JD, Wang BE. The effect of compound 861 on hepatic stellate cell proliferation and collagen synthesis. *Linchuang He Shiyuan Yixue Zazhi* 2003; **3**: 145-148
- 19 Huang C, Ding HG, Xu YL, Tang SZ, Wang BE, Jia JD, Zhao CH. Effect of somatostatin on calcium concentration in hepatic stellate cells and its signification. *Zhonghua Xiaohua Zazhi* 2002; **22**: 508-509

• CLINICAL RESEARCH •

Synergistic effects of interferon-alpha in combination with chemoradiation on human pancreatic adenocarcinoma

Jian-Hua Ma, Emilia Patrut, Jan Schmidt, Hanns-Peter Knaebel, Markus W. Büchler, Angela Märten

Jian-Hua Ma, Emilia Patrut, Jan Schmidt, Hanns-Peter Knaebel, Markus W. Büchler, Angela Märten, Department of Surgery, University of Heidelberg, Germany

Supported by a Generous Grant From the Joachim-Siebeneicher-Foundation

Co-first-authors: Emilia Patrut and Jan Schmidt

Correspondence to: Angela Märten, Department of Surgery, University of Heidelberg, Im Neuenheimer Feld 350, 69120 Heidelberg, Germany. angela.maerten@med.uni-heidelberg.de

Telephone: +49-6221-56-39890 Fax: +49-6221-56-8240

Received: 2004-08-25 Accepted: 2004-09-01

Abstract

AIM: To determine whether IFN- α is the agent that turns a slightly effective treatment (radiochemotherapy) into a potent therapy, we tested IFN- α for its synergistic properties.

METHODS: Eight pancreatic carcinoma cell lines were treated with the single agents and combinations of these. The role of IFN- α regarding a) direct inhibitory effects; b) radio and chemosensitizing effects; c) anti-angiogenic properties and d) enhancement of immunogenicity was investigated.

RESULTS: Our results show that IFN- α has direct inhibitory properties and some synergistic influence as determined by AnnexinV/PI stain and cell count. IFN- α is also able to prevent the increase in proliferation rate and VEGF secretion of CDDP resistant cells. Having taken the results from immunogenicity experiments together, we found cells that can be influenced by IFN- α but were less susceptible against T cells. Furthermore, high expression of MHC molecules, CD118, EGF-R and Fas was predictive for a good response.

CONCLUSION: In conclusion, IFN- α has direct cytotoxic effects, acts as a radiosensitizer and circumvents tumor cell-regrowth after CDDP treatment. These mechanisms may be responsible for the good clinical outcome of CapRI.

© 2005 The WJG Press and Elsevier Inc. All rights reserved.

Key words: Interferon-alpha; Pancreatic adenocarcinoma; Synergistic effects; Combination therapy

Ma JH, Patrut E, Schmidt J, Knaebel HP, Büchler MW, Märten A. Synergistic effects of interferon-alpha in combination with chemoradiation on human pancreatic adenocarcinoma. *World J Gastroenterol* 2005; 11(10): 1521-1528

<http://www.wjgnet.com/1007-9327/11/1521.asp>

INTRODUCTION

Carcinoma of the exocrine pancreas has an especially bad prognosis. The five-year survival rate is <1% with a median survival of 4-6 mo. Even after surgical intervention with a curative intention, the two-year survival rate in specialized centers is at best 25%^[1].

Investigators from the Virginia Mason Clinic have recently published data from a phase II trial of postoperative cisplatin (CDDP), 5-fluorouracil (5-FU), interferon alpha-2b (IFN- α), and external-beam radiation (RT) (that was) administered following pancreaticoduodenectomy. We termed this regimen CapRI for adjuvant treatment of pancreatic adenocarcinoma with ChemoRadioImmunotherapy. They treated 43 patients with mainly stage III tumors. Eighty-four percent had positive lymph nodes and 19% had positive cut margins. After a mean follow-up of 31.9 mo, 67% of the patients were still alive. Actuarial overall survival for the 1, 2, and 5-year survival rates were 95%, 64%, and 55% respectively. The treatment was quite toxic and 42% of the patients were hospitalized during the treatment, but there were no treatment-related deaths^[2].

Various chemo and/or radiation regimens have been tested in small studies for treatment of adjuvant resected pancreatic carcinoma. Most of them use 5-FU or gemcitabine as the chemotherapeutic agent, sometimes in combination with other agents such as CDDP. These protocols are often combined with radiation^[3]. The ESPAC-1 trial is the only trial to date that enrolled large numbers of patients (550 patients). The trial tested the hypothesis that chemoradiotherapy (40 Gy and weekly 5-FU) with or without 6 mo additional chemotherapy (5 FU, 425 mg/m², day 1-5 and folinic acid, 20 mg/m², d1-5, repeated monthly) provided an improvement in survival benefits compared to no adjuvant treatment. In a 2×2 factorial design, the 5-year survival rate for patients receiving chemoradiation was 10% and 19.6% without, and 21.1% for patients receiving chemotherapy and 8.4% without. The authors concluded from this that radiochemotherapy shows only limited success^[4].

Comparing the data from CapRI and ESPAC-1, we hypothesize that IFN- α is the agent that turns a slightly effective treatment (chemoradiotherapy) into a potent therapy. Several mechanisms are described which might explain why IFN- α plays a potential role in combination therapies.

IFN- α belongs to the group of type I interferons, which are already being used in cancer therapy (e.g. malignant melanoma, renal cell carcinoma, hairy cell leukemia and chronic myeloid leukemia)^[5,6]. IFN- α is produced by

monocytes/macrophages, lymphoblastoid cells, fibroblasts and plasmacytoid dendritic cells^[7]. Several other cell types are known to produce type I interferons after viral infections. IFN- α binds to the IFN- α receptor CD118; binding to the EBV-receptor CD21 is also described^[8]. The IFN receptor is coupled to a Janus-family tyrosine kinase, which phosphorylates signal-transducing activators of transcription (STATs), which translocate to the nucleus where they activate the transcription of several different genes inducing the synthesis of host cell proteins that contribute to the inhibition of viral replication^[9,10].

In addition to its anti-viral properties, IFN- α exhibits several other features that might be of interest especially for the use in combination treatments of cancer. Some of these features are: (1) direct inhibitory effects on tumor cell growth through prolongation of the cell cycle time of malignant cells, induction/inhibition of the expression of specific genes which lead to increased RNA degradation, inhibition of protein synthesis, down-regulation of oncogene expression, induction of tumor suppressor genes, and antagonism of the growth stimulatory effects of epidermal growth factor (EGF) and platelet-derived growth factor by down-regulation of cell surface receptors for the growth factors was reported^[11,12]; (2) radio and chemosensitizing effects (described for 5-FU, cisplatin and dacarbazine)^[13,14]; (3) anti-angiogenic properties. The latter is mainly due to the down-regulation of VEGF and by inhibiting the expression of pro-angiogenic molecules, basic fibroblast growth factor, and matrix metalloproteinase-9^[15-17]; (4) enhancement of immunogenicity of tumors. This phenomenon is provoked by an increase of MHC class I expression which enhances immune recognition^[12] and (5) modulation of the immune system. IFN- α plays an essential role in the differentiation, maturation and function of dendritic cells (DC), enhances the survival of T cells by expression of anti-apoptotic genes, induces the generation of CD8⁺ memory cells, enhances macrophage activities, and activates natural killer (NK) cells thus releasing cytokines^[12,18-20].

Therefore, we investigated the influence of IFN- α in the CapRI-regimen in eight human ductal pancreatic carcinoma cell lines regarding direct cytotoxic effects of IFN- α , radio and/or chemosensitizing effects, anti-angiogenic properties and expression of MHC molecules and IFN-receptors.

MATERIALS AND METHODS

Cell lines

Human pancreatic cancer cell lines ASPC-1, CAPAN-2, DAN-G, KciMoh-1, MiaPaCa-1, PANC-1, PatScl and PK 9 were obtained from ATCC, USA and cultured in RPMI 1 640 medium supplemented with 10% fetal bovine serum, 100 units/mL penicillin, and 100 μ g/mL streptomycin (PAA laboratories GmbH, Austria). They were maintained at 37 °C under 50 mL/L CO₂ in a humidified atmosphere.

Treatment to cell lines

Cells were subdivided into nine groups, each of which was treated with one of the following regimens almost in accordance with the protocol used in the CapRI scheme: (1) Untreated; (2) 5-FU 65 μ g/mL continuously, d 1-5; f

5-FU +IFN- α ; (3) CDDP 3 μ g/mL on d 1, for 60 min; (4) CDDP +IFN- α ; (5) RT 1.8 Gy/d, d 1-5; (6) RT+IFN- α ; (7) IFN- α 1 000 U/mL, d 1, 3, and 5; (8) 5-FU+CDDP+IFN- α +RT (CapRI).

Determination of apoptosis, cell death and cell numbers

Cells were investigated on day five of treatment. Apoptotic cells were detected on an Epics®XL.MCL flow cytometer (Beckman-Coulter, Krefeld, Germany) by AnnexinV staining using the AnnexinV/PI staining kit (BD Pharmingen™, Heidelberg, Germany) according to the manufacturer's instructions. Cells were analyzed immediately after staining. Unstained cells were used to set up controls. Cell numbers of viable cells were determined by trypan blue exclusion.

Flow cytometric analysis

Human pancreatic cancer cell lines were stained after treatment using various monoclonal antibodies directed against human cell surface antigens, including those against human HLA-ABC, HLA-DR, CD21, EGF-R, CD118, CD95 (Fas) and FasL (BD Biosciences, Heidelberg, Germany). For each flow cytometry measurement, gates for negative control were set to less than 2%. Data from at least 10 000 cells were collected and analyzed. Negative controls consisted of the cells labeled with a corresponding isotype control. Mean fluorescence was normalized to mean fluorescence of the control antibodies. To distinguish whether an up-regulation of surface molecules has occurred or negative cells for that marker were preferentially killed; cells were stained before treatment, 24 h later analyzed, re-stained and re-analyzed. An increase in positive cells that was not seen in the control group was termed up-regulation. To distinguish between down-regulation of a specific surface marker and preferential killing of positive cells, we compared the percentage of marker and PI double-positive cells of cells with an adequate control.

MTT assay for cell proliferation

The non-radioactive proliferation assay "EZ4U" kit (Biomedica, Vienna, Austria) was used according to the manufacturer's instructions. Tumor cells were seeded out at a density of 2 000 cells per well in triplicate in a 96-well plate. The proliferation rate was determined after 5 h of incubation as the amount of turnover of yellow tetrazolium salt to red formazan. Absorbance at 450 nm with 620 nm as a reference was measured with an ELISA reader; the absorbance of a medium blank was subtracted. The proliferation index was calculated by setting the proliferation of untreated cells to 1.

Determination of VEGF secretion by ELISA

After a four-day treatment, the cells were seeded out at a density of 1×10^5 living cells in 2 mL. After 24 h, the cell culture supernatant was collected for each group and stored at -80 °C for further analysis. Amounts of VEGF were determined by usage of the DuoSet ELISA Development kit (R&D Systems, Inc., USA). The assay was performed in duplicate according to the manufacturer's instructions.

Statistical analysis

Non-parametrical analysis (Mann-Whitney-U test) and

parametrical correlation (Pearson) on SPSS 11.5 was used to analyze statistical significance. A P -value <0.05 was considered as significant.

RESULTS

Cell survival

First, we determined the cell survival index (i.e., numbers of viable cells normalized to untreated cells [=1]) of eight cell lines by counting of viable cells after five-day treatment (Figure 1A). We found a statistically significant reduction of living cells after all treatments, which were more pronounced in 5-FU containing regimens. IFN- α alone decreased the cell survival index from 1 to 0.43 ± 0.24 ($P < 0.002$). With regard to radio or chemosensitizing effects, we found significant decrease of the index after adding IFN- α to radiotherapy (0.29 ± 0.14 compared to 0.21 ± 0.16 ; $P < 0.01$; Figure 1B). A significant chemosensitizing effect was found in three out of eight cell lines (two times for 5-FU, one time for CDDP); however, it failed to be significant after taking the mean from all cell lines.

Induction of apoptosis

We determined apoptosis and necrosis of eight cell lines after five-day treatment by measuring AnnexinV and PI

(Figure 2A). Results were normalized to values of untreated cells. We found a statistically significant increase of necrosis after all treatments. Late apoptosis (AnnexinV⁺/PI⁺) increased as well (significant for all but not for IFN- α treated cells). The sum of the dying cells was significantly increased after 5-FU and combination treatments as well as after CDDP+IFN- α treatment. Early apoptosis was not enhanced after treatments since it was determined after five days of treatment.

Regarding radio or chemosensitizing effects, we found a tendency towards sensitizing effects for adding of IFN- α to CDDP or radiotherapy. However, this was not significant (Figure 2B).

Inhibition of proliferation

We determined the proliferation index (proliferation normalized to untreated cells [=1]) of eight cell lines by MTT assay after five-day treatment (Figure 3A). We found a statistically significant reduction in proliferation after treatments including 5-FU. IFN- α alone inhibited proliferation but not in a significant way. Interestingly, we observed an increase in proliferation after treatment with CDDP ($P < 0.005$). This could be prevented by the addition of IFN- α (0.71 ± 0.77 compared to -0.11 ± 0.5 ; $P < 0.02$; Figure 3B). Other radio or chemosensitizing effects could not be found.

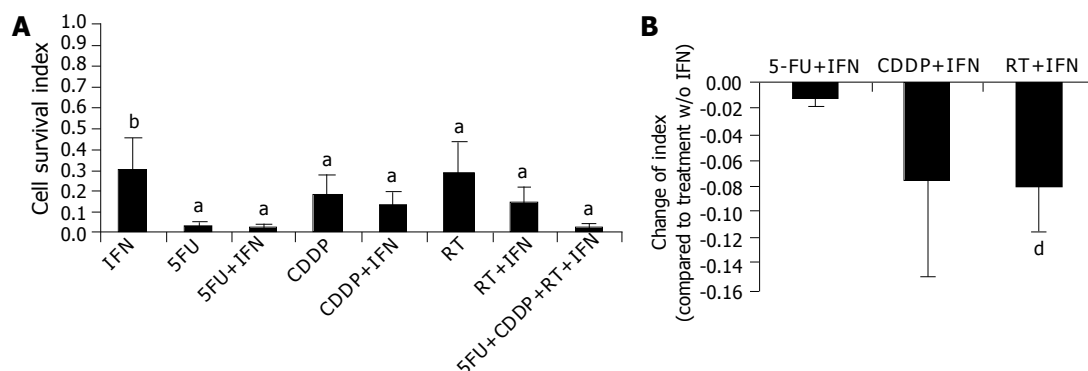


Figure 1 Influence on cell survival. Equal amount of cells were seeded out on day +1. A: Numbers of viable cells were determined after five-day treatment. Cell numbers of untreated cells were set to '1' and cell survival index was calculated. B: Shows the influence of IFN- α in combination treatments. Values of treatments without IFN- α were subtracted from values after combination treatment. Data is shown as mean \pm SD error from eight cell lines with at least three separate experiments. ^a $P < 0.05$ was labeled with an asterisk; ^b $P < 0.01$ with two asterisks and ^d $P < 0.001$ with three asterisks.

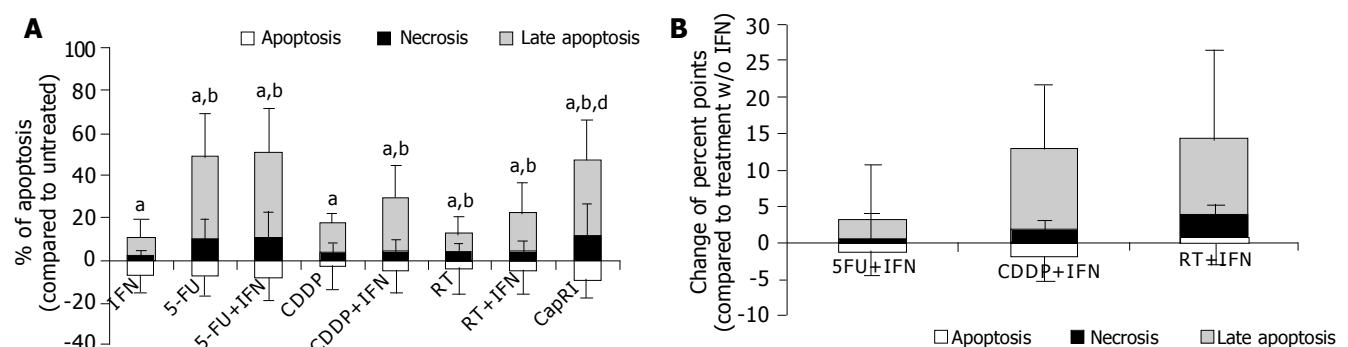


Figure 2 Induction of apoptosis. Apoptosis was determined after five-day treatment by staining for AnnexinV⁺ using flow cytometry (A). Late apoptosis is defined as AnnexinV⁺/PI⁺, necrosis as PI⁺. B) shows the influence of IFN- α in combination treatments. Values of treatments without IFN- α were subtracted from values after combination treatment. Data is shown as mean \pm SD error from eight cell lines with at least three separate experiments. ^a $P < 0.05$ was labeled with an asterisk; ^b $P < 0.01$ with two asterisks and ^d $P < 0.001$ with three asterisks.

Secretion of VEGF

Just in three out of eight cell lines, detectable VEGF concentrations could be found in the supernatant. After treatment with 5-FU and combinations VEGF levels were mostly below the detection level (<62.5 pg/mL, Figure 4A). CDDP increases VEGF secretion (102.7 ± 25.9 pg/mL/ 10^5 cells/24 h *vs* 204.7 ± 6.4 after CDDP treatment, $P < 0.05$). The addition of IFN- α to CDDP normalizes the amount of VEGF (104.2 ± 47.8 pg/mL/ 10^5 cells/24 h, $P < 0.01$; Figure 4B).

Immunophenotyping of treated tumor cells

Next, we analyzed the influence of IFN- α on immunogenicity of tumor cells. Therefore, we determined constitutive and inducible MHC expression. Mean expression of MHC class I was significantly increased after IFN- α treatment (data not shown). However, we were not able to detect any influence of IFN- α at this concentration on the percentage of MHC positive cells (Figure 5A). After five-day treatment with 5-FU and combinations, we found a significant reduction in MHC-positive cells. This was due to down-regulation of MHC molecules. In five out of eight cell lines, this effect could be significantly softened when IFN- α is added to 5-FU. However, it failed to be significant after taking the mean from all cell lines (Figure 5B). There was a

tendency towards higher MHC expression and mean fluorescence after adding IFN- α to chemo or radiotherapy; however, this was just significant for the mean fluorescence of HLA-ABC after adding IFN- α to CDDP.

Furthermore, we analyzed expression of EGF-R and IFN- α -receptors (Figure 6). EGF-R expression remained mainly unchanged by treatment. CD118 (IFN-R) was down-regulated after treatment, this was significant for treatment with 5-FU+IFN- α and CapRI scheme ($13.9 \pm 12.8\%$ on untreated cells *vs* $3.2 \pm 1.8\%$ or $3.5 \pm 2.7\%$, respectively). CD21, which is described to act as an IFN- α receptor was only slightly expressed on untreated cells and was significantly up-regulated after treatment with 5-FU and combinations ($7.8 \pm 3.5\%$ on untreated cells *vs* approximately 35% after treatment). IFN- α had no synergistic effect for any treatment. Furthermore, we observed a decrease of Fas-positive cells after treatment (data not shown).

Statistical analysis for predictive markers

Since we were interested in potentially predictive markers for treatment responsiveness, we analyzed expression of several markers on untreated cells for correlation with apoptosis/necrosis induction, decrease of cell survival and anti-proliferative effects. All parameters behaved in a similar

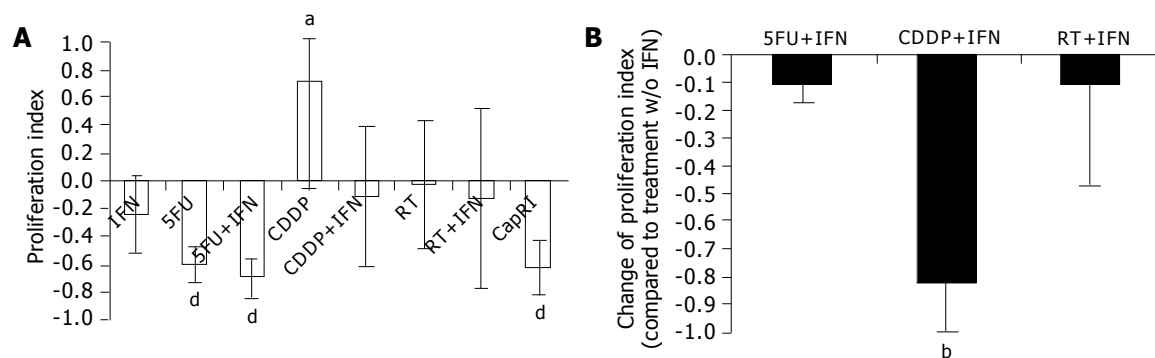


Figure 3 Inhibition of proliferation Proliferation rate was determined after five-day treatment by using a non-radioactive MTT assay. Proliferation rate of untreated cells was set to '1' and percentage of proliferation was calculated (A). B) shows the influence of IFN- α in combination treatments. Values of treatments without IFN- α were subtracted from values after combination treatment. Data is shown as mean \pm standard error from eight cell lines with at least three separate experiments. ^a $P < 0.05$ was labeled with an asterisk; ^b $P < 0.01$ with two asterisks and ^c $P < 0.001$ with three asterisks.

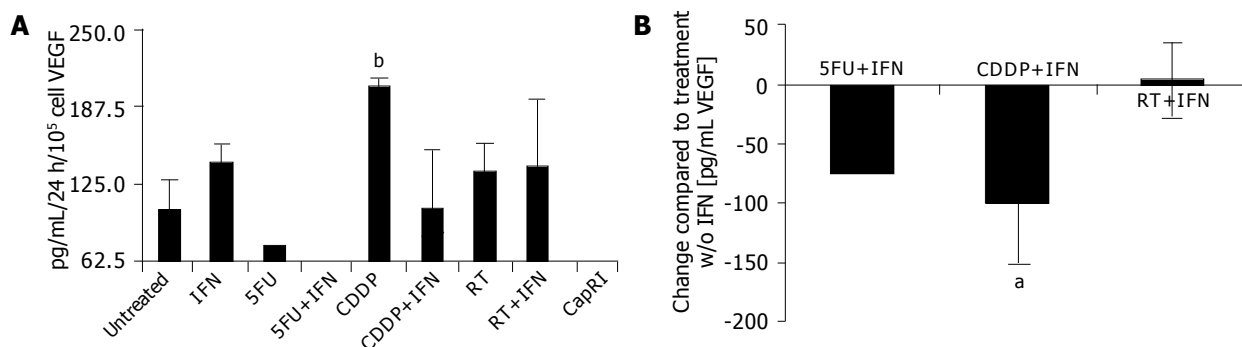


Figure 4 Secretion of VEGF Cells were seeded out after four-day treatment in a density of 1×10^5 living cells in 2 mL. Supernatants from treated and untreated tumor cells were collected after 24 h and stored at -80°C . VEGF concentration was determined by ELISA (A). B) shows the influence of IFN- α in combination treatments. Values of treatments without IFN- α were subtracted from values after combination treatment. Data from three cell lines are shown as mean \pm standard error from at least three separate experiments. ^a $P < 0.05$ was labeled with an asterisk and ^b $P < 0.01$ with two asterisks.

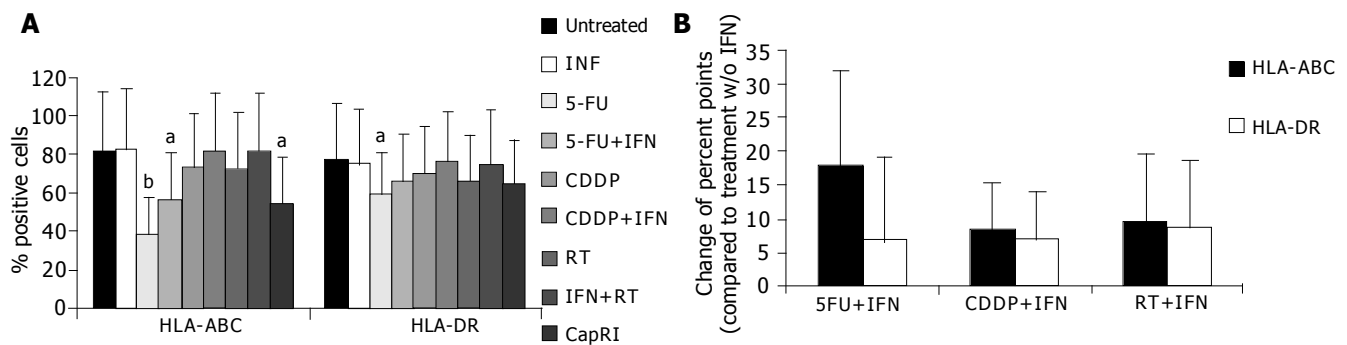


Figure 5 Immunophenotyping of tumor cells Tumor cells were treated as described. Expression of MHC molecules was analyzed after five-day treatment by flow cytometry (A). B) shows the influence of IFN- α in combination treatments. Values of treatments without IFN- α were subtracted from values after combination treatment. Data is shown as mean \pm SD error from eight cell lines each with at least four separate experiments. ^a P <0.05 was labeled with an asterisk and ^b P <0.01 with two asterisks.

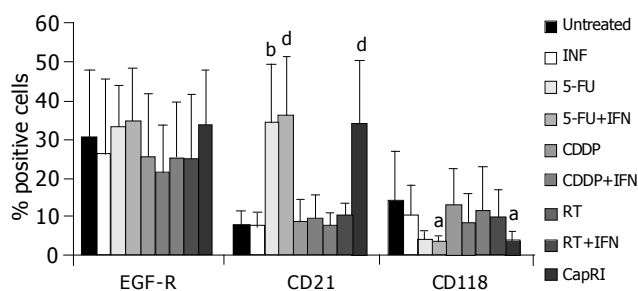


Figure 6 Expression of surface receptors Tumor cells were treated as described. Expressions of IFN and EGF receptors were analyzed after five-day treatment by flow cytometry. Data is shown as mean \pm SD error from eight cell lines each with at least four separate experiments. ^a P <0.05 was labeled with an asterisk; ^b P <0.01 with two asterisks and ^d P <0.001 with three asterisks.

way, mostly in a significant way (data from analysis of proliferation index correlated with induction of apoptosis/necrosis that correlated with late apoptosis, which in turn correlated with cell survival index).

We found a significant correlation between expression of MHC molecules, CD118, Fas and EGF-R on untreated cells with apoptosis/necrosis induction after treatment with the CapRI scheme (Figure 7A-E). Low expression of CD21 correlated with a low cell survival index (i.e., with low numbers of viable cells, Figure 7F).

Statistical analysis for correlation of marker

Next, we analyzed the treatment-response-pattern of parameters to define surrogate markers (Table 1). With regard to MHC molecules, IFN-receptors, EGF-receptor and Fas, almost all cell lines reacted in a similar way to the different treatments. The correlation was positive except for EGF-R and CD21 where we observed a negative correlation. Interestingly, treatments inducing apoptosis/necrosis also induce a decrease in MHC, CD118 and Fas-positive cells and an increase in CD21-positive cells. Treatments that inhibit proliferation also induce an increase of CD21-positive cells as well as a decrease of CD118 and Fas-positive cells and of VEGF secretion. Apoptosis/necrosis induction correlated with the anti-proliferative effect as well as with the number of surviving cells.

DISCUSSION

Carcinoma of the exocrine pancreas has an especially bad prognosis. Treatment after adjuvant resection prolongs the survival, but so far has failed to produce long-lasting benefits. Results from a phase II trial, where chemoradiotherapy was combined with IFN- α are very encouraging (55% 5-year survival compared to 10% in the ESPAC-1 trial).

Comparing the data from the CapRI and the ESPAC-1 trials, we hypothesize that IFN- α is the agent that turns a slightly effective treatment (radiochemotherapy) into a potent therapy. Several mechanisms are described that might explain why IFN- α could play a potential role in combination therapies. Here, we focused on the described mechanism of a) direct inhibitory effects on tumor cell growth^[12]; b) radio- and chemosensitizing effects^[13,14]; c) anti-angiogenic properties (as far as possible)^[15-17] and d) enhancement of immunogenicity of tumors^[12].

With regard to direct inhibitory effects we observed cytotoxic effects of IFN- α . A synergistic effect of IFN- α was observed after the addition to radiotherapy but not to chemotherapy. It is reported that IFN- α down-regulates EGF-R on renal cell carcinoma and breast cancer cells after 7 d of incubation and that this consequently results in cell growth inhibition^[11,12]. With a shorter incubation period, we were not able to confirm these data for pancreatic carcinoma. IFN- α treatment resulted only in a partial down-regulation of EGF-R. Similar observation was seen regarding the apoptosis rate after five days of treatment. In all cell lines, we found that only a few cells were in early apoptosis, some necrotic cells and the majority of the cells were in late apoptosis. Since there were many manipulations during the treatment period as well as for the untreated control group (e.g., daily harvesting for radiation), we had a high early apoptosis rate in untreated cells. But only treated cells showed remarkably high rates of late apoptosis and necrosis. This effect was not so pronounced in IFN- α treated cells. There was a tendency towards a synergistic effect of IFN- α ; however, it was not significant. Taken together, we must conclude that IFN- α has direct inhibitory properties and shows limited synergistic influence.

Next, we analyzed the proliferative capacity of surviving cells after five days of treatment. Interestingly, we found a significant increase in proliferation of CDDP resistant cells. This

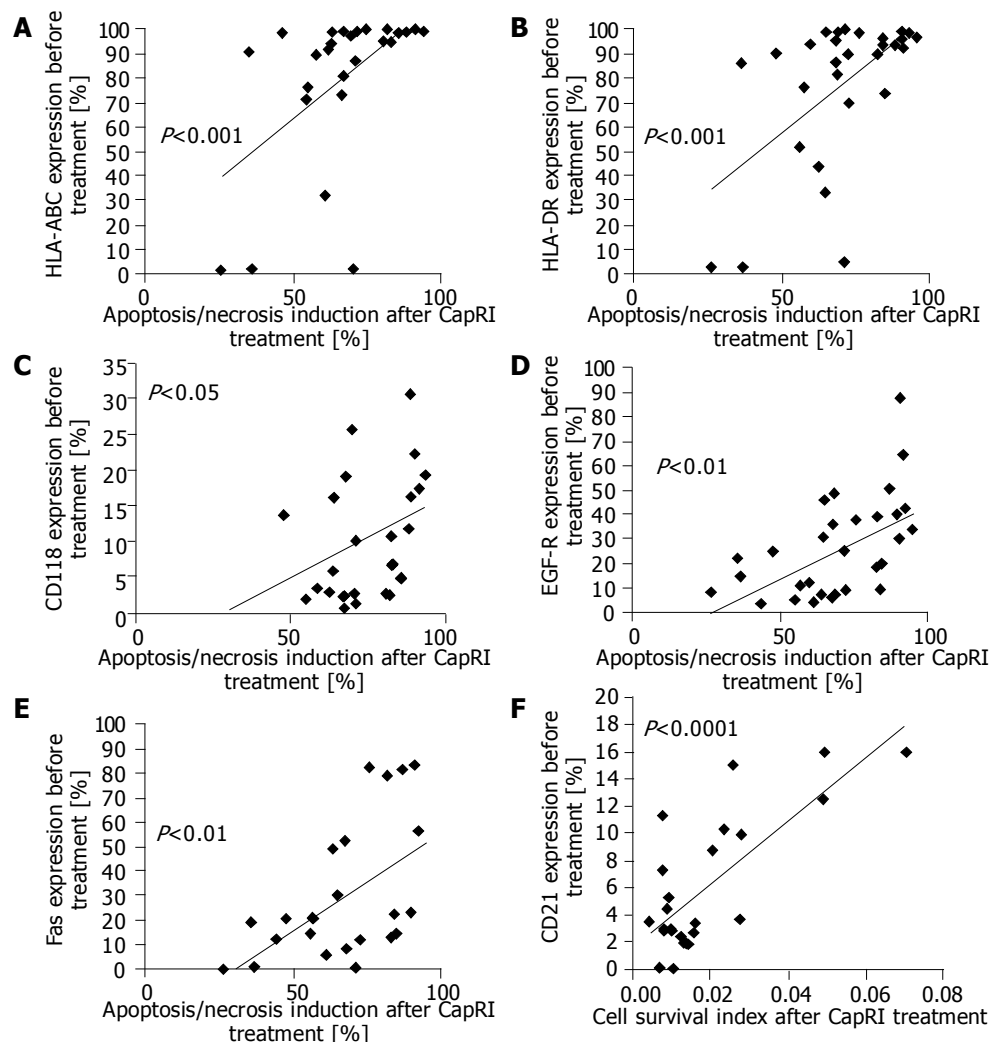


Figure 7 Statistical analysis Expression level on untreated cells were correlated with results from AnnexinV/PI stain, proliferation and cell survival index after treatment with the CapRI scheme and analyzed for use as predictive marker (A-F).

is in accordance with data from various groups who observed an accelerated tumor growth after chemotherapy^[21,22] *in vitro* as well as *in vivo*. IFN- α on its own has a slight inhibitory effect on proliferation rate, but was able to circumvent the accelerated tumor cell growth after CDDP treatment. Best results were seen again for treatments including 5-FU with no synergistic effect of IFN- α . Similar results could be observed for the secretion of VEGF. We tested this surrogate marker for *in vitro* analysis of anti-angiogenic effects. Only 3/8 cell lines secreted measurable amounts of VEGF. However, this significantly increased after treatment with CDDP; an effect which could again be circumvented by the addition of IFN- α . As Tannock concluded his article about 'Repopulation of tumor cells between cycles of chemotherapy: a neglected factor' with the sentence 'Biological agents with rapid onset and short duration of action, which can selectively inhibit tumor-cell repopulation, administered between cycles of chemotherapy, might improve the therapeutic index^[22]. Perhaps, IFN- α is one of these biological agents.

We also looked at effects of IFN- α on immunogenicity of the tumor cells. As expected, we observed an increase in

MHC molecules on the surface of the tumor cells after treatment with IFN- α . However, cell lines completely deficient for MHC did not change. Interestingly, we observed a significant decrease of MHC class I-positive cells after treatment with 5-FU and combinations. Our findings were different from what has been reported^[23-25] where an increase in MHC class I on various epithelial tumor cells after treatment with 5-FU was described. We can only speculate why we observed an opposite effect. Perhaps the continuous culture in the presence of high-dosed 5-FU over five days without any synergistic acting agent, such as levamisole, is responsible for our observations. This is supported by the observation that adding IFN- α to 5-FU at least diminishes the down-regulation and that treatment with 5-FU over 24 h had no effect. Abdalla *et al*^[24] described that 5-FU increase the steady state level of HLA class I mRNAs by about 80% but stated also a reduction of 20-57% in RNA synthesis. This could explain why after a 'long-time' treatment, MHC molecules were down-regulated.

As another feature of immunogenicity, we investigated the expression of IFN-R. Pancreatic tumor cells were always able to bind IFN- α . Although 5-FU down-regulates CD118, it provokes an increase of CD21, which acts as well as an

Table 1 Correlation of treatment response of various parameters. Various parameters of eight cell lines were determined after treatment with single agents and/or combinations. The response-pattern of parameters was investigated for correlation

	HLA-ABC	HLA-DR	HLA-ABC mean	HLA-DR mean	CD 21	CD 118	EGF-R	Fas	FasL	VEGF	Proliferation index	Apoptosis /necrosis	Cell survival index
HLA-ABC													
Pearson's correlation		0.928	0.783	0.777	-0.907	0.790	-0.769	0.887	0.867			-0.825	
P		0.001	0.012	0.014	0.001	0.011	0.015	0.001	0.002	NS	NS	0.006	NS
HLA-DR													
Pearson's	0.928		0.710	0.743	-0.753			0.762	0.782			-0.705	
P	0.001		0.032	0.022	0.019	NS	NS	0.017	0.013	NS	NS	0.034	NS
HLA-ABCmean													
Pearson's	0.783	0.710		0.939	-0.718		-0.892						
P	0.012	0.032		0.001	0.029	NS	0.001	NS	NS	NS	NS	NS	NS
HLA-DRmean													
Pearson's	0.777	0.743	0.939				-0.738						
P	0.014	0.022	0.001		NS	NS	0.023	NS	NS	NS	NS	NS	NS
CD 21													
Pearson's	-0.907	-0.753	-0.718			-0.926	0.850	-0.976	-0.957		-0.810	0.915	
P	0.001	0.019	0.029	NS		0.001	0.004	0.001	0.001	NS	0.008	0.001	NS
CD 118													
Pearson's	0.790				-0.926			0.966	0.946	0.596	0.898	-0.936	0.718
P	0.011	NS	NS	NS	0.001		NS	0.0001	0.0001	0.158	0.001	0.001	0.029
EGF-R													
Pearson's	-0.769		-0.892	-0.738	0.850			-0.764	-0.758				
P	0.015	NS	0.001	0.023	0.004	NS		0.017	0.018	NS	NS	NS	NS
Fas													
Pearson's	0.887	0.762			-0.976	0.966	-0.764		0.985		0.888	-0.922	
P	0.001	0.017	NS	NS	0.0001	0.0001	0.017		0.001	NS	0.001	0.001	NS
FasL													
Pearson's	0.867	0.782			-0.957	0.946	-0.758	0.985			0.875	-0.886	0.675
P	0.002	0.013	NS	NS	0.001	0.001	0.018	0.001		NS	0.002	0.001	0.046
VEGF													
Pearson's											0.800		
P	NS	NS	NS	NS	NS	NS	NS	NS	NS		0.031	NS	NS
Proliferation index													
Pearson's					-0.810	0.898		0.888	0.875	0.800			
P	NS	NS	NS	NS	0.008	0.001	NS	0.001	0.002	0.031		NS	NS
Apoptosis/necrosis													
Pearson's	-0.825	-0.705			0.915	-0.936		-0.922	-0.886		-0.721		-0.748
P	0.006	0.034	NS	NS	0.001	0.001	NS	0.001	0.001	NS	0.028		0.020
Cell survival index													
Pearson's						0.718			0.675			-0.748	
P	NS	NS	NS	NS	NS	0.029	NS	NS	0.046	NS	NS	0.020	

NS = not significant.

IFN-R. This up-regulation may be due to histone acetyltransferase activity of 5-FU that allows specific transcription factors access to the cognate DNA binding site^[26]. From the available results for immunogenicity, we observed cells that can be addressed by IFN- α but have a moderate reduction in T cell susceptibility.

We were also interested in predictive markers for response to the CapRI scheme. Therefore, we used apoptosis/necrosis induction, low cell survival index and negative proliferation index as parameters for good response; all parameters behaved very similar. For our *in vitro* experiments, we found a correlation between high expression in MHC molecules, CD118, EGF-R and Fas and apoptosis/necrosis induction. We do not know why MHC-positive cells are more susceptible to the treatment but the better response of Fas, CD118 and EGF-R-positive cells make sense. Fas-induced cell death may play a role in this treatment and CD118 expression is necessary for effects by IFN- α that is described to inhibit EGF-stimulated cell growth and

reduce EGF binding^[11]. Furthermore, we found a very similar reaction pattern to the different treatments with regard to most markers. Even if they are not dependent on each other, they could be used as surrogate markers.

In conclusion, we demonstrated that IFN- α has direct inhibitory properties with limited synergistic influence and that it reverts to the enhanced proliferation rate and VEGF secretion after CDDP treatment and the decreased MHC class I expression after 5-FU treatment. These results may be responsible for the positive outcome of the CapRI scheme. However, we hypothesize that the activation of the immune system by IFN- α plays a very important role in this treatment scheme, too. Further studies are started to investigate this mechanism.

ACKNOWLEDGEMENTS

We thank Karin Steybe for excellent technical assistance and Moustafa Kebbewar for proofreading of the manuscript.

REFERENCES

- 1 **Raraty MG**, Magee CJ, Ghaneh P, Neoptolemos JP. New techniques and agents in the adjuvant therapy of pancreatic cancer. *Acta Oncol* 2002; **41**: 582-595
- 2 **Picozzi VJ**, Kozarek RA, Traverso LW. Interferon-based adjuvant chemoradiation therapy after pancreaticoduodenectomy for pancreatic adenocarcinoma. *Am J Surg* 2003; **185**: 476-480
- 3 **Tsai JY**, Iannitti DA, Safran H. Combined modality therapy for pancreatic cancer. *Semin Oncol* 2003; **30**: 71-79
- 4 **Neoptolemos JP**, Stocken DD, Friess H, Bassi C, Dunn JA, Hickey H, Beger H, Fernandez-Cruz L, Dervenis C, Lacaine F, Falconi M, Pederzoli P, Pap A, Spooner D, Kerr DJ, Büchler MW. A randomized trial of chemoradiotherapy and chemotherapy after resection of pancreatic cancer. *N Engl J Med* 2004; **350**: 1200-1210
- 5 **Kirkwood J**. Cancer immunotherapy: the interferon-alpha experience. *Semin Oncol* 2002; **29**: 18-26
- 6 **Belardelli F**, Ferrantini M, Proietti E, Kirkwood JM. Interferon-alpha in tumor immunity and immunotherapy. *Cytokine Growth Factor Rev* 2002; **13**: 119-134
- 7 **Gutterman JU**. Cytokine therapeutics: lessons from interferon alpha. *Proc Natl Acad Sci USA* 1994; **91**: 1198-1205
- 8 **Delcayre AX**, Salas F, Mathur S, Kovats K, Lotz M, Lernhardt W. Epstein Barr virus/complement C3d receptor is an interferon alpha receptor. *EMBO J* 1991; **10**: 919-926
- 9 **Mogensen KE**, Lewerenz M, Reboul J, Lutfalla G, Uze G. The type I interferon receptor: structure, function, and evolution of a family business. *J Interferon Cytokine Res* 1999; **19**: 1069-1098
- 10 **Domanski P**, Witte M, Kellum M, Rubinstein M, Hackett R, Pitha P, Colamonici OR. Cloning and expression of a long form of the beta subunit of the interferon alpha beta receptor that is required for signaling. *J Biol Chem* 1995; **270**: 21606-21611
- 11 **Iacopino F**, Ferrandina G, Scambia G, Benedetti-Panici P, Mancuso S, Sica G. Interferons inhibit EGF-stimulated cell growth and reduce EGF binding in human breast cancer cells. *Anticancer Res* 1996; **16**: 1919-1924
- 12 **Pfeffer LM**, Dinarello CA, Herberman RB, Williams BR, Borden EC, Borden R, Walter MR, Nagabhushan TL, Trotta PP, Pestka S. Biological properties of recombinant alpha-interferons: 40th anniversary of the discovery of interferons. *Cancer Res* 1998; **58**: 2489-2499
- 13 **Kurzrock R**, Talpaz M, Guttermann J. Interferons: Clinical applications. Philadelphia: Lippincott; 1991
- 14 **Holsti LR**, Mattson K, Niiranen A, Standertskjöld-Nordenstam CG, Stenman S, Sovijärvi A, Cantell K. Enhancement of radiation effects by alpha interferon in the treatment of small cell carcinoma of the lung. *Int J Radiat Oncol Biol Phys* 1987; **13**: 1161-1166
- 15 **Decatris M**, Santhanam S, O'Byrne K. Potential of interferon-alpha in solid tumours: part 1. *BioDrugs* 2002; **16**: 261-281
- 16 **Solorzano CC**, Hwang R, Baker CH, Bucana CD, Pisters PW, Evans DB, Killian JJ, Fidler IJ. Administration of optimal biological dose and schedule of interferon alpha combined with gemcitabine induces apoptosis in tumor-associated endothelial cells and reduces growth of human pancreatic carcinoma implanted orthotopically in nude mice. *Clin Cancer Res* 2003; **9**: 1858-1867
- 17 **Wang L**, Wu WZ, Sun HC, Wu XF, Qin LX, Liu YK, Liu KD, Tang ZY. Mechanism of interferon alpha on inhibition of metastasis and angiogenesis of hepatocellular carcinoma after curative resection in nude mice. *J Gastrointest Surg* 2003; **7**: 587-594
- 18 **Paquette RL**, Hsu NC, Kiertscher SM, Park AN, Tran L, Roth MD, Glaspy JA. Interferon-alpha and granulocyte-macrophage colony-stimulating factor differentiate peripheral blood monocytes into potent antigen-presenting cells. *J Leukoc Biol* 1998; **64**: 358-367
- 19 **Matikainen S**, Sareneva T, Ronni T, Lehtonen A, Koskinen PJ, Julkunen I. Interferon-alpha activates multiple STAT proteins and upregulates proliferation-associated IL-2Ralpha, c-myc, and pim-1 genes in human T cells. *Blood* 1999; **93**: 1980-1991
- 20 **Marrack P**, Kappler J, Mitchell T. Type I interferons keep activated T cells alive. *J Exp Med* 1999; **189**: 521-530
- 21 **El Sharouni SY**, Kal HB, Battermann JJ. Accelerated regrowth of non-small-cell lung tumours after induction chemotherapy. *Br J Cancer* 2003; **89**: 2184-2189
- 22 **Davis AJ**, Tannock JF. Repopulation of tumour cells between cycles of chemotherapy: a neglected factor. *Lancet Oncol* 2000; **1**: 86-93
- 23 **Correale P**, Aquino A, Giuliani A, Pellegrini M, Micheli L, Cusi MG, Nencini C, Petrioli R, Prete SP, De Vecchis L, Turriziani M, Giorgi G, Bonmassar E, Francini G. Treatment of colon and breast carcinoma cells with 5-fluorouracil enhances expression of carcinoembryonic antigen and susceptibility to HLA-A(*)02.01 restricted, CEA-peptide-specific cytotoxic T cells in vitro. *Int J Cancer* 2003; **104**: 437-445
- 24 **Abdalla EE**, Blair GE, Jones RA, Sue-Ling HM, Johnston D. Mechanism of synergy of levamisole and fluorouracil: induction of human leukocyte antigen class I in a colorectal cancer cell line. *J Natl Cancer Inst* 1995; **87**: 489-496
- 25 **Ohtsukasa S**, Okabe S, Yamashita H, Iwai T, Sugihara K. Increased expression of CEA and MHC class I in colorectal cancer cell lines exposed to chemotherapy drugs. *J Cancer Res Clin Oncol* 2003; **129**: 719-726
- 26 **Zabel MD**, Weis JH. Cell-specific regulation of the CD21 gene. *Int Immunopharmacol* 2001; **1**: 483-493

• CLINICAL RESEARCH •

Aspartate aminotransferase-immunoglobulin complexes in patients with chronic liver disease

Masahiko Tameda, Katsuya Shiraki, Kinue Ooi, Koujiro Takase, Yoshitane Kosaka, Tsutomu Nobori, Yukihiro Tameda

Masahiko Tameda, Kinue Ooi, Tsutomu Nobori, Yukihiro Tameda, Department of Clinical Laboratory Medicine, School of Medicine, Mie University, Edobashi 2-174, Tsu, Mie-ken, 514 Japan
Katsuya Shiraki, Koujiro Takase, Yoshitane Kosaka, The First Department of Internal Medicine, School of Medicine, Mie University, Edobashi 2-174, Tsu, Mie-ken, 514 Japan

Correspondence to: Katsuya Shiraki, M.D., Ph.D., First Department of Internal Medicine, School of Medicine, Mie University, Edobashi 2-174, Tsu, Mie 514-8507 Japan. katsuyas@clin.medic.mie-u.ac.jp
Telephone: +81-59-231-5015 Fax: +81-59-232-5201

Received: 2004-04-30 Accepted: 2004-07-17

Abstract

AIM: To determine the complex of AST and immunoglobulin and to investigate its clinical significance in patients with liver disease.

METHODS: The complex of AST and immunoglobulin was determined by counter-immunoelectrophoresis and its clinical significance was investigated in 128 patients with liver disease.

RESULTS: AST was bound to immunoglobulin of anti-immunoglobulin A (IgA) class, but any binding to anti-immunoglobulin G and anti-immunoglobulin M classes was not observed. Although the incidence of AST-immunoglobulin complex was 41.8% in chronic hepatitis (CH), the incidences in liver cirrhosis and hepatocellular carcinoma were 62.2 and 90.0%, respectively. In alcoholic liver disease with high level of serum IgA, the incidence of the complex was 66.7%, which was higher than that in CH. The ratio of binding to lambda-chain of IgA was higher than that to kappa-chain of IgA. The serum level of IgA and the ratio of AST/alanine aminotransferase (ALT) were significantly higher in patients with AST-IgA complex than in those without complex.

CONCLUSION: These results suggest that AST-IgA complex in patients with progressive liver diseases and alcoholic liver injury can lead to elevation of the ratio of AST/ALT.

© 2005 The WJG Press and Elsevier Inc. All rights reserved.

Key words: Alcoholic liver disease; Aspartate aminotransferase; AST/ALT; Chronic hepatitis; Chronic liver disease; Hepatocellular carcinoma; Immunoglobulin; Liver cirrhosis

Tameda M, Shiraki K, Ooi K, Takase K, Kosaka Y, Nobori T,

Tameda Y. Aspartate aminotransferase-immunoglobulin complexes in patients with chronic liver disease. *World J Gastroenterol* 2005; 11(10): 1529-1531

<http://www.wjgnet.com/1007-9327/11/1529.asp>

INTRODUCTION

Complexes between serum enzyme and serum immunoglobulin sometimes influence the serum concentration of enzymes. Alkaline phosphatase (Al-P)^[1,2], amylase^[3,4], creatinine phosphokinase^[5] and lactate dehydrogenase (LDH)^[6] occasionally make complexes with serum immunoglobulins. Because the serum activities of the enzymes are higher in patients with enzyme-immunoglobulin complexes, which are frequently observed in patients with autoimmune diseases, it is important to evaluate enzyme-immunoglobulin complexes in clinical practice. Some investigators^[7-14] have reported that AST-immunoglobulin complexes are observed in several diseases, although the incidence is low. The ratio of AST to alanine aminotransferase (AST/ALT) increases with the progression of chronic liver diseases^[15]. When the ratio of AST/ALT is over 1.0, progression of chronic hepatitis (CH) to liver cirrhosis (LC) is strongly suspected. In this study, we evaluated the AST-immunoglobulin complexes in patients with chronic liver disease and whether the increase of the ratio of AST/ALT in patients with progressive chronic liver disease was related to the formation of complexes between AST and immunoglobulin.

MATERIALS AND METHODS

Patients

A total of 128 patients with liver disease were treated at the out-patient clinic or admitted to Mie University Hospital between July 1992 and June 1993. Sixty-seven patients were diagnosed as CH, 45 as LC, 10 as hepatocellular carcinoma (HCC) and 6 as alcoholic liver injury without cirrhosis (Alc). Details of the patients including the positive ratio of hepatitis B surface antigen (HBsAg) and antibodies to hepatitis C virus (HCV) are summarized in Table 1.

Methods

Immunoglobulin complexed with AST was determined by counter-immunoelectrophoresis^[8] on Titan III (Helena Ltd, Tokyo, Japan). Electrophoresis was performed in barbiturate buffer (pH 8.5) at a constant voltage of 300 V for 10 min, and then plates were washed with 0.9% sodium chloride to remove non-precipitated proteins. After the enzyme was stained at 37 °C for 60 min (Kokusai reagent, Tokyo, Japan),

Table 1 Clinical findings of 128 patients with liver disease

	Number of cases	Sex (M:F)	Mean of age (yr)	Positive rate of HBsAg, <i>n</i> (%)	Positive rate of anti-HCV, <i>n</i> (%)
Alcoholic liver injury	6	5:1	57±6	0	0
Chronic hepatitis	67	45:22	52±13	11 (16.4)	49 (73.1)
Liver cirrhosis	45	29:16	56±10	8 (17.8)	26 (57.8)
Hepatocellular carcinoma	10	9:1	66±7	3 (30.0)	5 (50.0)

Table 2 Comparison of clinical findings between the patients with and without AST-IgA complex in serum

	AST-IgA complex in serum		<i>P</i>
	(-)	(+)	
Number of cases	59	69	
Sex (M:F)	40:19	48:21	NS
Mean of age (yr)	52±13	58±12	<0.01
Number of patients with positive HBsAg	12	10	NS
Number of patients with positive anti-HCV	33	47	NS
Number of patients with liver cirrhosis	18	37	<0.02

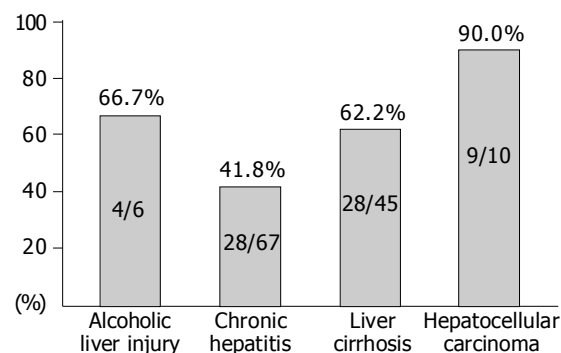
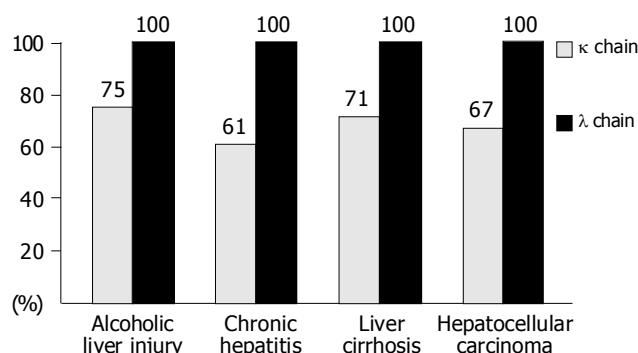
Table 3 Comparison of laboratory findings between the patients with and without AST-IgA complexes in serum (mean±SD)

	AST-IgA complex in serum		<i>P</i>
	(-)	(+)	
γ globulin (%)	21.0±5.8	24.5±6.5	<0.01
AST (IU/L)	55±25	115±50	<0.001
AST/ALT	1.16±0.56	1.37±0.61	<0.05
ChE (ΔpH)	0.79±0.25	0.61±0.27	<0.001
IgG (mg/dL)	1 980±568	2 211±532	NS
IgA (mg/dL)	299±150	397±195	<0.01
IgM (mg/dL)	178±114	195±101	NS

the plates were destained and fixed in 5% acetate. Anti-sera used to identify the immunoglobulin binding to AST were anti-immunoglobulin G (IgG), anti-immunoglobulin M (IgM), anti-immunoglobulin A (IgA), anti-Kappa chain and anti-lambda chain. The incidence of immunoglobulin-AST complexes and the types of immunoglobulin were discussed in various liver diseases. Furthermore, clinical findings and laboratory parameters were compared between patients with and without immunoglobulin-enzyme complexes. In this study, the data were expressed as mean±SD. Differences between mean values were tested for significance by Student's *t*-test and χ^2 test. $P<0.05$ was considered statistically significant.

Results

IgA was bound to AST. There were no complexes with IgG and IgM. Binding of IgA to AST was documented in 28 (41.8%) of 67 patients with CH, in 28 (62.2%) of 45 with LC, in 9 (90.0%) of 10 with HCC and 4 (66.7%) of 6 with Alc (Figure 1). When we investigated the type of immunoglobulin light chain that bound to AST, we found that AST-IgA complexes had binding to the kappa light chain in all patients. On the other hand, binding to the lambda light chain was documented in 61% of CH, 71% of LC,

**Figure 1** Incidence of AST-IgA complex in various liver diseases.**Figure 2** Investigation of light chains of AST-bound immunoglobulins in liver disease.

67% of HCC and 75% of Alc (Figure 2). When the clinical findings were compared between the patients with and without AST-IgA complexes (Table 2), there were no significant differences in sex, positive rates of HBsAg and anti-HCV. The incidence of LC in patients with AST-IgA complexes was 53.6%, which was significantly higher than 30.5% in patients without complexes ($P<0.02$). Comparisons of biochemical parameters among 69 patients with AST-IgA complexes and 59 without are summarized in Table 3. Gammaglobulin, AST, ALT, gamma-glutamyl transpeptidase and IgA in the patients with complexes were significantly higher than in those without complexes.

DISCUSSION

ALT and AST serum values have been widely used as sensitive laboratory parameters in clinical practice to evaluate the degree of liver injury^[10]. However, the serum values of these enzymes do not correctly reflect the degree of hepatic cell necrosis. Elevated serum AST and ALT may be observed when cells containing these enzymes are injured or the

permeability of cell membranes increases^[16]. Although serum levels of both ALT and AST are elevated when liver cells are injured, the degree of elevation is not parallel to the degree of injury. The mechanism of the elevation is affected by many factors, such as etiology of the liver disease or severity of the liver cell necrosis. The ratio of AST to ALT is a useful parameter, which can predict the severity of liver disease^[15]. On the other hand, some investigators^[17] have suggested that the ratio of AST/ALT is not useful in differentiating liver diseases because elevated AST/ALT is observed in many liver diseases. However, elevated AST/ALT ratio is sometimes observed in patients who heavily consume alcohol^[18]. When the ratio is over 2.0, alcoholic liver disease is strongly suspected. Furthermore, when the ratio is under 1.0, CH, chronic intrahepatic cholestasis or other liver diseases are suggested. Williams *et al.*^[17] reported that among patients who had chronic liver disease but no alcoholic aggravation, LC is suspected if the serum ratio of AST/ALT is over 1.0. The discrepancy in serum AST and ALT remains controversial. In general, the serum value of enzyme is regulated by factors such as degree of relapse from the organ containing large quantities of enzyme or degree of disappearance of enzyme from serum. The following mechanisms underlying the high AST/ALT values in patients with alcoholic liver disease have been speculated. (1) The injury to liver cell mitochondria in patients with alcoholic liver disease leads to dominant elevation of serum AST^[19]; (2) The production of aminotransferase in hepatocytes is more disturbed in ALT than in AST^[20]; (3) Patients are defined as having alcoholic liver disease based on pyridoxal 5' phosphatase deficiency, which is important in maintaining aminotransferase activity, especially that of ALT. Although these hypotheses can explain the mechanism of AST/ALT elevation in alcoholic liver disease, AST/ALT elevation cannot be elucidated in cirrhotic patients who do not consume alcohol. Williams *et al.*^[17] reported that in cirrhotic patients with elevated AST/ALT, there is impairment of AST excretion from kidney or the ability of AST intake in hepatic sinus is markedly disturbed. However, there are no reports to support their hypotheses. Enzymes, which in serum are sometimes complexed with serum immunoglobulin, might affect the elevation of serum enzyme activity. Binding of serum enzyme to serum immunoglobulin is well known in amylase, LDH, and ALP^[1-6]. Because AST is also complexed with immunoglobulins such as IgG and IgA^[7-12], markedly high values of serum AST are sometimes observed whether liver disease exists or not.

In this study, we have confirmed that binding of AST to immunoglobulin in liver disease is frequently encountered. Binding of AST to IgA was more frequently observed in LC than that in CH. The purpose of this study was to investigate whether complex formation of AST with serum immunoglobulin was related to the elevation of serum AST in LC. Based on the reports that the incidence of ALT-immunoglobulin complexes was lower in liver disease, it is suggested that the elevation of AST/ALT in LC is closely related to the binding of AST to serum immunoglobulin, especially to IgA. High serum IgA levels correlative with the progression of chronic and alcoholic liver diseases support this speculation. However, in this study there was

no significant difference in the incidence of complex formation of AST with IgA between LC and CH. This result cannot explain the mechanism of the elevated AST/ALT in LC. Finally, the activity of AST binding to IgA, the subclass of IgA and the degree of complex formation of ALT with immunoglobulin should be investigated.

REFERENCES

- 1 **Nagamine M**, Okuma S. Serum alkaline phosphatase isoenzymes linked to immunoglobulin G. *Clin Chim Acta* 1975; **65**: 39-46
- 2 **Crofton PM**, Smith AF. The properties and clinical significance of some electrophoretically slow forms of alkaline phosphatase. *Clin Chim Acta* 1978; **83**: 235-247
- 3 **Levitt MD**, Cooperband SR. Hyperamylasemia from the binding of serum amylase by an 11S IgA globulin. *N Engl J Med* 1968; **278**: 474-479
- 4 **Wilding P**, Cooke WT, Nicholson GI. Globulin bound amylase. A cause of persistently elevated levels in serum. *Ann Int Med* 1964; **60**: 1053-1056
- 5 **Urdal P**, Landaas S. Macro creatine kinase BB in serum, and some data on its prevalence. *Clin Chem* 1979; **25**: 461-465
- 6 **Biewenga J**, Feltkamp TE. LDH-IgA immunoglobulin complexes in human serum. *Clin Chim Acta* 1975; **58**: 239-249
- 7 **Weidner N**, Lott JA, Yale VD, Wahl RL, Little RA. Immunoglobulin-complexed aspartate aminotransferase. *Clin Chem* 1983; **29**: 382-384
- 8 **Nagamine M**, Okochi K. Complexes of immunoglobulins A and G with aspartate aminotransferase isoenzymes in serum. *Clin Chem* 1983; **29**: 379-381
- 9 **Kanemitsu F**. Aspartate aminotransferase-immunoglobulin G complexes in sera of two patients with acute hepatitis and immunoblastic lymphadenopathy. *Clin Chim Acta* 1986; **161**: 353-354
- 10 **Fex G**, Berntorp K. A circulating complex between ASAT and IgG in serum in an apparently healthy woman. *Clin Chim Acta* 1987; **164**: 11-15
- 11 **Kontinen A**, Murros J, Ojala K, Salaspuro M, Somer H, Rasanen J. A new cause of increased serum aspartate aminotransferase activity. *Clin Chim Acta* 1978; **84**: 145-147
- 12 **Nakajima M**, Ito K, Kuwa K, Nakayama T, Kitamura M. Occurrence of persistent elevated levels of serum glutamic oxaloacetic transaminase as a result of enzyme-immunoglobulin complex formation --with a report of two cases--. *Gastroenterol Jpn* 1980; **15**: 330-336
- 13 **Matama S**, Ito H, Tanabe S, Shibuya A, Shibata H, Saigenji K, Sakurai K, Hasegawa M. Immunoglobulin-complexed aspartate aminotransferase. *Intern Med* 1993; **32**: 156-159
- 14 **Stasia MJ**, Surla A, Renversez JC, Pene F, Morel-Femelez A, Morel F. Aspartate aminotransferase macroenzyme complex in serum identified and characterized. *Clin Chem* 1994; **40**: 1340-1343
- 15 **De Ritis F**, Coltorti M, Giusti G. Serum transaminase activities in liver disease. *Lancet* 1972; **1**: 685-687
- 16 **Kaplan MM**. Understanding serum enzyme tests in clinical liver disease. In: Davidson CS, ed. Problems in liver diseases. New York: Stratton Intercontinental Medical Book, 1979: 79-85
- 17 **Williams AL**, Hoofnagle JH. Ratio of serum aspartate to alanine aminotransferase in chronic hepatitis. Relationship to cirrhosis. *Gastroenterology* 1988; **95**: 734-739
- 18 **Cohen JA**, Kaplan MM. The SGOT/SGPT ratio- an indicator of alcoholic liver disease. *Dig Dis Sci* 1979; **24**: 835-838
- 19 **Nalpas B**, Vassault A, Le Guillou A, Lesgourgues B, Ferry N, Lacour B, Berthelot P. Serum activity of mitochondrial aspartate aminotransferase: a sensitive marker of alcoholism with or without alcoholic hepatitis. *Hepatology* 1986; **4**: 893-896
- 20 **Matloff DS**, Selinger MJ, Kaplan MM. Hepatic transaminase activity in alcoholic liver disease. *Gastroenterology* 1980; **78**: 1389-1392

• CLINICAL RESEARCH •

Efficacy of multislice computed tomography for gastroenteric and hepatic surgeries

Hiroshi Ohtani, Hidemi Kawajiri, Yuichi Arimoto, Koichi Ohno, Yasuhisa Fujimoto, Hiroko Oba, Kenji Adachi, Masaya Hirano, Shoichi Terakawa, Mitsuo Tsubakimoto

Hiroshi Ohtani, Hidemi Kawajiri, Yuichi Arimoto, Koichi Ohno, Yasuhisa Fujimoto, Department of Surgery, Osaka City Sumiyoshi Hospital, 1-2-16, Higashi-Kagaya, Suminoe-ku, Osaka 559-0012, Japan

Hiroko Oba, Kenji Adachi, Masaya Hirano, Department of Gastroenterology, Osaka City Sumiyoshi Hospital, 1-2-16, Higashi-Kagaya, Suminoe-ku, Osaka 559-0012, Japan

Shoichi Terakawa, Mitsuo Tsubakimoto, Department of Radiology, Osaka City Sumiyoshi Hospital, 1-2-16, Higashi-Kagaya, Suminoe-ku, Osaka 559-0012, Japan

Correspondence to: Dr. Hiroshi Ohtani, Department of Surgery, Osaka City Sumiyoshi Hospital, 1-2-16, Higashi-Kagaya, Suminoe-ku, Osaka 559-0012, Japan. m5051923@msic.med.osaka-cu.ac.jp
Telephone: +81-6-6681-1000 Fax: +81-6-6686-1547

Received: 2004-08-14 Accepted: 2004-10-18

Abstract

AIM: To determine the efficacy of multislice CT for gastroenteric and hepatic surgery.

METHODS: Dual-phase helical computed tomography was performed in 50 of 51 patients who underwent gastroenteric and hepatic surgeries. Twenty-eight, eighteen and four patients suffering from colorectal cancer, gastric cancer, and liver cancer respectively underwent colorectal surgery (laparoscopic surgery: 6 cases), gastrectomy, and hepatectomy. Three-dimensional computed tomography imaging of the inferior mesenteric artery, celiac artery and hepatic artery was performed. And in the follow-up examination of postoperative patients, multiplanar reconstruction image was made in case of need.

RESULTS: Scans in 50 patients were technically satisfactory and included in the analysis. Depiction of major visceral arteries, which were important for surgery and other treatments, could be done in all patients. Preoperative visualization of the left colic artery and sigmoidal arteries, the celiac artery and its branches, and hepatic artery was very useful to lymph node dissection, the planning of a reservoir and hepatectomy. And multiplanar reconstruction image was helpful to diagnosis for the postoperative follow-up of patients.

CONCLUSION: Three-dimensional volume rendering or multiplanar reconstruction imaging performed by multislice computed tomography was very useful for gastroenteric and hepatic surgeries.

Key words: Multislice CT; Three-dimensional CT; MPR; Gastroenteric surgery; Hepatic surgery

Ohtani H, Kawajiri H, Arimoto Y, Ohno K, Fujimoto Y, Oba H, Adachi K, Hirano M, Terakawa S, Tsubakimoto M. Efficacy of multislice computed tomography for gastroenteric and hepatic surgeries. *World J Gastroenterol* 2005; 11(10): 1532-1534
<http://www.wjgnet.com/1007-9327/11/1532.asp>

INTRODUCTION

Computed tomography (CT) is one of the most useful imaging techniques for the evaluation of original and metastatic lesions in gastroenteric and hepatic cancer. Contrast-enhanced CT (CECT) in particular has extraordinary precision. At our hospital, CECT is routinely performed to screen intra-abdominal malignancies. Recently, a helical CT scanner was developed, which permits scanning of the whole abdomen in a single breath-hold in each scanning phase. Multislice helical CT, which performs multiplanar reconstruction (MPR), maximum intensity projection (MIP), and shaded surface display (SSD), was first used at our institution in November of 2002^[1,2]. Arterial phase helical CT can immediately display the major visceral arteries, such as the celiac artery (CA), superior mesenteric artery (SMA), inferior mesenteric artery (IMA), and hepatic artery (HA)^[3-5]. Preoperative visualization of these vessels is useful for lymph node dissection, preservation of the left colic artery (LCA), planning of the reservoir, and hepatectomy.

MATERIALS AND METHODS

Dual-phase helical CT was performed with a high-speed scanner (Aquilion M8, Toshiba Medical Systems Co., Ltd., Tokyo, Japan) on 50 patients (28 male and 22 female) between December of 2002 and July of 2004. The ages of the patients ranged from 36 to 81 years (mean 65.9). One patient was unable to undergo CECT due to renal dysfunction. Twenty-eight, eighteen and four patients suffering from colorectal cancer, gastric cancer and liver cancer respectively underwent colorectal surgery (laparoscopic surgery: 6 cases), gastrectomy and hepatectomy respectively. A 20-gauge cannula was inserted into an antecubital and dual-phase helical CT was then performed after power injection of 1.5 mL/kg of iohexol at a rate of 3 mL/s. An automatic bolus-tracking program (Surestart, Toshiba Medical) was used to automatically start the arterial phase scan after the injection of iohexol. The CT values of

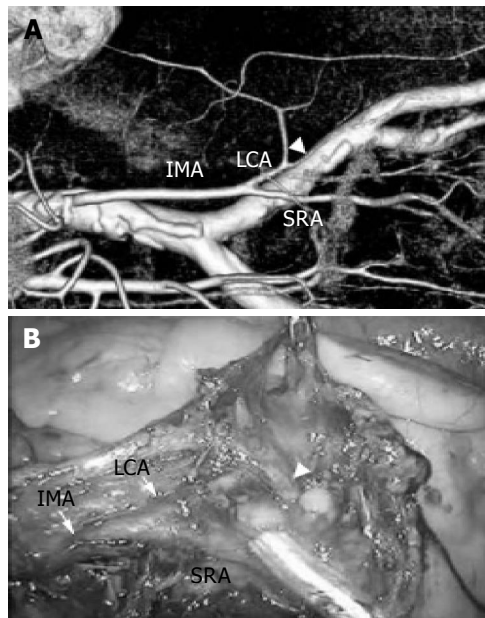


Figure 1 A case of sigmoid colon cancer who underwent a laparoscopic sigmoidectomy. **A:** Three-dimensional volume-rendered CT (3DCT) angiographic reconstructions show the IMA and its branches; **B:** The intraoperative findings similar to the preoperative visualization of the IMA were obtained. White arrowheads show the sigmoidal artery.

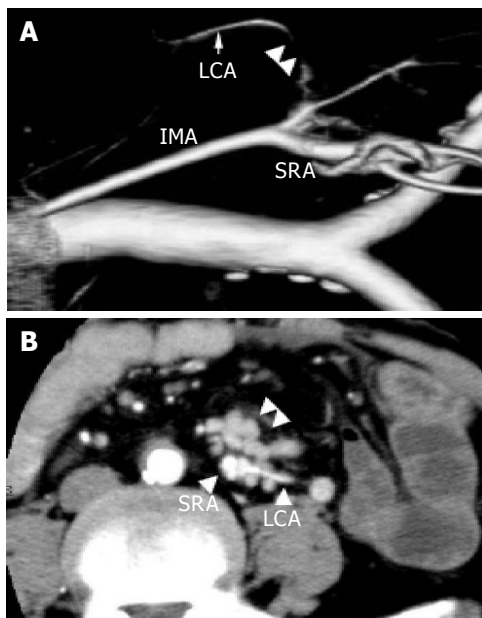


Figure 2 **A:** 3DCT image of the LCA is partially indistinct (two arrowheads); **B:** Swollen lymph nodes adhered to the LCA (two arrowheads).

the region of interest specified in the abdominal aorta were automatically calculated. The trigger for starting the diagnostic scan was set at an increase in aortic enhancement of 50 H, and the arterial phase helical CT scan started automatically at 17 s after the trigger level had been reached. Late phase scanning was initiated at 60 s after the arterial phase scan^[6]. After the state of the original region was estimated, metastatic or other lesions were examined. During each phase, scanning was performed in a single breath-hold.

Dual-phase helical CT data were then transferred to a Zio M900 workstation (ZioSoft, Inc., Morgan Hill, CA, USA), and three-dimensional CT (3DCT) images of IMA, CA or HA were reconstructed. Bones, large untargeted vessels and background tissues could be eliminated from the image. If necessary, the MPR or MIP image was reconstructed.

Dual phase helical CT is often performed to follow up postoperative patients, too. It is useful in diagnosis and screening.

RESULTS

Before surgery for sigmoid colon or rectal cancer, 3DCT of the IMA was performed for dissection of the lymph nodes around the root of the IMA. In all patients except two, the LCA was easily preserved in open and laparoscopic surgery (Figure 1). In the two cases, the root of the IMA was resected because macroscopically metastatic lymph nodes adhered to the LCA. The adhesion had been preoperatively identified on 3DCT (Figure 2) and was confirmed in intraoperative findings. In one patient, a slight deformity of the SRA was noticed (Figure 3), but preoperative 3DCT enabled us to recognize the superior rectal artery (SRA) and LCA easily. In gastrectomy for gastric cancer, CT imaging was useful in examining the variation of the major vessels. Preoperative visualization of the common hepatic artery (CHA) diverging from the SMA (Figure 4A), and of the right hepatic artery (RHA) branching from the SMA (Figure 4B) was extremely helpful in lymph node dissection and in the planning of a reservoir in cases of multiple metastatic liver cancer. In hepatectomy, 3DCT was of particular use in a patient who could not undergo angiography due to severe arteriosclerosis (Figure 5).

It was difficult to distinguish in the axial view whether a patient who underwent right hemicolectomy for ascending colon cancer suffered from dissemination or liver metastases (Figure 6A), however, he was diagnosed with dissemination by MPR image (Figure 6B).

DISCUSSION

Multislice CT has many merits including the short scanning time^[7,8], ease of data acquisition for 3D volume rendering, MPR, SSD and MIP performance. In gastroenteric and hepatic surgery, multislice CT is highly useful, particularly for preoperative visualization of the regional arteries, and in gastroenteric surgery visualization of the major visceral arteries is extremely helpful in lymph node dissection in open and laparoscopic surgery. Until recently, preoperative definition of the vascular anatomy was achieved by conventional catheter angiography. However, at our hospital, dual-phase helical CT during the arterial and late phases of contrast material enhancement is now performed before gastroenteric and hepatic surgery. In resection of advanced sigmoid colon and rectal cancer, we routinely dissect the lymph nodes around the root of the IMA while preserving the LCA because resection of the root of the IMA occasionally causes ischemia of the oral side of the sigmoid colon, sometimes leading to anastomotic leakage^[9]. In gastrectomy, preoperative imaging of arterial anomalies such as the anomalous RHA or the CHA arising from the SMA

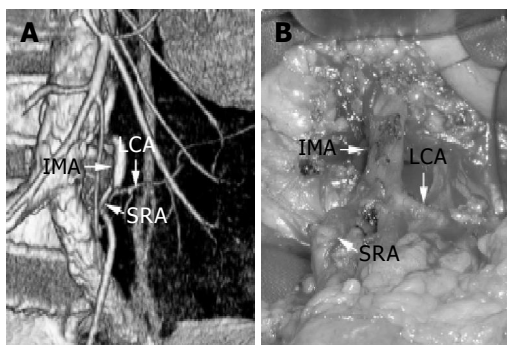


Figure 3 A: A slight deformity of the SRA was showed by 3DCT; B: In intraoperative findings, a slight deformity of the SRA was confirmed.

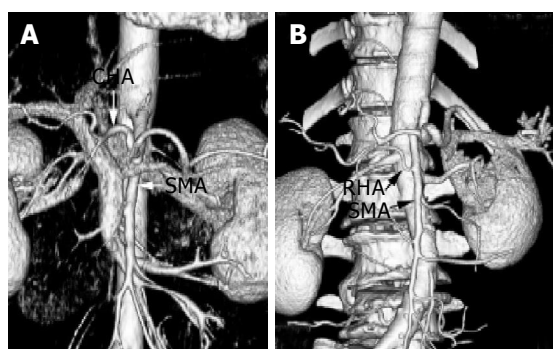


Figure 4 3DCT scans showed the CHA diverging from the SMA (A) and the RHA branching from the SMA (B).

is helpful in lymph node dissection and in planning the reservoir in cases of metastatic liver cancer. It is important to recognize the anomalous left hepatic artery arising from the left gastric artery in lymph node dissection, and in hepatic surgery, imaging of the HA is important. 3DCT is especially useful in patients who cannot undergo angiography due to certain conditions such as severe arteriosclerosis.

Intra-abdominal lesions are screened in the axial view by dual-phase helical CT at our hospital. In some cases, additional MPR such as sagittal or coronal view is helpful to identify the specific condition of a tumor.

In the present study, we found no disagreement between 3DCT images and findings upon operation. 3DCT is able to show exactly the surrounding vascular structures and it is minimally invasive compared to conventional catheter angiography^[10]. 3D volume-rendered image reconstruction such as MPR, SSD and MIP is easily and immediately acquired after the axial CT data are transferred to the Zio M900 workstation. 3DCT is a relatively simple technique, which provides many advantages, and dual-phase helical CT is useful not only in diagnosis and screening, but also in follow-up examination of postoperative patients.

In the future, 3DCT will prove to be essential in gastroenteric and hepatic surgeries.

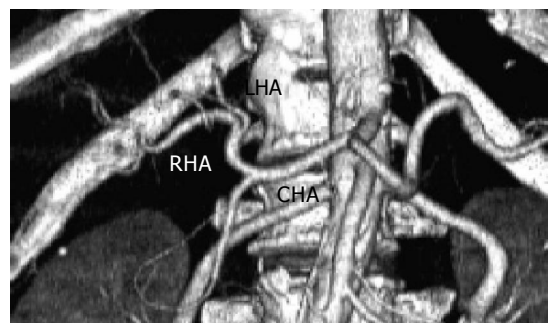


Figure 5 A case of hepatocellular carcinoma who could not undergo angiography due to severe arteriosclerosis. Preoperative visualization of the HA was obtained.

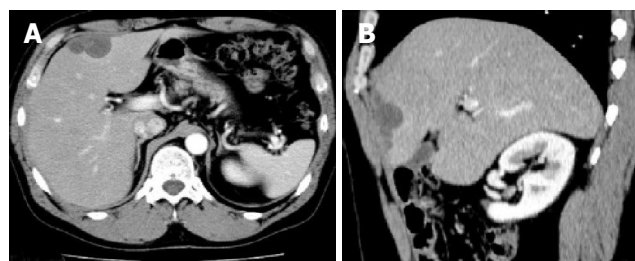


Figure 6 The follow-up patient who underwent right hemicolectomy for ascending colon cancer: A: In the axial view, it was difficult to distinguish whether low density area (LDA) in the lateral segment of the liver was dissemination or liver metastasis; B: The LDA was diagnosed as dissemination by MPR image (a sagittal view).

REFERENCES

- 1 Hu H. Multi-slice helical CT: scan and reconstruction. *Med Phys* 1999; **26**: 5-18
- 2 Hong KC, Freeny PC. Pancreaticoduodenal arcades and dorsal pancreatic artery: comparison of CT angiography with three-dimensional volume rendering, maximum intensity projection, and shaded-surface display. *AJR Am J Roentgenol* 1999; **172**: 925-931
- 3 Chong M, Freeny PC, Schmiedl UP. Pancreatic arterial anatomy: depiction with dual-phase helical CT. *Radiology* 1998; **208**: 537-542
- 4 Winter TC, Freeny PC, Nghiem HV, Hommeyer SC, Barr D, Croghan AM, Coldwell DM, Althaus SJ, Mack LA. Hepatic arterial anatomy in transplantation candidates: evaluation with three-dimensional CT arteriography. *Radiology* 1995; **195**: 363-370
- 5 Smith PA, Klein AS, Heath DG, Chavin K, Fishman EK. Dual-phase spiral CT angiography with volumetric 3D rendering for preoperative liver transplant evaluation: preliminary observations. *J Comput Assist Tomogr* 1998; **22**: 868-874
- 6 Kim T, Murakami T, Hori M, Takamura M, Takahashi S, Okada A, Kawata S, Cruz M, Federle MP, Nakamura H. Small hypervascular hepatocellular carcinoma revealed by double arterial phase CT performed with single breath-hold scanning and automatic bolus tracking. *AJR Am J Roentgenol* 2002; **178**: 899-904
- 7 Heiken JP, Brink JA, Vannier MW. Spiral (helical) CT. *Radiology* 1993; **189**: 647-656
- 8 Zeman RK, Fox SH, Silverman PM, Davros WJ, Carter LM, Griego D, Weltman DL, Ascher SM, Cooper CJ. Helical (spiral) CT of the abdomen. *AJR Am J Roentgenol* 1993; **160**: 719-725
- 9 Okuda J, Tanigawa N. Laparoscopic surgery for rectal and sigmoid colon cancer. *Nihon Rinsho* 2003; **61** Suppl 7: 391-395
- 10 Bluemke DA, Chambers TP. Spiral CT angiography: an alternative to conventional angiography. *Radiology* 1995; **195**: 317-319

• CLINICAL RESEARCH •

Hypoxia-inducible factor 1 alpha and vascular endothelial growth factor overexpression in ischemic colitis

Tomoyuki Okuda, Takeshi Azuma, Masahiro Ohtani, Ryuho Masaki, Yoshiyuki Ito, Yukinao Yamazaki, Shigeji Ito, Masaru Kuriyama

Tomoyuki Okuda, Takeshi Azuma, Yoshiyuki Ito, Masaru Kuriyama, Second Department of Internal Medicine, Faculty of Medical Sciences, University of Fukui, Matsuoka-cho, Fukui 9101193, Japan

Masahiro Ohtani, Yukinao Yamazaki, Department of Endoscopic Medicine, Faculty of Medical Sciences, University of Fukui, Matsuoka-cho, Fukui 9101193, Japan

Ryuho Masaki, Shigeji Ito, Department of Internal Medicine, Tannan Regional Medical Center, Sabae, Fukui 9168515, Japan

Correspondence to: Takeshi Azuma, M.D., Second Department of Internal Medicine, Faculty of Medical Sciences, University of Fukui, Matsuoka-cho, Yoshida-gun, Fukui 9101193, Japan. azuma@fmsrsa.fukui-med.ac.jp

Telephone: +81-776-61-8351 Fax: +81-776-61-8110

Received: 2004-08-24 Accepted: 2004-12-01

Okuda T, Azuma T, Ohtani M, Masaki R, Ito Y, Yamazaki Y, Ito S, Kuriyama M. Hypoxia-inducible factor 1 alpha and vascular endothelial growth factor overexpression in ischemic colitis. *World J Gastroenterol* 2005; 11(10): 1535-1539

<http://www.wjgnet.com/1007-9327/11/1535.asp>

INTRODUCTION

Ischemic colitis is a vascular condition of inadequate blood flow in the colon, which leads to colonic inflammation and can produce significant morbidity and mortality. Two well-known risks -factors of ischemic colitis are vascular factors and bowel factors^[1,2]. The vascular factors are related to systemic arteriosclerosis based on hypertension, diabetes mellitus, hyperlipidemia and thrombus, embolus, and vasculitis. It is also associated with hypovolemia, hypotension and the use of vasoconstricting drugs^[1,3]. The bowel factors are colon spasm, constipation, fecal impaction and prior history of abdominal surgery^[1,2]. The well-known pathological findings are degeneration, decudation, necrosis, regeneration of the epithelial layer, congestion, fibrin thrombus in blood capillaries, leukocyte invasion in the lamina propria and bleeding, edema, and exudates in the submucosal layer^[4]. Ischemic crisis is believed to occur in the tissue in ischemic colitis. However, there is no precise pathophysiological examination for so called "ischemic crisis" in this disease.

Drastic adaptation reactions are quickly induced to maintain homeostasis and preserve life, when the tissues are in an ischemic condition. Recently, several important discoveries have been made; the detection of hypoxia inducible factor 1 alpha (HIF-1 alpha and vascular endothelial growth factor (VEGF)^[5,6]. Increased concentrations of intracellular HIF-1 alpha molecules occur after hypoxia as a result of reduced degradation by the ubiquitin proteasome pathway^[7,8]. Binding HIF-1 alpha to the hypoxia response element of several "HIF-regulated genes" results in the increased transcription of several proteins involved in angiogenesis, glycolysis, erythropoiesis, the inhibition of apoptosis, and monocyte-related inflammation^[9,10]. VEGF is one of the most important factors for angiogenesis. VEGF is produced by the promoter signals from the HIF-1 alpha complex, secreted as a paracrine factor to the extracellular space, and binds to specific receptors, KDR/Flk-1^[11-13]. The signal transduction after self-phosphorylation of the VEGF receptor leads to angiogenesis due to endothelial cell proliferation^[14].

The aim of the present study was to examine the etiology

Abstract

AIM: To examine the etiology and pathophysiology in human ischemic colitis from the viewpoint of ischemic factors such as hypoxia-inducible factor 1 alpha (HIF-1 alpha and vascular endothelial growth factor (VEGF).

METHODS: Thirteen patients with ischemic colitis and 21 normal controls underwent colonoscopy. The follow-up colonoscopy was performed in 8 patients at 7 to 10 d after the occurrence of ischemic colitis. Biopsy samples were subjected to real-time RT-PCR and immunohistochemistry to detect the expression of HIF-1 alpha and VEGF.

RESULTS: HIF-1 alpha and VEGF expression were found in the normal colon tissues by RT-PCR and immunohistochemistry. HIF-1 alpha and VEGF were overexpressed in the lesions of ischemic colitis. Overexpressed HIF-1 alpha and VEGF RNA quickly decreased to the normal level in the scar regions at 7 to 10 d after the occurrence of ischemic colitis.

CONCLUSION: Constant expression of HIF-1 alpha and VEGF in normal human colon tissue suggested that HIF-1 alpha and VEGF play an important role in maintaining tissue integrity. We confirmed the ischemic crisis in ischemic colitis at the molecular level, demonstrating overexpression of HIF-1 alpha and VEGF in ischemic lesions. These ischemic factors may play an important role in the pathophysiology of ischemic colitis.

© 2005 The WJG Press and Elsevier Inc. All rights reserved.

Key words: Ischemic colitis; HIF-1 alpha; VEGF

and pathophysiology in human ischemic colitis from the viewpoint of these ischemic factors.

MATERIALS AND METHODS

Thirteen patients with ischemic colitis diagnosed by endoscopy (3 males and 10 females, mean age 63.2) participated in the present study. The ischemic lesion was located from the descending to the sigmoid colon in twelve cases and from the ascending to the transverse colon in one case. A total of three biopsy specimens (two from the lesion and one from normal rectal mucosa) were taken from each patient. One tissue specimen from the lesion and one from the normal rectal mucosa were put into a 1.5 mL Microfuge tube with 100 uL of RNA stabilizer agent (RNAlater, Qiagen, Valencia, CA, USA), stored at -80 °C, and subjected to real-time RT-PCR analysis. One specimen from the lesion was fixed in 10% buffered formalin (pH 7.2). Ordinary paraffin sections were cut, stained with hematoxylin and eosin and subjected to histological analysis. The follow-up colonoscopy was performed in 8 patients at 7-10 d after the first endoscopy. In these cases, two biopsy specimens (one for real-time RT-PCR and one for histological analysis) were taken from the cured lesion. Twenty-one normal controls (14 males and 7 females, mean age 67.1) were also chosen from subjects, who received total colonoscopy for colon cancer screening, performed by the Second Department of Internal Medicine, Faculty of Medical Sciences, University of Fukui or Department of Internal Medicine, and Tannan Regional Medical Center. All normal controls had normal findings in total colonoscopy. A total of eight biopsy specimens (two from the terminal ileum, two from the ascending colon, two from the descending colon and two from the rectum) were taken from normal controls. One specimen from each region was subjected to real-time RT-PCR and one to histology. This work was performed according to the principles of the Declaration of Helsinki and consent was obtained from each individual after a full description of the nature and protocol of the study.

Real-time quantitative PCR analysis

The tissue specimens were homogenized and an RNA extracted using RNA extraction kit (RNeasy Mini Kit, Qiagen, Valencia, CA, USA), according to the manufacturer's protocol. HIF-1 alpha and VEGF expression levels were assessed by real-time quantitative RT-PCR methods with the ABI prism 7700 system (TaqMan PCR, Applied Biosystems, Foster city, CA, USA) using Assays-on-Demand primers and probe sets Hs00153153m1 and Pre-developed TaqMan Assay reagent 4339277F respectively. The thermal cycling conditions included 48 °C for 30 min and 95 °C for 10 min, followed by 50 cycles of amplification at 95 °C

for 15 s and 60 °C for one minute. The PCR products were also examined by 2% agarose gel electrophoresis. The gels were stained with ethidium bromide to confirm successful amplification of the expected sequences. Human glyceraldehydes-3-phosphate dehydrogenase (GAPDH) RNA was measured as a control using Pre-developed TaqMan Assay reagent 4310884E (Applied Biosystems, Foster City, CA, USA). RNA for GAPDH was used as an endogenous control. The amount of HIF-1 alpha or VEGF RNA was normalized to the level of GAPDH by the ratio of HIF-1 alpha or VEGF to GAPDH.

Immunohistochemistry

HIF-1 alpha and VEGF expression were analyzed using a DAKO Envision plus kit (Dako Cytomation, Carpinteria, CA, USA). The primary antibodies used in this study were sc-10790 (rabbit, 1:50 dilution) (Santa Cruz Biotechnology, Santa Cruz, CA, USA) for HIF-1 alpha and sc-152 (rabbit, 1:25 dilution) (Santa Cruz Biotechnology, Santa Cruz, CA) for VEGF. Sections (4 um thick) were dewaxed and endogenous peroxidase activity was quenched with 3% H₂O₂ for 30 min. Antigen retrieval was achieved by heat treatment at 70 °C for 3 h. Sections were incubated with a blocking agent (Protein Block Serum-free: ×0909, Dako Cytomation, Carpinteria, CA, USA) for 20 min to reduce non-specific reactions. After washing with tris buffered saline (TBS), the primary antibodies were applied for 2 h and washed in TBS. Sections were incubated with a secondary goat anti-rabbit antibody for 60 min and washed in TBS. The color was developed by 7 min incubation with DAB solution and the sections were weakly counterstained with hematoxylin. Normal rabbit immunoglobulin G was substituted for the primary antibody as the negative control at the same concentration. As positive controls, we used advanced gastric or colon cancer cases with intense cancer cells of HIF-1 alpha and VEGF expression.

Statistical analysis

Statistical analysis was performed using the Statistical Package for the Biosciences (SPBS) version 9.44 software (Murata, Kyoto, Japan). Differences among groups were assessed using the non-parametric Mann-Whitney *U* test and the Kruskal-Wallis rank-sum test. Significance was set at *P*<0.05.

RESULTS

HIF-1 alpha and VEGF RNA in the normal colon tissues

HIF-1 alpha and VEGF PCR products were found in the normal colon tissues (Figure 1) and the relative amounts of expression in each region of the colon were shown in Table 1. There were no significant differences in the expression levels among the regions.

Table 1 HIF-1 alpha and VEGF RNA expression in the normal colon tissues

	Terminal ileum	Ascending colon	Descending colon	Rectum	<i>P</i> ¹
HIF-1 alpha/GAPDH	1.18±0.45	1.01±0.38	1.12±0.49	1.40±0.71	0.180 (NS)
VEGF/GAPDH	2.49±2.61	1.32±0.98	1.54±1.26	1.55±1.28	0.479 (NS)

¹Kruskal-Wallis rank-sum test.

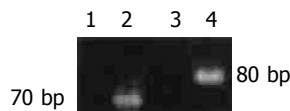


Figure 1 RT-PCR analysis of HIF-1 alpha (lane 1: negative control; lane 2: rectal mucosa) and VEGF (lane 3: negative control; lane 4: rectal mucosa).

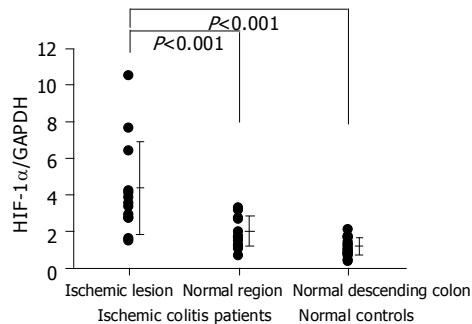


Figure 2 HIF-1 alpha RNA expression levels in the colon tissues.

Quantitative analysis of HIF-1 alpha and VEGF RNA in the colon tissues of patients with ischemic colitis

HIF-1 alpha was overexpressed in the lesions of ischemic colitis patients. The relative amounts of HIF-1 alpha RNA levels were significantly higher in the ischemic lesions than in the normal region in the same patient or in the normal descending colon tissues of the normal controls (Figure 2). VEGF was also overexpressed in the lesions of ischemic colitis patients. The relative amounts of VEGF RNA levels were significantly higher in the ischemic lesions than in a normal region in the same patient or in the normal descending colon tissues of the normal controls (Figure 3).

The colonoscopic findings returned to almost the normal state with scars at 7 to 10 d after the occurrence of ischemic colitis. Overexpressed HIF-1 alpha and VEGF RNA quickly decreased to normal levels in the scar regions (Figure 4).

Immunohistochemical analysis

Weak HIF-1 alpha or VEGF immunoreactive cells were scattered in epithelial and interstitial cells in normal colon tissue (Figure 5A, B). In contrast, strong HIF-1 alpha or VEGF immunoreactive cells were diffusely seen in the epithelial and interstitial cells, including inflammatory cells in the ischemic colitis lesions (Figure 5C, D).

DISCUSSION

The first ischemic colitis report was a case report by Boley *et al*^[15] in 1963, which founded the concept that was later accurately classified by Marston *et al*^[16] in 1966. It has since become a well-recognized clinical entity. Most patients experience a sudden onset of mild, left-sided lower abdominal pain. Hematochezia may occur within 24 h. The most susceptible areas of the colon to ischemic damage are the “watershed regions”, which include the splenic flexure, descending and sigmoid colons. The endoscopic features are non-specific; erythematous and edematous mucosa,

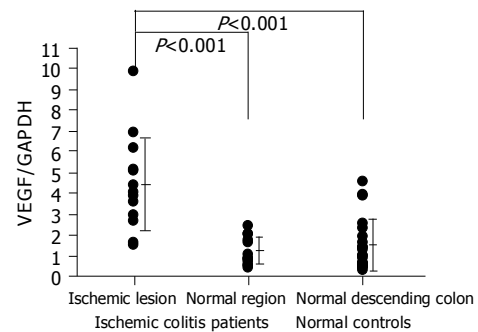


Figure 3 VEGF RNA expression levels in the colon tissues.

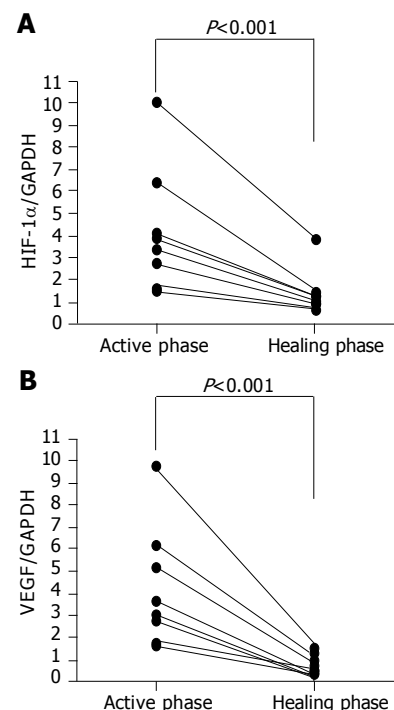


Figure 4 HIF-1 alpha and VEGF RNA expression levels in the colon tissues in the active and healing phases of ischemic colitis.

submucosal hemorrhages, and scattered areas of mucosal ulceration^[1]. The well known pathological findings are degeneration, decidual, necrosis, regeneration of the epithelial layer, congestion, fibrin thrombus in blood capillaries, leukocyte invasion in the lamina propria and bleeding, edema and exudates in the submucosal layer^[4]. Ischemic crisis is believed to occur in ischemic colitis tissue. However, there is no precise pathophysiological examination for so-called “ischemic crisis” in this disease.

Semenza *et al*^[5,17] discovered a new transcriptional factor; HIF-1 alpha in 1995. HIF-1 alpha is induced by tissue ischemia and promotes gene transcription^[18]. HIF-1 alpha increases and activates some important proteins and enzymes, providing a strong defense against apoptosis subsequent to severe hypoxia. HIF-1 alpha has important roles in the production of erythropoietin in the kidneys, induction of anaerobic glycolysis, angiogenesis via VEGF and activation of myeloid cell-mediated inflammatory reactions^[9,10]. Senger *et al*^[19] reported a vascular permeability factor (VPF) in 1983 and Ferrara *et al*^[20,23] independently identified a new

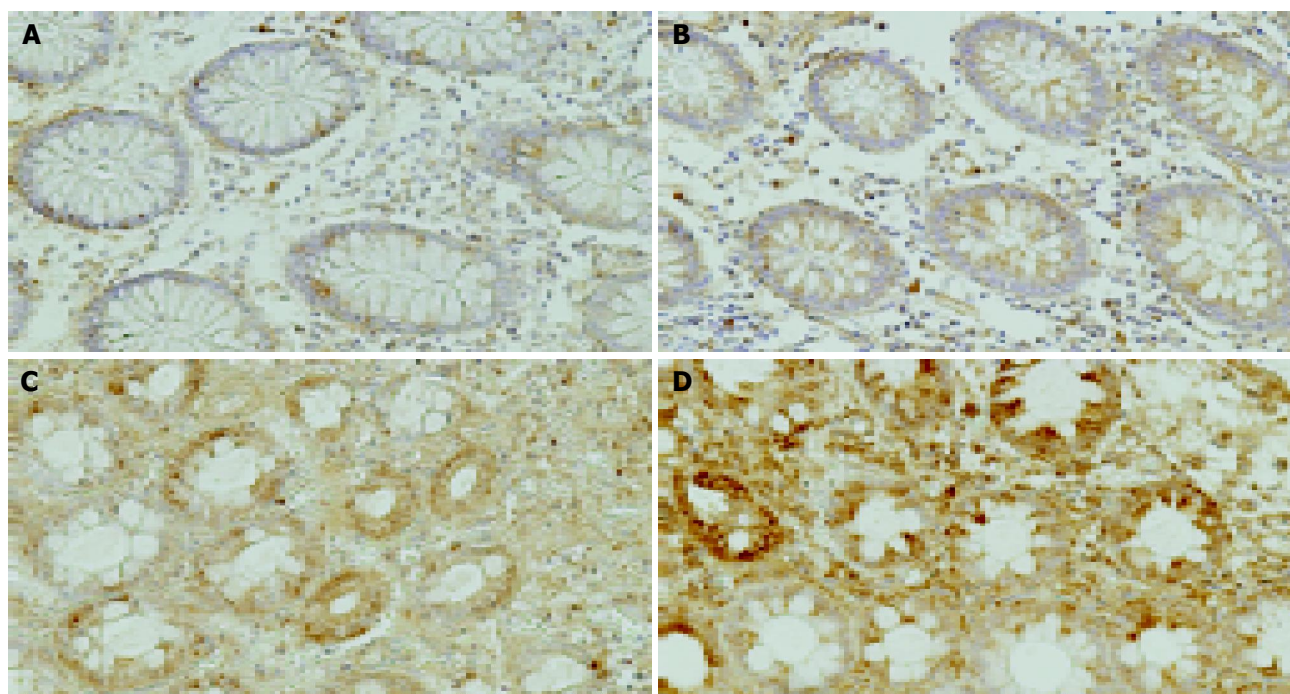


Figure 5 Immunostaining of HIF-1 alpha or VEGF in the colon tissues. Weak HIF-1 alpha or VEGF immunoreactive cells were scattered in epithelial cells and interstitial cells in normal colon tissue (A: HIF-1 alpha; B: VEGF). In contrast, strong HIF-1 alpha or VEGF immunoreactive cells were diffusely seen in the epithelial and intestinal cells, including inflammatory cells in the ischemic colitis lesions (C: HIF-1 alpha; D: VEGF). Scale bars represent 100 μ m.

angiogenic factor called VEGF in 1989. VEGF was the same as VPF, and it has been accepted that VEGF is one of the most important factors for angiogenesis^[6]. VEGF has the functions of epithelial cell floating, proliferation and increasing the vascular permeability. VEGF is produced by the promoter signals from the HIF-1 alpha complex, secreted as a paracrine factor to extracellular space and binds to specific receptors, KDR/Flk-1 and Flt-1^[12,13]. Then, the endothelial cell proliferation is promoted and finally angiogenesis is achieved under the hypoxic condition. In the present study, we demonstrated that two ischemic factors, HIF-1 alpha and VEGF, were constantly expressed in human colon tissue and were overexpressed in the ischemic colitis lesions. Our findings are the first molecular evidence of ischemia in ischemic colitis.

In addition, the overexpressed HIF-1 alpha and VEGF in the acute phase of ischemic colitis decreased to normal levels after 7 to 10 d. The colonoscopic findings also showed scarring in the lesion. These drastic changes suggest that when the ischemic crisis occurred, HIF-1 alpha and VEGF were induced immediately to prevent the expansion of tissue damage and to start quick repair to damaged tissue. Subsequently, these ischemic factors finished their role and their expression decreased to the ordinary state after the tissue recovered. This rapid change in the expression seems to differ from the continuous overexpression in inflammatory bowel disease^[21,22].

We confirmed the ischemic crisis in ischemic colitis at the molecular level by analyzing the expression of HIF-1 alpha and VEGF. These ischemic factors may play an important role in the pathophysiology of ischemic colitis. We also demonstrated that HIF-1 alpha and VEGF were

constantly expressed in normal human colon tissue including terminal ileum. The expression level of these factors was the same among regions of the colon, even though it is the descending colon where ischemic changes often occur. These ischemic factors were seen in epithelial cells and submucosal components. These results suggested that HIF-1 alpha and VEGF may play important roles in maintaining tissue integrity by regulating the delicate balance between proliferation and apoptosis. Further analysis of the function of these ischemic factors in the pathophysiology of the disease will be necessary in the future.

REFERENCES

- 1 **Sreenarasimhaiah J.** Diagnosis and management of intestinal ischaemic disorders. *BMJ* 2003; **326**: 1372-1376
- 2 **MacDonald PH.** Ischaemic colitis. *Best Pract Res Clin Gastroenterol* 2002; **16**: 51-61
- 3 **Hunt RH, Buchanan JD.** Transient ischaemic colitis--colonoscopy and biopsy in diagnosis. *J R Nav Med Serv* 1979; **65**: 15-19
- 4 **Habu Y, Tahashi Y, Kiyota K, Matsumura K, Hirota M, Inokuchi H, Kawai K.** Reevaluation of clinical features of ischemic colitis. Analysis of 68 consecutive cases diagnosed by early colonoscopy. *Scand J Gastroenterol* 1996; **31**: 881-886
- 5 **Wang GL, Jiang BH, Rue EA, Semenza GL.** Hypoxia-inducible factor 1 is a basic-helix-loop-helix-PAS heterodimer regulated by cellular O₂ tension. *Proc Natl Acad Sci USA* 1995; **92**: 5510-5514
- 6 **Shibuya M.** Role of VEGF-flt receptor system in normal and tumor angiogenesis. *Adv Cancer Res* 1995; **67**: 281-316
- 7 **Huang LE, Gu J, Schau M, Bunn HF.** Regulation of hypoxia-inducible factor 1 alpha is mediated by an O₂-dependent degradation domain via the ubiquitin-proteasome pathway. *Proc Natl Acad Sci USA* 1998; **95**: 7987-7992
- 8 **Kallio PJ, Pongratz I, Gradin K, McGuire J, Poellinger L.**

- Activation of hypoxia-inducible factor 1 alpha: posttranscriptional regulation and conformational change by recruitment of the Arnt transcription factor. *Proc Natl Acad Sci USA* 1997; **94**: 5667-5672
- 9 **Semenza GL**. Hypoxia-inducible factor 1: master regulator of O₂ homeostasis. *Curr Opin Genet Dev* 1998; **8**: 588-594
- 10 **Cramer T**, Yamanishi Y, Clausen BE, Forster I, Pawlinski R, Mackman N, Haase VH, Jaenisch R, Corr M, Nizet V, Firestein GS, Gerber HP, Ferrara N, Johnson RS. HIF-1 alpha is essential for myeloid cell-mediated inflammation. *Cell* 2003; **112**: 645-657
- 11 **Forsythe JA**, Jiang BH, Iyer NV, Agani F, Leung SW, Koos RD, Semenza GL. Activation of vascular endothelial growth factor gene transcription by hypoxia-inducible factor 1. *Mol Cell Biol* 1996; **16**: 4604-4613
- 12 **Millauer B**, Wizigmann-Voos S, Schnurch H, Martinez R, Moller NP, Risau W, Ullrich A. High affinity VEGF binding and developmental expression suggest Flk-1 as a major regulator of vasculogenesis and angiogenesis. *Cell* 1993; **72**: 835-846
- 13 **Hiratsuka S**, Minowa O, Kuno J, Noda T, Shibuya M. Flt-1 lacking the tyrosine kinase domain is sufficient for normal development and angiogenesis in mice. *Proc Natl Acad Sci USA* 1998; **95**: 9349-9354
- 14 **Takahashi T**, Ueno H, Shibuya M. VEGF activates protein kinase C-dependent, but Ras-independent Raf-MEK-MAP kinase pathway for DNA synthesis in primary endothelial cells. *Oncogene* 1999; **18**: 2221-2230
- 15 **Boley SJ**, Schwartz S, Lash J, Sternhill V. Reversible vascular occlusion of the colon. *Surg Gynecol Obstet* 1963; **116**: 53-60
- 16 **Marston A**, Pheils MT, Thomas ML, Morson BC. Ischaemic colitis. *Gut* 1966; **7**: 1-15
- 17 **Semenza GL**, Wang GL. A nuclear factor induced by hypoxia via de novo protein synthesis binds to the human erythropoietin gene enhancer at a site required for transcriptional activation. *Mol Cell Biol* 1992; **12**: 5447-5454
- 18 **Furuta GT**, Turner JR, Taylor CT, Hershberg RM, Comerford K, Narravula S, Podolsky DK, Colgan SP. Hypoxia-inducible factor 1-dependent induction of intestinal trefoil factor protects barrier function during hypoxia. *J Exp Med* 2001; **193**: 1027-1034
- 19 **Senger DR**, Galli SJ, Dvorak AM, Perruzzi CA, Harvey VS, Dvorak HF. Tumor cells secrete a vascular permeability factor that promotes accumulation of ascites fluid. *Science* 1983; **219**: 983-985
- 20 **Leung DW**, Cachianes G, Kuang WJ, Goeddel DV, Ferrara N. Vascular endothelial growth factor is a secreted angiogenic mitogen. *Science* 1989; **246**: 1306-1309
- 21 **Giatromanolaki A**, Sivridis E, Maltezos E, Papazoglou D, Simopoulos C, Gatter KC, Harris AL, Koukourakis MI. Hypoxia inducible factor 1 alpha and 2 alpha overexpression in inflammatory bowel disease. *J Clin Pathol* 2003; **56**: 209-213
- 22 **Kapsoritakis A**, Sfiridaki A, Maltezos E, Simopoulos K, Giatromanolaki A, Sivridis E, Koukourakis MI. Vascular endothelial growth factor in inflammatory bowel disease. *Int J Colorectal Dis* 2003; **18**: 418-422
- 23 **Ferrara N**, Houck KA, Jakeman LB, Winer J, Leung DW. The vascular endothelial growth factor family of polypeptides. *J Cell Biochem* 1991; **47**: 211-218

Edited by Li WZ Language Editor Elsevier HK

• CLINICAL RESEARCH •

A blind, randomized comparison of racecadotril and loperamide for stopping acute diarrhea in adults

Hwang-Huei Wang, Ming-Jium Shieh, Kuan-Fu Liao

Hwang-Huei Wang, Medical Faculty, Division of Gastroenterology, Department of Internal Medicine, China Medical University Hospital, Taichung, Taiwan, China

Kuan-Fu Liao, Medical Faculty, Division of Gastroenterology, Department of Internal Medicine, China Medical University Hospital, Taichung, Taiwan, China

Ming-Jium Shieh, Medical Faculty, Department of Internal Medicine, National Taiwan University Hospital, Taipei, Taiwan, China

Correspondence to: Kuan-Fu Liao, M.D., Division of Gastroenterology, Department of Internal Medicine, China Medical University Hospital, 2 Yuh-Der Road, Taichung, Taiwan, China. kuanfu.liao@msa.hinet.net

Telephone: +886-4-22062121 Fax: +886-4-22023119

Received: 2004-09-29 Accepted: 2004-10-18

but loperamide treatment is associated with a higher incidence of treatment-related constipation.

© 2005 The WJG Press and Elsevier Inc. All rights reserved.

Key words: Racecadotril; Loperamide; Acute diarrhea

Wang HH, Shieh MJ, Liao KF. A blind, randomized comparison of racecadotril and loperamide for stopping acute diarrhea in adults. *World J Gastroenterol* 2005; 11(10): 1540-1543
<http://www.wjgnet.com/1007-9327/11/1540.asp>

Abstract

AIM: Racecadotril is a specific enkephalinase inhibitor that exhibits intestinal antisecretory activity without affecting intestinal transit. Loperamide is an effective anti-diarrheal agent, but it usually induces constipation. This study is to compare the efficacy, safety, and tolerability of racecadotril versus loperamide in the outpatient treatment of acute diarrhea in adults.

METHODS: A two-center, randomized, parallel-group, single-blind study was carried out to compare the efficacy, tolerability, and safety of racecadotril (100 mg thrice daily) and loperamide (2.0 mg 2 twice daily) in 62 adult patients suffering from acute diarrhea. The main efficacy criterion used was the duration of diarrhea after beginning the treatment (in hours). Other signs and symptoms were also evaluated.

RESULTS: The clinical success rates for these anti-diarrheal treatments were 95.7% and 92.0% for racecadotril and loperamide respectively. Patients on racecadotril had a median duration of diarrhea of 19.5 h compared with a median of 13 h for patients on loperamide. Rapid improvement in anal burn and nausea was found for each drug. However, more patients on loperamide suffered from reactive constipation (29.0% vs 12.9%). Itching, another adverse event was notably higher in the racecadotril group (28.6% vs 0%). With regard to other adverse events, the two medications showed similar occurrence rates and similar concomitant medication usage rates.

CONCLUSION: Racecadotril and loperamide are rapid, equally effective treatments for acute diarrhea in adults,

INTRODUCTION

Infections of the gastrointestinal tract, especially infectious diarrhea, are among the most common debilitating infectious diseases, afflicting people of all ages around the world^[1]. Diarrhea remains the third most frequent syndrome seen in general practice^[2]. Although an etiologic agent is not found in many cases, microbial infection is the most common cause of most acute diarrheal diseases. The underlying pathophysiological problem of acute diarrhea is generally attributed to hypersecretion by the intestinal mucosa. Edelman commented that the ideal treatment for acute diarrhea should combine replacement of water and electrolytes with a medication able to inhibit intestinal hypersecretion while not slowing gastrointestinal transit^[3]. Despite possessing effective anti-diarrheal properties, the μ -receptor agonist, loperamide and other opiates, may cause adverse effects such as reactive constipation and abdominal distension^[4]. Their mode of action is through disrupting forward propulsive motility, increasing gut capacity, and delaying passage of fluid through the intestine.

The enkephalins were discovered in 1975, and act as neurotransmitters along the gastrointestinal tract where they are found in high levels in the mucosal cells^[5]. Enkephalins, endogenous opiate substances contributing to antisecretory activity, play an important physiological role acting as neurotransmitters, notably along the digestive tract. These substances can elicit intestinal antisecretory activity without affecting intestinal transit. Racecadotril, a specific enkephalinase inhibitor, exhibits intestinal antisecretory activity not only in animal models but also in humans, without contributing to intestinal transit time^[6]. Although several studies about this drug have been reported in the literature, no study has been reported in the oriental country; so this study was designed to compare the efficacy, safety and tolerability of racecadotril with loperamide in the treatment of acute diarrhea in adult patients.

MATERIALS AND METHODS

Male or female adults over 18 years of age who were suffering from acute diarrhea of presumed infectious origin were eligible for inclusion in the study. Acute diarrhea was defined as the passing of at least 3 watery stools in a minimum of 24 h and for the duration of less than five days.

Exclusion criteria were the presence of chronic, iatrogenic, or bloody diarrhea, having received antibiotic treatment for other medical or surgical problems, having a history of renal or hepatic dysfunction, having a concomitant infection, or being otherwise immunocompromised. Patients receiving treatment with an anti-diarrheal drug in the five days prior to the study were also excluded. Pregnant or lactating women and women planning pregnancy were also ineligible for study participation.

The study was a randomized, single-blind, and parallel group design implemented in two separate centers in Taiwan from April 2001 to December 2001. Before treatment, the patients collected one stool for culture, and gave blood for a blood cell count. Patients were randomly allocated to receive either 100 mg tablets of racecadotril three times daily (half an hour before or one hour after meal), or 2.0 mg tablets of loperamide twice daily.

The drugs are prepared with the same color of capsule in the outer appearance and given (drugs) by pharmacist according to a randomized controlled (sheet) schedule.

Patients were treated until recovery, defined as the production of 2 consecutive normal stools or no stool production for a period of 12 h. If recovery did not occur in 7 d, this treatment was discontinued. The first dose of the medication was taken under the supervision of a designated study physician or nurse.

No additional anti-diarrheal therapies or concomitant medications were permitted during the study.

Efficacy was documented by the physician and in a diary card filled in by the patient. The time, number, and stool characteristics were recorded, as were the occurrence of several adverse signs and symptoms. Formal evaluation by the physician occurred on conclusion and at the end of the treatment visit occurring 10–14 d after entering the study. Patients withdrawn from the study were to attend a follow-up visit three weeks after withdrawal to monitor adverse experiences and concomitant medication changes.

The primary efficacy criterion was the duration of diarrhea in hours, from the first treatment dose to recovery. Secondary efficacy criterion consisted of duration of abdominal pain and abdominal distension. The overall clinical response as a success or failure was assessed by physicians.

Tolerability and safety were assessed by recording the adverse events experienced during treatment and by the occurrence of constipation. The signs and symptoms evaluated were pain on abdominal palpation, anorexia, nausea, and anal burning.

The study was approved by the Institutional Review Board or Ethics Committee prior to each center's initiation and conducted in accordance with ICH and the local Government's Clinical Practices and the Declaration of Helsinki; all patients gave their informed consent.

Statistical analysis

Statistical analysis was performed using SAS vision 8. Both intent-to-treat (ITT) and per protocol (PP) analyses were performed for primary and secondary parameters. Estimates of the survival distribution of the duration of diarrhea were analyzed using Kaplan-Meier survival analysis techniques. The overall clinical response of treatment groups was compared using the Cochran-Mantel-Haenszel test, as was the comparison of treatment group changes from inclusion to the end of treatment visit.

RESULTS

A total of 62 patients were entered into the study, and all received at least one dose of study medication under supervision at the investigator site. All patients who had valid baseline data and were used in the ITT analysis are shown in Table 1.

The full data set consisted of 62 patients, with the 48 patients who participated fully making up the per protocol population (77.4%). Two patients (6.5%) did not complete the study due to adverse experiences, 11 patients (17.7%) were considered non-completers due to deviation from protocol, and 2 patients (3.2%) were lost to follow-up.

Of the initial 31 patients who received racecadotril, there were 15 males and 16 females. Thirty-one received loperamide (17 males and 14 females). The mean ages were 38.4 ± 15.1 years for racecadotril and 34.7 ± 12.3 years for loperamide. Patients in the 2 groups were comparable on other demographic variables (Table 1).

Based on the ITT population, the mean duration of diarrhea in the racecadotril group ($n = 31$) was 19.5 h and for the loperamide group ($n = 31$) was 13.0 h ($P = 0.23$). Based on PP analysis, the mean duration of diarrhea was 19 h in the racecadotril group ($n = 23$) compared to 13.0 h for the loperamide group ($n = 25$, $P = 0.37$). Both results are shown in Figure 1.

The mean duration of abdominal pain in the ITT population was 16 h for racecadotril and 14 h for loperamide. In the PP population, the median duration of abdominal pain was 16 h for racecadotril and 15 h for loperamide. The median duration of abdominal distension for the racecadotril group was 12 h in both the ITT and the PP analyses, but 12 and 14 h respectively in these populations on loperamide (Table 2).

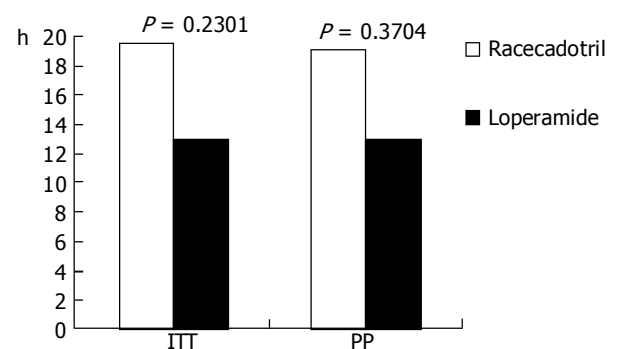


Figure 1 Mean duration of diarrhea (h). ITT (intent-to-treat); PP (per protocol).

Therapeutic improvement rates in the anal burning sensation were 71.0% (ITT) and 78.3% (PP) in the racecadotril group; 74.2% (ITT) and 76.0% (PP) in the loperamide group. For symptoms of nausea, the clinical improvement rates were 74.2% (ITT) and 78.3% (PP) in racecadotril group, 77.4% (ITT) and 80.0% (PP) in loperamide group (Table 3).

Treatment in the majority of patients was judged clinically successful. The percentages of successful treatments were 87.1% (ITT) and 95.6% (PP) in the racecadotril group and 87.1% (ITT) and 92.0% (PP) in the loperamide group (Table 4).

There were 14 (24.0%) patients who experienced at least one adverse event during the study: 8 (25.0%) in the racecadotril group and 7 (22.0%) in the loperamide group. The most frequently occurring adverse events were constipation (16.7%), bloody stool (11.1%), and itching (11.1%). A significantly greater number of patients experienced constipation in the loperamide treatment group (29.0% *vs* 12.9%, Table 5).

Table 1 Baseline patient characteristics (mean±SD)

Characteristics	Racecadotril (n = 31)	Loperamide (n = 31)	P
Male/Female	15 (48.4)/16 (51.6%)	17 (54.8%)/14 (45.2)	0.7997
Oriental	31 (100%)	31 (100%)	1.0000
Age (yr)	38.4±15.1	34.7±12.3	0.2961
Weight (kg)	57.4±12.7	59.6±9.0	0.4339
Height (cm)	162.6±9.6	164.8±9.6	0.357
BMI	21.5±3.3	22.0±2.9	0.6074

Table 2 Mean duration of symptom (h)

Symptom	Population	Racecadotril	Loperamide	P
Abdominal pain	ITT	16.0	14.0	0.9509
	PP	16.0	15.0	0.7177
Abdominal distension	ITT	12.0	14.0	0.5602
	PP	12.0	12.0	0.5250

Table 3 Rates of improvement in anal burn and nausea

Symptom	Population	Racecadotril (%)	Loperamide (%)	P
Anal burn	ITT	22/31 (71.0)	23/31 (74.2)	0.7353
	PP	18/23 (78.3)	19/25 (76.0)	0.7428
Nausea	ITT	23/31 (74.2)	24/31 (77.4)	0.6590
	PP	18/23 (78.3)	20/25 (80.0)	0.6475

Table 4 Clinical response by treatment group

Population	Racecadotril (%)	Loperamide (%)	P
ITT			
Clinical success	22/31 (87.1)	27/31 (87.1)	0.7212
PP			
Clinical success	22/23 (95.6)	23/25 (92.0)	0.6248

Table 5 Treatment-related adverse events with an incidence of more than 1 %

Population event	Racecadotril (n = 31) (%)	Loperamide (n = 21) (%)
Constipation	4 (12.9)	9 (29.0)
Bloody stool	1 (14.2)	1 (9.1)
Skin itching	2 (28.6)	0 (0.0)
Abdominal pain on palpation	1 (14.3)	0 (0.0)

DISCUSSION

The results of this randomized, parallel, controlled study confirm that the efficacy, tolerability, and safety of racecadotril are comparable to those of loperamide in treating acute diarrhea in adults, but racecadotril treatment is less associated with the adverse event of constipation.

In clinical practice, we usually use anti-diarrheal agents for patients suffering from acute diarrhea. In principle, because the mechanisms of stopping diarrhea are different in loperamide and racecadotril, there might be reason to choose one before the other. Loperamide activates the μ -receptor, prolonging the orocecal and colonic transit times by disrupting the gut's electrical activity, increasing gut capacity, and delaying the passage of fluids through the small intestine; it has no direct effect on absorption^[12]. Racecadotril is a specific inhibitor of enkephalinase. It activates the δ -receptor to reduce secretory activity in the gut^[16], thereby prolonging the antisecretory effect of the endogenous enkephalins.

Of the 62 patients randomized (ITT population), 48 patients (23 in racecadotril group and 25 in loperamide group) were considered valid as per protocol. The results of the study showed that no statistically significant differences were found in the effects of these medications on the duration of diarrhea (19.5 h *vs* 13.0 h), the duration of abdominal pain ($P = 0.95$, ITT and $P = 0.71$, PP), or on the duration of abdominal distension ($P = 0.56$, ITT and $P = 0.52$, PP) for the racecadotril groups and the loperamide groups respectively. The clinical improvement rates in anal burning sensation and nausea were greater than seventy percent in both the racecadotril group and the loperamide group, but the differences between the two groups did not reach statistical significance.

Therefore, the estimated clinical success rates, including duration of abdominal pain, abdominal distension, diarrhea, and anal burning sensation, were high in both the racecadotril and loperamide treatment groups in per protocol populations (95.6% and 92.0% respectively).

These two different medications show similar adverse events such as constipation, bloody stool, abdominal pain, skin itching, palpitation, dizziness, cold sweating, and headache. Skin itching was somewhat more frequent in the racecadotril group, but there was no statistically significant difference. This may be due to the relatively small study population, and needs further confirmation with a larger population. The adverse event of constipation in the racecadotril group is lower than in the loperamide treated group (12.9% and 29.0%) although there was no statistical significance.

The *in vivo* study by Hinterleitner *et al* also showed that plasma enkephalinase was significantly inhibited within the first 30 min of administration of racecadotril, and maximum inhibition was seen after 60 min. The inhibition of intestinal fluid secretion by racecadotril was confirmed by studying the effect of racecadotril on cholera-induced hypersecretion in the jejunum of 6 healthy subjects, which showed that racecadotril had no influence on basal water and electrolyte absorption (133 *vs* 140 mL/30 cm × h). But in control group, significant water secretion was induced (131 mL/30 cm × h). Racecadotril completely prevented this

secretion by leaving an absorption rate of 27 mL/30 cm \times h^[17].

There also demonstrated inhibition of intestinal secretion by racecadotril in diarrhea induced by castor oil, a model of hypersecretory diarrhea^[7]. In a study by Hamza *et al*^[18], racecadotril produced a significant ($P = 0.025$) decrease in stool weight during the first day of treatment compared with placebo, and was also associated with significantly fewer diarrhoeic stools than placebo after 1 d of treatment ($P = 0.027$), but less abdominal distension was found on racecadotril group than placebo group (5.6% *vs* 18.2%).

The anti-motility mechanism of action of many traditional drugs used to treat diarrhea can lead to adverse effects such as constipation, abdominal pain, and abdominal distension, which limits the potential use of these drugs^[14,19,20]. This study revealed that racecadotril is associated with a somewhat lower incidence of treatment-related constipation than that of loperamide. The study of the result in Rouge' *et al* showed racecadotril and loperamide were both rapidly and similarly effective, diarrhea resolving in both cases in nearly 2 d. With racecadotril, however, abdominal distension vanished significantly more rapidly (50.0% *vs* 27.0%; $P < 0.05$), and reactive constipation was less frequent (31.1% *vs* 8.1%; $P < 0.02$). These differences can be accounted for by the distinct mechanisms of antidiarrheal activity of the two drugs^[8]. In our study the mean duration of stopping diarrhea is 19.5 h on racecadotril treated group that is better than Rouge' *et al* study. So this study showed racecadotril has better effective for stopping diarrhea in oriental population, but has the same safety between oriental population and western population. However, multicenter-trial with a larger cohort of patients are required before racecadotril can be recommended as the drug of choice in acute diarrhea in oriental population.

In summary, the results of our study have confirmed that racecadotril is an effective antihypersecretory agent for the safe, outpatient treatment of acute diarrhea in adults, and are consistent with a previous study in showing a lower incidence of treatment-related constipation for this medication, compared to loperamide.

REFERENCES

- 1 Sheeby TW. Digestive disease as a national problem. VI. Enteric disease among United States troops in Vietnam. *Gastroenterology* 1968; **55**: 105-112
- 2 Sprinz H. Pathogenesis of intestinal infections. *Arch Pathol* 1969; **87**: 556-562
- 3 Edelman R. Prevention and treatment of infectious diarrhea: Speculations on the next 10 years. *Am J Med* 1985; **78**: 99-106
- 4 Schiller LR, Santa Ana CA, Morawski SG, Fordtran JS. Mechanism of the antidiarrheal effect of loperamide. *Gastroenterology* 1984; **86**: 1475-1480
- 5 Pollard H, Moreau J, Ronco P, Verroust P, Schwartz JC. Immunoautoradiographic localisation of enkephalinase (EC 3.4.24.11) in rat gastrointestinal tract. *Neuropeptides* 1991; **19**: 169-178
- 6 Primi MP, Bueno L, Baumer P, Berard H, Lecomte JM. Racecadotril demonstrates intestinal antisecretory activity *in vivo*. *Aliment Pharmacol Ther* 1999; **13** Suppl 6: 3-7
- 7 Baumer P, Danquechin Dorval E, Bertrand J, Vetel JM, Schwartz JC, Lecomte JM. Effects of acetorphan, an enkephalinase inhibitor, on experimental and acute diarrhoea. *Gut* 1992; **33**: 753-758
- 8 Roge J, Baumer P, Berard H, Schwartz JC, Lecomte JM. The enkephalinase inhibitor, acetorphan, in acute diarrhoea. A double-blind, controlled clinical trial versus loperamide. *Scand J Gastroenterol* 1993; **28**: 352-354
- 9 Vetel JM, Berard H, Fretault N, Lecomte JM. Comparison of racecadotril and loperamide in adults with acute diarrhoea. *Aliment Pharmacol Ther* 1999; **13** Suppl 6: 21-26
- 10 Lecomte JM. An overview of clinical studies with racecadotril in adults. *Int J Antimicrob Agents* 2000; **14**: 81-87
- 11 Prado D. A multinational comparison of racecadotril and loperamide in the treatment of acute watery diarrhoea in adults. *Scand J Gastroenterol* 2002; **37**: 656-661
- 12 Basilisco G, Camboni G, Bozzani A, Paravicini M, Bianchi PA. Oral naloxone antagonizes loperamide-induced delay of oro-cecal transit. *Dig Dis Sci* 1987; **32**: 829-832
- 13 Kachel G, Ruppin H, Hagel J, Barina W, Meinhardt M, Domschke W. Human intestinal motor activity and transport: effects of a synthetic opiate. *Gastroenterology* 1986; **90**: 85-93
- 14 Ruppin H. Review: loperamide—a potent antidiarrhoeal drug with actions along the alimentary tract. *Aliment Pharmacol Ther* 1987; **1**: 179-190
- 15 Schiller LR, Santa Ana CA, Morawski SG, Fordtran JS. Mechanism of the antidiarrhoeal effect of loperamide. *Gastroenterology* 1984; **86**: 1475-1480
- 16 Shook JE, Lemcke PK, Gehring CA, Hrubt VJ, Burks TF. Antidiarrhoeal properties of supraspinal mu and delta and peripheral mu, delta and kappa opioid receptor: Inhibition of diarrhea without constipation. *J Pharmacol Exp Ther* 1989; **249**: 83-90
- 17 Hinterleitner TA, Petritsch W, Dimsity G, Berard H, Lecomte JM, Krejs GJ. Acetorphan prevents cholera-toxin induced water and electrolyte secretion in the human jejunum. *Eur J Gastroenterol Hepatol* 1997; **9**: 887-891
- 18 Vetel JM, Berard H, Fretault N, Lecomte JM. Comparison of racecadotril and loperamide in adults with acute diarrhoea. *Aliment Pharmacol Ther* 1999; **13** Suppl 6: 21-26
- 19 DuPont HL, Hornick RB. Adverse effect of lomotil therapy in shigellosis. *JAMA* 1973; **226**: 1525-1528
- 20 Brown JW. Toxic megacolon associated with loperamide therapy. *JAMA* 1979; **226**: 301-302

Edited by Guo SY Language Editor Elsevier HK

• BRIEF REPORTS •

Connexin 26 correlates with Bcl-xL and Bax proteins expression in colorectal cancer

Luiza Kanczuga-Koda, Stanislaw Sulkowski, Mariusz Koda, Elzbieta Skrzydlewska, Mariola Sulkowska

Luiza Kanczuga-Koda, Stanislaw Sulkowski, Mariusz Koda, Mariola Sulkowska, Department of Pathology, Medical University of Bialystok, Poland
Elzbieta Skrzydlewska, Department of Analytical Chemistry, Medical University of Bialystok, Poland
Supported by the Polish State Committee for Scientific Research (3 PO5B 07922)

Correspondence to: Professor Stanislaw Sulkowski, Ph.D., Department of Pathology, Medical University of Bialystok, Waszyngtona 13, 15-269 Bialystok, Poland. sulek@zeus.amb.edu.pl
Telephone: +48-85-7485944 Fax: +48-85-7485944
Received: 2004-08-14 Accepted: 2004-09-24

Abstract

AIM: To evaluate of Cx26 in correlation with Bcl-xL and Bax proteins in colorectal cancer.

METHODS: Immunohistochemical staining using specific antibodies was performed to evaluate the protein expression of Cx26, Bax and Bcl-xL in 152 colorectal cancer samples and the correlations among studied proteins as well as the relationships between the expression of Cx26, Bax, Bcl-xL and clinicopathological features were analyzed.

RESULTS: Both normal epithelial cells and carcinoma cells expressed Cx26, Bax and Bcl-xL, but Cx26 in cancer cells showed aberrant, mainly cytoplasmic staining. Expression of Cx26, Bax and Bcl-xL was observed in 55.9%, 55.5% and 72.4% of evaluated colorectal cancers respectively. We found the positive correlation between Cx26 and Bax expression ($r = 0.561$, $P < 0.0001$), Cx26 and Bcl-xL ($r = 0.409$, $P < 0.0001$) as well as between Bax and Bcl-xL ($r = 0.486$, $P < 0.0001$). Association of Cx26, Bax and Bcl-xL expression with histological G2 grade of tumors was noted ($P < 0.005$, $P < 0.001$ and $P < 0.002$ respectively).

CONCLUSION: Cytoplasmic presence of Cx26 and its association with apoptotic markers could indicate a distinct role from physiological functions of Cx26 in cancer cells and it could suggest that connexins might be a target point for modulations of apoptosis with therapeutic implications.

© 2005 The WJG Press and Elsevier Inc. All rights reserved.

Key words: Cx26; Bcl-xL; Bax; Apoptosis; Colorectal cancer; Immunohistochemistry

Kanczuga-Koda L, Sulkowski S, Koda M, Skrzydlewska E, Sulkowska M. Connexin 26 correlates with Bcl-xL and Bax

proteins expression in colorectal cancer. *World J Gastroenterol* 2005; 11(10): 1544-1548

<http://www.wjgnet.com/1007-9327/11/1544.asp>

INTRODUCTION

The most common way of communication between cells is gap junctional intercellular communication (GJIC) mediated by gap junctions (GJs), which are formed from transmembrane proteins called connexins (Cx). A hexameric unit of connexins in one cell (a connexon) couples with a corresponding connexon in a contiguous cell to join the cytoplasm^[1]. This allows synchronizing different functions of cells within a tissue. The connexin proteins are encoded by a multigene family, and so far 20 different human Cx genes have been identified^[2]. Gap junctions may be heterotypic (each connexon composed of different Cx isotypes) or heteromeric (each connexon composed of more than one Cx isotype)^[3]. Gap junction channels allow the exchange of ions, nucleotides, metabolites and other small molecules (<1 ku) including second messengers such as cAMP, IP₃ and Ca²⁺ between adjacent cells^[3,4]. GJIC plays an important role in the maintenance of tissue homeostasis probably also by regulating the balance between cell gain and cell loss^[5]. Cancers are considered to be the result of a disruption of the homeostatic regulation of a cell's ability to respond appropriately to extracellular signals of the body, which trigger intracellular signal transduction mechanisms. Cancer cells, among others, have altered ability to program cell death. On the other hand, the cancer cells of solid tissues appear to have either dysfunctional homologous or heterologous GJIC^[6,7]. Altered expression of connexins has been observed in various cancers and forced expression of members of this gene family suppresses tumor growth^[6,8,9].

The normal human epithelial cells in the colon express Cx32 and Cx43^[10]. In previous studies we also observed for the first time Cx26 expression in the normal colon epithelium as well as in the colorectal cancer^[11,12]. However, the involvement of these connexins in apoptosis during colorectal carcinogenesis has not been investigated.

Dysregulation of apoptosis plays an important role in a colorectal carcinogenesis^[13,14]. Apoptosis is a complex physiological process that plays a crucial role in tissue homeostasis. Recent data suggest that modulation of molecules involved in the regulation of cell death by apoptosis may be equally important. The main group of genes controlling apoptosis is the Bcl-2 family, which includes both promoters (Bax, Bak, Bad and Bcl-xS) and inhibitors

(Bcl-2, Bcl-xL and Mcl-1)^[15]. Bcl-xL is able to form heterodimers with Bak and Bax. The elevated expression of this protein seems to be an early event in colorectal carcinogenesis^[16]. Bax is a proapoptotic factor^[15] and shows a high similarity with some Bcl-2 family proteins such as Bcl-xL, Bcl-w or Bid. As far as now, immunohistochemical studies have shown both lacks of statistically significant differences between expression of Bax in normal epithelial cells of colorectal mucosa and colorectal cancer cells^[16] as well as overexpression of Bax in primary colorectal cancer vs normal mucosa^[17].

Previous studies of apoptosis have focused mainly on the role of intracellular signaling pathways in the regulation of apoptosis. However, some studies have demonstrated correlation between intercellular communication and apoptosis^[18,19]. On the other hand, interactions between members of Bcl-2 family and gap junction proteins, -connexins, in colorectal cancer have not been investigated; thus, we examined the expression of Cx26, Bcl-xL and Bax by immunohistochemistry and correlations between Cx26 and studied apoptotic markers in colorectal cancer patients.

MATERIALS AND METHODS

Tissue samples were obtained from 152 patients (78 men and 74 women) who underwent surgical resection because of colon (84 cases) and rectal (68) carcinomas. Our study included 128 colorectal cancers classified histopathologically as adenocarcinoma and 24 as mucinous adenocarcinoma: 108 cases in G2 grade and 44 cases in G3 grade. There were 14 tumors in pT2 stage and 138 in pT3 stage. 82/152 (53.9%) patients had involved lymph nodes at the time of diagnosis. The age of patients ranged from 35 to 92 years old (mean 65.4 years). Tumor samples with adjacent normal colon mucosa were collected immediately after tumor removal, fixed in 10% buffered formaldehyde solution for 48 h and then embedded in paraffin blocks at 56 °C according to standard procedures. The resected tumors were histopathologically examined using standard hematoxylin-eosin staining.

Immunohistochemistry

Paraffin-embedded tissue sections were subjected to immunostaining, using goat polyclonal anti-Cx26, goat polyclonal anti-Bax and goat polyclonal anti-Bcl-xL antibodies (Abs) (Santa Cruz Biotechnology, USA) in dilution rate: 1:400, 1:200 and 1:300 respectively. All primary Abs were diluted in PBS with 1.5% normal blocking serum. The studies were performed with avidin-biotin-peroxidase complex (ABC Staining System, SCBt, USA). Slides were counterstained with hematoxylin. In negative controls sections known to stain positively with studied Abs were included in each run with buffer instead of primary antibodies.

The evaluation of immunostaining for Cx26, Bax and Bcl-xL was analyzed in 10 different tumor fields and the mean percentage of tumor cells with positive staining was evaluated. The sections were classified as positive when at least 10% of cancer cells expressed the studied antigens.

Statistical analysis

The significance of the associations was determined using Spearman correlation analysis and the χ^2 test. Probabilities of $P < 0.05$ were assumed as statistically significant.

RESULTS

Immunohistochemical analysis of the colorectal cancer sections revealed in 85/152 (55.9%) cases mainly cytoplasmic localization for Cx26. In a few cancer cases (15/152), classified in G2 grade, we focally observed punctate intercellular staining (Figure 1A-D). The adjacent colorectal mucosa also revealed positive immunostaining for this protein, but only punctate immunoreactivity was seen (Figure 1C). Cytoplasmic localization and microgranular staining for Bax (Figure 1E, F) and Bcl-xL (Figure 1G, H) proteins was noted in colorectal cancer sections. The adjacent colorectal mucosa also revealed positive immunostaining for these proteins. The studied markers were not detected in control samples, where immunostaining was performed with the omission of the primary antibodies. The positive expression of Bax and Bcl-xL was found in 55.5% and 72.4% of the tumors respectively.

Analysis of correlations among assessed proteins revealed the positive correlation between Cx26 and Bax expression ($r = 0.561$, $P < 0.0001$), between Cx26 and Bcl-xL ($r = 0.409$, $P < 0.0001$) as well as between Bax and Bcl-xL ($r = 0.486$, $P < 0.0001$) (Table 1). Interestingly, correlation between Cx26 and Bax was stronger in better differentiated (G2) than in poorly differentiated (G3) tumors ($P < 0.0001$ and $P < 0.006$ respectively).

Table 1 Correlations among Cx26, Bax and Bcl-xL expressions in human colorectal cancer

Comparative factors		R	P
Cx26	Bax	0.561	<0.0001
Cx26	Bcl-xL	0.409	<0.0001
Bax	Bcl-xL	0.486	<0.0001

The expression of Cx26, Bax and Bcl-xL did not correlate with age, sex of patient, tumor localization or tumor size. In our study, we noted a tendency toward association between Cx26, Bax expression and adenocarcinoma, but not mucinous adenocarcinoma type ($P = 0.07$ and $P = 0.064$ respectively) as well as positive association between Bcl-xL expression and adenocarcinoma type of cancer ($P < 0.02$). The subgroup of patients without involved lymph nodes showed unquestionable positive association between Cx26, Bax, Bcl-xL expression and adenocarcinoma type of tumor ($P < 0.001$, $P < 0.02$, $P < 0.0007$ respectively). On the other hand in the case of mucinous adenocarcinoma we did not find similar relationships. In better differentiated tumors (G2) we observed more Cx26, Bax and Bcl-xL-positive cases ($P < 0.005$, $P < 0.001$ and $P < 0.002$ respectively) than in poorly differentiated tumors (G3). A tendency towards negative association between Bax expression and lymph node status ($P = 0.063$), but not between Cx26, Bcl-xL and lymph node status was observed.

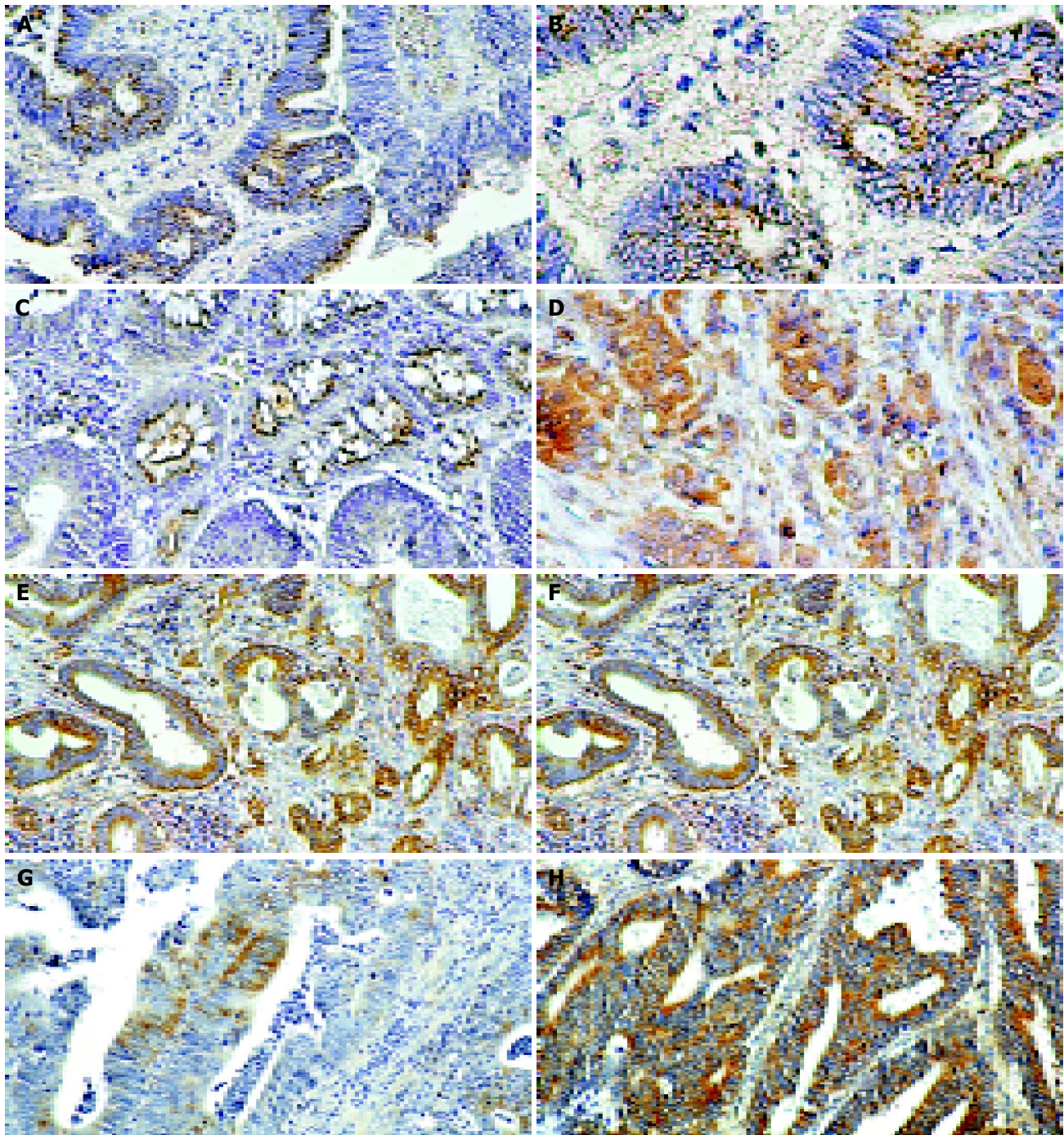


Figure 1 Immunohistochemical detection of Cx26 in the human colorectal cancer. A and B: Granular staining of Cx26 localized mainly between the colorectal cancer cells in the tumor classified in G2 grade; C: Immunopositive deposits in the form of granules are seen in the normal epithelium adjacent to the tumor; D: Strong cytoplasmic immunostaining of Cx26 in G3 grade colorectal cancer. Original magnification: A, C, and D $\times 200$, B $\times 400$; E: Cytoplasmic localization of Bax immunostaining in colorectal cancer classified as G2 grade; F: Strong cytoplasmic immunostaining of Bax in the majority cells of G3 grade colorectal cancer. Original magnification: E $\times 100$, F $\times 200$; G: Cytoplasmic localization of Bcl-xL immunostaining is focally seen in G2 grade colorectal cancer; H: Strong cytoplasmic immunostaining of Bcl-xL in the majority of colorectal cancer cells. Original magnification: G $\times 200$, H $\times 100$.

DISCUSSION

Connexins are typically localized in the cell membrane and normally show a punctate pattern of expression^[4,20]. Aberrant localization of connexins may contribute to the loss of intercellular communication via gap junctions^[21]. Our previous observations^[11] and present results suggest that impaired communication between neoplastic cells may depend on the subcellular disturbance in the synthesis and

localization of Cx26. Consequently, Cx26 protein accumulates in the cytoplasm of cancer cells and it is possible that Cx26 in this localization could play a distinct role from physiological functions.

Cytoplasmic localization of Cx26 might reflect a transcriptional or posttranscriptional defect of this protein during a colorectal carcinogenesis. Previous studies revealed mutations in the extracellular or transmembrane regions of connexins, which contributed to alteration in connexins

localization as well as to loss of GJIC^[22,23]. Immunohistochemical studies of the mutant Cx43 protein revealed nuclear and cytoplasmic localization and no sign of Cx43 in the intercellular area of mutant cells. Furthermore Krutovskikh *et al*^[22] revealed that subcellular localization of Cx43 in tumor cells could play a role in the regulation of tumor growth. In the other study^[25] mutations in the second extracellular region prevented localization to the plasma membrane but did not decrease the ability of Cx43 to inhibit the growth of tumor cells *in vitro*. Olbina and Eckhart^[24] concluded that regulation of cellular growth by Cx43 does not necessarily require GJIC. It could suggest that cytoplasmic connexins might control tumor progression by the influence on the expression of genes, which are responsible for regulation of cancer cell's functions. Basing on above findings and on our previous^[11,20] as well as present results it could be concluded that Cxs localized in the cytoplasm and in the plasma membrane between cells could play different roles in malignant and normal cells, but additional functional studies of the role of Cxs in signalling pathways are required.

Considerable data demonstrate that connexins could play a tumor suppressor role. Currently it is accepted that the tumor suppressive effect of connexins is associated with inhibition of cell growth and regulation of tissue differentiation. On the other hand, it has been shown that enhancing of apoptosis by a transfer of signalling molecules via gap junctions^[5] can contribute to the tumor suppression, but mechanisms, which regulate these processes are still unclear and it concern connexins localized in the plasma membrane. We suppose that regulation of apoptosis by connexins could be, among others, a result of a control of apoptotic markers such as Bcl-2 family proteins. This theory might explain subcellular localization of connexins in cytoplasmic or nuclear compartments of tumor cells. Krutovskikh *et al*^[22] proposed that connexins localized in cytoplasm have different signalling activity than those localized in the plasma membrane. Moreover, they supposed that signal transduction functions of connexins require interactions with other intracellular proteins. In fact Huang *et al*^[18] observed decreased expression of Bcl-2 in Cx43-transfected malignant cells compared to non-transfected cells. They suggested that connexin genes could regulate expression of other genes in tumor cells. Similarly Tanaka and Grossman^[19] found that forced expression of Cx26 (transfected cells with a Cx26 adenovirus vector) in prostate cancer cells suppressed the growth of cancer cells, induced cell cycle arrest at the G2/M phase as well as decreased the expression of Bcl-2 and enhanced apoptosis.

Although the role of connexins in cell growth regulation has been extensively studied, their involvements in apoptosis remain unclear. It has been postulated that GJIC plays a significant role in the regulation of apoptosis in cancerous cells. Krutovskikh *et al*^[5] have found that due to intercellular communication via gap junctions, cancer cells can spread cell death signals between themselves, and the messenger molecules, which initiate apoptotic process in neighboring cancer cells are probably Ca^{2+} ions. The ability of cells to kill each other through GJ channels has been shown in "bystander death" experiments, where toxin spreads via GJ

channels from affected cells into neighboring unaffected cells and eventually kills them^[26,27]. On the other hand, cancer disease is characterized by dysfunction of both, intercellular communication as well as apoptosis^[5,18,27]. Huang *et al*^[18] found that expression of Cx43 in human glioblastoma cells increased sensitivity of cells to chemotherapeutic agents, which resulted from apoptosis. They reported that Cx43-mediated apoptosis to chemotherapeutic agents is regulated in part through the down-regulation of Bcl-2 expression. It is important to notice that these authors suggested that increased apoptosis after re-expression of Cx43 might not be linked to increased gap junctional communication. In the present study we observed cytoplasmic expression of Cx26, which we consider to be with altered function. Analysis of correlations revealed the positive correlation between Cx26 and proapoptotic Bax as well as between Cx26 and antiapoptotic Bcl-xL. It suggests that cytoplasmic Cx26 could perform additional functions in malignant cell, for example, it might be involved in the control of apoptotic process, but functional relationships between cytoplasmic Cx26 and proteins involved in apoptosis require additional studies.

In the present study, we also analyzed correlations between expression of Cx26, Bax, Bcl-xL and some clinicopathological features. As described previously^[11], we did not find correlation between Cx26 expression and lymph node status. But we observed a tendency toward negative association between Bax expression and lymph node status. Furthermore, we found that in better differentiated tumors (G2), more Cx26-positive cases were present than in poorly differentiated tumors (G3), but mostly cytoplasmic staining was observed. In some cases of G2 carcinomas punctate immunostaining for Cx26 was seen. These observations indicate that during carcinogenesis in colon and rectum there are possible alterations in Cx26 expression, localization and probably decrease of functional gap junctions. Interestingly, we also observed positive association between Cx26 expression and adenocarcinoma type of tumor. It is well known that mucinous adenocarcinoma is associated with poorer outcome of patients than adenocarcinoma, so the presence of Cx26 in cytoplasm of colorectal tumors could be a good prognostic factor.

Our results showed aberrant expression and localization of connexin 26. Furthermore, cytoplasmic presence of Cx26 and its association with apoptotic markers could indicate a different role of Cx26 in neoplastic cells than participation in gap junctional intercellular communication and it could suggest that connexins might be a target point for modulations of apoptosis with therapeutic implications.

ACKNOWLEDGEMENTS

We are grateful to Edyta Jelska and Wojciech Mytnik for expert technical assistance.

REFERENCES

- 1 Duan L, Yuan H, Su CJ, Liu YY, Rao ZR. Ultrastructure of junction areas between neurons and astrocytes in rat supraoptic nuclei. *World J Gastroenterol* 2004; **10**: 117-121
- 2 Willecke K, Eiberger J, Degen J, Eckardt D, Romualdi A, Guldenagel M, Deutsch U, Sohl G. Structural and functional

- diversity of connexin genes in the mouse and human genome. *Biol Chem* 2002; **383**: 725-737
- 3 **Kumar NM**, Gilula NB. The gap junction communication channel. *Cell* 1996; **84**: 381-388
- 4 **Bruzzone R**, White TW, Paul DL. Connections with connexins: the molecular basis of direct intercellular signaling. *Eur J Biochem* 1996; **238**: 1-27
- 5 **Krutovskikh VA**, Piccoli C, Yamasaki H. Gap junction intercellular communication propagates cell death in cancerous cells. *Oncogene* 2002; **21**: 1989-1999
- 6 **Locke D**. Gap junctions in normal and neoplastic mammary gland. *J Pathol* 1998; **186**: 343-349
- 7 **Trosko JE**, Ruch RJ. Cell-cell communication in carcinogenesis. *Front Biosci* 1998; **3**: d208-d236
- 8 **Hirschi KK**, Xu CE, Tsukamoto T, Sager R. Gap junction genes Cx26 and Cx43 individually suppress the cancer phenotype of human mammary carcinoma cells and restore differentiation potential. *Cell Growth Differ* 1996; **7**: 861-870
- 9 **Mehta PP**, Perez-Stable C, Nadji M, Mian M, Asotra K, Roos BA. Suppression of human prostate cancer cell growth by forced expression of connexin genes. *Dev Genet* 1999; **24**: 91-110
- 10 **Dubina MV**, Iatckii NA, Popov DE, Vasil'ev SV, Krutovskikh VA. Connexin 43, but not connexin 32, is mutated at advanced stages of human sporadic colon cancer. *Oncogene* 2002; **21**: 4992-4996
- 11 **Kanczuga-Koda L**, Sulkowski S, Koda M, Sulkowska M. Alterations in connexin 26 expression during colorectal carcinogenesis. *Oncology* 2005; **68**: 217-222
- 12 **Kanczuga-Koda L**, Sulkowski S, Koda M, Sobaniec-Lotowska M, Sulkowska M. Expression of connexins 26, 32 and 43 in the human colon -an immunohistochemical study. *Folia Histochem Cytobiol* 2004; **42**: 203-207
- 13 **Gryfe R**, Swallow C, Bapat B, Redston M, Gallinger S, Couture J. Molecular biology of colorectal cancer. *Curr Probl Cancer* 1997; **21**: 233-300
- 14 **Watson DS**, Brotherick I, Shenton BK, Wilson RG, Campbell FC. Growth dysregulation and p53 accumulation in human primary colorectal cancer. *Br J Cancer* 1999; **80**: 1062-1068
- 15 **Reed JC**. Bcl-2 family proteins. *Oncogene* 1998; **17**: 3225-3236
- 16 **Krajewska M**, Moss SF, Krajewski S, Song K, Holt PR, Reed JC. Elevated expression of Bcl-X and reduced Bak in primary colorectal adenocarcinomas. *Cancer Res* 1996; **56**: 2422-2427
- 17 **Jansson A**, Sun XF. Bax expression decreases significantly from primary tumor to metastasis in colorectal cancer. *J Clin Oncol* 2002; **20**: 811-816
- 18 **Huang RP**, Hossain MZ, Huang R, Gano J, Fan Y, Boynton AL. Connexin 43 (cx43) enhances chemotherapy-induced apoptosis in human glioblastoma cells. *Int J Cancer* 2001; **92**: 130-138
- 19 **Tanaka M**, Grossman HB. Connexin 26 induces growth suppression, apoptosis and increased efficacy of doxorubicin in prostate cancer cells. *Oncol Rep* 2004; **11**: 537-541
- 20 **Kanczuga-Koda L**, Sulkowska M, Koda M, Reszec J, Famulski W, Baltaziak M, Sulkowski S. Expression of connexin 43 in breast cancer in comparison with mammary dysplasia and the normal mammary gland. *Folia Morphol (Warsz)* 2003; **62**: 439-442
- 21 **Krutovskikh V**, Mazzoleni G, Mironov N, Omori Y, Aguelon AM, Mesnil M, Berger F, Partensky C, Yamasaki H. Altered homologous and heterologous gap-junctional intercellular communication in primary human liver tumors associated with aberrant protein localization but not gene mutation of connexin 32. *Int J Cancer* 1994; **56**: 87-94
- 22 **Krutovskikh VA**, Troyanovsky SM, Piccoli C, Tsuda H, Asamoto M, Yamasaki H. Differential effect of subcellular localization of communication impairing gap junction protein connexin43 on tumor cell growth *in vivo*. *Oncogene* 2000; **19**: 505-513
- 23 **Defamie N**, Mograbi B, Roger C, Cronier L, Malassine A, Brucker-Davis F, Fenichel P, Segretain D, Pointis G. Disruption of gap junctional intercellular communication by lindane is associated with aberrant localization of connexin43 and zonula occludens-1 in 42GPA9 Sertoli cells. *Carcinogenesis* 2001; **22**: 1537-1542
- 24 **Olbins G**, Eckhart W. Mutations in the second extracellular region of connexin 43 prevent localization to the plasma membrane, but do not affect its ability to suppress cell growth. *Mol Cancer Res* 2003; **1**: 690-700
- 25 **Kalvelyte A**, Imbrasaitė A, Bukauskiene A, Verselis VK, Bukauskas FF. Connexins and apoptotic transformation. *Biochem Pharmacol* 2003; **66**: 1661-1672
- 26 **Mesnil M**, Yamasaki H. Bystander effect in herpes simplex virus-thymidine kinase/ganciclovir cancer gene therapy: role of gap-junctional intercellular communication. *Cancer Res* 2000; **60**: 3989-3999
- 27 **Tanaka M**, Grossman HB. Connexin 26 gene therapy of human bladder cancer: induction of growth suppression, apoptosis, and synergy with Cisplatin. *Hum Gene Ther* 2001; **12**: 2225-2236

• BRIEF REPORTS •

***Helicobacter pylori* strain-specific modulation of gastric inflammation in Mongolian gerbils**

Ken Ohnita, Hajime Isomoto, Shoji Honda, Akihiro Wada, Chun-Yang Wen, Yoshito Nishi, Yohei Mizuta, Toshiya Hirayama, Shigeru Kohno

Ken Ohnita, Hajime Isomoto, Yoshito Nishi, Yohei Mizuta, Shigeru Kohno, Second Department of Internal Medicine, Nagasaki University School of Medicine, Sakamoto 1-7-1, Nagasaki, Japan
Shoji Honda, Second Department of Internal Medicine, Oita Medical University, 1-1 Hasama, Oita 987-5593, Japan
Akihiro Wada, Toshiya Hirayama, Department of Bacteriology, Institute of Tropical Medicine, Nagasaki University School of Medicine, Sakamoto 12-4, Nagasaki, Japan
Chun-Yang Wen, Department of Molecular Pathology, Atomic Bomb Disease Institute, Nagasaki University School of Medicine, Sakamoto 12-4, Nagasaki, Japan
Correspondence to: Dr. Hajime Isomoto, Second Department of Internal Medicine, Nagasaki University School of Medicine, 1-7-1 Sakamoto, Nagasaki, Japan. hajime2002@yahoo.co.jp
Telephone: +81-95-849-7567 Fax: +81-95-849-7568
Received: 2004-09-02 Accepted: 2004-09-15

Abstract

AIM: The *cag* pathogenicity island (PAI) is one of potential virulence determinants of *Helicobacter pylori*. The Mongolian gerbil is a suitable experimental animal for the screening of virulence factors of *H. pylori*.

METHODS: Five-week-old Mongolian gerbils were inoculated with a standard *H. pylori* strain (ATCC 43504) possessing the *cag* PAI or a clinical isolate lacking the genes' cluster (OHPC-0002). The animals were killed at 2, 4, 8, 24 and 48 wk after inoculation ($n = 5$ each), and macroscopic and histopathological findings in the stomachs were compared.

RESULTS: In gerbils infected with ATCC 43504, a more severe degree of infiltration of polynuclear and mononuclear cells and lymphoid follicles was observed from 4 wk after inoculation compared to gerbils infected with OHPC-0002 especially in the antrum and transitional zone from the fundic to pyloric gland area. In addition, glandular atrophy, intestinal metaplasia, gastric ulcer and hyperplastic polyps were noted in gerbils infected with ATCC 43504, whereas only mild gastric erosions occurred in those infected with OHPC-0002.

CONCLUSION: Our results indicate that the *cag* PAI could be directly involved in gastric immune and inflammatory responses in the Mongolian gerbils, leading to a more advanced gastric disease.

Key words: *Helicobacter pylori*; Mongolian gerbil; *cag* pathogenicity island

Ohnita K, Isomoto H, Honda S, Wada A, Wen CY, Nishi Y, Mizuta Y, Hirayama T, Kohno S. *Helicobacter pylori* strain-specific modulation of gastric inflammation in Mongolian gerbils. *World J Gastroenterol* 2005; 11(10): 1549-1553
<http://www.wjgnet.com/1007-9327/11/1549.asp>

INTRODUCTION

Helicobacter pylori (*H. pylori*) is a Gram-negative, spiral-shaped, microaerophilic bacterium that colonizes the human gastric mucosa^[1-3]. The prevalence of *H. pylori* infection is still high in Asian countries including Japan, and this organism is now recognized as a major cause of chronic active gastritis^[1-4], peptic ulcers^[2-6] and gastric malignancies^[4,5,7,8]. However, the clinical manifestation of *H. pylori* infection varies widely in infected individuals and most persons are asymptomatic all their life^[9]. The pathogenic mechanism of this pleomorphism is not completely understood, but might be explained, in part, by strain diversity^[10-13].

Several factors have been proposed as possible virulence determinants^[14-18]. Among them, the *cag* pathogenicity island (*cag* PAI), a 40-kb cluster of ~30 genes of supposedly extraneous origin^[19], is reportedly associated with advanced gastroduodenal diseases including gastric cancer^[11-14].

In an effort to develop a model that would parallel as close as possible the course of infection as it occurs in humans, Hirayama *et al.*^[20] established an experimental model of inbred Mongolian gerbils with persistent *H. pylori* infection. Infection of Mongolian gerbils with *H. pylori* results in chronic active gastritis, gastric ulcer, intestinal metaplasia and gastric cancer^[21-24]. The Mongolian gerbil model may be valuable not only in elucidating *H. pylori*-related neoplasia but also in evaluating virulence factors^[11,12]. We sought to investigate the chronological and spatial changes of gastric inflammation after inoculation of *H. pylori* strains possessing or lacking the *cag* PAI.

MATERIALS AND METHODS

Animals

Five-week-old male specific pathogen-free Mongolian gerbils (MGS/Sea, male) weighting 27-43 g (Seac Yoshitomi, Fukuoka, Japan) were used. They were housed four per cage in stainless-steel cages on hardwood chip bedding in an air-conditioned room (12/12 h light/dark cycle) at 24 °C. They were fasted for 24 h prior to *H. pylori* inoculation, and

then fed with chow (CE-2; Clea Japan Co., Tokyo, Japan) and distilled water *ad libitum* 12 h after inoculation. Experiments were performed according to the guidelines of Ethics Committee for Animal Experiments at Nagasaki University.

Bacteria

We used the ATCC 43504 standard strain of *H. pylori* known to possess *cag* PAI and the *cag* PAI-totally deleted strain OHPC-0002^[25]. The *H. pylori* strains were cultivated on Muller Hinton II agar plate with 7% horse blood at 37 °C for 3 d under microaerophilic conditions^[25]. Bacteria harvested from the plates were incubated in 200 mL of *Brucella* broth (DIFCO Laboratories, Detroit, MI) with 10% horse serum at 37 °C for 24 h with vigorous shaking under controlled microaerophilic atmosphere^[23,25]. The inoculum size was adjusted with sterile saline to produce the optical density of McFarland 4 at 540 nm^[23].

Experimental design

A total of 75 Mongolian gerbils were randomly assigned to three experimental groups (25 each group). The animals were challenged with the vehicle (group A), 10⁹ colony-forming units (CFU) ATCC 43504 (group B) or OHPC-0002 (group C) in 1 mL of *Brucella* broth with 10% horse serum by intragastric gavage. Five gerbils in each experimental group were sacrificed under anesthesia at 2, 4, 8, 24 and 48 wk after inoculation. The stomachs were quickly removed, opened along the greater curvature, divided into two, and used for histopathological and culture examinations.

Histopathological examination

Half the stomach was fixed in 10% neutral buffered formalin and embedded in paraffin. Four µm thick sections were stained with hematoxylin and eosin. According to the Sydney system, each histological parameter of activity (neutrophils), chronic inflammation (mononuclear cells), glandular atrophy and intestinal metaplasia was graded into none, mild, moderate or severe^[26]. Intestinal metaplasia was defined by the presence of goblet cells in glandular mucosa with Alcian blue (pH 2.5)/periodic acid-Schiff staining^[27]. The biopsy specimens were examined blindly without knowledge of the results of the experimental group.

Culture study

The remaining half of the stomach was minced in 2 mL of

Brucella broth, placed on the blood agar and incubated for 4 d at 37 °C under the microaerophilic conditions^[23].

RESULTS

H. pylori colonization

H. pylori was recovered from almost all gerbils of groups B and C from 4 wk after inoculation throughout the whole observation period. The bacterial densities assessed by Giemsa staining did not differ significantly between groups B and C.

Macroscopic findings

There were no visible changes in the stomach of Mongolian gerbils of group A throughout the whole observation period. Until 4 wk after inoculation, no gross appearance was noted in the stomach of both groups B and C. At 8 wk, erosions with bleeding appeared in the antrum and transitional zone extending from fundic to pyloric mucosa in all the animals of group B. In one gerbil of the group B, the stomach contained an ulcer in the vicinity of the transitional zone at 8 wk post-inoculation. The erosive lesions were noted in the transitional mucosa of 3 and 4 animals of group B at 24 and 48 wk respectively. Sessile polyps with occasional apical erosions, which were classified histopathologically as hyperplastic polyps, were seen in the antrum of one Mongolian gerbil of group B. On the other hand, there were no visible macroscopic findings in the stomach of Mongolian gerbils of group C until 24 wk after inoculation. Mild erosions were seen in the antrum of one gerbil and in the transitional zone of 2 gerbils of group C at 48 wk.

Histopathological findings

No histopathological changes were noted in the stomach of Mongolian gerbils of group A throughout the whole observation period. Table 1 compares the histopathological grades of gastritis noted in the mucosa of gerbils of groups B and C based on the Sydney classification. At 2 wk after inoculation, mild mucosal infiltration of polynuclear and mononuclear cells appeared in the antrum of one gerbil of group B. At 4 wk, moderate to severe chronic active gastritis consisting of mononuclear and polynuclear cells was noted in the lamina propria of the antrum and transitional zone of group B. The histopathological changes in group B reached peak levels between 8 to 24 wk (Figure 1A). Lymphoid follicles were especially conspicuous in the

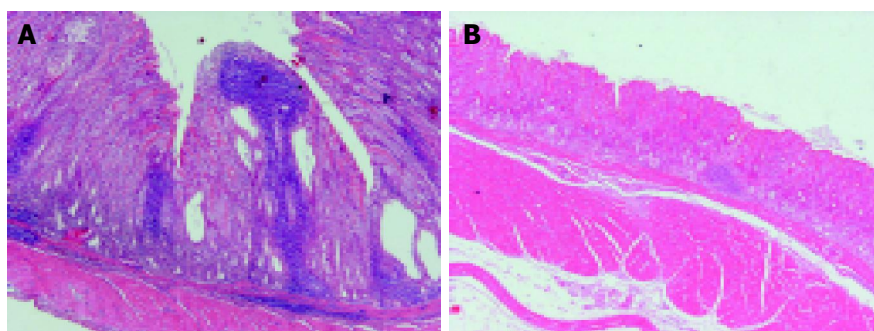


Figure 1 A: Severe chronic active gastritis was seen in the antrum of Mongolian gerbils infected with ATCC 43504 at 24 wk after inoculation (magnification, 40-fold); B: Mild chronic gastritis was noted in the antrum of Mongolian gerbils infected with OHPC-0002 at 24 wk after inoculation (magnification, 40-fold).

Table 1 Chronological and spatial changes of various parameters of histopathological gastritis in Mongolian gerbils infected with two species of *H pylori*

	Post-inoculation interval (wk)														
	Antrum					Transitional zone					Corpus				
	2	4	8	24	48	2	4	8	24	48	2	4	8	24	48
ATCC 43504-infected mongolian gerbils															
Activity															
None	4	0	0	0	1	5	0	0	0	1	5	3	2	3	4
Mild	1	2	2	2	4	0	2	0	1	2	0	2	2	2	0
Moderate	0	3	2	3	0	0	2	2	4	2	0	0	1	0	1
Severe	0	0	1	0	0	0	1	3	0	0	0	0	0	0	0
Chronic inflammation															
None	4	0	0	0	0	5	0	0	0	0	5	2	0	2	2
Mild	1	0	0	0	0	0	2	0	0	1	0	3	3	1	3
Moderate	0	2	1	2	2	0	3	3	1	2	0	0	2	2	0
Severe	0	3	4	3	3	0	0	2	4	2	0	0	0	0	0
Glandular atrophy															
None	5	2	2	2	2	5	4	2	2	1	5	5	5	4	5
Mild	0	3	3	3	3	0	1	3	3	4	0	0	0	1	0
Moderate	0	0	0	0	0	0	0	0	0	0	0	0	0	0	0
Severe	0	0	0	0	0	0	0	0	0	0	0	0	0	0	0
Intestinal metaplasia															
None	5	5	5	5	4	5	5	5	5	5	5	5	5	5	5
Mild	0	0	0	0	1	0	0	0	0	0	0	0	0	0	0
Moderate	0	0	0	0	0	0	0	0	0	0	0	0	0	0	0
Severe	0	0	0	0	0	0	0	0	0	0	0	0	0	0	0
OHPC-0002-infected mongolian gerbils															
Activity															
None	5	5	4	5	3	5	5	5	5	3	5	5	5	5	4
Mild	0	0	1	0	2	0	0	0	0	2	0	0	0	0	1
Moderate	0	0	0	0	0	0	0	0	0	0	0	0	0	0	0
Severe	0	0	0	0	0	0	0	0	0	0	0	0	0	0	0
Chronic inflammation															
None	5	5	4	2	1	5	5	5	4	3	5	5	5	5	4
Mild	0	0	1	3	2	0	0	0	1	0	0	0	0	0	1
Moderate	0	0	0	0	2	0	0	0	0	2	0	0	0	0	0
Severe	0	0	0	0	0	0	0	0	0	0	0	0	0	0	0
Glandular atrophy															
None	5	5	4	3	4	5	5	5	4	3	5	5	5	4	5
Mild	0	0	1	2	1	0	0	0	1	2	0	0	0	1	0
Moderate	0	0	0	0	0	0	0	0	0	0	0	0	0	0	0
Severe	0	0	0	0	0	0	0	0	0	0	0	0	0	0	0
Intestinal metaplasia															
None	5	5	5	5	5	5	5	5	5	5	5	5	5	5	5
Mild	0	0	0	0	0	0	0	0	0	0	0	0	0	0	0
Moderate	0	0	0	0	0	0	0	0	0	0	0	0	0	0	0
Severe	0	0	0	0	0	0	0	0	0	0	0	0	0	0	0

Data represents number of animals.

submucosa but they were also found in the deep portion of the mucosa of almost all animals of group B from 4 wk after inoculation. In the fundic mucosa of group B, mild mononuclear and polynuclear cell infiltration appeared at 4 wk. Mild to moderate infiltration of neutrophils and mononuclear cells was noted in the corpus of some gerbils of group B up to 48 wk, but the grades of gastritis were less severe than those in the antrum and the transitional zone. Mild atrophic gastritis appeared in the antrum and transitional zone of Mongolian gerbils of group B at 4 wk after inoculation, but seen in the corpus of only one gerbil at 24 wk. Intestinal metaplasia of incomplete type was found in the antrum of one gerbil of group B.

On the other hand, some Mongolian gerbils of group C

showed mild mononuclear and polynuclear cell infiltration in the antral mucosa at 8 wk after inoculation (Figure 1B). Furthermore, mild to moderate chronic active gastritis was noted in the antrum and transitional zone at 48 wk in some animals. Glandular atrophy appeared in the antral and transitional mucosa at 8 wk but was exclusively mild. No intestinal metaplasia was present anywhere in the animals of group C.

DISCUSSION

Various animals have been used for studying experimental *H pylori* infection including monkeys, dogs, piglets, domestic cats, rats and nude mice^[28-31]. These animal models had

disadvantages such as low infection rates, instability, immunodeficiency and high costs^[11,32]. Infection of conventional mice with *H pylori* strain SS1 overcame many of the above problems, but gastritis in mice induced by this infection is less intense than in humans^[33]. In 1996, Hirayama *et al*^[20] reported the development of a successful Mongolian gerbil model with persistent *H pylori* infection. Several investigators confirmed successively the progression from chronic active gastritis to atrophic gastritis and then to intestinal metaplasia and the occurrence of gastric ulcer in the Mongolian gerbil model^[22,23]. In addition, long-term *H pylori* infection by itself resulted even in the development of gastric adenocarcinoma^[24]. Thus, the gerbil seems to be the best experimental model for *H pylori* infection, and we employed the Mongolian gerbil to unravel the impact of *cag* PAI status, an important virulence determinant, on gastric pathogenesis *in vivo*.

In Mongolian gerbils infected with ATCC 43504 with total *cag* PAI, mild infiltration of neutrophils and mononuclear cells appeared in the antrum at 2 wk after inoculation. From 4 wk, moderate to severe chronic active gastritis, often accompanied by lymphoid follicle formation, was noted predominantly in the antrum and transitional zone. In the fundic mucosa, the severity of gastritis worsened to moderate from 8 wk. Such chronological changes of histological gastritis and spatial shift from antral to corporeal mucosa observed in gerbils infected with ATCC 43504 were consistent with previous results in Mongolian gerbils inoculated with other standard or clinical strains possessing intact *cag* PAI^[11,12,22,23].

The major finding of the present study is that the strain possessing the *cag* PAI induced more severe degree of gastritis in Mongolian gerbils than clinical strain lacking the genes' cluster^[25]. Because there were no differences in the susceptibility and bacterial density between the two strains, ATCC 43504 and OHPC-0002, the deletion did not change the ability of bacterial colonization or proliferation but affected the inflammatory reactions in the stomach of Mongolian gerbils. Akanuma *et al*^[12] cited similar results; a genetically handled mutant lacking total *cag* PAI or knockout strain of *cagE*, one of the functional genes in *cag* PAI, ameliorated histopathological gastritis in this animal. In addition, glandular atrophy, incomplete intestinal metaplasia, gastric ulcer and hyperplastic polyps were noted in gerbils infected with the *cag* PAI-positive strains, whereas only mild gastric erosions concomitant with slight infiltration of inflammatory cells occurred in animals infected with the *cag* PAI-negative strains. These findings indicate that intact *cag* PAI could be directly involved in the host immune and inflammatory processes and cause more advanced gastric diseases.

Deletions of the *cag* PAI and several *cag* insertion mutations reportedly block the induction of proinflammatory cytokine, interleukin-8, in gastric epithelial cell lines^[19,34]. The expression of interleukin-8 gene is up-regulated by nuclear factor kappa B (NF- κ B), which is involved in various inflammatory conditions such as inflammatory bowel diseases, rheumatoid arthritis and *H pylori*-associated gastritis through the regulation of a plethora of genes that encode bioactive molecules that mediate various immune and

inflammatory responses^[35-37]. In fact, accumulating evidence indicates that intact *cag* PAI is a prerequisite for the activation of NF- κ B^[34]. Considered together, these results suggest that the *cag* PAI-mediated activation of NF- κ B plays an important role in the pathogenesis of gastritis in Mongolian gerbils.

The VacA protein, which causes vacuolation in cultured cells^[17,18], is responsible for the virulence of *H pylori* and ulcer formation in the stomach and duodenum^[10,38]. However, since the VacA-positive strains often have intact *cag* PAI, the involvement of VacA in inducing gastritis is still controversial^[11,39]. In this regard, the *VacA*-disrupted *H pylori* strain could cause inflammatory changes in the stomach of Mongolian gerbils to a degree similar to those seen in Mongolian gerbils infected with the wild strain^[11], indicating that VacA is not crucial for gastric inflammation. Several other candidate genes outside the *cag* PAI^[15,16] should be validated in this reliable rodent model for the screening of determinants of virulence of *H pylori*.

REFERENCES

- 1 Blaser MJ. *Helicobacter pylori* and the pathogenesis of gastroduodenal inflammation. *J Infect Dis* 1990; **161**: 626-633
- 2 Ernst PB, Gold BD. The disease spectrum of *Helicobacter pylori*: the immunopathogenesis of gastroduodenal ulcer and gastric cancer. *Annu Rev Microbiol* 2000; **54**: 615-640
- 3 Gotz JM, Veenendaal RA, Biemond I, Muller ES, Veselic M, Lamers CB. Serum gastrin and mucosal somatostatin in *Helicobacter pylori*-associated gastritis. *Scand J Gastroenterol* 1995; **30**: 1064-1068
- 4 Parsonnet J, Friedman GD, Vandersteen DP, Chang Y, Vogelstein JH, Orentreich N, Sibley RK. *Helicobacter pylori* infection and the risk of gastric carcinoma. *N Engl J Med* 1991; **325**: 1127-1131
- 5 Nomura A, Stemmermann GN, Chyou PH, Kato I, Perez-Perez GI, Blaser MJ. *Helicobacter pylori* infection and gastric carcinoma among Japanese Americans in Hawaii. *N Engl J Med* 1991; **325**: 1132-1136
- 6 Graham DY, Lew GM, Klein PD, Evans DG, Evans DJ, Saeed ZA, Malaty HM. Effect of treatment of *Helicobacter pylori* infection on the long-term recurrence of gastric or duodenal ulcer: A randomized, controlled study. *Ann Intern Med* 1992; **116**: 705-708
- 7 Wotherspoon AC, Doglioni C, Diss TC, Pan L, Moschini A, de Boni M, Isaacson PG. Regression of primary low-grade B-cell gastric lymphoma of mucosa-associated lymphoid tissue type after eradication of *Helicobacter pylori*. *Lancet* 1993; **342**: 575-577
- 8 Morris A, Nicholson G. Ingestion of *Campylobacter pyloridis* causes gastritis and raised fasting gastric pH. *Am J Gastroenterol* 1987; **82**: 192-199
- 9 Dooley CP, Cohen H, Fitzgibbons PL, Bauer M, Appleman MD, Perez-Perez GI, Blaser MJ. Prevalence of *Helicobacter pylori* infection and histologic gastritis in asymptomatic persons. *N Engl J Med* 1989; **321**: 1562-1566
- 10 Blaser MJ, Atherton JC. *Helicobacter pylori* persistence: biology and disease. *J Clin Invest* 2004; **113**: 321-333
- 11 Ogura K, Maeda S, Nakao M, Watanabe T, Tada M, Kyutoku T, Yoshida H, Shiratori Y, Omata M. Virulence factors of *Helicobacter pylori* responsible for gastric diseases in Mongolian gerbil. *J Exp Med* 2000; **192**: 1601-1610
- 12 Akanuma M, Maeda S, Ogura K, Mitsuno Y, Hirata Y, Ikenoue T, Otsuka M, Watanabe T, Yamaji Y, Yoshida H, Kawabe T, Shiratori Y, Omata M. The evaluation of putative virulence factors of *Helicobacter pylori* for gastroduodenal disease by use of a short-term Mongolian gerbil infection model. *J Infect Dis* 2002; **185**: 341-347
- 13 Azuma T, Ohtani M, Yamazaki Y, Higashi H, Hatakeyama

- M. Meta-analysis of the relationship between CagA seropositivity and gastric cancer. *Gastroenterology* 2004; **126**: 1926-1927; author reply 1927-1928
- 14 **Azuma T**, Yamazaki S, Yamakawa A, Ohtani M, Muramatsu A, Suto H, Ito Y, Dojo M, Yamazaki Y, Kuriyama M, Keida Y, Higashi H, Hatakeyama M. Association between diversity in the Src homology 2 domain--containing tyrosine phosphatase binding site of *Helicobacter pylori* CagA protein and gastric atrophy and cancer. *J Infect Dis* 2004; **189**: 820-827
 - 15 **Dorrell N**, Martino MC, Stabler RA, Ward SJ, Zhang ZW, McColm AA, Farthing MJ, Wren BW. Characterization of *Helicobacter pylori* PldA, a phospholipase with a role in colonization of the gastric mucosa. *Gastroenterology* 1999; **117**: 1098-1104
 - 16 **Yamaoka Y**, Kwon DH, Graham DY. A M(r) 34,000 proinflammatory outer membrane protein (*oipA*) of *Helicobacter pylori*. *Proc Natl Acad Sci USA* 2000; **97**: 7533-7538
 - 17 **Padilla PI**, Wada A, Yahiro K, Kimura M, Niidome T, Aoyagi H, Kumatori A, Anami M, Hayashi T, Fujisawa J, Saito H, Moss J, Hirayama T. Morphologic differentiation of HL-60 cells is associated with appearance of RPTPbeta and induction of *Helicobacter pylori* VacA sensitivity. *J Biol Chem* 2000; **275**: 15200-15206
 - 18 **Wada A**, Yahiro K, Hirayama T. *Helicobacter pylori* vacuolating cytotoxin (VacA) and its modulatory effects in host cells. *Tanpakushitsu Kakusan Koso* 2001; **46**: 519-523
 - 19 **Censini S**, Lange C, Xiang Z, Crabtree JE, Ghiara P, Borodovsky M, Rappuoli R, Covacci A. *cagA*, a pathogenicity island of *Helicobacter pylori*, encodes type I-specific and disease-associated virulence factors. *Proc Natl Acad Sci USA* 1996; **93**: 14648-14653
 - 20 **Hirayama F**, Takagi S, Kusuhara H, Iwao E, Yokoyama Y, Ikeda Y. Induction of gastric ulcer and intestinal metaplasia in mongolian gerbils infected with *Helicobacter pylori*. *J Gastroenterol* 1996; **31**: 755-757
 - 21 **Fujioka T**, Honda S, Tokieda M. *Helicobacter pylori* infection and gastric carcinoma in animal models. *J Gastroenterol Hepatol* 2000; **15** Suppl: D55-D59
 - 22 **Ikeno T**, Ota H, Sugiyama A, Ishida K, Katsuyama T, Genta RM, Kawasaki S. *Helicobacter pylori*-induced chronic active gastritis, intestinal metaplasia and gastric ulcer in Mongolian gerbils. *Am J Pathol* 1999; **154**: 951-960
 - 23 **Honda S**, Fujioka T, Tokieda M, Gotoh T, Nishizono A, Nasu M. Gastric ulcer, atrophic gastritis, and intestinal metaplasia caused by *Helicobacter pylori* infection in Mongolian gerbils. *Scand J Gastroenterol* 1998; **33**: 454-460
 - 24 **Honda S**, Fujioka T, Tokieda M, Satoh R, Nishizono A, Nasu M. Development of *Helicobacter pylori*-induced gastric carcinoma in Mongolian gerbils. *Cancer Res* 1998; **58**: 4255-4259
 - 25 **Wada A**, Mori N, Oishi K, Hojo H, Nakahara Y, Hamanaka Y, Nagashima M, Sekine I, Ogushi K, Niidome T, Nagatake T, Moss J, Hirayama T. Induction of human beta-defensin-2 mRNA expression by *Helicobacter pylori* in human gastric cell line MKN45 cells on *cag* pathogenicity island. *Biochem Biophys Res Commun* 1999; **263**: 770-774
 - 26 **Price AB**. The Sydney System: histological division. *J Gastroenterol Hepatol* 1991; **6**: 209-222
 - 27 **Isomoto H**, Mizuta Y, Inoue K, Matsuo T, Hayakawa T, Miyazaki M, Onita K, Takeshima F, Murase K, Shimokawa I, Kohno S. A close relationship between *Helicobacter pylori* infection and gastric xanthoma. *Scand J Gastroenterol* 1999; **34**: 346-352
 - 28 **Karita M**, Li Q, Cantero D, Okita K. Establishment of a small animal model for human *Helicobacter pylori* infection using germ-free mouse. *Am J Gastroenterol* 1994; **89**: 208-213
 - 29 **Lambert JR**, Borromeo M, Pinkard KJ, Turner H, Chapman CB, Smith ML. Colonization of gnotobiotic piglets with *Campylobacter Pyloridis*--an animal model? *J Infect Dis* 1987; **155**: 1344
 - 30 **Radin MJ**, Eaton KA, Krakowka S, Morgan DR, Lee A, Otto G, Fox J. *Helicobacter pylori* gastric infection in gnotobiotic beagle dogs. *Infect Immun* 1990; **58**: 2606-2612
 - 31 **Shuto R**, Fujioka T, Kubota T, Nasu M. Experimental gastritis induced by *Helicobacter pylori* in Japanese monkeys. *Infect Immun* 1993; **61**: 933-939
 - 32 **Yan J**, Luo YH, Mao YF. Establishment of *Helicobacter pylori* infection model in Mongolian gerbils. *World J Gastroenterol* 2004; **10**: 852-855
 - 33 **Lee A**, O'Rourke J, De Ungria MC, Robertson B, Daskalopoulos G, Dixon MF. A standardized mouse model of *Helicobacter pylori* infection: inducing the Sydney strain. *Gastroenterology* 1997; **112**: 1386-1397
 - 34 **Ogura K**, Takahashi M, Maeda S, Ikenoue T, Kanai F, Yoshida H, Shiratori Y, Mori K, Mafune KI, Omata M. Interleukin-8 production in primary cultures of human gastric epithelial cells induced by *Helicobacter pylori*. *Dig Dis Sci* 1998; **43**: 2738-2743
 - 35 **Hirata Y**, Maeda S, Mitsuno Y, Tateishi K, Yanai A, Akanuma M, Yoshida H, Kawabe T, Shiratori Y, Omata M. *Helicobacter pylori* CagA protein activates serum response element-driven transcription independently of tyrosine phosphorylation. *Gastroenterology* 2002; **123**: 1962-1971
 - 36 **Baeuerle PA**, Baltimore D. NF-kappa B: ten years after. *Cell* 1996; **87**: 13-20
 - 37 **Isomoto H**, Mizuta Y, Miyazaki M, Takeshima F, Omagari K, Murase K, Nishiyama T, Inoue K, Murata I, Kohno S. Implication of NF-kappaB in *Helicobacter pylori*-associated gastritis. *Am J Gastroenterol* 2000; **95**: 2768-2776
 - 38 **Fujikawa A**, Shirasaka D, Yamamoto S, Ota H, Yahiro K, Fukada M, Shintani T, Wada A, Aoyama N, Hirayama T, Fukamachi H, Noda M. Mice deficient in protein tyrosine phosphatase receptor type Z are resistant to gastric ulcer induction by VacA of *Helicobacter pylori*. *Nat Genet* 2003; **33**: 375-381
 - 39 **Maeda S**, Ogura K, Yoshida H, Kanai F, Ikenoue T, Kato N, Shiratori Y, Omata M. Major virulence factors, VacA and CagA, are commonly positive in *Helicobacter pylori* isolates in Japan. *Gut* 1998; **42**: 338-343

• BRIEF REPORTS •

Anatomic and technical skill factor of gastroduodenal complication in post-transarterial embolization for hepatocellular carcinoma: A retrospective study of 280 cases

Ting-Kai Leung, Chi-Ming Lee, Hsin-Chi Chen

Ting-Kai Leung, Chi-Ming Lee, Hsin-Chi Chen, Department of Diagnostic Radiology, Taipei Medical University Hospital, Taipei, Taiwan, China

Correspondence to: Chi-Ming Lee, M.D., Department of Diagnostic Radiology, Taipei Medical University Hospital, 252, Wu Hsing Street, Taipei 110, Taiwan, China. vd142098@yahoo.com.tw

Telephone: +886-2-27372181-1131 Fax: +886-2-23780943

Received: 2004-08-13 Accepted: 2004-10-05

embolization; Gastroduodenal complication

Leung TK, Lee CM, Chen HC. Anatomic and technical skill factor of gastroduodenal complication in post-transarterial embolization for hepatocellular carcinoma: A retrospective study of 280 cases. *World J Gastroenterol* 2005; 11(10): 1554-1557

<http://www.wjgnet.com/1007-9327/11/1554.asp>

Abstract

AIM: To reduce the possibility of gastroduodenal complications. The purpose of this retrospective study was to survey the literature and compare and discuss the incidence of post-transarterial embolization (TAE) gastroduodenal complications.

METHODS: We found reports describing 280 cases of hepatocellular carcinoma with TAE procedures done during the past 4 years and selected all of them for our study. Amongst these cases, 86 were suspected of suffering gastroduodenal complications within one month of post-TAE treatment. Fifteen of these cases were proved by pan-endoscopy to have gastroduodenal erosions or ulcerations. We reviewed the angiographic pictures in patient records to evaluate the possibility that anatomic and technical skill factors could explain the complications.

RESULTS: Amongst the 15 cases, 9 were primary lesions of the antrum and prepylorus; 4 had duodenal ulcer or erosions; 2 had mid-body lesions; none showed a lesion at the fundus or cardia region. Three cases had not received TAEs using our ideal method, and may be associated with possible regurgitation of gel-foam pieces into the right or left gastric arteries. Two cases involved sub-selective embolization at a distal point on the hepatic artery; one case was found by angiography to have complete occlusion of the celiac trunk.

CONCLUSION: Comparing our results with past cases of post-TAE gastroduodenal complications, we surmise that our relatively low incidence (5.3%) of gastric complications might be explained by our concerted efforts to improve our technical skills in multi-sequential, selective and super-selective approaches to the embolization of tumor vessels.

© 2005 The WJG Press and Elsevier Inc. All rights reserved.

Key words: Post-TAE complication; Transarterial

INTRODUCTION

Transcatheter embolization for hepatocellular tumors has been performed worldwide for over 20 years. A Japanese study^[1,2] suggested that post-transarterial embolization (TAE) complications are mainly due to reflux of gel-foam pieces into the right gastric artery and to special anatomic factors (e.g., the right gastric artery is located too distal from the proper hepatic artery). In our 4-year study, we evaluated cases that had been reported in the literature and which resulted in post-TAE-induced gastroduodenal complications, as seen on endoscopy. In the current study we compare and discuss these cases.

MATERIALS AND METHODS

From January of 2000 to December of 2003, hundreds of cases in our hospital were diagnosed as hepatocellular carcinoma by fine needle biopsy, characteristic elevation of alpha-fetoprotein, or characteristic imaging findings (including three phases CT scans and diagnostic angiography). These patients received our TAE or transarterial chemotherapeutic embolization (TACE). In order to prevent the possible influence of adverse gastroduodenal effects due to anticancer drugs^[3], we excluded cases of combined treatment with chemotherapeutic, anticancer drugs (TACE). A total of 280 TAE cases were evaluated in this retrospective study.

Our TAE procedures involved administration of a mixture of lipiodol and 2 mg of gentamicin in a 20 cc syringe and a mixture of gel-foam pieces with contrast medium in another 20 cc syringe.

In order to prevent gastroduodenal complications, to preserve hepatic function and to decrease other possible adverse effects, most procedures involved placement of a 4- to 5-fr. catheter or a microcatheter, superselectively or selectively, so that embolization was as close as possible to the tumor vessels. The mixtures were transferred into smaller 2 cc syringes to achieve a slow and steady controlled injection.

The procedures were closely monitored under fluoroscopy in order to minimize backflow of lipiodol and gel-foam powder into the right gastric, left gastric or gastroduodenal arteries.

As part of our retrospective study, we recorded cases where patients had suffered gastric discomfort after the TAE procedure. There were 86 cases that received pan-endoscopy of the upper gastrointestinal tract (from esophagus to duodenum). Fifteen cases were chosen with positive findings of acute gastroduodenal erosions and ulcerations and which met the following criteria: (1) no history of peptic ulcer in the past 3 years; (2) patients began to have epigastric pain, nausea, black color stool or other gastric symptoms less than one month after TAE.

RESULTS

General observation

Amongst the 15 cases, 11 (73%) were suffering from GI symptoms and received pan-endoscopy with positive findings less than one week after TAE; 4 (27%) received pan-endoscopy more than one week but less than one month after TAE.

Endoscopic findings for the above study group included active stages of erosion and ulceration. None were found to involve active bleeding. The location of the main gastroduodenal lesions^[3-5] we found, is listed in Table 1.

Table 1 Upper GI endoscopic findings of mucosal erosion or ulceration among 15 TAE cases

Location	Case number
Fundus and cardia	0
Mid-body	2
Antrum and pre-pylorus	9
Duodenal ulcer or erosions	4
P	0.77

Anatomic and technical skill observation

Under arterial phase imaging, different patterns of anatomy of the proper hepatic artery, right hepatic artery and right gastric artery were found^[6]:

(1) Ten of the fifteen cases (66.7%) showed the most common anatomic form of three branches arising from the celiac trunk. The right gastric artery arose from the proper hepatic artery. The left hepatic artery divided from the proper hepatic artery. Amongst these patients, there were 4 cases with combined left and right lobe hepatic tumors. Each TAE procedure was done using the super-selective or selective principle (Figure 1A and B) with slow steady injection under fluoroscopic monitoring. Placement of the catheter was into the branches or the main trunk of the right hepatic artery (8 cases) or the left hepatic artery (4 cases). The observation reports are as follows: (1) two cases were completed using a non-ideal method, the sub-selective principle, where injection was made into the distal portion of the proper hepatic artery. Post-TAE angiographic injections of the above cases showed no diminished blood flow of the original, visible, right and left gastric arteries;

(2) Two cases (13.3%) showed complete displacement of the origin of the right hepatic artery to the superior mesenteric artery. The left hepatic and left gastric artery divided from the common hepatic artery. The right gastric artery arose from the left hepatic artery. TAE procedures were completed with selective injection (slow steady injection under fluoroscopic monitoring) into the right hepatic artery. Post-TAE angiographic injections showed no diminished blood flow in the right and left gastric arteries; (3) Two cases (13.3%) showed a three-branched celiac trunk with the right gastric artery arising from the left hepatic artery. The right hepatic artery divided from the proper hepatic artery. TAE procedures were completed with selective or super-selective injections into the right hepatic artery, again with slow steady injection under fluoroscopic monitoring. Post-TAE angiographic injections showed no diminished blood flow in the right and left gastric arteries; (4) there was one case (6.7%) with complete occlusion of the celiac trunk. Arterial angiography showed the absence of the common hepatic artery and its branches. The catheter was inserted so as to approach the right lobe of the hepatic tumor via a collateral branch of the SMA. The TAE procedure was completed without angiographic mapping of the right and left gastric arteries.

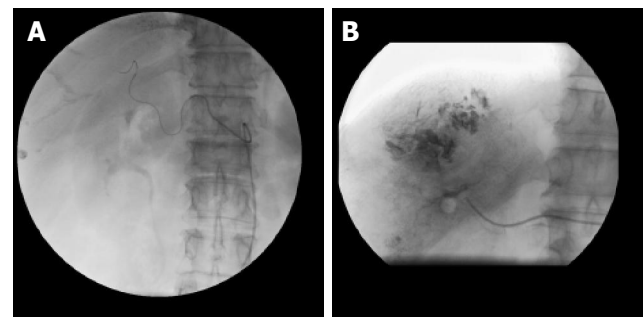


Figure 1 Some of our TAEs were superselective as close as by using microcatheter to approach as close as possible to the tumor vessel (A) and finished the embolization (B).

DISCUSSION

Technical analysis

Three patients did not receive TAE under ideal standard conditions. Of these three, 2 were in group 1 and 1 in group 4. All of them were associated with higher risk for gastroduodenal complications because of the imperfect technique that was used. A χ^2 , comparing these 3 to the other 12 cases, which had involved the use of the selective or super-selective TAE techniques, indicated that there was no statistically significant difference in the outcomes ($P = 0.16$; Table 2).

Table 2 P value between the number of cases of nonsuperselective/nonselective and superselective/selective is >0.05. There is no significant difference

Technique	Non-superselective/nonselective TAE	Super-selective-or selective TAE	P
Case number	3	12	0.16 (>0.05)

Anatomic analysis (Figure 2)^[7]

Usually, celiac trunk (A) gives rise to the common hepatic artery (B) and continue with proper hepatic artery (D), following the origin of the gastroduodenal artery (C). This artery is usually short and divides into the right (F), left (E) and, occasionally middle hepatic arteries. In others, one or more of the hepatic artery branches have a partially or totally displaced origin. The proper hepatic artery also frequently gives rise to the right gastric artery (H). Rarely, the origin of the entire hepatic blood supply is displaced to the superior mesenteric artery.

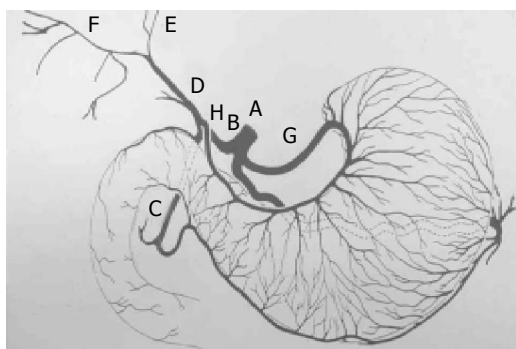


Figure 2 Description above.

The right gastric artery is not always visible at angiography unless it is providing a collateral blood supply to the left gastric artery^[6]. It is a small vessel that arises from the proper hepatic artery shortly after the origin of the gastroduodenal artery (C). It may also arise from the proximal left hepatic artery, especially when the right hepatic circulation is displaced to the superior mesenteric artery. The right gastric arteries are mostly anastomoses with the posterior branches of the left gastric artery (G). They mainly supply the pylorus and distal posterior surface of the stomach.

Tsuchigame and Takahashi^[1] suggested that post-TAE gastric lesions are basically due to the backflow of the embolic materials into the gastric artery and the consequent decrease in gastric mucosal blood flow may complicate gastric erosion or ulceration. According to their study, the incidence of post-TAE gastric complication is about 9%.

Nakamura and Hashimoto also discussed post-TAE gastric complications^[8]. They concluded that some anatomic variations - such as, the right gastric artery branches distally from the proper artery or its branch, or the accessory left gastric artery arises from the left hepatic artery - are the ones that are most likely to be associated with a high incidence of post-TAE gastric lesion.

Amongst the 15 cases of post-TAE gastroduodenal lesions, none showed complications in the gastric fundus and cardia region, suggesting a lesser association of complications with the left gastric artery. A high incidence of lesions was found at the antrum and prepylorus, which may reflect a greater association with the right gastric artery embolization^[9,10].

However, these differences in the incidence of post-TAE complication and the gastroduodenal locations were

not significant (Table 1).

According to our retrospective study of angiographic findings, only the two cases involving subselective proper hepatic artery embolization in Group 1 appear to complicate non-observable gel-foam^[11] reflux into the right gastric artery. On the other hand, the post-TAE consequence of gastroduodenal complications in Group 4 is unavoidable due to the unusual anatomic situation.

Angiographic reviews of Groups 2 and 3 appeared to involve the technical skills and safety factors during the embolization procedures and were proved by post-TAE angiographic views of the normal right gastric artery.

From January of 2000 to December of 2003, we improved our TAE procedure by incorporating segmental or sub-segmental embolizations. We strictly obeyed the principle of selective or superselective procedures during the embolizations. We achieved a rather low incidence (5.3%) of post-TAE gastroduodenal complications, which compared favorably to the 9% rate we found for published reports. In these reports, 3 of 280 cases (-1%) could be explained by non-ideal technical skills and anatomic factors, but 12 cases (4.3%) could not be explained.

Our findings indicate that there is no significant correlation between gastroduodenal complications^[12] and our imperfect technical embolization procedures (Table 2).

However, there still remain gastroduodenal complications^[13] (4.3%), beyond those attributable to anatomic factors^[14] and technical skills^[6].

Stress ulcer is one other possible etiology. There are at least five types of stress ulcers^[15] causing disturbances in the stomach and intestines. The pathogenesis of stress-induced lesions is probably multifactorial. We deduce that post-TAE pain sensation may be one stress-inducing factor. During stressful events^[16], normal protective mechanisms are altered, including epithelial turnover in the gastric mucosa and secretion of mucus and bicarbonate. These events, combined with the release of various mediators (e.g., arachidonic acid metabolites, cytokines, oxygen-free radicals), result in erosions that may progress to ulceration and bleeding^[15,16]. Reductions in mucosal blood flow may also be important in ulcer formation. Alterations in blood flow at the microcirculatory level may initiate changes that result in erosions that can progress to ulceration and bleeding.

REFERENCES

- 1 Tsuchigame T, Takahashi M, Watanabe O, Yoshimatsu S, Yamashita Y, Uozumi H, Ueno S, Hirota Y. Pathogenesis and prevention of gastrointestinal complications following transcatheter arterial embolization. *Nihon Igaku Hoshasen Gakkai Zasshi* 1990; **50**: 798-803
- 2 Ishigaki H, Suto T, Sasaki D, Tsushima K, Higuchi S, Baba T, Sano M, Munakata A, Yoshida Y, Takagi S. Factors of gastric lesions following after transcatheter arterial embolization for primary hepatoma. *Nihon Shokakibyo Gakkai Zasshi* 1990; **87**: 57-61
- 3 Matsuura T, Tsukamoto Y, Nakata H, Nakayama T, Shirakawa F, Okazaki I, Suzuki H. Complication of therapeutic transcatheter hepatic artery embolization for hepatoma-case of developing an extensive acute gastric ulcer. *Gan No Rinsho* 1983; **29**: A-11, 164-167
- 4 Sakamoto I, Aso N, Nagaoki K, Matsuoka Y, Uetani M, Ashizawa K, Iwanaga S, Mori M, Morikawa M, Fukuda T,

- Hayashi K, Matsunaga N. Complications associated with transcatheter arterial embolization for hepatic tumors. *Radiographics* 1998; **18**: 605–619
- 5 **Hirakawa M**, Iida M, Aoyagi K, Matsui T, Akagi K, Fujishima M. Gastroduodenal lesions after transcatheter arterial chemoembolization in patients with hepatocellular carcinoma. *Am J Gastroenterol* 1988; **83**: 837–840
- 6 **Lee KH**, Sung KB, Lee DY, Park SJ, Kim KW, Yu JS. Transcatheter arterial chemoembolization for hepatocellular carcinoma: anatomic and hemodynamic considerations in the hepatic artery and portal vein. *Radiographics* 2002; **22**: 1077–1091
- 7 **Stewart R**. Reuter, M.D. *Gastrointestinal Radiology* 1986: 1 (Saunders monographs in clinical radiology)
- 8 **Nakamura H**, Hashimoto T, Oi H, Sawada S, Furui S. Prevention of gastric complications in hepatic arterial chemoembolization. Balloon catheter occlusion technique. *Acta Radiol* 1991; **32**: 81–82
- 9 **Bradley EL**, Goldman ML. Gastric infarction after therapeutic embolization. *Surgery* 1976; **79**: 421–424
- 10 **Wells JJ**, Nostrant TT, Wilson JA, Gyves JW. Gastroduodenal ulcerations in patients receiving selective hepatic artery infusion chemotherapy. *Am J Gastroenterol* 1985; **80**: 425–429
- 11 **Tamura S**, Kihara Y, Yuki Y, Sugimura H, Shimizu T, Nishikawa T, Asato M, Adjei ON, Tong XQ, Watanabe K, Hasui Y. Lipiodolized gelatin sponge: a simple method to make gelatin sponge radiopaque. *Radiat Med* 1998; **16**: 13–15
- 12 **Hall DA**, Clouse ME, Gramm HF. Gastroduodenal ulceration after hepatic arterial infusion chemotherapy. *AJR Am J Roentgenol* 1981; **136**: 1216–1218
- 13 **Tsuchigame T**, Takahashi M, Bussaka H, Miyawaki M, Fukui K, Yasunaga T, Nanakawa S, Miyao M. Acute gastric lesions following transcatheter arterial embolization of hepatic malignancies. *Nihon Igaku Hoshasen Gakkai Zasshi* 1984; **44**: 1501–1507
- 14 **Charnsangavej C**, Carrasco CH, Wallace S, Richli W, Haynie TP. Hepatic arterial flow distribution with hepatic neoplasms: significance in infusion chemotherapy. *Radiology* 1987; **165**: 71–73
- 15 **Wightkin WT**. Stress ulcer: pathophysiology and prevention. *Am J Hosp Pharm* 1980; **37**: 1651–1655
- 16 **Liu GS**, Huang YX, Li SW, Pan BR, Wang X, Sun DY, Wang QL. Experimental study on mechanism and protection of stress ulcer produced by explosive noise. *World J Gastroenterol* 1998; **4**: 519–523

Edited by Guo SY Language Editor Elsevier HK

• BRIEF REPORTS •

Laparoscopic Heller myotomy with or without partial fundoplication: A matter of debate

G Ramacciato, FA D'Angelo, P Aurello, M Del Gaudio, G Varotti, P Mercantini, R Bellagamba, G Ercolani

G Ramacciato, FA D'Angelo, P Aurello, M Del Gaudio, G Varotti, P Mercantini, R Bellagamba, G Ercolani, Università degli Studi di Roma "La Sapienza" - II Facoltà di Medicina e Chirurgia. Ospedale Sant'Andrea - UOC Chirurgia "D", Via di Grottarossa n°1035-1037, 00189 Roma, Italia

Correspondence to: D'Angelo FA, MD. Università degli Studi di Roma "La Sapienza" - II Facoltà di Medicina e Chirurgia. Ospedale Sant'Andrea - UOC Chirurgia "D". Via di Grottarossa n°1035-1037, 00189 Roma, Italia. francesco.dangelo@uniroma1.it

Telephone: +39-680345693 Fax: +39-80345001

Received: 2004-08-31 Accepted: 2004-10-07

Abstract

AIM: To present our experience of laparoscopic Heller stretching myotomy followed by His angle reconstruction as surgical approach to esophageal achalasia.

METHODS: Thirty-two patients underwent laparoscopic Heller myotomy; an anterior partial fundoplication in 17, and angle of His reconstruction in 15 cases represented the antireflux procedure of choice.

RESULTS: There were no morbidity and mortality recorded in both anterior fundoplication and angle of His reconstruction groups. No differences were detected in terms of recurrent dysphagia, p.o. reflux or medical therapy.

CONCLUSION: To reduce the incidence of recurrent achalasia after laparoscopic Heller myotomy, we believe that His' angle reconstruction is a safe and effective alternative to the anterior fundoplication.

© 2005 The WJG Press and Elsevier Inc. All rights reserved.

Key words: Achalasia; Gastroesophageal reflux; Laparoscopic Heller myotomy

Ramacciato G, D'Angelo FA, Aurello P, Del Gaudio M, Varotti G, Mercantini P, Bellagamba R, Ercolani G. Laparoscopic Heller myotomy with or without partial fundoplication: A matter of debate. *World J Gastroenterol* 2005; 11(10): 1558-1561 <http://www.wjgnet.com/1007-9327/11/1558.asp>

INTRODUCTION

Achalasia is a rare esophageal disease characterized by incomplete and uncoordinated relaxation of the lower esophageal sphincter associated with aperistaltic esophagus.^[1,2]

This condition causes typical symptoms of dysphagia and regurgitation, heartburn, postprandial chest pain, malnutrition and aspiration, all leading to a poor quality of life.^[3] Treatment is directed to reduce the resting pressure of the lower esophageal sphincter which can be achieved in different ways: 1 pharmacologically, with the use of calcium channel blockers; 2 endoscopically, by means of balloon dilatation or botulinum toxin injection; 3 surgically, performing an esophageal myotomy^[4].

Extramucosal myotomy was first described by Heller in 1913, who performed two complete myotomies on opposite sides of the esophagus with an open access. Later in 1923, Zaaier restricted this procedure to a single anterior myotomy. However, surgical section of the muscular layers of the lower esophageal sphincter normally exposes the esophageal mucosa to gastroesophageal reflux, thus requiring an antireflux procedure^[5].

Since 1991, thoracoscopic and laparoscopic approaches to Heller myotomy have shown equal efficacy compared to open procedure, eventually making the laparoscopic Heller myotomy followed by an antireflux procedure, the treatment of choice for achalasia.^[6] Since several authors have eventually reported some lack of success of this procedure in terms of recurrent achalasia^[7,8], which required additional endoscopic or surgical maneuvers, the selective application of different antireflux procedures started to be put in place^[9-13].

Aim of this study is to present our experience of laparoscopic Heller stretching myotomy followed by His angle reconstruction, as surgical approach to esophageal achalasia.

MATERIALS AND METHODS

After a cumulative experience of more than 75 patients treated over a 20-year period with either open Heller-Nissen or Heller-Belsey fundoplication MKIV and a previous series of 16 cases treated with thoracoscopic Heller Myotomy,^[14] a total of 32 patients between 1997 and 2004 underwent Laparoscopic Heller Myotomy at the Department of Surgery "P. Valdoni" of the University of Rome "La Sapienza". In 17 patients an anterior partial fundoplication was associated to the myotomy (Heller - Dor, HD), whereas in 15 cases the angle of His reconstruction (Heller - His, HH) was the chosen antireflux procedure.

Pre-operative work-up consisted of patient's clinical history, barium swallow, upper GI endoscopy, and esophageal Ph-manometry. There were 16 males and 16 females with a mean age of 42.0 (range 14-77) and the mean symptoms-duration was 73.4 mo. The disease was graded according

to esophageal diameter: stage I (<4 cm): 1 patient, stage II (4-6 cm): 22 patients, stage III (>6 cm): 9 patients; median LES pressure was 32.8 mmHg (mean 32.8 ± 5.9 mmHg). Esophageal peristalsis was absent in all patients. None of them had undergone previous abdominal surgery.

Surgical technique: five trocars are required as previously described.^[14] After incision of the phrenoesophageal ligament, the dissection is performed selectively over the anterior aspect of the esophagus and the superior part of the diaphragmatic crura. The anterior vagus nerve is identified and its branches preserved. The short gastric vessels are not divided and the esophagus is not encircled, in order to preserve the anatomical attachments of the cardia. The esophageal dissection is prolonged into the mediastinum, 6-8 cm above the gastroesophageal junction (GEJ). The esophagomyotomy is then extended proximally to the GEJ for about 6 cm and distally for 2 cm below the cardia on the gastric wall. We found advantageous and safe performing the myotomy by stretching and tearing the circular muscle fibers with two laparoscopic graspers directed in opposite direction. Once the submucosal plane is reached, the muscular layer is separated bluntly from the submucosa and the stretching myotomy is easily extended proximally and distally. Bleeding from the esophageal musculature is minimal and no attempt is made to diathermy the bleeding. All surgical maneuvers are performed, with the esophagoscope placed in the esophagus, in order to assess the completeness of the myotomy and ensure mucosal integrity.

After completion of the myotomy once the partial anterior fundoplication has been performed, the anterior wall of the gastric fundus is sutured first to the left, then to the right muscular edges of the myotomy with three interrupted stitches for each side in H-D series (17 cases). The proximal suture of the right side also includes the superior part of the right crus. In 15 patients, we only reconstruct the angle of His, (H-H) tying two or three interrupted stitches between the gastric fundus and the left wall of the esophagus.

A barium swallow is routinely performed post-operatively on D1 to confirm mucosal integrity before starting oral fluid intake. Patients were discharged as soon as comfortable and when a soft diet was tolerated, usually on D2 or 3.

Patients were evaluated clinically at 1, 6, 12 mo after surgery, in order to assess recurrent achalasia or heartburn. This was achieved by handing out a standard validated questionnaire. Endoscopy and esophageal pH-manometry were carried out when indicated. All the patients received Proton-Pump-Inhibitors (PPI) medication in the perioperative period and for the first months after surgery.

Statistical analysis

SPSS statistical package was used to generate frequency distribution for demographic variables. The Fisher- exact test for comparison of patient subgroups for categorical variable was used. Results are expressed as mean \pm SD and median. Differences were considered significant at $P < 0.05$.

RESULTS

Among HD patients there was 1 esophageal perforation

identified at the time of surgery by intraoperative endoscopy and repaired laparoscopically with the anterior partial fundoplication protecting the suture. Mean operative time was 150 min (range 60-192 min). Mean blood -loss was less than 50 mL. No p.o. morbidity and mortality were recorded. Post-operative mean hospital stay was 2.0 ± 1.0 d. Occasional dysphagia and regurgitation were reported in 1 patient. Post-operative heartburn occurred in 1 patient, who was successfully treated with medical therapy. Barium swallow examination showed a decrease in mean esophageal diameter from 54.5 ± 5.7 to 27.1 ± 3.3 mm ($P = 0.0001$).

Among HH patients no esophageal perforation were identified at the time of surgery. Mean operative time was 130 min (range 60-145 min) and mean blood -loss was less than 50 mL. Neither p.o. morbidity nor mortality was recorded. Post-operative hospital stay was 2.0 ± 1.0 d. No p.o. dysphagia has been noticed. Post-operative occasional heartburn occurred in 3 cases, although only 1 required medical treatment.

Barium swallow examination showed a decrease in mean esophageal diameter from 55.3 ± 5.1 to 28.5 ± 2.9 mm ($P = 0.0001$).

When comparing p.o. dysphagia rates between HD *vs* HH group, no significant differences ($P = 1.0$) (Table 1) were found.

Post-operative gastroesophageal reflux following HD and HH occurred in 1 and 3 patients respectively, $P = 0.30$ (Table 2), only one patient submitted to HH operation required continuous medical treatment $P = 0.45$ (Table 3).

Table 1 Dysphagia after Heller-Dor vs Heller-His operation

	Dysphagia Yes patients (n)	%	No patients (n)	%	Total patients (n)
Heller-Dor	1	5.9	16	94.1	17
Heller-His			15	100	15
					32

$P = 1.0$.

Table 2 Gastroesophageal reflux Heller-Dor vs Heller-His operation

	Reflux Yes patients (n)	%	No patients (n)	%	Total patients (n)
Heller-Dor	1	5.9	16	94.1	17
Heller-His	3	20	12	80	15
					32

$P = 0.30$.

Table 3 Chronic PPI Therapy after Heller-Dor vs Heller-His operation

	PPI Medical Yes patients (n)	Therapy %	No patients (n)	%	Total patients (n)
Heller-Dor			17	100	17
Heller-His	1	6.6	14	93.4	15
					32

$P = 0.45$.

DISCUSSION

Heller myotomy is the most effective treatment of dysphagia due to achalasia, and the laparoscopic approach allows extending the myotomy well below the GEJ. Some aspects of this procedure, however, have yet to be defined. Firstly, there is no agreement about how much the myotomy should be extended in order to be effective. Secondly, it is still not clear to what extent the myotomy causes gastroesophageal reflux. Another unresolved issue is the need to add an antireflux procedure to the myotomy and what type of procedure should be performed. Finally, there is still debate about the incidence of recurrent achalasia following the antireflux procedure, and what are the reasons for this. Topart, in 1992, reported an incidence of 30% of redo-surgery for recurrent dysphagia following Heller myotomy associated with Nissen fundoplication^[12].

Oelschlager *et al*^[8] recently reported recurrence of dysphagia up to 17.3% in patients treated with myotomies extended for 1.5 cm or less below the GEJ, and only of 3.4% when extended for 3 cm below this mark.

Shiino *et al* reported severe dysphagia after myotomy in 16% of patients, requiring either surgical or endoscopic treatment. The myotomy was extended for 2 cm below the GEJ and an antireflux procedure was performed^[15]. Zaninotto *et al* reported an incidence of recurrent dysphagia of 8.8% after laparoscopic Heller myotomy followed by anterior partial fundoplication (Dor). According to the authors, this was due to either an incomplete section of the muscle fibers or to the fibrotic scar of the myotomy edges^[13]. The hypothesis that scarring between the fundoplication and esophageal mucosa in the anterior wrap may account for the poorer result after Dor procedure is also argued by Lyass^[11].

Oelschlager compared Dor *vs* Toupet fundoplication following Heller myotomy reporting an incidence of recurrent achalasia of 17.3% and 3.4%, respectively ($P = 0.001$).^[8] This could be due to the fact, that covering the myotomy site with the Dor fundoplication could lead to adhesions formation between the two surfaces and provoke recurrent achalasia;^[13] the Toupet fundoplication keeps the myotomy edges apart by keeping fixed the fundus to each side thus reducing the risk of fibrosis.^[8] Toupet fundoplication also requires dissection of the posterior esophageal attachments and the section of some of the short gastric vessels, which could reduce the GEJ competence with subsequent p.o. reflux. However, there are cases in which a partial fundoplication may be beneficial. In patients with hiatal hernia, fundoplication may prevent stomach herniation. When an unnoticed mucosal perforation occurs during myotomy, a partial fundoplication may be used to cover the repair.^[6] Clearly neither of the two approaches (Toupet or Dor fundoplication) resulted in a completely competent cardia and normal acid exposure^[5,8,11].

On the other hand Raiss reported a 2% incidence of recurrent achalasia after laparotomic Heller myotomy without fundoplication.^[16] Lyass, in a review of literature from 1991 to 2001, analyzed persistent dysphagia and p.o. gastroesophageal reflux after laparoscopic Heller myotomy associated or not to antireflux procedures.^[11] In this paper, an incidence of abnormal esophageal pH-manometry is reported in 35-36% of patients who underwent trans-

abdominal open Heller myotomy without fundoplication and 10-16% of patients who had a partial fundoplication. In the presented laparoscopic series, the rate of abnormal pH-manometry findings in the antireflux *vs* no antireflux procedures groups were 10% and 7.9%, respectively.^[11] This may be explained by the different technical aspects of the procedures. The extent of esophageal dissection performed in open surgery may be more disruptive. The angle of His, a natural barrier to reflux, is often destroyed by the extensive dissection performed in open surgery. The laparoscopic approach is less traumatic to this area and more often preserves this angle. Also, the length of the myotomy may be shorter, especially on the gastric side.^[11] Bloomston *et al* compared the results of laparoscopic Heller myotomy with or without concomitant fundoplication (Dor). The dysphagia rate was of 14% among patients who underwent myotomy alone compared to 26% of patients received concomitant Dor fundoplication. The incidence of anti-acid treatment required post-operatively in the two groups were 13% *vs* 10%, respectively (data non statistically significant)^[11,11] Diener *et al* and Douard reported 10% incidence of p.o. dysphagia^[17,18], and Ackroyd *et al*^[3] 13%. The incidence of p.o. dysphagia reported in literature varies between 17.3% and 30% after short myotomy compared to 3.4-16% after long myotomy^[15,19,20]. Kumar *et al* reported a 6% incidence of endoscopic proved esophagitis after laparoscopic cardiomyotomy using the Dundee technique which limits the mobilization to the anterior wall of the abdominal and thoracic esophagus, stating that the routine addition of an anti-reflux operation is not justified in patients undergoing laparoscopic cardiomyotomy, provided that the lateral and posterior attachment of the esophagus are kept intact^[21].

In striving to reduce the incidence of recurrent achalasia after Heller myotomy, we decided not to perform any type fundoplication over the raw mucosal surface. Furthermore, we did not dissect the posterior aspect of the esophagus as the Toupet fundoplication requires, in order to reduce the surgical modifications of the posterior elements of fixation of the GEJ. To control the gastroesophageal reflux, we decided to reconstruct the angle of His forcing the gastroesophageal gas valve mechanism described by Hill.^[22] Our technique requires the suture of the right side of the gastric dome to the adjacent left side of the esophageal myotomy with three interrupted, non absorbable stitches. In our series, we performed a 2 cm extended myotomy on the gastric side and we recorded only 1 case of p.o. occasional dysphagia (1/32) 3.1%, which was in the HD group (1/17, 5.8%). No recurrence of dysphagia was recorded among HH patients. Among the 3 patients who experience occasional episodes of p.o. heartburn, only 1 required medical therapy (PPI) to control the reflux. The association of a Dor antireflux procedure was necessarily performed in a case where a mucosal perforation was noticed at the time of surgery, whereas a different antireflux procedure could be chosen if the mucosal layer resulted intact after completion of the myotomy.^[11,20] Decker reported 17% p.o. dysphagia after myotomy and partial posterior or anterior fundoplication and 7% of mucosal perforation^[2]. Luketich and co-workers reported an overall incidence of 9.6% of intraoperative mucosal perforation

despite the use epinephrine injection to lift up the muscular layers and recurrent dysphagia rate of 12.9%, with 4.8% of redo myotomy^[7].

Mucosal tear rates vary from author to author: Luketich^[7] reported a rate of 9.6%, Bloomston^[1] of 6%, Decker^[2] 5.4%, Donahue^[20] 13.5%, Diener^[18] 5%, Ackroyd^[3] 12%, Raiss^[16] 4%. In our personal experience, intra-operative mucosal perforation decreased from 12.5% (thoracoscopic approach) to 5.9% (laparoscopic approach)^[14]. In the present series mucosal tearing occurred in 3.1%. Even if the laparoscopic approach offers better exposure of the GEJ injuries to the mucosa still occur especially when extending the myotomy on the gastric side, where the plane between the submucosa and the muscle layer is less evident and bleeding is more profuse^[13]. In order to reduce incidence of mucosal perforation we performed the myotomy by stretching and tearing the circular muscle fibers with two laparoscopic graspers directed in opposite directions, with no attempt to diathermy small bleeding or to perform the myotomy with monopolar hook or ultrasonic shears. Diathermy and division of circular muscle fibers with these instruments may increase the risk of intra-operative or delayed mucosal perforation. Since the use of this stretching technique, the incidence of mucosal perforation has decreased from 12.5% to 3.1% (1/32). Although mucosal tearing could not be completely abolished after stretching myotomy, 3.1% rate appears to be one of the lowest reported, even less than the one reported after open Heller procedure.^[16] Further improvement could be achieved in the future using robot-assisted laparoscopic cardiomyotomy as suggested by Shah *et al*, with the possibility of scaling down of movements allowing to be carry out the myotomy with greater precision, eliminating the surgeon's natural tremor too.

In conclusion, recurrent achalasia seems to be the major problem after laparoscopic Heller myotomy. In striving to reduce the incidence of this complication, we decided not to perform any type of fundoplication, in order to avoid adhesions formation and scarring between the row mucosal surface of the esophagus and the overlapped gastric wall.

Our antireflux procedure consisted in suturing the right side of the gastric fundus to the left side of the esophageal myotomy, stressing the His' angle flap valve. In this subgroup, no cases of recurrent achalasia were recorded, although when comparing the HH and HD groups no significant differences could be detected in respect to this issue. Before deciding not to perform an anterior fundoplication it is essential to rule out esophageal mucosa perforation at the time of surgery. In our experience, laparoscopic stretching myotomy is associated with a total incidence of mucosal perforation of 3.1% compared to 13.5-4% reported in literature.

REFERENCES

- 1 **Bloomston M**, Rosemurgy AS. Selective application of fundoplication during laparoscopic heller myotomy ensures favorable outcomes. *Surg Laparosc Endosc Percutan Tech* 2002; **12**: 309-315
- 2 **Decker G**, Borie F, Bouamrine D, Veyrac M, Guillon F, Fingerhut A, Millat B. Gastrointestinal quality of life before and after laparoscopic heller myotomy with partial posterior fundoplication. *Ann Surg* 2002; **236**: 750-758; discussion 758

- 3 **Ackroyd R**, Watson DI, Devitt PG, Jamieson GG. Laparoscopic cardiomyotomy and anterior partial fundoplication for achalasia. *Surg Endosc* 2001; **15**: 683-686
- 4 **Patti MG**, Fisichella PM, Perretta S, Galvani C, Gorodner MV, Robinson T, Way LW. Impact of minimally invasive surgery on the treatment of esophageal achalasia: a decade of change. *J Am Coll Surg* 2003; **196**: 698-703; discussion 703-705
- 5 **Richards WO**, Clements RH, Wang PC, Lind CD, Mertz H, Ladipo JK, Holzman MD, Sharp KW. Prevalence of gastroesophageal reflux after laparoscopic Heller myotomy. *Surg Endosc* 1999; **13**: 1010-1014
- 6 **Shimi S**, Nathanson LK, Cuschieri A. Laparoscopic cardiomyotomy for achalasia. *J R Coll Surg Edinb* 1991; **36**: 152-154
- 7 **Luketich JD**, Fernando HC, Christie NA, Buenaventura PO, Keenan RJ, Ikramuddin S, Schauer PR. Outcomes after minimally invasive esophagomyotomy. *Ann Thorac Surg* 2001; **72**: 1909-1912; discussion 1912-1913
- 8 **Oelschlager BK**, Chang L, Pellegrini CA. Improved outcome after extended gastric myotomy for achalasia. *Arch Surg* 2003; **138**: 490-495; discussion 495-497
- 9 **Chipponi J**. Should fundoplication be added to Heller's myotomy? *Ann Chir* 2002; **127**: 743-744
- 10 **Hagedorn C**, Jonson C, Lonroth H, Ruth M, Thune A, Lundell L. Efficacy of an anterior as compared with a posterior laparoscopic partial fundoplication: results of a randomized, controlled clinical trial. *Ann Surg* 2003; **238**: 189-196
- 11 **Lyass S**, Thoman D, Steiner JP, Phillips E. Current status of an antireflux procedure in laparoscopic Heller myotomy. *Surg Endosc* 2003; **17**: 554-558
- 12 **Topart P**, Deschamps C, Taillefer R, Duranceau A. Long-term effect of total fundoplication on the myotomized esophagus. *Ann Thorac Surg* 1992; **54**: 1046-1051; discussion 1051-1052
- 13 **Zaninotto G**, Costantini M, Portale G, Battaglia G, Molena D, Carta A, Costantino M, Nicoletti L, Ancona E. Etiology, diagnosis, and treatment of failures after laparoscopic Heller myotomy for achalasia. *Ann Surg* 2002; **235**: 186-192
- 14 **Ramacciato G**, Mercantini P, Amodio PM, Corigliano N, Barreca M, Stipa F, Ziparo V. The laparoscopic approach with antireflux surgery is superior to the thoracoscopic approach for the treatment of esophageal achalasia. Experience of a single surgical unit. *Surg Endosc* 2002; **16**: 1431-1437
- 15 **Shiino Y**, Awad ZT, Haynatzki GR, Davis RE, Hinder RA, Filipi CJ. Postmyotomy dysphagia after laparoscopic surgery for achalasia. *World J Gastroenterol* 2003; **9**: 1129-1131
- 16 **Raiss M**, Hraa A, Menfaa M, Al Baroudi S, Ahallat M, Hosni K, Halhal A, Tounsi A. Heller's myotomy without fundoplication: a series of 123 patients. *Ann Chir* 2002; **127**: 771-775
- 17 **Douard R**, Gaudric M, Chaussade S, Couturier D, Houssin D, Dousset B. Functional results after laparoscopic Heller myotomy for achalasia: A comparative study to open surgery. *Surgery* 2004; **136**: 16-24
- 18 **Diener U**, Patti MG, Molena D, Tamburini A, Fisichella PM, Whang K, Way LW. Laparoscopic Heller myotomy relieves dysphagia in patients with achalasia and low LES pressure following pneumatic dilatation. *Surg Endosc* 2001; **15**: 687-690
- 19 **Chen LQ**, Chughtai T, Sideris L, Nastos D, Taillefer R, Ferraro P, Duranceau A. Long-term effects of myotomy and partial fundoplication for esophageal achalasia. *Dis Esophagus* 2002; **15**: 171-179
- 20 **Donahue PE**, Horgan S, Liu KJ, Madura JA. Floppy Dor fundoplication after esophagocardiomyotomy for achalasia. *Surgery* 2002; **132**: 716-722; discussion 722-723
- 21 **Kumar V**, Shimi SM, Cuschieri A. Does laparoscopic cardiomyotomy require an antireflux procedure? *Endoscopy* 1998; **30**: 8-11
- 22 **Hill LD**, Aye RW, Nilsson C. The Hill Repair. In: Griffith Pearson F, Cooper JD, Deslauriers J, Ginsberg RJ, Hiebert CA, Alexander Patterson G, Hirschel Jr HC (eds): *Esophageal Surgery* (2nd ed.). Philadelphia: Churchill Livingstone; 2002, chapter 22: 345-356. Elsevier Science, PA, USA

• BRIEF REPORTS •

Immunocytochemical detection of HoxD9 and Pbx1 homeodomain protein expression in Chinese esophageal squamous cell carcinomas

De-Bin Liu, Zhen-Dong Gu, Xiao-Zhe Cao, Hong Liu, Ji-You Li

De-Bin Liu, Zhen-Dong Gu, Hong Liu, Department of Thoracic Surgery, Peking University School of Oncology, Beijing Cancer Hospital, Beijing Institute for Cancer Research, Beijing 100036, China

Xiao-Zhe Cao, Department of Pathology, Lanzhou General Hospital of PLA, Lanzhou 730030, Gansu Province, China

Ji-You Li, Department of Pathology, Peking University School of Oncology, Beijing Cancer Hospital, Beijing Institute for Cancer Research, Beijing 100036, China

Supported by Beijing New Star of Science and Technology Plan from Beijing Municipal Science and Technology Commission, No. 954813600, and by Institutional Research Fund of Peking University School of Oncology, Beijing Cancer Hospital; and partially supported by Research Fund of Beijing Municipal Science and Technology Commission, No. H020920030390

Correspondence to: De-Bin Liu, Department of Thoracic Surgery, Peking University School of Oncology, Beijing Cancer Hospital, Beijing Institute for Cancer Research, Beijing 100036, China. dbliumd@sohu.com

Telephone: +86-10-88121122 Fax: +86-10-88122437

Received: 2004-08-16 Accepted: 2004-10-18

© 2005 The WJG Press and Elsevier Inc. All rights reserved.

Key words: Esophageal squamous cell carcinoma; Homeobox genes; Homeodomain; HoxD9; Pbx1

Liu DB, Gu ZD, Cao XZ, Liu H, Li JY. Immunocytochemical detection of HoxD9 and Pbx1 homeodomain protein expression in Chinese esophageal squamous cell carcinomas. *World J Gastroenterol* 2005; 11(10): 1562-1566

<http://www.wjgnet.com/1007-9327/11/1562.asp>

INTRODUCTION

Esophageal squamous cell carcinoma (ESCC) is one of the most common fatal cancers worldwide, and the highest rates of esophageal cancer in the world occur in north-central China. Although tremendous advances in diagnosis and treatment have been achieved recently, esophageal cancer is still one of the most lethal malignancies mainly because of its later discovery. However, many cases of esophageal carcinoma could be cured and even prevented if there were better screening methods to uncover the disease when it is limited and most responsive to intervention. A possibility is to screen patients for the expression of various regulatory genes. The etiology of esophageal cancer has been partially elucidated using recently devised molecular biological techniques. The homeobox (Hox) genes are a family of regulatory genes that contain a common 183-nucleotide sequence and code for specific nuclear proteins (homeoproteins) that act as transcription factors. In addition to their roles in axial patterning during embryonic development^[1-4], Hox genes help control the normal cellular proliferation and differentiation of several adult tissues^[5-7] and the proliferation and oncogenic transformation in some neoplasms and cancers^[8-11].

HoxD9 is the member of Abd-B related HoxD genes located closest to the 3' end of the chromosome. It is involved in the development and patterning of the forelimb and axial skeleton^[12]. HoxD9 gene is also known to be a potential transcription factor that not only autoregulates itself but also transactivates other Hox genes and certain members of other gene families^[13,14].

The Pbx1 proto-oncogene, another transcription factor, was originally identified at the site of t(1;19) chromosomal translocations in acute pre-B-cell leukemia. The Pbx1 gene codes for two isoforms of the homeodomain (HD) DNA-binding motif^[15,16]. Human pre-B-cell acute leukemias are frequently associated with t(1;19)(q23; p13,3) chromosomal

Abstract

AIM: To evaluate the expression pattern of two novel oncofetal antigens, the HoxD9 and Pbx1 homeoproteins in esophageal squamous cell carcinomas (ESCCs) to determine what role they would play in the carcinogenesis of ESCC.

METHODS: We obtained tissue samples of ESCC from 56 patients who underwent esophagectomy but not preoperative chemotherapy or radiotherapy. The diagnosis of ESCC was established and confirmed by staff pathologists. We used a highly sensitive, indirect, immunocytochemical method to detect HoxD9 and Pbx1 proteins. We qualitatively and quantitatively evaluated cells that exhibited and staining using a light microscope.

RESULTS: In all observed carcinoma tissue samples, more than 60% of neoplastic cells stained lightly or strongly for HoxD9, and more than 50% of neoplastic cells stained lightly or strongly for Pbx1.

CONCLUSION: Our data suggest that HoxD9 and Pbx1 are inappropriately expressed in most human esophageal squamous cell carcinoma. Understanding the role of Hox genes in esophageal epithelial cell carcinogenesis may not only augment early detection but also offer new avenues for treatment of this disease.

rearrangement, which creates a chimeric gene encoding a fused E2a and Pbx1 proteins^[17-20]. Aberrant E2a transcripts lacking the helix-loop-helix DNA-binding motif have been detected in several stable cell lines carrying the translocation^[16]. Fusion cDNAs have been shown to encode an 85 KDa protein composed of the N-terminal two-thirds transactivation domain of the E2a protein fused to a homeoprotein termed Pbx1^[16-18]. Thus Pbx1 is a class II Hox gene. Although homeoprotein can bind to DNA as monomers, dimerization with Pbx homeoproteins substantially increases the DNA-binding activity of these transcription factors^[21].

We examined expression pattern of two novel oncofetal antigens, the HoxD9 and Pbx1 homeoproteins in ESCC by using a sensitive immunocytochemical method to evaluate if they could be a screening tool for esophageal cancer.

MATERIALS AND METHODS

Tissue handling and storage

All 56 ESCC from patients whose tissues used in the retrospective study were formalin-fixed, paraffin-embedded archival specimens obtained from the pathology tissue banks. The patients underwent esophagectomy at Peking University School of Oncology, Beijing Cancer Hospital without preoperative chemotherapy or radiotherapy. These tissues were fixed in 10% formalin buffered with phosphate to pH 7.4 and were then embedded in paraffin. The diagnosis of ESCC was established and confirmed by staff pathologists in the Department of Pathology of Beijing Cancer Hospital. This study was approved by the Institutional Board for Clinical Research.

Antibodies

Anti-HoxD9 antibody (H-342; Santa Cruz Biotechnology, Santa Cruz, CA) is a rabbit polyclonal antibody raised against a recombinant protein corresponding to amino acids 1-342, a sequence that represents full-length HoxD9 of human origin. This antibody is recommended by the company for detection of HoxD9, HoxC9, HoxA9 and HoxB9 of mouse, rat, and human origin by Western blotting, immunoprecipitation, and immunohistochemistry. Anti-Pbx1 antibody (P-20; Santa Cruz Biotechnology) is an affinity-purified rabbit polyclonal antibody raised against a peptide mapped to the amino terminus of Pbx1 of human origin. This antibody reacts with Pbx1 of mouse, rat, and human origin as detected by Western blotting and immunohistochemistry, and it does not cross-react with Pbx2 or Pbx3.

Immunocytochemical antigen-detection technique

We used a highly sensitive, indirect four-step immunocytochemical method^[22-26] in formalin-fixed, paraffin-embedded ESCC tissue samples to detect HoxD9 and Pbx1 proteins. Briefly, the samples were deparaffinized by three changes of xylene substitute for 20-30 min, and then rehydrated using decreasing dilutions of alcohol (100%, 95%, 85%, 70%, and 50% to PBS). An initial blocking step using 1% hydrogen peroxide was necessary to eliminate endogenous alkaline phosphatase activity. A second blocking step was conducted with purified goat serum for antigenic epitopes and excess serum was removed from the area

surrounding the sections. The tissue sections were incubated with primary anti-HoxD9 or anti-Pbx1 antibodies for 90-120 min, and then with the secondary antibody for 20 min. Immunostaining of the antigen primary antibody complex was performed using the avidin-biotin-peroxidase complex with the LSAB kit, peroxidase (Dako, Kyoto, Japan) to allow formation of a stable yellow-brown precipitate and was followed by light hematoxylin counterstaining. Finally, short- and long-term morphologic clearings were carried out with two changes of xylene substitute.

As a control, some sections of each tissue sample were not incubated with primary antibody. Other sections were not treated with hydrogen peroxide so we could confirm the presence of endogenous alkaline phosphatase activity.

Tissue evaluation

Qualitative and quantitative evaluation of the percentage of antigen-positive cells as determined by their yellow-brown color and intensity of staining were conducted using a light microscope (Olympus, Kyoto, Japan). For each section, we counted 100-200 cells each from five distinct areas in non-necrotic, non-hemorrhagic ESCC tissues. Artifacts were avoided, and areas with morphologic characteristics of interest were identified. The intensity of staining was characterized as very intense, strong, light, or negative^[22]. We calculated the percentage of cells that exhibited any staining^[22]. (+++++) indicates that >90% of the total cell number are positive; (++++) indicates that 51-90% of the total cell number are positive; (++) indicates 11-50% of the total cell number are positive; (+) indicates 1-10% of the total cell number are positive; (-) are negative.

RESULTS

HoxD9 and Pbx1 were both observed in the nuclei and cytoplasm of the ESCC cells (Figure 1A). In all sections, more than 60% of neoplastic cells lightly or strongly stained for HoxD9. More than 50% of neoplastic cells also stained lightly or strongly for Pbx1 (Figure 1B).

DISCUSSION

The presence of HoxD9 and Pbx1 demonstrated the re-expression of these transcriptional regulators of oncogenesis and histogenesis after neoplastic transformation of esophageal epithelium and its cellular differentiation. Bodey and his colleagues established the expression pattern of three homeoproteins (Hox-B3, -B4, and -C6) in human lung carcinoma^[23], osteosarcoma^[24], breast carcinoma^[25], and childhood medulloblastoma^[26] tissues. Using the same immunocytochemical technique we did two Hox gene products in human ESCC cells. Thus re-expression of Hox gene products occurs in a wide variety of neoplastically transformed cells, and homeoproteins appear to be a family of oncofetal antigens involved in both normal cellular development and in cellular carcinogenesis and tumor progression.

Genes that have been shown to be controlled by homeoproteins encode adhesion molecules, transcription factors (in particular the Hox genes themselves), and growth

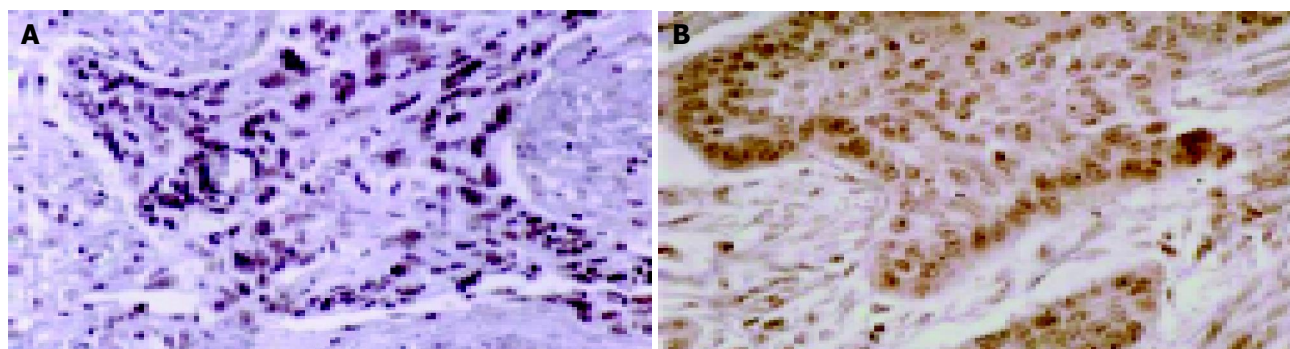


Figure 1 Tissue sections of human ESCC. A: Strongly staining for HoxD9 can be seen in the nuclei and cytoplasm of the ESCC cells (×400); B: Strongly staining for Pbx1 can be seen in the nuclei and cytoplasm of the ESCC cells (×400).

factors. At present, the putative targets of HoxD9 include other members of the Hox family and adhesion molecules, such as the liver cell adhesion molecule^[13,14]. At least one Hox gene, HoxB7, has been shown to activate basic fibroblast growth factor (bFGF) transcription in melanomas by binding to the promoter of bFGF gene^[27]. Moreover, transduction of the breast carcinoma cell line with the HoxB7 gene induces bFGF expression and increases cell proliferation of teratocarcinoma cells^[28]. Whether HoxD9 directly affects the regulation of bFGF and c-Fos, important factors for cell proliferation and transformation is uncertain and needs further investigation. However, bFGF and c-Fos were found to be up-regulated in HoxD9 transfected synoviocytes. HoxD9 appears to play a role in bFGF-induced proliferation, but not so much so in the tumor necrosis factor pathway^[29].

Pbx proteins comprise a functionally and biochemically distinct subclass of homeoproteins. A similar role for Pbx is indicated by this protein's potential involvement in a highly conserved autoregulatory loop that controls HoxB1 expression in the mouse hindbrain^[30]. Pbx1 was discovered as a fusion with the E2a gene after chromosomal translocations in a subset of acute leukemias. The resulting E2a-Pbx1 chimeric proteins display potent oncogenic properties that appear to require dimerization with Hox DNA-binding partners. E2a-Pbx1 heterodimerizes with Hox but not with MEIS proteins (members of the TALE family of homeoproteins), produces acute myeloid leukemia in mice, and blocks differentiation of cultured murine myeloid progenitors. Calvo *et al*^[31] reported that a 25-residue predicted alpha-helix preceding the Pbx1 HD bound this HD and prevented both its binding to DNA and its ability to heterodimerize with Hox proteins. Addition of 39 residues at the N terminus to this inhibitory helix revealed a Pbx dimerization interface that orchestrated cooperative DNA-binding of E2a-Pbx1 and exposed all Pbx proteins as homodimers and heterodimers. Sequences inhibiting DNA-binding and mediating Pbx dimerization coincided with those reported to have nuclear export function. An additional 103 residues at the N terminus side of the Pbx dimerization interface restored heterodimerization with Hox and MEIS1 proteins. This negative switch domain comprising of the inhibitory helix and N-terminal regions required for its partner-mediated derepression was dispensable to myeloid immortalization by E2a-Pbx1. Although the heterodimer

was stabilized, the 310 helix C terminus to the Pbx1 HD was also dispensable to E2a-Pbx1's ability to heterodimerize with Hox proteins and immortalize myeloblasts. Retention of myeloid immortalization by E2a-Pbx1 proteins lacking all Pbx1 sequences for the N or C terminus to the HD indicates that Hox proteins cooperate with E2a-Pbx1 in myeloid immortalization^[31].

The DNA-binding affinity and specificity of homeoproteins is augmented by cofactor interactions. Hox cofactors in mammals include Pbx^[32] and MEIS^[33]. Pbx proteins bind DNA cooperatively as heterodimers with MEIS family members and also with homeoproteins from paralog groups 1 to 10. MEIS proteins cooperatively bind DNA with the Abd-B class of homeoproteins groups 9 and 10. The most important aspects of this binding are that most of the Pbx N terminus to the HD is required for efficient cooperative binding with HoxD4 and HoxD9; MEIS and Pbx proteins form higher-order complexes on a heterodimeric binding site; MEIS forms a similar trimer with DNA-bound Pbx-HoxD9; and an additional trimer class involving non-DNA-bound Pbx and DNA-bound MEIS-HoxD9 or MEIS-HoxD10 heterodimers is enhanced by mutation of the Pbx HD^[34]. These findings suggest novel functions for Pbx and MEIS in modulating the function of DNA-bound MEIS-Hox and Pbx-Hox heterodimers, respectively.

Retinoic acid induces expression of genes encoding the Hox family of transcription factors, whose differential expression orchestrates developmental programs specifying anterior-posterior structures during embryogenesis, thereby possibly inducing various effects on Hox gene expression based on the subset organization of its receptors^[35]. Homeoproteins bind DNA as monomers and Pbx proteins as heterodimers. Retinoic acid up-regulated Pbx expression coincident with transcriptional activation of Hox genes in P19 embryonal carcinoma cells undergoing neuronal differentiation. However, in contrast to Hox induction, Pbx up-regulation was predominantly a result of post-transcriptional mechanisms. Pbx1, as well as its highly related family members Pbx2 and Pbx3, exhibited different profiles of up-regulation, suggesting possible functional divergence^[35]. The parallel up-regulation of Pbx and Hox proteins in this model suggests an important role for transcriptional control by Pbx-Hox heterodimers during neurogenesis and provide evidence of precise control by retinoic acid^[36].

The function of homeoproteins may be modulated by various secreted factors, such as growth factors, cytokines, and hormones. The involvement of HoxD9 in the regulation of cellular growth might be mediated, at least in part, by up-regulation of growth factors such as bFGF and c-Fos or might result from increased transcription activity by its regulators^[34]. The expression of HoxC6 in osteosarcomas and neuroblastomas is differentially regulated by rhBMP-2, tumor growth factor-beta, and activin-A, which suggests that specific Hox genes may be target genes for tumor growth factor-beta superfamily members and may represent a way in which growth factors exert their immense effects on development and carcinogenesis^[37].

Many adjuvant therapies and surgical procedures have been examined to improve survival among patients with esophageal cancer. Surgical resection rates have improved strikingly, and operative mortality has decreased markedly. However, the curative potential of surgery is likely highest when the disease is detected while it is still in early stage. Our data suggest that two Hox genes, HoxD9 and Pbx1, are inappropriately expressed in most ESCCs. The exact mechanisms that regulate the re-expression of these oncofetal antigens in ESCC, as well as other solid tumors, should be elucidated through further basic research. Understanding the role of Hox genes in esophageal epithelial cell carcinogenesis may not only increase early detection but also offer new avenues of treatment for this disease.

ACKNOWLEDGEMENTS

We appreciate the excellent immunocytochemical induction provided by Professor De-Wen Wang and Ms. Ya-Bin Gao.

REFERENCES

- 1 **Gehring WJ**, Hiromi Y. Homeotic genes and the homeobox. *Annu Rev Genet* 1986; **20**: 147-173
- 2 **McGinnis W**, Krumlauf R. Homeobox genes and axial patterning. *Cell* 1992; **68**: 283-302
- 3 **Lewis EB**. A gene complex controlling segmentation in *Drosophila*. *Nature* 1978; **276**: 565-570
- 4 **Krumlauf R**. Hox genes in vertebrate development. *Cell* 1994; **78**: 191-201
- 5 **Quaranta MT**, Petrini M, Tritarelli E, Samoggia P, Care A, Bottero L, Testa U, Peschle C. HOXB cluster genes in activated natural killer lymphocytes: expression from 3'-->5' cluster side and proliferative function. *J Immunol* 1996; **157**: 2462-2469
- 6 **Care A**, Testa U, Bassani A, Tritarelli E, Montesoro E, Samoggia P, Cianetti L, Peschle C. Coordinate expression and proliferative role of HOXB genes in activated adult T lymphocytes. *Mol Cell Biol* 1994; **14**: 4872-4877
- 7 **Magli MC**, Largman C, Lawrence HJ. Effects of HOX homeobox genes in blood cell differentiation. *J Cell Physiol* 1997; **173**: 168-177
- 8 **Cillo C**, Barba P, Freschi G, Bucciarelli G, Magli MC, Boncinelli E. HOX gene expression in normal and neoplastic human kidney. *Int J Cancer* 1992; **51**: 892-897
- 9 **De Vita G**, Barba P, Odartchenko N, Givel JC, Freschi G, Bucciarelli G, Magli MC, Boncinelli E, Cillo C. Expression of homeobox-containing genes in primary and metastatic colorectal cancer. *Eur J Cancer* 1993; **29A**: 887-893
- 10 **Thorsteinsdottir U**, Sauvageau G, Humphries RK. Hox homeobox genes as regulators of normal and leukemic hematopoiesis. *Hematol Oncol Clin North Am* 1997; **11**: 1221-1237
- 11 **Duboule D**. *Guidebook to the Homeobox Genes*. Oxford: Oxford University Press, 1994
- 12 **Fromental-Ramain C**, Warot X, Lakkaraju S, Favier B, Haack H, Birling C, Dierich A, Doll e P, Chambon P. Specific and redundant functions of the paralogous Hoxa-9 and Hoxd-9 genes in forelimb and axial skeleton patterning. *Development* 1996; **122**: 461-472
- 13 **Zappavigna V**, Renucci A, Izpisua-Belmonte JC, Urier G, Peschle C, Duboule D. HOX4 genes encode transcription factors with potential auto- and cross-regulatory capacities. *EMBO J* 1991; **10**: 4177-4187
- 14 **Goomer RS**, Holst BD, Wood IC, Jones FS, Edelman GM. Regulation *in vitro* of an L-CAM enhancer by homeobox genes HoxD9 and HNF-1. *Proc Natl Acad Sci USA* 1994; **91**: 7985-7989
- 15 **Kamps MP**, Murre C, Sun XH, Baltimore D. A new homeobox gene contributes the DNA binding domain of the t(1;19) translocation protein in pre-B ALL. *Cell* 1990; **60**: 547-555
- 16 **Nourse J**, Mellentin JD, Galili N, Wilkinson J, Stanbridge E, Smith SD, Cleary ML. Chromosomal translocation t(1;19) results in synthesis of a homeobox fusion mRNA that codes for a potential chimeric transcription factor. *Cell* 1990; **60**: 535-545
- 17 **Monica K**, Galili N, Nourse J, Saltman D, Cleary ML. PBX2 and PBX3, new homeobox genes with extensive homology to the human proto-oncogene PBX1. *Mol Cell Biol* 1991; **11**: 6149-6157
- 18 **Monica K**, LeBrun DP, Dederda DA, Brown R, Cleary ML. Transformation properties of the E2a-Pbx1 chimeric oncoprotein: fusion with E2a is essential, but the Pbx1 homeodomain is dispensable. *Mol Cell Biol* 1994; **14**: 8304-8314
- 19 **Lu Q**, Wright DD, Kamps MP. Fusion with E2A converts the Pbx1 homeodomain protein into a constitutive transcriptional activator in human leukemias carrying the t(1;19) translocation. *Mol Cell Biol* 1994; **14**: 3938-3948
- 20 **LeBrun DP**, Cleary ML. Fusion with E2A alters the transcriptional properties of the homeodomain protein PBX1 in t(1;19) leukemias. *Oncogene* 1994; **9**: 1641-1647
- 21 **Phelan ML**, Featherstone MS. Distinct HOX N-terminal arm residues are responsible for specificity of DNA recognition by HOX monomers and HOX.PBX heterodimers. *J Biol Chem* 1997; **272**: 8635-8643
- 22 **Bodey B**, Zeltzer PM, Saldivar V, Kemshead J. Immunophenotyping of childhood astrocytomas with a library of monoclonal antibodies. *Int J Cancer* 1990; **45**: 1079-1087
- 23 **Bodey B**, Bodey B, Groger AM, Siegel SE, Kaiser HE. Immunocytochemical detection of homeobox B3, B4, and C6 gene product expression in lung carcinomas. *Anticancer Res* 2000; **20**: 2711-2716
- 24 **Bodey B**, Bodey B, Siegel SE, Luck JV, Kaiser HE. Homeobox B3, B4, and C6 gene product expression in osteosarcomas as detected by immunocytochemistry. *Anticancer Res* 2000; **20**: 2717-2721
- 25 **Bodey B**, Bodey B, Siegel SE, Kaiser HE. Immunocytochemical detection of the homeobox B3, B4, and C6 gene products in breast carcinomas. *Anticancer Res* 2000; **20**: 3281-3286
- 26 **Bodey B**, Bodey B, Siegel SE, Kaiser HE. Immunocytochemical detection of the homeobox B3, B4, and C6 gene products in childhood medulloblastomas/primitive neuroectodermal tumors. *Anticancer Res* 2000; **20**: 1769-1780
- 27 **Care A**, Silvani A, Meccia E, Mattia G, Stoppacciaro A, Parmiani G, Peschle C, Colombo MP. HOXB7 constitutively activates basic fibroblast growth factor in melanomas. *Mol Cell Biol* 1996; **16**: 4842-4851
- 28 **Nakajima T**, Aono H, Hasunuma T, Yamamoto K, Maruyama I, Nosaka T, Hatanaka M, Nishioka K. Overgrowth of human synovial cells driven by the human T cell leukemia virus type I tax gene. *J Clin Invest* 1993; **92**: 186-193
- 29 **Khoa ND**, Nakazawa M, Hasunuma T, Nakajima T,

- Nakamura H, Kobata T, Nishioka K. Potential role of HOXD9 in synoviocyte proliferation. *Arthritis Rheum* 2001; **44**: 1013-1021
- 30 **Slupsky CM**, Sykes DB, Gay GL, Sykes BD. The HoxB1 hexapeptide is a prefolded domain: implications for the Pbx1/Hox interaction. *Protein Sci* 2001; **10**: 1244-1253
- 31 **Calvo KR**, Knoepfler P, McGrath S, Kamps MP. An inhibitory switch derepressed by pbx, hox, and Meis/Prep1 partners regulates DNA-binding by pbx1 and E2a-pbx1 and is dispensable for myeloid immortalization by E2a-pbx1. *Oncogene* 1999; **18**: 8033-8043
- 32 **Phelan ML**, Rambaldi I, Featherstone MS. Cooperative interactions between HOX and PBX proteins mediated by a conserved peptide motif. *Mol Cell Biol* 1995; **15**: 3989-3997
- 33 **Shen WF**, Montgomery JC, Rozenfeld S, Moskow JJ, Lawrence HJ, Buchberg AM, Largman C. AbdB-like Hox proteins stabilize DNA binding by the Meis1 homeodomain proteins. *Mol Cell Biol* 1997; **17**: 6448-6458
- 34 **Shanmugam K**, Green NC, Rambaldi I, Saragovi HU, Featherstone MS. PBX and MEIS as non-DNA-binding partners in trimeric complexes with HOX proteins. *Mol Cell Biol* 1999; **19**: 7577-7588
- 35 **Langston AW**, Gudas LJ. Retinoic acid and homeobox gene regulation. *Curr Opin Genet Dev* 1994; **4**: 550-555
- 36 **Knoepfler PS**, Kamps MP. The Pbx family of proteins is strongly upregulated by a post-transcriptional mechanism during retinoic acid-induced differentiation of P19 embryonal carcinoma cells. *Mech Dev* 1997; **63**: 5-14
- 37 **Kloen P**, Visker MH, Olijve W, van Zoelen EJ, Boersma CJ. Cell-type-specific modulation of Hox gene expression by members of the TGF-beta superfamily: a comparison between human osteosarcoma and neuroblastoma cell lines. *Biochem Biophys Res Commun* 1997; **233**: 365-369

Edited by Guo SY Language Editor Elsevier HK

• CASE REPORT •

Effect of *Helicobacter pylori* eradication on gastric hyperplastic polyposis in Cowden's disease

Hajime Isomoto, Hisashi Furusu, Ken Ohnita, Yusuke Takehara, Chun-Yang Wen, Shigeru Kohno

Hajime Isomoto, Hisashi Furusu, Ken Ohnita, Yusuke Takehara, Shigeru Kohno, Second Department of Internal Medicine, Nagasaki University School of Medicine 1-7-1 Sakamoto, Nagasaki, Japan

Chun-Yang Wen, Department of Molecular Pathology, Atomic Bomb Disease Institute, Nagasaki University School of Medicine, Sakamoto 12-4, Nagasaki, Japan

Chun-Yang Wen, Department of Digestive Disease, Nanjing Drum Tower Hospital, Medical School of Nanjing University, Nanjing 210008, Jiangsu Province, China

Correspondence to: Dr. Hajime Isomoto, Second Department of Internal Medicine, Nagasaki University School of Medicine 1-7-1 Sakamoto, Nagasaki, Japan. hajimei2002@yahoo.co.jp

Telephone: +81-95-8497567 Fax: +81-95-8497568

Received: 2004-08-14 Accepted: 2004-09-30

Abstract

A 21-year-old woman with complaints of hematochezia was diagnosed as having Cowden's disease (CD), an autosomal dominant condition characterized by multiple hamartomas, since facial papules and gingival papillomas were identified. On endoscopy, multiple hyperplastic polyps were seen in the rectum and left-side colon. There were also esophageal glycogenic acanthosis and hyperplastic polyposis in the antrum accompanied by *Helicobacter pylori*-related gastritis. Although gastric hyperplastic polyposis had by no means regressed with unsuccessful first-line eradication therapy for *H. pylori*, following cure of the infection with salvage therapy consisting of rabeprazole, amoxicillin and metronidazole, the polyposis lesions almost disappeared. Follow-up gastroscopy 2 and 3 years after cessation of the second-line eradication therapy revealed almost complete regression of the polyposis lesions with no evidence of *H. pylori* infection. We recommend eradication treatment for CD patients with gastric hyperplastic polyps and the infection, as the occurrence of gastric carcinoma among hyperplastic polyps has been described.

© 2005 The WJG Press and Elsevier Inc. All rights reserved.

Key words: Cowden's disease; *Helicobacter pylori*; Hyperplastic polyposis

Isomoto H, Furusu H, Ohnita K, Takehara Y, Wen CY, Kohno S. Effect of *Helicobacter pylori* eradication on gastric hyperplastic polyposis in Cowden's disease. *World J Gastroenterol* 2005; 11(10): 1567-1569

<http://www.wjgnet.com/1007-9327/11/1567.asp>

INTRODUCTION

Cowden's disease (CD) is a rare autosomally dominant inherited cancer predisposition syndrome characterized by multiple hamartomas involving various organ systems derived from all three germ cell layers^[1]. Pathognomonic mucocutaneous features include facial papules that are especially prominent around the nasal labial folds and perioral area; acral keratoses of the palms and soles; and mucous papillomas^[1,2]. Alimentary tract abnormalities found in CD primarily appear as multiple polyps of various histopathologic features including hamartomatous, hyperplastic, inflammatory, juvenile, lymphomatous and adenomatous polyps^[3-6]. Hyperplastic polyp is the most common gastric polyp seen in CD^[6].

Although hyperplastic polyp itself is non-neoplastic, the risk of dysplastic changes and/or carcinomatous conversion is now recognized^[7]. Patients with gastric polyps may present with bleeding, abdominal pain or gastric outlet obstruction^[8]. Therefore, most clinicians agree that the large gastric polyps or polyps associated with complications should be removed endoscopically or surgically^[9]. Recently, the strong relationship between gastric hyperplastic polyp and *Helicobacter pylori* (*H. pylori*) infection has been demonstrated^[10-13]. Ohkusa *et al*^[10] reported that most hyperplastic polyps disappeared after cure of the infection. Eradication of *H. pylori* may, therefore, be a therapeutic option for hyperplastic polyps occurring in association with *H. pylori* gastritis^[10-12]. Herein, we describe a patient with CD in whom hyperplastic gastric polyposis with concomitant *H. pylori* infection almost disappeared following successful eradication.

CASE REPORT

A 21-year-old Japanese woman presented with hematochezia of 2-wk duration. The past and family histories were unremarkable. Laboratory tests were normal except for positive fecal occult blood. On physical examination with dermatological consultation, multiple facial papules and gingival papillomas were identified. Thus, a definite diagnosis of CD was made, fulfilling the two major clinical criteria^[14]. However, no abnormalities involving the thyroid, breast, skeleton and genitourinary tract were found. Upper gastrointestinal endoscopy revealed numerous sessile or hemispheric polyps up to 5 mm in size within the antrum (Figure 1). Biopsies obtained from the polyposis revealed hyperplasia of foveolar epithelium, along with neutrophil and mononuclear cell infiltration, consistent with histological characteristics of hyperplastic polyp^[11]. In addition, multiple, whitish, minute protrusions, which showed positive staining



Figure 1 Endoscopy revealed numerous sessile polyps up to 5 mm in size within the antrum.

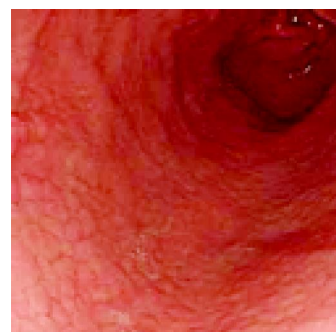


Figure 2 Note the near disappearance of polyposis on repeat gastroscopy 2 years after the commencement of anti-*Helicobacter pylori* second-line therapy.

with iodine, were observed throughout the esophagus. Biopsies from these lesions showed glycogenic acanthosis. Colonoscopy showed multiple, whitish, sessile polyps ranging in size from 2 to 8 mm, which extended from the rectum to the descending colon but exhibited a predilection for the rectosigmoid area. These polyps were histopathologically judged to be hyperplastic. Barium contrast study of the small bowel and computed tomograms of the brain, neck, chest, abdomen and pelvis showed no abnormalities.

H. pylori infection was detected both in the antrum and corpus by Giemsa staining and rapid urease test using biopsy samples obtained during gastroscopy. The patient was treated with a 1-wk course of triple therapy consisting of lansoprazole 30 mg twice daily, amoxicillin 750 mg twice daily and clarithromycin 200 mg twice daily, but repeat gastroscopy 3 mo after commencement of the initial treatment showed no regression or disappearance of the gastric hyperplastic polyposis. Histopathological examination of biopsy samples from the antrum and corpus showed persistent infection by the same organism and chronic active gastritis. The patient was subsequently treated with a 1-wk triple therapy consisting of rabeprazole 10 mg twice daily, amoxicillin 750 mg twice daily and metronidazole 250 mg twice daily^[15]. Four weeks after cessation of the salvage treatment, the ¹³C-urea breath test was negative. Three months later, repeat gastroscopy showed substantial decrease in size and number of the polyposis. A 2-year follow-up gastroscopy revealed almost complete regression of the lesions (Figure 2). *H. pylori* infection was still negative (urea breath test) at the last follow-up, 3 years after commencement of the eradication treatment. However, the morphology of esophageal and colonic lesions remains unchanged.

DISCUSSION

Gastrointestinal involvement is common in CD^[3-6]. Histopathologically different types of gastrointestinal polyps have been observed frequently in patients with CD^[3-6]. In this regard, gastrointestinal hamartoma is considered as a criterion in the extensive set of formal criteria required for the diagnosis of CD proposed by International Cowden Consortium^[14]. In one series of 51 individuals of whom 20 had a gastrointestinal workup, 16 had gastrointestinal lesions including 13 colonic polyps^[16]. Typically, multiple polyps of

the distal colon and rectum were seen with relative sparing of the proximal colon^[16]. Multiple small polyps in the stomach and duodenum were also common^[6,16]. Esophageal glycogenic acanthosis is a distinct lesion of affected patients with diffuse papillomatosis^[3,17], as noted in our case. Gastroenterologists should consider the diagnosis of CD in any patient with such lesions in the digestive tract.

To date, there is little information on the association of *H. pylori* infection with gastric manifestations of CD. Lee *et al*^[18] reported the first case of CD with gastric hamartomatous polyposis accompanied by *H. pylori*-related gastritis, albeit antibiotic treatment for the infection was not applied. In our patient, following cure of *H. pylori* infection with salvage therapy, polyposis lesions significantly regressed, although polyposis had by no means regressed with unsuccessful first-line triple therapy. This relation provided further support for recent studies indicating a close relationship between hyperplastic polyp and persistent *H. pylori* infection; cure of the infection results in regression or disappearance of most hyperplastic polyps^[10,12,13].

One can speculate that the inflammatory cell infiltration and acceleration of epithelial cell turnover induced by *H. pylori* infection contributes to the development and/or progression of hyperplastic polyps^[10,11]. Most CD patients have been shown to carry germ line or somatic mutations of *PTEN* (*protein tyrosine phosphatase and tensin homolog*), which is a tumor suppressor gene located on chromosome 10q23^[19,20]. This lipid phosphatase activity of *PTEN* products plays a role in the regulation of phosphoinositol 3-kinase and is relevant in limiting cell cycle progression and promoting apoptosis and thus suppressing cell cycle^[2,4,19]. Therefore, in the formation of gastric hyperplastic polyps of CD, such *H. pylori*-associated effect may facilitate the inherent tendency of cell proliferation and tissue disorganization predisposed by genetic alteration representative of *PTEN* mutation^[2,4,19].

The risk that patients with hyperplastic polyps would develop gastric carcinoma was reported to be as high as 3.6%^[21]. Hyperplastic polyps develop in atrophic mucosa in 40-75% of cases^[22], and it is possible that in many cases of hyperplastic polyps, chronic atrophic gastritis, which is mostly the consequence of *H. pylori* infection, increases the risk of developing gastric carcinoma^[11,22,23]. In addition, the incidence of malignant transformation of gastric hyperplastic polyps is estimated at 1.5 to 3%^[7]. In fact,

gastric carcinoma *in situ* among hyperplastic polyps has been described in a CD woman^[24]. Therefore, we recommend anti-*H. pylori* eradication treatment for patients with CD manifesting gastric hyperplastic polyps, when they present with concomitant *H. pylori* infection.

Once the diagnosis of CD is made, affected patients have to be considered as high- risk patients for developing malignancies^[2,5]. The most common associated malignancies are breast, thyroid and endometrial carcinomas^[2,5]. A life-long follow-up is necessary for this CD woman. Colonic adenocarcinomas have been reported in patients with CD^[25], albeit their association with this disease at molecular levels remains unclear. Therefore, the existing polyps should be addressed by repeat endoscopic surveillance in the present case.

REFERENCES

- Lloyd KM, Denis M. Cowden's disease: A possible new symptom complex with multiple system involvement. *Ann Intern Med* 1963; **58**: 136-142
- Fistarol SK, Anliker MD, Itin PH. Cowden disease or multiple hamartoma syndrome-cutaneous clue to internal malignancy. *Eur J Dermatol* 2002; **12**: 411-421
- Kay PS, Soetikno RM, Mindelzun R, Young HS. Diffuse esophageal glycogenic acanthosis: an endoscopic marker of Cowden's disease. *Am J Gastroenterol* 1997; **92**: 1038-1040
- Corredor J, Wambach J, Barnard J. Gastrointestinal polyps in children: advances in molecular genetics, diagnosis, and management. *J Pediatr* 2001; **138**: 621-628
- Wirtzfeld DA, Petrelli NJ, Rodriguez-Bigas MA. Hamartomatous polyposis syndromes: molecular genetics, neoplastic risk, and surveillance recommendations. *Ann Surg Oncol* 2001; **8**: 319-327
- Hizawa K, Iida M, Matsumoto T, Kohrogi N, Suekane H, Yao T, Fujishima M. Gastrointestinal manifestations of Cowden's disease. Report of four cases. *J Clin Gastroenterol* 1994; **18**: 13-18
- Daibo M, Itabashi M, Hirota T. Malignant transformation of gastric hyperplastic polyps. *Am J Gastroenterol* 1987; **82**: 1016-1025
- Neimark S, Rogers AI. Gastric polyps: a review. *Am J Gastroenterol* 1982; **77**: 585-587
- Isomoto H, Inoue K, Furusu H, Enjoji A, Fujimoto C, Yamakawa M, Hirakata Y, Omagari K, Mizuta Y, Murase K, Shimada S, Murata I, Kohno S. The role of endoscopy in the surveillance of premalignant condition of the upper gastrointestinal tract. Guidelines for clinical applications. *Gastrointestinal Endosc* 1998; **34**(Suppl 3): 18-20
- Ohkusa T, Takashimizu I, Fujiki K, Suzuki S, Shimoi K, Horiuchi T, Sakurazawa T, Ariake K, Ishii K, Kumagai J, Tanizawa T. Disappearance of hyperplastic polyps in the stomach after eradication of *Helicobacter pylori*. A randomized, clinical trial. *Ann Intern Med* 1998; **129**: 712-715
- Oberhuber G, Stolte M. Gastric polyps: an update of their pathology and biological significance. *Virchows Arch* 2000; **437**: 581-590
- Ljubicic N, Banic M, Kujundzic M, Antic Z, Vrkljan M, Kovacevic I, Hrabar D, Doko M, Zovak M, Mihatov S. The effect of eradicating *Helicobacter pylori* infection on the course of adenomatous and hyperplastic gastric polyps. *Eur J Gastroenterol Hepatol* 1999; **11**: 727-730
- Mocek FW, Ward WW, Wolfson SE, Ramage WT, Wieman TJ. Elimination of recurrent hyperplastic polyps by eradication of *Helicobacter pylori*. *Ann Intern Med* 1994; **120**: 1007-1008
- Eng C. Will the real Cowden syndrome please stand up: revised diagnostic criteria. *J Med Genet* 2000; **37**: 828-830
- Isomoto H, Inoue K, Furusu H, Enjoji A, Fujimoto C, Yamakawa M, Hirakata Y, Omagari K, Mizuta Y, Murase K, Shimada S, Murata I, Kohno S. High-dose rabeprazole-amoxicillin versus rabeprazole-amoxicillin-metronidazole as second-line treatment after failure of the Japanese standard regimen for *Helicobacter pylori* infection. *Aliment Pharmacol Ther* 2003; **18**: 101-107
- Starink TM, van der Veen JP, Arwert F, de Waal LP, de Lange GG, Gille JJ, Eriksson AW. The Cowden syndrome: a clinical and genetic study in 21 patients. *Clin Genet* 1986; **29**: 222-233
- McGarrity TJ, Wagner-Baker MJ, Ruggiero FM, Thiboutot DM, Hampel H, Zhou XP, Eng C. GI polyposis and glycogenic acanthosis of the esophagus associated with *PTEN* mutation positive Cowden syndrome in the absence of cutaneous manifestations. *Am J Gastroenterol* 2003; **98**: 1429-1434
- Lee HR, Moon YS, Yeom CH, Kim KW, Chun JY, Kim HK, Choi HS, Kim DK, Chung TS. Cowden's disease-a report on the first case in Korea and literature review. *J Korean Med Sci* 1997; **12**: 570-575
- Liaw D, Marsh DJ, Li J, Dahia PL, Wang SI, Zheng Z, Bose S, Call KM, Tsou HC, Peacocke M, Eng C, Parsons R. Germline mutations of the *PTEN* gene in Cowden disease, an inherited breast and thyroid cancer syndrome. *Nat Genet* 1997; **16**: 64-67
- Chi SG, Kim HJ, Park BJ, Min HJ, Park JH, Kim YW, Dong SH, Kim BH, Lee JL, Chang YW, Chang R, Kim WK, Yang MH. Mutational abrogation of the *PTEN/MMAC1* gene in gastrointestinal polyps in patients with Cowden disease. *Gastroenterology* 1998; **115**: 1084-1089
- Stolte M, Bethke B, Sticht T, Burkhard U. Differentiation of focal foveolar hyperplasia from hyperplastic polyps in gastric biopsy material. *Pathol Res Pract* 1995; **191**: 1198-1202
- Laxen F, Kekki M, Sipponen P, Siurala M. The gastric mucosa in stomachs with polyps: morphologic and dynamic evaluation. *Scand J Gastroenterol* 1983; **18**: 503-511
- Veereman Wauters G, Ferrell L, Ostroff JW, Heyman MB. Hyperplastic gastric polyps associated with persistent *Helicobacter pylori* infection and active gastritis. *Am J Gastroenterol* 1990; **85**: 1395-1397
- Hamby LS, Lee EY, Schwarz RW. Parathyroid adenoma and gastric carcinoma as manifestations of Cowden's disease. *Surgery* 1995; **118**: 115-117
- Carlson GJ, Nivatvongs S, Snover DC. Colorectal polyps in Cowden's disease (multiple hamartoma syndrome). *Am J Surg Pathol* 1984; **8**: 763-770

• ACKNOWLEDGEMENTS •

Acknowledgements to Reviewers of *World Journal of Gastroenterology*

Many reviewers have contributed their expertise and time to the peer review, a critical process to ensure the quality of *World Journal of Gastroenterology*. The editors and authors of the articles submitted to the journal are grateful to the following reviewers for evaluating the articles (including those were published and those were rejected in this issue) during the last editing period of time.

Ke-Ji Chen, Professor

Xiyuan Hospital, Chinese Traditional Medicine University, Beijing 100091, China

Zong-Jie Cui, Professor

Institute of Cell Biology, Beijing Normal University, Beijing 100875, China

Dai-Ming Fan, Professor

Director of Department of Gastroenterology, Xijing Hospital, Fourth Military Medical University, Xi'an 710032, China

Xue-Gong Fan, Professor

Xiangya Hospital, Changsha 410008, China

Gan-Sheng Feng, M.D.

Huazhong University of Science and Technology, Tongji Medical College, Union Hospital, Wuhan 430032, Hubei Province, China

Zhi-Qiang Huang, Professor

Abdominal Surgery Institute of General Hospital of PLA, Fuxing Road, Beijing 100853, China

Joseph B Kirsner, M.D.

Department of Medicine/GI, Univ. of Chicago Hospitals & Clinics, University of Chicago Hosp. & Clinics, 5841 S. Maryland Ave., Mail Code 2100. Chicago IL 60637-1470, United States

Ai- Ping Lu, Professor

China Academy of Traditional Chinese Medicine, Dongzhimen Nei, 18 Beixincang, Beijing 100700, China

Shou-Dong Lee, Professor

Department of Medicine, Taipei Veterans General Hospital, 201 Shih-Pai Road, Sec. 2. Taipei 112, Taiwan

Peter Malfertheiner, M.D.

Clinic of Gastroenterology Hepatology and Infectious Disease, Otto-von-Guericke-University, Leipziger Str. 44, Magdeburg 39120, Germany

Mikio Nishioka, M.D.

Ehime Rosai Hospital, 13-27 Minami Komatsubara, Niihama 792-8550, Japan

Lun-Xiu Qin, Professor

Liver Cancer Institute and Zhongshan Hospital, Fudan University, 180 Feng Lin Road, Shanghai 200032, China

Christian Rabe, M.D.

Resident, Department of Medicine 1, University of Bonn Sigumund-Freud-Strasse, 25 D 53105 Bonn, Germany

Vasiliy Ivanovich Reshetnyak, Professor

Institute of General Reanimatology, 25-2, Petrovka Str., Moscow 107031, Russian Federation

Michael Steer, Professor

Department of Surgery, Tufts-Nemc, 860 Washington St, Boston, Ma 02111, United States

Ken Shirabe, M.D.

Department of surgery, Aso Iizuka Hospital, 3-83 Yoshio Machi, Iizuka City 820-8205, Japan

Bertram Wiedenmann, M.D.

Department of Internal Medicine, Division of Hepatology and Gastroenterology and Interdisciplinary Center for Metabolism, Endocrinology and Diabetes Mellitus, Augustenburger Platz 1, Berlin D-13353, Germany

Howard J. Worman, M.D.

Department of Medicine, College of Physicians and Surgeons Columbia University, 630 West 168th Street, New York, NY 10032, United States

George Y Wu, Professor

Department of Medicine, Division of Gastroenterology-Hepatology, University of Connecticut Health Center, 263 Farmington Ave, Farmington, CT 06030, United States

Eddie Wisse, Professor

Irisweg 16, Keerbergen 3140, Belgium

Ming-Shiang Wu, Associate Professor

Department of Internal Medicine, National Taiwan University Hospital, No 7, Chung-Shan S. Rd., Taipei 100, Taiwan

Jia-Yu Xu, Professor

Shanghai Second Medical University, Rui Jin Hospital, 197 Rui Jin Er Road, Shanghai 200025, China

Zhi-Rong Zhang, Professor

West China School of Pharmacy, Sichuan University, 17 South Renmin Road, Chengdu 610041, Sichuan Province, China

Wei-Guo Zhu, M.D.

Peking University Health Science Center, Beijing 100083, China

Meetings

Major meetings coming up

**Digestive Disease Week
106th Annual Meeting of AGA, The
American Gastroenterology Association**
May 14-19, 2005
www.ddw.org/
Chicago, Illinois

13th World Congress of Gastroenterology
September 10-14, 2005
www.wcog2005.org/
Montreal, Canada

**13th United European Gastroenterology
Week, UEGW**
October 15-20, 2005
www.uegf.org/
Copenhagen, Denmark

**American College of Gastroenterology
Annual Scientific Meeting**
October 28-November 2, 2005
www.acg.gi.org/
Honolulu Convention Center, Honolulu,
Hawaii

Events and Meetings in the upcoming 6 months

EASL 2005 the 40th annual meeting
April 13-17, 2005
www.easl.ch/easl2005/
Paris, France

**21st annual international congress of
Pakistan society of Gastroenterology &
GI Endoscopy**
March 25-27, 2005
www.psgc2005.com
Peshawar

**World Congress on Gastrointestinal
Cancer**
June 15-18, 2005
Barcelona

**British Society of Gastroenterology
Conference (BSG)**
March 14-17, 2005
www.bsg.org.uk
Birmingham

**Digestive Disease Week DDW 106th
Annual Meeting**

May 15-18, 2005
www.ddw.org
Chicago, Illinois

Events and meetings in 2005

**Canadian Digestive Disease Week
Conference**
February 26-March 6, 2005
www.cag-acg.org
Banff, AB

2005 World Congress of Gastroenterology
September 12-14, 2005
Montreal, Canada

**International Colorectal Disease
Symposium 2005**
February 3-5, 2005
Hong Kong

**13th UEGW meeting United European
Gastroenterology Week**
October 15-20, 2005
www.webasistent.cz/guarant/uegw2005/
Copenhagen-Malmoe

**7th International Workshop on Thera-
peutic Endoscopy**
September 10-12, 2005
www.alfamedical.com
Theodor Bilharz Research Institute

EASL 2005 the 40th annual meeting
April 13-17, 2005
www.easl.ch/easl2005/
Paris, France

**Pediatric Gastroenterology, Hepatology
and Nutrition**
March 13, 2005
Jakarta, Indonesia

**21st annual international congress of
Pakistan society of Gastroenterology &
GI Endoscopy**
March 25-27, 2005
www.psgc2005.com
Peshawar

**8th Congress of the Asian Society of
HepatoBiliary Pancreatic Surgery**
February 10-13, 2005
Mandaluyong, Philippines

**APDW 2005 - Asia Pacific Digestive
Week 2005**
September 25-28, 2005
www.apdw2005.org
Seoul, Korea

**World Congress on Gastrointestinal
Cancer**
June 15-18, 2005
Barcelona

**British Society of Gastroenterology
Conference (BSG)**
March 14-17, 2005
www.bsg.org.uk
Birmingham

**Digestive Disease Week DDW 106th
Annual Meeting**
May 15-18, 2005
www.ddw.org
Chicago, Illinois

**70th ACG Annual Scientific Meeting
and Postgraduate Course**
October 28-November 2, 2005
Honolulu Convention Center, Honolulu,
Hawaii

Events and Meetings in 2006

**EASL 2006 - THE 41ST ANNUAL
MEETING**
April 26-30, 2006
Vienna, Austria

**Canadian Digestive Disease Week
Conference**
March 4-12, 2006
www.cag-acg.org
Quebec City

**XXX pan-american congress of digestive
diseases XXX congreso panamericano de
enfermedades digestivas**
November 25-December 1, 2006
www.gastro.org.mx
Cancun

**World Congress on Gastrointestinal
Cancer**
June 14-17, 2006
Barcelona, Spain

**7th World Congress of the International
Hepato-Pancreato-Biliary Association**
September 3-7, 2006
www.edinburgh.org/conference
Edinburgh

**71st ACG Annual Scientific Meeting
and Postgraduate Course**
October 20-25, 2006
Venetian Hotel, Las Vegas, Nevada

Instructions to authors

GENERAL INFORMATION

World Journal of Gastroenterology (WJG, ISSN 1007-9327) is a weekly journal of more than 48 000 circulation, published on the 7th, 14th, 21st and 28th of every month.

Original Research, Clinical Trials, Reviews, Comments, and Case Reports in esophageal cancer, gastric cancer, colon cancer, liver cancer, viral liver diseases, *etc.*, from all over the world are welcome on the condition that they have not been published previously and have not been submitted simultaneously elsewhere.

Published jointly by

The WJG Press and Elsevier Inc.

SUBMISSION OF MANUSCRIPTS

Manuscripts should be typed double-spaced on A4 (297×210 mm) white paper with outer margins of 2.5 cm. Number all pages consecutively, and start each of the following sections on a new page: Title Page, Abstract, Introduction, Materials and Methods, Results, Discussion, Acknowledgements, References, Tables, Figures and Figure Legends. Neither the Editors nor the Publisher is responsible for the opinions expressed by contributors. Manuscripts formally accepted for publication become the permanent property of The WJG Press and Elsevier Inc., and may not be reproduced by any means, in whole or in part without the written permission of both the Authors and the Publisher. We reserve the right to put onto our website and copy-edit accepted manuscripts. Authors should also follow the guidelines for the care and use of laboratory animals of their institution or national animal welfare committee.

Authors should retain one copy of the text, tables, photographs and illustrations, as rejected manuscripts will not be returned to the author(s) and the editors will not be responsible for the loss or damage to photographs and illustrations.

Online submission

Online submission is strongly advised. Manuscripts should be submitted through the Online Submission System at: <http://www.wjgnet.com/index.jsp>. Authors are highly recommended to consult the ONLINE INSTRUCTIONS TO AUTHORS (<http://www.wjgnet.com/wjg/help/instructions.jsp>) before attempting to submit online. Authors encountering problems with the Online Submission System may send an email describing the problem to wjg@wjgnet.com for assistance. If you submit manuscript online, do not make a postal contribution. A repeated online submission for the same manuscript is strictly prohibited.

Postal submission

Send 3 duplicate hard copies of the full-text manuscript typed double-spaced on A4(297×210 mm) white paper together with any original photographs or illustrations and a 3.5 inch computer diskette or CD-ROM containing an electronic copy of the manuscript including all the figures, graphs and tables in native Microsoft Word format or *.rtf format to:

World Journal of Gastroenterology

Room 1066, Yishou Garden,
No.58, North Langxinzhuang Road,
PO Box 2345, Beijing 100023, China
E-mail: wjg@wjgnet.com
<http://www.wjgnet.com>

MANUSCRIPT PREPARATION

All contributions should be written in English. All articles must be submitted using a word-processing software. All submissions must be typed in 1.5 line spacing and in word size 12 with ample margins. The letter font is Tahoma. For authors originating from China, one copy of the Chinese translation of the manuscript is also required (excluding references). Style should conform to our house format. Required information for each of the manuscript sections is as follows:

Title page

Full manuscript title, running title, all author(s) name(s), affiliations, institution(s) and/or department(s) where the work was accomplished, disclosure of any financial support for the research, and the name, full address, telephone and fax numbers and email address of the corresponding author should be involved. Titles should be concise and informative (removing all unnecessary words), emphasize what is NEW, and avoid abbreviations. A short running title of less than 40 letters should be provided. List the author(s)' name(s) as follows: initials and/or first name, middle name or initial(s) and full family name.

Abstract

An informative, structured abstract of no more than 250 words should accompany each manuscript. Abstracts for original contributions should be structured into the following sections: AIM: Only the purpose should be included. METHODS: The materials, techniques, instruments and equipments, and the experimental procedures should be included. RESULTS: The observatory and experimental results, including data, effects, outcome, *etc.* should be included. Authors should present *P* value where necessary, and the significant data should accompany. CONCLUSION: Accurate view and the value of the results should be included.

The format of structured abstracts is at: <http://www.wjgnet.com/wjg/help/11.doc>

Key words

Please list 3-10 key words that could reflect content of the study.

Text

For most article types, the main text should be structured into the following sections: INTRODUCTION, MATERIALS AND METHODS, RESULTS AND DISCUSSION, and should include appropriate Figures and Tables. Data should be presented in the body text or Figures and Tables, not both.

Illustrations

Figures should be numbered as 1, 2, 3 and so on, and mentioned clearly in the main text. Provide a brief title for each figure on a separate page. No detailed legend should be involved under the figures. This part should add into the text where the figures are applicable. Digital images: black and white photographs should be scanned and saved in TIFF format at a resolution of 300 dpi; color images should be saved as CMYK (print files) and not RGB (screen-viewing files). Place each photograph in a separate file. Print images: supply images of size no smaller than 126×76 mm printed on smooth surface paper; label the image by writing the Figure number and orientation using an arrow. Photomicrographs: indicate the original magnification and stain in the legend. Digital Drawings: supply files in EPS if created by Freehand and Illustrator, or TIFF from Photoshop. EPS files must be accompanied by a version in native file format for editing purposes. Scans of existing line drawings should be scanned at a resolution of 1200 dpi and as close as possible to the size at which they will appear when printed, not smaller. Please use uniform legends for the same subjects. For example: Figure 1 Pathological changes of atrophic gastritis after treatment. A: ...; B: ...; C: ...; D: ...; E: ...; F: ...; G: ...

Tables

Three-line tables should be numbered as 1, 2, 3 and so on, and mentioned clearly in the main text. Provide a brief title for each table. No detailed legend should be involved under the tables. This part should add into the text where the tables are applicable. The information should complement but not duplicate that contained in the text. Use one horizontal line under the title, a second under the column heads, and a third below the Table, above any footnotes. Vertical and italic lines should be omitted.

Notes in tables and illustrations

Data which is not statistically significant should not be noted. ^a*P*<0.05, ^b*P*<0.01 (*P*>0.05 should not be noted). If there are other series of *P* values, ^c*P*<0.05 and ^d*P*<0.01 are used; Third series of *P* values can be expressed as ^e*P*<0.05 and ^f*P*<0.01. Other notes in tables or under

illustrations should be expressed as 1F , 2F , 3F ; or some other symbols with a superscript (Arabic numerals) in the upper left corner. In a multi-curve illustration, each curve should be labeled with ●, ○, ■, □, ▲, △, etc. in a certain sequence.

Acknowledgments

Brief acknowledgments of persons who have made genuine contributions to the manuscripts and who endorse the data and conclusions are included. Authors are responsible for obtaining written permission to use any copyrighted text and/or illustrations.

References

Cited references should mainly be drawn from journals covered in the Science Citation Index (<http://www.isinet.com>) and/or Index Medicus (<http://www.ncbi.nlm.nih.gov/PubMed>) databases. Mention all references in the text, tables and figure legends, and set off by consecutive, superscripted Arabic numerals. References should be numbered consecutively in the order in which they appear in the text. Abbreviate journal title names according to the Index Medicus style (<http://www.ncbi.nlm.nih.gov/entrez/query.fcgi?db=journals>). Unpublished observations and personal communications are not listed as references. The style and punctuation of the references conform to ISO standard and the Vancouver style (5th edition); see examples below. Reference lists not conforming to this style could lead to delayed or even rejected publication status. Examples:

Standard journal article (list all authors and include the PubMed ID [PMID] where applicable)

- 1 **Das KM**, Farag SA. Current medical therapy of inflammatory bowel disease. *World J Gastroenterol* 2000; 6: 483-489 [PMID: 11819634]
- 2 **Pan BR**, Hodgson HJF, Kalsi J. Hyperglobulinemia in chronic liver disease: Relationships between *in vitro* immunoglobulin synthesis, short lived suppressor cell activity and serum immunoglobulin levels. *Clin Exp Immunol* 1984; 55: 546-551 [PMID: 6231144]
- 3 **Lin GZ**, Wang XZ, Wang P, Lin J, Yang FD. Immunologic effect of Jianpi Yishen decoction in treatment of Pixu-diarrhoea. *Shijie Huaren Xiaohua Zazhi* 1999; 7: 285-287 [CMFAID:1082371101835979]

Books and other monographs (list all authors)

- 4 **Sherlock S**, Dooley J. Diseases of the liver and biliary system. 9th ed. Oxford: Blackwell Sci Pub, 1993: 258-296

Chapter in a book (list all authors)

- 5 **Lam SK**. Academic investigator's perspectives of medical treatment for peptic ulcer. In: Swabb EA, Azabo S. Ulcer disease: investigation and basis for therapy. New York: Marcel Dekker, 1991: 431-450

Electronic journal (list all authors)

- 6 **Morse SS**. Factors in the emergence of infectious diseases. *Emerg Infect Dis serial online*, 1995-01-03, cited 1996-06-05; 1(1):24 screens. Available from: URL: <http://www.cdc.gov/ncidod/EID/eid.htm>

PMID requirement

From the full reference list, please submit a separate list of those references embodied in PubMed, keeping the same order as in the full reference list, with the following information only: (1) abbreviated journal name and citation (e.g. *World J Gastroenterol* 2003;9(11): 2400-2403; (2) article title (e.g. Epidemiology of gastroenterologic cancer in Henan Province, China); (3) full author list (e.g. Lu JB, Sun XB, Dai DX, Zhu SK, Chang QL, Liu SZ, Duan WJ); (4) PMID (e.g. 14606064). Provide the full abstracts of these references, as quoted from PubMed on a 3.5 inch disk or CD-ROM in Microsoft Word format and send by post to the *WJG* Press. For those references taken from journals not indexed by *Index Medicus*, a printed copy of the first page of the full reference should be submitted. Attach these references to the end of the manuscript in their order of appearance in the text.

Inappropriate references

Authors should always cite references that are relevant to their article, and avoid any inappropriate references. Inappropriate references include those that are linked with a hyphen and the difference between the two numbers at two sides of the hyphen is more than 5. For example, [1-6], [2-14] and [1,3,4-10,22] are all considered as inappropriate references. Authors should not cite their own unrelated published articles.

Statistical data

Present as mean±SD and mean±SE.

Statistical expression

Express *t* test as *t*(in italics), *F* test as *F*(in italics), chi square test as χ^2 (in Greek), related coefficient as *r*(in italics), degree of freedom as γ (in Greek), sample number as *n*(in italics), and probability as *P*(in italics).

Units

Use SI units. For example: body mass, *m*(B) = 78 kg; blood pressure, *p* (B)=16.2/12.3 kPa; incubation time, *t*(incubation)=96 h, blood glucose concentration, *c*(glucose) 6.4±2.1 mmol/L; blood CEA mass concentration, *p*(CEA) = 8.6 24.5 μg/L; CO₂ volume fraction, 50 mL/L CO₂ not 5% CO₂; likewise for 40 g/L formaldehyde, not 10% formalin; and mass fraction, 8 ng/g, etc. Arabic numerals such as 23,243,641 should be read 23 243 641.

The format about how to accurately write common units and quantum is at: <http://www.wjgnet.com/wjg/help/15.doc>

Abbreviations

Standard abbreviations should be defined in the abstract and on first mention in the text. In general, terms should not be abbreviated unless they are used repeatedly and the abbreviation is helpful to the reader. Permissible abbreviations are listed in Units, Symbols and Abbreviations: A Guide for Biological and Medical Editors and Authors (Ed. Baron DN, 1988) published by The Royal Society of Medicine, London. Certain commonly used abbreviations, such as DNA, RNA, HIV, LD50, PCR, HBV, ECG, WBC, RBC, CT, ESR, CSF, IgG, ELISA, PBS, ATP, EDTA, mAb, can be used directly without further mention.

Italicization

Quantities: *t* time or temperature, *c* concentration, *A* area, *l* length, *m* mass, *V* volume.

Genotypes: *gyrA*, *arg 1*, *c myc*, *c fos*, etc.

Restriction enzymes: *EcoRI*, *HindI*, *BamHI*, *Kbo I*, *Kpn I*, etc.

Biology: *Helicobacter pylori*, *H pylori*, *E coli*, etc.

SUBMISSION OF THE REVISED MANUSCRIPTS AFTER ACCEPTED

Please revise your article according to the revision policies of *WJG*. The revised version including manuscript and high-resolution image figures (if any) should be copied on a floppy or compact disk. Author should send the revised manuscript, along with printed high-resolution color or black and white photos, copyright transfer letter, the final check list for authors, and responses to reviewers by a courier (such as EMS) (submission of revised manuscript by e-mail or on the *WJG* Editorial Office Online System is NOT available at present).

Language evaluation

The language of a manuscript will be graded before sending for revision. (1) Grade A: priority publishing; (2) Grade B: minor language polishing; (3) Grade C: a great deal of language polishing; (4) Grade D: rejected. The revised articles should be in grade B or grade A.

Copyright assignment form

It is the policy of *WJG* to acquire copyright in all contributions. Papers accepted for publication become the copyright of *WJG* and authors will be asked to sign a transfer of copyright form. All authors must read and agree to the conditions outlined in the Copyright Assignment Form (which can be downloaded from <http://www.wjgnet.com/wjg/help/9.doc>).

Final check list for authors

The format is at: <http://www.wjgnet.com/wjg/help/13.doc>

Responses to reviewers

Please revise your article according to the comments/suggestions of reviewers. The format for responses to the reviewers' comments is at: <http://www.wjgnet.com/wjg/help/10.doc>

Proof of financial support

For paper supported by a foundation, authors should provide a copy of the document and serial number of the foundation.

Publication fee

Authors of accepted articles must pay publication fee.

World Journal of Gastroenterology standard of quantities and units

Number	Nonstandard	Standard	Notice
1	4 days	4 d	In figures, tables and numerical narration
2	4 days	four days	In text narration
3	day	d	After Arabic numerals
4	Four d	Four days	At the beginning of a sentence
5	2 hours	2 h	After Arabic numerals
6	2 hs	2 h	After Arabic numerals
7	hr, hrs,	h	After Arabic numerals
8	10 seconds	10 s	After Arabic numerals
9	10 year	10 years	In text narration
10	Ten yr	Ten years	At the beginning of a sentence
11	0,1,2 years	0,1,2 yr	In figures and tables
12	0,1,2 year	0,1,2 yr	In figures and tables
13	4 weeks	4 wk	
14	Four wk	Four weeks	At the beginning of a sentence
15	2 months	2 mo	In figures and tables
16	Two mo	Two months	At the beginning of a sentence
17	10 minutes	10 min	
18	Ten min	Ten minutes	At the beginning of a sentence
19	50% (V/V)	500 mL/L	
20	50% (m/V)	500 g/L	
21	1 M	1 mol/L	
22	10 μM	10 μmol/L	
23	1NHCl	1 mol/L HCl	
24	1NH ₂ SO ₄	0.5 mol/L H ₂ SO ₄	
25	4rd edition	4 th edition	
26	15 year experience	15- year experience	
27	18.5 kDa	18.5 ku, 18 500u or M _r 18 500	
28	25 g·kg ⁻¹ /d ⁻¹	25 g/(kg·d) or 25 g/kg per day	
29	6900	6 900	
30	1000 rpm	1 000 r/min	
31	sec	s	After Arabic numerals
32	1 pg·L ⁻¹	1 pg/L	
33	10 kilograms	10 kg	
34	13 000 rpm	13 000 g	High speed; g should be in italic and suitable conversion.
35	1000 g	1 000 r/min	Low speed. g cannot be used.
36	Gene bank	GeneBank	International classified genetic materials collection bank
37	Ten L	Ten liters	At the beginning of a sentence
38	Ten mL	Ten milliliters	At the beginning of a sentence
39	umol	μmol	
40	30 sec	30 s	
41	1 g/dl	10 g/L	10-fold conversion
42	OD ₂₆₀	A ₂₆₀	"OD" has been abandoned.
43	Oneg/L	One microgram per liter	At the beginning of a sentence
44	A ₂₆₀ nm ^b P<0.05	A ₂₆₀ nm ^a P<0.05	A should be in italic. In Table, no note is needed if there is no significance in statistics: ^a P<0.05, ^b P<0.01 (no note if P>0.05). If there is a second set of P value in the same table, ^c P<0.05 and ^d P<0.01 are used for a third set: ^e P<0.05, ^f P<0.01.
45	*F=9.87, [§] F=25.9, [#] F=67.4	¹ F=9.87, ² F=25.9, ³ F=67.4	Notices in or under a table
46	KM	km	kilometer
47	CM	cm	centimeter
48	MM	mm	millimeter
49	Kg, KG	kg	kilogram
50	Gm, gr	g	gram
51	nt	N	newton
52	l	L	liter
53	db	dB	decibel
54	rpm	r/min	rotation per minute
55	bq	Bq	becquerel, a unit symbol
56	amp	A	ampere
57	coul	C	coulomb
58	HZ	Hz	
59	w	W	watt
60	KPa	kPa	kilo-pascal
61	p	Pa	pascal
62	ev	EV	volt (electronic unit)
63	Jonle	J	joule
64	J/mmol	kJ/mol	kilojoule per mole
65	10×10×10cm ³	10 cm×10 cm×10 cm	
66	N·km	KN·m	moment
67	$\bar{x} \pm s$	mean±SD	In figures, tables or text narration
68	Mean±SEM	mean±SE	In figures, tables or text narration
69	im	im	intramuscular injection
70	iv	iv	intravenous injection
71	Wang et al	Wang et al.	
72	EcoRI	EcoRI	Eco in italic and RI in positive. Restriction endonuclease has its prescript form of writing.
73	Ecoli	E.coli	Bacteria and other biologic terms have their specific expression.
74	Hp	H pylori	
75	Iga	Iga	writing form of genes
76	igA	IgA	writing form of proteins
77	~70 kDa	~70 ku	